

Dirk Praetorius

Lubomír Bañas



TECHNISCHE
UNIVERSITÄT
WIEN
Vienna University of Technology

DISSERTATION

On Dynamical Micromagnetism

ausgeführt zum Zwecke der Erlangung des akademischen Grades
eines Doktors der Naturwissenschaften unter der Leitung von

Ao. Univ.-Prof. Dipl.-Math. Dr.techn. Dirk Praetorius

E101 - Institut für Analysis und Scientific Computing, TU Wien

und

Prof. Dr. Ľubomír Bañas

Fakultät für Mathematik, Universität Bielefeld

eingereicht an der Technischen Universität Wien

Fakultät für Mathematik und Geoinformation

von

Marcus Page, M.Sc.

Matrikelnummer: 0847860

Rienöfßgasse 9/10a

1040 Wien

Wien, am 1. Okt. 2013

gewidmet meinen Eltern
Monika Page und Wolfgang Page

Kurzfassung

Magnetische Prozesse spielen eine wichtige Rolle in einer Vielzahl technologischer Anwendungen. Speziell im Mikroskalenbereich basieren viele Geräte auf der Ausnutzung des dynamischen Verhaltens der Magnetisierung \mathbf{m} eines ferromagnetischen Körpers, etwa zur Datensicherung auf magnetischen Festplatten. In diesen Größenbereichen wird das Verhalten der Magnetisierung von einer Vielzahl physikalischer Effekte beeinflusst. Um diese Effekte ausreichend gut vorausszusagen, und damit die Kosten für die Entwicklung und Verbesserung solcher Hardware niedrig zu halten, bedarf es zuverlässiger numerischer Simulationen.

Die Grundlage für diese Simulationen bildet die *Landau-Lifshitz-Gilbert* Gleichung (LLG). Diese modelliert die Dynamik der Magnetisierung eines ferromagnetischen Körpers Ω über einem Zeitintervall $(0, T)$ und unter dem Einfluss des sogenannten *effektiven Feldes*. Die verschiedenen physikalischen Effekte tragen in Form von Operatoren zu diesem effektiven Feld und damit dem Verhalten der Magnetisierung bei. Mathematische Herausforderungen bei dieser zeitabhängigen partiellen Differentialgleichung liegen in ihrer starken Nichtlinearität, etwaigen komplexen und nichtlokalen Feldbeiträgen, sowie einer inhärenten nichtkonvexen Nebenbedingung zur Längenerhaltung der Magnetisierung.

Ausgangspunkt der vorliegenden Arbeit bildet die Arbeit [ALOUGES, Disc. Cont. Dyn. Sys. Ser. S, 2008], sowie deren Erweiterungen [ALOUGES et al., Physica B, 2011] und [GOLDENITS, Dissertation, TU Wien, 2012]. Im erstgenannten Beitrag leitet der Autor ein Finite-Elemente-Schema für die LLG Gleichung her, welches nur die Lösung eines linearen Gleichungssystems pro Zeitschritt erfordert und dabei unbedingte Konvergenz sicherstellt.

In dieser Arbeit behandeln wir multiple Erweiterungen der Analysis von ALOUGES. Zunächst untersuchen wir die reine LLG Gleichung für ein allgemeines effektives Feld, während ALOUGES und die genannten Nachfolgearbeiten nur klassische Feldbeiträge betrachten. Dadurch gewinnen wir zwei abstrakte Voraussetzungen an die einzelnen Feldbeiträge, welche die unbedingte Konvergenz des Verfahrens garantieren. Wir weisen nach, dass die klassischen Feldbeiträge durch unseren abstrakten Zugang abgedeckt sind und auch ein neuer Mehrskalenzugang aus [BRUCKNER, Dissertation, TU Wien, 2013] in diesen Rahmen fällt.

Im zweiten Schritt betrachten wir gekoppelte Probleme, d.h. wir koppeln LLG mit einer weiteren Evolutionsgleichung, um zusätzliche Effekte simulieren zu können. Konkret untersuchen wir Kopplung zum vollen Maxwell-System (als Modellbeispiel für hyperbolische Gleichungen zweiter Ordnung) und der eddy-current Gleichung (als Modellbeispiel für eine parabolische Gleichung zweiter Ordnung) zum besseren Verständnis magnetischer Felder, sowie der Impulserhaltungsgleichung (als Modellbeispiel für einen nichtlinearen Kopplungsoperator) für magnetoelastische Effekte. In allen Fällen schlagen wir Algorithmen vor, welche die Gleichungen numerisch entkoppeln, d.h. statt eines großen (nichtlinearen) Systems lösen wir pro Zeitschritt nacheinander zwei kleinere lineare Systeme, eines für LLG und eines für die gekoppelte Gleichung. Trotz dieser Entkopplung, die in der Praxis große Vorteile bietet, erhalten wir keine zusätzliche Anforderung an Orts- und Zeitschrittweite und können jeweils unbedingte Konvergenz nachweisen. Unsere Analysis liefert ferner konstruktive Beweise für die Existenz von (schwachen) Lösungen, d.h. wir zeigen, dass die berechenbaren diskreten Lösungen gegen eine schwache Lösung des Gesamtsystems konvergieren.

Numerische Simulationen runden die Arbeit ab.

Abstract

Magnetic processes play an important role in a variety of technological applications. Especially on a microscale, many devices rely on the exploitation of the dynamic behaviour of the magnetization \mathbf{m} of a ferromagnetic body. This is used, for example, for data storage in magnetic hard drives. Within these length scales, the behaviour of the magnetization is influenced by a multitude of physical effects. In order to reliably predict these effects, and thus lower the production costs for development and/or improvement of such devices, we require reliable numerical simulations.

The foundation for those simulations is the *Landau-Lifshitz-Gilbert* equation (LLG). This equation models the dynamics of the magnetization of a ferromagnetic body Ω on some time intervall $(0, T)$ under the influence of the so-called *effective field*. The different physical effects contribute to this effective field, and hence the behaviour of \mathbf{m} , in form of operators on suitable Banach spaces. Mathematical challenges of this time-dependent partial differential equation are given by a strong nonlinearity, possible complicated and nonlocal field contributions, as well as an inherent non-convex side constraint which enforces length preservation of \mathbf{m} .

Starting point for this thesis is the work [ALOUGES, Disc. Cont. Dyn. Sys. Ser. S, 2008] as well as the subsequent contributions [ALOUGES et al., Physica B, 2011] and [GOLDENITS, PhD thesis, Vienna UT, 2012]. In the first one, the author constructs a finite-element-scheme for the LLG equation which only requires the solution of one linear system per time step. Moreover, unconditional convergence is proved.

In this work, we consider multiple extensions of ALOUGES' analysis. First, we investigate the pure LLG equation with an abstract effective field, while ALOUGES and the mentioned subsequent works only consider classical field contributions. Via this approach, we derive two conditions which guarantee unconditional convergence provided that they are satisfied by all contributions of the effective field. We further show that all classical field contributions are covered by this general advance, and that even a new multiscale model from [BRUCKNER, PhD thesis, Vienna UT, 2013] falls into this setting.

In a second step, we deal with coupled problems, i.e. problems where LLG is coupled to a second evolution equation, in order to include even more physical effects. More precisely, we investigate coupling to the full Maxwell system (as a model problem for hyperbolic second order PDEs) and the eddy-current equation (as a model problem for parabolic second order PDEs) for a more precise modeling of the occurring magnetic fields. Moreover, we consider coupling to the conservation of momentum equation (as a model problem for nonlinear coupling operators) to account for magnetostriction, i.e. magnetoelastic effects. In all cases, we propose algorithms that numerically decouple both equations, i.e. instead of one large (and possibly nonlinear) system, we subsequently solve two smaller linear systems in each time step, one for LLG and one for the coupled PDE. Despite this decoupling, which provides major advantages in practice, we still prove unconditional convergence. Moreover, in all cases, our analysis yields constructive proofs of the existence of (weak) solutions in the sense that the computable discrete solutions converge towards some weak solution of the overall PDE system.

Numerical simulations complete the work.

Danksagung

An dieser Stelle möchte ich mich gerne bei den vielen lieben Menschen bedanken, ohne die die vorliegende Arbeit sicherlich nicht in dieser Form möglich gewesen wäre.

Allen voran gilt mein Dank meinem Betreuer und Lehrer Dirk Praetorius. Sicherlich bedanke ich mich für die Vergabe dieses Themas und die Einführung in einen spannenden Forschungsbereich den ich alleine niemals hätte wählen können. Mein aufrichtiger Dank gilt ihm jedoch für all die anderen Dinge durch die er mich in den letzten Jahren, nicht nur fachlich, unterstützt hat. Er hat mich aufgebaut als es den Anschein hatte, dass nichts so funktioniert wie es sollte, mir viele Reisen zu spannenden Konferenzen und Orten ermöglicht, und als Bindeglied unserer Arbeitsgruppe einfach dafür gesorgt dass man sich hier wohl fühlt. Vielen vielen Dank dafür.

Auch Ľubomír Bañas gilt mein besonderer Dank. Im Laufe dieser Arbeit haben die Gespräche mit ihm mehrfach genau den richtigen Hinweis zur richtigen Zeit geliefert. Außerdem hatte er für meine (naiven) Fragen stets ein offenes Ohr. Er hat mich zu Forschungsaufenthalten, spannenden Diskussionen und lustigen Abenden eingeladen, und sicherlich sehr viel Zeit mit dem Lesen dieser Arbeit verbracht. Vielen Dank dafür.

Ich bin stets in den Genuss gekommen, mich auf eine tolle Arbeitsgruppe verlassen zu können. Dies gilt sowohl für die bitteren Momenten des Doktorats als auch für die lustigen. Allen voran steht hier Michael Feischl der immer für jeden Spaß und Froyo zu haben war. Aber auch den ganzen Rest, Michael Karkulik, Thomas Führer, Josef Kemetmüller, Michele Ruggeri, Markus Faustmann und Markus Mayr möchte ich erwähnen. Nicht unerwähnt bleiben darf hier auch meine Leidensgenossin Petra Goldenits mit der ich viele gute und schlechte Zeiten erlebt habe und die meine Dissertationszeit, zumindest zu Beginn, maßgeblich mitgeprägt hat.

Nicht minder lustig, wenn auch nicht zu meiner Arbeitsgruppe gehörend, war die Zusammenarbeit mit Florian Bruckner und Jonathan Rochat. Danke und macht weiter so.

Auch von privater Seite habe ich in den letzten Jahren unendlich viel Unterstützung erhalten. Es ist schwer in Worte zu fassen, wie wichtig es ist, einen guten Freundeskreis zu haben damit man nicht vergisst, dass es auch noch ein Leben neben der Uni gibt. Ich möchte mich daher ausdrücklich bei all meinen Freunden bedanken. Ihr wart immer für mich da und ich freue mich schon auf alles was noch kommt ;).

Abschließend möchte ich mich von ganzem Herzen bei Susanne und meiner Familie, mit meinen Eltern und meinem Bruder Sven, bedanken. Ihr seid bedingungslos auf meiner Seite und gebt mir immer wieder Kraft und Ausdauer. Danke, dass es euch gibt!

Contents

1. Introduction	1
1.1. What is all about	3
1.2. The Landau-Lifshitz-Gilbert equation and the effective field	4
1.3. Classical field contributions	8
1.4. Extended contributions	11
1.4.1. Multiscale modeling	11
1.4.2. The Maxwell system	12
1.4.3. Magnetoelastic interactions	14
1.5. Preliminaries & Notation	14
1.6. Overview over the current literature	17
1.7. Structure of this thesis and main results	21
2. Problem formulation and discretization	23
2.1. What are we trying to do	23
2.1.1. Numerical framework	25
2.2. Abstract algorithm	27
2.3. Abstract convergence analysis	31
2.3.1. Time-dependent energy contributions	44
2.4. Improved energy estimate	55
3. Application to field contributions	61
3.1. Classical contributions	61
3.1.1. Magnetocrystalline anisotropy and pointwise operators	61
3.1.2. Applied exterior field	63
3.1.3. Linear and continuous contributions, e.g., the strayfield operator	63
3.2. Uniformly monotone operators	68
3.2.1. Multiscale problems	71
3.3. Numerical experiments	78
3.3.1. General performance	78
3.3.2. Finite time blowup in 2D	82
3.3.3. The case $\alpha = 0$	87

4. Coupling to full Maxwell system	95
4.1. The Maxwell-Landau-Lifshitz-Gilbert system	95
4.2. Preliminaries and numerical algorithms	98
4.2.1. Analysis of coupled Algorithm 4.2.1	104
4.2.2. Analysis of fully decoupled Algorithm 4.2.2	109
4.2.3. Improved energy estimates	115
5. Coupling to the eddy-current equation	123
5.1. The eddy-current-LLG system	123
5.2. Preliminaries and numerical algorithm	125
5.3. Convergence analysis	126
5.3.1. Improved energy estimate	130
5.4. Numerical experiments	132
5.4.1. General performance	133
5.4.2. Finite time blowup in 3D	136
5.4.3. Remarks on known stable states	142
6. LLG with magnetostriction	149
6.1. Elasticity model and problem formulation	149
6.2. Preliminaries and numerical integrator	153
6.2.1. Convergence analysis	155
6.3. Numerical experiments	165
6.3.1. General performance	165
6.3.2. Some thoughts on energy	173
6.3.3. Effects on hysteresis	176
7. Outlook and open questions	179
A. Appendix	183
A.1. Equalities and inequalities	183
A.2. Functional analytic facts	185
A.3. What else?	189
Bibliography	197
Author's CV	204

Chapter 1

Introduction

MAGNETISM accompanied mankind throughout the centuries. From the first reference by THALES OF MILETUS (around 585 B.C.), who thought that certain materials attracted each other because they have souls, to the construction and initial operation of the high-speed Transrapid Maglev train in Shanghai in 2004, it shaped our understanding of the world. The exploitation of magnetism, while not fully understood, led to the development of the compass and its use in navigation which revolutionized travel sometime between the 9th and 11th century. The first comprehensive scientific contribution to the understanding of magnetism goes back to WILLIAM GILBERT around 1600 with the famous work *De Magnete, Magneticisque Corporibus, et de Magno Magnete Tellure* [Gil00]. In this work, GILBERT even experimentally concluded that the earth itself is a giant magnet. Over time, more and more scientists, among others CARL FRIEDRICH GAUSS and MICHAEL FARADAY, contributed to the physical understanding and the mathematical modeling of magnetic fields and their relationship to electric currents. Finally, in 1865, JAMES CLERK MAXWELL proposed a set of equations which describe the interactions of electricity and magnetism and laid the foundation to the study of electromagnetism, cf. [Max65]. Today, we count the electromagnetic force as one of the four fundamental interactions between physical bodies. The unification of the forces *gravitation*, *electromagnetism*, *weak nuclear force*, and *strong nuclear force* into a unifying *theory of everything* is one of the major open problems in modern physics and subject to comprehensive research. The history of magnetism is thus far from being over and will undoubtedly influence science and technology for many more generations [Ver93].

In this work, we consider magnetic interactions of very small magnetic bodies. The magnetic condition of such a body at a given time is described by a physical quantity called *magnetization*. Magnetic effects to control the behaviour of the magnetization are exploited in various technological devices throughout all areas. In magnetic recording devices, e.g. hard drives, for example, the magnetization of Ironoxid or Cobalt is used to store data. To that end, a very thin layer of the magnetic material is applied to a slice. Via a magnetic field, the magnetization of the material can now be aligned almost parallel into one direction (e.g. left or right) in certain areas of the slice. The recording head which emits the magnetic field, can then be utilized to change the direction of the magnetization in a specific area at any time. Employing the interpretation, e.g., *left* $\hat{=}$ 1 and *right* $\hat{=}$ 0, any data can be stored in this way. This basic functionality is visualized in Figure 1.1

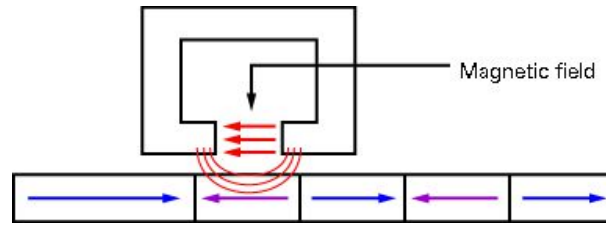


Figure 1.1.: Basic functionality of a magnetic hard drive. *Picture taken from www.elektronik-kompandium.de, copyright of Patrick Schnabel is thankfully acknowledged.*

On a microscale, the dynamical behaviour of the magnetization depends on a variety of physical influences that exceed the simple response to a magnetic field. Instead, on this scale one even needs to consider interactions on the atomistic level as well as the alignment of the different molecules within the crystal lattice. The dynamical behaviour of a magnetization then follows the Landau-Lifshitz-Gilbert equation which is a strongly nonlinear partial differential equation which inherently includes some non-convex side constraint. The interpretation and mathematical modeling of this equation as well as the influential effects are described in detail below. Over time, the size of technological devices tends to get smaller under the same requirements like e.g. storage capacity. In order to guarantee progress and working technology while avoiding unnecessary costs, reliable and fast computer simulations, that take into account as many physical effects as possible, are thus required.

In this thesis, we contribute to this requirement and construct an unconditionally convergent numerical scheme to simulate micromagnetic problems. The main leitmotif of this thesis is always the generality of the discretization approach. To be more precise, we investigate and give answers to the following questions:

- What is the set of assumptions that an influential effect needs to fulfill in order to be reliably included into the numerical scheme? Here, we always ensure that the scheme remains unconditionally convergent. In particular, this includes:
 - Can linear effects be included?
 - Can nonlinear effects be included?
 - Can time dependent effects be included?
 - What can we say about the energy of the system?
- Are the effects considered in the classical literature compatible with our requirements?
- Are multiscale problems compatible with our requirements?
- Some effects require coupling of the Landau-Lifshitz-Gilbert equation to yet another PDE. We show that those problems are also compatible with our scheme. This includes:
 - Can we couple linear parabolic PDEs, e.g., the eddy-current formulation?
 - Can we couple linear hyperbolic PDEs, e.g., the full Maxwell system?
 - Can we include couplings, where the coupling operator is nonlinear, e.g., the magnetostrictive effect?

- Can the individual problems be decoupled for the numerical simulation without posing a condition on the discretization parameters?
- How can we make the overall integrator computationally attractive?

1.1. What is all about

The basic goal of this work, which coincides with the goal of many other works in the area of dynamical micromagnetism, is to gain knowledge about the magnetization of a ferromagnetic material of very small size. The magnetization of such a magnet is a physically measurable quantity which basically states how magnetic the material is at a certain point and into a certain direction. In principle, information about the state of the magnetization (or any other physical quantity) can be gained in three ways.

- (i) Experimentally
- (ii) Analytically / Theoretically
- (iii) Computationally (i.e. by means of a computer simulation)

While the second and third possibilities require a suitable model that describes the behaviour of the magnetization under the influence of certain effects, the first one merely uses observation in order to derive those very models. It therefore has to be completed before the other two steps. As usually (and so in micromagnetics), this was done by experimental physicists, and the reader is referred to the pioneering works [LL35] and [Gil55] from 1935 and 1955, respectively, as well as to the monograph [HS08] and the references therein. The work of the mathematician then begins in step (ii) as well-posedness of the model, existence of solutions, and regularity properties are investigated. Here, we refer to the pioneering works [Vis85] and [AS92] to name only a few. Finally, one is interested in the prediction of the behaviour of the magnetization in certain setups in order to make the physical effects usable in, e.g., technological devices like magnetic hard drives. This prediction is usually done by means of computer simulations, and thus the need for reliable and fast solvers of the given model arises. To that end, a variety of work has been done, and the reader is referred to the overview articles [KP06, Cim07a, GC09], the monograph [Pro01], and the references therein. A brief overview is also given in Section 1.6.

The contributions of this thesis are located between (ii) and (iii) as we construct reliable numerical schemes which are then rigorously analyzed and thus also give insight into the properties of the solution.

Mathematically speaking, a magnet is modeled by a bounded, polyhedral domain $\Omega \subset \mathbb{R}^3$ with boundary $\Gamma = \partial\Omega$. The dynamics of the magnetization is investigated on the finite time interval $[0, T]$ for some $T > 0$. The magnetization \mathbf{M} in $[A/m]$ is then given as a function

$$\mathbf{M} : \Omega_T := (0, T) \times \Omega \longrightarrow \{\mathbf{x} \in \mathbb{R}^3 : |\mathbf{x}| = M_s\}. \quad (1.1.1)$$

Here, M_s denotes the saturation magnetization in $[A/m]$. This models the fact that the ferromagnet is saturated, i.e. that the magnetization cannot be increased any further by applying a stronger magnetic field. The strength of the magnetization in a saturated material, mathematically the length of \mathbf{M} at any point, is actually temperature dependent. In our setting, we

thus implicitly assume that the temperature does not change over time, i.e. the length of the magnetization remains constant over time. Moreover, we assume that the temperature is below the Curie point, where the magnet loses its ferromagnetic properties. The magnetization can thus be written as $\mathbf{M} = M_s \mathbf{m}$ for some dimensionless direction \mathbf{m} of unit length.

Remark . *The inclusion of variable temperature into both, the simulations as well as the development of recording devices, for so-called heat-assisted-recording, is currently an active field of research. It is, however, beyond the scope of this work, and we refer to e.g. [BPS08, BPS12] and the references therein for further information.*

In physics literature, one often deals with the polarization \mathbf{J} instead of \mathbf{M} as the relevant quantity, cf. e.g. [SSS⁺01]. This is, however, equivalent as it describes only some scaling with the permeability of vacuum $\mu_0 = 4\pi \cdot 10^{-7}$ in $[Tm/A]$. This rescaling allows to work with magnetic fields given in $[T]$, rather than $[A/m]$ which is more suitable in some situations. Together with the polarization \mathbf{J} , one has the saturation polarization J_s , and there holds

$$\mathbf{J} = \mu_0 \mathbf{M}, \quad J_s = \mu_0 M_s, \quad \text{and} \quad \mathbf{J} = J_s \mathbf{m}.$$

As mentioned above, various physical effects have an influence on the polarization resp. the magnetization. Those effects now contribute to the so-called total effective field \mathbf{H}_{eff} in the form of operators (on suitable Banach spaces). This effective field then drives the dynamical behaviour of \mathbf{J} via the Landau-Lifshitz-Gilbert equation which is described in the next section.

From a physical point of view, one often argues with energies rather than operators. Such an approach is also possible here, since one can assign a certain energy to each physical effect. The sum of all energies then denotes the total energy $\mathcal{E}_{\text{total}}$ in $[J]$ of the polarization. The effective field is then simply given by the first variation of the total energy after the polarization. As one expects, the magnetization pursues a state of minimal energy and the stationary solutions of the upcoming Landau-Lifshitz-Gilbert equation minimize the total energy $\mathcal{E}_{\text{total}}$, cf. e.g. [Alo08b].

1.2. The Landau-Lifshitz-Gilbert equation and the effective field

The dynamical behaviour of a magnetic polarization \mathbf{J} over time and under the influence of an effective magnetic field \mathbf{H}_{eff} is described by the Landau-Lifshitz-Gilbert (LLG) equation

$$\mathbf{J}_t = -\frac{\gamma_0}{1 + \alpha^2} \mathbf{J} \times \mathbf{H}_{\text{eff}} - \frac{\alpha \gamma_0}{(1 + \alpha^2) J_s} \mathbf{J} \times (\mathbf{J} \times \mathbf{H}_{\text{eff}}). \quad (1.2.1)$$

Here, $\gamma_0 = 2.210173 \cdot 10^5$ in $[m/(As)]$ denotes the gyromagnetic ratio, and \mathbf{H}_{eff} in $[A/m]$ denotes the total effective field which accounts for all the included physical effects below. The effective field is given as the negative variation

$$\mathbf{H}_{\text{eff}} = -\frac{\partial \mathcal{E}_{\text{total}}}{\partial \mathbf{J}} \quad (1.2.2)$$

of the total energy $\mathcal{E}_{\text{total}}$ in $[J]$ after the polarization \mathbf{J} . To ease the presentation, one usually considers a non-dimensional formulation of LLG. We refer to [Gol12, Section 1.1], where the derivation of this formulation is comprehensively discussed. As dimensionless equation, (1.2.1) takes the form

$$\mathbf{m}_t = -\frac{1}{1 + \alpha^2} \mathbf{m} \times \mathbf{h}_{\text{eff}} - \frac{\alpha}{1 + \alpha^2} \mathbf{m} \times (\mathbf{m} \times \mathbf{h}_{\text{eff}}), \quad (1.2.3)$$

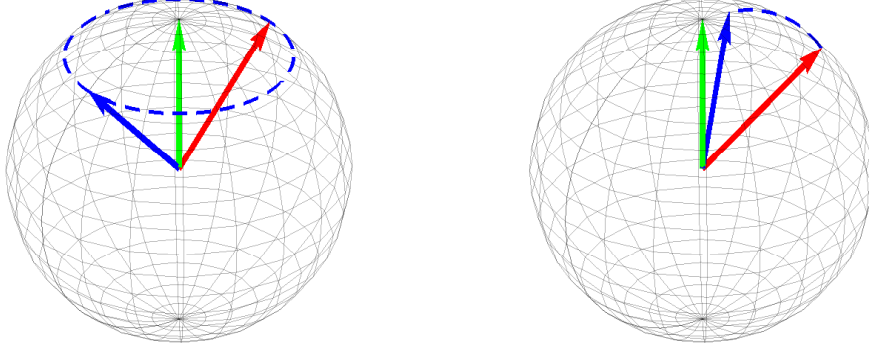


Figure 1.2.: Precession part (*left*) and damping part (*right*) of the LLG equation.

for some dimensionless magnetization

$$\mathbf{m} : \Omega_T \longrightarrow \mathbb{S}^2 := \{\mathbf{x} \in \mathbb{R}^3 : |\mathbf{x}| = 1\}.$$

In addition, (1.2.3) is supplemented by the following initial and boundary conditions

$$\mathbf{m}(0) = \mathbf{m}_0 \quad \in \mathbf{H}^1(\Omega, \mathbb{S}^2), \quad (1.2.4)$$

$$\partial_n \mathbf{m} = 0 \quad \text{on } \partial\Omega_T := (0, T) \times \partial\Omega. \quad (1.2.5)$$

In the following, we will investigate this equation a little bit closer.

The precession term

The first term on the right hand side of (1.2.3) denotes the so-called precession and can be rigorously derived from quantum mechanical concepts. Starting from Schrödinger's equation

$$\frac{d}{dt} \langle M_i \rangle = \frac{1}{i\hbar} \langle [M_i, \hat{\mathcal{E}}] \rangle, \quad i = 1, 2, 3 \quad (1.2.6)$$

for the Hamiltonian $\hat{\mathcal{E}}$, a technical derivation yields

$$\mathbf{m}_t = -\mathbf{m} \times \mathbf{h}_{\text{eff}}, \quad (1.2.7)$$

which is the classical undamped Landau-Lifshitz equation. For details on the derivation of equation (1.2.7), we refer to [Hrk05, GD08, Woh10]. The solution of Equation (1.2.7) describes a rotation of the magnetization \mathbf{m} around the effective field \mathbf{h}_{eff} . This behaviour is visualized in Figure 1.2 (*left*), where \mathbf{h}_{eff} is visualized by the green arrow and the magnetization at two points in time, t_1 and t_2 , is plotted in red and blue, respectively.

The damping term

The second part of (1.2.3) cannot be motivated mathematically. It was phenomenologically introduced by LANDAU and LIFSHITZ in [LL35] for some damping parameter λ to account for

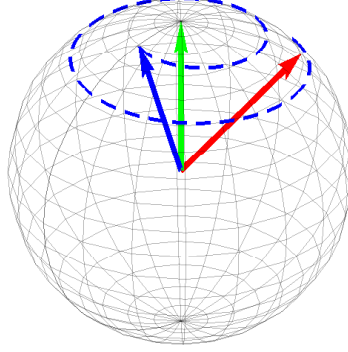


Figure 1.3.: Evolution of the magnetization, where precession and damping are taken into account.

friction effects. Consequently, the equation

$$\mathbf{m}_t = -\lambda \mathbf{m} \times (\mathbf{m} \times \mathbf{h}_{\text{eff}}) \quad (1.2.8)$$

describes damping of the magnetization towards the effective field. This behaviour is visualized in Figure 1.2 (*right*).

Combining both equations (1.2.7) and (1.2.8), one derives the classical Landau-Lifshitz equation

$$\mathbf{m}_t = -\mathbf{m} \times \mathbf{h}_{\text{eff}} - \lambda \mathbf{m} \times (\mathbf{m} \times \mathbf{h}_{\text{eff}}) \quad (1.2.9)$$

from [LL35]. Taking both effects into account, it describes a magnetization that rotates around the effective field while being damped towards it. This behaviour is visualized in Figure 1.3.

Gilbert's contribution

By 1955, a number of different damping mechanisms had been studied, and we refer to [Gil04] and the references therein for further information. It turned out, however, that while the commonly used Landau-Lifshitz damping term was very feasible for small damping $0 < \lambda \ll 1$, it failed to produce useful results as damping grows larger $\lambda \gg 1$. To that end, GILBERT introduced a new phenomenological damping term which allowed to take into account larger (especially non-eddy-current) damping as it occurs, for example, in thin Permalloy sheets, cf. [Gil55, Gil04]. He derived the equation

$$\mathbf{m}_t = -\mathbf{m} \times (\mathbf{h}_{\text{eff}} - \alpha \mathbf{m}_t), \quad (1.2.10)$$

which is equivalent to

$$\mathbf{m}_t = -\frac{1}{1 + \alpha^2} \mathbf{m} \times \mathbf{h}_{\text{eff}} - \frac{\alpha}{1 + \alpha^2} \mathbf{m} \times (\mathbf{m} \times \mathbf{h}_{\text{eff}}). \quad (1.2.11)$$

The last equation turns out to be much more suitable for larger damping $\alpha \gg 1$. For small damping $\alpha \ll 1$, on the other hand, the term α^2 is negligible, and the LLG equation (1.2.11) is a very good approximation of (1.2.9) for $\lambda = \alpha$.

Throughout this work, we will switch between various different equivalent formulations of LLG as they have distinct advantages and disadvantages. In addition to the equations (1.2.10) and (1.2.11), there is yet another equivalent formulation and for sake of readability, we collect all formulations in the following lemma.

Lemma 1.2.1. *Let LLG be supplemented with the initial and boundary conditions*

$$\begin{aligned} \mathbf{m}(0) &= \mathbf{m}_0 && \in H^1(\Omega, \mathbb{S}^2) \\ \partial_n \mathbf{m} &= 0 && \text{on } \partial\Omega_T. \end{aligned}$$

Then, the following formulations of LLG are equivalent:

$$a) \quad \mathbf{m}_t = -\frac{1}{1+\alpha^2} \mathbf{m} \times \mathbf{h}_{\text{eff}} - \frac{\alpha}{1+\alpha^2} \mathbf{m} \times (\mathbf{m} \times \mathbf{h}_{\text{eff}}) \quad (1.2.12)$$

$$b) \quad \alpha \mathbf{m}_t + \mathbf{m} \times \mathbf{m}_t = \mathbf{h}_{\text{eff}} - \mathbf{m}(\mathbf{m} \cdot \mathbf{h}_{\text{eff}}) \quad \text{and} \quad |\mathbf{m}| = 1 \text{ a.e. in } \Omega_T \quad (1.2.13)$$

$$c) \quad \mathbf{m}_t - \alpha \mathbf{m} \times \mathbf{m}_t = \mathbf{h}_{\text{eff}} \times \mathbf{m}. \quad (1.2.14)$$

Proof. The proof is done by straightforward calculations and exploits properties of the cross product. The elaborated arguments can be found in [Gol12, Lemma 1.2.1]. \square

While equation *a)* is suitable for the interpretation and physical understanding of the two different effects (precession and damping) that drive the magnetization, it will not be used for the upcoming analysis. Instead, equation *b)* will be used for the construction of a numerical scheme below. In order to be consistent with the available literature, equation *c)* will finally serve for the definition of a weak solution.

We close this short section with an observation that directly follows from the LLG equation (1.2.12). Scalar multiplication with \mathbf{m} almost everywhere on Ω_T yields

$$\mathbf{m}_t \cdot \mathbf{m} = -\frac{1}{1+\alpha^2} \mathbf{m} \times \mathbf{h}_{\text{eff}} \cdot \mathbf{m} - \frac{\alpha}{1+\alpha^2} \mathbf{m} \times (\mathbf{m} \times \mathbf{h}_{\text{eff}}) \cdot \mathbf{m}.$$

In combination with the cross product property $(a \times b) \cdot a = 0$ for any $a, b \in \mathbb{R}^3$, this yields

$$\frac{1}{2} \partial_t |\mathbf{m}|^2 = \mathbf{m}_t \cdot \mathbf{m} = 0 \text{ pointwise almost everywhere in } \Omega_T. \quad (1.2.15)$$

The equation thus preserves the length of the vector-valued magnetization at almost every point of the computational domain Ω_T which is in good agreement with (1.1.1). From $|\mathbf{m}_0| = 1$, we thus conclude $|\mathbf{m}| = 1$ almost everywhere in Ω_T . Moreover, we conclude that the time derivative \mathbf{m}_t of the magnetization is pointwise orthogonal to \mathbf{m} . This property will massively enter the construction of our numerical integrator below. Note, however, that this property only follows from the formulations *a)* and *c)* of LLG and has to be explicitly supposed for formulation *b)*.

1.3. Classical field contributions

After we shed some more light on the LLG equation, we take a closer look at the physical effects which influence the dynamic behaviour of the magnetization. In the first part, we consider the classical field contributions

- Exchange
- Microcrystalline anisotropy
- External field
- Strayfield

which are well-known throughout the literature and for which various analytical and numerical results are available. In the next section, we then consider physical effects that extend this classical scheme.

Exchange

The exchange effect describes the property of a ferromagnet that it prefers a constant magnetization. If the sample Ω is large enough, this leads to the formation of domain structures, i.e. subregions of Ω where the magnetization is aligned in parallel, but allows jumps along the walls. Since the investigation of magnetic domains in nanostructures is beyond the scope of this work, we refer to the works [Get08, HS08] and the references therein. The corresponding energy contribution reads

$$\mathcal{E}_{\text{exch}} = \frac{1}{2}C_e \int_{\Omega} |\nabla \mathbf{m}|^2, \quad (1.3.1)$$

where $C_e > 0$ denotes the material dependent exchange constant. The contribution to the effective field caused by the exchange is then given by the Laplacian of the magnetization

$$\mathbf{h}_{\text{exch}} = C_e \Delta \mathbf{m}. \quad (1.3.2)$$

As this contribution involves not only the magnetization, but also its spatial derivative, it requires special treatment. In order to guarantee unconditional convergence of the upcoming scheme, this contribution will thus be treated implicitly.

Microcrystalline anisotropy

In each ferromagnetic material, the particles are aligned in a crystal lattice in which certain directions may be distinguished. A magnetization which is not aligned with those *easy axes*, has a higher energetic value. Consequently, the magnetization prefers the easy directions over the others. This material dependent effect is called microcrystalline anisotropy. A magnetic material may have one (uniaxial) or more (multiaxial) easy directions and the preference of the magnetization might even be inhomogeneously distributed between the different easy axes. For more details and illustrations, the interested reader is referred to [HS08, Section 3.2.3]. For a given anisotropy density

$$\phi : \mathbb{B} := \{\mathbf{x} \in \mathbb{R}^3 : |\mathbf{x}| \leq 1\} \longrightarrow \mathbb{R}^3, \quad (1.3.3)$$

the corresponding anisotropy energy reads

$$\mathcal{E}_{\text{ani}} = C_{\text{ani}} \int_{\Omega} \phi(\mathbf{m}), \quad (1.3.4)$$

where C_{ani} denotes the anisotropy constant. Prominent examples for ϕ are the uniaxial density

$$\phi(x) = -\frac{1}{2} (x \cdot \mathbf{e})^2,$$

with the easy axis \mathbf{e} , or the cubic density

$$\phi(x) = K_1(x_1^2x_2^2 + x_2^2x_3^2 + x_3^2x_1^2) + K_2x_1^2x_2^2x_3^2.$$

The corresponding field contribution is then given by $\mathbf{h}_{\text{ani}} = -C_{\text{ani}} D\phi(\mathbf{m})$.

External field

The magnetization of a ferromagnetic body can obviously be influenced if it is exposed to an external magnetic field \mathbf{f} . This effect is called *Zeeman* contribution. It states that the magnetization will prefer alignment with the external field. The corresponding energy contribution is given by

$$\mathcal{E}_{\text{ext}} = - \int_{\Omega} \mathbf{f} \cdot \mathbf{m}, \quad (1.3.5)$$

and the field contribution to \mathbf{h}_{eff} simply by \mathbf{f} . Depending on the regularity of $\mathbf{h}_{\text{ext}} = \mathbf{f}$, different approximations can be used for a numerical integrator, and we refer to [Gol12] for details.

Strayfield

The last of the classical contributions considered in micromagnetic theory is the so-called *strayfield* or *demagnetizing field*. It accounts for the fact that each magnetized body itself induces a magnetic field in the whole space \mathbb{R}^3 which then again influences the magnetization until an equilibrium is reached. Formally, this field \mathbf{H} follows Maxwell's equations, but oftentimes, it suffices to utilize only a simplified, stationary version. Instead of solving the full Maxwell system from Section 1.4.2 below, one only solves

$$\begin{aligned} \nabla \times \mathbf{H} &= 0, \\ \nabla \cdot \mathbf{B} &= \nabla \cdot \mu_0(\mathbf{H} + \mathbf{m}) = 0, \end{aligned}$$

where \mathbf{B} denotes the magnetic induction. Since \mathbf{H} is curl-free, there exists some scalar potential $u \in H^1(\mathbb{R}^3)$ such that $\mathbf{H} = \nabla u$. Additionally, the above equations are supplemented by boundary conditions and a radiation condition, cf. e.g. [Hrk05, Section 4.2.3]. Altogether, one derives the transmission problem

$$\begin{aligned} \Delta u &= \text{div } \mathbf{m} && \text{in } \Omega, \\ \Delta u &= 0 && \text{in } \mathbb{R}^3 \setminus \overline{\Omega}, \\ [u] &= 0 && \text{on } \partial\Omega, \\ [\partial_{\mathbf{n}} u] &= -\mathbf{m} \cdot \mathbf{n} && \text{on } \partial\Omega, \\ u(\mathbf{x}) &= \mathcal{O}(1/|\mathbf{x}|) && \text{for } |\mathbf{x}| \rightarrow \infty. \end{aligned} \quad (1.3.6)$$

Here, $[\cdot]$ denotes the jump operator. The energy contribution is then given by

$$\mathcal{E}_{\text{stray}} = \frac{1}{2} \int_{\mathbb{R}^3} |\mathbf{H}|^2 = \frac{1}{2} \int_{\mathbb{R}^3} |\nabla u|^2 = \frac{1}{2} \int_{\mathbb{R}^3} |\mathcal{P}(\mathbf{m})|^2,$$

where $\mathcal{P}(\mathbf{m}) = \nabla u$ denotes the strayfield operator and expresses the dependence on \mathbf{m} . This contribution can be further simplified since $\mathcal{P}(\cdot)$ is the L^2 -orthogonal projection onto the space

$$\mathbf{L}_{\nabla}^2(\mathbb{R}^3) = \{\mathbf{f} \in \mathbf{L}^2(\mathbb{R}^3) : \exists u \in H^1(\mathbb{R}^3), \quad \nabla u = \mathbf{f}\},$$

cf. e.g. [Pra04, Proposition 3.1]. This yields

$$(\mathcal{P}(\mathbf{m}), \mathcal{P}(\mathbf{m})) = (\mathcal{P}(\mathbf{m}), \mathbf{m}) + \underbrace{(\mathcal{P}(\mathbf{m}), \mathcal{P}(\mathbf{m}) - \mathbf{m})}_{=0}.$$

Since the magnetization vanishes outside the computational domain Ω , one deduces

$$\mathcal{E}_{\text{stray}} = \frac{1}{2} \int_{\Omega} \mathcal{P}(\mathbf{m}) \cdot \mathbf{m}, \quad (1.3.7)$$

and the corresponding field contribution is given by $\mathbf{h}_{\text{stray}} = \mathcal{P}(\mathbf{m})$. Moreover, there holds boundedness

$$\|\mathcal{P}(\mathbf{m})\|_{\mathbf{L}^p(\mathbb{R}^3)} \leq C(p) \|\mathbf{m}\|_{\mathbf{L}^p(\Omega)} \quad (1.3.8)$$

for all $3/2 < p < \infty$, cf. e.g. [Pra04, Theorem 5.1]. In particular, $\mathcal{P}(\cdot)$ is self-adjoint and there holds

$$(\mathcal{P}(\mathbf{u}), \mathbf{v}) = (\mathbf{u}, \mathcal{P}(\mathbf{v})) \quad \text{for all } \mathbf{u}, \mathbf{v} \in \mathbf{L}^2(\mathbb{R}^3). \quad (1.3.9)$$

These last two estimates will be exploited below to gain improved energy estimates.

The energy functional and the effective field

Altogether, the total energy, which is classically considered throughout the literature, is thus given by

$$\begin{aligned} \mathcal{E}_{\text{total}} &= \mathcal{E}_{\text{exch}} + \mathcal{E}_{\text{ani}} + \mathcal{E}_{\text{ext}} + \mathcal{E}_{\text{stray}} \\ &= \frac{1}{2} C_e \int_{\Omega} |\nabla \mathbf{m}|^2 + C_{\text{ani}} \int_{\Omega} \phi(\mathbf{m}) - \int_{\Omega} \mathbf{f} \cdot \mathbf{m} + \frac{1}{2} \int_{\Omega} \mathcal{P}(\mathbf{m}) \cdot \mathbf{m}. \end{aligned} \quad (1.3.10)$$

This total energy is also called *Gibb's free energy*. The corresponding magnetic field is then given by

$$\begin{aligned} \mathbf{h}_{\text{eff}} &= \mathbf{h}_{\text{exch}} + \mathbf{h}_{\text{ani}} + \mathbf{h}_{\text{ext}} + \mathbf{h}_{\text{stray}} \\ &= C_e \Delta \mathbf{m} - C_{\text{ani}} D\phi(\mathbf{m}) + \mathbf{f} - \mathcal{P}(\mathbf{m}). \end{aligned} \quad (1.3.11)$$

In the subsequent sections and chapters, we follow a more general approach, where we introduce an abstract field operator $\boldsymbol{\pi}(\cdot)$. Via this approach, we derive two simple conditions that a field contribution needs to fulfill, to guarantee convergence of our scheme. In this context, we also consider the energy of the general operator given by

$$\mathcal{E}_{\text{general}} = \int_{\Omega} \boldsymbol{\pi}(\mathbf{m}) \cdot \mathbf{m}. \quad (1.3.12)$$

This ansatz particularly includes the classic energy functionals and leads to the desired field contribution $\boldsymbol{\pi}(\mathbf{m})$ (up to some constant) if $\boldsymbol{\pi}(\mathbf{m})$ is, e.g., polynomial with respect to \mathbf{m} .

1.4. Extended contributions

In the following, we introduce physical effects that extend the classical scheme from above as they require the inclusion of multiple domains on different scales or even coupling to other PDEs. The construction and analysis of a convergent scheme for those coupled problems is one of the main contributions of this thesis.

1.4.1. Multiscale modeling

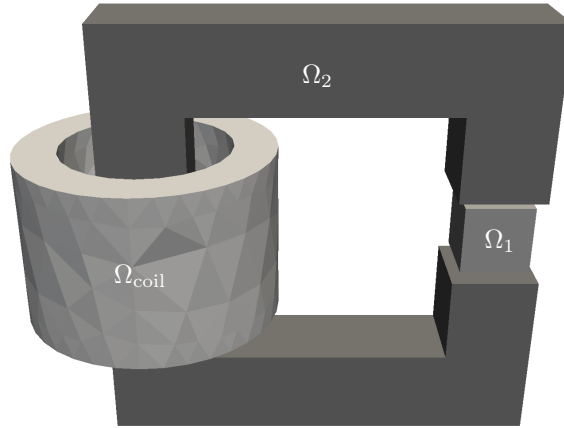


Figure 1.4.: Example geometry which demonstrates model separation into LLG region Ω_1 and Maxwell region Ω_2 (and in this case in an electric coil region Ω_{coil}). Here, Ω_1 represents one grain of a recording media and Ω_2 shows a simple model of a recording head. — Picture taken from [BFF⁺12], copyright of Florian Bruckner is thankfully acknowledged.

Many devices that rely on micromagnetic interactions, contain several parts on several different length scales. Often, the magnetization dynamics after the LLG equation are important only on a small domain, whereas for the magnetization on other parts, rough estimates are sufficient. We face such a problem, if we want to simulate a complete read/write head of a magnetic hard disk, for example, as it is visualized in Figure 1.4. Here, one is interested in the detailed remagnetization process of the magnetic grains, simplified by Ω_1 . For the other domains, however, it is sufficient to have an approximation of the magnetization such that the magnetic field that they induce, and which then reacts back on Ω_1 , can be approximated. In this thesis, we consider a model by BRUCKNER which was introduced in [Bru13]. On the small domain Ω_1 , we are interested in the magnetization dynamics of \mathbf{m}_1 given by the LLG equation. On the macroscopic domain Ω_2 , on the other hand, the model involves some (possibly nonlinear) material law

$$\mathbf{m}_2 = \chi(|\mathbf{H}|)\mathbf{H}.$$

Suitable material laws can be found, e.g., in [RZMP81]. The corresponding strayfields $\nabla u_1 = \mathcal{P}(\mathbf{m}_1)$ and $\nabla u_2 = \mathcal{P}(\mathbf{m}_2)$ are then computed and both contribute to the effective field \mathbf{h}_{eff} of the LLG domain Ω_1 .

1.4.2. The Maxwell system

As mentioned above, the magnetostatic strayfield is only an approximation of the magnetic field generated by the magnetization \mathbf{m} . The complete field \mathbf{H} , which is really induced, is the solution of the full Maxwell system which is then coupled to the LLG equation. Depending on the material and the considered timescale, it is not always necessary to solve the full system, and there are different approximation levels that suit different situations. Besides the magnetostatic approximation, we consider the full system, as well as the eddy-current simplification in this thesis. For many situations, the classic strayfield already gives sufficiently good approximations, but this is not always the case, see e.g. [MV01, Hrk05]. In the following, we briefly present the additional equations.

The full Maxwell system

We start with the Maxwell's equations as they are given in [Mon08, Section 1.2]. The four vector-valued quantities E (electric field intensity), D (electric displacement), H (magnetic field intensity), and B (magnetic induction) fulfill

$$\partial_t B + \nabla \times \mathbf{E} = 0, \quad (1.4.1a)$$

$$\nabla \cdot D = \rho, \quad (1.4.1b)$$

$$\partial_t D - \nabla \times \mathbf{H} = -\tilde{J}, \quad (1.4.1c)$$

$$\nabla \cdot B = 0. \quad (1.4.1d)$$

Equation (1.4.1a) is called Faraday's law and describes the influence of a changing magnetic field on the electric field. Condition (1.4.1b) goes back to Gauss and gives the effect of the charge density ρ on the electric displacement. Equation (1.4.1c) is Ampère's circuital law (modified by MAXWELL) and finally, condition (1.4.1d) takes into account that B is solenoidal. In the above equations, \tilde{J} denotes the electric current density. The Maxwell equations are computed on some domain $\hat{\Omega}$ into which the magnet Ω is embedded.

Depending on the presence, respectively absence of media, the relations between the above quantities are given by certain material laws. To ease the presentation, we assume the magnet $\Omega \subset \hat{\Omega}$ to be much smaller than the Maxwell domain $\hat{\Omega}$. Moreover, as is usually done in practice, we assume the difference $\hat{\Omega} \setminus \Omega$ to be vacuum. For the electric field and the displacement, we then get the relation

$$D = \varepsilon_0 \mathbf{E}, \quad (1.4.2)$$

where ε_0 denotes the electric permittivity of free space. Since the magnetic induction is obviously influenced by the magnetization of the ferromagnetic body Ω , we need to employ the slightly more involved material law

$$B = \mu \mathbf{H} = \mu_0 (\mathbf{H} + \mathbf{m}). \quad (1.4.3)$$

Here, μ denotes the magnetic permeability and μ_0 the permeability of vacuum. Plugging (1.4.2) and (1.4.3) into the equations (1.4.1a)–(1.4.1d), we derive

$$\mu_0 \partial_t \mathbf{H} + \nabla \times \mathbf{E} = -\mu_0 \mathbf{m}_t, \quad (1.4.4a)$$

$$\varepsilon_0 \nabla \cdot \mathbf{E} = \rho, \quad (1.4.4b)$$

$$\varepsilon_0 \partial_t \mathbf{E} - \nabla \times \mathbf{H} = -\tilde{J}, \quad (1.4.4c)$$

$$\nabla \cdot \mathbf{H} = -\nabla \cdot \mathbf{m}. \quad (1.4.4d)$$

Next, according to [Hrk05, Section 6.1.1], the electric current density can be further split into

$$\tilde{\mathbf{J}} = J_s + J_{\text{free}} + J_{\text{mat}}, \quad (1.4.5)$$

denoting an independent current source term J_s , the free currents J_{free} , and the material currents J_{mat} . Furthermore, the material currents and the magnetization are connected via the relation

$$\nabla \times \mathbf{m} = J_{\text{mat}} = \chi_\Omega \sigma \mathbf{E}, \quad (1.4.6)$$

where χ_Ω denotes the magnetic susceptibility. We note that in a non-dimensional formulation of the Maxwell system, χ_Ω coincides with the characteristic function of Ω , since the susceptibility of vacuum is zero. Employing this relation, we finally end up with

$$\mu_0 \partial_t \mathbf{H} + \nabla \times \mathbf{E} = -\mu_0 \mathbf{m}_t, \quad (1.4.7a)$$

$$\varepsilon_0 \nabla \cdot \mathbf{E} = \rho, \quad (1.4.7b)$$

$$\varepsilon_0 \partial_t \mathbf{E} - \nabla \times \mathbf{H} + \sigma \chi_\Omega \mathbf{E} = -J, \quad (1.4.7c)$$

$$\nabla \cdot \mathbf{H} = -\nabla \cdot \mathbf{m}, \quad (1.4.7d)$$

where $J = J_s + J_{\text{free}}$ consists of the source currents and the free currents.

The eddy-current simplification

Starting from the equations (1.4.7), we aim to derive the so-called eddy-current equation which is a simplification of the Maxwell system for good conductors. More precisely, this is modeled by the condition

$$\varepsilon_0 \partial_t \mathbf{E} \ll \sigma \mathbf{E}, \quad (1.4.8)$$

cf. e.g. [ABN00, Hrk05]. Taking into account the relation

$$J_{\text{free}} + J_{\text{mat}} = \sigma \mathbf{E}, \quad (1.4.9)$$

and $J_{\text{mat}} = \sigma \chi_\Omega \mathbf{E}$, from (1.4.7c) we obtain

$$\varepsilon_0 \partial_t \mathbf{E} - \nabla \times \mathbf{H} + \sigma \mathbf{E} = -J_s. \quad (1.4.10)$$

Exploiting (1.4.8) and neglecting the source currents, we derive

$$\nabla \times \mathbf{H} = \sigma \mathbf{E}. \quad (1.4.11)$$

Plugging this equation into (1.4.7a), we finally derive

$$\mu_0 \partial_t \mathbf{H} + \frac{1}{\sigma} \nabla \times (\nabla \times \mathbf{H}) = -\mu_0 \mathbf{m}_t, \quad (1.4.12)$$

which is the desired eddy-current equation.

1.4.3. Magnetoelastic interactions

Magnetoelastic properties are intrinsic to all magnetic materials. In ferromagnetic materials, like Terfenol-D, they are particularly more enhanced and the elasticity is exploited in many technical devices like positioning sensors and actuators. The effect that models the deformation of a ferromagnetic body under the influence of a magnetic field is called *magnetostriction*. The inclusion of this effect after [Vis85, Bañ05b] relies on the coupling of LLG to the conservation of momentum equation

$$\varrho \mathbf{u}_{tt} - \nabla \cdot \boldsymbol{\sigma} = 0 \quad \text{in } \Omega_T, \quad (1.4.13)$$

supplemented by the initial and boundary conditions

$$\begin{aligned} \mathbf{u}(0) &= \mathbf{u}_0 & \text{in } \Omega, \\ \mathbf{u}_t(0) &= \dot{\mathbf{u}}_0 & \text{in } \Omega, \text{ and} \\ \mathbf{u} &= 0 & \text{on } \Gamma. \end{aligned}$$

Here, ϱ denotes the material density, and the vector-valued quantity \mathbf{u} is the displacement. The stress tensor $\boldsymbol{\sigma}$ is given by

$$\begin{aligned} \boldsymbol{\sigma} &:= \boldsymbol{\lambda}^e \boldsymbol{\varepsilon}^e(\mathbf{u}, \mathbf{m}), \quad \sigma_{ij} = \sum_{p,q=1}^3 \lambda_{ijpq}^e \varepsilon_{pq}^e, \\ \boldsymbol{\varepsilon}^e(\mathbf{u}, \mathbf{m}) &:= \boldsymbol{\varepsilon}(\mathbf{u}) - \boldsymbol{\varepsilon}^m(\mathbf{m}) \end{aligned}$$

for some material tensor $\boldsymbol{\lambda}^e$. The total strain tensor is defined as the symmetric part of the gradient

$$\varepsilon_{ij}(\mathbf{u}) := \frac{1}{2} \left(\frac{\partial u_i}{\partial x_j} + \frac{\partial u_j}{\partial x_i} \right),$$

and the magnetic part is given by

$$\boldsymbol{\varepsilon}^m(\mathbf{m}) := \boldsymbol{\lambda}^m \mathbf{m} \mathbf{m}^T,$$

where $\boldsymbol{\lambda}^m$ denotes another material tensor. The elastic effect is finally incorporated into the effective field by means of the operator

$$(\mathbf{h}_m)_q = (\mathbf{h}_m(\mathbf{u}, \mathbf{m}))_q := \sum_{i,j,p=1}^3 \lambda_{ijpq}^m \sigma_{ij}(\mathbf{m})_p, \quad q = 1, 2, 3,$$

where $(\cdot)_q$ denotes the q -th component.

1.5. Preliminaries & Notation

In this short section, we aim to fix some notation that is widely used throughout the work. Additional notation will be explained as the need arises.

Norms

Throughout this thesis, we investigate functions in various Banach spaces which may or may not be time-dependent. For a better overview, we collect the notation of the corresponding norms here. Before the actual definition of those norms and spaces, however, we like to address the issue of dimension, since we will mostly work in three-dimensional space. To prevent confusion with scalar-valued functions, multidimensional functions will be indicated by bold letters. In addition, we will also use bold letters for function spaces consisting of multidimensional functions. The \mathbf{L}^2 -norm of a square integrable three-dimensional function $\mathbf{u} : \mathbb{R}^3 \rightarrow \mathbb{R}^3$ on some domain $\Omega \subseteq \mathbb{R}^3$ with $\mathbf{u} = (u_1, u_2, u_3)$, for example, will thus be denoted by

$$\|\mathbf{u}\|_{\mathbf{L}^2(\Omega)}^2 = \int_{\Omega} |\mathbf{u}(\mathbf{x})|^2 d\mathbf{x} = \int_{\Omega} |u_1(\mathbf{x})|^2 + |u_2(\mathbf{x})|^2 + |u_3(\mathbf{x})|^2 d\mathbf{x}.$$

Next, we define some frequently used spaces and their corresponding norms in the multidimensional setting. We denote the space of square-integrable functions on some space-time domain Ω_T by $\mathbf{L}^2(\Omega_T)$ equipped with the norm

$$\begin{aligned} \|\mathbf{u}\|_{\mathbf{L}^2(\Omega_T)}^2 &:= \int_{\Omega_T} |\mathbf{u}(t, \mathbf{x})|^2 d\mathbf{x} dt = \int_0^T \int_{\Omega} |\mathbf{u}(t, \mathbf{x})|^2 d\mathbf{x} dt = \int_0^T \|\mathbf{u}(t)\|_{\mathbf{L}^2(\Omega)}^2 dt \\ &= \|\mathbf{u}\|_{L^2([0,T], \mathbf{L}^2(\Omega))}^2, \end{aligned}$$

where the last equality is in analogy to the definition from [Eva02, § 5.9.2]. For the second equality, we employed Fubini's theorem. Those functions in $\mathbf{L}^2(\Omega_T)$ that admit a weak derivative which is again in $\mathbf{L}^2(\Omega_T)$, are denoted by $\mathbf{H}^1(\Omega_T)$, with

$$\|\mathbf{u}\|_{\mathbf{H}^1(\Omega_T)}^2 := \|\mathbf{u}\|_{\mathbf{L}^2(\Omega_T)}^2 + \|\nabla \mathbf{u}\|_{\mathbf{L}^2(\Omega_T)}^2 + \|\partial_t \mathbf{u}\|_{\mathbf{L}^2(\Omega_T)}^2,$$

where $\nabla(\cdot)$ denotes the weak spatial gradient operator and $\partial_t(\cdot)$, sometimes also denoted by $(\cdot)_t$ is the (weak) time derivative. Note that the weak derivative of $\mathbf{H}^1(\Omega_T)$ -functions even includes one weak time derivative. In addition, we define the $\mathbf{L}^2(\Omega_T)$ -functions which admit a weak derivative in $\mathbf{L}^2(\Omega_T)$ only in time by $H^1((0, T); \mathbf{L}^2(\Omega))$, and those that admit one weak derivative only in space, by $L^2((0, T); \mathbf{H}^1(\Omega))$. The corresponding norms are given by

$$\|\mathbf{u}\|_{H^1((0,T); \mathbf{L}^2(\Omega))}^2 := \int_0^T \|\mathbf{u}(t)\|_{\mathbf{L}^2(\Omega)}^2 + \|\partial_t \mathbf{u}(t)\|_{\mathbf{L}^2(\Omega)}^2 dt$$

and

$$\|\mathbf{u}\|_{L^2((0,T); \mathbf{H}^1(\Omega))}^2 := \int_0^T \|\mathbf{u}(t)\|_{\mathbf{L}^2(\Omega)}^2 + \|\nabla \mathbf{u}(t)\|_{\mathbf{L}^2(\Omega)}^2 dt.$$

Finally, and in analogy to [Eva02, §5.9.2], we define the functions that are H^1 in time and map each t to a function in $\mathbf{H}^1(\Omega)$, by

$$\begin{aligned} \|\mathbf{u}\|_{H^1((0,T); \mathbf{H}^1(\Omega))}^2 &:= \int_0^T \|\mathbf{u}(t)\|_{\mathbf{H}^1(\Omega)}^2 + \|\partial_t \mathbf{u}(t)\|_{\mathbf{H}^1(\Omega)}^2 dt \\ &= \int_0^T \|\mathbf{u}(t)\|_{\mathbf{L}^2(\Omega)}^2 + \|\nabla \mathbf{u}(t)\|_{\mathbf{L}^2(\Omega)}^2 + \|\partial_t \mathbf{u}(t)\|_{\mathbf{L}^2(\Omega)}^2 + \|\nabla \partial_t \mathbf{u}(t)\|_{\mathbf{L}^2(\Omega)}^2 dt. \end{aligned}$$

Note carefully that $\mathbf{H}^1(\Omega_T) \neq H^1((0, T); \mathbf{H}^1(\Omega))$ since the latter additionally involves the spatial gradient of the weak time-derivative. To ease the presentation as well as the readability, we will omit the time- and spatial domains if the context is clear and thus use the following abbreviations throughout:

$$\begin{aligned} H^1((0, T); \mathbf{L}^2(\Omega)) &=: H^1(\mathbf{L}^2), \\ L^2((0, T); \mathbf{H}^1(\Omega)) &=: L^2(\mathbf{H}^1), \\ H^1((0, T); \mathbf{H}^1(\Omega)) &=: H^1(\mathbf{H}^1). \end{aligned}$$

Moreover, if no confusion is possible, we will omit explicitly stating the integration variable, e.g.

$$\begin{aligned} \int_0^T \|\mathbf{u}\|_{\mathbf{L}^2(\Omega)}^2 dt &= \int_0^T \|\mathbf{u}\|_{\mathbf{L}^2(\Omega)}^2, \quad \text{and} \\ \int_{\Omega} |\mathbf{u}(t, \mathbf{x})| d\mathbf{x} &= \int_{\Omega} |\mathbf{u}(t, \mathbf{x})| \quad \text{for } t \in [0, T]. \end{aligned}$$

Finally, the scalar products of two functions $\phi, \psi \in \mathbf{L}^2(\Omega_T)$ or $\mathbf{L}^2(\Omega)$ are denoted by (ϕ, ψ) . Sometimes, to avoid confusion, also $\langle \phi, \psi \rangle$ is utilized. We stress, however, that ambiguity is never an issue. For two vectors $\mathbf{x}, \mathbf{y} \in \mathbb{R}^3$, the scalar product is denoted by $\mathbf{x} \cdot \mathbf{y}$.

Representations of time-dependent spaces

Formally, $\mathbf{L}^2(\Omega_T)$ and $L^2(\mathbf{L}^2)$ denote different spaces. The first one simply involves the square-integrable functions over the time-space cone Ω_T , whereas the second space involves the square-integrable functions over $[0, T]$ with values in $\mathbf{L}^2(\Omega)$. Therefore, a function $u \in \mathbf{L}^2(\Omega_T)$ maps from Ω_T to \mathbb{R}^3 , i.e. almost everywhere in Ω_T , we have

$$\begin{aligned} u : \Omega_T &\rightarrow \mathbb{R}^3 \text{ with} \\ (t, x) &\mapsto u(t, x) \in \mathbb{R}^3. \end{aligned}$$

A function $\tilde{u} \in L^2(\mathbf{L}^2)$, on the other hand, maps from $[0, T]$ into the space of square-integrable functions $\mathbf{L}^2(\Omega)$, i.e.

$$\begin{aligned} \tilde{u} : [0, T] &\rightarrow \mathbf{L}^2(\Omega) \text{ with} \\ t &\mapsto \tilde{u}(t) \in \mathbf{L}^2(\Omega). \end{aligned}$$

We like to emphasize that, due to the Fubini theorem, both spaces essentially coincide. Moreover, there is a natural identification, since $\tilde{u} \in L^2(\mathbf{L}^2)$ implicitly yields a function \hat{u} with

$$\begin{aligned} \hat{u} : \Omega_T &\rightarrow \mathbb{R}^3 \text{ with} \\ (t, x) &\mapsto \hat{u}(t, x) := \tilde{u}(t)(x) \end{aligned}$$

and $u := \hat{u}$.

We may thus consider a square-integrable function as a function on the time-space cone, or as a time-dependent function with values in $\mathbf{L}^2(\Omega)$. In the following, both representations will prove suitable in different situations, and we will switch between the two possibilities with no notational distinction. Obviously, though, time evaluations are to be understood almost everywhere, if we do not have any information on the smoothness of the corresponding function.

Convergence

We frequently work with subconvergent sequences, i.e. sequences that admit the extraction of a convergent subsequence. This is due to the fact that most of the upcoming convergence proofs rely on compactness arguments. To clarify the presentation, we therefore introduce a special notation for this case. To that end, let X be a normed vector space. If a sequence $(a_n) \subseteq X$ admits a subsequence a_{n_ℓ} that converges towards some $a \in X$ for $\ell \rightarrow \infty$, i.e. $\lim_{\ell \rightarrow \infty} \|a_{n_\ell} - a\|_X = 0$, we write

$$a_n \xrightarrow{\text{sub}} a \text{ in } X.$$

If the sequence is only weakly subconvergent, i.e. it admits a weakly convergent subsequence, we write

$$a_n \xrightarrow{\text{sub}} a \text{ in } X.$$

What else?

In the upcoming results, we will always state constants and their dependencies. Throughout the proofs, however, we omit multiplicative constants for sake of readability. As a remedy, we use the notations \lesssim and \gtrsim to denote *smaller or equal* and *larger or equal*, respectively, up to a multiplicative constant, i.e. for two quantities A, B and a constant $c > 0$, we write $A \lesssim B$ if $A \leq cB$. Here, the constant $c > 0$ is always independent of the time- and spatial parameter if not explicitly stated otherwise. In the case $A \lesssim B$ and $B \lesssim A$, we write $A \sim B$.

1.6. Overview over the current literature

The Landau-Lifshitz-Gilbert equation poses a problem of equal interest for the physical as well as for the mathematical community. Its great applicability and necessity for the simulation and construction of technological devices cannot be overestimated. On the other hand, the equation itself poses a whole set of mathematical difficulties such as

- a strong nonlinearity,
- the non-convex side constraint $|\mathbf{m}| = 1$ almost everywhere,
- possible nonlocal field contributions,
- inclusion of coupled problems, or
- possibly nonlinear coupling to other PDEs.

All those problems complicate the construction and analysis of numerical integrators for LLG and yet, make the equation that much more interesting. Consequently, many contributions to the analysis and numerics of LLG have been made in the recent years. In this section, we aim to give a brief overview over the current state of the art and also embed our contribution into the bigger context.

Obviously, we cannot cover the complete literature, so we will restrict ourselves to those works which are in direct correlation to this thesis. First of all, this includes only the mathematical literature. For a comprehensive overview over the state of the art in the physics

literature, we refer to [Kro07, HS08] and the references therein. Next, we consider only those works that contribute to the analysis and numerics of weak solutions. For literature on strong solutions, we refer to the overview articles [KP06, Cim07a, GC09] as well as the monographs [Pro01, Bañ05b, Cim05] and the references therein. A nice overview is also given in [Gol12]. For details on strong solutions of LLG with magnetostriction, we refer to [BS05] and [BS06], where also numerical schemes are considered. In [Bañ08], even a posteriori estimates for LLG with magnetostriction can be found and an adaptive algorithm is proposed. For strong solutions of the Maxwell-LLG system, we refer to [MV99, dSM⁺05]. The works [Cim07b, Cim07c, Cim08] consider strong error estimates for the Maxwell-LLG system and even provide an analysis of the regularity properties of periodic solutions.

First results on the existence of weak solutions of LLG, even in the presence of the full Maxwell system and the magnetostrictive effect, go back to VISINTIN [Vis85]. Here, however, the notion of a weak solution was different from what is used nowadays. In [AS92], the authors first defined a weak solution that is also the foundation for this thesis. There, a function \mathbf{m} is a weak solution of the Landau-Lifshitz equation (1.2.9) for the simplified field $\mathbf{h}_{\text{eff}} = \mathbf{h}_{\text{exch}}$, if it fulfills the following definition.

Definition 1.6.1. *Let $\mathbf{m}_0 \in \mathbf{H}^1(\Omega)$ with $|\mathbf{m}_0| = 1$ almost everywhere, then \mathbf{m} is a weak solution of LLG if*

- (i) *for all $T > 0$, $\mathbf{m} \in \mathbf{H}^1(\Omega_T)$, $|\mathbf{m}| = 1$ almost everywhere;*
- (ii) *for all $\varphi \in \mathbf{H}^1(\Omega_T)$, there holds*

$$\int_{\Omega_T} \mathbf{m}_t \cdot \varphi + \lambda \int_{\Omega_T} (\mathbf{m} \times \mathbf{m}_t) = -(1 + \lambda^2) \int_{\Omega_T} (\mathbf{m} \times \nabla \mathbf{m}) \cdot \nabla \varphi;$$

- (iii) *$\mathbf{m}(\mathbf{x}, 0) = \mathbf{m}_0(\mathbf{x})$ in the sense of traces;*
- (iv) *for all $T > 0$,*

$$\int_{\Omega} \frac{|\nabla \mathbf{m}(T)|^2}{2} + \frac{\lambda}{1 + \lambda^2} \int_{\Omega_T} \mathbf{m}_t^2 \leq \int_{\Omega} \frac{|\nabla \mathbf{m}_0|^2}{2}$$

Moreover, ALOUGES and SOYEUR showed in this work, that weak solutions exist and are, in general, not unique. To that end, they showed the existence of a weak solution \mathbf{m} and then constructed another (stationary solution) \mathbf{m}_0 which is weakly harmonic, i.e. it satisfies

$$-\Delta \mathbf{m}_0 = \mathbf{m}_0 |\nabla \mathbf{m}_0|^2$$

in the distributional sense. Given the additional length preservation constraint, this function is a weak solution of the Landau-Lifshitz equation. In a next step they proved that $\mathbf{m} \neq \mathbf{m}_0$ and even constructed a continuum of weak solutions by

$$\begin{aligned} \mathbf{m}^t(s) &= \mathbf{m}_0 & \text{if } s \leq t, \\ \mathbf{m}^t(s) &= \mathbf{m}(s - t) & \text{otherwise,} \end{aligned}$$

for all $t > 0$ and where \mathbf{m} is the constructed solution with $\mathbf{m}(0) = \mathbf{m}_0$. In [AS92], however, the authors only treat the LL equation, rather than LLG and consider an effective field with exchange only. For those reasons, our notion of a weak solution 2.1.1 is slightly different. The existence of weak solutions of the Maxwell-LLG system is shown in [CF98], and for the existence of weak solutions of LLG with magnetostriction, we refer to [CEF11].

Next, we consider works which provide (convergent) numerical integrators for the LLG equation. Those integrators can be divided into two groups depending on how they treat the geometric side constraint. More precisely, we distinguish between

- projection based integrators and
- non-projection based integrators.

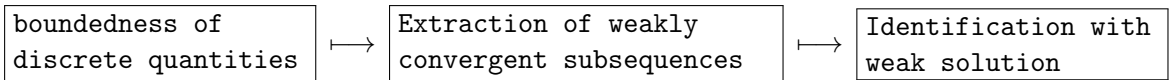
In the case of non-projection based schemes, the side constraint has to be implicitly enforced by the algorithm, whereas in the other case, it is explicitly enforced by normalization. For both cases, there exist *prototype schemes* which inspired a whole bunch of future publications. Concerning the projection based integrators, the pioneering work is the one by ALOUGES and JAISSE [AJ06]. They considered an explicit finite element scheme for the original LL equation, where they employed the equivalent formulation similar to (1.2.13). Introducing a free variable \mathbf{v} which approximates the time derivative and testing in the pointwise tangent space $\mathcal{K}_{\mathbf{m}_h^j}$, they derive the scheme

$$\lambda(\mathbf{v}_h^j, \varphi) - ((\mathbf{m}_h^j \times \mathbf{v}_h^j), \varphi) = -(\nabla \mathbf{v}_h^j, \nabla \varphi) + (\mathbf{h}_{\text{eff}}, \varphi), \quad \text{for all } \varphi \in \mathcal{K}_{\mathbf{m}_h^j},$$

where \mathbf{m}_h^j is assumed to be given. In a second step, the node constraint is enforced by nodewise normalization, i.e.

$$\mathbf{m}_h^{j+1}(z) = \frac{\mathbf{m}_h^j(z) + k\mathbf{v}_h^j(z)}{|\mathbf{m}_h^j(z) + k\mathbf{v}_h^j(z)|}, \quad (1.6.1)$$

for all nodes $z \in \mathcal{N}_h$. Here and throughout, $h, k > 0$ denote the spatial and temporal mesh parameters. A major advantage of this scheme, which will also be found in all follow-up works, is that, despite the nonlinearity of LL resp. LLG, only one linear system needs to be solved per timestep. In [AJ06], the authors prove, that the (in time interpolated) discrete solutions provide a subsequence \mathbf{m}_{hk} that weakly converges towards a weak solution \mathbf{m} of LL in the sense of Definition 1.6.1, provided that first k , and afterwards h is driven to 0. We emphasize that here, as well as in all inspired works, the proof is constructive in that it even yields existence of weak solutions without any regularity assumptions. Throughout, the line of proof is always given by the three steps:



In 2008, the result from above was improved by BARTELS, KO, and PROHL in [BKP08]. Here, the authors prove that the integrator from [AJ06] provides a weakly subconvergent sequence of discrete solutions as $(h, k) \rightarrow (0, 0)$, provided $kh^{-1-d/2} \rightarrow 0$. Moreover, the efficiency of the scheme was further increased by incorporating mass-lumping, i.e. reduced integration. The authors did, however, only consider a reduced effective field $\mathbf{h}_{\text{eff}} = \Delta \mathbf{m}$. In [BKP08],

the authors specifically employed the Alouges-Jaisson *tangent plane scheme* because of its stability for small damping parameters λ , as their focus was on a numerical study of finite time blow-up for small damping. In this thesis, we will also contribute to those studies.

The next improvement to the tangent plane scheme was provided by ALOUGES in 2008, cf. [Alo08a]. Here, the author managed to circumvent the disadvantages of an explicit discretization by utilizing the implicit discretization

$$\alpha(\mathbf{v}_h^j, \varphi) - (\mathbf{m}_h^j \times \mathbf{v}_h^j, \varphi) = -(1 + \alpha^2)(\nabla(\mathbf{m}_h^j + \theta k \mathbf{v}_h^j), \nabla \varphi) \quad \text{for all } \mathbf{v}_h^j \in \mathcal{K}_{\mathbf{m}_h^j},$$

where $\theta \in [0, 1]$ is used to steer the scheme. That is to say, $\theta = 0$ denotes the explicit scheme from above, $\theta = 1$ denotes a fully implicit scheme, and $\theta = 1/2$ is a Crank-Nicholson type discretization. The modulus constraint is again enforced by nodewise normalization, i.e. (1.6.1). In this work, the author proves existence of a weakly convergent subsequence as $(h, k) \rightarrow 0$ independently of each other, provided $\theta \in (1/2, 1]$. This work again inspired multiple sequels, among others this thesis. In [Gol12], the scheme was extended to cover all of the classic field contributions from Section 1.3, where only the exchange contribution is treated implicitly, and all the other contributions are treated explicitly. Moreover, reduced integration to enhance the scheme's efficiency was rigorously included into the analysis. In total, the derived scheme is given by

$$\alpha(\mathbf{v}_h^j, \varphi)_h + (\mathbf{m}_h^j \times \mathbf{v}_h^j, \varphi)_h = -C_e(\nabla(\mathbf{m}_h^j + \theta k \mathbf{v}_h^j), \nabla \varphi) + (\mathbf{h}_{\text{low}}(\mathbf{m}_h^j), \varphi) \quad \text{for all } \varphi \in \mathcal{K}_{\mathbf{m}_h^j}$$

and subsequent normalization. Here, the advantages from the implicit scheme could be carried over and the author proves unconditional weak subconvergence towards a weak solution. Independently of [Gol12], the authors of the work [AKT11] also extended the implicit tangent plane scheme to a semi-implicit scheme for the full effective field with an unconditional convergence result. Unlike [Gol12], however, [AKT11] does not study the influence of additional discretization errors which arise, e.g., for the strayfield computation. Moreover, they even propose a first second order in time formulation without convergence analysis. In [AKST12], the authors propose the second order in time scheme

$$\begin{aligned} (\psi_m(\mathbf{m}_h^j) \mathbf{v}_h^j, \varphi) + (\mathbf{m}_h^j \times \mathbf{v}_h^j, \varphi) + \frac{k}{2}((1 + \rho(k)) \nabla \mathbf{v}_h^j, \nabla \varphi) - (\mathbf{h}_{\text{stray}}(\mathbf{v}_h^j), \varphi) - (D\phi(\mathbf{v}_h^j), \varphi) \\ = -(\nabla \mathbf{m}_h^j, \nabla \varphi) + (\mathbf{h}_{\text{stray}}(\mathbf{m}_h^j) + \mathbf{h}_{\text{ext}} + D\phi(\mathbf{m}_h^j), \varphi), \end{aligned}$$

for all $\varphi \in \mathcal{K}_{\mathbf{m}_h^j}$. Here, ψ_m denotes a cut-off function, and $\rho(k) \rightarrow 0$ as $k \rightarrow 0$. The scheme is motivated by not simply taking \mathbf{v}_h^j as the approximation of \mathbf{m}_t at t_j , but rather as a higher order Taylor expansion. The drawback is, however, that the scheme requires implicit treatment of all field contributions. The original work [Alo08a] of ALOUGES also inspired the work [LT12], where coupling to the eddy-current equation is considered, as well as [GLT13], which deals with the stochastic LLG equation. Finally, it is the main foundation of this thesis, where the original results are extended in multiple ways while still maintaining the initial advantages.

As prototype scheme for non-projection based methods serves the work [BP06] from BARTELS and PROHL from 2006. The authors combine reduced integration with a midpoint based approach and derive

$$(\mathbf{d}_t \mathbf{m}_h^{j+1}, \varphi)_h + \alpha(\mathbf{m}_h^{j+1} \times \mathbf{d}_t \mathbf{m}_h^{j+1}, \varphi)_h = (1 + \alpha^2)(\bar{\mathbf{m}}_h^{j+1/2} \times \tilde{\Delta}_h \bar{\mathbf{m}}_h^{j+1/2}, \varphi)_h \quad \forall \varphi \in \mathcal{S}^1(\mathcal{T}_h).$$

Here, $d_t \mathbf{m}_h^{j+1} = (\mathbf{m}_h^{j+1} - \mathbf{m}_h^j)/k$ denotes the first order difference quotient, $\bar{\mathbf{m}}_h^{j+1/2} = 1/2(\mathbf{m}_h^{j+1} + \mathbf{m}_h^j)$ the midpoint evaluation, and $\tilde{\Delta}_h$ the discrete Laplacian defined by

$$-(\tilde{\Delta}_h \phi, \varphi_h)_h = (\nabla \phi, \nabla \varphi_h) \quad \text{for all } \varphi_h \in \mathcal{S}^1(\mathcal{T}_h).$$

One easily verifies that the mass lumping is employed here not only for efficiency reasons, but rather ensures the modulus constraint provided the initial data fulfills $|\mathbf{m}_0| = 1$ almost everywhere. Given the exact solvability of the above system of equations, the authors prove unconditional convergence towards (and hence existence of) a weak solution of LLG. The system is, however, nonlinear and thus requires an iterative solution. To that end, in [BP06], a fixed point iteration is proposed which again leads to a coupling of the mesh parameters and allows convergence only if $k \leq Ch^2$.

In [BBP08], the authors extend the midpoint scheme to the Maxwell-LLG problem and derive

$$\begin{aligned} (d_t \mathbf{m}_h^{j+1}, \varphi)_h + \alpha(\mathbf{m}_h^j \times d_t \mathbf{m}_h^{j+1}, \varphi)_h \\ = (1 + \alpha^2)(\bar{\mathbf{m}}_h^{j+1/2} \times (\tilde{\Delta}_h \bar{\mathbf{m}}_h^{j+1/2} + P_{V_h} \bar{\mathbf{H}}_h^{j+1/2}))_h \quad \text{for all } \varphi \in \mathcal{S}^1(\mathcal{T}_h), \\ \varepsilon_0(d_t \mathbf{E}_h^{j+1}, \psi) - (\bar{\mathbf{H}}_h^{j+1/2}, \nabla \times \psi) + \sigma(\chi_\Omega \bar{\mathbf{E}}_h^{j+1/2}, \psi) \\ = -(\bar{\mathbf{J}}_h^{j+1/2}, \psi) \quad \text{for all } \psi \in X_h, \\ \mu_0(d_t \mathbf{H}_h^{j+1}, \zeta) + (\nabla \times \bar{\mathbf{E}}_h^{j+1/2}, \zeta) = \mu_0(d_t \mathbf{m}_h^{j+1}, \zeta) \quad \text{for all } \zeta \in Y_h. \end{aligned}$$

Here, X_h and Y_h are suitable conforming finite element spaces and ε_0, μ_0 denote the electric and magnetic permeability. Again, unconditional convergence is proved theoretically, but the proposed fixed point iteration imposes $k \leq Ch^2$. Moreover, the algorithm couples Maxwell's equations with LLG even numerically, such that in each step a large system of nonlinear equations needs to be solved. In [Roc12], the author extends the midpoint scheme to magnetostriuctive effects, and convergence under the same conditions is proved. An application of the midpoint scheme to thermally assisted recording is found in [BPS08] and as before, unconditional convergence is theoretically proved. Very recently, in [BBP13], the authors presented computational studies of the stochastic LLG equation using a midpoint-based algorithm.

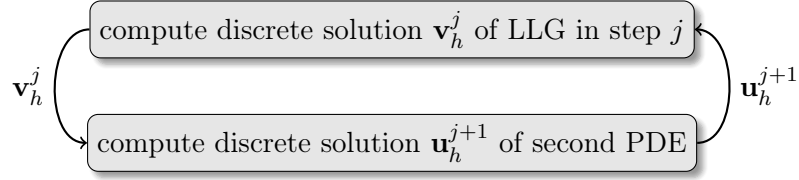
Finally, a computational comparison between the tangent plane scheme and the midpoint scheme for a 2D blowup-benchmark problem can be found in [BPPR13].

1.7. Structure of this thesis and main results

The remainder of this work is organized as follows:

- In **Chapter 2**, we present our numerical integrator, which is based on the work [Alo08a] of ALOUGES, for the pure LLG equation in the most general form. We derive a set of two assumptions, namely boundedness and some weak convergence property, that a stationary field contribution needs to fulfill in order to guarantee unconditional convergence of the scheme. Moreover, we investigate time dependent contributions and show convergence via a Riemann-sum approach. As a side effect, we prove that for a fixed spatial mesh size $h > 0$, the sequence of discrete solutions converges towards some limit \mathbf{m}_h as the temporal mesh size $k > 0$ tends to zero, and that this convergence is uniform. Finally, we take a closer look at the energy of the system and derive improved energy estimates.

- **Chapter 3** considers the conditions from the general analysis in concrete applications. First, we show that all classic field contributions are covered by our general theory. In the next step, we investigate the multiscale approach from [Bru13] and show that it also fits into our setting. In particular, we show that the desired conditions for convergence are guaranteed by a certain class of monotone operators. Numerical experiments conclude this chapter and shed particular new light on the development of singularities in the solution of LLG. The results have partially been published in [BFF⁺12].
- Next, we leave the pure LLG case and consider the coupled problem of LLG with the full Maxwell system in **Chapter 4**. This serves as a model problem for a coupling of LLG with a second order linear hyperbolic PDE. We propose two numerical schemes, one of which is fully decoupled, i.e. instead of one large nonlinear system, one subsequently solves two smaller linear systems in an iterated scheme:



Even though, this approach comprises major advantages with respect to analysis and implementation, it does not impose additional conditions, and unconditional convergence can still be proved. This is the first fully decoupled and rigorously analyzed algorithm for the Maxwell-LLG system in the literature. The idea of decoupling will also accompany us through the subsequent chapters. The results from this chapter have partially been published in [BPP13].

- **Chapter 5** considers coupling of LLG to the eddy-current equation, i.e. coupling of LLG with a second order parabolic PDE. Again, we propose a fully decoupled scheme and derive unconditional convergence. Moreover, an improved energy estimate is shown. Numerical experiments conclude the chapter. The results have partially been published in [LPPT13].
- In **Chapter 6**, we include the magnetostrictive effect into our simulation which imposes coupling to the conservation of momentum equation. Again, this serves as a model problem. Here, the coupling operator, i.e. the corresponding field contribution, is nonlinear and one thus has to be careful with the weak limits. As before, we can show unconditional convergence of a fully decoupled scheme even in this case. The results from this chapter have partially been published in [BPPR13]. Numerical experiments conclude this section.
- A short outlook and discussion of open questions is finally given in **Chapter 7**.

Problem formulation and discretization

In this chapter, we present our first extension of the original work [Alo08a] of ALOUGES. We consider the pure LLG equation, but our ambitions go beyond incorporating only the classical field contributions from Section 1.3 which has been discussed in e.g. [AKT11, Gol12]. Instead, the goal of this chapter is to provide a set of assumptions that guarantee unconditional convergence of the numerical integrator provided that they are fulfilled for all field contributions. To that end, we perform an abstract convergence analysis where we only distinguish between time dependent and stationary contributions. Unlike [AKT11] and in the spirit of [Gol12], we even incorporate a possible discretization of the field contributions.

2.1. What are we trying to do

We aim for the construction and rigorous analysis of an unconditionally convergent integrator for the LLG equation (1.2.12)

$$\mathbf{m}_t = -\frac{1}{1+\alpha^2}\mathbf{m} \times \mathbf{h}_{\text{eff}} - \frac{\alpha}{1+\alpha^2}\mathbf{m} \times (\mathbf{m} \times \mathbf{h}_{\text{eff}})$$

subject to the initial and boundary conditions

$$\begin{aligned} \mathbf{m}(0) &= \mathbf{m}_0 && \text{in } \mathbf{H}^1(\Omega, \mathbb{S}^2) \\ \partial_n \mathbf{m} &= 0 && \text{on } \partial\Omega_T. \end{aligned}$$

In order to derive a general result, we do not consider the standard field contributions, but rather an effective field with general operators

$$\mathbf{h}_{\text{eff}} = C_e \Delta \mathbf{m} + C_1 \boldsymbol{\pi}(\mathbf{m}) + C_2 \boldsymbol{\chi}(\mathbf{m}). \quad (2.1.1)$$

The contributions $\boldsymbol{\pi}(\cdot)$ and $\boldsymbol{\chi}(\cdot)$ denote stationary, respectively time-dependent operators, and we refer to Section 2.2 below for a detailed description. Throughout this work, we only deal with weak solvers and seek convergence towards a weak solution. To that end, we follow the approaches from the literature and employ the equivalent formulation (1.2.14)

$$\mathbf{m}_t - \alpha \mathbf{m} \times \mathbf{m}_t = \mathbf{h}_{\text{eff}} \times \mathbf{m}.$$

In the spirit of ALOUGES and SOYEUR [AS92], our notion of a weak solution of LLG then reads as follows:

Definition 2.1.1. A function \mathbf{m} is called a weak solution of LLG, if

- (i) $\mathbf{m} \in \mathbf{H}^1(\Omega_T)$ with $|\mathbf{m}| = 1$ almost everywhere in Ω_T ;
- (ii) For all $\phi \in C^\infty(\overline{\Omega_T})$, there holds

$$\int_{\Omega_T} \mathbf{m}_t \cdot \phi - \alpha \int_{\Omega_T} (\mathbf{m} \times \mathbf{m}_t) \cdot \phi = \quad (2.1.2)$$

$$- C_e \int_{\Omega_T} (\nabla \times \mathbf{m}) \cdot \nabla \phi + C_1 \int_{\Omega_T} (\boldsymbol{\pi}(\mathbf{m}) \times \mathbf{m}) \cdot \phi + C_2 \int_{\Omega_T} (\boldsymbol{\chi}(\mathbf{m}) \times \mathbf{m}, \phi); \quad (2.1.3)$$

- (iii) We have $\mathbf{m}(0, \cdot) = \mathbf{m}_0$ in the sense of traces;
- (iv) For almost all $t' \in (0, T)$, there holds

$$\|\nabla \mathbf{m}(t')\|_{\mathbf{L}^2(\Omega)}^2 + \|\mathbf{m}_t\|_{\mathbf{L}^2(\Omega_{t'})}^2 \leq C, \quad (2.1.4)$$

for some constant $C > 0$ which depends only on \mathbf{m}_0 , as well as on the constants C_π and C_χ from below.

As mentioned above, we follow the steps of ALOUGES [Alo08a] for the construction of our numerical integrator. To that end, we utilize the third equivalent formulation (1.2.13)

$$\alpha \mathbf{m}_t + \mathbf{m} \times \mathbf{m}_t = \mathbf{h}_{\text{eff}} - \mathbf{m}(\mathbf{m} \cdot \mathbf{h}_{\text{eff}}) \quad \text{and} \quad |\mathbf{m}| = 1 \text{ a.e. in } \Omega_T$$

subject to the above initial and boundary conditions. The main observation from [Alo08a] now is that the equation is nonlinear with respect to the magnetization \mathbf{m} , but linear with respect to the time derivative \mathbf{m}_t of the magnetization. Consequently, we introduce a new free variable \mathbf{v} , which will approximate \mathbf{m}_t . Via this approach, even though LLG is nonlinear, a scheme can be derived which requires the solution of only one linear system per time step. The adjusted equation then reads

$$\alpha \mathbf{v} + \mathbf{m} \times \mathbf{v} = \mathbf{h}_{\text{eff}} - \mathbf{m}(\mathbf{m} \cdot \mathbf{h}_{\text{eff}})$$

This equation is advantageous for yet another reason. We already know from (1.2.15), that the magnetization \mathbf{m} and its time derivative \mathbf{m}_t are pointwise orthogonal on the continuous level. For the construction of the upcoming finite-element scheme, this is taken into account for the choice of the test functions. Since the sought solution \mathbf{v} should be in the tangent space of \mathbf{m} in order to be a useful replacement for \mathbf{m}_t , the above equation is tested with functions from the tangent space

$$\mathcal{K}_{\mathbf{m}} := \{ \phi \in C^\infty(\overline{\Omega_T}) : \phi \cdot \mathbf{m} = 0 \text{ almost everywhere in } \Omega_T \}, \quad (2.1.5)$$

and the upcoming integrator is therefore called *tangent plane scheme*. This, however, yields

$$\alpha(\mathbf{v}, \phi) + (\mathbf{m} \times \mathbf{v}, \phi) = (\mathbf{h}_{\text{eff}}, \phi) \quad \text{for all } \phi \in \mathcal{K}_{\mathbf{m}}, \quad (2.1.6)$$

i.e. the second term on the right hand side vanishes. Moreover, and for stability reasons, the exchange contribution (here hidden in the notation \mathbf{h}_{eff}) is treated implicitly. For sake of efficiency, however, all the other contributions will be treated explicitly, cf. [AKT11, Gol12]. Finally, we emphasize, that all the upcoming convergence proofs are constructive, i.e. they even provide existence of weak solutions without any further regularity assumptions.

2.1.1. Numerical framework

Throughout this work, let $\Omega \subset \mathbb{R}^3$ denote a polyhedral domain. For the discretization of (2.1.6), we employ a regular triangulation \mathcal{T} of Ω after the following definition.

Definition 2.1.2. *A set $\mathcal{T} = \{T_1, \dots, T_P\}$ is called a triangulation of Ω if and only if*

- \mathcal{T} is a finite set of non-degenerated tetrahedra,
- Ω is fully covered by \mathcal{T} , i.e. $\bar{\Omega} = \bigcup \mathcal{T}$,
- for two elements $T, T' \in \mathcal{T}$ with $T \neq T'$, there holds $|T \cap T'| = 0$.

We call a triangulation further *regular* (in the sense of Ciarlet), if the intersection of two elements $T, T' \in \mathcal{T}$ with $T \neq T'$ is either

- empty,
- a common node,
- a common edge, or
- a common face.

Throughout, the set of nodes of the triangulation is denoted by \mathcal{N} . For a given triangulation \mathcal{T} , the local mesh size is given by

$$h_T := \text{diam}(T) := \sup \{|\mathbf{x} - \mathbf{y}| : \mathbf{x}, \mathbf{y} \in T\}.$$

Moreover, let ρ_T be the radius of the largest sphere within T , and define by

$$\sigma(\mathcal{T}) := \max_{T \in \mathcal{T}} \frac{h_T}{\rho_T} \geq 1$$

the so-called *form regularity constant*. A triangulation $\mathcal{T} = \mathcal{T}_h$ subordinate to the global mesh-size

$$h := \max_{T \in \mathcal{T}} h_T$$

will be denoted by \mathcal{T}_h and its nodes by \mathcal{N}_h . For many results concerning finite element methods, it is very important that the form regularity constant remains bounded as $h \rightarrow 0$. This will be the case here as well and has to be ensured by the mesh refinement strategy. Throughout this work, we employ the refinement strategy from [Ver96, Section 4.1]. When refined, the tetrahedron is subdivided into 8 smaller tetrahedra as follows: First, we cut off the four apices and get four tetrahedra. The remainder forms an octahedron at the center of the original tetrahedron and is further subdivided into four more tetrahedra. A more detailed description

including a visualization of the scheme is found in [Gol12, Section 2.1.1]. We stress, that this refinement strategy guarantees that the shape regularity constant remains bounded.

For the discretization of (2.1.6), we now employ the standard P1-FEM space of piecewise affine and globally continuous functions

$$\mathcal{S}^1(\mathcal{T}_h) := \{\phi_h : \bar{\Omega} \rightarrow \mathbb{R}^3 \text{ continuous} : \phi_h|_T \text{ is affine for all } T \in \mathcal{T}_h\}. \quad (2.1.7)$$

Note, that a basis for the three-dimensional space $\mathcal{S}^1(\mathcal{T}_h)$ can be obtained from the one-dimensional hat functions. To that end, let $\{\eta_1, \dots, \eta_N\}$ be a basis for the scalar P1-FEM space $\tilde{\mathcal{S}}^1(\mathcal{T}_h)$. Then a basis for the three-dimensional case is given by

$$\left\{ \begin{pmatrix} \eta_i \\ 0 \\ 0 \end{pmatrix}, \begin{pmatrix} 0 \\ \eta_i \\ 0 \end{pmatrix}, \begin{pmatrix} 0 \\ 0 \\ \eta_i \end{pmatrix} : i = 1, \dots, N \right\}. \quad (2.1.8)$$

Due to the modulus constraint, we further introduce the set

$$\mathcal{M}_h := \{\phi \in \mathcal{S}^1(\mathcal{T}_h) : |\phi_h| = 1 \text{ for all nodes } \mathbf{z} \in \mathcal{N}_h\}, \quad (2.1.9)$$

which will be used to approximate the magnetization. Finally, to account for the fact that the sought quantity \mathbf{v} is orthogonal to the magnetization, we define the discrete counterpart of (2.1.5) by

$$\mathcal{K}_{\mathbf{m}_h^j} := \{\phi_h \in \mathcal{S}^1(\mathcal{T}_h) : \phi_h(\mathbf{z}) \cdot \mathbf{m}_h^j(\mathbf{z}) = 0 \text{ for all nodes } \mathbf{z} \in \mathcal{N}_h\}. \quad (2.1.10)$$

This space will be utilized for the discretized function $\mathbf{v}_h^j \approx \mathbf{v}(t_j) = \mathbf{m}_t(t_j)$ at a given time $t_j \in (0, T)$.

For the time discretization, we finally impose a uniform partition \mathcal{I}_k with $0 = t_0 < t_1 < \dots < t_N = T$ of the time interval $[0, T]$. The time step is then denoted by $k = k_j := t_j - t_{j-1}$ for $j = 1, \dots, N$, i.e. $t_j = jk$.

In many of the upcoming proofs, a certain angle condition

$$\int_{\Omega} \nabla \eta_i \cdot \nabla \eta_j \quad \text{for all basis functions } \eta_i, \eta_j \in \mathcal{S}^1(\mathcal{T}_h) \text{ with } i \neq j$$

is required. We emphasize that this condition only needs to be enforced for the initial mesh \mathcal{T}_0 . If the refinement strategy from above is used, and \mathcal{T}_j fulfills the angle condition, then it is also satisfied by \mathcal{T}_{j+1} , cf. [Bar05]. Moreover, the angle condition is automatically fulfilled if the dihedral angles of the triangulation are smaller than $\pi/2$.

We close this section with a technical result that correlates the $\mathbf{L}^p(\Omega)$ -norm with the degrees of freedom at the nodes of the triangulation.

Lemma 2.1.3. *Let $\phi_h \in V_h$ be a discrete function. For any $1 \leq p < \infty$, we then have*

$$\frac{1}{C} \|\phi_h\|_{\mathbf{L}^p(\Omega)}^p \leq h^d \sum_{\mathbf{z} \in \mathcal{N}_h} |\phi_h(\mathbf{z})|^p \leq C \|\phi_h\|_{\mathbf{L}^p(\Omega)}^p, \quad (2.1.11)$$

where $d \in \mathbb{N}_0$ denotes the spatial dimension, and the constant $C > 0$ depends only on d and the shape regularity constant $\sigma(\mathcal{T}_h)$.

Proof. The proof basically relies on norm equivalence on finite dimensional spaces and scaling arguments. The elaborated arguments can be found e.g. in [Gol12, Lemma 3.1.1]. \square

2.2. Abstract algorithm

In this section, we present our LLG-integrator in an abstract setting, where the effective field consists of the exchange contribution as well as the two general field contributions

$$\begin{aligned}\pi &: \mathbf{L}^2(\Omega) \rightarrow \mathbf{L}^2(\Omega) \quad \text{and} \\ \chi &: \mathbf{L}^2(\Omega_T) \rightarrow \mathbf{L}^2(\Omega_T).\end{aligned}\tag{2.2.1}$$

Since the first operator $\pi(\cdot)$ is not time-dependent, we implicitly understand time evaluations by $\pi(\mathbf{f})(t) = \pi(\mathbf{f}(t))$ for $\mathbf{f} \in \mathbf{L}^2(\Omega_T)$. Note that such an equality is not true in general for the time-dependent contribution $\chi(\cdot)$, i.e. $\chi(\mathbf{f})(t) \neq \chi(\mathbf{f}(t))$ as $\chi(\mathbf{f}(t))$ is not even well-defined, since $\mathbf{f}(t) \notin \mathbf{L}^2(\Omega_T)$. Even if we would implicitly understand $\mathbf{f}(t)$ as a constant function in time, i.e. $\mathbf{f}(t)(t') = \mathbf{f}(t) \in \mathbf{L}^2(\Omega)$ for almost all $t' \in [0, T]$, such an equality would generally not be true. If $\chi(\cdot)$ is given by $\chi(\mathbf{f}) = \mathbf{g}\mathbf{f}$ for some $\mathbf{g} \in \mathbf{L}^\infty(\Omega_T)$, for example, then we have $\chi(\mathbf{f})(t, \mathbf{x}) = \mathbf{g}(t, \mathbf{x})\mathbf{f}(t, \mathbf{x})$, but $\chi(\mathbf{f}(t'))(t, \mathbf{x}) = \mathbf{g}(t, \mathbf{x})\mathbf{f}(t', \mathbf{x})$. This circumstance complicates the upcoming convergence analysis. In addition, for any given $h > 0$, let

$$\pi_h : \mathbf{L}^2(\Omega) \rightarrow \mathbf{L}^2(\Omega)\tag{2.2.2}$$

be a numerical realization of π . Unlike [AKT11], this will allow us to rigorously include the inevitable approximation error that occurs when computing the different field contributions, into the convergence analysis. For sake of readability, we neglect a numerical approximation of the time-dependent contribution $\chi(\cdot)$ and assume that this is computed exactly. Obviously, we cannot prove convergence for completely arbitrary operators, and we will specify the required properties down below in (2.3.2)–(2.3.4). In Section 3 we will then investigate some classical field contributions and show that they fit into our abstract framework. We first state our general integrator.

Algorithm 2.2.1 (General algorithm). *Input: initial approximation $\mathbf{m}_h^0 \in \mathcal{M}_h$, damping parameter $\alpha > 0$, parameter $\theta \in [0, 1]$, $C_1, C_2 \geq 0$.*

For $j = 0, \dots, N - 1$ iterate:

(i) Find $\mathbf{v}_h^j \in \mathcal{K}_{\mathbf{m}_h^j}$ such that for all test functions $\psi_h \in \mathcal{K}_{\mathbf{m}_h^j}$, we have

$$\begin{aligned}\alpha \int_{\Omega} \mathbf{v}_h^j \cdot \psi_h + \int_{\Omega} (\mathbf{m}_h^j \times \mathbf{v}_h^j) \cdot \psi_h &= -C_e \int_{\Omega} \nabla(\mathbf{m}_h^j + \theta k \mathbf{v}_h^j) \cdot \nabla \psi_h \\ &+ C_1 \int_{\Omega} \pi_h(\mathbf{m}_h^j) \cdot \psi_h + C_2 \int_{\Omega} \chi(\mathbf{m}_{hk})(t_j) \cdot \psi_h.\end{aligned}\tag{2.2.3}$$

(ii) Define $\mathbf{m}_h^{j+1} \in \mathcal{M}_h$ nodewise by $\mathbf{m}_h^{j+1} = \sum_{i=0}^{\mathcal{N}_h} \mathbf{m}_i^{j+1} \eta_i$ with $\mathbf{m}_i^{j+1} = \frac{\mathbf{m}_i^j + k \mathbf{v}_i^j}{|\mathbf{m}_i^j + k \mathbf{v}_i^j|}$.

Output: Sequence of discrete time derivatives $\mathbf{v}_h^j \in \mathcal{K}_{\mathbf{m}_h^j}$ and magnetizations $\mathbf{m}_h^{j+1} \in \mathcal{M}_h$.

For $t \in [t_j, t_{j+1})$ the function $\mathbf{m}_{hk} \in \mathbf{L}^2(\Omega_T)$ is defined by

$$\begin{aligned}\mathbf{m}_{hk}(t, \mathbf{x}) &:= \frac{t - jk}{k} \mathbf{m}_h^{j+1}(\mathbf{x}) + \frac{(j+1)k - t}{k} \mathbf{m}_h^j(\mathbf{x}), \\ &= \mathbf{m}_h^j(\mathbf{x}) + (t - t_j) \mathbf{d}_t \mathbf{m}_h^{j+1}(\mathbf{x}),\end{aligned}\tag{2.2.4}$$

where the equality can be established as in (2.2.13) below, and $d_t \mathbf{m}_h^{j+1}$ denotes the first order difference quotient, i.e.

$$d_t \mathbf{m}_h^{j+1} = \frac{\mathbf{m}_h^{j+1} - \mathbf{m}_h^j}{k}.$$

The evaluation of $\chi(\mathbf{m}_{hk})$ in step j of the above algorithm is to be understood successively, i.e. \mathbf{m}_{hk} is constructed successively and $\chi(\mathbf{m}_{hk})$ denotes the application of χ to the so far constructed function \mathbf{m}_{hk} . In the upcoming proof, this leads to some technical issue. Since \mathbf{m}_{hk} is constructed on the fly during execution of the above algorithm, it is a priori not defined on the full time interval $[0, T]$ in each step. We therefore need to assume, that χ is well defined on shorter time intervals as well, so that $\chi(\mathbf{m}_{hk})$ makes sense. Furthermore, we assume that $\chi(\mathbf{m}_{hk})(t)$ depends only on \mathbf{m}_{hk} at time t or earlier, but not on later times. If \mathbf{m}_{hk} denotes the full function on $[0, T]$ and $\tilde{\mathbf{m}}_{hk}$ denotes the successively generated function on $[0, T/2]$, we thus have

$$\chi(\mathbf{m}_{hk})(t) = \chi(\tilde{\mathbf{m}}_{hk})(t) \quad \text{for almost all } t \in [0, T/2]. \quad (2.2.5)$$

This assumption is, however, quite natural, since the field contributions usually stem from physical effects and equations and should thus fulfill such a property. Moreover, to ensure that our algorithm is well-defined, we assume that $\chi(\cdot)$ is sufficiently smooth in time in order for the time evaluation $\chi(\mathbf{m}_{hk})(t_j)$ to make sense. More precisely, we assume that $\chi(\mathbf{f}) : [0, T] \rightarrow \mathbf{L}^2(\Omega)$ is continuous, if $\mathbf{f} : [0, T] \rightarrow \mathbf{L}^2(\Omega)$ is continuous. We stress that our convergence analysis only requires Riemann integrability of χ in time. For sake of simplicity, however, we assume time-continuity here. Finally, for the initial step, $\chi(\mathbf{m}_{hk})(0)$ has to be meaningful, i.e. there exists some suitable spatial operator $\chi_0 : \mathbf{L}^2(\Omega) \rightarrow \mathbf{L}^2(\Omega)$ such that $\chi(\mathbf{m}_{hk})(0) = \chi_0(\mathbf{m}_h^0)$.

For sake of readability, we recall the three assumptions on the time-dependent contribution $\chi(\cdot)$.

- We assume that $\chi(\cdot)$ is well defined even on smaller time-intervals and that $\chi(\mathbf{m}_{hk})(t)$ does not depend on values of \mathbf{m}_{hk} at any time $t' > t$.
- We assume that $\chi(\mathbf{f})$ is continuous in time if \mathbf{f} is continuous in time.
- We assume that there exists some suitable initial value $\chi(\mathbf{m}_{hk})(0) = \chi_0(\mathbf{m}_h^0)$.

In addition to the linear time-interpolation \mathbf{m}_{hk} , we also define the piecewise constant time-approximations for $t \in [t_j, t_{j+1})$ by

$$\begin{aligned} \mathbf{m}_{hk}^-(t, \mathbf{x}) &:= \mathbf{m}_h^j(\mathbf{x}), \\ \mathbf{m}_{hk}^+(t, \mathbf{x}) &:= \mathbf{m}_h^{j+1}(\mathbf{x}). \end{aligned} \quad (2.2.6)$$

Since our ansatz treats the time derivative of the magnetization as independent variable, we also define its piecewise constant time-approximation for $t \in [t_j, t_{j+1})$ by

$$\mathbf{v}_{hk}^-(t, \mathbf{x}) := \mathbf{v}_h^j(\mathbf{x}). \quad (2.2.7)$$

Before moving on to a general convergence analysis of the above algorithm, we write down some results that immediately follow from the definition of the discrete approximations and Algorithm 2.2.1, respectively. First of all, we show that the above algorithm is well-defined.

Lemma 2.2.2. *Algorithm 2.2.1 presented above is well defined, i.e. it admits a unique solution $\mathbf{v}_h^j \in \mathcal{K}_{\mathbf{m}_h^j}$ in each step of the loop. In particular there holds $\|\mathbf{m}_h^j\|_{\mathbf{L}^\infty(\Omega)} = 1$ and $\|\mathbf{m}_{hk}\|_{\mathbf{L}^\infty(\Omega_T)} = 1$.*

Proof. We define the bilinear form $a^j(\cdot, \cdot) : \mathcal{K}_{\mathbf{m}_h^j} \times \mathcal{K}_{\mathbf{m}_h^j} \rightarrow \mathbb{R}$ by

$$a^j(\varphi, \psi) := \alpha(\varphi, \psi) + ((\mathbf{m}_h^j \times \varphi), \psi) + \theta C_e k (\nabla \varphi, \nabla \psi)$$

and the functional

$$L^j(\psi) := -C_e (\nabla \mathbf{m}_h^j, \nabla \psi) + C_1(\pi(\mathbf{m}_h^j), \psi) + C_2(\chi(\mathbf{m}_{hk})(t_j), \psi).$$

Then, (2.2.3) can equivalently be stated as

$$a^j(\mathbf{v}_h^j, \psi) = L^j(\psi) \quad \text{for all } \psi \in \mathcal{K}_{\mathbf{m}_h^j}.$$

Clearly $L^j(\cdot)$ is a linear functional in ψ and $a^j(\cdot, \cdot)$ is positive definite, since

$$a^j(\psi, \psi) = \alpha\|\psi\|_{\mathbf{L}^2(\Omega)}^2 + \theta C_e k \|\nabla \psi\|_{\mathbf{L}^2(\Omega)}^2.$$

Due to finite dimension, we conclude the existence of a unique solution $\mathbf{v}_h^j \in \mathcal{K}_{\mathbf{m}_h^j}$ in each time step. Finally, from the definition of \mathbf{v}_h^j and the Pythagoras theorem, we get

$$|\mathbf{m}_h^j(\mathbf{z}) + k\mathbf{v}_h^j(\mathbf{z})|^2 = |\mathbf{m}_h^j(\mathbf{z})|^2 + k|\mathbf{v}_h^j(\mathbf{z})|^2 \geq 1.$$

Therefore, also the normalization from step (ii) of the above algorithm is well-defined. The boundedness of $\|\mathbf{m}_h^j\|_{\mathbf{L}^\infty(\Omega)} = \|\mathbf{m}_{hk}\|_{\mathbf{L}^\infty(\Omega_T)} = 1$ finally follows from normalization at the grid points and use of barycentric coordinates, cf. [Gol12, Lemma 3.2.6]. \square

The next two statements relate the time derivative of the discrete magnetization \mathbf{m}_{hk} with the quantity \mathbf{v}_{hk}^- , i.e. the variable that approximates the time-derivative of the continuous solution \mathbf{m} . In fact, we have a relation of those two quantities on each time step.

Lemma 2.2.3. *The time derivative of the discrete magnetization \mathbf{m}_{hk} is a lower bound for the approximation \mathbf{v}_{hk}^- of the time derivative of the continuous magnetization \mathbf{m} in each time step, i.e. for $t \in [t_j, t_{j+1})$, there holds*

$$\|\partial_t \mathbf{m}_{hk}(t)\|_{\mathbf{L}^2(\Omega)} = \left\| \frac{\mathbf{m}_h^{j+1} - \mathbf{m}_h^j}{k} \right\|_{\mathbf{L}^2(\Omega)} \leq C_v \|\mathbf{v}_h^j\|_{\mathbf{L}^2(\Omega)} \quad (2.2.8)$$

for each $j = 0, \dots, N-1$. Here, the constant $C_v \geq 0$ is a norm equivalence constant of a finite dimensional space.

Proof. The proof is a simple consequence of the orthogonality relation between \mathbf{v}_h^j and \mathbf{m}_h^j . The elaborated arguments can be found in [Gol12, Lemma 3.3.2]. \square

Lemma 2.2.4. *For any $j = 0, \dots, N-1$ and any node $\mathbf{z} \in \mathcal{N}_h$, there holds*

$$|\mathbf{m}_h^{j+1}(\mathbf{z}) - \mathbf{m}_h^j(\mathbf{z}) - k\mathbf{v}_h^j(\mathbf{z})| \leq \frac{1}{2} |k\mathbf{v}_h^j(\mathbf{z})|^2. \quad (2.2.9)$$

Proof. The proof is found e.g. in [Gol12, Lemma 3.3.3]. \square

The following abstract result concerns the difference of the piecewise linear and piecewise constant interpolations in time of some continuous quantity $\mathbf{g} \in \mathbf{L}^2(\Omega)$. We consider functions $\mathbf{g}_{hk}, \mathbf{g}_{hk}^-$, and \mathbf{g}_{hk}^+ of the form (2.2.4) resp. (2.2.6). As expected, we find that the difference can be estimated from above by means of the weak time derivative.

Lemma 2.2.5. *Let $\mathbf{g}_h^j \in \mathcal{S}^1(\mathcal{T}_h)$ be a spatial discretization of the quantity $\mathbf{g}(t_j) \in \mathbf{L}^2(\Omega)$ for any $j = 0, \dots, N-1$. Analogously to the above definitions, we set*

$$\begin{aligned} \mathbf{g}_{hk}(t, \mathbf{x}) &:= \frac{t-jk}{k} \mathbf{g}_h^{j+1}(\mathbf{x}) + \frac{(j+1)k-t}{k} \mathbf{g}_h^j(\mathbf{x}), \quad \text{and} \\ \mathbf{g}_{hk}^-(t, \mathbf{x}) &:= \mathbf{g}_h^j(\mathbf{x}), \quad \mathbf{g}_{hk}^+(t, \mathbf{x}) := \mathbf{g}_h^{j+1}(\mathbf{x}) \quad \text{for } t \in (t_j, t_{j+1}]. \end{aligned}$$

Then, for almost all $t \in [0, T]$, there holds

$$\|(\mathbf{g}_{hk} - \mathbf{g}_{hk}^-)(t)\|_{\mathbf{L}^2(\Omega)} \leq k \|\partial_t \mathbf{g}_{hk}(t)\|_{\mathbf{L}^2(\Omega)} \quad \text{and} \quad (2.2.10)$$

$$\|(\mathbf{g}_{hk} - \mathbf{g}_{hk}^+)(t)\|_{\mathbf{L}^2(\Omega)} \leq 2k \|\partial_t \mathbf{g}_{hk}(t)\|_{\mathbf{L}^2(\Omega)}. \quad (2.2.11)$$

In particular, we thus get

$$\|\mathbf{g}_{hk} - \mathbf{g}_{hk}^\pm\|_{\mathbf{L}^2(\Omega_T)}^2 \leq Ck \sum_{j=0}^{N-1} \|\mathbf{g}_h^{j+1} - \mathbf{g}_h^j\|_{\mathbf{L}^2(\Omega)}^2 = Ck^3 \|\partial_t \mathbf{g}_{hk}\|_{\mathbf{L}^2(\Omega_T)}^2, \quad (2.2.12)$$

where $C > 0$ is either 1 or 2, depending on the approximation \mathbf{g}_{hk}^- resp. \mathbf{g}_{hk}^+ . Moreover, if the discrete time derivative $\partial_t \mathbf{g}_{hk}$ is bounded in $\mathbf{L}^2(\Omega_T)$, then we have $\|\mathbf{g}_{hk} - \mathbf{g}_{hk}^\pm\|_{\mathbf{L}^2(\Omega_T)}^2 \rightarrow 0$.

Proof. First of all, we see that for $t \in [t_j, t_{j+1}]$, we have

$$\begin{aligned} \mathbf{g}_{hk}(t) &= \frac{t-jk}{k} \mathbf{g}_h^{j+1} + \frac{(j+1)k-t}{k} \mathbf{g}_h^j \\ &= \frac{t-t_j}{k} \mathbf{g}_h^{j+1} + \frac{k-(t-t_j)}{k} \mathbf{g}_h^j \\ &= \mathbf{g}_h^j + \frac{t-t_j}{k} (\mathbf{g}_h^{j+1} - \mathbf{g}_h^j) \\ &= \mathbf{g}_h^j + (t-t_j) \mathbf{d}_t \mathbf{g}_h^{j+1}. \end{aligned} \quad (2.2.13)$$

For $t \in [t_j, t_{j+1})$, we thus get

$$\begin{aligned} \|(\mathbf{g}_{hk} - \mathbf{g}_{hk}^-)(t)\|_{\mathbf{L}^2(\Omega)} &= \|\mathbf{g}_h^j + (t-t_j) \mathbf{d}_t \mathbf{g}_h^{j+1} - \mathbf{g}_h^j\|_{\mathbf{L}^2(\Omega)} \\ &= |t-t_j| \|\mathbf{d}_t \mathbf{g}_h^{j+1}\|_{\mathbf{L}^2(\Omega)} \\ &\leq k \|\mathbf{d}_t \mathbf{g}_h^{j+1}\|_{\mathbf{L}^2(\Omega)} \\ &= k \|\partial_t \mathbf{g}_{hk}(t)\|_{\mathbf{L}^2(\Omega)}, \end{aligned}$$

and

$$\begin{aligned} \|(\mathbf{g}_{hk} - \mathbf{g}_{hk}^+)(t)\|_{\mathbf{L}^2(\Omega)} &= \|\mathbf{g}_h^j + (t-t_j) \mathbf{d}_t \mathbf{g}_h^{j+1} - \mathbf{g}_h^{j+1}\|_{\mathbf{L}^2(\Omega)} \\ &\leq \|\mathbf{g}_h^{j+1} - \mathbf{g}_h^j\|_{\mathbf{L}^2(\Omega)} + |t-t_j| \|\mathbf{d}_t \mathbf{g}_h^{j+1}\|_{\mathbf{L}^2(\Omega)} \\ &\leq 2k \|\mathbf{d}_t \mathbf{g}_h^{j+1}\|_{\mathbf{L}^2(\Omega)} \\ &= 2k \|\partial_t \mathbf{g}_{hk}(t)\|_{\mathbf{L}^2(\Omega)}, \end{aligned}$$

which proves (2.2.10)–(2.2.11). The desired estimate (2.2.12) for the $\mathbf{L}^2(\Omega_T)$ -norm simply follows from summing up over all timesteps, i.e.

$$\begin{aligned} \|\mathbf{g}_{hk} - \mathbf{g}_{hk}^\pm\|_{\mathbf{L}^2(\Omega_T)}^2 &= \sum_{j=0}^{N-1} \int_{t_j}^{t_{j+1}} \|(\mathbf{g}_{hk} - \mathbf{g}_{hk}^\pm)(t)\|_{\mathbf{L}^2(\Omega)}^2 dt \\ &\leq k \sum_{j=0}^{N-1} C \|\mathbf{g}_h^{j+1} - \mathbf{g}_h^j\|_{\mathbf{L}^2(\Omega)}^2 \\ &= Ck^3 \|\partial_t \mathbf{g}_{hk}\|_{\mathbf{L}^2(\Omega_T)}^2. \end{aligned}$$

This completes the proof. \square

Remark. For most of the upcoming discrete quantities, we can show

$$\|\mathbf{g}_{hk} - \mathbf{g}_{hk}^\pm\|_{\mathbf{L}^2(\Omega_T)}^2 \lesssim k \sum_{j=0}^{N-1} \|\mathbf{g}_h^{j+1} - \mathbf{g}_h^j\|_{\mathbf{L}^2(\Omega)}^2 \longrightarrow 0,$$

whence the above Lemma allows us to unify the limits of \mathbf{g}_{hk} and \mathbf{g}_{hk}^\pm as long as they exist.

We are now ready to give a first convergence result based on the abstract framework of the above algorithm.

2.3. Abstract convergence analysis

In this section, we give a detailed convergence analysis of the abstract Algorithm 2.2.1. The proof follows the lines of [Alo08a, Gol12], but the analysis is widened and generalized at several points to capture the general field contributions $\boldsymbol{\pi}$ and $\boldsymbol{\chi}$. The following theorem is the main result of this Section and states convergence of the scheme in the abstract framework, under some assumptions on the field contributions. Afterwards, we will explicitly investigate certain field contributions and show that they fall into our general setting. In particular, all field contributions from Chapter 1 are covered by this theory.

Theorem 2.3.1. (a) Let $\theta \in (1/2, 1]$ and suppose that the spatial meshes \mathcal{T}_h are uniformly shape regular and satisfy the angle condition

$$\int_{\Omega} \nabla \eta_i \cdot \nabla \eta_j \quad \text{for all basis functions } \eta_i, \eta_j \in \mathcal{S}^1(\mathcal{T}_h) \text{ with } i \neq j. \quad (2.3.1)$$

Moreover, suppose that the general field contributions $\boldsymbol{\pi}_h(\cdot)$ and $\boldsymbol{\chi}(\cdot)(\cdot)$ are uniformly bounded, i.e. for all $\mathbf{n} \in \mathbf{L}^2(\Omega)$ with $|\mathbf{n}| \leq 1$ pointwise almost everywhere and $\tilde{\mathbf{n}} \in C(\mathbf{L}^2)$ with $|\tilde{\mathbf{n}}| \leq 1$ pointwise almost everywhere, there holds

$$\begin{aligned} \|\boldsymbol{\pi}_h(\mathbf{n})\|_{\mathbf{L}^2(\Omega)} &\leq C_{\boldsymbol{\pi}} < \infty \\ \|\boldsymbol{\chi}(\tilde{\mathbf{n}})(t)\|_{\mathbf{L}^2(\Omega)} &\leq C_{\boldsymbol{\chi}} < \infty. \end{aligned} \quad (2.3.2)$$

The constants $C_{\boldsymbol{\pi}}, C_{\boldsymbol{\chi}} > 0$ may depend only on Ω and are, in particular, assumed to be independent of the time step- and spatial mesh-sizes k and h . Finally, suppose weak convergence of the initial data, i.e.

$$\mathbf{m}_h^0 \rightharpoonup \mathbf{m}^0 \quad \text{weakly in } \mathbf{H}^1(\Omega) \quad (2.3.3)$$

as $h \rightarrow 0$. Under these assumptions, we have strong subconvergence of \mathbf{m}_{hk}^- towards some function \mathbf{m} in $\mathbf{L}^2(\Omega_T)$ as $(h, k) \rightarrow (0, 0)$ independently of each other.

(b) In addition to the above, we assume

$$\begin{aligned} \pi_h(\mathbf{m}_{hk}^-) &\xrightarrow{\text{sub}} \pi(\mathbf{m}) \quad \text{weakly subconvergent in } \mathbf{L}^2(\Omega_T), \text{ and} \\ k \sum_{j=0}^{N-1} \int_{\Omega} \chi(\mathbf{m}_{hk})(t_j) \cdot ((\mathbf{m}_{hk}^- \times \Psi)(t_j)) &\xrightarrow{\text{sub}} \int_{\Omega_T} \chi(\mathbf{m}) \cdot (\mathbf{m} \times \Psi), \end{aligned} \quad (2.3.4)$$

for all $\Psi \in C^\infty(\Omega_T)$. Then, the computed FE solutions \mathbf{m}_{hk} are weakly subconvergent in $\mathbf{H}^1(\Omega_T)$ towards a weak solution $\mathbf{m} \in \mathbf{H}^1(\Omega_T)$ of LLG in the sense of 2.1.1. In particular, this yields existence of weak solutions and each accumulation point of \mathbf{m}_{hk} is a weak solution of LLG.

Remark. The second assumption in (2.3.4) seems hard to verify at first glance. It is, however, exactly the property that is needed for the convergence analysis. In a more detailed investigation, we propose some more suitable conditions (2.3.30)–(2.3.31) which guarantee the above convergence property. As the proof is quite involved and requires considering the h - and k -limits separately, details are postponed to Section 2.3.1.

The proof of Theorem 2.3.1 basically relies on the following three steps which will be elaborated subsequently.

- **Step 1:** Boundedness of the discrete quantities and energies.
- **Step 2:** Existence of weakly convergent subsequences via compactness.
- **Step 3:** Identification of the limits with weak solutions of LLG.

Before we move on to the actual convergence analysis, we would like to comment on the somewhat technical angle condition (2.3.1). While it may seem arbitrary at first sight, this condition is a crucial ingredient to prove a certain energy decay on a discrete level. Starting from the energy decay relation

$$\int_{\Omega} \left| \nabla \left(\frac{\mathbf{m}}{|\mathbf{m}|} \right) \right|^2 \leq \int_{\Omega} |\nabla \mathbf{m}|^2$$

it has been shown by BARTELS in [Bar05] that (2.3.1) and nodewise projection ensures the decay even on a discrete level, i.e.

$$\int_{\Omega} \left| \nabla \mathcal{I}_h \left(\frac{\mathbf{m}}{|\mathbf{m}|} \right) \right|^2 \leq \int_{\Omega} |\nabla \mathcal{I}_h \mathbf{m}|^2. \quad (2.3.5)$$

This yields the following lemma by definition of \mathbf{m}_h^{j+1} .

Lemma 2.3.2. Assume the angle condition (2.3.1). Then, we have the energy decay relation

$$\|\nabla \mathbf{m}_h^{j+1}\|_{\mathbf{L}^2(\Omega)}^2 \leq \|\nabla(\mathbf{m}_h^j + k\mathbf{v}_h^j)\|_{\mathbf{L}^2(\Omega)}^2 \quad (2.3.6)$$

in each step $j = 0, \dots, N-1$ of Algorithm 2.2.1. □

Remark . As mentioned in Section 2.1.1, (2.3.1) is automatically fulfilled for tetrahedral meshes with dihedral angles that are smaller than $\pi/2$. If the condition is satisfied by \mathcal{T}_0 , it can be ensured for the refined meshes as well, provided that, e.g., the refinement strategy from Section 2.1.1 is used.

We now elaborate the above steps of the convergence proof.

Step 1: The discrete quantities \mathbf{m}_{hk} , \mathbf{m}_{hk}^\pm , and \mathbf{v}_{hk}^- are uniformly bounded.

Lemma 2.3.3. For any $j = 0, \dots, N$, there holds

$$\frac{1}{2} \|\nabla \mathbf{m}_h^j\|_{L^2(\Omega)}^2 + k \sum_{i=0}^{j-1} \|\mathbf{v}_h^i\|_{L^2(\Omega)}^2 + (\theta - 1/2) k^2 \sum_{i=0}^{j-1} \|\nabla \mathbf{v}_h^i\|_{L^2(\Omega)}^2 \leq C_3, \quad (2.3.7)$$

where $C_3 > 0$ depends only on C_π and C_χ from (2.3.2), C_1 , C_2 , and C_e as well as $|\Omega|$.

Proof. We consider (2.2.3) with the special testfunction $\boldsymbol{\psi}_h = \mathbf{v}_h^i \in \mathcal{K}_{\mathbf{m}_h^i}$ to see

$$\begin{aligned} \alpha(\mathbf{v}_h^i, \mathbf{v}_h^i) + \underbrace{(\mathbf{m}_h^i \times \mathbf{v}_h^i, \mathbf{v}_h^i)}_{=0} &= -C_e (\nabla(\mathbf{m}_h^i + \theta k \mathbf{v}_h^i), \nabla \mathbf{v}_h^i) \\ &\quad + C_1 (\pi_h(\mathbf{m}_h^i), \mathbf{v}_h^i) \\ &\quad + C_2 (\chi(\mathbf{m}_{hk})(t_i), \mathbf{v}_h^i), \end{aligned}$$

and therefore

$$\begin{aligned} \alpha \|\mathbf{v}_h^i\|_{L^2(\Omega)}^2 + C_e \theta k \|\nabla \mathbf{v}_h^i\|_{L^2(\Omega)}^2 &= -C_e (\nabla \mathbf{m}_h^i, \nabla \mathbf{v}_h^i) \\ &\quad + C_1 (\pi_h(\mathbf{m}_h^i), \mathbf{v}_h^i) \\ &\quad + C_2 (\chi(\mathbf{m}_{hk})(t_i), \mathbf{v}_h^i). \end{aligned} \quad (2.3.8)$$

Next, we use

$$\frac{1}{2} \|\nabla \mathbf{m}_h^{i+1}\|_{L^2(\Omega)}^2 \leq \frac{1}{2} \|\nabla(\mathbf{m}_h^i + k \mathbf{v}_h^i)\|_{L^2(\Omega)}^2$$

from Lemma 2.3.2 to deduce

$$\begin{aligned} \frac{1}{2} \|\nabla \mathbf{m}_h^{i+1}\|_{L^2(\Omega)}^2 &\leq \frac{1}{2} \|\nabla \mathbf{m}_h^i + k \nabla \mathbf{v}_h^i\|_{L^2(\Omega)}^2 \\ &= \frac{1}{2} \|\nabla \mathbf{m}_h^i\|_{L^2(\Omega)}^2 + k (\nabla \mathbf{m}_h^i, \nabla \mathbf{v}_h^i) + \frac{k^2}{2} \|\nabla \mathbf{v}_h^i\|_{L^2(\Omega)}^2 \\ &= \frac{1}{2} \|\nabla \mathbf{m}_h^i\|_{L^2(\Omega)}^2 + \frac{k^2}{2} \|\nabla \mathbf{v}_h^i\|_{L^2(\Omega)}^2 - \frac{\alpha k}{C_e} \|\mathbf{v}_h^i\|_{L^2(\Omega)}^2 \\ &\quad - \theta k^2 \|\nabla \mathbf{v}_h^i\|_{L^2(\Omega)}^2 + \frac{k C_1}{C_e} (\pi_h(\mathbf{m}_h^i), \mathbf{v}_h^i) + \frac{k C_2}{C_e} (\chi(\mathbf{m}_{hk})(t_i), \mathbf{v}_h^i) \\ &= \frac{1}{2} \|\nabla \mathbf{m}_h^i\|_{L^2(\Omega)}^2 - (\theta - \frac{1}{2}) k^2 \|\nabla \mathbf{v}_h^i\|_{L^2(\Omega)}^2 - \frac{\alpha k}{C_e} \|\mathbf{v}_h^i\|_{L^2(\Omega)}^2 \\ &\quad + \frac{k C_1}{C_e} (\pi_h(\mathbf{m}_h^i), \mathbf{v}_h^i) + \frac{k C_2}{C_e} (\chi(\mathbf{m}_{hk})(t_i), \mathbf{v}_h^i). \end{aligned} \quad (2.3.9)$$

Summation over $i = 0, \dots, j-1$ and exploiting the telescopic sum leads to

$$\begin{aligned} \frac{1}{2} \|\nabla \mathbf{m}_h^j\|_{L^2(\Omega)}^2 &\leq \frac{1}{2} \|\nabla \mathbf{m}_h^0\|_{L^2(\Omega)}^2 - (\theta - \frac{1}{2}) k^2 \sum_{i=0}^{j-1} \|\nabla \mathbf{v}_h^i\|_{L^2(\Omega)}^2 - \frac{\alpha k}{C_e} \sum_{i=0}^{j-1} \|\mathbf{v}_h^i\|_{L^2(\Omega)}^2 \\ &\quad + \frac{k C_1}{C_e} \sum_{i=0}^{j-1} (\boldsymbol{\pi}_h(\mathbf{m}_h^i), \mathbf{v}_h^i) + \frac{k C_2}{C_e} \sum_{i=0}^{j-1} (\boldsymbol{\chi}(\mathbf{m}_{hk})(t_i), \mathbf{v}_h^i). \end{aligned}$$

Hölders inequality in combination with (2.3.2) now yields

$$\begin{aligned} \frac{1}{2} \|\nabla \mathbf{m}_h^j\|_{L^2(\Omega)}^2 &+ \frac{\alpha k}{C_e} \sum_{i=0}^{j-1} \|\mathbf{v}_h^i\|_{L^2(\Omega)}^2 + (\theta - \frac{1}{2}) k^2 \sum_{i=0}^{j-1} \|\nabla \mathbf{v}_h^i\|_{L^2(\Omega)}^2 \\ &\leq \frac{1}{2} \|\nabla \mathbf{m}_h^0\|_{L^2(\Omega)}^2 + \frac{k C_1}{C_e} \sum_{i=0}^{j-1} \|\boldsymbol{\pi}_h(\mathbf{m}_h^i)\|_{L^2(\Omega)} \|\mathbf{v}_h^i\|_{L^2(\Omega)} \\ &\quad + \frac{k C_2}{C_e} \sum_{i=0}^{j-1} \|\boldsymbol{\chi}(\mathbf{m}_{hk})(t_i)\|_{L^2(\Omega)} \|\mathbf{v}_h^i\|_{L^2(\Omega)} \\ &\leq \frac{1}{2} \|\nabla \mathbf{m}_h^0\|_{L^2(\Omega)}^2 \\ &\quad + \frac{2k}{C_e} \sum_{i=0}^{j-1} \max\{C_1 C_\pi, C_2 C_\chi\} \|\mathbf{v}_h^i\|_{L^2(\Omega)}, \end{aligned}$$

Exploiting Youngs inequality, this reveals for any $\varepsilon > 0$

$$\begin{aligned} \frac{1}{2} \|\nabla \mathbf{m}_h^j\|_{L^2(\Omega)}^2 &+ \frac{\alpha k}{C_e} \sum_{i=0}^{j-1} \|\mathbf{v}_h^i\|_{L^2(\Omega)}^2 + (\theta - \frac{1}{2}) k^2 \sum_{i=0}^{j-1} \|\nabla \mathbf{v}_h^i\|_{L^2(\Omega)}^2 \\ &\leq \frac{1}{2} \|\nabla \mathbf{m}_h^0\|_{L^2(\Omega)}^2 + \frac{k}{C_e} \sum_{i=0}^{j-1} \left(\frac{1}{2\varepsilon} \max\{C_1 C_\pi, C_2 C_\chi\}^2 + \varepsilon \|\mathbf{v}_h^i\|_{L^2(\Omega)}^2 \right) \end{aligned}$$

and therefore

$$\begin{aligned} \frac{1}{2} \|\nabla \mathbf{m}_h^j\|_{L^2(\Omega)}^2 &+ \frac{k}{C_e} (\alpha - \varepsilon) \sum_{i=0}^{j-1} \|\mathbf{v}_h^i\|_{L^2(\Omega)}^2 + (\theta - \frac{1}{2}) k^2 \sum_{i=0}^{j-1} \|\nabla \mathbf{v}_h^i\|_{L^2(\Omega)}^2 \\ &\leq \frac{1}{2} \|\nabla \mathbf{m}_h^0\|_{L^2(\Omega)}^2 + \frac{k}{C_e} \sum_{i=0}^{j-1} \frac{1}{2\varepsilon} \max\{C_1 C_\pi, C_2 C_\chi\}^2. \end{aligned}$$

Altogether we have thus proved

$$\begin{aligned} \frac{1}{2} \|\nabla \mathbf{m}_h^j\|_{L^2(\Omega)}^2 &+ \frac{k}{C_e} (\alpha - \varepsilon) \sum_{i=0}^{j-1} \|\mathbf{v}_h^i\|_{L^2(\Omega)}^2 + (\theta - \frac{1}{2}) k^2 \sum_{i=0}^{j-1} \|\nabla \mathbf{v}_h^i\|_{L^2(\Omega)}^2 \\ &\leq \frac{1}{2} \|\nabla \mathbf{m}_h^0\|_{L^2(\Omega)}^2 + \frac{T}{2\varepsilon C_e} \max\{C_1 C_\pi, C_2 C_\chi\}^2, \end{aligned}$$

which is a stability result that depends on $\varepsilon > 0$. The choice $\varepsilon < \alpha$ thus yields the desired result (2.3.7). \square

The last result is all that is necessary to show boundedness of the discrete magnetizations \mathbf{m}_{hk} and \mathbf{m}_{hk}^\pm , as well as of the discrete time derivative \mathbf{v}_{hk}^- .

Corollary 2.3.4. *The discrete quantities from (2.2.4) and (2.2.6)–(2.2.7) are uniformly bounded in $\mathbf{H}^1(\Omega_T)$ resp. $\mathbf{L}^2(\Omega_T)$, i.e.*

$$\|\mathbf{m}_{hk}\|_{\mathbf{H}^1(\Omega_T)} \leq C_4 < \infty \quad (2.3.10)$$

$$\|\mathbf{m}_{hk}^\pm\|_{\mathbf{L}^2(\mathbf{H}^1)} \leq C_4 < \infty, \text{ and} \quad (2.3.11)$$

$$\|\mathbf{v}_{hk}^-\|_{\mathbf{L}^2(\Omega_T)} \leq C_4 < \infty, \quad (2.3.12)$$

where the constant $C_4 > 0$ depends only on C_3 from Lemma 2.3.3, C_v from Lemma 2.2.3, and $|\Omega|$.

Proof. From Lemma 2.3.3, we get boundedness of $\|\mathbf{m}_h^j\|_{\mathbf{H}^1(\Omega)}$, and $k \sum_{i=0}^{j-1} \|\mathbf{v}_h^i\|_{\mathbf{L}^2(\Omega)}$ in each time step $j = 0, \dots, N$. First, we thus get

$$\|\mathbf{v}_{hk}^-\|_{\mathbf{L}^2(\Omega_T)}^2 = \sum_{i=0}^{N-1} \int_{t_i}^{t_{i+1}} \|\mathbf{v}_h^i\|_{\mathbf{L}^2(\Omega)}^2 = k \sum_{i=0}^{N-1} \|\mathbf{v}_h^i\|_{\mathbf{L}^2(\Omega)}^2 \leq C_3.$$

Second, we consider boundedness of the discrete magnetizations. A bound for the $\mathbf{L}^2(\Omega_T)$ part was already given in Lemma 2.2.2. We therefore consider the gradient contributions. To that end, the above boundedness of \mathbf{m}_h^j directly implies

$$\begin{aligned} \|\nabla \mathbf{m}_{hk}\|_{\mathbf{L}^2(\mathbf{L}^2)}^2 &= \sum_{i=0}^{N-1} \int_{t_i}^{t_{i+1}} \|\nabla \mathbf{m}_h^i + (t - t_i) \mathrm{d}_t \nabla \mathbf{m}_h^{i+1}\|_{\mathbf{L}^2(\Omega)}^2 \\ &\leq 2 \sum_{i=0}^{N-1} \int_{t_i}^{t_{i+1}} \|\nabla \mathbf{m}_h^i\|_{\mathbf{L}^2(\Omega)}^2 + \|\nabla \mathbf{m}_h^{i+1}\|_{\mathbf{L}^2(\Omega)}^2 \\ &= 2k \sum_{i=0}^{N-1} (\|\nabla \mathbf{m}_h^{i+1}\|_{\mathbf{L}^2(\Omega)}^2 + \|\nabla \mathbf{m}_h^i\|_{\mathbf{L}^2(\Omega)}^2) \\ &\leq 4TC_3. \end{aligned}$$

By definition of the $\mathbf{H}^1(\Omega_T)$ -norm, it only remains to investigate $\|\partial_t \mathbf{m}_{hk}\|_{\mathbf{L}^2(\Omega_T)}$. To that end, we use Lemma 2.2.3 and conclude from the definition of \mathbf{m}_{hk}

$$\begin{aligned} \|\partial_t \mathbf{m}_{hk}\|_{\mathbf{L}^2(\Omega_T)}^2 &= \int_0^T \|\partial_t \mathbf{m}_{hk}(t)\|_{\mathbf{L}^2(\Omega)}^2 = \sum_{i=0}^{N-1} \int_{t_i}^{t_{i+1}} \|\partial_t \mathbf{m}_{hk}(t)\|_{\mathbf{L}^2(\Omega)}^2 \\ &= \sum_{i=0}^{N-1} \int_{t_i}^{t_{i+1}} \left\| \frac{\mathbf{m}_h^{i+1} - \mathbf{m}_h^i}{k} \right\|_{\mathbf{L}^2(\Omega)}^2 \\ &\leq C_v^2 \sum_{i=0}^{N-1} \|\mathbf{v}_h^i\|_{\mathbf{L}^2(\Omega)}^2 \int_{t_i}^{t_{i+1}} 1 \\ &= kC_v^2 \sum_{i=0}^{N-1} \|\mathbf{v}_h^i\|_{\mathbf{L}^2(\Omega)}^2 \leq C_v^2 C_3. \end{aligned}$$

Finally, the bound for $\|\mathbf{m}_{hk}^+\|_{\mathbf{L}^2(\mathbf{H}^1)}$ and $\|\mathbf{m}_{hk}^-\|_{\mathbf{L}^2(\mathbf{H}^1)}$ follows analogously. \square

With the last result, step 1 of the proof of our main theorem is completed.

Step 2:

In this short part, we show the existence of weakly convergent subsequences of our discretizations \mathbf{m}_{hk} , \mathbf{m}_{hk}^\pm and \mathbf{v}_{hk}^- . Here, the main ingredient is an abstract compactness argument which shows mere existence of those subsequences. Therefore, we do not get any information on whether or not those sequences converge towards a useful limit at this point. However, we can already promise that this will be the case. The limit, though, still has to be formally identified with a weak solution of LLG. This will be done in step 3 below.

Lemma 2.3.5. *There exist functions $\mathbf{m} \in H^1(\Omega_T; \mathbb{S}^2)$ and $\mathbf{v} \in L^2(\Omega_T)$, as well as subsequences of \mathbf{m}_{hk} , \mathbf{m}_{hk}^\pm and \mathbf{v}_{hk}^- such that there holds*

$$\mathbf{m}_{hk} \xrightarrow{\text{sub}} \mathbf{m} \quad \text{weakly in } \mathbf{H}^1(\Omega_T) \text{ for } (h, k) \longrightarrow (0, 0), \quad (2.3.13)$$

$$\mathbf{m}_{hk}, \mathbf{m}_{hk}^\pm \xrightarrow{\text{sub}} \mathbf{m} \quad \text{weakly in } L^2(\mathbf{H}^1) \text{ for } (h, k) \longrightarrow (0, 0), \quad (2.3.14)$$

$$\mathbf{m}_{hk}, \mathbf{m}_{hk}^\pm \xrightarrow{\text{sub}} \mathbf{m} \quad \text{strongly in } \mathbf{L}^2(\Omega_T) \text{ for } (h, k) \longrightarrow (0, 0), \quad (2.3.15)$$

$$\mathbf{m}_{hk}, \mathbf{m}_{hk}^\pm \xrightarrow{\text{sub}} \mathbf{m} \quad \text{pointwise a.e. in } \Omega_T \text{ for } (h, k) \longrightarrow (0, 0), \quad (2.3.16)$$

$$\mathbf{v}_{hk}^- \xrightarrow{\text{sub}} \mathbf{v} \quad \text{weakly in } \mathbf{L}^2(\Omega_T) \text{ for } (h, k) \longrightarrow (0, 0). \quad (2.3.17)$$

In particular, there exists one subsequence (h_m, k_n) of (h, k) such that all the above limits hold simultaneously. Moreover, the limit function \mathbf{m} is continuous in time.

Proof. Since all the considered spaces are reflexive, the boundedness from Corollary 2.3.4 in combination with the theorem of Eberlein-Smulian A.2.1 proves the existence of limit functions $\mathbf{m} \in \mathbf{H}^1(\Omega_T)$, $(\tilde{\mathbf{m}}^-, \tilde{\mathbf{m}}^+) \in L^2(\mathbf{H}^1)$, and $\mathbf{v} \in \mathbf{L}^2(\Omega_T)$, as well as subsequences, such that there holds

$$\begin{aligned} \mathbf{m}_{hk} &\xrightarrow{\text{sub}} \mathbf{m} \quad \text{weakly in } \mathbf{H}^1(\Omega_T), \\ \mathbf{m}_{hk}^- &\xrightarrow{\text{sub}} \tilde{\mathbf{m}}^- \quad \text{weakly in } L^2(\mathbf{H}^1), \\ \mathbf{m}_{hk}^+ &\xrightarrow{\text{sub}} \tilde{\mathbf{m}}^+ \quad \text{weakly in } L^2(\mathbf{H}^1), \\ \mathbf{v}_{hk}^- &\xrightarrow{\text{sub}} \mathbf{v} \quad \text{weakly in } \mathbf{L}^2(\Omega_T). \end{aligned}$$

Successive extraction of those subsequences shows that there exists a subsequence of the indices (h, k) for which all limit processes hold simultaneously. Due to the Rellich-Kondrachov compactness theorem, we get the compact embedding $\mathbf{H}^1(\Omega_T) \Subset \mathbf{L}^2(\Omega_T)$ and thus the strong subconvergence

$$\mathbf{m}_{hk} \xrightarrow{\text{sub}} \mathbf{m} \quad \text{strongly in } \mathbf{L}^2(\Omega_T).$$

Uniqueness of weak limits (Lemma A.2.9) and the continuous inclusion $\mathbf{H}^1(\Omega_T) \subseteq L^2(\mathbf{H}^1)$ further shows

$$\mathbf{m}_{hk} \xrightarrow{\text{sub}} \mathbf{m} \quad \text{weakly in } L^2(\mathbf{H}^1).$$

Moreover, boundedness also proves

$$\begin{aligned} \mathbf{m}_{hk}^- &\xrightarrow{\text{sub}} \tilde{\mathbf{m}}^- \quad \text{weakly in } \mathbf{L}^2(\Omega_T) \text{ and} \\ \mathbf{m}_{hk}^+ &\xrightarrow{\text{sub}} \tilde{\mathbf{m}}^+ \quad \text{weakly in } \mathbf{L}^2(\Omega_T). \end{aligned}$$

It thus only remains to show that the limits \mathbf{m} , $\tilde{\mathbf{m}}^-$ and $\tilde{\mathbf{m}}^+$ coincide, i.e.

$$\mathbf{m} = \tilde{\mathbf{m}}^- = \tilde{\mathbf{m}}^+ \quad \text{almost everywhere in } \Omega_T.$$

To that end, Lemma 2.2.5 shows

$$\|\mathbf{m}_{hk} - \mathbf{m}_{hk}^\pm\|_{\mathbf{L}^2(\Omega_T)} \leq k^{3/2} \|\partial_t \mathbf{m}_{hk}\|_{\mathbf{L}^2(\Omega_T)} \longrightarrow 0.$$

In particular, the last statement proves subconvergence of \mathbf{m}_{hk}^\pm towards \mathbf{m} even strongly in $\mathbf{L}^2(\Omega_T)$, since

$$\|\mathbf{m}_{hk}^\pm - \mathbf{m}\|_{\mathbf{L}^2(\Omega_T)} \leq \|\mathbf{m}_{hk}^\pm - \mathbf{m}_{hk}\|_{\mathbf{L}^2(\Omega_T)} + \|\mathbf{m}_{hk} - \mathbf{m}\|_{\mathbf{L}^2(\Omega_T)} \xrightarrow{\text{sub}} 0.$$

The Weyl Lemma A.2.7 now shows the pointwise convergence (2.3.16). Finally, from

$$\| |\mathbf{m}| - 1 \|_{\mathbf{L}^2(\Omega_T)} \leq \| |\mathbf{m}| - |\mathbf{m}_{hk}^-| \|_{\mathbf{L}^2(\Omega_T)} + \| |\mathbf{m}_{hk}^-| - 1 \|_{\mathbf{L}^2(\Omega_T)}$$

and

$$\| |\mathbf{m}_{hk}^-|(t, \cdot) - 1 \|_{\mathbf{L}^2(\Omega)} \leq h \max_{t_j} \|\nabla \mathbf{m}_h^j\|_{\mathbf{L}^2(\Omega)},$$

we deduce $|\mathbf{m}| = 1$ almost everywhere in Ω_T . For the last estimate, we exploited $\mathbf{m}_h^j \in \mathcal{S}^1(\mathcal{T}_h)$. Finally, it remains to show the desired time-continuity. From $\mathbf{m} \in \mathbf{H}^1(\Omega_T)$, we deduce

$$\|\mathbf{m}\|_{H^1([0,T]; \mathbf{L}^2(\Omega))}^2 = \int_0^T (\|\mathbf{m}(t)\|_{\mathbf{L}^2(\Omega)}^2 + \|\mathbf{m}_t(t)\|_{\mathbf{L}^2(\Omega)}^2) \leq \|\mathbf{m}\|_{\mathbf{H}^1(\Omega_T)} \leq C,$$

and thus $\mathbf{m} \in H^1([0,T]; \mathbf{L}^2(\Omega))$. Exploiting [Eva02, § 5.9.2, Theorem 2], we particularly conclude $\mathbf{m} \in C([0,T]; \mathbf{L}^2(\Omega))$. \square

This concludes the proof of part (a) of Theorem 2.3.1.

Step 3:

In the remainder of this section, we aim to identify the functions \mathbf{m}, \mathbf{v} , whose existence was shown in Lemma 2.3.5, with a weak solution of LLG and its time derivative, respectively. First of all, we ignore the dependency on the LLG equation and simply show that the limit function \mathbf{v} is indeed the weak time derivative of \mathbf{m} .

Lemma 2.3.6. *The function $\mathbf{v} \in \mathbf{L}^2(\Omega_T)$ is the weak time derivative of $\mathbf{m} \in \mathbf{H}^1(\Omega_T)$, i.e. $\mathbf{v} = \partial_t \mathbf{m}$ almost everywhere on Ω_T .*

Proof. The proof was already given in [Alo08a, Gol12], and we therefore only sketch it. The elaborated arguments can be found in [Gol12, Lemma 3.3.13]. Simple geometric estimates show the inequality

$$\|\partial_t \mathbf{m}_{hk} - \mathbf{v}_{hk}^-\|_{\mathbf{L}^1(\Omega_T)} \lesssim k \|\mathbf{v}_{hk}^-\|_{\mathbf{L}^2(\Omega_T)}^2,$$

which, in combination with the weak lower semicontinuity of the norm, yields

$$\|\partial_t \mathbf{m} - \mathbf{v}\|_{\mathbf{L}^1(\Omega_T)} \leq \liminf \|\partial_t \mathbf{m}_{hk} - \mathbf{v}_{hk}^-\|_{\mathbf{L}^1(\Omega_T)} = 0, \quad \text{for } (h, k) \rightarrow (0, 0).$$

This reveals $\mathbf{v} = \partial_t \mathbf{m}$ in $\mathbf{L}^1(\Omega_T)$ and thus almost everywhere in Ω_T . \square

With the identification of \mathbf{v} with the time derivative $\partial_t \mathbf{m}$ of \mathbf{m} , reuse of the lower semicontinuity now shows boundedness of the energy.

Lemma 2.3.7. *The energy is bounded in the sense of the weak solution from Definition 2.1.1, i.e. for almost any $t' \in [0, T]$ we have*

$$\|\nabla \mathbf{m}(t')\|_{\mathbf{L}^2(\Omega)}^2 + \|\partial_t \mathbf{m}\|_{\mathbf{L}^2(\Omega_{t'})}^2 \leq C_3, \quad (2.3.18)$$

with $C_3 > 0$ from Lemma 2.3.3.

Proof. From the discrete energy estimate (2.3.7), we get for any $t' \in [0, T]$ with $t' \in [t_j, t_{j+1})$

$$\begin{aligned} \|\nabla \mathbf{m}_{hk}^+(t')\|_{\mathbf{L}^2(\Omega)}^2 + \|\mathbf{v}_{hk}^-\|_{\mathbf{L}^2(\Omega_{t'})}^2 &= \|\nabla \mathbf{m}_{hk}^+(t')\|_{\mathbf{L}^2(\Omega)}^2 + \int_0^{t'} \|\mathbf{v}_{hk}^-\|_{\mathbf{L}^2(\Omega)}^2 \\ &\leq \|\nabla \mathbf{m}_{hk}^+(t')\|_{\mathbf{L}^2(\Omega)}^2 + \int_0^{t_{j+1}} \|\mathbf{v}_{hk}^-\|_{\mathbf{L}^2(\Omega)}^2 \\ &= \|\nabla \mathbf{m}_h^{j+1}\|_{\mathbf{L}^2(\Omega)}^2 + \sum_{i=0}^j \int_{t_i}^{t_{i+1}} \|\mathbf{v}_h^i\|_{\mathbf{L}^2(\Omega)}^2 \\ &= \|\nabla \mathbf{m}_h^{j+1}\|_{\mathbf{L}^2(\Omega)}^2 + k \sum_{i=0}^j \|\mathbf{v}_h^i\|_{\mathbf{L}^2(\Omega)}^2 \\ &\leq C_3 \end{aligned}$$

Integration in time thus yields for any measurable set $\mathfrak{T} \subseteq [0, T]$

$$\int_{\mathfrak{T}} \|\nabla \mathbf{m}_{hk}^+(t')\|_{\mathbf{L}^2(\Omega)}^2 + \int_{\mathfrak{T}} \|\mathbf{v}_{hk}^-\|_{\mathbf{L}^2(\Omega_{t'})}^2 \leq \int_{\mathfrak{T}} C_3.$$

Finally, by use of weak lower semicontinuity, we deduce

$$\int_{\mathfrak{T}} \|\nabla \mathbf{m}(t')\|_{\mathbf{L}^2(\Omega)}^2 + \int_{\mathfrak{T}} \|\partial_t \mathbf{m}\|_{\mathbf{L}^2(\Omega_{t'})}^2 \leq \int_{\mathfrak{T}} C_3.$$

Note that we can pass to the limit also on the (potentially small) time set \mathfrak{T} , since $\mathbf{L}^2(\Omega_{\mathfrak{T}})$ can always be bounded from above by $\mathbf{L}^2(\Omega_T)$. Since the above inequality is true for any measurable set $\mathfrak{T} \subseteq [0, T]$, the desired result follows from standard measure theory, see e.g. [Els11, Section IV, Theorem 4.4]. \square

Before completing the proof, we need two somewhat technical lemmata. The first one deals with nodal interpolation estimates which arise due to usage of discrete test functions. The second one considers the limit process of some concrete terms which are treated separately for sake of readability. Let us first recall the definition of the piecewise constant in time approximation of a given smooth function.

For $\Psi \in \mathcal{C}^\infty(\overline{\Omega_T})$, let Ψ_k^- be defined by

$$\Psi_k^-(t, \mathbf{x}) := \Psi(t_j, \mathbf{x}) \quad \text{for } t \in [t_j, t_{j+1}). \quad (2.3.19)$$

Then, we have the following statement:

Lemma 2.3.8. *There holds the estimate*

$$\begin{aligned}
 & \int_0^T (\alpha \mathbf{v}_{hk}^- + \mathbf{m}_{hk}^- \times \mathbf{v}_{hk}^-, (\mathcal{I}_h - 1)(\mathbf{m}_{hk}^- \times \Psi_k^-)) + C_e \theta k \int_0^T (\nabla \mathbf{v}_{hk}^-, \nabla (\mathcal{I}_h - 1)(\mathbf{m}_{hk}^- \times \Psi_k^-)) \\
 & + C_e \int_0^T (\nabla \mathbf{m}_{hk}^-, \nabla (\mathcal{I}_h - 1)(\mathbf{m}_{hk}^- \times \Psi_k^-)) \\
 & - C_1 \int_0^T (\pi_h(\mathbf{m}_{hk}^-), (\mathcal{I}_h - 1)(\mathbf{m}_{hk}^- \times \Psi_k^-)) \\
 & - C_2 k \sum_{j=0}^{n-1} \int_{\Omega} \chi(\mathbf{m}_{hk})(t_j) \cdot (\mathcal{I}_h - 1)((\mathbf{m}_{hk}^- \times \Psi)(t_j)) \\
 & = \mathcal{O}(h)
 \end{aligned} \tag{2.3.20}$$

for any $\Psi \in C^\infty(\overline{\Omega_T})$.

Proof. The proof follows the lines of [Alo08a] and [Gol12, Lemma 3.3.16]. From the approximation theorem [Bra07, Theorem 6.4], we get

$$\begin{aligned}
 & \|\mathbf{m}_{hk}^-(t, \cdot) \times \Psi_k^-(t, \cdot) - \mathcal{I}_h(\mathbf{m}_{hk}^-(t, \cdot) \times \Psi_k^-(t, \cdot))\|_{\mathbf{H}^1(K)}^2 \\
 & \lesssim h^2 \|D^2(\mathbf{m}_{hk}^-(t, \cdot) \times \Psi_k^-(t, \cdot))\|_{\mathbf{L}^2(K)}^2 \\
 & \lesssim h^2 \|\mathbf{m}_{hk}^-(t, \cdot)\|_{\mathbf{H}^1(K)}^2 \|\Psi_k^-(t, \cdot)\|_{\mathbf{W}^{2,\infty}(K)}^2 \\
 & = h^2 \|\mathbf{m}_{hk}^-(t, \cdot)\|_{\mathbf{H}^1(K)}^2 \|\Psi(t_j, \cdot)\|_{\mathbf{W}^{2,\infty}(K)}^2 \\
 & \lesssim h^2 \|\mathbf{m}_{hk}^-(t, \cdot)\|_{\mathbf{H}^1(K)}^2 \|\Psi\|_{\mathbf{W}^{2,\infty}([0,T] \times K)}^2,
 \end{aligned}$$

for any $K \in \mathcal{T}_h(\Omega)$. Here, we have used that \mathbf{m}_{hk}^- is an affine function on each element $K \in \mathcal{T}_h(\Omega)$. Summation over all elements and integration in time thus leads to

$$\|\mathbf{m}_{hk}^- \times \Psi_k^- - \mathcal{I}_h(\mathbf{m}_{hk}^- \times \Psi_k^-)\|_{L^2(\mathbf{H}^1)} \lesssim h \|\mathbf{m}_{hk}^-\|_{L^2(\mathbf{H}^1)} \|\Psi\|_{\mathbf{W}^{2,\infty}(\Omega_T)}.$$

Using this statement, we see

$$\begin{aligned}
 & (\alpha \mathbf{v}_{hk}^- + \mathbf{m}_{hk}^- \times \mathbf{v}_{hk}^-, (\mathcal{I}_h - 1)(\mathbf{m}_{hk}^- \times \Psi_k^-)) \\
 & \leq \alpha \|\mathbf{v}_{hk}^- + \mathbf{m}_{hk}^- \times \mathbf{v}_{hk}^-\|_{L^2(\Omega_T)} \|(\mathcal{I}_h - 1)(\mathbf{m}_{hk}^- \times \Psi_k^-)\|_{L^2(\Omega_T)} \\
 & = \mathcal{O}(h),
 \end{aligned}$$

$$\begin{aligned}
 & k(\nabla \mathbf{v}_{hk}^-, \nabla (\mathcal{I}_h - 1)(\mathbf{m}_{hk}^- \times \Psi_k^-)) \\
 & \leq \|k \nabla \mathbf{v}_{hk}^-\|_{L^2(\Omega_T)} \|(\mathcal{I}_h - 1)(\mathbf{m}_{hk}^- \times \Psi_k^-)\|_{L^2(\mathbf{H}^1)} \\
 & = \mathcal{O}(h), \quad \text{and}
 \end{aligned}$$

$$(\nabla \mathbf{m}_{hk}^-, \nabla (\mathcal{I}_h - 1)(\mathbf{m}_{hk}^- \times \Psi_k^-)) = \mathcal{O}(h),$$

where we have used the boundedness of $k \|\nabla \mathbf{v}_{hk}^-\|_{L^2(\Omega_T)}$ from Lemma 2.3.3 for $\theta \in (1/2, 1]$ in the second estimate. Using the boundedness of the general contributions from assumption (2.3.2), we deduce

$$(\pi_h(\mathbf{m}_{hk}^-), (\mathcal{I}_h - 1)(\mathbf{m}_{hk}^- \times \Psi_k^-)) = \mathcal{O}(h),$$

as well as

$$\begin{aligned}
 & k \sum_{j=0}^{N-1} \langle \chi(\mathbf{m}_{hk})(t_j), (\mathcal{I}_h - 1)((\mathbf{m}_{hk}^- \times \Psi)(t_j)) \rangle \\
 & \lesssim k \sum_{j=0}^{N-1} \|(\mathcal{I}_h - 1)((\mathbf{m}_{hk}^- \times \Psi)(t_j))\|_{\mathbf{L}^2(\Omega)} \\
 & \leq hk \sum_{j=0}^{N-1} \|\mathbf{m}_h^j\|_{\mathbf{H}^1(\Omega)} \|\Psi\|_{\mathbf{W}^{2,\infty}(\Omega_T)} \\
 & \lesssim h \|\Psi\|_{\mathbf{W}^{2,\infty}(\Omega_T)} k \sum_{j=0}^{N-1} 1 \\
 & \lesssim h \|\Psi\|_{\mathbf{W}^{2,\infty}(\Omega_T)} \\
 & = \mathcal{O}(h).
 \end{aligned}$$

The combination of the above results concludes the proof. \square

In order to ease the presentation as well as the readability of the convergence proof, we consider the following limits separately:

Lemma 2.3.9. *There holds*

$$\alpha(\mathbf{v}_{hk}^- + \mathbf{m}_{hk}^- \times \mathbf{v}_{hk}^-, \mathbf{m}_{hk}^- \times \Psi_k^-) \xrightarrow{\text{sub}} \alpha(\mathbf{m}_t + \mathbf{m} \times \mathbf{m}_t, \mathbf{m} \times \Psi) \quad (2.3.21)$$

$$C_e \theta k (\nabla \mathbf{v}_{hk}^-, \nabla(\mathbf{m}_{hk}^- \times \Psi_k^-)) \xrightarrow{\text{sub}} 0 \quad \text{and} \quad (2.3.22)$$

$$C_e (\nabla \mathbf{m}_{hk}^-, \nabla(\mathbf{m}_{hk}^- \times \Psi_k^-)) \xrightarrow{\text{sub}} C_e (\nabla \mathbf{m}, \nabla(\mathbf{m} \times \Psi)), \quad (2.3.23)$$

for $(h, k) \rightarrow (0, 0)$. Moreover, there holds

$$\mathbf{m}_{hk}^- \times \Psi_k^- \xrightarrow{\text{sub}} \mathbf{m} \times \Psi \quad (2.3.24)$$

strongly in $\mathbf{L}^2(\Omega_T)$ as $(h, k) \rightarrow (0, 0)$.

Proof. The proof is done in analogously to [Alo08a] and [Gol12, Lemma 3.3.17–3.3.19]. The only difference is that, in our case, we also have to deal with a piecewise constant approximation of Ψ in time. We therefore only have to show

$$\begin{aligned}
 & \mathbf{m}_{hk}^- \times \Psi_k^- \xrightarrow{\text{sub}} \mathbf{m} \times \Psi \quad \text{strongly in } \mathbf{L}^2(\Omega_T) \text{ and} \\
 & \nabla(\mathbf{m}_{hk}^- \times \Psi_k^-) \xrightarrow{\text{sub}} \mathbf{m} \times \nabla \Psi \quad \text{strongly in } \mathbf{L}^2(\Omega_T).
 \end{aligned}$$

Let us now consider those convergence properties individually. From Lemma 2.3.5, we already know the pointwise convergence of \mathbf{m}_{hk}^- towards \mathbf{m} almost everywhere in Ω_T . Moreover, from the continuity of Ψ and the compactness of $\overline{\Omega_T}$, we conclude that Ψ is even uniformly continuous on $\overline{\Omega_T}$. Now let $\varepsilon > 0$ be arbitrary and let $\delta = \delta(\varepsilon)$ be the parameter of uniform continuity, i.e.

$$\forall (t_1, \mathbf{x}_1), (t_2, \mathbf{x}_2) \in \Omega_T : \quad |(t_1, \mathbf{x}_1) - (t_2, \mathbf{x}_2)| \leq \delta \implies |\Psi(t_1, \mathbf{x}_1) - \Psi(t_2, \mathbf{x}_2)| \leq \varepsilon.$$

By definition this yields for $k \leq \delta$ and $t \in [t_j, t_{j+1})$

$$|\Psi_k^-(t, \mathbf{x}) - \Psi(t, \mathbf{x})| = |\Psi(t_j, \mathbf{x}) - \Psi(t, \mathbf{x})| \leq \varepsilon,$$

whence the pointwise convergence of Ψ_k^- to Ψ . By definition, we thus get $(\mathbf{m}_{hk}^- \times \Psi_k^-) \xrightarrow{\text{sub}} (\mathbf{m} \times \Psi)$ pointwise almost everywhere in Ω_T . Due to the boundedness

$$|\mathbf{m}_{hk}^-(t, \mathbf{x}) \times \Psi_k^-(t, \mathbf{x})| \leq \|\mathbf{m}_{hk}^-\|_{\mathbf{L}^\infty(\Omega_T)} \|\Psi\|_{\mathbf{L}^\infty(\Omega_T)} = \|\Psi\|_{\mathbf{L}^\infty(\Omega_T)},$$

the Lebesgue dominated convergence theorem A.2.3 yields $(\mathbf{m}_{hk}^- \times \Psi_k^-) \xrightarrow{\text{sub}} (\mathbf{m} \times \Psi)$ even strongly in $\mathbf{L}^2(\Omega_T)$ whence (2.3.24). For the other convergence properties, we exploit the result of Lemma A.1.6 to see

$$\begin{aligned} (\nabla \mathbf{v}_{hk}^-, \nabla(\mathbf{m}_{hk}^- \times \Psi_k^-)) &= (\nabla \mathbf{v}_{hk}^-, \mathbf{m}_{hk}^- \times \nabla \Psi_k^-), \quad \text{as well as} \\ (\nabla \mathbf{m}_{hk}^-, \nabla(\mathbf{m}_{hk}^- \times \Psi_k^-)) &= (\nabla \mathbf{m}_{hk}^-, \mathbf{m}_{hk}^- \times \nabla \Psi_k^-). \end{aligned}$$

From the above elaborations, we already know the pointwise convergence of \mathbf{m}_{hk}^- . It thus remains to show pointwise convergence of $\nabla \Psi_k^-$ to $\nabla \Psi$ almost everywhere in Ω_T . Since Ψ is smooth, we also get uniform continuity of $\nabla \Psi$, where we again denote the continuity parameter by $\delta = \delta(\varepsilon)$ for any $\varepsilon > 0$. Use of Lemma A.2.12 now allows us to interchange the spatial gradient with the time evaluation of Ψ , and for $k \leq \delta$ and $t \in [t_j, t_{j+1})$ shows

$$\begin{aligned} |(\nabla \Psi_k^-)(t, \mathbf{x}) - (\nabla \Psi)(t, \mathbf{x})| &= |(\nabla \Psi_k^-(t))(\mathbf{x}) - (\nabla \Psi)(t, \mathbf{x})| \\ &= |(\nabla \Psi(t_j))(\mathbf{x}) - (\nabla \Psi)(t, \mathbf{x})| \\ &= |(\nabla \Psi)(t_j, \mathbf{x}) - (\nabla \Psi)(t, \mathbf{x})| \leq \varepsilon. \end{aligned}$$

We therefore conclude pointwise convergence of $\nabla \Psi_k^-$ to $\nabla \Psi$ almost everywhere in Ω_T . Analogously to [Gol12, Lemma 3.3.17–3.3.19], we conclude the proof. \square

We are now ready to conclude the proof of part **(b)** of the main theorem from this section, i.e. we identify the function $\mathbf{m} \in \mathbf{H}^1(\Omega_T)$ with a weak solution of the general LLG equation.

Proof of part (b) of Theorem 2.3.1. We choose any function $\Psi \in C^\infty(\overline{\Omega_T})$ and in (2.2.3) test with $\varphi_h^j := \mathcal{I}_h((\mathbf{m}_{hk}^- \times \Psi)(t_j)) \in \mathcal{K}_{\mathbf{m}_h^j}$. Note that by definition of \mathbf{m}_{hk}^- and $\mathcal{K}_{\mathbf{m}_h^j}$, we have $\varphi_h^j \in \mathcal{K}_{\mathbf{m}_h^j}$. Plugging into our Algorithm 2.2.1 now yields

$$\begin{aligned} \alpha \int_{\Omega} \mathbf{v}_h^j \cdot \mathcal{I}_h((\mathbf{m}_{hk}^- \times \Psi)(t_j)) &+ \int_{\Omega} (\mathbf{m}_h^j \times \mathbf{v}_h^j) \cdot \mathcal{I}_h(\mathbf{m}_{hk}^- \times \Psi)(t_j) \\ &= -C_e \int_{\Omega} \nabla(\mathbf{m}_h^j + \theta k \mathbf{v}_h^j) \cdot \nabla \mathcal{I}_h((\mathbf{m}_{hk}^- \times \Psi)(t_j)) \\ &\quad + C_1 \int_{\Omega} \pi_h(\mathbf{m}_h^j) \cdot \mathcal{I}_h((\mathbf{m}_{hk}^- \times \Psi)(t_j)) \\ &\quad + C_2 \int_{\Omega} \chi(\mathbf{m}_{hk})(t_j) \cdot \mathcal{I}_h((\mathbf{m}_{hk}^- \times \Psi)(t_j)). \end{aligned}$$

Next, multiplication by k and summation over all time intervals $j = 0, \dots, N-1$ show

$$\begin{aligned}
 & \int_{\Omega_T} (\alpha \mathbf{v}_{hk}^- + \mathbf{m}_{hk}^- \times \mathbf{v}_{hk}^-) \cdot \mathcal{I}_h(\mathbf{m}_{hk}^- \times \Psi_k^-) \\
 &= -C_e \int_{\Omega_T} \nabla(\mathbf{m}_{hk}^- + \theta k \mathbf{v}_{hk}^-) \cdot \nabla \mathcal{I}_h(\mathbf{m}_{hk}^- \times \Psi_k^-) \\
 &+ C_1 \int_{\Omega_T} \pi_h(\mathbf{m}_{hk}^-) \cdot \mathcal{I}_h(\mathbf{m}_{hk}^- \times \Psi_k^-) \\
 &+ C_2 k \sum_{j=0}^{N-1} \int_{\Omega} \chi(\mathbf{m}_{hk})(t_j) \cdot \mathcal{I}_h((\mathbf{m}_{hk}^- \times \Psi)(t_j)).
 \end{aligned} \tag{2.3.25}$$

For the term on the left-hand side, this equality can be seen as follows:

$$\begin{aligned}
 & k \sum_{j=0}^{N-1} \left(\mathbf{v}_h^j + \mathbf{m}_h^j \times \mathbf{v}_h^j, \mathcal{I}_h((\mathbf{m}_{hk}^- \times \Psi)(t_j)) \right) \\
 &= \sum_{j=0}^{N-1} \int_{t_j}^{t_{j+1}} \left(\mathbf{v}_h^j + \mathbf{m}_h^j \times \mathbf{v}_h^j, \mathcal{I}_h((\mathbf{m}_{hk}^- \times \Psi)(t_j)) \right) \\
 &= \sum_{j=0}^{N-1} \int_{t_j}^{t_{j+1}} \left(\mathbf{v}_{hk}^-(t) + \mathbf{m}_{hk}^-(t) \times \mathbf{v}_{hk}^-(t), \mathcal{I}_h((\mathbf{m}_{hk}^- \times \Psi_k^-)(t)) \right) \\
 &= \int_0^T (\mathbf{v}_{hk}^- + \mathbf{m}_{hk}^- \times \mathbf{v}_{hk}^-, \mathcal{I}_h(\mathbf{m}_{hk}^- \times \Psi_k^-)).
 \end{aligned}$$

The other time-independent terms, in particular nonlinear ones, can be treated analogously.

Next, we rewrite (2.3.25) as

$$\begin{aligned}
 0 &= \int_{\Omega_T} (\alpha \mathbf{v}_{hk}^- + \mathbf{m}_{hk}^- \times \mathbf{v}_{hk}^-) \cdot \mathcal{I}_h(\mathbf{m}_{hk}^- \times \Psi_k^-) + C_e \int_{\Omega_T} \nabla(\mathbf{m}_{hk}^- + \theta k \mathbf{v}_{hk}^-) \cdot \nabla \mathcal{I}_h(\mathbf{m}_{hk}^- \times \Psi_k^-) \\
 &- C_1 \int_{\Omega_T} \pi_h(\mathbf{m}_{hk}^-) \cdot \mathcal{I}_h(\mathbf{m}_{hk}^- \times \Psi_k^-) - C_2 k \sum_{j=0}^{N-1} \int_{\Omega} \chi(\mathbf{m}_{hk})(t_j) \cdot \mathcal{I}_h((\mathbf{m}_{hk}^- \times \Psi)(t_j)) \\
 &= \int_{\Omega_T} (\alpha \mathbf{v}_{hk}^- + \mathbf{m}_{hk}^- \times \mathbf{v}_{hk}^-) \cdot (\mathcal{I}_h - 1)(\mathbf{m}_{hk}^- \times \Psi_k^-) + C_e \int_{\Omega_T} \nabla(\mathbf{m}_{hk}^- + \theta k \mathbf{v}_{hk}^-) \cdot \nabla (\mathcal{I}_h - 1)(\mathbf{m}_{hk}^- \times \Psi_k^-) \\
 &- C_1 \int_{\Omega_T} \pi_h(\mathbf{m}_{hk}^-) \cdot (\mathcal{I}_h - 1)(\mathbf{m}_{hk}^- \times \Psi_k^-) - C_2 k \sum_{j=0}^{N-1} \int_{\Omega} \chi(\mathbf{m}_{hk})(t_j) \cdot (\mathcal{I}_h - 1)((\mathbf{m}_{hk}^- \times \Psi)(t_j)) \\
 &+ \int_{\Omega_T} (\alpha \mathbf{v}_{hk}^- + \mathbf{m}_{hk}^- \times \mathbf{v}_{hk}^-) \cdot (\mathbf{m}_{hk}^- \times \Psi_k^-) + C_e \int_{\Omega_T} \nabla(\mathbf{m}_{hk}^- + \theta k \mathbf{v}_{hk}^-) \cdot \nabla(\mathbf{m}_{hk}^- \times \Psi_k^-) \\
 &- C_1 \int_{\Omega_T} \pi_h(\mathbf{m}_{hk}^-) \cdot (\mathbf{m}_{hk}^- \times \Psi_k^-) - C_2 k \sum_{j=0}^{N-1} \int_{\Omega} \chi(\mathbf{m}_{hk})(t_j) \cdot ((\mathbf{m}_{hk}^- \times \Psi)(t_j)) \\
 &= \mathcal{O}(h) + \int_{\Omega_T} (\alpha \mathbf{v}_{hk}^- + \mathbf{m}_{hk}^- \times \mathbf{v}_{hk}^-) \cdot (\mathbf{m}_{hk}^- \times \Psi_k^-) + C_e \int_{\Omega_T} \nabla(\mathbf{m}_{hk}^- + \theta k \mathbf{v}_{hk}^-) \cdot \nabla(\mathbf{m}_{hk}^- \times \Psi_k^-) \\
 &- C_1 \int_{\Omega_T} \pi_h(\mathbf{m}_{hk}^-) \cdot (\mathbf{m}_{hk}^- \times \Psi_k^-) - C_2 k \sum_{j=0}^{N-1} \int_{\Omega} \chi(\mathbf{m}_{hk})(t_j) \cdot ((\mathbf{m}_{hk}^- \times \Psi)(t_j)),
 \end{aligned}$$

where we have used Lemma 2.3.8 for the last step. Passing to the limit while using the convergence properties from Lemma 2.3.9, strong subconvergence (2.3.24), as well as the convergence assumption (2.3.4) for the general field contributions, we see

$$\begin{aligned} \alpha \int_{\Omega_T} \mathbf{m}_t \cdot (\mathbf{m} \times \Psi) + \int_{\Omega_T} (\mathbf{m} \times \mathbf{m}_t) \cdot (\mathbf{m} \times \Psi) &= -C_e \int_{\Omega_T} \nabla \mathbf{m} \cdot \nabla (\mathbf{m} \times \Psi) \\ &+ C_1 \int_{\Omega_T} \boldsymbol{\pi}(\mathbf{m}) \cdot (\mathbf{m} \times \Psi) \\ &+ C_2 \int_{\Omega_T} \boldsymbol{\chi}(\mathbf{m}) \cdot (\mathbf{m} \times \Psi). \end{aligned}$$

Technical but elementary calculations (see e.g. [Gol12, Proof of Thm. 3.3.7]) show the identities

$$\begin{aligned} (\mathbf{m} \times \mathbf{m}_t) \cdot (\mathbf{m} \times \Psi) &= \mathbf{m}_t \cdot \Psi \quad \text{and} \\ \mathbf{m}_t \cdot (\mathbf{m} \times \Psi) &= -(\mathbf{m} \times \mathbf{m}_t) \cdot \Psi \end{aligned}$$

whence

$$\begin{aligned} \int_{\Omega_T} \mathbf{m}_t \cdot \Psi - \alpha \int_{\Omega_T} (\mathbf{m} \times \mathbf{m}_t) \cdot \Psi &= -C_e \int_{\Omega_T} \nabla \mathbf{m} \cdot \nabla (\mathbf{m} \times \Psi) \\ &+ C_1 \int_{\Omega_T} \boldsymbol{\pi}(\mathbf{m}) \cdot (\mathbf{m} \times \Psi) \\ &+ C_2 \int_{\Omega_T} \boldsymbol{\chi}(\mathbf{m}) \cdot (\mathbf{m} \times \Psi). \end{aligned}$$

Exploiting the identities

$$\begin{aligned} \mathbf{a} \cdot (\mathbf{b} \times \mathbf{c}) &= (\mathbf{a} \times \mathbf{b}) \cdot \mathbf{c} \quad \text{and} \\ \int_{\Omega_T} \nabla \mathbf{m} \cdot \nabla (\mathbf{m} \times \Psi) &= \int_{\Omega_T} \nabla \mathbf{m} \cdot (\mathbf{m} \times \nabla \Psi) \end{aligned}$$

for any $\mathbf{a}, \mathbf{b}, \mathbf{c} \in \mathbb{R}^3$, cf. Lemma A.1.6–A.1.7, we deduce (2.1.2). The energy estimate was already shown in Lemma 2.3.7. Finally, it remains to show $\mathbf{m}(0, \cdot) = \mathbf{m}^0$ in the sense of traces. This, however, follows from the weak convergence $\mathbf{m}_{hk} \xrightarrow{\text{sub}} \mathbf{m}$ in $\mathbf{H}^1(\Omega_T)$ and hence the weak convergence of the traces. Here, due to continuity in time (Lemma 2.3.5), the lower trace of \mathbf{m}_{hk} and \mathbf{m} , respectively, is simply given by the evaluation at $t = 0$, i.e. we get

$$\begin{array}{ccc} \mathbf{m}_{hk}(0, \cdot) & \xrightarrow{\text{trace theorem}} & \mathbf{m}(0, \cdot) \\ \text{definition} \parallel & & \parallel \heartsuit \\ \mathbf{m}_h^0 & \xrightarrow{\text{assumption (2.3.3)}} & \mathbf{m}^0(\cdot) \end{array}$$

From the assumed convergence property $\mathbf{m}_h^0 \rightharpoonup \mathbf{m}^0$ in $\mathbf{H}^1(\Omega)$ and the uniqueness of weak limits, we conclude the equality \heartsuit and thus the desired result. \square

In the remaining part of this chapter, we further investigate the time-dependent energy contribution $\boldsymbol{\chi}(\cdot)$. In (2.3.30)–(2.3.31), we propose two verifiable conditions that are sufficient to prove convergence of the sum in (2.3.4). A special case, in which the analysis simplifies, is considered individually.

2.3.1. Time-dependent energy contributions

We now investigate the time-dependent field contribution and take a closer look at the desired convergence property

$$k \sum_{j=0}^{N-1} \int_{\Omega} \chi_h(\mathbf{m}_{hk})(t_j) \cdot ((\mathbf{m}_{hk}^- \times \Psi)(t_j)) \xrightarrow{\text{sub}} \int_{\Omega_T} \chi(\mathbf{m}) \cdot (\mathbf{m} \times \Psi), \quad (2.3.26)$$

which is very much needed in the above convergence analysis. We start with a simple case where we assume additional apriori knowledge..

Time-dependent but a priori convergent contributions

The main problem with time-dependent contributions is that the above sum can a priori not be written as time integral over $\chi(\mathbf{m}_{hk}^-)$. It is, however, still possible to approximate the whole operator $\chi(\cdot)$ piecewise constant in time and thus deduce a representation of the form

$$k \sum_{j=0}^{n-1} \int_{\Omega} \chi(\mathbf{m}_{hk})(t_j) \cdot ((\mathbf{m}_{hk}^- \times \Psi)(t_j)) = \int_{\Omega_T} \chi_{hk}^- \cdot (\mathbf{m}_{hk}^- \times \Psi_k^-), \quad (2.3.27)$$

with $\chi_{hk}^-(t) := \chi(\mathbf{m}_{hk})(t_j)$ for $t \in [t_j, t_{j+1})$. For now, let us assume that we even have some weak convergence property for this approximation, i.e.

$$\chi_{hk}^- \xrightarrow{\text{sub}} \chi(\mathbf{m}) \quad \text{weakly in } \mathbf{L}^1(\Omega_T). \quad (2.3.28)$$

In this case, from the strong convergence

$$(\mathbf{m}_{hk}^- \times \Psi_k^-) \xrightarrow{\text{sub}} (\mathbf{m} \times \Psi),$$

we immediately get

$$\int_{\Omega_T} \chi_{hk}^- \cdot (\mathbf{m}_{hk}^- \times \Psi_k^-) \xrightarrow{\text{sub}} \int_{\Omega_T} \chi(\mathbf{m}) \cdot (\mathbf{m} \times \Psi) \quad (2.3.29)$$

from Lemma A.2.10.

In this case, the weak convergence property refers to the weak convergence of the approximation of the entire operator χ as opposed to the time-independent case, where we only needed the application of the operator π to the weakly convergent subsequence. It may thus be quite difficult to derive such a convergence property, which is the main reason for the analysis in the next section. This case is, however, still relevant as one can see, for example, by considering the approximation of a continuous external field $\chi \in \mathcal{C}(\overline{\Omega_T})$. In this case, χ_{hk}^- is, independently of \mathbf{m}_{hk} , given by the time evaluation $\chi_{hk}^-(t) = \chi(t_j)$ for $t \in [t_j, t_{j+1})$ and we have that χ_{hk}^- converges towards χ even strongly in $\mathbf{L}^2(\Omega_T)$. This can be seen as follows: As in the proof of Lemma 2.3.9, from uniform continuity we immediately see that $\chi_{hk}^- \rightarrow \chi$ even pointwise and almost everywhere. Lebesgue's dominated convergence Theorem A.2.3 would now directly show the desired convergence.

For sake of motivation, however, we choose a different approach here. From [Els11, VI, Theorem 5.9] and the pointwise convergence, we deduce $\chi_{hk}^- \rightharpoonup \chi$ weakly in $\mathbf{L}^2(\Omega_T)$. Moreover,

from the continuity of $\|\chi\|_{\mathbf{L}^2(\Omega)}$ (and thus Riemann integrability) in time, we see

$$\|\chi_{hk}^-\|_{\mathbf{L}^2(\Omega_T)}^2 = \sum_{i=0}^{N-1} \int_{t_i}^{t_{i+1}} \|\chi(t_i)\|_{\mathbf{L}^2(\Omega)}^2 = k \sum_{i=0}^{N-1} \|\chi(t_i)\|_{\mathbf{L}^2(\Omega)}^2 \longrightarrow \int_0^T \|\chi(t)\|_{\mathbf{L}^2(\Omega)}^2 = \|\chi\|_{\mathbf{L}^2(\Omega_T)}^2.$$

The combination of weak convergence and convergence of the norms in \mathbb{R} yield the convergence $\chi_{hk}^- \longrightarrow \chi$ even strongly in $\mathbf{L}^2(\Omega_T)$. It turns out that the Riemann sum approach, while it may be unexpected in the first place, carries quite far. In the following, we will pick up on this idea and extend it to cover more general cases.

If we know even less ...

As we have seen in the last section, weak $\mathbf{L}^1(\Omega_T)$ resp. $\mathbf{L}^2(\Omega_T)$ convergence is not obvious for time-dependent operators. One approach that was chosen above is considering a corresponding Riemann sum. In this section, we allow more general operators and extend the Riemann sum concept in two ways. First, we drop the assumption $\chi_{hk} \rightharpoonup \chi$ of weak convergence. Second, we allow operators that change with h and k inside our Riemann-type sum. Those two changes make the convergence analysis much more complicated. We will, however, still derive unconditional convergence and can thus treat very general field contributions within our LLG integrator. In this section, we therefore finally investigate the limiting process

$$k \sum_{j=0}^{n-1} \int_{\Omega} \chi(\mathbf{m}_{hk})(t_j) \cdot ((\mathbf{m}_{hk}^- \times \Psi)(t_j)) \xrightarrow{\text{sub}} \int_{\Omega_T} \chi(\mathbf{m}) \cdot (\mathbf{m} \times \Psi)$$

for completely general field contributions. In particular, we allow contributions χ which do not only depend on \mathbf{m}_h^j at a certain time t_j , but rather on the whole evolution \mathbf{m}_{hk} up to t_j . As promised, the upcoming analysis will lead to unconditional convergence of our integrator as $(h, k) \rightarrow (0, 0)$. Some technical details, however, require separate consideration of the h - and k -limit. Besides the necessity that arises due to the proof, this approach is very interesting, as for fixed $h > 0$, it yields existence of a function $\mathbf{m}_h \in \mathbf{L}^2(\Omega_T)$ with $\mathbf{m}_{hk} \xrightarrow{\text{sub}} \mathbf{m}_h$ in $\mathbf{L}^2(\Omega_T)$ and even uniformly in time. Using this ansatz, we thus gain additional information about our numerical integrator that goes way beyond the simple fact that it is convergent.

Obviously, it is impossible to show convergence for fully arbitrary operators. Therefore, we assume the following two conditions to be fulfilled by the contributions χ . Those assumptions will prove to be sufficient for the desired property (2.3.26).

$$\chi(\mathbf{m}_h) \xrightarrow{\text{sub}} \chi(\mathbf{m}) \quad \text{weakly in } \mathbf{L}^1(\Omega_T) \quad \text{and} \quad (2.3.30)$$

$$\begin{aligned} \|\chi(\mathbf{m}_{hk})(t) - \chi(\mathbf{m}_h)(t)\|_{\mathbf{L}^2(\Omega)}^2 &\lesssim \|\mathbf{m}_{hk}(t) - \mathbf{m}_h(t)\|_{\mathbf{L}^2(\Omega)}^2 \\ &\quad + \|\mathbf{m}_{hk} - \mathbf{m}_h\|_{\mathbf{L}^2(\Omega_T)}^2 + \|\mathbf{m}_{hk}^- - \mathbf{m}_h\|_{\mathbf{L}^2(\Omega_T)}^2 \\ &\quad + \|\mathbf{m}_{hk}^+ - \mathbf{m}_h\|_{\mathbf{L}^2(\Omega_T)}^2, \end{aligned} \quad (2.3.31)$$

where $\mathbf{m}_h \in \mathbf{L}^2(\Omega_T)$ denotes the k -limit of \mathbf{m}_{hk} . While existence of this function formally still has to be shown, we can already assure that it does exist. Moreover, we will also see, that \mathbf{m}_h is continuous with respect to time. We like to emphasize that time-continuity of \mathbf{m}_{hk} and \mathbf{m}_h and the assumption on χ guarantee that the time evaluation in (2.3.31) is well-defined.

Remark . At first glance, the above conditions (2.3.30)–(2.3.31) seem to be equally strong as in the previous section. We stress, however, that in this case, we only need convergence properties of the operator χ applied to the discrete magnetizations. In this section, we thus completely circumvent the approximation of the operator itself. More precisely, there holds $\chi(\mathbf{m}_{hk}) \neq \chi_{hk}$.

In the following, we will show that there indeed exists a function $\mathbf{m}_h \in \mathbf{L}^2(\Omega_T)$ such that \mathbf{m}_{hk} , and even \mathbf{m}_{hk}^\pm , admit strongly convergent subsequences with

$$\begin{aligned} \mathbf{m}_{hk} &\xrightarrow{\text{sub}} \mathbf{m}_h \text{ strongly in } \mathbf{L}^2(\Omega_T), \\ \mathbf{m}_{hk}^- &\xrightarrow{\text{sub}} \mathbf{m}_h \text{ strongly in } \mathbf{L}^2(\Omega_T), \text{ and} \\ \mathbf{m}_{hk}^+ &\xrightarrow{\text{sub}} \mathbf{m}_h \text{ strongly in } \mathbf{L}^2(\Omega_T), \end{aligned} \tag{2.3.32}$$

as $k \rightarrow 0$. In particular, this limit process is even uniformly in time. The main argument will be the application of the Arzela-Ascoli theorem which basically classifies compact sets within the continuous functions. First we need a technical lemma.

Lemma 2.3.10. *Let $h > 0$ be fixed and $\alpha > 0$. Then, the set $\{\|\mathbf{v}_h^j\|_{\mathbf{L}^2(\Omega)}\}_j$ is uniformly bounded as $k \rightarrow 0$, i.e.*

$$\sup_{k>0} \|\mathbf{v}_h^j\|_{\mathbf{L}^2(\Omega)} \leq C_5(h) < \infty,$$

where $C_5(h) > 0$ depends only on C_π and C_χ from (2.3.2), $\alpha > 0$, the current mesh-width $h > 0$, as well as the shape regularity constant $\sigma(\mathcal{T}_h) > 0$. In particular, $C_5(h)$ is independent of k .

Proof. From (2.3.8), we immediately get

$$\begin{aligned} \alpha \int_{\Omega} |\mathbf{v}_h^j|^2 &\leq -C_e \int_{\Omega} \nabla \mathbf{m}_h^j \cdot \nabla \mathbf{v}_h^j \\ &\quad + C_1 \int_{\Omega} \pi_h(\mathbf{m}_h^j) \cdot \mathbf{v}_h^j \\ &\quad + C_2 \int_{\Omega} \chi(\mathbf{m}_{hk})(t_j) \cdot \mathbf{v}_h^j \end{aligned}$$

whence

$$\begin{aligned} \alpha \|\mathbf{v}_h^j\|_{\mathbf{L}^2(\Omega)}^2 &\lesssim \|\nabla \mathbf{m}_h^j\|_{\mathbf{L}^2(\Omega)} \|\nabla \mathbf{v}_h^j\|_{\mathbf{L}^2(\Omega)} + C_1 C_\pi \|\mathbf{v}_h^j\|_{\mathbf{L}^2(\Omega)} \\ &\quad + C_2 C_\chi \|\mathbf{v}_h^j\|_{\mathbf{L}^2(\Omega)}. \end{aligned}$$

Next, we apply an inverse estimate (see e.g. [Bra07, II, Theorem 6.8]) for the first term on the right-hand side to see

$$\begin{aligned} \alpha \|\mathbf{v}_h^j\|_{\mathbf{L}^2(\Omega)}^2 &\lesssim \frac{1}{h^2} \|\mathbf{m}_h^j\|_{\mathbf{L}^2(\Omega)} \|\mathbf{v}_h^j\|_{\mathbf{L}^2(\Omega)} + (C_1 C_\pi + C_2 C_\chi) \|\mathbf{v}_h^j\|_{\mathbf{L}^2(\Omega)} \\ &= \left(\frac{1}{h^2} \|\mathbf{m}_h^j\|_{\mathbf{L}^2(\Omega)} + (C_1 C_\pi + C_2 C_\chi) \right) \|\mathbf{v}_h^j\|_{\mathbf{L}^2(\Omega)}. \end{aligned}$$

Altogether, using the compactness of Ω , we derive

$$\begin{aligned}\|\mathbf{v}_h^j\|_{L^2(\Omega)} &\lesssim \frac{1}{h^2} \|\mathbf{m}_h^j\|_{L^2(\Omega)} + (C_1 C_\pi + C_2 C_\chi) \\ &\leq \frac{1}{h^2} |\Omega|^{1/2} + (C_1 C_\pi + C_2 C_\chi) \\ &=: C_5(h),\end{aligned}$$

and therefore the k -independent boundedness of $\|\mathbf{v}_h^j\|_{L^2(\Omega)}$. \square

The previous lemma now allows us to uniformly bound \mathbf{m}_{hk} for $k \rightarrow 0$. In addition, this allows us to prove that the sequence \mathbf{m}_{hk} is even equicontinuous for any fixed $h > 0$. This, however, yields the possibility of applying the Arzelà-Ascoli theorem to see that for fixed $h > 0$, \mathbf{m}_{hk} is even uniformly convergent in time. The reader might know the Arzelà-Ascoli theorem only for functions $g : [0, T] \rightarrow \mathbb{R}$. There are, however, several extensions to function spaces, one of which will be applied here. The following result can be found e.g. in [Pop74, Chapter 4, Cor. 4.48], and the interested reader is referred to that work for further studies.

Proposition 2.3.11 (Arzelà-Ascoli). *Let (X, d_X) and (Y, d_Y) be metric spaces. Let further X be compact and $H \subset C(X, Y)$. Then, H is relatively compact in $C(X, Y)$ if and only if*

- (a) $H(x) := \{h(x) : h \in H\}$ is relatively compact in Y for any $x \in X$ and
- (b) H is equicontinuous, i.e.

$$\forall \varepsilon > 0 \exists \delta > 0 \forall h \in H \forall x_1, x_2 \in X : d_X(x_1, x_2) \leq \delta \Rightarrow d_Y(h(x_1), h(x_2)) \leq \varepsilon.$$

\square

Exploiting this result, we now investigate the limiting process for $k \rightarrow 0$.

Lemma 2.3.12. *Let $h > 0$ be fixed. Then, there exists a function $\mathbf{m}_h \in \mathbf{L}^2(\Omega_T)$, such that a subsequence of \mathbf{m}_{hk} converges uniformly in time towards \mathbf{m}_h for $k \rightarrow 0$, i.e.*

$$\|\mathbf{m}_{hk} - \mathbf{m}_h\|_{C([0, T]; L^2(\Omega))} \xrightarrow{\text{sub}} 0. \quad (2.3.33)$$

In particular, there holds

$$\|\mathbf{m}_{hk} - \mathbf{m}_h\|_{L^2(\Omega_T)} \xrightarrow{\text{sub}} 0 \quad (2.3.34)$$

$$\|\mathbf{m}_{hk}(t) - \mathbf{m}_h(t)\|_{L^2(\Omega)} \xrightarrow{\text{sub}} 0. \quad (2.3.35)$$

for the same subsequence as above. Moreover, the limit function \mathbf{m}_h is continuous in time for any $h > 0$.

Proof. We aim to use the Arzelà-Ascoli theorem for the following quantities:

$$\begin{aligned}(X, d_X) &= ([0, T], |\cdot|), \\ (Y, d_Y) &= (\mathcal{S}^1(\mathcal{T}_h), \|\cdot\|_{L^2(\Omega)}), \\ H &= \mathbf{m}_{hk}(\cdot) \subset C(X, Y) \quad \text{for fixed } h.\end{aligned}$$

First, we note that obviously, one has $\mathbf{m}_{hk}(\cdot) \in C([0, T], (\mathcal{S}^1(\mathcal{T}_h), \|\cdot\|_{L^2(\Omega)}))$. Next, we want to apply Proposition 2.3.11. We first show assumption (b), i.e. the equicontinuity of \mathbf{m}_{hk} . To that end, let $\varepsilon > 0$ be arbitrary and $C_5(h) = C_5(h, |\Omega|, C_\pi, C_\chi)$ be the constant from Lemma 2.3.10. We now choose $\delta = \frac{\varepsilon}{C_v C_5} > 0$ (independent of $k > 0$) and consider $t, t' \in [0, T]$ with $|t - t'| \leq \delta$. For any $k > 0$, we have to distinguish two cases.

Case 1: $t, t' \in [t_j, t_{j+1}]$. There holds

$$\begin{aligned}
 & \|\mathbf{m}_{hk}(t, \cdot) - \mathbf{m}_{hk}(t', \cdot)\|_{L^2(\Omega)} \\
 &= \left\| \frac{t - jk}{k} \mathbf{m}_h^{j+1} + \frac{(j+1)k - t}{k} \mathbf{m}_h^j - \frac{t' - jk}{k} \mathbf{m}_h^{j+1} - \frac{(j+1)k - t'}{k} \mathbf{m}_h^j \right\|_{L^2(\Omega)} \\
 &= \left\| \frac{t - t'}{k} \mathbf{m}_h^{j+1} - \frac{t - t'}{k} \mathbf{m}_h^j \right\|_{L^2(\Omega)} \\
 &= \frac{|t - t'|}{k} \|\mathbf{m}_h^{j+1} - \mathbf{m}_h^j\|_{L^2(\Omega)} \\
 &\leq \frac{|t - t'|}{k} k C_v \|\mathbf{v}_h^j\|_{L^2(\Omega)} \\
 &\leq |t - t'| C_v C_5 \\
 &\leq \frac{\varepsilon}{C_v C_5} C_v C_5 = \varepsilon,
 \end{aligned}$$

with $C_5 = C_5(h)$ (see Lemma 2.3.10). In particular, C_5 is independent of k . For the first inequality, we additionally exploited Lemma 2.2.3.

Case 2: t and t' are from 'different time intervals', i.e. $t \in [j_1 k, (j_1 + 1)k]$ and $t' \in [j_2 k, (j_2 + 1)k]$ with $j_1 < j_2$. Then we have

$$|t' - t| = |t - t_{j_1+1}| + \sum_{i=j_1+1}^{j_2-1} |t_i - t_{i+1}| + |t' - t_{j_2}|.$$

The triangle inequality in $L^2(\Omega)$ further shows

$$\begin{aligned}
 \|\mathbf{m}_{hk}(t', \cdot) - \mathbf{m}_{hk}(t, \cdot)\|_{L^2(\Omega)} &\leq \|\mathbf{m}_{hk}(t', \cdot) - \mathbf{m}_{hk}(t_{j_2}, \cdot)\|_{L^2(\Omega)} \\
 &\quad + \sum_{i=j_1+1}^{j_2-1} \|\mathbf{m}_{hk}(t_{i+1}, \cdot) - \mathbf{m}_{hk}(t_i, \cdot)\|_{L^2(\Omega)} \\
 &\quad + \|\mathbf{m}_{hk}(t_{j_1+1}, \cdot) - \mathbf{m}_{hk}(t, \cdot)\|_{L^2(\Omega)}.
 \end{aligned}$$

Using case 1 above now yields

$$\begin{aligned}
 \|\mathbf{m}_{hk}(t', \cdot) - \mathbf{m}_{hk}(t, \cdot)\|_{L^2(\Omega)} &\leq (|t' - t_{j_2}| + \sum_{i=j_1+1}^{j_2-1} |t_i - t_{i+1}| + |t_{j_1+1} - t|) C_v C_5, \\
 &= |t' - t| C_v C_5 \leq \varepsilon
 \end{aligned}$$

which is the equicontinuity of $\{\mathbf{m}_{hk} : k > 0\}$. It remains to show assumption (a). To that end, we show that $\|\mathbf{m}_{hk}(t, \cdot)\|_{H^1(\Omega)}$ is bounded independently of k . Exploiting the Rellich-Kondrachov compactness theorem A.2.4, we then conclude relative compactness of $\{\mathbf{m}_{hk}(t, \cdot) : k > 0\}$ in $L^2(\Omega)$. Again, we distinguish between two cases.

Case 1: We first consider $t = t_j = jk$ for any $j \in 1, \dots, N$. Then, we have

$$\|\mathbf{m}_{hk}(t_j, \cdot)\|_{\mathbf{L}^2(\Omega)}^2 = \|\mathbf{m}_h^j\|_{\mathbf{L}^2(\Omega)}^2 \leq |\Omega| \|\mathbf{m}_h^j\|_{L^\infty(\Omega)}^2 = |\Omega|.$$

The uniform boundedness of $\|\nabla \mathbf{m}_h^j\|_{\mathbf{L}^2(\Omega)}^2$ directly follows from Lemma 2.3.3.

Case 2: Now, let $t \neq t_j$ with $t \in [jk, (j+1)k]$. Then, we have

$$\begin{aligned} \|\mathbf{m}_{hk}(t, \cdot)\|_{\mathbf{H}^1(\Omega)}^2 &= \|\mathbf{m}_{hk}(t, \cdot)\|_{\mathbf{L}^2(\Omega)}^2 + \|\nabla \mathbf{m}_{hk}(t, \cdot)\|_{\mathbf{L}^2(\Omega)}^2 \\ &= \left\| \frac{t-jk}{k} \mathbf{m}_h^j + \frac{(j+1)k-t}{k} \mathbf{m}_h^{j+1} \right\|_{\mathbf{L}^2(\Omega)}^2 \\ &\quad + \left\| \frac{t-jk}{k} \nabla \mathbf{m}_h^j + \frac{(j+1)k-t}{k} \nabla \mathbf{m}_h^{j+1} \right\|_{\mathbf{L}^2(\Omega)}^2 \\ &\leq \frac{|t-jk|}{k} \|\mathbf{m}_h^j\|_{\mathbf{L}^2(\Omega)}^2 + \frac{|(j+1)k-t|}{k} \|\mathbf{m}_h^{j+1}\|_{\mathbf{L}^2(\Omega)}^2 \\ &\quad + \frac{|t-jk|}{k} \|\nabla \mathbf{m}_h^j\|_{\mathbf{L}^2(\Omega)}^2 + \frac{|(j+1)k-t|}{k} \|\nabla \mathbf{m}_h^{j+1}\|_{\mathbf{L}^2(\Omega)}^2 \\ &\leq \frac{k}{k} (\|\mathbf{m}_h^j\|_{\mathbf{L}^2(\Omega)}^2 + \|\mathbf{m}_h^{j+1}\|_{\mathbf{L}^2(\Omega)}^2 + \|\nabla \mathbf{m}_h^j\|_{\mathbf{L}^2(\Omega)}^2 + \|\nabla \mathbf{m}_h^{j+1}\|_{\mathbf{L}^2(\Omega)}^2) \\ &\leq C. \end{aligned}$$

This bound is even independent of h . Altogether, we derived relative compactness of $\{\mathbf{m}_{hk}(\cdot) : k > 0\}$ in $C(X, Y)$ and thus the existence of a subsequence that converges towards a function \mathbf{m}_h in $C(X, Y)$. Since uniform limits of continuous functions are continuous, we conclude continuity of \mathbf{m}_h in time. The pointwise convergence (2.3.35) directly follows from uniform convergence. Since $[0, T]$ is a compact interval, we finally get

$$\|\mathbf{m}_{hk} - \mathbf{m}_h\|_{\mathbf{L}^2(\Omega_T)}^2 = \|\mathbf{m}_{hk} - \mathbf{m}_h\|_{L^2([0, T]; \mathbf{L}^2(\Omega))}^2 \leq |T| \|\mathbf{m}_{hk} - \mathbf{m}_h\|_{L^\infty([0, T]; \mathbf{L}^2(\Omega))}^2 \xrightarrow{\text{sub}} 0$$

and thus the desired result. \square

In the following, we mostly work with the discretizations \mathbf{m}_{hk}^- resp. \mathbf{m}_{hk}^+ , which are constant in time. Therefore, we like to have a corresponding result for those functions. Luckily, the uniform convergence can be transferred, which is the result of the upcoming corollary.

Corollary 2.3.13. *The uniform convergence property can be transferred to \mathbf{m}_{hk}^- and \mathbf{m}_{hk}^+ , i.e. for fixed $h > 0$, we have*

$$\|\mathbf{m}_{hk}^- - \mathbf{m}_h\|_{L^\infty([0, T]; \mathbf{L}^2(\Omega))} \xrightarrow{\text{sub}} 0 \quad \text{and} \quad (2.3.36)$$

$$\|\mathbf{m}_{hk}^+ - \mathbf{m}_h\|_{L^\infty([0, T]; \mathbf{L}^2(\Omega))} \xrightarrow{\text{sub}} 0 \quad (2.3.37)$$

as $k \rightarrow 0$, for the same subsequence as above.

Proof. The Lemmata 2.2.3 and 2.3.10 show the uniform boundedness of

$$\|\partial_t \mathbf{m}_{hk}(t)\|_{\mathbf{L}^2(\Omega)} = \left\| \frac{\mathbf{m}_h^{j+1} - \mathbf{m}_h^j}{k} \right\|_{\mathbf{L}^2(\Omega)} \leq C_v \|\mathbf{v}_h^j\|_{\mathbf{L}^2(\Omega)} \leq C_v C_5(h), \quad (2.3.38)$$

for any $t \in [t_j, t_{j+1}]$. Next, we know from Lemma 2.2.5

$$\begin{aligned}
 \|\mathbf{m}_{hk} - \mathbf{m}_{hk}^-\|_{L^\infty([0,T];L^2(\Omega))}^2 &= \sup_{t \in [0,T]} \|\mathbf{m}_{hk}(t) - \mathbf{m}_{hk}^-(t)\|_{L^2(\Omega)}^2 \\
 &= \sup_{t \in [0,T]} \int_{\Omega} |\mathbf{m}_{hk}(t, \mathbf{x}) - \mathbf{m}_{hk}^-(t, \mathbf{x})|^2 dx \\
 &= \sup_{t \in [0,T]} k^2 \int_{\Omega} |\partial_t \mathbf{m}_{hk}(t, \mathbf{x})|^2 dx \\
 &= \sup_{t \in [0,T]} k^2 \|\partial_t \mathbf{m}_{hk}(t)\|_{L^2(\Omega)}^2 \\
 &\leq k^2 C_v^2 C_5(h)^2 \longrightarrow 0.
 \end{aligned}$$

This, however, directly yields

$$\begin{aligned}
 \|\mathbf{m}_{hk}^- - \mathbf{m}_h\|_{L^\infty([0,T];L^2(\Omega))} &\leq \|\mathbf{m}_{hk}^- - \mathbf{m}_{hk}\|_{L^\infty([0,T];L^2(\Omega))} \\
 &\quad + \|\mathbf{m}_{hk} - \mathbf{m}_h\|_{L^\infty([0,T];L^2(\Omega))} \xrightarrow{\text{sub}} 0,
 \end{aligned}$$

due to Lemma 2.3.12. The result (2.3.37) for \mathbf{m}_{hk}^+ is derived analogously. \square

With the above statements, we have a pretty good understanding of the limiting process of the discrete magnetizations for $k \rightarrow 0$. It thus remains to investigate the one for $h \rightarrow 0$ and the corresponding question on whether or not it makes sense to treat those limiting processes separately. The next lemma gives some insight into that regard.

Lemma 2.3.14. *There holds $\|\mathbf{m}_h - \mathbf{m}\|_{L^2(\Omega_T)} \rightarrow 0$ for $h \rightarrow 0$, i.e. we have*

$$\begin{array}{ccc}
 \mathbf{m}_{hk} & \xrightarrow{k} & \mathbf{m}_h \\
 & \searrow (k,h) & \downarrow h \\
 & & \mathbf{m}
 \end{array}$$

Without loss of generality, the convergence is to be understood for yet another subsequence in the sense of Lemma 2.3.12, i.e. there exists a subsequence of the index set (h, k) such that all the above convergence properties hold simultaneously.

Proof. We only have to show the convergence property $\|\mathbf{m}_h - \mathbf{m}\|_{L^2(\Omega_T)}$ for $h \rightarrow 0$, as the other terms have already been treated before. To that end, we write

$$\|\mathbf{m} - \mathbf{m}_h\|_{L^2(\Omega_T)}^2 \leq 2\|\mathbf{m} - \mathbf{m}_{hk}\|_{L^2(\Omega_T)}^2 + 2\|\mathbf{m}_{hk} - \mathbf{m}_h\|_{L^2(\Omega_T)}^2.$$

Now, let $\varepsilon > 0$ be arbitrary. From the unconditional convergence of \mathbf{m}_{hk} towards \mathbf{m} , we deduce the existence of (h_0, k_0) such that $\|\mathbf{m} - \mathbf{m}_{hk}\|_{L^2(\Omega_T)}^2 \leq \varepsilon$ for all $h \leq h_0, k \leq k_0$. This yields

$$\begin{aligned}
 \|\mathbf{m} - \mathbf{m}_h\|_{L^2(\Omega_T)}^2 &= \limsup_{k \rightarrow 0} \|\mathbf{m} - \mathbf{m}_h\|_{L^2(\Omega_T)}^2 \\
 &\leq \limsup_{k \rightarrow 0} (2\|\mathbf{m} - \mathbf{m}_{hk}\|_{L^2(\Omega_T)}^2 + 2\|\mathbf{m}_{hk} - \mathbf{m}_h\|_{L^2(\Omega_T)}^2) \\
 &\leq 2 \limsup_{k \rightarrow 0} \|\mathbf{m} - \mathbf{m}_{hk}\|_{L^2(\Omega_T)}^2 + 2 \limsup_{k \rightarrow 0} \|\mathbf{m}_{hk} - \mathbf{m}_h\|_{L^2(\Omega_T)}^2 \\
 &\leq 2\varepsilon + 0 = 2\varepsilon,
 \end{aligned}$$

for all $h \leq h_0$. Here, we used that there exists a subsequence of \mathbf{m}_{hk} such that there holds

$$\|\mathbf{m}_{hk} - \mathbf{m}_h\|_{\mathbf{L}^2(\Omega_T)}^2 \longrightarrow 0 \quad \text{for any fixed } h < h_0 \text{ and } k \rightarrow 0.$$

This can be seen by construction of a diagonal sequence in the following sense: First, we choose a subsequence of the time-index k such that we have $\mathbf{m}_{h_0 k_0^n} \rightarrow \mathbf{m}_{h_0}$ for $n \rightarrow \infty$. Then, we choose a further subsequence satisfying $\mathbf{m}_{h_1 k_1^n} \rightarrow \mathbf{m}_{h_1}$, as well as $\mathbf{m}_{h_0 k_1^n} \rightarrow \mathbf{m}_{h_0}$ as $n \rightarrow \infty$, and so on. For the time-index k , we now choose the diagonal sequence $\mathbf{m}_{hk} := \mathbf{m}_{h_k k_n^n}$ to see

$$\mathbf{m}_{hk} \xrightarrow{\text{sub}} \mathbf{m}_h \quad \text{for any } h < h_0, \quad \text{as } k \rightarrow 0. \quad (2.3.39)$$

This concludes the proof. \square

Up to now, we investigated both, the limiting process for $k \rightarrow 0$, as well as the one for $h \rightarrow 0$, and we saw that indeed, the discrete quantities behave the way we anticipated. The next lemma carries those convergence properties over to a pointwise level. Recall that all involved quantities are continuous in time, cf. Lemmata 2.3.5 and 2.3.12.

Corollary 2.3.15. *For any $t \in [0, T]$, we have*

$$\|\mathbf{m}_{hk}(t) - \mathbf{m}(t)\|_{\mathbf{L}^2(\Omega)} \xrightarrow{\text{sub}} 0 \text{ and} \quad (2.3.40)$$

$$\|\mathbf{m}_h(t) - \mathbf{m}(t)\|_{\mathbf{L}^2(\Omega)} \xrightarrow{\text{sub}} 0, \quad (2.3.41)$$

as $(k, h) \rightarrow (0, 0)$ resp. $h \rightarrow 0$.

Proof. We only show the first statement since the second one follows completely analogously. For the moment, we assume that there existed some $t \in [0, T]$, such that the above convergence property does not hold, i.e.

$$\exists C > 0 \forall (h, k) : \|\mathbf{m}_{hk}(t) - \mathbf{m}(t)\|_{\mathbf{L}^2(\Omega)} \geq C.$$

Due to continuity of the involved functions (Lemma 2.3.5 and 2.3.12), there exists a neighborhood $B_\varepsilon(t)$ around t , such that

$$\|\mathbf{m}_{hk}(t) - \mathbf{m}(t)\|_{\mathbf{L}^2(\Omega)} > 0$$

for any $t \in B_\varepsilon(t)$ and for all (h, k) . This, however, yields

$$\|\mathbf{m}_{hk} - \mathbf{m}\|_{\mathbf{L}^2(\Omega_T)}^2 = \int_0^T \|\mathbf{m}_{hk}(s) - \mathbf{m}(s)\|_{\mathbf{L}^2(\Omega)}^2 ds > 0$$

for all (h, k) which contradicts the assumption. \square

We finally collected all the necessary ingredients to prove assumption (2.3.26). The proof consists of one lemma and two propositions, and considers the limiting processes for $k \rightarrow 0$ and $h \rightarrow 0$ separately. In order to ease readability, the following lemma was extracted from the proof. The upcoming propositions 2.3.17 and 2.3.18 then deal with one limiting process each, and thus combine all the previous results.

Lemma 2.3.16. *There holds*

$$k \sum_{j=0}^{N-1} \|\chi(\mathbf{m}_{hk})(t_j) - \chi(\mathbf{m}_h)(t_j)\|_{\mathbf{L}^2(\Omega)} \xrightarrow{sub} 0 \quad (2.3.42)$$

as $k \rightarrow 0$, where the subsequence is the same as for the limiting process $\mathbf{m}_{hk} \xrightarrow{sub} \mathbf{m}_h$.

Proof. By assumption (2.3.31), we have

$$\begin{aligned} k \sum_{j=0}^{N-1} \|\chi(\mathbf{m}_{hk})(t_j) - \chi(\mathbf{m}_h)(t_j)\|_{\mathbf{L}^2(\Omega)} & \\ & \lesssim k \sum_{j=0}^{N-1} \left(\|\mathbf{m}_{hk}(t_j) - \mathbf{m}_h(t_j)\|_{\mathbf{L}^2(\Omega)}^2 + \|\mathbf{m}_{hk} - \mathbf{m}_h\|_{\mathbf{L}^2(\Omega_T)}^2 \right. \\ & \quad \left. + \|\mathbf{m}_{hk}^- - \mathbf{m}_h\|_{\mathbf{L}^2(\Omega_T)}^2 + \|\mathbf{m}_{hk}^+ - \mathbf{m}_h\|_{\mathbf{L}^2(\Omega_T)}^2 \right)^{1/2} \\ & \lesssim |T| \left(\|\mathbf{m}_{hk} - \mathbf{m}_h\|_{L^\infty(\mathbf{L}^2)}^2 + \|\mathbf{m}_{hk}^- - \mathbf{m}_h\|_{L^\infty(\mathbf{L}^2)}^2 + \|\mathbf{m}_{hk}^+ - \mathbf{m}_h\|_{L^\infty(\mathbf{L}^2)}^2 \right)^{1/2} \\ & \xrightarrow{sub} 0, \end{aligned}$$

where we have used Lemma 2.3.12 and Corollary 2.3.13. □

Remark. *The convergence analysis in this section could be greatly simplified, if we could proof uniform convergence of \mathbf{m}_{hk} to \mathbf{m} in time. This is, however, not the case.*

Proposition 2.3.17. *For any fixed $h > 0$, there holds*

$$k \sum_{j=0}^{N-1} \int_{\Omega} \chi(\mathbf{m}_{hk})(t_j) \cdot (\mathbf{m}_{hk}^- \times \Psi)(t_j) \xrightarrow{sub} \int_{\Omega_T} \chi(\mathbf{m}_h) \cdot (\mathbf{m}_h \times \Psi) \quad (2.3.43)$$

as $k \rightarrow 0$.

Proof. We obviously have

$$\begin{aligned}
 & \left| k \sum_{j=0}^{N-1} \int_{\Omega} \chi(\mathbf{m}_{hk})(t_j) \cdot (\mathbf{m}_{hk}^- \times \Psi)(t_j) - \int_{\Omega_T} \chi(\mathbf{m}_h) \cdot (\mathbf{m}_h \times \Psi) \right| \\
 &= \left| k \sum_{j=0}^{N-1} \int_{\Omega} \chi(\mathbf{m}_h)(t_j) \cdot (\mathbf{m}_h \times \Psi)(t_j) - \int_{\Omega_T} \chi(\mathbf{m}_h) \cdot (\mathbf{m}_h \times \Psi) \right. \\
 &\quad - k \sum_{j=0}^{N-1} \int_{\Omega} \chi(\mathbf{m}_h)(t_j) \cdot (\mathbf{m}_h \times \Psi)(t_j) + k \sum_{j=0}^{N-1} \int_{\Omega} \chi(\mathbf{m}_h)(t_j) \cdot (\mathbf{m}_{hk}^- \times \Psi)(t_j) \\
 &\quad \left. + k \sum_{j=0}^{N-1} \int_{\Omega} \chi(\mathbf{m}_{hk})(t_j) \cdot (\mathbf{m}_{hk}^- \times \Psi)(t_j) - k \sum_{j=0}^{N-1} \int_{\Omega} \chi(\mathbf{m}_h)(t_j) \cdot (\mathbf{m}_{hk}^- \times \Psi)(t_j) \right| \\
 &\leq \left| k \sum_{j=0}^{N-1} \int_{\Omega} \chi(\mathbf{m}_h)(t_j) \cdot (\mathbf{m}_h \times \Psi)(t_j) - \int_{\Omega_T} \chi(\mathbf{m}_h) \cdot (\mathbf{m}_h \times \Psi) \right| \\
 &\quad + \left| k \sum_{j=0}^{N-1} \int_{\Omega} \chi(\mathbf{m}_{hk})(t_j) \cdot (\mathbf{m}_{hk}^- \times \Psi)(t_j) - k \sum_{j=0}^{N-1} \int_{\Omega} \chi(\mathbf{m}_h)(t_j) \cdot (\mathbf{m}_{hk}^- \times \Psi)(t_j) \right| \\
 &\quad + \left| k \sum_{j=0}^{N-1} \int_{\Omega} \chi(\mathbf{m}_h)(t_j) \cdot (\mathbf{m}_{hk}^- \times \Psi)(t_j) - k \sum_{j=0}^{N-1} \int_{\Omega} \chi(\mathbf{m}_h)(t_j) \cdot (\mathbf{m}_h \times \Psi)(t_j) \right| \\
 &= |I_1| + |I_2| + |I_3|.
 \end{aligned}$$

In the following, we will investigate each of those three contributions separately. First, we have

$$|I_1| \longrightarrow 0$$

by definition of the Riemann integral. Note, that $\int_{\Omega} \chi(\mathbf{m}_h)(\cdot) \cdot (\mathbf{m}_h \times \Psi)(\cdot)$ is Riemann integrable in time due to continuity of \mathbf{m}_h and thus, by assumption, continuity of $\chi(\mathbf{m}_h)(\cdot)$ in time. For the second term, we use Lemma 2.3.16 to deduce

$$\begin{aligned}
 |I_2| &\leq k \sum_{j=0}^{N-1} \int_{\Omega} |[\chi(\mathbf{m}_{hk})(t_j) - \chi(\mathbf{m}_h)(t_j)] \cdot (\mathbf{m}_{hk}^- \times \Psi)(t_j)| \\
 &\leq k \sum_{j=0}^{N-1} \|\chi(\mathbf{m}_{hk})(t_j) - \chi(\mathbf{m}_h)(t_j)\|_{L^2(\Omega)} \|(\mathbf{m}_{hk}^- \times \Psi)(t_j)\|_{L^2(\Omega)} \\
 &\lesssim k \sum_{j=0}^{N-1} \|\chi(\mathbf{m}_{hk})(t_j) - \chi(\mathbf{m}_h)(t_j)\|_{L^2(\Omega)} \xrightarrow{\text{sub}} 0, \quad \text{für } k \rightarrow 0
 \end{aligned}$$

Finally, it remains to consider the third term. Here, we have

$$\begin{aligned}
 |I_3| &\leq k \sum_{j=0}^{N-1} \|\chi(\mathbf{m}_h)(t_j)\|_{L^2(\Omega)} \|[(\mathbf{m}_{hk}^- \times \Psi) - (\mathbf{m}_h \times \Psi)](t_j)\|_{L^2(\Omega)} \\
 &\lesssim \sup_{t_j} \|[(\mathbf{m}_{hk}^- \times \Psi) - (\mathbf{m}_h \times \Psi)](t_j)\|_{L^2(\Omega)} \\
 &\lesssim \|(\mathbf{m}_{hk}^- \times \Psi) - (\mathbf{m}_h \times \Psi)\|_{L^\infty([0,T];L^2(\Omega))} \\
 &= \|(\mathbf{m}_{hk}^- - \mathbf{m}_h) \times \Psi\|_{L^\infty(L^2)} \\
 &\lesssim \|\mathbf{m}_{hk}^- - \mathbf{m}_h\|_{L^\infty(L^2)} \|\Psi\|_{L^\infty(L^2)} \xrightarrow{\text{sub}} 0.
 \end{aligned}$$

For the first estimate, we used the assumed time-continuity of $\chi(\mathbf{m}_h)$ and thus

$$k \sum_{j=0}^{n-1} \|\chi(\mathbf{m}_h)(t_j)\|_{L^2(\Omega)} \longrightarrow \int_0^T \|\chi(\mathbf{m}_h)(t)\|_{L^2(\Omega)}.$$

This concludes the proof. \square

Remark. In the proof of the previous result, we used the Riemann sum $k \sum_{j=0}^{N-1} \int_{\Omega} \chi(\mathbf{m}_{hk})(t_j)$ for the convergence analysis. The quantity \mathbf{m}_{hk} , however, is successively constructed by our scheme. Implicitly, we thus assumed, that $\chi(\mathbf{m}_{hk})(t_j)$ depends only on \mathbf{m}_{hk} at time t_j or earlier, i.e. it does not depend on later time evaluations. This is where we used assumption (2.2.5), which is a quite natural one, since the involved quantities usually stem from physical processes of some kind.

With the last statement, we can finally describe the h -limit and thus show (2.3.26).

Proposition 2.3.18. *Assumption (2.3.26) holds, i.e. we have*

$$k \sum_{j=0}^{N-1} \int_{\Omega} \chi(\mathbf{m}_{hk})(t_j) \cdot ((\mathbf{m}_{hk}^- \times \Psi)(t_j)) \longrightarrow \int_{\Omega_T} \chi(\mathbf{m}) \cdot (\mathbf{m} \times \Psi) \quad (2.3.44)$$

as $(h, k) \rightarrow (0, 0)$.

Proof. We define the real-valued sequence

$$a_{hk} := k \sum_{j=0}^{N-1} \int_{\Omega} \chi(\mathbf{m}_{hk})(t_j) \cdot (\mathbf{m}_{hk}^- \times \Psi)(t_j).$$

Then, there holds

$$|a_{hk}| \leq k \sum_{j=0}^{N-1} \|\chi(\mathbf{m}_{hk})(t_j)\|_{L^2(\Omega)} \|(\mathbf{m}_{hk}^- \times \Psi)(t_j)\|_{L^2(\Omega)} \lesssim C_{\chi} T,$$

whence boundedness of a_{hk} . Due to the Bolzano-Weierstrass theorem, there exists some value $a \in \mathbb{R}$ and a subsequence of a_{hk} (notationally unchanged) with

$$\lim_{\substack{h \rightarrow 0 \\ k \rightarrow 0}} a_{hk} =: a.$$

Proposition 2.3.17, assumption (2.3.30), and Lemma A.2.10 now show

$$\lim_{h \rightarrow 0} \lim_{k \rightarrow 0} a_{hk} = \lim_{h \rightarrow 0} \int_{\Omega_T} \chi(\mathbf{m}_h) \cdot (\mathbf{m}_h \times \Psi) = \int_{\Omega_T} \chi(\mathbf{m}) \cdot (\mathbf{m} \times \Psi).$$

From the uniqueness of limits and Lemma A.3.1, we finally deduce

$$a = \int_{\Omega_T} \chi(\mathbf{m}) \cdot (\mathbf{m} \times \Psi),$$

which concludes the proof. \square

This statement concludes the general convergence analysis. In the next chapter, we will investigate certain concrete field contributions from the literature and show that those fulfill our assumptions and are thus covered by the theory. Later on, we will show that it is even possible to couple the general LLG integrator with other PDEs and still derive an unconditionally convergent scheme. Before proceeding to those investigations, however, we shed some light on further aspects of our integrator: We discuss improved and physically more relevant energy estimates.

2.4. Improved energy estimate

In this section, we like to comment on our energy decay estimates in comparison to those available throughout the literature. In our notion of a weak solution of LLG, we are satisfied with a simple energy bound in the sense of (2.1.4). Put explicitly, we only assume the energy to be bounded by some time- and space-independent constant $C \geq 0$, i.e.

$$\|\nabla \mathbf{m}(t')\|_{\mathbf{L}^2(\Omega)}^2 + \|\mathbf{m}_{t'}\|_{\mathbf{L}^2(\Omega_{t'})}^2 \leq C, \text{ for almost all } t' \in [0, T].$$

We stress that such an energy bound is sufficient to show convergence of our respective algorithms towards a weak solution. Furthermore, from a mathematical point of view, more than this boundedness is not to be expected. This is true mainly due to the fact that — as mathematicians — we try to prove convergence with as little as possible assumptions on the involved operators, i.e. we try to figure out the set of minimal assumptions to still have unconditional convergence towards some useful notion of a solution.

In contrast to this approach, in many works available throughout the literature (especially physically related ones), we find energy estimates of the form

$$\mathcal{E}(t') + \|\mathbf{m}_{t'}\|_{\mathbf{L}^2(\Omega_{t'})}^2 \leq \mathcal{E}(0)$$

for some meaningful energy term $\mathcal{E}(\cdot)$ and $t' \in [0, T]$. This means that as time progresses, the total energy of the system can never increase, which is certainly a property one would expect from any physically motivated simulation. We like to emphasize, however, that estimates of this form are thus a physical relevance rather than a mathematical necessity. The reason why such estimates can still be obtained in practice is that the contributions of the effective field usually stem from physical observations, as well. Those operators then fulfill more properties than the bare minimum that is needed to obtain convergence. Given such additional properties, those *improved energy estimates* can be deduced with our LLG integrator as well, which is the result of this section. As mentioned in Section 1.3, we define the energy term

$$\mathcal{E}(t) := \mathcal{E}(\mathbf{m}(t)) := C_e \|\nabla \mathbf{m}(t)\|_{\mathbf{L}^2(\Omega)}^2 - \langle \boldsymbol{\pi}(\mathbf{m}(t)), \mathbf{m}(t) \rangle - \langle \mathbf{f}(t), \mathbf{m}(t) \rangle \quad (2.4.1)$$

and its discrete version

$$\mathcal{E}(\mathbf{m}_h^j) := C_e \|\nabla \mathbf{m}_h^j\|_{\mathbf{L}^2(\Omega)}^2 - \langle \pi_h(\mathbf{m}_h^j), \mathbf{m}_h^j \rangle - \langle \mathbf{f}_h^j, \mathbf{m}_h^j \rangle. \quad (2.4.2)$$

To obtain a result which is comparable to the available literature, we omit the time-dependent contribution χ . Moreover, since externally applied fields are relevant in many physical simulations and have a special impact on the energy landscape, we especially consider this contribution modeled by the function $\mathbf{f} : \mathbf{L}^2(\Omega_T) \rightarrow \mathbf{L}^2(\Omega_T)$. The term \mathbf{f}_h^j denotes some suitable approximation of the applied field, and we assume strong convergence of $\mathbf{f}_{hk}^\pm \rightarrow \mathbf{f}$ in $\mathbf{L}^2(\Omega_T)$. The reader is referred to Section 3.1.2 for details.

With those notions, we can derive an energy result in the spirit of e.g. [AKST12], which weakly depends on the spatial dimension and has partially been published in [BFF⁺12]. Even though this work mainly deals with 3D domains, we also give a result for 2D since this might be of general interest.

Lemma 2.4.1 (improved energy estimate). *Let $\pi(\cdot)$ and $\pi_h(\cdot)$ be uniformly Lipschitz-continuous with Lipschitz constant C_L , and let the applied field $\mathbf{f} \in \mathbf{L}^2(\Omega_T)$ be constant in time and hence $\mathbf{f}_h^i = \mathbf{f}_h^{i+1}$ for all time-steps $i = 0, \dots, N-1$ of the integrator. Furthermore, for the 3D case, let \mathbf{f} be in $\mathbf{L}^4(\Omega_T)$ and let $\pi_h(\cdot)$ be uniformly bounded in $\mathbf{L}^4(\Omega)$. Then, there holds*

$$\mathcal{E}(\mathbf{m}(t')) + 2(\alpha - 3/2C_v^2\varepsilon)\|\mathbf{m}_t\|_{\mathbf{L}^2(\Omega_{t'})}^2 \leq \mathcal{E}(\mathbf{m}(0)) + \frac{1}{4\varepsilon}\|\mathbf{f}\|_{\mathbf{L}^2(\Omega_T)}^2 + \frac{|T|(C_\pi^2 + C_L^2)}{4\varepsilon}$$

for any $\varepsilon > 0$ and almost every $t' \in [0, T]$. For vanishing applied field \mathbf{f} and self-adjoint operators $\pi(\cdot)$ and $\pi_h(\cdot)$, it even holds that

$$\mathcal{E}(\mathbf{m}(t')) + 2\alpha\|\mathbf{m}_t\|_{\mathbf{L}^2(\Omega_{t'})}^2 \leq \mathcal{E}(\mathbf{m}(0))$$

for almost every $t' \in [0, T]$.

Proof. To abbreviate notation, we define

$$H(\mathbf{m}_h^i) := -\pi_h(\mathbf{m}_h^i) - \mathbf{f}_h^i.$$

Together with $\mathbf{f}_h^i = \mathbf{f}_h^{i+1}$, this implies

$$H(\mathbf{m}_h^{i+1}) - H(\mathbf{m}_h^i) = -\pi_h(\mathbf{m}_h^{i+1}) + \pi_h(\mathbf{m}_h^i).$$

In complete analogy to (2.3.9), we get

$$\begin{aligned} \mathcal{E}(\mathbf{m}_h^{i+1}) - \mathcal{E}(\mathbf{m}_h^i) &= C_e \|\nabla \mathbf{m}_h^{i+1}\|_{\mathbf{L}^2(\Omega_1)}^2 + \langle H(\mathbf{m}_h^{i+1}), \mathbf{m}_h^{i+1} \rangle - C_e \|\nabla \mathbf{m}_h^i\|_{\mathbf{L}^2(\Omega_1)}^2 - \langle H(\mathbf{m}_h^i), \mathbf{m}_h^i \rangle \\ &\leq C_e \|\nabla \mathbf{m}_h^i\|_{\mathbf{L}^2(\Omega_1)}^2 - 2C_e(\theta - 1/2)k^2 \|\nabla \mathbf{v}_h^i\|_{\mathbf{L}^2(\Omega_1)}^2 - 2\alpha k \|\mathbf{v}_h^i\|_{\mathbf{L}^2(\Omega_1)}^2 \\ &\quad - 2k \langle H(\mathbf{m}_h^i), \mathbf{v}_h^i \rangle + \langle H(\mathbf{m}_h^{i+1}), \mathbf{m}_h^{i+1} \rangle - C_e \|\nabla \mathbf{m}_h^i\|_{\mathbf{L}^2(\Omega_1)}^2 \\ &\quad - \langle H(\mathbf{m}_h^i), \mathbf{m}_h^i \rangle \\ &= -2C_e(\theta - 1/2)k^2 \|\nabla \mathbf{v}_h^i\|_{\mathbf{L}^2(\Omega_1)}^2 - 2\alpha k \|\mathbf{v}_h^i\|_{\mathbf{L}^2(\Omega_1)}^2 + 2k \langle H(\mathbf{m}_h^i), \mathbf{v}_h^i \rangle \\ &\quad + \langle H(\mathbf{m}_h^{i+1}), \mathbf{m}_h^{i+1} \rangle - \langle H(\mathbf{m}_h^i), \mathbf{m}_h^i \rangle. \end{aligned}$$

Straightforward calculations now show

$$\begin{aligned} & -2k\langle H(\mathbf{m}_h^i), \mathbf{v}_h^i \rangle + \langle H(\mathbf{m}_h^{i+1}) + H(\mathbf{m}_h^i), \mathbf{m}_h^{i+1} - \mathbf{m}_h^i \rangle \\ & = 2\langle H(\mathbf{m}_h^i), \mathbf{m}_h^{i+1} - \mathbf{m}_h^i - k\mathbf{v}_h^i \rangle + \langle H(\mathbf{m}_h^{i+1}) - H(\mathbf{m}_h^i), \mathbf{m}_h^{i+1} - \mathbf{m}_h^i \rangle. \end{aligned}$$

Next, the exploitation of $|\mathbf{m}_h^{i+1}(\mathbf{z}) - \mathbf{m}_h^i(\mathbf{z}) - k\mathbf{v}_h^i(\mathbf{z})| \leq 1/2|k\mathbf{v}_h^i(\mathbf{z})|^2$ for all nodes $\mathbf{z} \in \mathcal{N}_h$, cf. Lemma 2.2.4 in combination with the norm equivalence from Proposition 2.1.3, we get for the 2D case

$$\begin{aligned} \|\mathbf{m}_h^{i+1} - \mathbf{m}_h^i - k\mathbf{v}_h^i\|_{\mathbf{L}^2(\Omega)}^2 & \leq h^2 \sum_{\mathbf{z} \in \mathcal{N}_h} |\mathbf{m}_h^{i+1}(\mathbf{z}) - \mathbf{m}_h^i(\mathbf{z}) - k\mathbf{v}_h^i(\mathbf{z})|^2 \\ & \lesssim \frac{h^2}{4} \sum_{\mathbf{z} \in \mathcal{N}_h} k^4 |\mathbf{v}_h^i(\mathbf{z})|^4 \\ & \lesssim k^4 \|\mathbf{v}_h^i\|_{\mathbf{L}^4(\Omega)}^4 \end{aligned}$$

whence

$$\begin{aligned} 2\langle H(\mathbf{m}_h^i), \mathbf{m}_h^{i+1} - \mathbf{m}_h^i - k\mathbf{v}_h^i \rangle & \leq 2\|H(\mathbf{m}_h^i)\|_{\mathbf{L}^2(\Omega)} \|\mathbf{m}_h^{i+1} - \mathbf{m}_h^i - k\mathbf{v}_h^i\|_{\mathbf{L}^2(\Omega)} \\ & \lesssim k^2 \|\mathbf{v}_h^i\|_{\mathbf{L}^4(\Omega)}^2. \end{aligned}$$

For the 3D case, we get

$$\begin{aligned} \|\mathbf{m}_h^{i+1} - \mathbf{m}_h^i - k\mathbf{v}_h^i\|_{\mathbf{L}^{4/3}(\Omega)}^{4/3} & \lesssim h^3 \sum_{\mathbf{z} \in \mathcal{N}_h} |\mathbf{m}_h^{i+1}(\mathbf{z}) - \mathbf{m}_h^i(\mathbf{z}) - k\mathbf{v}_h^i(\mathbf{z})|^{4/3} \\ & \lesssim h^3 \sum_{\mathbf{z} \in \mathcal{N}_h} k^{8/3} |\mathbf{v}_h^i(\mathbf{z})|^{8/3} \\ & \lesssim k^{8/3} \|\mathbf{v}_h^i\|_{\mathbf{L}^{8/3}(\Omega)}^{8/3} \end{aligned}$$

whence

$$\|\mathbf{m}_h^{i+1} - \mathbf{m}_h^i - k\mathbf{v}_h^i\|_{\mathbf{L}^{4/3}(\Omega)} \leq k^2 \|\mathbf{v}_h^i\|_{\mathbf{L}^{8/3}(\Omega)}^2.$$

Next, we use $\|H(\mathbf{m}_h^i)\|_{\mathbf{L}^4(\Omega)} \leq C$ to see

$$\begin{aligned} 2\langle H(\mathbf{m}_h^i), \mathbf{m}_h^{i+1} - \mathbf{m}_h^i - k\mathbf{v}_h^i \rangle & \leq 2\|H(\mathbf{m}_h^i)\|_{\mathbf{L}^4(\Omega)} \|\mathbf{m}_h^{i+1} - \mathbf{m}_h^i - k\mathbf{v}_h^i\|_{\mathbf{L}^{4/3}(\Omega)} \\ & \lesssim k^2 \|\mathbf{v}_h^i\|_{\mathbf{L}^{8/3}(\Omega)}^2 \\ & \lesssim k^2 \|\mathbf{v}_h^i\|_{\mathbf{L}^3(\Omega)}^2, \end{aligned}$$

and make use of the Sobolev embeddings

$$\begin{aligned} \|\mathbf{v}_h^i\|_{\mathbf{L}^4(\Omega)}^2 & \lesssim \|\mathbf{v}_h^i\|_{\mathbf{H}^1(\Omega)} \|\mathbf{v}_h^i\|_{\mathbf{L}^2(\Omega)} & \text{for 2D} \\ \|\mathbf{v}_h^i\|_{\mathbf{L}^3(\Omega)}^2 & \lesssim \|\mathbf{v}_h^i\|_{\mathbf{H}^1(\Omega)} \|\mathbf{v}_h^i\|_{\mathbf{L}^2(\Omega)} & \text{for 3D.} \end{aligned}$$

Altogether we have thus shown

$$2\langle H(\mathbf{m}_h^i), \mathbf{m}_h^{i+1} - \mathbf{m}_h^i - k\mathbf{v}_h^i \rangle \lesssim k^2 \|\mathbf{v}_h^i\|_{\mathbf{L}^2(\Omega)} (\|\mathbf{v}_h^i\|_{\mathbf{L}^2(\Omega)} + \|\nabla \mathbf{v}_h^i\|_{\mathbf{L}^2(\Omega)}).$$

Using Lipschitz-continuity of $H(\cdot)$ together with Lemma 2.2.3, we further estimate

$$\begin{aligned} \langle H(\mathbf{m}_h^{i+1}) - H(\mathbf{m}_h^i), \mathbf{m}_h^{i+1} - \mathbf{m}_h^i \rangle &\leq \|H(\mathbf{m}_h^{i+1}) - H(\mathbf{m}_h^i)\|_{\mathbf{L}^2(\Omega)} \|\mathbf{m}_h^{i+1} - \mathbf{m}_h^i\|_{\mathbf{L}^2(\Omega)} \\ &\leq C_L \|\mathbf{m}_h^{i+1} - \mathbf{m}_h^i\|_{\mathbf{L}^2(\Omega)}^2 \\ &\leq C_v^2 C_L k^2 \|\mathbf{v}_h^i\|_{\mathbf{L}^2(\Omega)}^2. \end{aligned}$$

We have thus derived

$$\begin{aligned} \mathcal{E}(\mathbf{m}_h^{i+1}) - \mathcal{E}(\mathbf{m}_h^i) &\leq -C_e 2(\theta - 1/2) k^2 \|\nabla \mathbf{v}_h^i\|_{\mathbf{L}^2(\Omega)}^2 + \widehat{C} k^2 (\|\mathbf{v}_h^i\|_{\mathbf{L}^2(\Omega)} \|\nabla \mathbf{v}_h^i\|_{\mathbf{L}^2(\Omega)} + \|\mathbf{v}_h^i\|_{\mathbf{L}^2(\Omega)}^2) \\ &\quad - 2\alpha k \|\mathbf{v}_h^i\|_{\mathbf{L}^2(\Omega)}^2 + \langle H(\mathbf{m}_h^{i+1}), \mathbf{m}_h^i \rangle - \langle H(\mathbf{m}_h^i), \mathbf{m}_h^{i+1} \rangle. \end{aligned}$$

Summing up over $i = 0, \dots, j-1$ and using the Cauchy-Schwarz inequality, we get for any $j = 0, \dots, N$ and for $\theta \in [1/2, 1]$

$$\begin{aligned} \mathcal{E}(\mathbf{m}_h^j) - \mathcal{E}(\mathbf{m}_h^0) + 2\alpha k \sum_{i=0}^{j-1} \|\mathbf{v}_h^i\|_{\mathbf{L}^2(\Omega_1)}^2 &\leq Ck (\|\mathbf{v}_{hk}^-\|_{\mathbf{L}^2(\Omega_T)} \|\nabla \mathbf{v}_{hk}^-\|_{\mathbf{L}^2(\Omega_T)} + \|\mathbf{v}_{hk}^-\|_{\mathbf{L}^2(\Omega_T)}^2) \\ &\quad + \sum_{i=0}^{j-1} \langle H(\mathbf{m}_h^{i+1}), \mathbf{m}_h^i \rangle - \sum_{i=0}^{j-1} \langle H(\mathbf{m}_h^i), \mathbf{m}_h^{i+1} \rangle \\ &= k (\|\mathbf{v}_{hk}^-\|_{\mathbf{L}^2(\Omega_T)} \|\nabla \mathbf{v}_{hk}^-\|_{\mathbf{L}^2(\Omega_T)} + \|\mathbf{v}_{hk}^-\|_{\mathbf{L}^2(\Omega_T)}^2) \\ &\quad + \sum_{i=0}^{j-1} (\langle H(\mathbf{m}_h^{i+1}) - H(\mathbf{m}_h^i), \mathbf{m}_h^i \rangle - \langle H(\mathbf{m}_h^i), \mathbf{m}_h^{i+1} - \mathbf{m}_h^i \rangle), \end{aligned} \tag{2.4.3}$$

where we have used

$$\langle H(\mathbf{m}_h^{i+1}), \mathbf{m}_h^i \rangle = \langle H(\mathbf{m}_h^{i+1}) - H(\mathbf{m}_h^i), \mathbf{m}_h^i \rangle + \langle H(\mathbf{m}_h^i), \mathbf{m}_h^i \rangle$$

and

$$-\langle H(\mathbf{m}_h^i), \mathbf{m}_h^{i+1} \rangle = -\langle H(\mathbf{m}_h^i), \mathbf{m}_h^{i+1} - \mathbf{m}_h^i \rangle - \langle H(\mathbf{m}_h^i), \mathbf{m}_h^i \rangle,$$

respectively, for the last inequality. Next, we again exploit Lipschitz-continuity and Young's inequality to see for any $\varepsilon > 0$

$$\begin{aligned} \sum_{i=0}^{j-1} (\langle H(\mathbf{m}_h^{i+1}) - H(\mathbf{m}_h^i), \mathbf{m}_h^i \rangle - \langle H(\mathbf{m}_h^i), \mathbf{m}_h^{i+1} - \mathbf{m}_h^i \rangle) \\ \leq C_v C_L \sum_{i=0}^{j-1} \|k \mathbf{v}_h^i\|_{\mathbf{L}^2(\Omega)} \|\mathbf{m}_h^i\|_{\mathbf{L}^2(\Omega)} + C_v \sum_{i=0}^{j-1} \|k \mathbf{v}_h^i\|_{\mathbf{L}^2(\Omega)} \|\mathbf{f}_h^i\|_{\mathbf{L}^2(\Omega)} + C_v C_\pi \sum_{i=0}^{j-1} \|k \mathbf{v}_h^i\|_{\mathbf{L}^2(\Omega)} \\ \leq 3C_v^2 \varepsilon k \sum_{i=0}^{j-1} \|\mathbf{v}_h^i\|_{\mathbf{L}^2(\Omega)}^2 + \frac{k}{4\varepsilon} \sum_{i=0}^{j-1} \|\mathbf{f}_h^i\|_{\mathbf{L}^2(\Omega)}^2 + \frac{|T|(C_\pi^2 + C_L^2)}{4\varepsilon}. \end{aligned}$$

We thus get

$$\begin{aligned} \mathcal{E}(\mathbf{m}_h^j) + 2k(\alpha - 3/2 C_v^2 \varepsilon) \sum_{i=0}^{j-1} \|\mathbf{v}_h^i\|_{\mathbf{L}^2(\Omega)}^2 &\leq \mathcal{E}(\mathbf{m}_h^0) + C_2 k (\|\mathbf{v}_{hk}^-\|_{\mathbf{L}^2(\Omega_T)} \|\nabla \mathbf{v}_{hk}^-\|_{\mathbf{L}^2(\Omega_T)} + \|\mathbf{v}_{hk}^-\|_{\mathbf{L}^2(\Omega_T)}^2) \\ &\quad + \frac{1}{4\varepsilon} \|\mathbf{f}_{hk}^-\|_{\mathbf{L}^2(\Omega_T)}^2 + \frac{|T|(C_\pi^2 + C_L^2)}{4\varepsilon}. \end{aligned}$$

As in the proof of Lemma 2.3.7, we conclude for any measurable set $\mathfrak{T} \in [0, T]$

$$\begin{aligned} \int_{\mathfrak{T}} \mathcal{E}(\mathbf{m}_{hk}^+(t')) + 2(\alpha - 3/2C_v^2\varepsilon) \int_{\mathfrak{T}} \|\mathbf{v}_{hk}^-\|_{\mathbf{L}^2(\Omega_{t'})}^2 &\leq \int_{\mathfrak{T}} \mathcal{E}(\mathbf{m}_h^0) + Ck \int_{\mathfrak{T}} \|\mathbf{v}_{hk}^-\|_{\mathbf{L}^2(\Omega_T)} \|\nabla \mathbf{v}_{hk}^-\|_{\mathbf{L}^2(\Omega_T)} \\ &\quad + Ck \int_{\mathfrak{T}} \|\mathbf{v}_{hk}^-\|_{\mathbf{L}^2(\Omega_T)}^2 + \int_{\mathfrak{T}} \frac{1}{4\varepsilon} \|\mathbf{f}_{hk}^-\|_{\mathbf{L}^2(\Omega_T)}^2 \\ &\quad + \int_{\mathfrak{T}} \frac{|T|(C_\pi^2 + C_L^2)}{4\varepsilon}. \end{aligned}$$

Passing to the limit as $(h, k) \rightarrow (0, 0)$, this finally yields

$$\int_{\mathfrak{T}} \mathcal{E}(\mathbf{m}(t)) + 2(\alpha - 3/2C_v^2\varepsilon) \int_{\mathfrak{T}} \|\mathbf{m}_t\|_{\mathbf{L}^2(\Omega_t)}^2 \leq \int_{\mathfrak{T}} \mathcal{E}(\mathbf{m}(0)) + \int_{\mathfrak{T}} \frac{1}{4\varepsilon} \|\mathbf{f}\|_{\mathbf{L}^2(\Omega_T)}^2 + \int_{\mathfrak{T}} \frac{|T|(C_\pi^2 + C_L^2)}{4\varepsilon}.$$

Here, we have used the boundedness of $\sqrt{k}\|\nabla \mathbf{v}_{hk}^-\|_{\mathbf{L}^2(\Omega_T)}$. Since $\mathfrak{T} \in [0, T]$ was arbitrary, we derive the desired result from standard measure theory, cf. e.g. [Els11, IV, Theorem 4.4]. Note that for vanishing \mathbf{f} and self-adjoint operators, the terms

$$\sum_{i=0}^j \langle H(\mathbf{m}_h^{i+1}), \mathbf{m}_h^i \rangle - \sum_{i=0}^j \langle H(\mathbf{m}_h^i), \mathbf{m}_h^{i+1} \rangle$$

in (2.4.3) vanish. This immediately yields the corresponding result. \square

Chapter 3

Application to field contributions

In this section, we finally consider concrete contributions of the effective field which stem from actual physical processes. We investigate the classical field contributions

- magnetocrystalline anisotropy,
- magnetostatic strayfield, and
- exterior magnetic field

and show that they indeed fulfill the assumptions (2.3.2) and (2.3.4). For sake of readability, we repeat those here:

$$\begin{aligned} \|\pi_h(\mathbf{m}_h^j)\|_{L^2(\Omega)} &\leq C_\pi < \infty, \quad \text{and} \\ \pi_h(\mathbf{m}_{hk}^-) &\xrightarrow{\text{sub}} \pi(\mathbf{m}) \quad \text{weakly subconvergent in } L^2(\Omega_T), \end{aligned}$$

i.e. we concentrate on the classical contributions, and neglect a possible time-dependence $\chi(\cdot)$ here. We thus give particular examples for our general field contribution $\pi_h(\cdot)$ and show that the classical micromagnetic field theory is covered by our general approach. Moreover, in a second step, we exceed the classical field contributions and show that our framework even covers a multiscale model as introduced in Section 1.4.1. The results from this chapter have partially been published in [BFF⁺12].

3.1. Classical contributions

We now consider each of the classic field contributions individually. We start with the anisotropy contribution from Section 1.3.

3.1.1. Magnetocrystalline anisotropy and pointwise operators

Let $\mathbb{B} := \{x \in \mathbb{R}^3 : |x| \leq 1\}$ be the compact unit ball in \mathbb{R}^3 , and let $\phi : \mathbb{B} \rightarrow \mathbb{R}$ be a Lipschitz continuous anisotropy density. This particularly includes the uniaxial density

$$\phi(x) = -\frac{1}{2}(x \cdot \mathbf{e})^2,$$

with a given easy axis $\mathbf{e} \in \mathbb{S} := \{x \in \mathbb{R}^3 : |x| = 1\}$ as it occurs, for example, in Cobalt (*Co*) or Hematite (Fe_2O_3). Furthermore, the general approach also covers nonlinear anisotropy densities like the cubic density

$$\phi(x) = K_1(x_1^2x_2^2 + x_2^2x_3^2 + x_3^2x_1^2) + K_2x_1^2x_2^2x_3^2,$$

with certain constants $K_1, K_2 \geq 0$, which is relevant for Iron (*Fe*) and Nickel (*Ni*), for example.

According to Rademacher's theorem, ϕ is differentiable pointwise almost everywhere with $D\phi \in \mathbf{L}^\infty(\mathbb{B})$. The anisotropy contribution to the effective field now reads

$$\boldsymbol{\pi}(\mathbf{n})(x) = D\phi(\mathbf{n}(x)) \quad \text{for } \mathbf{n} \in \mathbf{L}^2(\Omega) \text{ and almost all } x \in \Omega, \quad (3.1.1)$$

and $\boldsymbol{\pi}_h(\cdot) = \boldsymbol{\pi}(\cdot)$. The next result states that, for this classic field contribution, all assumptions to guarantee convergence are fulfilled.

Proposition 3.1.1. *Suppose that $\Phi \in \mathbf{L}^\infty(\mathbb{B})$, e.g. $\Phi(x) = D\phi(x)$, and $\boldsymbol{\pi}_h(\mathbf{n}) := \boldsymbol{\pi}(\mathbf{n}) := \Phi \circ \mathbf{n}$ such that the pointwise operation is continuous (but might be nonlinear). Then, there exists a constant $C_6 > 0$ such that*

$$\|\boldsymbol{\pi}(\mathbf{n})\|_{\mathbf{L}^\infty(\Omega)} \leq C_6 \quad \text{for all } \mathbf{n} \in \mathbf{L}^2(\Omega) \text{ with } |\mathbf{n}| \leq 1 \text{ almost everywhere.} \quad (3.1.2)$$

Moreover, there holds strong subconvergence $\boldsymbol{\pi}(\mathbf{m}_{hk}^-) \xrightarrow{\text{sub}} \boldsymbol{\pi}(\mathbf{m})$ in $\mathbf{L}^2(\Omega_T)$ as $(h, k) \rightarrow (0, 0)$. In particular, the assumptions (2.3.2)–(2.3.4) of Theorem 2.3.1 are satisfied.

Proof. Clearly, (3.1.2) holds with $C_6 = \|\Phi\|_{\mathbf{L}^\infty(\Omega)}$. Lemma 2.3.5 thus predicts strong subconvergence $\mathbf{m}_{hk}^- \rightarrow \mathbf{m}$ in $\mathbf{L}^2(\Omega_T)$. Now, choose sequences $h_\ell \rightarrow 0$, $k_\ell \rightarrow 0$ such that $\mathbf{m}_\ell := \mathbf{m}_{h_\ell k_\ell}^-$ converges strongly in $\mathbf{L}^2(\Omega_T)$ to \mathbf{m} . According to the Weyl Lemma A.2.7, by extracting a subsequence, we may in particular assume that \mathbf{m}_ℓ converges to \mathbf{m} even pointwise almost everywhere in Ω_T . By pointwise continuity, this implies $\boldsymbol{\pi}(\mathbf{m}_\ell) \rightarrow \boldsymbol{\pi}(\mathbf{m})$ pointwise almost everywhere in Ω_T . In particular, $|\mathbf{m}_\ell| \leq 1$ also implies $|\mathbf{m}| \leq 1$ almost everywhere. Moreover and because of (3.1.2), $|\boldsymbol{\pi}(\mathbf{m}) - \boldsymbol{\pi}(\mathbf{m}_\ell)| \leq 2C_6$ is uniformly bounded in $\mathbf{L}^\infty(\Omega_T)$. Finally, the Lebesgue dominated convergence theorem A.2.3 thus applies and proves even strong convergence of $\boldsymbol{\pi}(\mathbf{m}_\ell)$ to $\boldsymbol{\pi}(\mathbf{m})$ in $\mathbf{L}^2(\Omega_T)$. \square

Remark . *We emphasize that – at least the uniaxial anisotropy – fulfills the additional assumptions required for the improved energy estimate from Lemma 2.4.1. Here, we have*

$$D\phi(\mathbf{m}) = (\mathbf{m}, \mathbf{e})\mathbf{m},$$

whence the \mathbf{L}^4 -boundedness of $D\phi(\cdot)$. Moreover, the operator is self-adjoint in $\mathbf{L}^2(\Omega)$ as

$$((\mathbf{e}, \mathbf{u})\mathbf{e}, \mathbf{v}) = (\mathbf{e}, \mathbf{u})(\mathbf{e}, \mathbf{v}) = ((\mathbf{e}, \mathbf{v})\mathbf{e}, \mathbf{u})$$

for all $\mathbf{u}, \mathbf{v} \in \mathbf{L}^2(\Omega)$.

3.1.2. Applied exterior field

For the applied exterior field contribution \mathbf{f} , the general operators π_h resp. π is actually independent of the magnetization. The analysis does, however, cover a numerical approximation \mathbf{f}_{hk} of \mathbf{f} . In this short section, we thus consider

$$\pi_h(\mathbf{m}_{hk}^-) := \mathbf{f}_{hk}^-, \quad (3.1.3)$$

where \mathbf{f}_{hk}^- , analogously to above, is defined by

$$\mathbf{f}_{hk}^-(t) := \mathbf{f}_h^j \quad \text{for any } t \in [t_j, t_{j+1}). \quad (3.1.4)$$

Depending on the actual smoothness of \mathbf{f} , different discretizations are possible. Those include time discretization and time-space discretization and, for $\mathbf{f} \in C(\Omega_T)$ read

$$\mathbf{f}_h^j(\cdot) := \mathbf{f}(t_j, \cdot) \quad \text{and} \quad \mathbf{f}_h^j := \mathcal{I}_h(\mathbf{f}(t_j, \cdot)), \quad (3.1.5)$$

respectively. For functions with less regularity, corresponding integral formulations can be used, see e.g. [Gol12, Section 3.4]. For all those discretizations, the assumptions (2.3.2)–(2.3.4) of Theorem 2.3.1 are satisfied. Furthermore, one usually even gets strong convergence

$$\|\mathbf{f}_{hk}^- - \mathbf{f}\|_{L^2(\Omega_T)} \rightarrow 0. \quad (3.1.6)$$

For further information and proof, the reader is referred to [Gol12, Lemma 3.4.1].

3.1.3. Linear and continuous contributions, e.g., the strayfield operator

In this subsection, we consider the strayfield- or demagnetization operator. Basically, this is an application of a more general result for linear and continuous operators which is stated below. For a given linear and continuous $\pi \in L(\mathbf{L}^2(\Omega); \mathbf{L}^2(\Omega))$, we assume that the discretization $\pi_h(\cdot)$ is also linear and continuous and satisfies

$$\pi_h(\mathbf{n}) \rightharpoonup \pi(\mathbf{n}) \quad \text{weakly in } \mathbf{L}^2(\Omega) \quad (3.1.7)$$

for all $\mathbf{n} \in \mathbf{L}^2(\Omega)$.

Lemma 3.1.2. *Under the foregoing assumptions, it holds that*

$$\|\pi_h(\mathbf{n})\|_{\mathbf{L}^2(\Omega)} \leq C_7 \quad \text{for all } \mathbf{n} \in \mathbf{L}^2(\Omega) \text{ with } |\mathbf{n}| \leq 1 \text{ almost everywhere} \quad (3.1.8)$$

and for all $h > 0$, with an independent constant $C_7 > 0$. Moreover, strong subconvergence $\mathbf{m}_{hk}^- \xrightarrow{\text{sub}} \mathbf{m}$ in $\mathbf{L}^2(\Omega_T)$ implies weak subconvergence $\pi_h(\mathbf{m}_{hk}^-) \xrightarrow{\text{sub}} \pi(\mathbf{m})$ in $\mathbf{L}^2(\Omega_T)$ as $h, k \rightarrow 0$. In particular, the assumptions (2.3.2)–(2.3.4) of Theorem 2.3.1 are satisfied.

Proof. Weak convergence in (3.1.7) implies the boundedness $\sup_{h>0} \|\pi_h(\mathbf{n})\|_{\mathbf{L}^2(\Omega)} < \infty$ for all $\mathbf{n} \in \mathbf{L}^2(\Omega)$. Therefore, the Banach-Steinhaus theorem [Wer00, Theorem IV 2.1] applies and predicts uniform boundedness of the operator norms

$$C := \sup_{h>0} \|\pi_h\| < \infty.$$

In particular, this guarantees $\|\pi_h(\mathbf{n})\|_{\mathbf{L}^2(\Omega)} \leq C \|\mathbf{n}\|_{\mathbf{L}^2(\Omega)} \leq C |\Omega|^{1/2}$ for all $\mathbf{n} \in \mathbf{L}^2(\Omega)$ with $|\mathbf{n}| \leq 1$ almost everywhere and thus verifies (3.1.8). Finally, it remains to prove weak $\mathbf{L}^2(\Omega_T)$ -subconvergence of $\pi_h(\mathbf{m}_{hk}^-)$ to $\pi(\mathbf{m})$.

To this end, choose sequences $h_\ell \rightarrow 0$, $k_\ell \rightarrow 0$ such that $\mathbf{m}_\ell := \mathbf{m}_{h_\ell k_\ell}^-$ converges strongly in $\mathbf{L}^2(\Omega_T)$ to \mathbf{m} . Define $\pi_\ell := \pi_{h_\ell}$ and let $\phi \in \mathbf{L}^2(\Omega_T)$. Then,

$$(\pi_\ell(\mathbf{m}_\ell) - \pi(\mathbf{m}), \phi) = (\pi_\ell(\mathbf{m}) - \pi(\mathbf{m}), \phi) - (\pi_\ell(\mathbf{m}) - \pi_\ell(\mathbf{m}_\ell), \phi) \quad (3.1.9)$$

We rewrite the first duality bracket in the form

$$(\pi_\ell(\mathbf{m}) - \pi(\mathbf{m}), \phi) = \int_0^T \langle \pi_\ell(\mathbf{m}(t)) - \pi(\mathbf{m}(t)), \phi(t) \rangle dt.$$

By use of (3.1.7), the integrand tends to zero pointwise almost everywhere as $\ell \rightarrow \infty$. Moreover, the uniform stability of the linear operator $\pi_\ell - \pi$ and $|\mathbf{m}| \leq 1$ almost everywhere in Ω_T yields

$$\begin{aligned} \langle \pi_\ell(\mathbf{m}(t)) - \pi(\mathbf{m}(t)), \phi(t) \rangle &\leq \|\pi_\ell(\mathbf{m}(t)) - \pi(\mathbf{m}(t))\|_{\mathbf{L}^2(\Omega)} \|\phi(t)\|_{\mathbf{L}^2(\Omega)} \\ &\lesssim \|\mathbf{m}(t)\|_{\mathbf{L}^2(\Omega)} \|\phi(t)\|_{\mathbf{L}^2(\Omega)} := g(t). \end{aligned}$$

Since $g \in L^1(0, T)$, the Lebesgue dominated convergence theorem proves that the first scalar product in (3.1.9) tends to zero as $\ell \rightarrow 0$. For the second scalar product, we argue similarly. We write

$$\begin{aligned} (\pi_\ell(\mathbf{m}) - \pi_\ell(\mathbf{m}_\ell), \phi) &= \int_0^T \langle \pi_\ell(\mathbf{m}(t) - \mathbf{m}_\ell(t)), \phi(t) \rangle dt \\ &\lesssim \int_0^T \|\mathbf{m}(t) - \mathbf{m}_\ell(t)\|_{\mathbf{L}^2(\Omega)} \|\phi(t)\|_{\mathbf{L}^2(\Omega)} dt \\ &\leq \|\mathbf{m} - \mathbf{m}_\ell\|_{\mathbf{L}^2(\Omega_T)} \|\phi\|_{\mathbf{L}^2(\Omega_T)}, \end{aligned}$$

since the operators π_ℓ are linear and uniformly stable and the integrands are positive. Altogether, we have seen that the scalar product in (3.1.9) tends to zero as $\ell \rightarrow \infty$. We thus conclude weak convergence in $\mathbf{L}^2(\Omega_T)$. \square

Remark. Similar arguments to those in the proof of Lemma 3.1.2 show that strong $\mathbf{L}^2(\Omega)$ -convergence $\pi_h(\mathbf{n}) \rightarrow \pi(\mathbf{n})$ for all $\mathbf{n} \in \mathbf{L}^2(\Omega)$ instead of (3.1.7) also yields strong convergence $\pi_h(\mathbf{m}_{hk}^-) \rightarrow \pi(\mathbf{m})$ in $\mathbf{L}^2(\Omega)$.

Remark. A result similar to Lemma 3.1.2 is also given in [Gol12, Lemma 4.0.2]. We emphasize, however, that we consider an abstract framework, whereas in [Gol12], only the strayfield contribution was considered. Moreover, the result from [Gol12] requires stronger assumptions.

Before we come to the actual algorithm for strayfield computation and the more involved multiscale problem, we briefly recall some integral operators and their mapping properties.

Integral operators and mapping properties

The following applications need two integral operators for either Γ , namely the double-layer potential \tilde{K} and the simple-layer potential \tilde{V} , which formally read

$$(\tilde{K}v)(x) = \frac{1}{4\pi} \int_{\Gamma} \frac{(x-y) \cdot \mathbf{n}(y)}{|x-y|^3} v(y) d\Gamma(y), \quad (3.1.10)$$

$$(\tilde{V}\phi)(x) = \frac{1}{4\pi} \int_{\Gamma} \frac{1}{|x-y|} \phi(y) d\Gamma(y), \quad (3.1.11)$$

for all $x \in \mathbb{R}^3 \setminus \Gamma$. These operators allow extension to bounded, linear operators $\tilde{K} : H^{1/2}(\Gamma) \rightarrow H^1(\mathbb{R}^3 \setminus \Gamma)$ and $\tilde{V} : H^{-1/2}(\Gamma) \rightarrow H^1(\mathbb{R}^3)$, see e.g. [McL00, HW08, SS11]. There holds

$$\Delta \tilde{K}v = \Delta \tilde{V}\phi = 0 \quad \text{on } \mathbb{R}^3 \setminus \Gamma \quad \text{and} \quad \tilde{K}v, \tilde{V}\phi \in C^\infty(\mathbb{R}^3 \setminus \Gamma) \quad (3.1.12)$$

at least if ϕ admits the additional regularity $\phi \in L^2(\Gamma)$. Via restriction to the boundary Γ , one obtains

$$(\tilde{K}v)^{\text{int}} = (K - 1/2)v \quad \text{and} \quad (\tilde{V}\phi)^{\text{int}} = V\phi, \quad (3.1.13)$$

where the operators $K : H^{1/2}(\Gamma) \rightarrow H^{1/2}(\Gamma)$ and $V : H^{-1/2}(\Gamma) \rightarrow H^{1/2}(\Gamma)$ coincide formally with \tilde{K} and \tilde{V} , but are evaluated on the boundary Γ . There hold the following jump properties across the boundary Γ , cf. e.g. [SS11, Theorem 3.3.1]:

$$(\tilde{K}v)^{\text{ext}} - (\tilde{K}v)^{\text{int}} = v, \quad \partial_{\mathbf{n}}^{\text{ext}} \tilde{K}v - \partial_{\mathbf{n}}^{\text{int}} \tilde{K}v = 0, \quad (3.1.14)$$

$$(\tilde{V}\phi)^{\text{ext}} - (\tilde{V}\phi)^{\text{int}} = 0, \quad \partial_{\mathbf{n}}^{\text{ext}} \tilde{V}\phi - \partial_{\mathbf{n}}^{\text{int}} \tilde{V}\phi = -\phi. \quad (3.1.15)$$

Here, the superscripts *int* and *ext* indicate whether the trace is considered from inside Ω or the exterior domain $\mathbb{R}^3 \setminus \overline{\Omega}$.

Fredkin/Koehler approach for strayfield computation

In the following, we present the approach of FREDKIN and KOEHLER [FK90] for the approximate computation of the strayfield contribution and show that it satisfies the desired properties.

Let $\mathbf{m} \in L^2(\Omega)$ be given. We aim to solve the transmission problem

$$\begin{aligned} \Delta u &= \nabla \cdot \mathbf{m} && \text{in } \Omega, \\ \Delta u &= 0 && \text{in } \mathbb{R}^3 \setminus \overline{\Omega}, \\ u^{\text{ext}} - u^{\text{int}} &= 0 && \text{on } \Gamma, \\ \partial_{\mathbf{n}} u^{\text{ext}} - \partial_{\mathbf{n}} u^{\text{int}} &= -\mathbf{m} \cdot \mathbf{n} && \text{on } \Gamma, \\ u(x) &= \mathcal{O}(1/|x|) && \text{as } |x| \rightarrow \infty \end{aligned} \quad (3.1.16)$$

from (1.3.6). To that end, We split the solution u into two partial solutions u_1 and u_2 . In a first step, let $u_1 \in H^1(\Omega)$ with $\int_{\Omega} u_1 dx = 0$ be the unique solution of the Neumann problem

$$\begin{aligned} \Delta u_1 &= \nabla \cdot \mathbf{m} && \text{in } \Omega, \\ \partial_{\mathbf{n}} u_1 &= \mathbf{m} \cdot \mathbf{n} && \text{on } \Gamma, \end{aligned} \quad (3.1.17)$$

and extend u_1 by zero to the entire space $\mathbb{R}^3 \setminus \overline{\Omega}$. Then, the remainder $u_2 = u - u_1$ satisfies

$$\begin{aligned} \Delta u_2 &= 0 && \text{in } \Omega, \\ \Delta u_2 &= 0 && \text{in } \mathbb{R}^3 \setminus \overline{\Omega}, \\ u_2^{\text{ext}} - u_2^{\text{int}} &= u_1^{\text{int}} && \text{on } \Gamma, \\ \partial_{\mathbf{n}} u_2^{\text{ext}} - \partial_{\mathbf{n}} u_2^{\text{int}} &= 0 && \text{on } \Gamma, \\ u_2(x) &= \mathcal{O}(1/|x|) && \text{as } |x| \rightarrow \infty. \end{aligned} \quad (3.1.18)$$

It is well-known that the unique solution $u_2 \in H^1(\mathbb{R}^3 \setminus \Gamma)$ of the transmission problem (3.1.18) is the double-layer potential

$$u_2(x) = (\tilde{K}u_1^{\text{int}})(x) := \frac{1}{4\pi} \int_{\Gamma} \frac{(y-x) \cdot \mathbf{n}(y)}{|y-x|^3} u_1^{\text{int}}(y) d\Gamma(y) \quad \text{for all } x \in \mathbb{R}^3 \setminus \Gamma, \quad (3.1.19)$$

see e.g. [McL00]. The trace jump of the double-layer potential, where the integral operator K formally coincides to \tilde{K} , but is evaluated for $x \in \Gamma$, is given by $(\tilde{K}u_1^{\text{int}})^{\text{int}} = (K - 1/2)u_1^{\text{int}}$. From the combination of (3.1.12) and (3.1.19), we now get $\Delta u_2 = \Delta \tilde{K}u_1 = 0$ on $\mathbb{R}^3 \setminus \Gamma$. Consequently, u_2 on Ω is characterized by the inhomogeneous Dirichlet problem

$$\begin{aligned} \Delta u_2 &= 0 && \text{in } \Omega, \\ u_2^{\text{int}} &= (K - 1/2)u_1^{\text{int}} && \text{on } \Gamma, \end{aligned} \quad (3.1.20)$$

and we have $u = u_1 + u_2$. Altogether, the strayfield operator is then given by $\boldsymbol{\pi}(\mathbf{m}) = \mathcal{P}(\mathbf{m}) = \nabla u = \nabla u_1 + \nabla u_2$ in Ω .

To discretize these equations, we use lowest-order Courant finite elements: First, let $u_{1h} \in \mathcal{S}^1(\mathcal{T}_h)$ with $\int_{\Omega} u_{1h} dx = 0$ be the unique FE solution of

$$\int_{\Omega} \nabla u_{1h} \cdot \nabla v_h dx = \int_{\Omega} \mathbf{m} \cdot \nabla v_h dx \quad \text{for all } v_h \in \mathcal{S}^1(\mathcal{T}_h) \text{ with } \int_{\Omega} v_h dx = 0. \quad (3.1.21)$$

Note, that integration by parts was performed twice here, and the boundary data cancel out due to $\partial_{\mathbf{n}} u_1 = \mathbf{m} \cdot \mathbf{n}$. Moreover, since $\text{div } \mathbf{m}$ is employed in a weak sense, only $\mathbf{L}^2(\Omega)$ -regularity of \mathbf{m} is required instead of $\mathbf{m} \in \mathbf{H}(\text{div})$. Since a finite element solution $u_{2h} \in \mathcal{S}^1(\mathcal{T}_h)$ of (3.1.20) cannot satisfy continuous Dirichlet data $(K - 1/2)u_{1h}^{\text{int}}$, we employ a Clément-type quasi-interpolation operator $I_h : H^{1/2}(\Gamma) \rightarrow \mathcal{S}^1(\mathcal{T}_h|_{\Gamma})$, e.g. the Scott-Zhang projection [SZ80]. Then, we let $u_{2h} \in \mathcal{S}^1(\mathcal{T}_h)$ with $u_{2h}^{\text{int}} = I_h(K - 1/2)u_{1h}^{\text{int}}$ be the unique solution of the inhomogeneous Dirichlet problem

$$\int_{\Omega} \nabla u_{2h} \cdot \nabla v_h dx = 0 \quad \text{for all } v_h \in \mathcal{S}^1(\mathcal{T}_h) \text{ with } v_h^{\text{int}} = 0. \quad (3.1.22)$$

The following proposition is found in [Gol12, Lemma 4.3.5] and applies, in particular, for the Scott-Zhang projection.

Proposition 3.1.3. *Suppose that the operator $I_h : L^2(\Gamma) \rightarrow \mathcal{S}^1(\mathcal{T}_h|_{\Gamma})$ satisfies L^2 - and H^1 -stability*

$$\|I_h v\|_{L^2(\Gamma)} \leq C_8 \|v\|_{L^2(\Gamma)} \quad \text{resp.} \quad \|\nabla_{\Gamma} I_h v\|_{L^2(\Gamma)} \leq C_8 \|\nabla_{\Gamma} v\|_{L^2(\Gamma)} \quad (3.1.23)$$

as well as a first-order approximation property

$$\|(1 - I_h)v\|_{L^2(\Gamma)} \leq C_8 h \|\nabla_{\Gamma} v\|_{L^2(\Gamma)} \quad (3.1.24)$$

for all $v \in H^1(\Gamma)$. Here, ∇_Γ denotes the surface gradient, and we suppose that the constant $C_8 > 0$ stays bounded as $h \rightarrow 0$. Then, the operator $\pi_h(\mathbf{m}) := \nabla u_{1h} + \nabla u_{2h}$ defined via (3.1.21)–(3.1.22) satisfies $\pi_h \in L(\mathbf{L}^2(\Omega); \mathbf{L}^2(\Omega))$, and convergence (3.1.7) towards $\pi(\mathbf{m}) := \nabla u$ holds even strongly in $\mathbf{L}^2(\Omega)$. In particular, Lemma 3.1.2 applies and guarantees the assumptions (2.3.2) and (2.3.4). \square

Remark . Besides the famous FREDKIN/KOEHLER approach, there are other ways to approximatively compute the strayfield. Those include the analytic projection approach after PRAETORIUS [Pra04], the symmetric FEM-BEM coupling after COSTABEL [Cos88], as well as the JOHNSON/NÉDÉLEC coupling [JN80]. Moreover, all of those approaches are compatible with our general framework as they guarantee the assumptions (2.3.2) and (2.3.4) analogously to the FREDKIN/KOEHLER approach. The interested reader is referred to [Gol12, Chapter 4] where all the proofs can be found.

Remark . We like to emphasize that the results of this section are also covered by the more general result on uniformly monotone operators from the next section.

Remark . The strayfield contribution, as well as its discretization (if chosen wisely), fit well into the setting of improved energy estimates in the sense of Lemma 2.4.1. We have already seen in the introduction, that the strayfield operator $\mathcal{P}(\cdot)$ with $\mathcal{P}(\mathbf{m}) = \nabla u$ is uniformly bounded in \mathbf{L}^4 , cf. (1.3.8) and self-adjoint, cf. (1.3.9). Now, let us consider the projection approach after PRAETORIUS [Pra04]. Here, the discretized operator is given by

$$\mathcal{P}_h := \Pi_h \mathcal{P} \Pi_h : \mathbf{L}^2(\Omega) \longrightarrow \mathcal{P}^0(\mathcal{T}_h),$$

where the operator Π_h denotes the \mathbf{L}^2 -orthogonal projection onto the piecewise constant functions $\mathcal{P}^0(\mathcal{T}_h)$, i.e. the elementwise integral mean. We refer to [Pra04, Gol12] for details. By definition, we thus even get self-adjointness as well as uniform \mathbf{L}^4 -boundedness of the discrete operator \mathcal{P}_h . This can be seen as follows: For each element T_i , the Jensen inequality [Eva02, B.1, Theorem 2] yields for the convex function $(\cdot)^4$

$$\begin{aligned} \|\Pi_h \mathbf{n}\|_{\mathbf{L}^4(T_i)} &= \left(\int_{T_i} \left(\frac{1}{|T_i|} \int_{T_i} \mathbf{n} \right)^4 \right)^{1/4} \\ &= \left(\left(\frac{1}{|T_i|} \int_{T_i} \mathbf{n} \right)^4 |T_i| \right)^{1/4} \\ &\leq \left(\frac{|T_i|}{|T_i|} \int_{T_i} \mathbf{n}^4 \right)^{1/4} \\ &= \|\mathbf{n}\|_{\mathbf{L}^4(T_i)}. \end{aligned}$$

In combination with

$$\|\Pi_h \mathbf{n}\|_{\mathbf{L}^4(\Omega)}^4 = \sum_{T_i} \|\Pi_h \mathbf{n}\|_{\mathbf{L}^4(T_i)}^4 \leq \sum_{T_i} \|\mathbf{n}\|_{\mathbf{L}^4(T_i)}^4 = \|\mathbf{n}\|_{\mathbf{L}^4(\Omega)}^4,$$

this yields

$$\|\Pi_h \mathcal{P} \Pi_h \mathbf{m}\|_{\mathbf{L}^4(\Omega)} \leq \|\mathcal{P} \Pi_h \mathbf{m}\|_{\mathbf{L}^4(\Omega)} \lesssim \|\Pi_h \mathbf{m}\|_{\mathbf{L}^4(\Omega)} \leq \|\mathbf{m}\|_{\mathbf{L}^4}.$$

Hence the additional assumptions for the improved energy estimate are fulfilled.

3.2. Uniformly monotone operators

In this section, we consider an extension of the above framework. We allow the general field contribution $\pi(\cdot)$ and its discretization $\pi_h(\cdot)$ to depend not only on the magnetization, but also an additional contribution $\zeta \in \mathbf{L}^2(Y_T) = L^2([0, T], Y)$ for some Banach space Y . In the showcase example of the next section, ζ will simply be the applied field \mathbf{f} . In particular, the analysis therefore includes a discretization \mathbf{f}_{hk}^- of \mathbf{f} . Suitable discretizations are discussed in Section 3.1.2. We stress, however, that more general ζ are possible. In total, the effective field thus reads

$$\mathbf{h}_{\text{eff}} = C_e \nabla \mathbf{m} + \pi(\mathbf{m}, \zeta). \quad (3.2.1)$$

Given this additional dependence, the assumptions (2.3.2) and (2.3.4) have to be slightly modified. Altogether we derive the following result which is stated in analogy to the main theorem 2.3.1.

Theorem 3.2.1. *(a) Let $\theta \in (1/2, 1]$ and suppose that the spatial meshes \mathcal{T}_h are uniformly shape regular and satisfy the angle condition*

$$\int_{\Omega} \nabla \eta_i \cdot \nabla \eta_j \leq 0 \quad \text{for all basis functions } \eta_i, \eta_j \in \mathcal{S}^1(\mathcal{T}_h^{\Omega}) \text{ with } i \neq j. \quad (3.2.2)$$

Define functions $\mathbf{f}_{hk}^- \in \mathcal{P}^0(\mathcal{I}_k; \mathbf{L}^2(\Omega))$ and $\zeta_{hk}^- \in \mathcal{P}^0(\mathcal{I}_k; Y)$ by $\mathbf{f}_{hk}^-(t) := \mathbf{f}_h^j$, $\zeta_{hk}^-(t) := \zeta_h^j$ for $t_j \leq t < t_{j+1}$. We suppose that

$$\mathbf{f}_{hk}^- \xrightarrow{\text{sub}} \mathbf{f} \quad \text{weakly convergent in } \mathbf{L}^2(\Omega_T) \quad (3.2.3)$$

Moreover, we suppose that the spatial discretization $\pi_h(\cdot, \cdot)$ of $\pi(\cdot, \cdot)$ satisfies

$$\|\pi_h(\mathbf{n}, y)\|_{\mathbf{L}^2(\Omega)} \leq C_{29} \quad (3.2.4)$$

for all $h, k > 0$ and all $\mathbf{n} \in \mathbf{L}^2(\Omega)$ with $|\mathbf{n}| \leq 1$ almost everywhere in Ω and $y \in Y$ with $\|y\|_Y \leq C_{10}$ for some y -independent constant $C_{10} > 0$. Here, $C_{29} > 0$ denotes a constant that is independent of h, k, \mathbf{n} , and y , but may depend on C_{10} and Ω . We further assume $\|\zeta_h^j\|_Y \leq C_{10}$ for all $j = 1, \dots, N$. Under these assumptions, we have strong $\mathbf{L}^2(\Omega_T)$ -subconvergence of \mathbf{m}_{hk}^- towards some function \mathbf{m} .

(b) In addition to the above, we assume $\mathbf{m}_h^0 \rightharpoonup \mathbf{m}^0$ weakly in $\mathbf{H}^1(\Omega)$ and

$$\pi_h(\mathbf{m}_{hk}^-, \zeta_{hk}^-) \xrightarrow{\text{sub}} \pi(\mathbf{m}, \zeta) \quad \text{weakly subconvergent in } \mathbf{L}^2(\Omega_T). \quad (3.2.5)$$

Then, the computed FE solutions \mathbf{m}_{hk} are weakly subconvergent in $\mathbf{H}^1(\Omega_T)$ to a weak solution $\mathbf{m} \in \mathbf{H}^1(\Omega_T)$ of general LLG.

Proof. The proof is verbatim to that of Theorem 2.3.1 without the time dependent field contribution. \square

Before we come to an example of this new field contribution, we investigate the criteria under which the assumptions (3.2.4) and (3.2.5) are valid. In contrast to the pointwise, respectively linear and continuous setting from before, we now extend the analysis to (possibly nonlinear)

uniformly monotone operators in the setting of the Browder Minty Theorem [Zei90, Section 26.2].

Let X be a separable Hilbert space, $A : X \rightarrow X^*$ be a uniformly monotone, coercive, and hemicontinuous (nonlinear) operator, and $b \in X^*$. We consider the operator equation

$$Aw = b \quad (3.2.6)$$

and the corresponding Galerkin formulation

$$\langle Aw_h, v_h \rangle_{X_h^* \times X_h} = \langle b_h, v_h \rangle_{X_h^* \times X_h} \quad \text{for all } v_h \in X_h, \quad (3.2.7)$$

for finite dimensional subspaces $X_h \subseteq X_{h'} \subset X$, as $h > h'$. Then, we get the following result which goes back to BROWDER and MINTY.

Theorem 3.2.2 (Browder & Minty, 1963). *The following statements are true:*

- (a) *For each $b \in X^*$, the operator equation (3.2.6) admits a unique solution $w \in X$.*
- (b) *For each $b_h \in X^*$, the Galerkin formulation (3.2.7) admits a unique solution $w_h \in X$.*
- (c) *If we have $\|b_h\|_{X^*} \leq M < \infty$, then the sequence of Galerkin solutions is bounded, i.e. $\|w_h\|_{X_h} \leq C < \infty$. Here, the h -independent constant $C > 0$ depends only on M and the coercivity of A . In particular, the sequence (w_h) is weakly subconvergent in X towards some limit $w \in X$. If $\lim_{h \rightarrow 0} \|b - b_h\|_{X_h^*} = 0$, this limit solves the operator equation (3.2.6).*
- (d) *Due to the uniform monotonicity of A , there even holds strong convergence $\lim_{h \rightarrow 0} \|w - w_h\|_X = 0$ of the entire sequence.*

Proof. The proof is along the lines of [Zei90, Theorem 26.A] with only minor modifications concerning the strong convergence $\|b_h - b\|_{X^*}$. \square

This framework is now used in the following lemma which guarantees the assumptions (3.2.4)–(3.2.5) of Theorem 3.2.1 for certain field contributions:

Lemma 3.2.3. *Let Y be a Banach space and let $S, S_h \in L(X, \mathbf{L}^2(\Omega))$, and $T, T_h \in L(\mathbf{L}^2(\Omega) \times Y, X^*)$ with*

$$S_h x \rightarrow Sx \quad \text{weakly in } \mathbf{L}^2(\Omega) \text{ for all } x \in X, \quad (3.2.8)$$

$$T_h(\mathbf{n}, y) \rightarrow T(\mathbf{n}, y) \quad \text{strongly in } X^* \text{ for all } \mathbf{n} \in \mathbf{L}^2(\Omega), y \in Y, \quad (3.2.9)$$

and $\pi(\cdot) := SA^{-1}T : \mathbf{L}^2(\Omega) \times Y \rightarrow \mathbf{L}^2(\Omega)$. For $h > 0$, $\mathbf{n} \in \mathbf{L}^2(\Omega)$, and $y \in Y$, define the approximate operator $\pi_h(\mathbf{n}, y) := S_h u_h$, where u_h is the unique Galerkin solution of

$$\langle Au_h, v_h \rangle_{X_h^* \times X_h} = \langle T_h(\mathbf{n}, y), v_h \rangle_{X_h^* \times X_h} \quad \text{for all } v_h \in X_h. \quad (3.2.10)$$

Under the foregoing assumptions, it holds that

$$\|\pi_h(\mathbf{n}, y)\|_{\mathbf{L}^2(\Omega)} \leq C_{12} \quad (3.2.11)$$

for all $\mathbf{n} \in \mathbf{L}^2(\Omega)$ with $|\mathbf{n}| \leq 1$ almost everywhere and all $y \in Y$ with $\|y\|_Y \leq C_{11}$ for some constant $C_{11} > 0$, and for all $h > 0$. The constant $C_{12} > 0$ does not depend on y and \mathbf{n} , but only on Ω and C_{11} . Moreover, strong subconvergence $(\mathbf{m}_{hk}^-, \zeta_{hk}^-) \rightarrow (\mathbf{m}, \zeta)$ in $\mathbf{L}^2([0, T]; (\mathbf{L}^2(\Omega) \times Y)) = \mathbf{L}^2(\mathbf{L}^2(\Omega) \times Y)$ for some sequence $\zeta_{hk}^- \in L^\infty(Y)$ implies weak subconvergence $\pi_h(\mathbf{m}_{hk}^-, \zeta_{hk}^-) \rightharpoonup \pi(\mathbf{m}, \zeta)$ in $\mathbf{L}^2(\Omega_T)$ as $(h, k) \rightarrow (0, 0)$. In particular, the assumptions (3.2.4) and (3.2.5) are satisfied.

Proof. The Banach-Steinhaus theorem implies uniform boundedness $C_S := \sup_{h>0} \|S_h\| < \infty$ and $C_T := \sup_{h>0} \|T_h\| < \infty$ of the respective operator norms. For fixed $\mathbf{n} \in \mathbf{L}^2(\Omega)$ with $|\mathbf{n}| \leq 1$ almost everywhere, $y \in Y$ with $\|y\|_Y \leq C_{11}$, and $b_h := T_h(\mathbf{n}, y)$, this implies

$$\|b_h\|_{X^*} \leq C_T \|(\mathbf{n}, y)\|_{\mathbf{L}^2(\Omega) \times Y} \leq C_T (|\Omega| + C_{11}^2)^{1/2} =: M < \infty.$$

Thus, from the Browder-Minty theorem, we infer $\|u_h\|_X \leq C < \infty$, where $C > 0$ does neither depend on h nor on (\mathbf{n}, y) , but only on M . Consequently, this proves (3.2.11) with $C_{12} = CC_S$.

Next, we aim to show that $\pi_h(\mathbf{n}_h, y_h) \rightharpoonup \pi(\mathbf{n}, y)$ weakly in $\mathbf{L}^2(\Omega)$ as $h \rightarrow 0$ provided that $(\mathbf{n}_h, y_h) \rightarrow (\mathbf{n}, y)$ strongly in $\mathbf{L}^2(\Omega) \times Y$. By assumption (3.2.9) on T_h , we have $T_h(\mathbf{n}, y) \rightarrow T(\mathbf{n}, y)$ strongly in X^* as $h \rightarrow 0$. Together with uniform boundedness of T_h , this implies

$$T_h(\mathbf{n}_h, y_h) = T_h(\mathbf{n}, y) - T_h(\mathbf{n} - \mathbf{n}_h, y - y_h) \rightarrow T(\mathbf{n}, y) \quad \text{strongly in } X^* \text{ as } h \rightarrow 0.$$

Therefore, the Browder-Minty theorem for uniformly monotone operators guarantees $u_h \rightarrow u$ strongly in X , where $u = A^{-1}T(\mathbf{n}, y)$ and $u_h \in X_h$ solves (3.2.10) with (\mathbf{n}, y) replaced by (\mathbf{n}_h, y_h) . The convergence assumption (3.2.8), the uniform boundedness of S_h , and the strong convergence $\|u_h - u\|_{\mathbf{L}^2(\Omega)} \rightarrow 0$ thus show

$$\pi_h(\mathbf{n}_h, y_h) = S_h u_h = S_h u - S_h(u - u_h) \rightharpoonup S u = \pi(\mathbf{n}, y) \text{ weakly in } \mathbf{L}^2(\Omega) \text{ as } h \rightarrow 0.$$

Finally, we prove weak subconvergence $\pi_h(\mathbf{m}_{hk}^-, \zeta_{hk}^-) \rightharpoonup \pi(\mathbf{m}, \zeta)$ in $\mathbf{L}^2(\Omega_T)$ as $(h, k) \rightarrow (0, 0)$. To that end, we choose sequences $h_\ell \rightarrow 0$, $k_\ell \rightarrow 0$ such that $(\mathbf{m}_\ell, \zeta_\ell) := (\mathbf{m}_{h_\ell k_\ell}^-, \zeta_{h_\ell k_\ell}^-)$ converges strongly in $L^2(\mathbf{L}^2(\Omega) \times Y)$ to (\mathbf{m}, ζ) . By extracting a further subsequence, we may assume that $\mathbf{m}_\ell(t) \rightarrow \mathbf{m}(t)$ strongly in $\mathbf{L}^2(\Omega)$ as well as $\zeta_\ell(t) \rightarrow \zeta(t)$ in Y , for almost all times t . Define $\pi_\ell := \pi_{h_\ell}$ and let $\phi \in \mathbf{L}^2(\Omega_T)$. Then,

$$(\pi_\ell((\mathbf{m}_\ell, \zeta_\ell)) - \pi((\mathbf{m}, \zeta)), \phi) = \int_0^T \langle \pi_\ell((\mathbf{m}_\ell(t), \zeta_\ell(t))) - \pi((\mathbf{m}(t), \zeta(t))), \phi(t) \rangle dt.$$

From weak convergence $\pi_\ell((\mathbf{m}_\ell(t), \zeta_\ell(t))) \rightharpoonup \pi((\mathbf{m}(t), \zeta(t)))$ as $\ell \rightarrow \infty$ for almost all times t , we see pointwise convergence of the integrand to zero. According to (3.2.11) and the assumption $\zeta_{hk}^- \in L^\infty(Y)$, the Lebesgue dominated convergence theorem thus proves

$$(\pi_\ell((\mathbf{m}_\ell, \zeta_\ell)) - \pi((\mathbf{m}, \zeta)), \phi) \rightarrow 0 \quad \text{as } \ell \rightarrow \infty.$$

This concludes the proof. \square

Remark. (i) Similar arguments as in the proof of Lemma 3.2.3 reveal that strong convergence $S_h x \rightarrow S x$ in (3.2.8) also results in strong convergence $\pi_h(\mathbf{m}_{hk}^-, \zeta_{hk}^-) \rightarrow \pi(\mathbf{m}, \zeta)$ in $\mathbf{L}^2(\Omega_T)$ as $h, k \rightarrow 0$.

(ii) The abstract framework applies, in particular, to linear contributions $\pi_h(\cdot) = S_h$ of the effective field \mathbf{h}_{eff} , where $X = \mathbf{L}^2(\Omega)$, $Y = \{0\}$, and the operators A and $T = T_h$ are just the identities. In this case, we have $\zeta_{hk}^- = 0$ for all $(h, k) > 0$ and thus $\mathbf{L}^2(\Omega) \hookrightarrow \mathbf{L}^2(\Omega) \times Y$ is the canonical embedding with $\mathbf{L}^2(\Omega) \cong \{(x, 0) : x \in \mathbf{L}^2(\Omega)\}$. In particular, we may therefore write $\pi_h(\mathbf{m}_{hk}^-, \zeta_{hk}^-) = \pi_h(\mathbf{m}_{hk}^-)$. The (linear) strayfield contribution is thus also covered by the more general result of Lemma 3.2.3.

(iii) For the upcoming multiscale example, we will use $Y = \mathbf{H}(\text{div}; \Omega_2)$ for some domain Ω_2 , $\zeta_{hk}^- = \mathbf{f}_{hk}^-$, and $\zeta = \mathbf{f}$, respectively.

In the next section, we finally present a nonlinear and uniformly monotone operator $\pi(\cdot, \cdot)$ which is covered by the theory of Lemma 3.2.3. This operator models a multiscale problem which was first introduced in [Bru13].

3.2.1. Multiscale problems

In our model, we consider two separated ferromagnetic bodies Ω_1 and Ω_2 as schematized in Figure 3.1. Let $\Omega_1, \Omega_2 \subset \mathbb{R}^3$ be bounded Lipschitz domains with Euclidean distance $\text{dist}(\Omega_1, \Omega_2) > 0$ and boundaries $\Gamma_1 = \partial\Omega_1$ resp. $\Gamma_2 = \partial\Omega_2$. On the microscopic part Ω_1 , we are interested in the domain configuration and thus solve the LLG equation to obtain the magnetization $\mathbf{m}_1 : \Omega_1 \rightarrow \mathbb{R}^3$. On Ω_2 , we will use the macroscopic Maxwell equations with a (possibly nonlinear) material law instead.

To motivate this setting, we consider a magnetic recording head (see Figure 3.1). The microscopic sensor element is based on the giant magnetoresistance (GMR) effect, and it requires the use of LLG in order to describe the short range interactions between the individual layers of the sensor accurately. On the other hand, the smaller these sensor elements, the more important becomes the shielding of the strayfield of neighboring data bits. In practice, this is achieved by means of some macroscopic softmagnetic shields located directly besides the GMR sensor. Describing these large components by use of LLG would lead to very large problem sizes, because the detailed domain structure within the magnetic shields would be calculated. The macroscopic Maxwell equations allow to overcome this limitation and thus provide a profound method to describe the influence of the shields in an averaged sense. For more details and motivation of this model, the interested reader is referred to [Bru13].

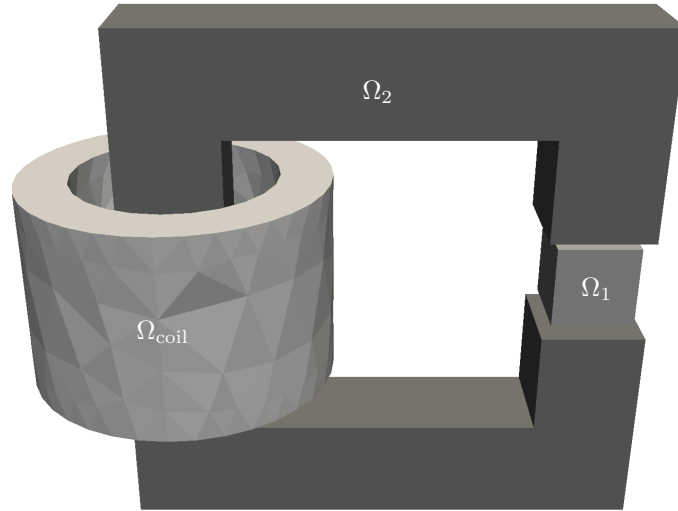


Figure 3.1.: Example geometry which demonstrates model separation into LLG region Ω_1 and Maxwell region Ω_2 (and in this case in an electric coil region Ω_{coil}). Here, Ω_1 represents one grain of a recording media and Ω_2 shows a simple model of a recording write head. — Picture taken from [BFF⁺12], copyright of Florian Bruckner is thankfully acknowledged.

Problem formulation

In this section, we present some details of the modeling, as well as the computation and discretization, of the multiscale operator. This was developed in joint work with THOMAS FÜHRER and is published in [BFF⁺12]. We start with the magnetostatic Maxwell's equations

(see e.g. [Mon08])

$$\nabla \times \mathbf{H} = \mathbf{j} \quad \text{and} \quad \nabla \cdot \mathbf{B} = 0 \quad \text{in } \mathbb{R}^3, \quad (3.2.12)$$

where $\mathbf{H} : \mathbb{R}^3 \rightarrow \mathbb{R}^3$ is the magnetic field strength and where the magnetic flux density $\mathbf{B} : \mathbb{R}^3 \rightarrow \mathbb{R}^3$ is given by

$$\mathbf{B} = \mu_0(\mathbf{H} + \mathbf{m}) \quad \text{in } \mathbb{R}^3. \quad (3.2.13)$$

Here, μ_0 denotes the permeability of vacuum. The current density \mathbf{j} is the source of the magnetic field strength \mathbf{H} . The magnetization field \mathbf{m} is non-trivial on the magnetic bodies $\Omega_1 \cup \Omega_2$, but vanishes in $\mathbb{R}^3 \setminus (\overline{\Omega_1 \cup \Omega_2})$. The total magnetic field is split into

$$\mathbf{H} = \mathbf{H}_1 + \mathbf{H}_2 + \mathbf{f}, \quad (3.2.14)$$

where $\mathbf{H}_j : \mathbb{R}^3 \rightarrow \mathbb{R}^3$ is the magnetic field induced by the magnetization \mathbf{m} on Ω_j and \mathbf{f} is the applied field generated by the current density \mathbf{j} in $\mathbb{R}^3 \setminus \overline{\Omega_1 \cup \Omega_2}$. We thus have

$$\nabla \times \mathbf{f} = \mathbf{j} \quad \text{and therefore} \quad \nabla \times \mathbf{H}_j = 0 \quad \text{in } \mathbb{R}^3. \quad (3.2.15)$$

In particular, the de Rham complex tells us that the induced fields are gradient fields $\mathbf{H}_j = -\nabla u_j$ with certain scalar potentials $u_j : \mathbb{R}^3 \rightarrow \mathbb{R}$. For this model, we assume that \mathbf{f} is induced by electric currents only, but not by magnetic monopoles, which yields

$$\nabla \cdot \mathbf{f} = 0 \quad \text{in } \mathbb{R}^3. \quad (3.2.16)$$

Moreover, the sources of \mathbf{H}_j lie inside Ω_j only and hence

$$\nabla \cdot \mathbf{H}_j = 0 \quad \text{in } \mathbb{R}^3 \setminus \overline{\Omega_j}. \quad (3.2.17)$$

Since we assumed no sources for \mathbf{B} , i.e. (3.2.12), we obtain

$$0 = \nabla \cdot \mathbf{B} = \mu_0(\nabla \cdot \mathbf{H} + \nabla \cdot \mathbf{m}) = \mu_0(\nabla \cdot \mathbf{H}_j + \nabla \cdot \mathbf{m}) \quad \text{on } \Omega_j. \quad (3.2.18)$$

Together with $\mathbf{H}_j = -\nabla u_j$ and (3.2.17), this reveals

$$\Delta u_j = \nabla \cdot \mathbf{m} \quad \text{in } \Omega_j, \quad (3.2.19a)$$

$$\Delta u_j = 0 \quad \text{in } \mathbb{R}^3 \setminus \overline{\Omega_j}. \quad (3.2.19b)$$

For the micromagnetic body Ω_1 , the respective magnetization $\mathbf{m}_1 = \mathbf{m}|_{\Omega_1}$ is computed by solving the LLG equation. The overall transmission problem (3.2.19) is then supplemented by boundary conditions as well as a radiation condition and reads

$$\Delta u_1 = \nabla \cdot \mathbf{m}_1 \quad \text{in } \Omega_1, \quad (3.2.20a)$$

$$\Delta u_1 = 0 \quad \text{in } \mathbb{R}^3 \setminus \overline{\Omega_1}. \quad (3.2.20b)$$

$$u_1^{\text{ext}} - u_1^{\text{int}} = 0 \quad \text{on } \Gamma_1, \quad (3.2.20c)$$

$$\partial_{\mathbf{n}} u_1^{\text{ext}} - \partial_{\mathbf{n}} u_1^{\text{int}} = -\mathbf{m}_1 \cdot \mathbf{n} \quad \text{on } \Gamma_1, \quad (3.2.20d)$$

$$u_1(x) = \mathcal{O}(1/|x|) \quad \text{as } |x| \rightarrow \infty. \quad (3.2.20e)$$

Again, the superscripts *int* and *ext* indicate whether the trace is considered from inside Ω_1 (resp. Ω_2 in (3.2.23) below) or the exterior domain $\mathbb{R}^3 \setminus \overline{\Omega}_1$ (resp. $\mathbb{R}^3 \setminus \overline{\Omega}_2$ in (3.2.23) below). Moreover, \mathbf{n} denotes the outer unit normal vector on Γ_1 (resp. Γ_2 in (3.2.23) below), which points from Ω_1 (resp. Ω_2 in (3.2.23) below) to the exterior domain. On the macroscopic domain, we are not interested in the dynamics on the microscale and thus do not utilize LLG here. Instead, we involve a nonlinear material law

$$\mathbf{m} = \chi(|\mathbf{H}|)\mathbf{H} \quad \text{on } \Omega_2 \quad (3.2.21)$$

with a scalar function $\chi : \mathbb{R}_{\geq 0} \rightarrow \mathbb{R}$ and $|\cdot|$ the modulus. Obviously, the results we aim for impose some restrictions on χ . Many physically relevant examples are, however, covered by the theory and some are exemplified below.

For the computation of the potential u_2 , we introduce an auxiliary potential u_{app} . Recall that $\nabla \times \mathbf{f} = 0$ in Ω_2 . If Ω_2 is simply connected, we infer $\mathbf{f} = -\nabla u_{\text{app}}$ on Ω_2 with some potential $u_{\text{app}} : \Omega_2 \rightarrow \mathbb{R}$. According to (3.2.16) and up to an additive constant, u_{app} can be obtained as the unique solution of the Neumann problem

$$\Delta u_{\text{app}} = 0 \quad \text{in } \Omega_2, \quad (3.2.22a)$$

$$\partial_{\mathbf{n}} u_{\text{app}}^{\text{int}} = -\mathbf{f}^{\text{int}} \cdot \mathbf{n} \quad \text{on } \Gamma_2, \quad (3.2.22b)$$

with $\int_{\Omega_2} u_{\text{app}} dx = 0$. Note, that here we need the additional regularity $\mathbf{f} \in \mathbf{H}(\text{div})$, as for those functions, the normal trace is well-defined, i.e. the map $\mathbf{m} \mapsto \mathbf{m} \cdot \mathbf{n}$ is well-defined for $\mathbf{m} \in \mathbf{H}(\text{div})$, cf. e.g. [Mon08, Theorem 3.24]. The transmission problem for the total potential $u = u_1 + u_2 + u_{\text{app}}$ of the total magnetic field $\mathbf{H} = -\nabla u$ in Ω_2 and for the potential u_2 in $\mathbb{R}^3 \setminus \overline{\Omega}_2$, supplemented by a radiation condition, reads

$$\nabla \cdot ((1 + \chi(|\nabla u|))\nabla u) = 0 \quad \text{on } \Omega_2, \quad (3.2.23a)$$

$$\Delta u_2 = 0 \quad \text{on } \mathbb{R}^3 \setminus \overline{\Omega}_2, \quad (3.2.23b)$$

$$u_2^{\text{ext}} - u^{\text{int}} = -u_1^{\text{int}} - u_{\text{app}}^{\text{int}} \quad \text{on } \Gamma_2, \quad (3.2.23c)$$

$$\partial_{\mathbf{n}} u_2^{\text{ext}} - (1 + \chi(|\nabla u^{\text{int}}|))\partial_{\mathbf{n}} u^{\text{int}} = (\mathbf{H}_1^{\text{ext}} + \mathbf{f}^{\text{ext}}) \cdot \mathbf{n} \quad \text{on } \Gamma_2, \quad (3.2.23d)$$

$$u_2(x) = \mathcal{O}(1/|x|) \quad \text{as } |x| \rightarrow \infty, \quad (3.2.23e)$$

where (3.2.23a) follows from (3.2.12)–(3.2.17) and (3.2.21). The boundary conditions of (3.2.23) are derived from (3.2.12), which leads to $(\mathbf{H}^{\text{ext}} - \mathbf{H}^{\text{int}}) \cdot \mathbf{n} = 0$ on Γ_2 , and the continuity of u_2 on Γ_2 . Details on the computation of the above quantities are postponed to the next section.

Remark. In case of a linear material law $\chi(|\mathbf{H}|) = \chi \in \mathbb{R}_{>0}$ in (3.2.21), the transmission problem (3.2.23) simplifies to $(1 + \chi)\Delta u_2 = 0$ in Ω_2 , $u_2^{\text{ext}} - u_2^{\text{int}} = 0$ on Γ_2 , and $\partial_{\mathbf{n}} u_2^{\text{ext}} - (1 + \chi)\partial_{\mathbf{n}} u_2^{\text{int}} = (\mathbf{H}_1^{\text{ext}} + \mathbf{f}^{\text{ext}}) \cdot \mathbf{n}$ on Γ_2 in (3.2.23a), (3.2.23c), and (3.2.23d), respectively. In particular, the Neumann problem (3.2.22) does not have to be solved.

In the next part, we will discuss how the above problem can actually be computed, i.e. we will divide it into subproblems which are then individually analyzed.

Computation of the multiscale operator

Our goal is to apply Proposition 3.2.3 to the model problem, i.e. the computation of $\boldsymbol{\pi}(\mathbf{m}, \mathbf{f}) = \nabla u_2$ on Ω_1 . We therefore need to bring it into the appropriate form $\boldsymbol{\pi}(\mathbf{m}, \mathbf{f}) = S\mathbf{A}^{-1}T(\mathbf{m}, \mathbf{f})$

for suitable operators S , A , and T . In the following we consider the individual subproblems needed for the computation of ∇u_2 as well as their discretizations and assign the corresponding operators.

The computation of the total potential u , and therefore of u_2 , relies on the computation of the auxiliary potential u_{app} and the strayfield potential on Ω_2 . For a magnetization $\mathbf{m} \in \mathbf{L}^2(\Omega_1)$, we compute $u_1 \in H^1(\Omega_1)$ via the FREDKIN/KOEHLER-approach from Section 3.1.3 as solution of the strayfield operator on the microscopic part. To that end, u_1 is separated into u_{11} and u_{12} , where u_{11} is the solution of (3.1.17). Recall that u_{11} is extended by zero on $\mathbb{R}^3 \setminus \overline{\Omega}_1$. We therefore have $u_1 = u_{12} = \tilde{K}_1 u_{11}^{\text{int}}$. Here and subsequently,

$$K_i : H^{-1/2}(\Gamma_i) \rightarrow H^{1/2}(\Gamma_i) \quad \text{and} \quad V_i : H^{1/2}(\Gamma_i) \rightarrow H^{1/2}(\Gamma_i)$$

denote the operators from (3.1.10) and (3.1.11) on the corresponding boundaries $\Gamma_i = \partial\Omega_i$ for $i = 1, 2$.

According to (3.1.12), u_1 on Ω_2 then solves the inhomogeneous Dirichlet problem

$$\begin{aligned} -\Delta u_1 &= 0 && \text{in } \Omega_2, \\ u_1^{\text{int}} &= (\tilde{K}_1 u_{11}^{\text{int}})^{\text{int}} && \text{on } \Gamma_2. \end{aligned} \tag{3.2.24}$$

For the auxiliary potential u_{app} , (3.2.22) can be solved directly on Ω_2 . With respect to the abstract notation of Lemma 3.2.3, we introduce the continuous linear operator

$$\begin{aligned} \tilde{T} : \mathbf{L}^2(\Omega_1) \times \mathbf{H}(\text{div}; \Omega_2) &\rightarrow H^{1/2}(\Gamma_2) \times H^{-1/2}(\Gamma_2), \\ \tilde{T}(\mathbf{m}, \mathbf{f}) &= (u_1^{\text{int}} + u_{\text{app}}^{\text{int}}, \mathbf{f} \cdot \mathbf{n} - \partial_{\mathbf{n}} u_1^{\text{int}}). \end{aligned} \tag{3.2.25}$$

The space Y from Lemma 3.2.3 is thus given by $\mathbf{H}(\text{div}; \Omega_2)$.

In the next step, we then compute the total magnetostatic potential $u = u_1 + u_2 + u_{\text{app}}$ related to the macroscopic domain Ω_2 . With $\chi(|\nabla u|) = \chi(|\mathbf{f} - \nabla u_1 - \nabla u_2|)$, (3.2.23) is equivalently stated by means of the Johnson-Nédélec coupling from [JN80, AFF⁺13],

$$\begin{aligned} \int_{\Omega_2} (1 + \chi(|\nabla u|)) \nabla u \cdot \nabla v - \int_{\Gamma_2} \phi v &= - \int_{\Gamma_2} (\mathbf{f} \cdot \mathbf{n} - \partial_{\mathbf{n}} u_1^{\text{ext}}) v, \\ V_2 \phi - (K_2 - 1/2) u^{\text{int}} &= -(K_2 - 1/2) (u_1^{\text{int}} + u_{\text{app}}^{\text{int}}), \end{aligned} \tag{3.2.26}$$

for all $v \in H^1(\Omega_2)$. For more details, the reader is referred to [BFF⁺12] and the references therein. Recall that $u_1 \in C^\infty(\mathbb{R}^3 \setminus \overline{\Omega}_1) \subseteq H^2(\Omega_2)$, cf. (3.1.12). Therefore, it holds

$$\partial_{\mathbf{n}} u_1^{\text{ext}} = \partial_{\mathbf{n}} u_1^{\text{int}}$$

on Γ_2 and hence on the right-hand side of (3.2.26). Again, we emphasize that – depending on χ – this problem might very well be nonlinear. The coupling formulation provides the total potential u on Ω_2 as well as the exterior normal derivative $\phi = \partial_{\mathbf{n}} u_2^{\text{ext}}$ of u_2 on Γ_2 .

Recall that the dual space $H^{-1/2}(\Gamma_2)$ of the trace space $H^{1/2}(\Gamma_2)$ is continuously embedded into the dual space $\tilde{H}^{-1}(\Omega_2)$ of $H^1(\Omega_2)$ by means of the trace operator which maps $H^1(\Omega_2)$ onto $H^{1/2}(\Gamma_2)$. Therefore, the operator \tilde{T} from (3.2.25) can also be considered as an operator to $H^{1/2}(\Gamma_2) \times \tilde{H}^{-1}(\Omega_2)$. With respect to the abstract notation of Lemma 3.2.3, the coupling formulation (3.2.26) gives rise to the nonlinear operator

$$\begin{aligned} \tilde{A} : H^{-1/2}(\Gamma_2) \times H^1(\Omega_2) &\rightarrow H^{1/2}(\Gamma_2) \times \tilde{H}^{-1}(\Omega_2) \\ \tilde{A}(\phi, u) &= (u_1^{\text{int}} + u_{\text{app}}^{\text{int}}, \mathbf{f} \cdot \mathbf{n} - \partial_{\mathbf{n}} u_1^{\text{ext}}). \end{aligned} \tag{3.2.27}$$

It is not obvious at all, that the coupling equation (3.2.26) admits a (unique) solution. This hinges strongly on the material law χ . To that end, we present some suitable and physically relevant choices in the following and consider material laws of the form

$$\chi(t) = C_{13} \tanh(C_{14}t)/t \quad \text{for } t > 0, \quad \chi(0) = C_{13}C_{14}, \quad (3.2.28)$$

with dimensionless constants $C_{13}, C_{14} > 0$ or

$$\chi(t) = \frac{C_{15} + C_{16}t}{1 + C_{17}t + C_{18}t^2} \quad (3.2.29)$$

with certain, material-dependent constants $C_{15}, C_{16}, C_{17}, C_{18} > 0$. Furthermore, the operator \tilde{A} itself is *not* uniformly monotone. To get into the setting of uniformly monotone operators, an additional linear shift is required, and we define $A = L\tilde{A}$ and $T = L\tilde{T}$ for some linear operator L . This does not change the solution of the operator equations and details are found in [BFF⁺12, Lemma 19]. In this setting, [BFF⁺12, Lemma 18,19] state unique solvability and thus well-posedness of the equations (3.2.25) and (3.2.27).

So far, we have computed the total potential u , and by simple postprocessing $u_2 = u - u_1 - u_{\text{app}}$ on Ω_2 is derived. The effective field \mathbf{h}_{eff} , however, relies on the gradient of u_2 on the microscopic part Ω_1 . Since u_2 solves $-\Delta u_2 = 0$ in $\mathbb{R}^3 \setminus \bar{\Omega}_2$, u_2 can theoretically be computed by means of the representation formula, cf. e.g. [SS11, Theorem 3.1.6],

$$u_2 = -\tilde{V}_2(\partial_{\mathbf{n}} u_2^{\text{ext}}) + \tilde{K}_2(u_2^{\text{ext}}) \quad \text{in } \mathbb{R}^3 \setminus \bar{\Omega}_2 \supset \Omega_1. \quad (3.2.30)$$

To lower the computational cost for an implementation, we will, however, not use the representation formula on Ω_1 , but only on Γ_1 and solve an inhomogeneous Dirichlet problem instead. With $u_2^{\text{ext}} = u_2^{\text{int}} = u^{\text{int}} - u_1^{\text{int}} - u_{\text{app}}^{\text{int}}$ as well as $\phi = \partial_{\mathbf{n}} u_2^{\text{ext}}$ on Γ_2 , we obtain

$$\begin{aligned} -\Delta u_2 &= 0 && \text{in } \Omega_1, \\ u_2^{\text{int}} &= (-\tilde{V}_2\phi + \tilde{K}_2(u^{\text{int}} - u_1^{\text{int}} - u_{\text{app}}^{\text{int}}))^{\text{int}} && \text{on } \Gamma_1, \end{aligned} \quad (3.2.31)$$

according to (3.1.12). Put into the abstract frame of Lemma 3.2.3, we consider the linear and continuous operator

$$\begin{aligned} S : H^{-1/2}(\Gamma_2) \times H^1(\Omega_2) &\rightarrow \mathbf{L}^2(\Omega_1) \\ S(\phi, u^{\text{int}}) &= \nabla u_2. \end{aligned} \quad (3.2.32)$$

Overall, the computation of $\boldsymbol{\pi}(\mathbf{m}, \mathbf{f}) = S\tilde{A}^{-1}\tilde{T}(\mathbf{m}, \mathbf{f}) = SA^{-1}T = \nabla u_2$ on Ω_1 is therefore done in five steps:

- (i) Solve (3.1.17) to compute u_{11} on Ω_1 .
- (ii) Solve (3.2.24) to compute ∇u_1 on Ω_2 .
- (iii) Solve (3.2.22) to compute u_{app} on Ω_2 .
- (iv) Solve (3.2.26) to provide u and $\phi = \partial_{\mathbf{n}} u_2^{\text{ext}}$ on Γ_2 .
- (v) Solve (3.2.31) to provide ∇u_2 on Ω_1 .

Remark. Note that the formal definition of the operator S once again requires the solution of (3.2.24)–(3.2.22) to provide $u_1^{\text{int}} + u_{\text{app}}^{\text{int}}$. Theoretically, this can be dealt with by considering the extended operators

$$\begin{aligned}\widehat{T}(\mathbf{m}, \mathbf{f}) &= (u_1^{\text{int}} + u_{\text{app}}^{\text{int}}, \mathbf{f} \cdot \mathbf{n} - \partial_{\mathbf{n}} u_1^{\text{ext}}, u_1^{\text{int}} + u_{\text{app}}^{\text{int}}), \\ \widehat{A}(\phi, u, u_1^{\text{int}} + u_{\text{app}}^{\text{int}}) &= (u_1^{\text{int}} + u_{\text{app}}^{\text{int}}, \mathbf{f} \cdot \mathbf{n} - \partial_{\mathbf{n}} u_1^{\text{ext}}, u_1^{\text{int}} + u_{\text{app}}^{\text{int}}), \\ \widehat{S}(\phi, u, u_1^{\text{int}} + u_{\text{app}}^{\text{int}}) &= \nabla u_2.\end{aligned}$$

Then, \widehat{S} and \widehat{T} are still linear and continuous. Provided A is uniformly monotone, the inverse of A is well-defined and continuous so that (an obvious extension of) Lemma 3.2.3 still applies.

Discretization of the multiscale operator

Discretization of \widetilde{T} :

Analogously to the strayfield operator from Section 3.1.3, we solve (3.1.21) to obtain an approximation $u_{11h} \in \mathcal{S}_*^1(\mathcal{T}_h^{\Omega_1})$ of u_{11} . We then proceed as in Section 3.1.3 and discretize the given Dirichlet data by means of the Scott-Zhang operator from [SZ80]. Note that $u_1 = \widetilde{K}_1 u_{11}^{\text{int}} \in C^\infty(\mathbb{R}^3 \setminus \overline{\Omega_1}) \subset H^2(\Omega_2)$. Therefore, the discretization of (3.2.24) then reads: Find $u_{1h} \in \mathcal{S}^1(\mathcal{T}_h^{\Omega_2})$ such that

$$\int_{\Omega_2} \nabla u_{1h} \cdot \nabla v_h \, dx = 0 \quad \text{for all } v_h \in \mathcal{S}_0^1(\mathcal{T}_h^{\Omega_2}) \quad \text{with } u_{1h}|_{\Gamma_2} = I_h^{\Gamma_2} K_1 u_{11h}^{\text{int}}. \quad (3.2.33)$$

Analogously to Proposition 3.1.3, one obtains the following result:

Lemma 3.2.4. *The operator $B_h : \mathbf{L}^2(\Omega_1) \rightarrow \mathcal{S}^1(\mathcal{T}_h^{\Omega_2})$ with $B_h \mathbf{m} := u_{1h}$, which uses the discrete solution of (3.1.21) to compute the solution $u_{1h} \in \mathcal{S}^1(\mathcal{T}_h^{\Omega_2})$ of (3.2.33), is well-defined, linear, and continuous. Moreover, there holds strong convergence $B_h \mathbf{m} \rightarrow B \mathbf{m}$ in $H^1(\Omega_2)$ as $h \rightarrow 0$ for all $\mathbf{m} \in \mathbf{L}^2(\Omega_1)$. Here, $B : \mathbf{L}^2(\Omega_1) \rightarrow H^1(\Omega_2)$ denotes the linear and continuous solution operator of (3.2.24). \square*

The discrete version of (3.2.22) reads as follows: Let $u_{\text{app},h} \in \mathcal{S}_*^1(\mathcal{T}_h^{\Omega_2})$ solve

$$\int_{\Omega_2} \nabla u_{\text{app},h} \cdot \nabla v_h \, dx = - \int_{\Gamma_2} \mathbf{f} \cdot \mathbf{n} \, d\Gamma_2 \quad \text{for all } v_h \in \mathcal{S}_*^1(\mathcal{T}_h^{\Omega_2}). \quad (3.2.34)$$

The following Lemma states a corresponding result for (3.2.34).

Lemma 3.2.5. *Let Ω_2 be convex. Then, the operator $B_h : \mathbf{H}(\text{div}; \Omega_2) \rightarrow \mathcal{S}_*^1(\mathcal{T}_h^{\Omega_2})$ which maps \mathbf{f} to the discrete solution of (3.2.34) is well-defined, linear, and continuous. Moreover, there holds strong convergence $B_h \mathbf{f} \rightarrow B \mathbf{f}$ in $\mathbf{H}^1(\Omega_2)$ as $h \rightarrow 0$ for all $\mathbf{f} \in \mathbf{H}(\text{div}; \Omega_2)$. Here, $B : \mathbf{H}(\text{div}; \Omega_2) \rightarrow H_*^1(\Omega_2)$ denotes the linear and continuous solution operator of (3.2.22). \square*

With respect to the definition of the operator \widetilde{T} in (3.2.25), it remains to prove convergence $\partial_{\mathbf{n}} u_{1h}^{\text{int}} \rightarrow \partial_{\mathbf{n}} u_1^{\text{int}}$ strongly in $H^{-1/2}(\Gamma_2)$ as $h \rightarrow 0$. To that end, let u_{1h}^* be the discrete solution of (3.2.33) with boundary data $u_{1h}^*|_{\Gamma_2} = I_h^{\Gamma_2} K_1 u_{11}^{\text{int}}$. Here, $I_h^{\Gamma_2} : H^{1/2}(\Gamma_2) \rightarrow \mathcal{S}^1(\mathcal{T}_h^{\Omega_2}|_{\Gamma_2})$ denotes the projection induced by the Scott-Zhang projection $I_h^{\Omega_2} : H^1(\Omega_2) \rightarrow \mathcal{S}^1(\mathcal{T}_h^{\Omega_2})$, now considered on Ω_2 instead of Ω_1 , cf. [BFF⁺12]. The Céa lemma proves

$$\|u_1 - u_{1h}^*\|_{H^1(\Omega_2)} \lesssim \|u_1 - I_h^{\Omega_2} u_1\|_{H^1(\Omega_2)} = \mathcal{O}(h).$$

For the term $\|u_{1h} - u_{1h}^*\|_{H^1(\Omega_2)}$, we get due to convexity of Ω_1 and thus $u_1 \in H^2(\Omega_1)$

$$\|u_{1h}^* - u_{1h}\|_{H^1(\Omega_2)} \lesssim \|u_{11}^{\text{int}} - u_{11h}^{\text{int}}\|_{H^{1/2}(\Gamma_1)} \lesssim \|u_{11} - u_{11h}\|_{H^1(\Omega_1)} = \mathcal{O}(h),$$

where we have used stability of $I_h^{\Omega_2}$ and \tilde{K}_1 as well as the trace theorem. Altogether, we see

$$\|u_1 - u_{1h}\|_{H^1(\Omega_2)} \leq \|u_1 - u_{1h}^*\|_{H^1(\Omega_2)} + \|u_{1h}^* - u_{1h}\|_{H^1(\Omega_2)} = \mathcal{O}(h).$$

The desired result now follows from $\|\Psi\|_{H^{-1/2}(\Gamma_2)} \leq \|\Psi\|_{L^2(\Gamma_2)}$ for all $\Psi \in L^2(\Gamma_2)$ and the next lemma, which can be found in [BFF⁺12, Lemma 24].

Lemma 3.2.6. *Let $w \in H^2(\Omega_2)$ and let $w_h \in \mathcal{S}^1(\mathcal{T}_h^{\Omega_2})$ be a sequence with*

$$\|\nabla(w - w_h)\|_{L^2(\Omega_2)} \leq C_{19}h^{1/2+\varepsilon} \quad \text{for all } h > 0$$

for some h -independent constants $C_{19} > 0$ and $\varepsilon > 0$. Then, there holds

$$\|\partial_\nu(w - w_h)\|_{L^2(\Gamma_2)} \leq C_{20}h^\varepsilon \quad \text{for all } h > 0$$

and a constant $C_{20} > 0$ which is independent of $h > 0$. □

Combining Lemma 3.2.4–3.2.6, we obtain the following proposition.

Proposition 3.2.7. *With $X = H^{-1/2}(\Gamma_2) \times H^1(\Omega_2)$ and $Y = \mathbf{H}(\text{div}; \Omega_2)$, the operator*

$$\begin{aligned} \tilde{T}_h : L^2(\Omega_1) \times \mathbf{H}(\text{div}; \Omega_2) &\rightarrow \mathcal{P}^0(\mathcal{E}_h^{\Gamma_2}) \times \mathcal{S}^1(\mathcal{T}_h^{\Omega_2}) \subseteq X^*, \\ \tilde{T}_h(\mathbf{m}, \mathbf{f}) &= (u_{1h}^{\text{int}} + u_{\text{app},h}^{\text{int}}, \mathbf{f} \cdot \mathbf{n} - \partial_{\mathbf{n}} u_{1h}^{\text{int}}) \end{aligned} \quad (3.2.35)$$

is well-defined, linear, and continuous and satisfies (3.2.9) with (T_h, T) replaced by (\tilde{T}_h, \tilde{T}) . □

Discretization of \tilde{A} :

For the numerical solution of (3.2.26), we use lowest-order finite elements combined with lowest-order boundary elements. The numerical approximation of the Johnson-Nédélec equations is then given by the following problem: Find $(\phi_h, u_h) \in X_h := \mathcal{P}^0(\mathcal{E}_h^{\Gamma_2}) \times \mathcal{S}^1(\mathcal{T}_h^{\Omega_2})$ such that

$$\begin{aligned} \int_{\Omega_2} (1 + \tilde{\chi}(|\nabla u_h|)) \nabla u_h \cdot \nabla v_h - \int_{\Gamma_2} \phi_h v_h^{\text{int}} &= - \int_{\Gamma_2} (\mathbf{f} \cdot \mathbf{n} - \partial_{\mathbf{n}} u_{1h}^{\text{int}}) v_h, \\ \int_{\Gamma_2} (V_2 \phi_h - (K_2 - 1/2) u_h^{\text{int}}) \psi_h &= - \int_{\Gamma_2} (K_2 - 1/2) (u_{1h}^{\text{int}} + u_{\text{app},h}^{\text{int}}) \psi_h \end{aligned} \quad (3.2.36)$$

for all $(\psi_h, v_h) \in X_h$, where $(u_{\text{app},h}, u_{1h})$ is the output of T_h . With the operator \tilde{A} from (3.2.27), the Galerkin formulation (3.2.36) is given by

$$\langle \tilde{A}(\phi_h, u_h), (\psi_h, v_h) \rangle_{X_h^* \times X_h} = \langle \tilde{T}_h(\mathbf{m}, \mathbf{f}), (\psi_h, v_h) \rangle_{X_h^* \times X_h} \quad \text{for all } (\psi_h, v_h) \in X_h. \quad (3.2.37)$$

Analogously to the linear case, (3.2.37) is equivalent to

$$\langle A(\phi_h, u_h), (\psi_h, v_h) \rangle_{X_h^* \times X_h} = \langle T_h(\mathbf{m}, \mathbf{f}), (\psi_h, v_h) \rangle_{X_h^* \times X_h} \quad \text{for all } (\psi_h, v_h) \in X_h, \quad (3.2.38)$$

for the uniformly monotone operator $A = L\tilde{A}$ and $T_h = L\tilde{T}_h$. For details, we again refer to [BFF⁺12] and [AFF⁺13]. Consequently, T_h satisfies assumption (3.2.9).

Discretization of S :

In analogy to (3.2.33), we use the Scott-Zhang operator $I_h^{\Gamma_1}$ to discretize the Dirichlet data in (3.2.31). The corresponding discretization thus reads: Find $u_{2h} \in \mathcal{S}^1(\mathcal{T}_h^{\Omega_1})$ with $u_{2h}|_{\Gamma_1} = I_h^{\Gamma_1}(-\tilde{V}_2\phi_h + \tilde{K}_2(u_h^{\text{int}} - u_{1h}^{\text{int}} - u_{\text{app},h}^{\text{int}}))^{\text{int}}$ such that

$$\int_{\Omega_1} \nabla u_{2h} \cdot \nabla v_h = 0 \quad \text{for all } v_h \in \mathcal{S}_0^1(\mathcal{T}_h^{\Omega_1}). \quad (3.2.39)$$

Completely analogously to before, the following result is true.

Proposition 3.2.8. *The operator $S_h : X = H^{-1/2}(\Gamma_2) \times H^1(\Omega_2) \rightarrow \mathcal{P}^0(\mathcal{T}_h^{\Omega_1})^3 \subseteq \mathbf{L}^2(\Omega_1)$, which computes the gradient of the solution of (3.2.39) is well-defined, linear, and continuous. Moreover, there holds $S_h x \rightarrow Sx$ strongly in $\mathbf{L}^2(\Omega_1)$ as $h \rightarrow 0$ for all $x \in X$. Here, $S : X \rightarrow \mathbf{L}^2(\Omega_1)$ denotes the exact solution operator of (3.2.31). In particular, S satisfies (3.2.8). \square*

Combining the last results, we ultimately conclude:

Proposition 3.2.9. *Suppose that the microscopic domain Ω_1 is convex, that the macroscopic domain Ω_2 is simply connected, and that the material law χ is of the form (3.2.28) or (3.2.29). Let $Y := \mathbf{H}(\text{div}; \Omega_2)$ and $\zeta_{hk}^- := \mathbf{f}_{hk}^-$. Assume further that $\mathbf{f}|_{\Omega_2}$ is sufficiently smooth, such that $\mathbf{f}_{hk}^- \rightarrow \mathbf{f}$ strongly in $L^2(\mathbf{H}(\text{div}; \Omega_2))$ and $\mathbf{f}_{hk}^- \in L^\infty(\mathbf{H}(\text{div}; \Omega_2))$. Then, the operator $\pi_h(\mathbf{m}, \mathbf{f}) = S_h A^{-1} T_h(\mathbf{m}, \mathbf{f}) = \nabla u_{2h}$ defined via the previous section satisfies all assumptions of Lemma 3.2.3. In particular, the assumptions (3.2.4)–(3.2.5) of Theorem 3.2.1 are satisfied. \square*

Remark. *Computational studies of the analyzed multiscale approach are beyond the scope of this thesis and can be found in [BVB⁺, Bru13].*

3.3. Numerical experiments

In this section, we give a first set of numerical experiments to underline the theoretical results from above and allow for a better understanding of the tangent plane scheme 2.2.1. Throughout, we consider various field contributions which will be individually specified in the different examples. As a starting point for our implementation, and hence the computational experiments, serve two different LLG implementations. For the 3D examples, we extend a MATLAB code written by PETRA GOLDENITS during her PhD thesis [Gol12]. For the upcoming 2D examples, a FREEFEM++ code from JONATHAN ROCHAT [Roc12] serves as starting point. Throughout, the 3D visualizations are carried out in PARAVIEW [Webc].

3.3.1. General performance

The basic implementation of this code has already been tested with μMAG problems from the National Institute of Standards and Technology [Webb], and we refer to [Gol12, Chapter 6] for details and documentation. Here, we thus concentrate on the performance as well as the investigation of the unique properties of this scheme. For the first example, we aim to investigate the convergence rate of the tangent plane scheme in both, time and space. To that

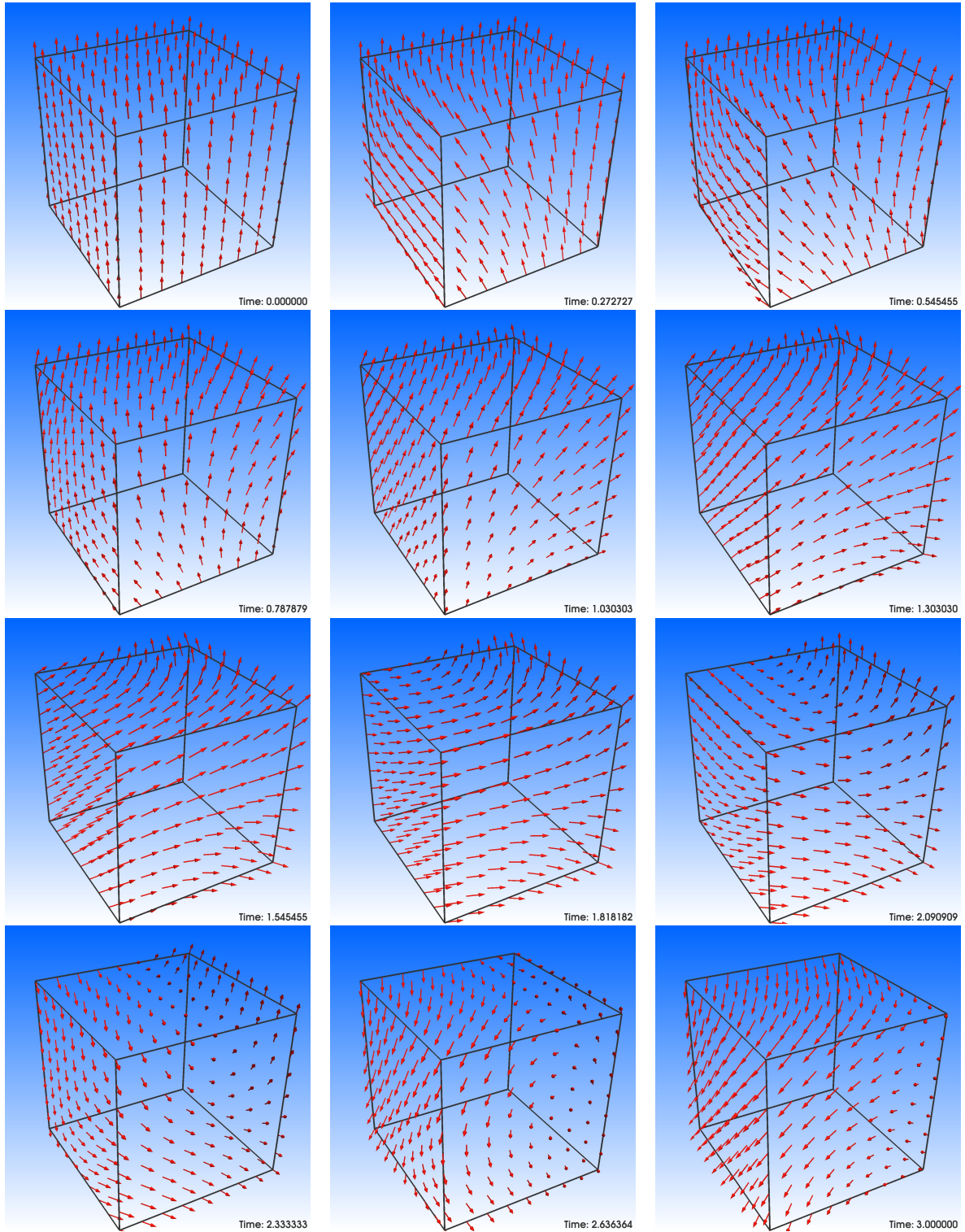


Figure 3.2.: Magnetization dynamics on $[0, 3]$ for the above example.

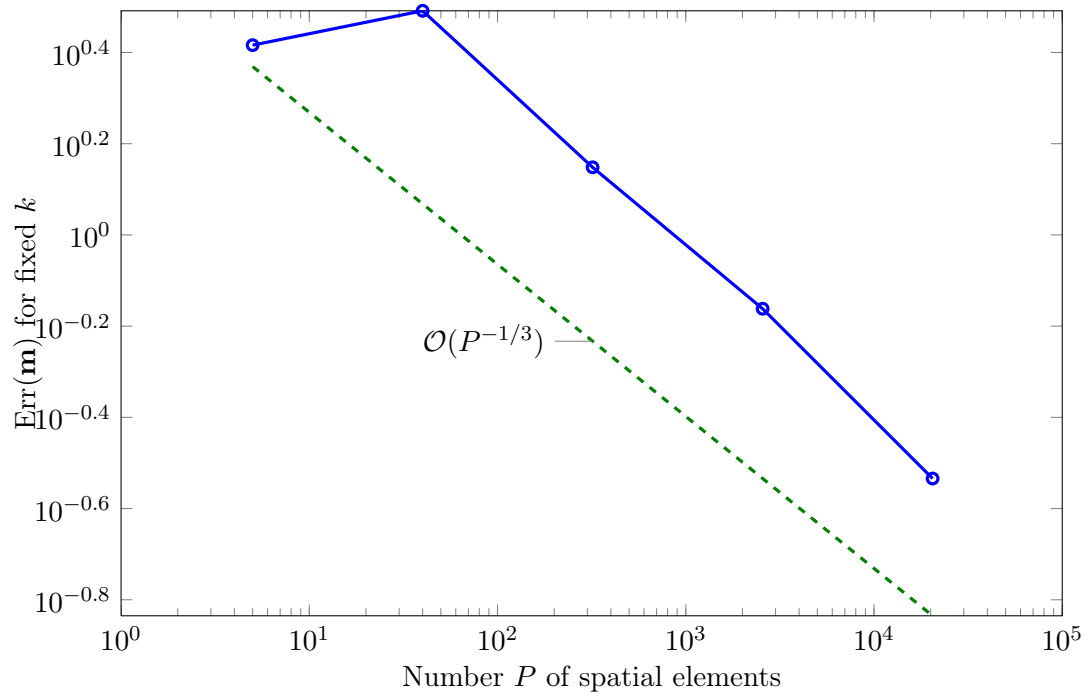


Figure 3.3.: Spatial error for $k = 0.01$. As expected, linear decay is observed.

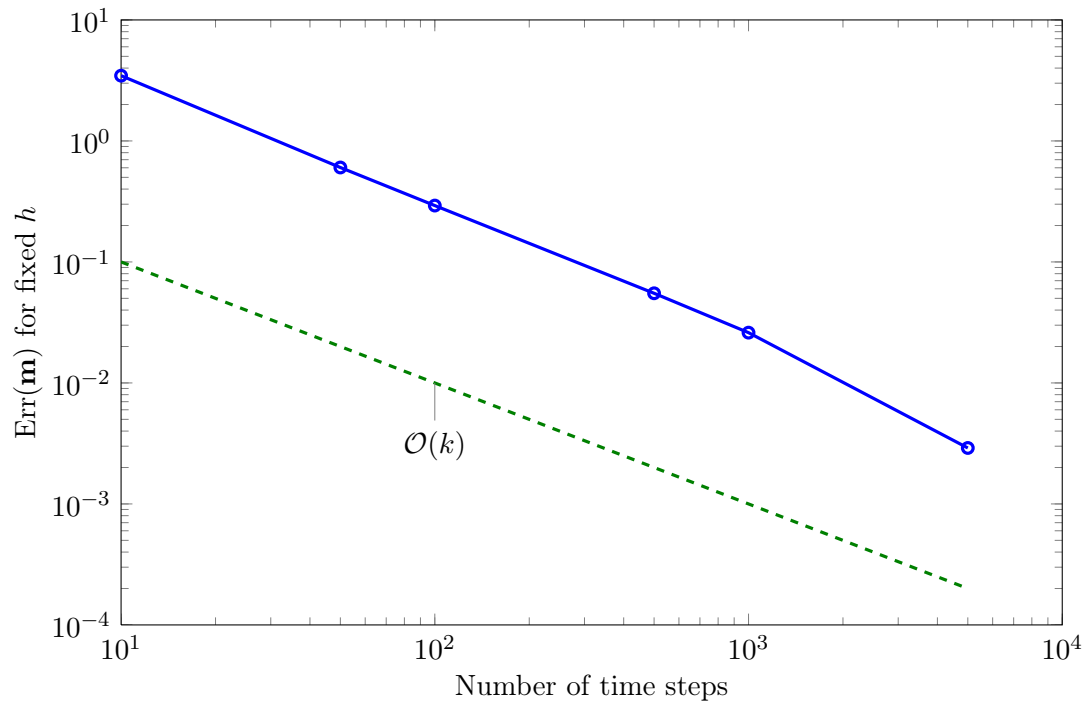


Figure 3.4.: Temporal error for $P = 20480$ spatial elements. As expected, linear decay is observed.

end, we consider a homogeneous magnetization in x_3 -direction on the scaled and shifted unit cube $[-1, 1]^3$. Onto this initial state, a rotating external field of the form

$$\mathbf{f}(t, x_1, x_2, x_3) := \begin{pmatrix} f_1 \\ f_2 \\ f_3 \end{pmatrix}(t, x_1, x_2, x_3),$$

with

$$\begin{aligned} f_1 &:= \alpha \cos(2t + x_1 + x_2 + x_3) + 3 \sin(t + x_1) \cos(t + x_2 + x_3) \\ &\quad + \sin(t + x_2 + x_3) \sin(2t + x_1 + x_2 + x_3) + \cos(t + x_1) \cos^2(t + x_2 + x_3), \\ f_2 &:= 3 \cos(t + x_1) \cos(t + x_2 + x_3) - (\alpha \sin(2t + x_1 + x_2 + x_3) \\ &\quad + \sin(t + x_1) \cos^2(t + x_2 + x_3) - \sin(t + x_2 + x_3) \cos(2t + x_1 + x_2 + x_3)), \text{ and} \\ f_3 &:= \alpha \cos(t + x_2 + x_3) + 2 \sin(t + x_2 + x_3) - \cos^2(t + x_2 + x_3) \end{aligned}$$

is applied. In addition, the exchange contribution is taken into account with $C_e = 1$, i.e. we consider

$$\mathbf{h}_{\text{eff}} = \Delta \mathbf{m} + \mathbf{f}.$$

The other input variables are chosen to be $\alpha = 1 = \theta$.

The evolution of the magnetization is computed on the time interval $[0, 3]$, and we are interested in the convergence rates of the scheme in time and space as $(h, k) \rightarrow (0, 0)$. Since no exact solution is known, we employ a reference solution \mathbf{m} on a fine grid with 20480 elements and 10000 time steps. The dynamic behaviour of the magnetization is visualized in Figure 3.2. A respective error table for different time- and spatial mesh sizes is given below in Table 3.1. Here, the error is given by

$$\text{Err}(\mathbf{m}) := \max_j \|\mathbf{m}_h^j - \mathbf{m}(t_j)\|_{L^2(\Omega)} + \|\nabla \mathbf{m}_h^j - \nabla \mathbf{m}(t_j)\|_{L^2(\Omega)}.$$

	Timesteps						
	10	50	100	500	1000	5000	10000
Spatial elements							
5	3.3592	2.6469	2.6067	2.5839	2.5816	2.5799	2.5797
40	4.1866	3.1576	3.1003	3.0767	3.0754	3.0746	3.0746
320	3.7968	1.6100	1.4067	1.2830	1.2707	1.2614	1.2603
2560	3.5580	0.9217	0.6890	0.5664	0.5568	0.5503	0.5496
20480	3.4629	0.6032	0.2923	0.0551	0.0260	0.0029	NA

Table 3.1.: $\text{Err}(\mathbf{m})$ for the above example computed with respect to a reference solution.

Due to construction, we expect the scheme to be of first order in both, time and space. Indeed, the error decay in space shows the desired behaviour if the time step is chosen sufficiently

small (≥ 100 steps). Note that for small amounts of spatial elements (≤ 2560 elements), the time error rarely decays, but is rather stuck at a certain value. This is in agreement with observations from e.g. [Roc12], and we conclude that in these ranges, the temporal error is dominated by the spatial error. The last line of Table 3.1, however, reveals even the desired convergence rate for the temporal error. The error seems to make an abrupt jump between the fourth and fifth line for small time steps. This is due to the fact, that the reference solution is computed on 20480 elements, as well. Therefore, the spatial resolution of the discrete- and the reference solution coincides in the last line and the spatial error is thus negligible. This spatial mesh, on the other hand, is a good opportunity to investigate the temporal error.

The decay of the spatial error for 100 time steps is visualized in Figure 3.3. Here, we plot the error over $P^{-1/3}$, where P denotes the number of elements. Notice that this is a 3D simulation, whence $h \sim P^{-1/3}$. On a double-logarithmic scale, we see that the error indeed behaves like $\mathcal{O}(h)$, as to be expected. Figure 3.4 visualizes the decay of the temporal error on a spatial grid of $P = 20480$ elements. Here, the error is plotted over the amount of time steps. Again, the experiment confirms a linear decay rate of $\mathcal{O}(k)$.

3.3.2. Finite time blowup in 2D

In the second experiment, we consider a 2-dimensional benchmark problem from [BP06], which is expected to produce a finite time blowup. On $\Omega = [-0.5, 0.5]^2$, we consider the initial magnetization

$$\mathbf{m}_0(\mathbf{x}) := \begin{cases} (0, 0, -1) & \text{for } |\mathbf{x}| \geq 1/2, \\ (2\mathbf{x}A, A^2 - |\mathbf{x}|^2)/(A^2 + |\mathbf{x}|^2) & \text{for } |\mathbf{x}| \leq 1/2, \end{cases}$$

with $A := (1 - 2|\mathbf{x}|^4)/s$ for some $s > 0$. Starting from this initial data, we run the simulation with

$$\mathbf{h}_{\text{eff}} = \Delta \mathbf{m}.$$

Put explicitly, we set $C_e = 1$ and neglect all field contributions besides the exchange part. In particular, no external field is employed. Moreover, we choose $\alpha = \theta = 1$ and $s = 4$ for now. The evolution of the magnetization on the time interval $[0, 0.03]$ for $h = 1/32$ and $k = 0.00001$ is visualized in Figure 3.5. A lateral view is given in Figure 3.6. As observed before in [BP06] and also [Roc12, BPPR13] in a different setting, we see that the magnetization heads towards an extremal state at around $t = 0.023$ and then gets aligned parallel. The goal of this benchmark problem is to pinpoint the time of this extremal *blowup point* which is defined as the time at which the gradient of \mathbf{m} takes its maximum. More precisely, we seek $t \in [0, T]$, such that

$$|\mathbf{m}(t)|_{W^{1,\infty}(\Omega)} = \|\nabla \mathbf{m}(t)\|_{L^\infty(\Omega)} = \max_{\tilde{t} \in [0, T]} \|\nabla \mathbf{m}(\tilde{t})\|_{L^\infty(\Omega)}.$$

In [BP06], the authors used the midpoint scheme to compute this problem. Therefore, however, they were restricted to comparatively large time steps, since the fixed point iteration enforces a coupling between h and k , namely $k \leq Ch^2$, for this algorithm. As a result, the most refined spatial mesh-size they could employ, was $h = 1/64$. For those computations, the empirical blowup time seemed to converge towards approximately 0.03. As we do not have any coupling

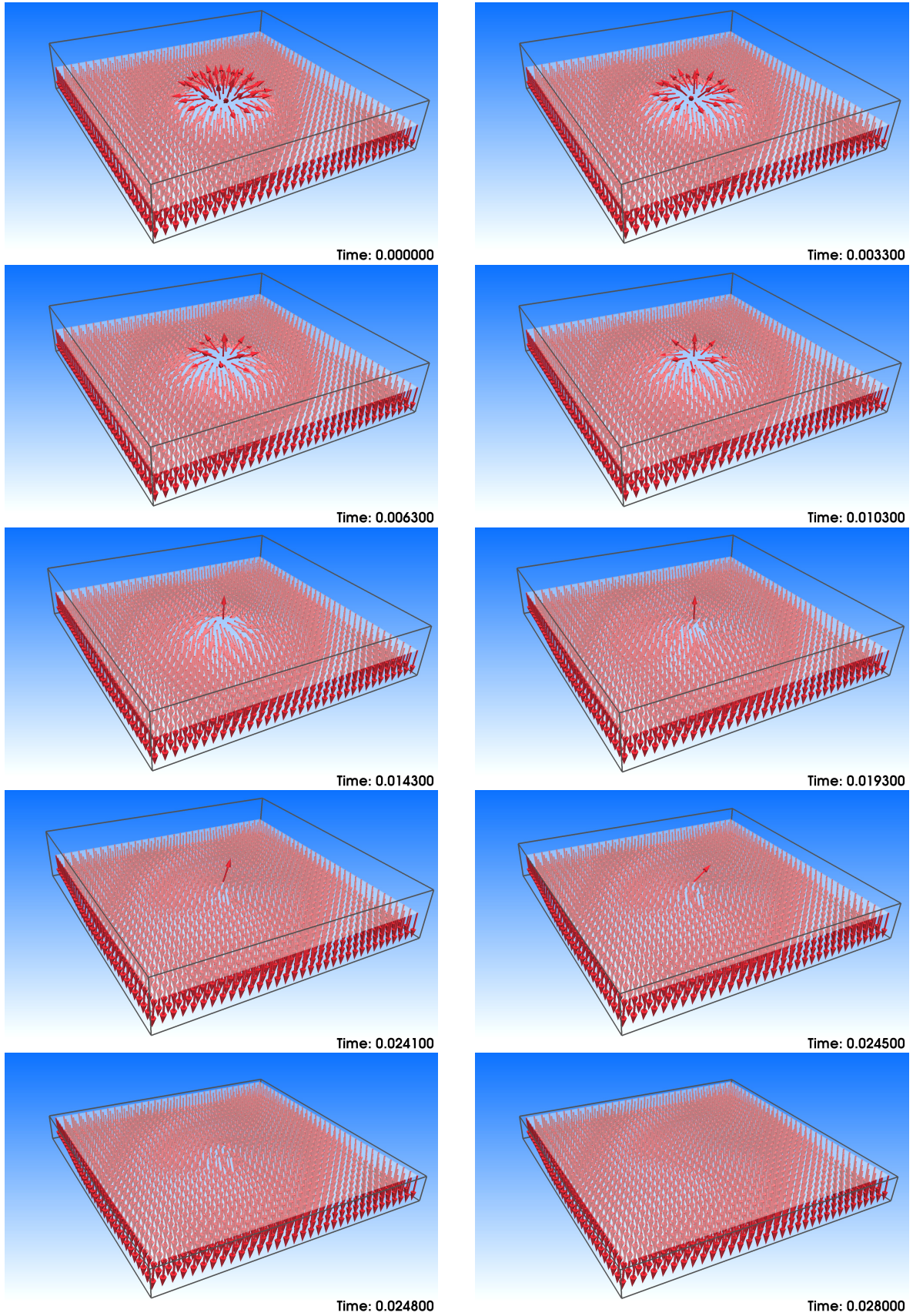
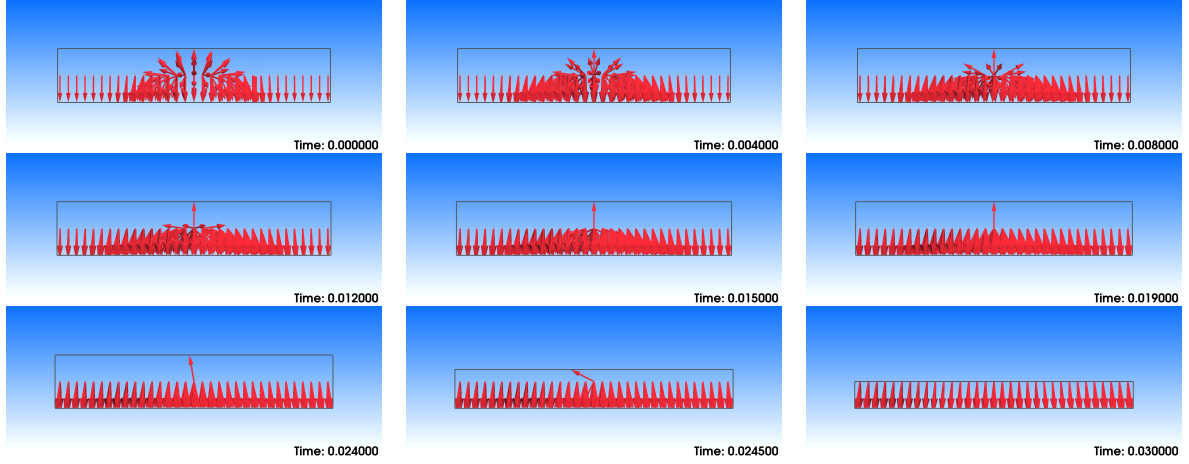


Figure 3.5.: Magnetization dynamics on $[0, 0.03]$ for $h = 1/32$ and $k = 0.00001$.


 Figure 3.6.: Magnetization dynamics on $[0, 0.03]$ in lateral view.

between h and k , the tangent plane scheme is very convenient for this problem, since we can compute much further than $h = 1/64$ which reveals some unexpected results.

In Figure 3.7, a comparison of the empirical blowup times is visualized for different $h \in \{1/8, 1/16, 1/32, 1/64, 1/96, 1/128\}$ and $k = 0.00001$. For large $h \geq 1/64$, the results from [BP06] are reproduced. For smaller h , however, we observe that the blowup time does not converge but rather approaches higher values. For $h = 1/128$ the blowup time even becomes as high as 0.09. These results are in agreement with first observations from [BKP08, BPPR13], where still coarser meshes were considered. We conclude that the empirical blowup time strongly depends on the mesh size and, contrary to [BP06], cannot observe convergence towards any point in time. In fact, finite time blowup in this example might even be a numerical artifact caused by insufficient mesh resolution.

Moreover, we find that for fixed spatial mesh size and varying time step size, the empirical blowup time changes again. This behaviour is visualized in Figure 3.8. Here, we observe that the blowup time approaches smaller values as k is decreased. In particular, for fixed $h = 1/32$, the blowup time seems to converge around 0.022. Since the blowup time is very sensitive with respect to the mesh-size parameters, however, we stress that additional computations are in order to fully clarify this benchmark example. In fact, it should be interesting to consider adaptively generated spatial meshes. In addition, we observe that, in contrast to Figure 3.7, the value of $\|\nabla \mathbf{m}(t)\|_{\mathbf{L}^\infty(\Omega)}$ at the time of the blowup is constant in this case. We therefore conclude that this value only depends on the spatial mesh-size and not particularly on the time step size k .

Next, we consider dependence of the blowup time on the two parameters α and s . The corresponding results are visualized in the Figures 3.9 and 3.10. We observe that, for small α , the blowup time seems to approach 0.038 and for $\alpha \leq 1/32$ the curves nearly coincide. Note that the choice of a very small α induces a strong rotation of the magnetization (not displayed) which causes the energy to not to drop to zero immediately after the blowup occurs.

For different values of s , we see that the blowup time decreases as s is increased. Again, our results are in good agreement with those from [BP06].

Finally, we consider the energy of the simulation for different values of k and h and for $\alpha = 1$ and $s = 4$. Since, besides the exchange contribution, no other field contribution is

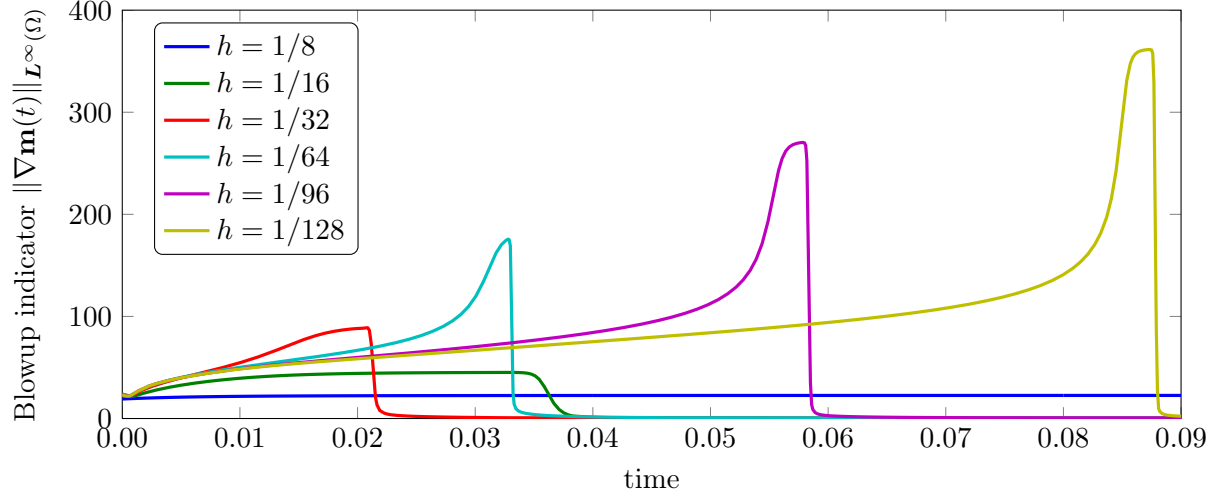


Figure 3.7.: Different empirical blowup times for $h \in \{1/8, 1/16, 1/32, 1/64, 1/96, 1/128\}$ and $k = 0.00001$.

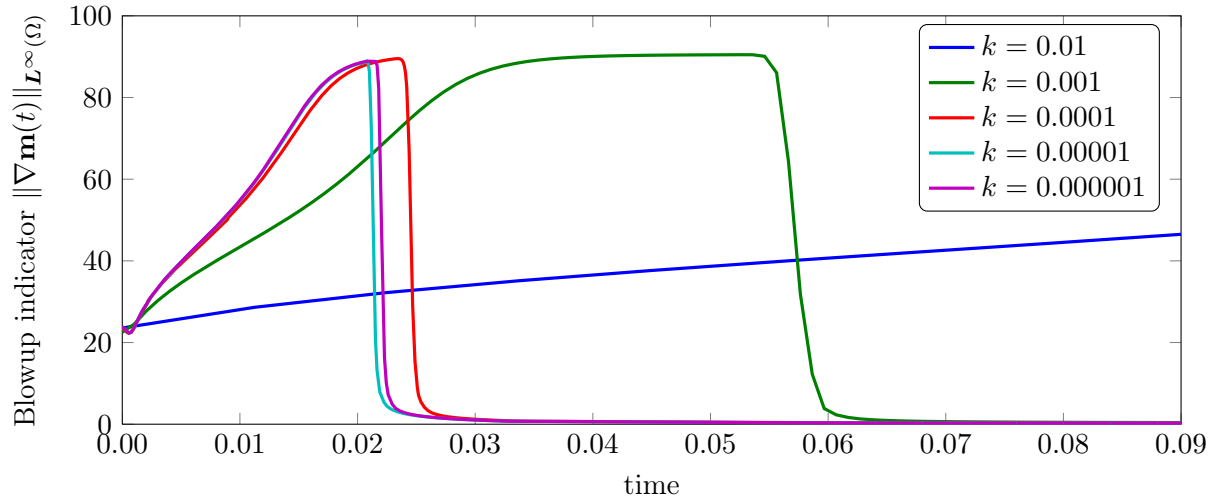


Figure 3.8.: Empirical blowup times for $k \in \{10^{-2}, 10^{-3}, 10^{-4}, 10^{-5}, 10^{-6}\}$ and $h = 1/32$.

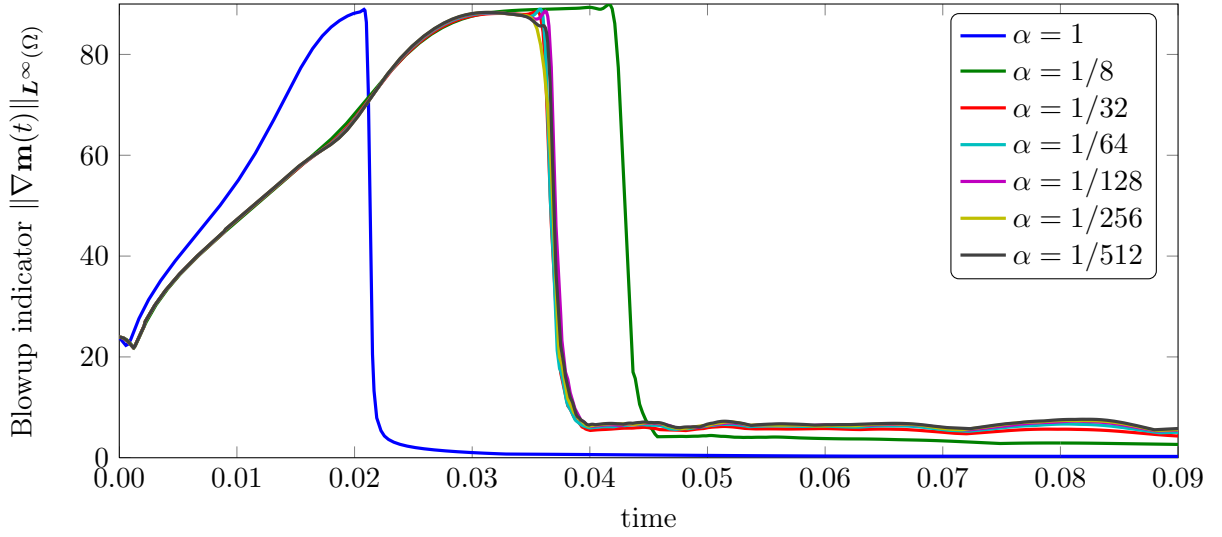


Figure 3.9.: Different empirical blowup times for $\alpha \in \{1, 1/32, 1/64, 1/128, 1/256, 1/512\}$, $k = 0.00001$, and $h = 1/32$.

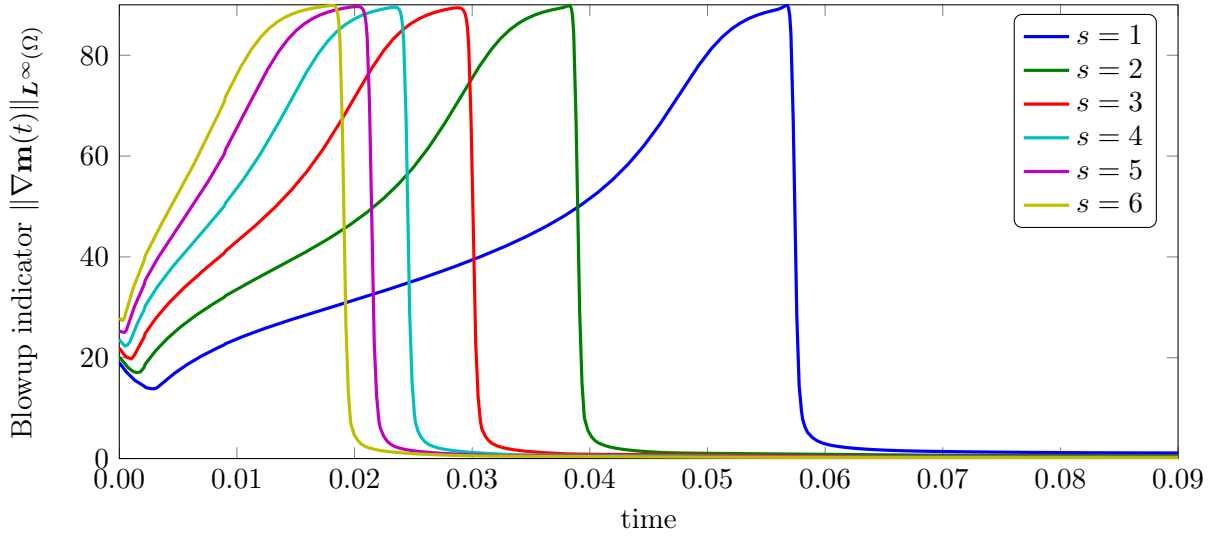


Figure 3.10.: Empirical blowup times for $s \in \{1, 2, 3, 4, 5, 6\}$, $\alpha = 1$, $k = 0.0001$, and $h = 1/32$.

considered, this term is given by

$$\mathcal{E}(\mathbf{m}, t) = \frac{1}{2} \|\nabla \mathbf{m}(t)\|_{\mathbf{L}^2(\Omega)}^2,$$

and the results are visualized in Figure 3.11. As expected, we observe a monotone decay of the energy for any set of mesh parameters. We like to emphasize that the energy, and hence the magnetization, behaves as predicted even for the cases $(k = 10^{-2}, h = 1/32)$, $(k = 10^{-3}, h = 1/32)$, and $(k = 10^{-3}, j = 1/64)$ for which the classical CFL condition $k < h^2$ is not satisfied. This empirical observation underlines the theoretical result of unconditional convergence which is a key advantage of the tangent plane scheme in comparison to other methods like the

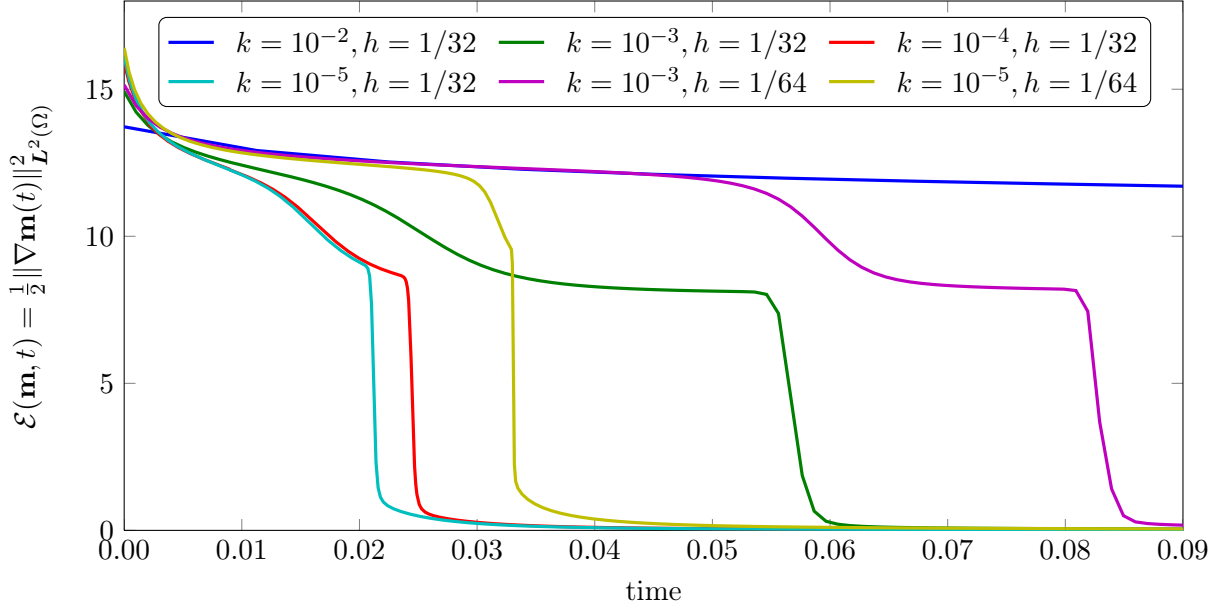


Figure 3.11.: Energy $\mathcal{E}(\mathbf{m}, t)$ for different configurations of mesh parameters and $\alpha = 1, s = 4$ plotted over time.

midpoint scheme. For the latter, unconditional convergence is only theoretically proved.

Altogether, usage of the tangent plane method allows a more thorough investigation of this benchmark problem since larger time steps and hence finer spatial meshes can be computed. This sheds new light on the blowup time in dependence of various input and mesh parameters. While it is expected that the blowup time varies for different parameters α and s , it is quite surprising that it seems to react fairly sensible to the mesh size parameters h and k . In particular, we cannot confirm the conjecture from [BP06] stating that the blowup time converges towards a specific point in time as those parameters decrease.

3.3.3. The case $\alpha = 0$

In the last experiment of this set, we address the special case where $\alpha = 0$, i.e. the case where no damping is considered. When we look at the general Algorithm 2.2.1, we see that the damping constant α is the coefficient of the \mathbf{L}^2 -contribution of our bilinear form

$$a^j(\varphi, \psi) = \alpha(\varphi, \psi) + (\mathbf{m}_h^j \times \varphi, \psi) + \theta C_e k (\nabla \varphi, \nabla \psi),$$

cf. Equation (2.2.3). With the arguments from Lemma 2.2.2, we immediately see that $a^j(\cdot, \cdot)$ is positive definite for $\alpha > 0$, since

$$a^j(\psi, \psi) = \alpha \|\psi\|_{\mathbf{L}^2(\Omega)}^2 + \theta C_e k \|\nabla \psi\|_{\mathbf{L}^2(\Omega)}^2.$$

This result is particularly true for all $\psi \in \mathcal{S}^1(\Omega)$ and we conclude that Algorithm 2.2.1 is well-defined for $\alpha > 0$, even without the tangent plane constraint. This result can directly be observed at the condition numbers of the corresponding system matrices. Concerning the implementation, the tangent space constraint is treated by means of a Lagrangian multiplier.

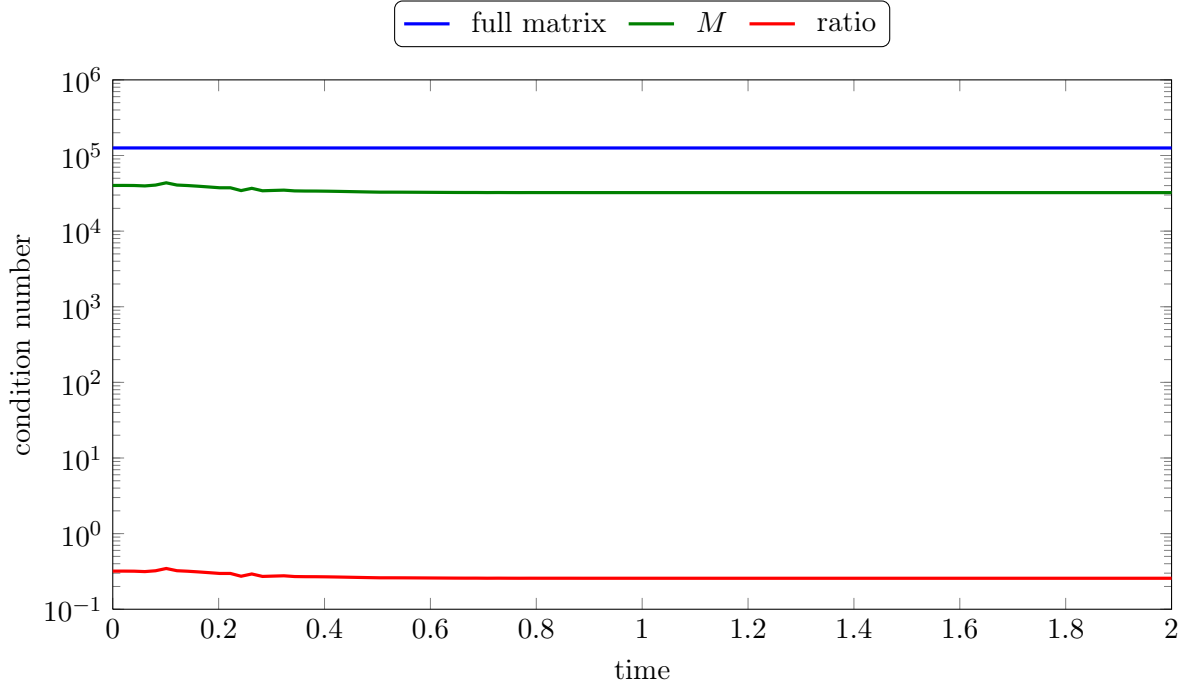


Figure 3.12.: Condition numbers of M and the full matrix from (3.3.1) for $\alpha = 1$ plotted over the simulation time.

In each time step, we thus solve a system of the form

$$\begin{pmatrix} M & \Lambda^T \\ \Lambda & 0 \end{pmatrix} \begin{pmatrix} \mathbf{v} \\ \boldsymbol{\lambda} \end{pmatrix} = \begin{pmatrix} \mathbf{b} \\ 0 \end{pmatrix}. \quad (3.3.1)$$

Here, $\mathbf{v}_h^j = \sum_{m=1}^{3N} \mathbf{v}_m \beta_m$ is the sought solution, and the Langrangian matrix Λ is up to some scaling factor given by

$$\Lambda = \begin{pmatrix} \Lambda^1 & \Lambda^2 & \Lambda^3 \end{pmatrix} \in \mathbb{R}^{N \times 3N},$$

with

$$\Lambda_{ii'}^\ell = \mathbf{m}_h^j(\mathbf{z}_i) \cdot \mathbf{e}_\ell \delta_{ii'}.$$

The line $\Lambda \mathbf{v} = 0$ thus realizes the tangent plane constraint $\mathbf{m}_h^j(\mathbf{z}) \cdot \mathbf{v}_h^j(\mathbf{z}) = 0$ for all $\mathbf{z} \in \mathcal{N}_h$. Finally, for the matrix $M \in \mathbb{R}^{3N \times 3N}$, we have $M = A + B$, where A and B denote the matrices stemming from the scaled \mathbf{H}^1 -scalar product and the cross product in (2.2.3), respectively. The vector \mathbf{b} denotes evaluation of the right-hand side $L^j(\cdot)$. The interested reader is referred to [GHPS, Section 3], for details. Solving $M \mathbf{v} = \mathbf{b}$ thus corresponds to a solution in the full space $\mathcal{S}^1(\Omega)$, whereas solving the full problem (3.3.1) corresponds to a solution in the tangent space. With the theoretical result from above, we expect both, M and the full matrix from (3.3.1) to be well conditioned for $\alpha > 0$. In a first experiment we now consider the cube $\Omega = [-1, 1]^3[nm]$ and an initial homogeneous magnetization in the direction $[1, 1, 1]$. The initial state is visualized in Figure 3.13 top left. We then consider the exchange contribution

as well as some uniaxial anisotropy with easy axis in x_3 -direction, i.e.

$$\mathbf{h}_{\text{eff}} = C_e \Delta \mathbf{m} + C_a D \Phi(\mathbf{m}).$$

The constants are chosen as in the NIST μMAG 3 problem as $C_e = 10^{-11}$ and $C_a = 39788.73455192433$, cf. [Webb]. The time interval is given by $[0, 2][ns]$ and we choose $\alpha = 1$. We observe a rotation of \mathbf{m} around the easy axis and a damping towards it, cf. Figure 3.13 (*white arrows*). The condition number of M and the full matrix from (3.3.1), as well as the ratio between $\text{cond}(M)$ and $\text{cond}(\text{full})$ are visualized in Figure 3.12. As predicted by theory, both matrices are well-conditioned and hence admit unique solvability.

This observation, however, leaves the obvious question of the case $\alpha = 0$. We stress that this case is well worth studying as it occurs in the study of spin torques [Ber02, HKC04], for example. In Figure 3.14, the condition numbers of the involved matrices for $\alpha = 0$ are visualized. We empirically observe unique solvability in the tangent space, whereas the matrix M is ill-conditioned in this case. In fact, the condition number of the full system is about 10^{11} times smaller and the system thus admits inversion.

The magnetization dynamics for this case are finally visualized in Figure 3.13 (*red arrows*). As expected, we observe a rotation around the effective magnetic field which—in this case—points into the direction of the easy axis.

Insight into this behaviour – at least for some cases – is indeed hidden in the tangent plane constraint. For $\alpha = 0$, at first sight, equation (2.2.3) breaks down to

$$C_e k \theta (\nabla \mathbf{v}_h^j, \nabla \boldsymbol{\psi}) + (\mathbf{m}_h^j \times \mathbf{v}_h^j, \boldsymbol{\psi}) = L^j(\boldsymbol{\psi}), \quad (3.3.2)$$

where $L^j(\cdot)$ denotes the right-hand side from (2.2.3). This yields

$$a^j(\boldsymbol{\psi}, \boldsymbol{\psi}) = C_e k \theta (\nabla \boldsymbol{\psi}, \nabla \boldsymbol{\psi}) + (\mathbf{m}_h^j \times \boldsymbol{\psi}, \boldsymbol{\psi}) = C_e k \theta \|\nabla \boldsymbol{\psi}\|_{L^2(\Omega)}^2,$$

which is not an equivalent norm on $\mathcal{S}^1(\Omega)$. This is not surprising, since the constant functions are within the kernel of $a^j(\cdot, \cdot)$ and (2.2.3) does therefore not admit a unique solution in $\mathcal{S}^1(\Omega)$ for $\alpha = 0$. The tangent plane constraint can, however, be exploited in order to improve the solvability result at least in some cases.

To that end, suppose that there exist three nodes $\mathbf{z}_1, \mathbf{z}_2, \mathbf{z}_3 \in \mathcal{N}_h$ such that the individual components of the magnetization evaluated at those nodes are linearly independent. That is to say

$$\left| c_1 \begin{pmatrix} m_1^j(\mathbf{z}_1) \\ m_1^j(\mathbf{z}_2) \\ m_1^j(\mathbf{z}_3) \end{pmatrix} + c_2 \begin{pmatrix} m_2^j(\mathbf{z}_1) \\ m_2^j(\mathbf{z}_2) \\ m_2^j(\mathbf{z}_3) \end{pmatrix} + c_3 \begin{pmatrix} m_3^j(\mathbf{z}_1) \\ m_3^j(\mathbf{z}_2) \\ m_3^j(\mathbf{z}_3) \end{pmatrix} \right| = 0$$

implies

$$\begin{pmatrix} c_1 \\ c_2 \\ c_3 \end{pmatrix} = 0$$

for constants $c_1, c_2, c_3 \in \mathbb{R}$ and where m_i^j denotes the i -th component of \mathbf{m}_h^j for $i = 1, 2, 3$. We emphasize that those three nodes $\mathbf{z}_1, \mathbf{z}_2, \mathbf{z}_3$ may be different for each $j > 0$ and we simply assume that three of those exist in each step of the algorithm.

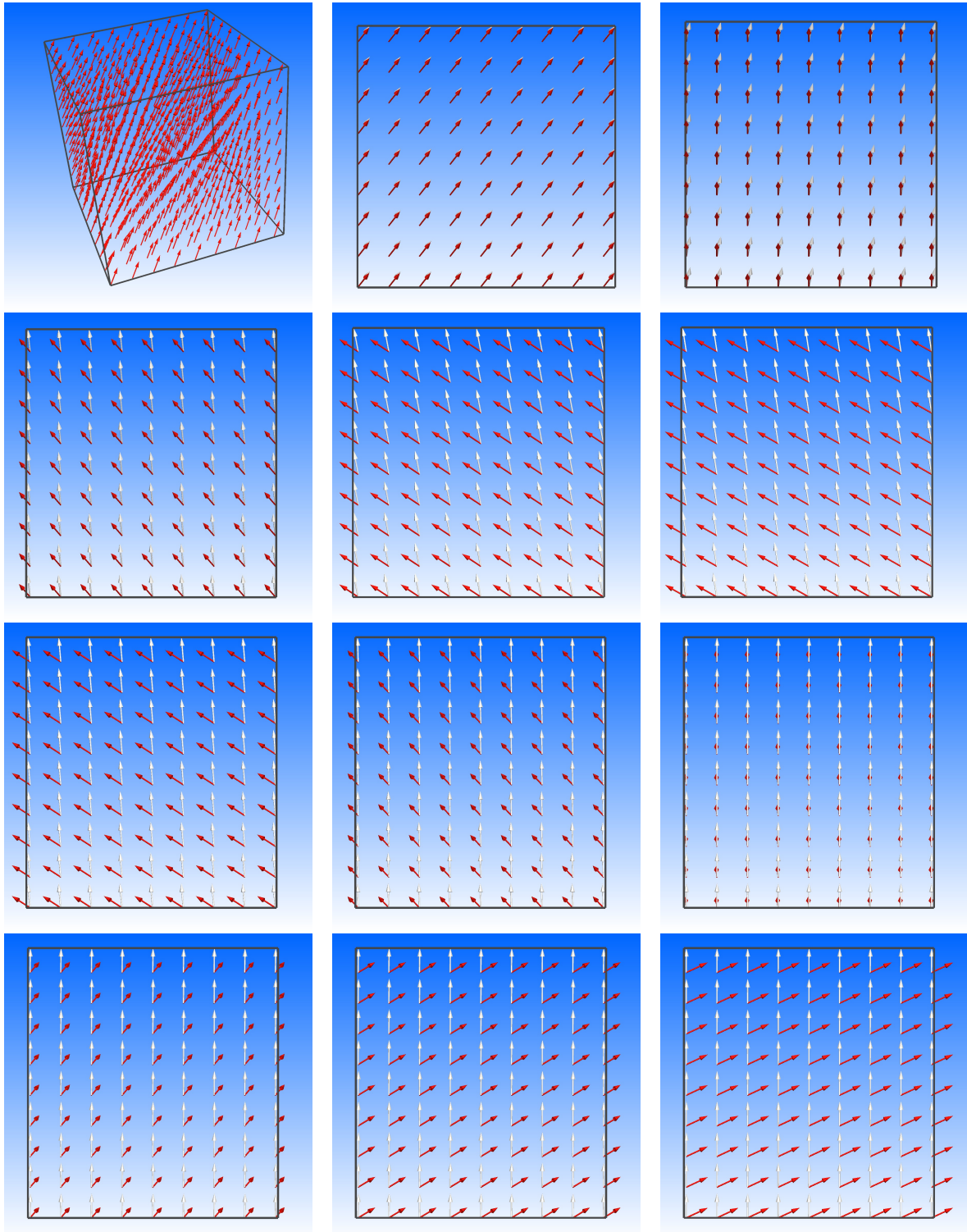


Figure 3.13.: Magnetization dynamics as 2D projection on $[0, 2]$ for $\alpha = 1$ (white) and $\alpha = 0$ (red). Initial state is visualized in the top left picture

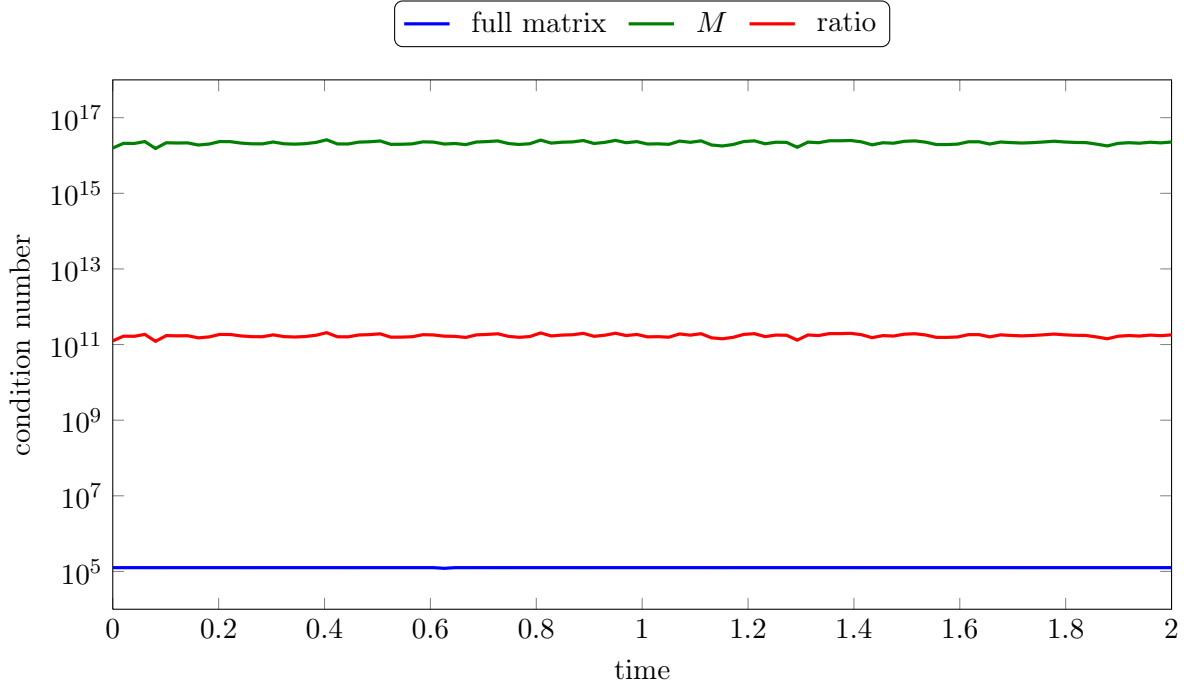


Figure 3.14.: Condition numbers of M and the full matrix from (3.3.1) for $\alpha = 0$ plotted over the simulation time.

Under this assumption, (3.3.2) admits a unique solution $\mathbf{v}_h^j \in \mathcal{K}_{\mathbf{m}_h^j}$ in each step j even for $\alpha = 0$. To see this, we define

$$\|\mathbf{v}\| := \|\nabla \mathbf{v}\|_{L^2(\Omega)} + \sum_{\mathbf{z} \in \mathcal{N}_h} |\mathbf{v}(\mathbf{z}) \cdot \mathbf{m}_h^j(\mathbf{z})|$$

for all $\mathbf{v} \in \mathcal{S}^1(\mathcal{T}_h)$. Obviously, $\|\cdot\|$ is a seminorm on $\mathcal{S}^1(\mathcal{T}_h)$, and from the tangent plane condition, we get

$$\|\mathbf{v}\| = \|\nabla \mathbf{v}\|_{L^2(\Omega)} \quad \text{for all } \mathbf{v} \in \mathcal{K}_{\mathbf{m}_h^j}.$$

It remains to show that $\|\cdot\|$ indeed defines a norm on $\mathcal{S}^1(\mathcal{T}_h)$. To that end, we only need to show that $\sum_{\mathbf{z} \in \mathcal{N}_h} |\mathbf{v}(\mathbf{z}) \cdot \mathbf{m}_h^j(\mathbf{z})|$ is definite on the constant functions. Now let $c \in \mathbb{R}^3$ be constant, i.e.

$$c = \begin{pmatrix} c_1 \\ c_2 \\ c_3 \end{pmatrix}$$

for some $c_1, c_2, c_3 \in \mathbb{R}$, and consider

$$\sum_{\mathbf{z} \in \mathcal{N}_h} |c \cdot \mathbf{m}_h^j(\mathbf{z})| = 0.$$

By definition, this yields

$$|c_1 m_1^j(\mathbf{z}) + c_2 m_2^j(\mathbf{z}) + c_3 m_3^j(\mathbf{z})| = 0 \quad \text{for all } \mathbf{z} \in \mathcal{N}_h$$

and thus also

$$\begin{aligned} 0 &= |c_1 m_1^j(\mathbf{z}_1) + c_2 m_2^j(\mathbf{z}_1) + c_3 m_3^j(\mathbf{z}_1)| \\ &\quad + |c_1 m_1^j(\mathbf{z}_2) + c_2 m_2^j(\mathbf{z}_2) + c_3 m_3^j(\mathbf{z}_2)| \\ &\quad + |c_1 m_1^j(\mathbf{z}_3) + c_2 m_2^j(\mathbf{z}_3) + c_3 m_3^j(\mathbf{z}_3)|, \end{aligned}$$

for the special nodes $\mathbf{z}_1, \mathbf{z}_2, \mathbf{z}_3$ from above. The last estimate is, however, equivalent to

$$\left| c_1 \begin{pmatrix} m_1^j(\mathbf{z}_1) \\ m_1^j(\mathbf{z}_2) \\ m_1^j(\mathbf{z}_3) \end{pmatrix} + c_2 \begin{pmatrix} m_2^j(\mathbf{z}_1) \\ m_2^j(\mathbf{z}_2) \\ m_2^j(\mathbf{z}_3) \end{pmatrix} + c_3 \begin{pmatrix} m_3^j(\mathbf{z}_1) \\ m_3^j(\mathbf{z}_2) \\ m_3^j(\mathbf{z}_3) \end{pmatrix} \right| = 0,$$

which yields $c_1 = c_2 = c_3 = 0$ by assumption. The quantity $\|\cdot\|$ thus defines a norm on $\mathcal{S}^1(\mathcal{T}_h)$, whence $\|\nabla(\cdot)\|_{\mathbf{L}^2(\Omega)}$ is a norm on $\mathcal{K}_{\mathbf{m}_h^j}$.

Even without \mathbf{L}^2 -contribution within the bilinear form, we thus deduce that (3.3.2) admits a unique solution $\mathbf{v}_h^j \in \mathcal{K}_{\mathbf{m}_h^j}$. Even though, this does not fully cover the experiment at hand, we observe that the scheme's solvability greatly benefits from the tangent test space. The experiment, however, empirically suggests that the tangent plane constraint allows unique solvability even under weaker assumptions.

Artificial damping

Within the context of neglected damping, there is one more thing to investigate, which is actually a drawback of the tangent plane algorithm: *artificial damping*. To that end, we go back to the 2D blowup example from before, i.e. we consider the exchange only case. For this particular effective field, in combination with $\alpha = 0$, the analysis from Lemma 2.3.3 reveals

$$\frac{1}{2} \|\nabla \mathbf{m}_h^{j+1}\|_{\mathbf{L}^2(\Omega)}^2 \leq \frac{1}{2} \|\nabla \mathbf{m}_h^j\|_{\mathbf{L}^2}^2 - (\theta - \frac{1}{2}) k^2 \|\nabla \mathbf{v}_h^j\|_{\mathbf{L}^2(\Omega)}^2. \quad (3.3.3)$$

Put explicitly, even for the $\alpha = 0$ case, we do not have an energy equality, but rather an inequality in each time step. Moreover, on the right-hand side, we get the additional term $(\theta - 1/2)k^2 \|\nabla \mathbf{v}_h^j\|_{\mathbf{L}^2(\Omega)}^2$ with a negative sign. We emphasize that this term rises simply from the construction of the scheme and by no means follows from the equation. For $\theta \in (1/2, 1]$, which is the interesting case, we therefore deduce

$$\frac{1}{2} \|\nabla \mathbf{m}_h^{j+1}\|_{\mathbf{L}^2(\Omega)}^2 < \frac{1}{2} \|\nabla \mathbf{m}_h^j\|_{\mathbf{L}^2(\Omega)}^2. \quad (3.3.4)$$

Even though, we chose the damping parameter to be zero, a certain term is subtracted from the energy in each step, and we thus cannot expect constant energy in the no-damping case. More precisely, using the semi-implicit tangent plane scheme, it is not straightforward to simulate a micromagnetic process without any damping at all. This is somehow the price for unconditional stability which was derived by introducing this additional energy term in the first place. In fact, we expect this behaviour to be stronger, the bigger we choose θ . Indeed, the predicted behaviour can be observed numerically and the energy for different values of θ , $\alpha = 0$, $h = 1/32$ and $k = 0.0001$ is plotted over the time in Figure 3.15. As expected, we can clearly see an energy decay in the no-damping case. Obviously, this is much smaller

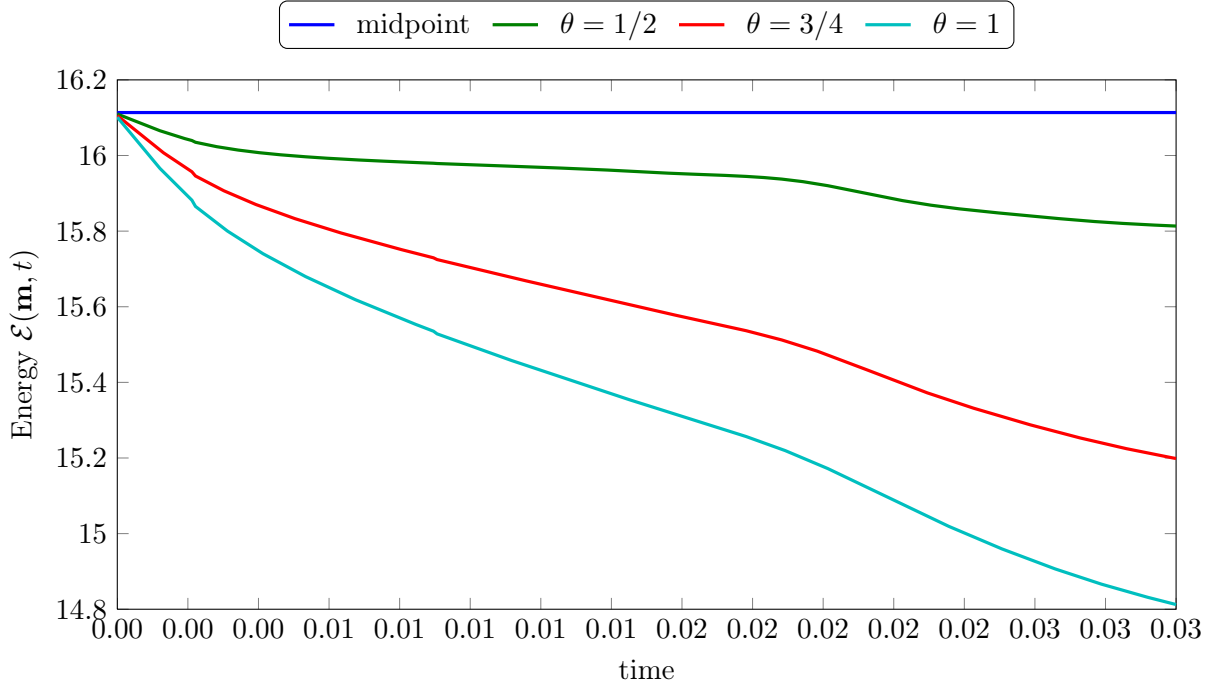


Figure 3.15.: Energy $\mathcal{E}(\mathbf{m}, t)$ for different values of θ plotted over time. Energy computed with the midpoint scheme is plotted for comparison (dark blue).

than in the case where damping is considered, but it is still not negligible. Moreover, the empirical observations confirm that the artificial energy decay becomes smaller the closer we get to $\theta = 1/2$. In this case the artificial damping term from above vanishes. Even in the case $\theta = 1/2$, we observe some damping of the energy which is, however, in agreement with our theory, as in none of the cases can we prove an energy equality. For sake of comparison, we also plot the energy of the midpoint scheme computation from [BP06] for the same setting (dark blue). Comparison data was provided by JONATHAN ROCHAT which is thankfully acknowledged. For this scheme, in the no-damping case, an energy equality can indeed be derived, and we observe the respective behaviour in this experiment. Altogether, we thus conclude that the artificial damping of the tangent plane scheme stems from the introduction of the implicit part in combination with the normalization step.

Coupling to full Maxwell system

In this chapter, we finally consider something other than the pure LLG equation and investigate coupling to other PDEs. First, we will analyze the coupling of LLG to the full Maxwell system. This allows us to treat the effects stemming from the magnetic strayfield more accurately than before. Moreover, via $\sigma \neq 0$ in (4.1.1) below, this ansatz allows to model conducting ferromagnets. The latter is unclear for the magnetostatic strayfield approximation which has been investigated so far [MV01]. The results of this chapter have partially been published in [BPP13].

4.1. The Maxwell-Landau-Lifshitz-Gilbert system

We consider the coupled Maxwell-Landau-Lifshitz-Gilbert system (MLLG) to accurately describe the effects of the self-induced magnetic strayfield onto the magnetization \mathbf{m} . To that end, we consider the two domains $\Omega \Subset \widehat{\Omega} \subseteq \mathbb{R}^3$, where the Maxwell system is solved on the larger domain $\widehat{\Omega}$, and the LLG equation is solved on the embedded domain Ω . This is due to the fact that the strayfield exists even outside the micromagnetic domain Ω and that its values outside of Ω again influence the magnetization \mathbf{m} . For given parameters $\alpha, \varepsilon_0, \mu_0, \sigma \geq 0$, the MLLG system reads

$$\mathbf{m}_t - \alpha \mathbf{m} \times \mathbf{m}_t = -\mathbf{m} \times \mathbf{h}_{\text{eff}} \quad \text{in } \Omega_T \tag{4.1.1a}$$

$$\varepsilon_0 \mathbf{E}_t - \nabla \times \mathbf{H} + \sigma \chi_\Omega \mathbf{E} = -\mathbf{J} \quad \text{in } \widehat{\Omega}_T := (0, T) \times \widehat{\Omega} \tag{4.1.1b}$$

$$\mu_0 \mathbf{H}_t + \nabla \times \mathbf{E} = -\mu_0 \mathbf{m}_t \quad \text{in } \widehat{\Omega}_T. \tag{4.1.1c}$$

Here, the variables $\mathbf{H} : \widehat{\Omega}_T \rightarrow \mathbb{R}^3$ and $\mathbf{E} : \widehat{\Omega}_T \rightarrow \mathbb{R}^3$ denote the sought electric and magnetic field, respectively. More details on the derivation of the System 4.1.1 are given in Section 1.4.2. In analogy to the Chapters 2 and 3, the effective field \mathbf{h}_{eff} consists of $\mathbf{h}_{\text{eff}} = C_e \Delta \mathbf{m} + \mathbf{H} + \boldsymbol{\pi}(\mathbf{m})$ for some general field contribution $\boldsymbol{\pi}$. For sake of simplicity, the time dependent field contribution χ is neglected here. Also, we neglect a possible spatial approximation $\boldsymbol{\pi}_h$ of $\boldsymbol{\pi}$. We stress, however, that using the techniques from Chapter 2, the inclusion of the approximation $\boldsymbol{\pi}_h$ is straightforward. We thus only assume the general contribution to be uniformly bounded and a priori weakly subconvergent, i.e. (4.2.7) and (4.2.11) below. As before, we emphasize that the case $\mathbf{h}_{\text{eff}} = C_e \Delta \mathbf{m} + \mathbf{H} + C_a D\Phi(\mathbf{m}) + \mathbf{f}$ is particularly covered. The constants $\varepsilon_0, \mu_0 \geq 0$ in (4.1.1) denote the electric and magnetic permeability of free space, respectively,

and the constant $\sigma \geq 0$ stands for the conductivity of the ferromagnetic domain Ω . The field $\mathbf{J} : \widehat{\Omega}_T \rightarrow \mathbb{R}^3$ describes a known applied current density and $\chi_\Omega : \widehat{\Omega} \rightarrow \{0, 1\}$ is the characteristic function of Ω . As is usually done for simplicity [BBP08], we assume $\widehat{\Omega} \subset \mathbb{R}^3$ to be bounded with perfectly conducting outer surface $\partial\widehat{\Omega}$ into which the ferromagnet $\Omega \Subset \widehat{\Omega}$ is embedded, and $\widehat{\Omega} \setminus \overline{\Omega}$ is assumed to be vacuum. In addition, the MLLG system (4.1.1) is supplemented by initial conditions

$$\mathbf{m}(0, \cdot) = \mathbf{m}^0 \text{ in } \Omega \quad \text{and} \quad \mathbf{E}(0, \cdot) = \mathbf{E}^0, \quad \mathbf{H}(0, \cdot) = \mathbf{H}^0 \text{ in } \widehat{\Omega} \quad (4.1.1d)$$

as well as boundary conditions

$$\partial_{\mathbf{n}} \mathbf{m} = 0 \text{ on } \partial\Omega_T, \quad \mathbf{E} \times \mathbf{n} = 0 \text{ on } \partial\widehat{\Omega}_T. \quad (4.1.1e)$$

In analogy to [CF98, BBP08], we assume the given data to satisfy

$$\mathbf{m}^0 \in \mathbf{H}^1(\Omega, \mathbb{S}^2), \quad \mathbf{H}^0, \mathbf{E}^0 \in \mathbf{L}^2(\widehat{\Omega}, \mathbb{R}^3), \quad \mathbf{J} \in \mathbf{L}^2(\widehat{\Omega}_T, \mathbb{R}^3) \quad (4.1.1f)$$

as well as

$$\operatorname{div}(\mathbf{H}^0 + \chi_\Omega \mathbf{m}^0) = 0 \quad \text{in } \widehat{\Omega}, \quad \langle \mathbf{H}^0 + \chi_\Omega \mathbf{m}^0, \mathbf{n} \rangle = 0 \quad \text{on } \partial\widehat{\Omega}. \quad (4.1.1g)$$

The latter stems from the material law (1.4.3) in combination with $\operatorname{div} B = 0$, i.e. (1.4.1d). Note that from (4.1.1c), one deduces $\partial_t \operatorname{div} B = 0$, whence $\operatorname{div} B(t) = \operatorname{div} B(0)$. It thus suffices to assume this property for the initial values. For the weak formulation of the Maxwell part, we introduce the space

$$\mathbf{H}_0(\operatorname{curl}, \widehat{\Omega}) := \{ \varphi \in \mathbf{L}^2(\widehat{\Omega}) : \nabla \times \varphi \in \mathbf{L}^2(\widehat{\Omega}), \varphi \times \mathbf{n} = 0 \text{ on } \Gamma \},$$

Next, we state the notion of a weak solution of the MLLG system (4.1.1) which goes back to [CF98].

Definition 4.1.1. Given (5.1.1e)–(5.1.1f), the tuple $(\mathbf{m}, \mathbf{E}, \mathbf{H})$ is called a weak solution of MLLG if,

- (i) $\mathbf{m} \in \mathbf{H}^1(\Omega_T)$ with $|\mathbf{m}| = 1$ almost everywhere in Ω_T and $(\mathbf{E}, \mathbf{H}) \in \mathbf{L}^2(\widehat{\Omega}_T)$;
- (ii) for all $\varphi \in C^\infty(\overline{\Omega_T})$ and $\zeta \in C_c^\infty([0, T]; C^\infty(\widehat{\Omega}) \cap \mathbf{H}_0(\text{curl}, \widehat{\Omega}))$ and $\xi \in C_c^\infty([0, T]; C^\infty(\widehat{\Omega}))$, we have

$$\int_{\Omega_T} \mathbf{m}_t \cdot \varphi - \alpha \int_{\Omega_T} (\mathbf{m} \times \mathbf{m}_t) \cdot \varphi = -C_e \int_{\Omega_T} (\nabla \mathbf{m} \times \mathbf{m}) \cdot \nabla \varphi \quad (4.1.2)$$

$$+ \int_{\Omega_T} (\mathbf{H} \times \mathbf{m}) \cdot \varphi + \int_{\Omega_T} (\boldsymbol{\pi}(\mathbf{m}) \times \mathbf{m}) \cdot \varphi, \quad (4.1.3)$$

$$- \varepsilon_0 \int_{\widehat{\Omega}_T} \mathbf{E} \cdot \zeta_t - \int_{\widehat{\Omega}_T} \mathbf{H} \cdot (\nabla \times \zeta) + \sigma \int_{\Omega_T} \mathbf{E} \cdot \zeta = - \int_{\widehat{\Omega}_T} \mathbf{J} \cdot \zeta + \varepsilon_0 \int_{\widehat{\Omega}} \mathbf{E}^0 \cdot \zeta(0, \cdot), \quad (4.1.3)$$

$$- \mu_0 \int_{\widehat{\Omega}_T} \mathbf{H} \cdot \xi_t + \int_{\widehat{\Omega}_T} \mathbf{E} \cdot (\nabla \times \xi) = -\mu_0 \int_{\Omega_T} \mathbf{m}_t \cdot \xi + \mu_0 \int_{\widehat{\Omega}} \mathbf{H}^0 \cdot \xi(0, \cdot); \quad (4.1.4)$$

- (iii) there holds $\mathbf{m}(0, \cdot) = \mathbf{m}^0$ in the sense of traces;

- (iv) for almost all $t' \in (0, T)$, we have bounded energy

$$\|\nabla \mathbf{m}(t')\|_{\mathbf{L}^2(\Omega)}^2 + \|\mathbf{m}_t\|_{\mathbf{L}^2(\Omega_t')}^2 + \|\mathbf{H}(t')\|_{\mathbf{L}^2(\widehat{\Omega})}^2 + \|\mathbf{E}(t')\|_{\mathbf{L}^2(\widehat{\Omega})}^2 \leq C, \quad (4.1.5)$$

where $C > 0$ is independent of t .

Note that the test functions for the Maxwell part are chosen from the space

$$C_c^\infty([0, T]; C^\infty(\widehat{\Omega})),$$

i.e. we impose a zero-condition for the upper time boundary. This is due to the fact that we only show boundedness of the involved quantities in $\mathbf{L}^2(\widehat{\Omega})$ and thus perform integration by parts in time to get rid of the time derivatives of \mathbf{E} and \mathbf{H} .

Existence of weak solutions was first shown in [CF98] for a simplified model. We stress, however, that our analysis is constructive in the sense that it also proves existence.

Remark. Under additional assumptions on the general contribution $\boldsymbol{\pi}(\cdot)$, namely that $\boldsymbol{\pi}(\cdot)$ is self-adjoint with $\|\boldsymbol{\pi}(\mathbf{n})\|_{\mathbf{L}^4(\Omega)} \leq C$ for all $\mathbf{n} \in \mathbf{L}^2(\Omega)$ with $|\mathbf{n}| \leq 1$ almost everywhere, the energy estimate (4.1.5) can be improved. The same techniques as in Lemma 2.4.1 then show for almost all $t' \in (0, T)$ and $\varepsilon > 0$

$$\mathcal{E}(\mathbf{m}, \mathbf{H}, \mathbf{E})(t') + 2(\alpha - \varepsilon)\mu_0 \|\mathbf{m}_t\|_{\mathbf{L}^2(\Omega_{t'})}^2 + 2\sigma \|\mathbf{E}\|_{\mathbf{L}^2(\Omega_{t'})}^2 \leq \mathcal{E}(\mathbf{m}, \mathbf{H}, \mathbf{E})(0) - \int_0^{t'} (\mathbf{J}, \mathbf{E}),$$

where

$$\mathcal{E}(\mathbf{m}, \mathbf{H}, \mathbf{E}) := \mu_0 C_e \|\nabla \mathbf{m}(t)\|_{\mathbf{L}^2(\Omega)}^2 + \mu_0 \|\mathbf{H}(t)\|_{\mathbf{L}^2(\widehat{\Omega})}^2 + \varepsilon_0 \|\mathbf{E}(t)\|_{\mathbf{L}^2(\widehat{\Omega})}^2 - \mu_0 \langle \boldsymbol{\pi}(\mathbf{m}(t)), \mathbf{m}(t) \rangle.$$

This is in analogy to [BBP08] and the result is formally stated and proved in Section 4.2.3. In particular, the above assumptions are fulfilled in case of vanishing applied field $\mathbf{f} \equiv 0$ and if $\boldsymbol{\pi}(\cdot)$ denotes the uniaxial anisotropy density.

4.2. Preliminaries and numerical algorithms

In this section, we present two numerical algorithms to treat the coupled Maxwell-LLG system (4.1.1). The first one follows the lines of BANAS, BARTELS & PROHL [BBP08] and describes a fully coupled system that may yield the possibility of a higher order extension by means of midpoint evaluations. The second one is fully decoupled which eases the analysis, the numerical implementation, as well as some possible preconditioning of the Maxwell part. Both algorithms are guaranteed to be unconditionally convergent towards a weak solution of the MLLG system in the sense of Definition 4.1.1. Before we come to the actual description of our numerical solvers, we like to fix some notation and preliminaries.

For the spatial discretization, let $\mathcal{T}_h^{\hat{\Omega}}$ be a regular triangulation of the polyhedral and bounded Lipschitz domain $\hat{\Omega} \subset \mathbb{R}^3$ into compact and non-degenerate tetrahedra. By \mathcal{T}_h , we denote its restriction to $\Omega \Subset \hat{\Omega}$, where we assume that Ω is resolved, i.e.

$$\mathcal{T}_h = \mathcal{T}_h^{\hat{\Omega}}|_{\Omega} = \{T \in \mathcal{T}_h^{\hat{\Omega}} : T \cap \Omega \neq \emptyset\} \quad \text{and} \quad \bar{\Omega} = \bigcup_{T \in \mathcal{T}_h} T.$$

As before (Section 2.1.1), we denote the standard \mathcal{P}^1 -FEM space of globally continuous and piecewise affine functions from Ω to \mathbb{R}^3 by $\mathcal{S}^1(\mathcal{T}_h)$ and by \mathcal{I}_h the nodal interpolation operator onto this space. By \mathcal{M}_h , we denote the set of admissible functions of unit length and by \mathcal{K}_{Φ_h} the pointwise orthogonal space of Φ_h for any $\Phi_h \in \mathcal{M}_h$.

For discretization of Maxwell's equations (4.1.1b)–(4.1.1c), we use conforming ansatz spaces $\mathcal{X}_h \subset \mathbf{H}_0(\text{curl}; \hat{\Omega})$, $\mathcal{Y}_h \subset \mathbf{L}^2(\hat{\Omega})$ subordinate to $\mathcal{T}_h^{\hat{\Omega}}$ which additionally fulfill $\nabla \times \mathcal{X}_h \subset \mathcal{Y}_h$. In analogy to [BBP08], one can choose e.g. first order edge elements

$$\mathcal{X}_h := \{\varphi_h \in \mathbf{H}_0(\text{curl}; \hat{\Omega}) : \varphi_h|_K \in \mathcal{P}_1(K) \text{ for all } K \in \mathcal{T}_h^{\hat{\Omega}}\}$$

and piecewise constants

$$\mathcal{Y}_h := \{\zeta_h \in \mathbf{L}^2(\hat{\Omega}) : \zeta_h|_K \in \mathcal{P}_0(K) \text{ for all } K \in \mathcal{T}_h^{\hat{\Omega}}\}.$$

We refer to [Mon08, Chapter 8.5] for more information and properties of these spaces. Associated with \mathcal{X}_h , let $\mathcal{I}_{\mathcal{X}_h} : \mathbf{H}^2(\hat{\Omega}) \rightarrow \mathcal{X}_h$ denote the corresponding nodal FEM interpolator. Moreover, let

$$\mathcal{I}_{\mathcal{Y}_h} : \mathbf{L}^2(\hat{\Omega}) \rightarrow \mathcal{Y}_h$$

denote the \mathbf{L}^2 -orthogonal projection, characterized by

$$(\zeta - \mathcal{I}_{\mathcal{Y}_h} \zeta, \mathbf{y}_h) = 0 \quad \text{for all } \zeta \in \mathbf{L}^2(\hat{\Omega}) \text{ and } \mathbf{y}_h \in \mathcal{Y}_h.$$

By standard estimates, see e.g. [Mon08], one derives the approximation properties

$$\|\varphi - \mathcal{I}_{\mathcal{X}_h} \varphi\|_{\mathbf{L}^2(\hat{\Omega})} + h \|\nabla \times (\varphi - \mathcal{I}_{\mathcal{X}_h} \varphi)\|_{\mathbf{L}^2(\hat{\Omega})} \leq C h^2 \|\nabla^2 \varphi\|_{\mathbf{L}^2(\hat{\Omega})} \quad (4.2.1)$$

$$\|\zeta - \mathcal{I}_{\mathcal{Y}_h} \zeta\|_{\mathbf{L}^2(\hat{\Omega})} \leq C h \|\zeta\|_{\mathbf{H}^1(\hat{\Omega})} \quad (4.2.2)$$

for all $\varphi \in \mathbf{H}^2(\hat{\Omega})$ and $\zeta \in \mathbf{H}^1(\hat{\Omega})$ and some h -independent constant $C > 0$.

For ease of presentation, we finally assume that the applied field \mathbf{J} is continuous in time, i.e. $\mathbf{J} \in C([0, T]; \mathbf{L}^2(\Omega))$ so that $\mathbf{J}^j := \mathbf{J}(t_j)$ is meaningful. We emphasize, however, that this

is not necessary for our convergence analysis. For discretization of the time derivative, we employ the difference quotient of first order, i.e.

$$d_t \phi^{j+1} = \frac{\phi^{j+1} - \phi^j}{k}.$$

Next, we propose two algorithms for the numerical integration of MLLG, where the first one follows the lines of [BBP08].

Algorithm 4.2.1. *Input: Initial data \mathbf{m}^0 , \mathbf{E}^0 , and \mathbf{H}^0 , parameter $\theta \in [0, 1]$, counter $j = 0$. For all $j = 0, \dots, N - 1$ iterate:*

(i) *Compute unique solution $(\mathbf{v}_h^j, \mathbf{E}_h^{j+1}, \mathbf{H}_h^{j+1}) \in (\mathcal{K}_{\mathbf{m}_h^j}, \mathcal{X}_h, \mathcal{Y}_h)$ such that for all $(\phi_h, \psi_h, \zeta_h) \in \mathcal{K}_{\mathbf{m}_h^j} \times \mathcal{X}_h \times \mathcal{Y}_h$, there holds*

$$\begin{aligned} \alpha(\mathbf{v}_h^j, \phi_h) + ((\mathbf{m}_h^j \times \mathbf{v}_h^j), \phi_h) &= -C_e(\nabla(\mathbf{m}_h^j + \theta k \mathbf{v}_h^j), \nabla \phi_h) \\ &\quad + (\mathbf{H}_h^{j+1/2}, \phi_h) + (\boldsymbol{\pi}(\mathbf{m}_h^j), \phi_h), \end{aligned} \quad (4.2.3a)$$

$$\varepsilon_0(d_t \mathbf{E}_h^{j+1}, \psi_h) - (\mathbf{H}_h^{j+1/2}, \nabla \times \psi_h) + \sigma(\chi_\Omega \mathbf{E}_h^{j+1/2}, \psi_h) = -(\mathbf{J}^{j+1/2}, \psi_h), \quad (4.2.3b)$$

$$\mu_0(d_t \mathbf{H}_h^{j+1}, \zeta_h) + (\nabla \times \mathbf{E}_h^{j+1/2}, \zeta_h) = -\mu_0(\mathbf{v}_h^j, \zeta_h). \quad (4.2.3c)$$

(ii) *Define $\mathbf{m}_h^{j+1} \in \mathcal{M}_h$ nodewise by $\mathbf{m}_h^{j+1}(z) = \frac{\mathbf{m}_h^j(z) + k \mathbf{v}_h^j(z)}{|\mathbf{m}_h^j(z) + k \mathbf{v}_h^j(z)|}$ for all $z \in \mathcal{N}_h$*

Note that the scalar product $(\mathbf{v}_h^j, \zeta_h)$ in (4.2.3b) is the $L^2(\widehat{\Omega})$ -scalar product. Here, we thus implicitly use the zero extension

$$\widetilde{\mathbf{v}}_h^j(\mathbf{x}) := \begin{cases} \mathbf{v}_h^j(\mathbf{x}) & \mathbf{x} \in \Omega \\ 0 & \text{else.} \end{cases} \quad (4.2.4)$$

For the sake of computational and implementational ease, LLG and Maxwell's equations can be decoupled, which leads to two smaller linear systems per time step. This modification is explicitly stated in the second algorithm.

Algorithm 4.2.2. *Input: Initial data \mathbf{m}^0 , \mathbf{E}^0 , and \mathbf{H}^0 , parameter $\theta \in [0, 1]$, counter $j = 0$. For all $j = 0, \dots, N - 1$ iterate:*

(i) *Compute unique solution $\mathbf{v}_h^j \in \mathcal{K}_{\mathbf{m}_h^j}$ such that for all $\phi_h \in \mathcal{K}_{\mathbf{m}_h^j}$, there holds*

$$\alpha(\mathbf{v}_h^j, \phi_h) + ((\mathbf{m}_h^j \times \mathbf{v}_h^j), \phi_h) = -C_e(\nabla(\mathbf{m}_h^j + \theta k \mathbf{v}_h^j), \nabla \phi_h) + (\mathbf{H}_h^j, \phi_h) + (\boldsymbol{\pi}(\mathbf{m}_h^j), \phi_h). \quad (4.2.5a)$$

(ii) *Compute unique solution $(\mathbf{E}_h^{j+1}, \mathbf{H}_h^{j+1}) \in (\mathcal{X}_h, \mathcal{Y}_h)$ such that for all $(\boldsymbol{\psi}_h, \boldsymbol{\zeta}_h) \in \mathcal{X}_h \times \mathcal{Y}_h$, there holds*

$$\varepsilon_0(d_t \mathbf{E}_h^{j+1}, \boldsymbol{\psi}_h) - (\mathbf{H}_h^{j+1}, \nabla \times \boldsymbol{\psi}_h) + \sigma(\chi_\Omega \mathbf{E}_h^{j+1}, \boldsymbol{\psi}_h) = -(\mathbf{J}^j, \boldsymbol{\psi}_h), \quad (4.2.5b)$$

$$\mu_0(d_t \mathbf{H}_h^{j+1}, \boldsymbol{\zeta}_h) + (\nabla \times \mathbf{E}_h^{j+1}, \boldsymbol{\zeta}_h) = -\mu_0(\mathbf{v}_h^j, \boldsymbol{\zeta}_h). \quad (4.2.5c)$$

(iii) *Define $\mathbf{m}_h^{j+1} \in \mathcal{M}_h$ nodewise by $\mathbf{m}_h^{j+1}(z) = \frac{\mathbf{m}_h^j(z) + k \mathbf{v}_h^j(z)}{|\mathbf{m}_h^j(z) + k \mathbf{v}_h^j(z)|}$ for all $z \in \mathcal{N}_h$.*

In the above algorithm, the scalar product in (4.2.5c) is again understood in the sense of (4.2.4).

Remark. *Before we come to the analysis of the two presented algorithms, we briefly want to remark on their quality and benefits. The first Algorithm 4.2.1 follows the ideas of [BBP08] and, due to the midpoint evaluation, might be extendable to a scheme which is of higher order in time. While the second Algorithm 4.2.2 seems to be only a minor extension of the first one, it provides major advantages. Besides simplifications in the analysis, this scheme seems to be vastly superior for an actual numerical implementation: First, since the two equations are decoupled, it can easily be added to an existing LLG solver. Second, since the Maxwell part can be treated separately, possible preconditioning techniques as in [Bañ10] can directly be applied.*

It is quite straightforward to see that both of the above algorithms are well-defined, i.e. admit unique solutions in each step of the respective loop. This result is formally stated and proved in the next two lemmata. We start with the coupled system of Algorithm 4.2.1.

Lemma 4.2.3. *Algorithm 4.2.1 is well-defined in the sense that in each step $j = 0, \dots, N - 1$ of the loop, there exist unique solutions $(\mathbf{m}_h^{j+1}, \mathbf{v}_h^j, \mathbf{E}_h^{j+1}, \mathbf{H}_h^{j+1})$.*

Proof. We multiply the first equation of (4.2.3) by μ_0 and the second and third equation by some free parameter $C_{21} > 0$, which will be fixed later, to define the bilinear form $a^j(\cdot, \cdot)$ on $(\mathcal{K}_{\mathbf{m}_h^j}, \mathcal{X}_h, \mathcal{Y}_h)$ by

$$\begin{aligned} a^j((\boldsymbol{\Phi}, \boldsymbol{\Psi}, \boldsymbol{\Theta}), (\phi, \boldsymbol{\psi}, \boldsymbol{\zeta})) &:= \alpha \mu_0(\boldsymbol{\Phi}, \phi) + \mu_0((\mathbf{m}_h^j \times \boldsymbol{\Phi}), \phi) + \mu_0 C_e \theta k (\nabla \boldsymbol{\Phi}, \nabla \phi) - \frac{\mu_0}{2}(\boldsymbol{\Theta}, \boldsymbol{\zeta}) \\ &+ \frac{C_{21} \varepsilon_0}{k}(\boldsymbol{\Psi}, \boldsymbol{\psi}) - \frac{C_{21}}{2}(\boldsymbol{\Theta}, \nabla \times \boldsymbol{\psi}) + \frac{C_{21} \sigma}{2}(\chi_\Omega \boldsymbol{\Psi}, \boldsymbol{\psi}) \\ &+ \frac{C_{21} \mu_0}{k}(\boldsymbol{\Theta}, \boldsymbol{\zeta}) + \frac{C_{21}}{2}(\nabla \times \boldsymbol{\Psi}, \boldsymbol{\zeta}) + C_{21} \mu_0(\boldsymbol{\Phi}, \boldsymbol{\zeta}) \end{aligned}$$

and the linear functional $L^j(\cdot)$ on $(\mathcal{K}_{\mathbf{m}_h^j}, \mathcal{X}_h, \mathcal{Y}_h)$ by

$$\begin{aligned} L^j((\phi, \psi, \zeta)) &:= -\mu_0 C_e (\nabla \mathbf{m}_h^j, \nabla \phi) + \frac{\mu_0}{2} (\mathbf{H}_h^j, \phi) + \mu_0 (\boldsymbol{\pi}(\mathbf{m}_h^j), \phi) \\ &\quad + \frac{C_{21}\varepsilon_0}{k} (\mathbf{E}_h^j, \psi) + \frac{C_{21}}{2} (\mathbf{H}_h^j, \nabla \times \psi) - \frac{C_{21}\sigma}{2} (\chi_\Omega \mathbf{E}_h^j, \psi) - C_{21} (\mathbf{J}^{j+1/2}, \psi) \\ &\quad + \frac{C_{21}\mu_0}{k} (\mathbf{H}_h^j, \zeta) - \frac{C_{21}}{2} (\nabla \times \mathbf{E}_h^j, \zeta). \end{aligned}$$

To ease the readability, the respective first lines of these definitions stem from (4.2.3a), the second from (4.2.3b), and the third from (4.2.3c). Clearly, (4.2.3) is equivalent to

$$a^j((\mathbf{v}_h^j, \mathbf{E}_h^{j+1}, \mathbf{H}_h^{j+1}), (\phi_h, \psi_h, \zeta_h)) = L^j((\phi_h, \psi_h, \zeta_h)) \quad \text{for all } (\phi_h, \psi_h, \zeta_h) \in \mathcal{K}_{\mathbf{m}_h^j} \times \mathcal{X}_h \times \mathcal{Y}_h.$$

Next, we aim to show that the bilinear form $a^j(\cdot, \cdot)$ is positive definite on $\mathcal{K}_{\mathbf{m}_h^j} \times \mathcal{X}_h \times \mathcal{Y}_h$. Usage of the Hölder inequality reveals that for all $(\phi, \psi, \zeta) \in \mathcal{K}_{\mathbf{m}_h^j} \times \mathcal{X}_h \times \mathcal{Y}_h$ it holds that

$$\begin{aligned} a^j((\phi, \psi, \zeta), (\phi, \psi, \zeta)) &= \alpha \mu_0 (\phi, \phi) + \underbrace{\mu_0 ((\mathbf{m}_h^j \times \phi), \phi)}_{=0} + \mu_0 C_e \theta k (\nabla \phi, \nabla \phi) - \frac{\mu_0}{2} (\phi, \zeta) \\ &\quad + \frac{C_{21}\varepsilon_0}{k} (\psi, \psi) - \frac{C_{21}}{2} (\zeta, \nabla \times \psi) + \frac{C_{21}\sigma}{2} (\chi_\Omega \psi, \psi) \\ &\quad + \frac{C_{21}\mu_0}{k} (\zeta, \zeta) + \frac{C_{21}}{2} (\nabla \times \psi, \zeta) + C_{21}\mu_0 (\phi, \zeta) \\ &= \alpha \mu_0 (\phi, \phi) + \mu_0 C_e \theta k (\nabla \phi, \nabla \phi) + (C_{21}\mu_0 - \frac{\mu_0}{2}) (\phi, \zeta) \\ &\quad + \frac{C_{21}\varepsilon_0}{k} (\psi, \psi) + \frac{C_{21}\sigma}{2} (\chi_\Omega \psi, \psi) + \frac{C_{21}\mu_0}{k} (\zeta, \zeta) \\ &\geq \underbrace{(\alpha - 2\varepsilon(C_{21} - 1/2))}_{=:a} \mu_0 \|\phi\|_{L^2(\Omega)}^2 + \frac{C_{21}\varepsilon_0}{k} \|\psi\|_{L^2(\hat{\Omega})}^2 \\ &\quad + \underbrace{(\frac{C_{21}}{k} - \frac{C_{21} - 1/2}{2\varepsilon})}_{=:b} \mu_0 \|\zeta\|_{L^2(\hat{\Omega})}^2, \end{aligned}$$

where we have used

$$(\phi, \zeta) \geq -2\varepsilon \|\phi\|_{L^2(\Omega)}^2 - \frac{1}{2\varepsilon} \|\zeta\|_{L^2(\hat{\Omega})}^2.$$

For the last inequality, we employed the zero extension of ϕ in the sense of (4.2.4). Choosing $C_{21} = 1/2$ now yields $a, b > 0$ and thus the desired result.

From $\mathbf{v}_h^j \in \mathcal{K}_{\mathbf{m}_h^j}$ and the Pythagoras theorem, we get $|\mathbf{m}_h^j(\mathbf{z}) + k\mathbf{v}_h^j(\mathbf{z})|^2 = |\mathbf{m}_h^j(\mathbf{z})|^2 + k|\mathbf{v}_h^j(\mathbf{z})|^2 \geq 1$. Hence, also step (ii) of Algorithm 4.2.1 is well-defined. This concludes the proof. \square

The next Lemma states that also the second, fully decoupled algorithm is well-defined.

Lemma 4.2.4. *Algorithm 4.2.2 is well-defined in the sense that it admits a unique solution $(\mathbf{m}_h^{j+1}, \mathbf{v}_h^j, \mathbf{E}_h^{j+1}, \mathbf{H}_h^{j+1})$ in each step $j = 0, \dots, N-1$ of the iterative loop.*

Proof. For the first equation (4.2.5a), we define the bilinear form $a^j(\cdot, \cdot) : \mathcal{K}_{\mathbf{m}_h^j} \times \mathcal{K}_{\mathbf{m}_h^j} \rightarrow \mathbb{R}$ by

$$a_1^j(\Phi, \phi) := \alpha(\Phi, \phi) + ((\mathbf{m}_h^j \times \Phi), \phi) + \theta C_e k (\nabla \Phi, \nabla \phi)$$

and the functional

$$L_1^j(\phi) := -C_e(\nabla \mathbf{m}_h^j, \nabla \phi) + (\mathbf{H}_h^j, \phi) + (\pi(\mathbf{m}_h^j), \phi).$$

Then, (4.2.5a) is equivalent to

$$a_1^j(\mathbf{v}_h^j, \phi) = L_1^j(\phi) \quad \forall \phi \in \mathcal{K}_{\mathbf{m}_h^j}.$$

Obviously, $L^j(\cdot)$ is linear, while $a^j(\cdot, \cdot)$ is bilinear and positive definite, since

$$a^j(\phi, \phi) = \alpha \|\phi\|_{L^2(\Omega)}^2 + \theta C_e k \|\nabla \phi\|_{L^2(\Omega)}^2.$$

We thus deduce existence of a unique $\mathbf{v}_h^j \in \mathcal{K}_{\mathbf{m}_h^j}$ solving (4.2.5a). For the second equation (4.2.5b), we have to consider the bilinear form $a_2(\cdot, \cdot) : (\mathcal{X}_h, \mathcal{Y}_h) \times (\mathcal{X}_h, \mathcal{Y}_h) \rightarrow \mathbb{R}$ defined by

$$a_2((\Psi, \Theta), (\psi, \zeta)) := \frac{\varepsilon_0}{k}(\Psi, \psi) - (\Theta, \nabla \times \psi) + \sigma(\chi_\Omega \Psi, \psi) + \frac{\mu_0}{k}(\Theta, \zeta) + (\nabla \times \Psi, \zeta)$$

which is continuous and positive definite. This is easily seen by

$$\begin{aligned} a_2((\psi, \zeta), (\psi, \zeta)) &= \frac{\varepsilon_0}{k}(\psi, \psi) - (\zeta, \nabla \times \psi) + \sigma(\chi_\Omega \psi, \psi) + \frac{\mu_0}{k}(\zeta, \zeta) + (\nabla \times \psi, \zeta) \\ &= \frac{\varepsilon_0}{k}(\psi, \psi) + \sigma(\chi_\Omega \psi, \psi) + \frac{\mu_0}{k}(\zeta, \zeta) \\ &= \frac{\varepsilon_0}{k} \|\psi\|_{L^2(\hat{\Omega})}^2 + \frac{\mu_0}{k} \|\zeta\|_{L^2(\hat{\Omega})}^2 + \sigma \|\psi\|_{L^2(\Omega)}^2. \end{aligned}$$

We further define the functional

$$L_2^j((\psi, \zeta)) := -(\mathbf{J}^j, \psi) - \frac{\varepsilon_0}{k}(\mathbf{E}_h^j, \psi) - \mu_0(\mathbf{v}_h^j, \zeta) - \frac{\mu_0}{k}(\mathbf{H}_h^j, \zeta)$$

which is obviously linear. Hence, the system (4.2.5b)–(4.2.5c) is equivalent to

$$a_2((\mathbf{E}_h^{j+1}, \mathbf{H}_h^{j+1}), (\psi, \zeta)) = L_2^j(\psi, \zeta) \quad \forall (\psi, \zeta) \in (\mathcal{X}_h, \mathcal{Y}_h).$$

Due to finite dimension, there is a unique solution $(\mathbf{E}_h^{j+1}, \mathbf{H}_h^{j+1})$ of (4.2.5b)–(4.2.5c). As in Lemma 6.2.2, we see that step (iii) of Algorithm 4.2.2 is also well-defined. \square

We will close this section with our main convergence theorem for the coupled Maxwell-LLG system which reads analogously to Theorem 2.3.1 and covers both algorithms 4.2.1 and 4.2.2 simultaneously. Since the proof is quite lengthy, it is postponed to the upcoming sections below.

We quickly recall the definition of our discrete quantities in the sense of Lemma 2.2.5. For $\mathbf{x} \in \Omega$ and $t \in [t_j, t_{j+1})$ and for $\gamma_h^\ell \in \{\mathbf{m}_h^\ell, \mathbf{H}_h^\ell, \mathbf{E}_h^\ell, \mathbf{J}^\ell, \mathbf{v}_h^\ell\}$ the discrete approximations are given by

$$\begin{aligned} \gamma_{hk}(t, \mathbf{x}) &:= \frac{t - t_j}{k} \gamma_h^{j+1}(\mathbf{x}) + \frac{t_{j+1} - t}{k} \gamma_h^j(\mathbf{x}) \\ \bar{\gamma}^-(t, \mathbf{x}) &:= \gamma_h^j(\mathbf{x}), \quad \bar{\gamma}^+(t, \mathbf{x}) := \gamma_h^{j+1}(\mathbf{x}). \end{aligned}$$

Furthermore, we define the midpoint evaluation by

$$\bar{\gamma}_{hk}(t, \mathbf{x}) := \gamma_h^{j+1/2}(\mathbf{x}) = \frac{\gamma_h^{j+1}(\mathbf{x}) + \gamma_h^j(\mathbf{x})}{2}.$$

The next statement is the main result of this chapter.

Theorem 4.2.5. (a) *Let $\theta \in (1/2, 1]$ and suppose that the spatial meshes \mathcal{T}_h are uniformly shape regular and satisfy the angle condition*

$$\int_{\Omega} \nabla \eta_i \cdot \nabla \eta_j \quad \text{for all basis functions } \eta_i, \eta_j \in \mathcal{S}^1(\mathcal{T}_h) \text{ with } i \neq j. \quad (4.2.6)$$

Moreover, suppose that the general field contribution $\boldsymbol{\pi}(\mathbf{n})$ is uniformly bounded, i.e.

$$\|\boldsymbol{\pi}(\mathbf{n})\|_{\mathbf{L}^2(\Omega)} \leq C_{\boldsymbol{\pi}} < \infty \quad (4.2.7)$$

for $\mathbf{n} \in \mathbf{L}^2(\Omega)$ with $|\mathbf{n}| \leq 1$ almost everywhere, and where the constants $C_{\boldsymbol{\pi}} > 0$ is independent of the timestep- and spatial mesh-sizes k and h . In particular, $C_{\boldsymbol{\pi}}$ may depend only on Ω . Assume additionally that we have convergence of the initial data, i.e.

$$\mathbf{m}_h^0 \rightharpoonup \mathbf{m}^0 \quad \text{weakly in } \mathbf{H}^1(\Omega) \quad (4.2.8)$$

as well as

$$\mathbf{H}_h^0 \rightharpoonup \mathbf{H}^0 \quad \text{and} \quad \mathbf{E}_h^0 \rightharpoonup \mathbf{E}^0 \quad \text{weakly in } \mathbf{L}^2(\hat{\Omega}). \quad (4.2.9)$$

Finally, for the field \mathbf{J} , we assume sufficient regularity, e.g. $\mathbf{J} \in C([0, T]; \mathbf{L}^2(\hat{\Omega}))$, such that

$$\mathbf{J}^{\pm} \rightharpoonup \mathbf{J} \quad \text{weakly in } \mathbf{L}^2(\hat{\Omega}_T). \quad (4.2.10)$$

Under these assumptions, we have strong subconvergence of \mathbf{m}_{hk}^- towards some function \mathbf{m} in $\mathbf{L}^2(\Omega_T)$.

(b) *In addition to the above, we assume the weak convergence property*

$$\boldsymbol{\pi}(\mathbf{m}_{hk}^-) \xrightarrow{\text{sub}} \boldsymbol{\pi}(\mathbf{m}) \quad \text{weakly subconvergent in } \mathbf{L}^2(\Omega_T). \quad (4.2.11)$$

Then, the computed FE solutions $(\mathbf{m}_{hk}, \mathbf{H}_{hk}, \mathbf{E}_{hk})$ of either Algorithm 4.2.1 or Algorithm 4.2.2 are weakly subconvergent in $\mathbf{H}^1(\Omega_T) \times \mathbf{L}^2(\hat{\Omega}_T) \times \mathbf{L}^2(\hat{\Omega}_T)$ towards a weak solution $(\mathbf{m}, \mathbf{H}, \mathbf{E})$ of the Maxwell-LLG system. In particular, this yields existence of weak solutions of MLLG and each accumulation point of $(\mathbf{m}_{hk}, \mathbf{E}_{hk}, \mathbf{H}_{hk})$ is a weak solution in the sense of Definition 4.1.1.

Remark. *As mentioned above, an approximation $\boldsymbol{\pi}_h(\cdot)$ of $\boldsymbol{\pi}(\cdot)$ can easily be included into the analysis. With the techniques from Chapter 2 the analysis directly carries over to this case and, in analogy to before, one then gets the constraints $\|\boldsymbol{\pi}_h(\mathbf{m}_h^j)\|_{\mathbf{L}^2(\hat{\Omega})} \leq C_{\boldsymbol{\pi}} < \infty$ as well as*

$$\boldsymbol{\pi}_h(\mathbf{m}_{hk}^-) \xrightarrow{\text{sub}} \boldsymbol{\pi}(\mathbf{m}) \quad \text{weakly subconvergent in } \mathbf{L}^2(\hat{\Omega}_T)$$

for the numerical approximation.

4.2.1. Analysis of coupled Algorithm 4.2.1

As in Section 2.3, the convergence analysis follows three steps.

- **Step 1:** Boundedness of the discrete quantities and energies.
- **Step 2:** Existence of weakly convergent subsequences.
- **Step 3:** Identification of the weak limits from Step 2 with a weak solution of the Maxwell-LLG system. This particularly shows existence of weak solutions.

We begin with the verification that the discrete quantities computed by Algorithm 4.2.1 are indeed uniformly bounded.

Step 1:

Lemma 4.2.6. *The discrete quantities $(\mathbf{m}_h^j, \mathbf{E}_h^j, \mathbf{H}_h^j) \in \mathcal{M}_h \times \mathcal{X}_h \times \mathcal{Y}_h$ fulfill*

$$\|\nabla \mathbf{m}_h^j\|_{\mathbf{L}^2(\Omega)}^2 + k \sum_{i=0}^{j-1} \|\mathbf{v}_h^i\|_{\mathbf{L}^2(\Omega)}^2 + \|\mathbf{H}_h^j\|_{\mathbf{L}^2(\widehat{\Omega})}^2 + \|\mathbf{E}_h^j\|_{\mathbf{L}^2(\widehat{\Omega})}^2 + (\theta - 1/2)k^2 \sum_{i=0}^{j-1} \|\nabla \mathbf{v}_h^i\|_{\mathbf{L}^2(\Omega)}^2 \leq C_{22} \quad (4.2.12)$$

for each $j = 0, \dots, N$ and some constant $C_{22} > 0$ that depends only on $|\widehat{\Omega}|$, $|\Omega|$, and C_π .

Proof. As for pure LLG, the proof relies on choosing of the correct test functions. For Maxwell's equations (4.2.3b)–(4.2.3c), we choose $(\boldsymbol{\psi}_h, \boldsymbol{\zeta}_h) = (\mathbf{E}_h^{i+1/2}, \mathbf{H}_h^{i+1/2})$ and obtain after summing up

$$\begin{aligned} d_t \left(\frac{\varepsilon_0}{2} \|\mathbf{E}_h^{i+1}\|_{\mathbf{L}^2(\widehat{\Omega})}^2 + \frac{\mu_0}{2} \|\mathbf{H}_h^{i+1}\|_{\mathbf{L}^2(\widehat{\Omega})}^2 \right) + \sigma \|\chi_\Omega \mathbf{E}_h^{i+1/2}\|_{\mathbf{L}^2(\widehat{\Omega})}^2 \\ = -(\mathbf{J}^{i+1/2}, \mathbf{E}_h^{i+1/2}) - \mu_0(\mathbf{v}_h^i, \mathbf{H}_h^{i+1/2}). \end{aligned}$$

The LLG equation (4.2.3a) is now tested with $\boldsymbol{\varphi}_i = \mathbf{v}_h^i \in \mathcal{K}_{\mathbf{m}_h^i}$. We get

$$\alpha(\mathbf{v}_h^i, \mathbf{v}_h^i) + \underbrace{((\mathbf{m}_h^i \times \mathbf{v}_h^i), \mathbf{v}_h^i)}_{=0} = -C_e(\nabla(\mathbf{m}_h^i + \theta k \mathbf{v}_h^i), \nabla \mathbf{v}_h^i) + (\mathbf{H}_h^{i+1/2}, \mathbf{v}_h^i) + (\boldsymbol{\pi}(\mathbf{m}_h^i), \mathbf{v}_h^i),$$

whence

$$\frac{\alpha k}{C_e} \|\mathbf{v}_h^i\|_{\mathbf{L}^2(\Omega)}^2 + \theta k^2 \|\nabla \mathbf{v}_h^i\|_{\mathbf{L}^2(\Omega)}^2 = -k(\nabla \mathbf{m}_h^i, \nabla \mathbf{v}_h^i) + \frac{k}{C_e} (\mathbf{H}_h^{i+1/2}, \mathbf{v}_h^i) + \frac{k}{C_e} (\boldsymbol{\pi}(\mathbf{m}_h^i), \mathbf{v}_h^i).$$

Next, we use $\|\nabla \mathbf{m}_h^{i+1}\|_{\mathbf{L}^2(\Omega)}^2 \leq \|\nabla(\mathbf{m}_h^i + k \mathbf{v}_h^i)\|_{\mathbf{L}^2(\Omega)}^2$ stemming from the mesh condition (4.2.6), cf. [Bar05], and argue as in the proof of Lemma 2.3.3 to see

$$\begin{aligned} \frac{1}{2} \|\nabla \mathbf{m}_h^{i+1}\|_{\mathbf{L}^2(\Omega)}^2 &\leq \frac{1}{2} \|\nabla \mathbf{m}_h^i\|_{\mathbf{L}^2(\Omega)}^2 + k(\nabla \mathbf{m}_h^i, \nabla \mathbf{v}_h^i) + \frac{k^2}{2} \|\nabla \mathbf{v}_h^i\|_{\mathbf{L}^2(\Omega)}^2 \\ &= \frac{1}{2} \|\nabla \mathbf{m}_h^i\|_{\mathbf{L}^2(\Omega)}^2 - (\theta - 1/2)k^2 \|\nabla \mathbf{v}_h^i\|_{\mathbf{L}^2(\Omega)}^2 \\ &\quad - \frac{\alpha k}{C_e} \|\mathbf{v}_h^i\|_{\mathbf{L}^2(\Omega)}^2 + \frac{k}{C_e} (\mathbf{H}_h^{i+1/2}, \mathbf{v}_h^i) + \frac{k}{C_e} (\boldsymbol{\pi}(\mathbf{m}_h^i), \mathbf{v}_h^i). \end{aligned}$$

Multiplication by μ_0/k thus yields

$$\begin{aligned} \frac{\mu_0}{2k} (\|\nabla \mathbf{m}_h^{i+1}\|_{\mathbf{L}^2(\Omega)}^2 - \|\nabla \mathbf{m}_h^i\|_{\mathbf{L}^2(\Omega)}^2) + \frac{\alpha\mu_0}{C_e} \|\mathbf{v}_h^i\|_{\mathbf{L}^2(\Omega)}^2 + (\theta - 1/2)\mu_0 k \|\nabla \mathbf{v}_h^i\|_{\mathbf{L}^2(\Omega)}^2 \\ \leq \frac{\mu_0}{C_e} (\mathbf{H}_h^{i+1/2}, \mathbf{v}_h^i) + \frac{\mu_0}{C_e} (\boldsymbol{\pi}(\mathbf{m}_h^i), \mathbf{v}_h^i). \end{aligned}$$

Adding up the two inequalities, we employ Cauchy's inequality A.1.5 and conclude for any $\varepsilon, \nu > 0$

$$\begin{aligned} d_t \left(\frac{\mu_0}{2} \|\nabla \mathbf{m}_h^{i+1}\|_{\mathbf{L}^2(\Omega)}^2 + \frac{\varepsilon_0}{2C_e} \|\mathbf{E}_h^{i+1}\|_{\mathbf{L}^2(\hat{\Omega})}^2 + \frac{\mu_0}{2C_e} \|\mathbf{H}_h^{i+1}\|_{\mathbf{L}^2(\hat{\Omega})}^2 \right) + \frac{\sigma}{C_e} \|\chi_\Omega \mathbf{E}_h^{i+1/2}\|_{\mathbf{L}^2(\hat{\Omega})}^2 \\ + (\theta - 1/2)\mu_0 k \|\nabla \mathbf{v}_h^i\|_{\mathbf{L}^2(\Omega)}^2 + \frac{\mu_0}{C_e} (\alpha - \varepsilon) \|\mathbf{v}_h^i\|_{\mathbf{L}^2(\Omega)}^2 \\ \leq \frac{1}{4\nu C_e} \|\mathbf{J}^{i+1/2}\|_{\mathbf{L}^2(\hat{\Omega})}^2 + \frac{\nu}{C_e} \|\mathbf{E}_h^{i+1/2}\|_{\mathbf{L}^2(\hat{\Omega})}^2 + \frac{\mu_0}{4\varepsilon C_e} \|\boldsymbol{\pi}(\mathbf{m}_h^i)\|_{\mathbf{L}^2(\Omega)}^2. \end{aligned}$$

Multiplying by k and summing over the time steps $i = 0, \dots, j-1$, we see

$$\begin{aligned} \frac{\mu_0}{2} \|\nabla \mathbf{m}_h^j\|_{\mathbf{L}^2(\Omega)}^2 + \frac{\varepsilon_0}{2C_e} \|\mathbf{E}_h^j\|_{\mathbf{L}^2(\hat{\Omega})}^2 + \frac{\mu_0}{2C_e} \|\mathbf{H}_h^j\|_{\mathbf{L}^2(\hat{\Omega})}^2 + \frac{k\sigma}{C_e} \sum_{i=0}^{j-1} \|\chi_\Omega \mathbf{E}_h^{i+1/2}\|_{\mathbf{L}^2(\hat{\Omega})}^2 \\ + (\theta - 1/2)\mu_0 k^2 \sum_{i=0}^{j-1} \|\nabla \mathbf{v}_h^i\|_{\mathbf{L}^2(\Omega)}^2 + \frac{\mu_0 k}{C_e} (\alpha - \varepsilon) \sum_{i=0}^{j-1} \|\mathbf{v}_h^i\|_{\mathbf{L}^2(\Omega)}^2 \\ \leq \frac{k}{4\nu C_e} \sum_{i=0}^{j-1} \|\mathbf{J}^{i+1/2}\|_{\mathbf{L}^2(\hat{\Omega})}^2 + \frac{\nu k}{C_e} \sum_{i=0}^{j-1} \|\mathbf{E}_h^{i+1/2}\|_{\mathbf{L}^2(\hat{\Omega})}^2 + \frac{k\mu_0}{4\varepsilon C_e} \sum_{i=0}^{j-1} \|\boldsymbol{\pi}(\mathbf{m}_h^i)\|_{\mathbf{L}^2(\Omega)}^2 \\ + \frac{\mu_0}{2} \|\nabla \mathbf{m}_h^0\|_{\mathbf{L}^2(\Omega)}^2 + \frac{\varepsilon_0}{2C_e} \|\mathbf{E}_h^0\|_{\mathbf{L}^2(\hat{\Omega})}^2 + \frac{\mu_0}{2C_e} \|\mathbf{H}_h^0\|_{\mathbf{L}^2(\hat{\Omega})}^2 \\ \leq C + \frac{k\nu}{C_e} \sum_{i=0}^{j-1} \|\mathbf{E}_h^{i+1/2}\|_{\mathbf{L}^2(\hat{\Omega})}^2. \end{aligned}$$

For the last inequality, we exploited boundedness of the general field contribution (2.3.2), as well as convergence (and hence boundedness) of the initial data.

Unfortunately, the term $\sum_{i=0}^{j-1} \|\mathbf{E}_h^{i+1/2}\|_{\mathbf{L}^2(\hat{\Omega})}^2$ cannot be absorbed by $\sum_{i=0}^{j-1} \|\chi_\Omega \mathbf{E}_h^{i+1/2}\|_{\mathbf{L}^2(\hat{\Omega})}^2$ on the left-hand side, since the latter is defined only on the smaller domain Ω . The remedy is to employ an artificial extension

$$\sum_{i=0}^{j-1} \|\mathbf{E}_h^{i+1/2}\|_{\mathbf{L}^2(\hat{\Omega})}^2 \leq \frac{1}{2} \sum_{i=0}^{j-1} (\|\mathbf{E}_h^{i+1}\|_{\mathbf{L}^2(\hat{\Omega})}^2 + \|\mathbf{E}_h^i\|_{\mathbf{L}^2(\hat{\Omega})}^2) \leq \frac{1}{2} \|\mathbf{E}_h^j\|_{\mathbf{L}^2(\hat{\Omega})}^2 + \sum_{i=0}^{j-1} \|\mathbf{E}_h^i\|_{\mathbf{L}^2(\hat{\Omega})}^2.$$

This yields

$$\begin{aligned} \frac{\mu_0}{2} \|\nabla \mathbf{m}_h^j\|_{\mathbf{L}^2(\Omega)}^2 + \frac{1}{2C_e} \underbrace{(\varepsilon_0 - k\nu)}_{=: C_E} \|\mathbf{E}_h^j\|_{\mathbf{L}^2(\hat{\Omega})}^2 + \frac{\mu_0}{2C_e} \|\mathbf{H}_h^j\|_{\mathbf{L}^2(\hat{\Omega})}^2 + \frac{k\sigma}{C_e} \sum_{i=0}^{j-1} \|\chi_\Omega \mathbf{E}_h^{i+1/2}\|_{\mathbf{L}^2(\hat{\Omega})}^2 \\ + (\theta - 1/2)\mu_0 k^2 \sum_{i=0}^{j-1} \|\nabla \mathbf{v}_h^i\|_{\mathbf{L}^2(\Omega)}^2 + \frac{\mu_0 k}{C_e} (\alpha - \varepsilon) \sum_{i=0}^{j-1} \|\mathbf{v}_h^i\|_{\mathbf{L}^2(\Omega)}^2 \\ \leq C + \frac{k\nu}{C_e} \sum_{i=0}^{j-1} \|\mathbf{E}_h^i\|_{\mathbf{L}^2(\hat{\Omega})}^2, \end{aligned}$$

where $C_{\mathbf{E}} > 0$ for $\nu < \varepsilon_0/k_0$. Hence, the assertion then follows by application of the discrete Gronwall's inequality A.1.2 for $\varepsilon \leq \alpha$. \square

Step 2: Analogously to Lemma 2.3.5, we conclude the existence of weakly convergent subsequences.

Lemma 4.2.7. *There exist functions $\mathbf{m} \in \mathbf{H}^1(\Omega_T, \mathbb{S}^2)$, $\mathbf{v} \in \mathbf{L}^2(\Omega_T)$, and $\mathbf{E}, \mathbf{H} \in \mathbf{L}^2(\widehat{\Omega}_T) \times \mathbf{L}^2(\widehat{\Omega}_T)$ such that*

$$\mathbf{m}_{hk} \xrightarrow{\text{sub}} \mathbf{m} \text{ in } \mathbf{H}^1(\Omega_T), \quad (4.2.13a)$$

$$\mathbf{m}_{hk}, \mathbf{m}_{hk}^\pm, \overline{\mathbf{m}}_{hk} \xrightarrow{\text{sub}} \mathbf{m} \text{ in } \mathbf{L}^2(\mathbf{H}^1), \quad (4.2.13b)$$

$$\mathbf{m}_{hk}, \mathbf{m}_{hk}^\pm, \overline{\mathbf{m}}_{hk} \xrightarrow{\text{sub}} \mathbf{m} \text{ in } \mathbf{L}^2(\Omega_T), \quad (4.2.13c)$$

$$\mathbf{H}_{hk}, \overline{\mathbf{H}}_{hk} \xrightarrow{\text{sub}} \mathbf{H} \text{ in } \mathbf{L}^2(\widehat{\Omega}_T), \quad (4.2.13d)$$

$$\mathbf{E}_{hk}, \overline{\mathbf{E}}_{hk} \xrightarrow{\text{sub}} \mathbf{E} \text{ in } \mathbf{L}^2(\widehat{\Omega}_T), \quad (4.2.13e)$$

$$\mathbf{v}_{hk}^- \xrightarrow{\text{sub}} \mathbf{v} \text{ in } \mathbf{L}^2(\Omega_T). \quad (4.2.13f)$$

In particular, there exists a subsequence (h_n, k_n) of (h, k) such that all the above limits hold simultaneously.

Proof. The limits concerning the magnetization \mathbf{m} as well as \mathbf{v} follow as in Lemma 2.3.5. Due to the boundedness of the discrete electric and magnetic field from Lemma 4.2.6, we conclude existence of $\mathbf{H}, \widetilde{\mathbf{H}}$ and $\mathbf{E}, \widetilde{\mathbf{E}}$ with

$$\mathbf{H}_{hk} \xrightarrow{\text{sub}} \mathbf{H}$$

$$\overline{\mathbf{H}}_{hk} \xrightarrow{\text{sub}} \widetilde{\mathbf{H}}$$

$$\mathbf{E}_{hk} \xrightarrow{\text{sub}} \mathbf{E}$$

$$\overline{\mathbf{E}}_{hk} \xrightarrow{\text{sub}} \widetilde{\mathbf{E}}$$

in $\mathbf{L}^2(\widehat{\Omega}_T)$. It thus only remains to show that the limits \mathbf{H} and $\widetilde{\mathbf{H}}$, resp. \mathbf{E} and $\widetilde{\mathbf{E}}$ coincide. This can be seen by some clever user of the midpoint rule. For $\Lambda \in C^\infty(\widehat{\Omega}_T)$, consider the piecewise constant approximation $\Lambda^- \in \mathcal{P}^0(\mathcal{I}_k, C^\infty(\widehat{\Omega}))$ with $\Lambda^-(t) = \Lambda(t_j)$ for $t \in [t_j, t_{j+1})$ and $\gamma_{hk} \in \{\mathbf{E}_{hk}, \mathbf{H}_{hk}\}$. Since the midpoint rule is exact for the (piecewise) affine function (γ_{hk}, Λ^-) , there holds

$$\begin{aligned} \int_0^T (\bar{\gamma}_{hk}, \Lambda^-) &= \sum_{j=0}^{N-1} \int_{t_j}^{t_{j+1}} \frac{1}{2} (\gamma_h^{j+1} + \gamma_h^j, \Lambda(t_j)) = k \sum_{j=0}^{N-1} (\gamma_{hk}, \Lambda^-) \left(\frac{t_{j+1} + t_j}{2} \right) \\ &= \sum_{j=0}^{N-1} \int_{t_j}^{t_{j+1}} (\gamma_{hk}, \Lambda^-) = \int_0^T (\gamma_{hk}, \Lambda^-). \end{aligned}$$

We thus deduce

$$\begin{aligned} (\bar{\gamma}_{hk}, \Lambda) &= (\bar{\gamma}_{hk}, \Lambda^-) + (\bar{\gamma}_{hk}, \Lambda - \Lambda^-) \\ &= (\gamma_{hk}, \Lambda^-) + (\bar{\gamma}_{hk}, \Lambda - \Lambda^-) \\ &= (\gamma_{hk}, \Lambda) + (\gamma_{hk}, \Lambda^- - \Lambda) + (\bar{\gamma}_{hk}, \Lambda - \Lambda^-). \end{aligned}$$

Pointwise convergence of Λ^- to Λ in combination with the Lebesgue theorem for dominated convergence A.2.3 yield $\Lambda^- \xrightarrow{\text{sub}} \Lambda$ strongly in $\mathbf{L}^2(\Omega_T)$. We thus get $\lim_{(h,k) \rightarrow 0} (\bar{\gamma}_{hk}, \Lambda) = \lim_{(h,k) \rightarrow 0} (\gamma_{hk}, \Lambda)$ and hence to coincidence of the two limits. \square

From Lemma 2.3.6, we conclude that the limiting function \mathbf{v} equals the time derivative of the magnetization \mathbf{m} almost everywhere in Ω_T . This concludes the proof of part *a* of Theorem 4.2.5. In the remainder, we aim to identify the limiting functions from Lemma 4.2.7 with weak solutions of the MLLG system, i.e. we prove part *b* of Theorem 4.2.5.

Step 3:

Proof of the convergence Theorem 4.2.5 for Algorithm 4.2.1. As special set of test functions serve $(\phi_h, \psi_h, \zeta_h)(t, \cdot) := (\mathcal{I}_h(\mathbf{m}_{hk}^- \times \varphi), \mathcal{I}_{\mathcal{X}_h} \psi, \mathcal{I}_{\mathcal{Y}_h} \zeta)(t, \cdot)$ for any $(\varphi, \psi, \zeta) \in C^\infty(\Omega_T) \times C_c^\infty([0, T]; C^\infty(\hat{\Omega}) \cap \mathbf{H}_0(\text{curl}, \hat{\Omega})) \times C_c^\infty([0, T]; C^\infty(\hat{\Omega}))$. Algorithm 4.2.1 implies

$$\begin{aligned} \alpha \int_0^T (\mathbf{v}_{hk}^-, \phi_h) + \int_0^T ((\mathbf{m}_{hk}^- \times \mathbf{v}_{hk}^-), \phi_h) &= -C_e \int_0^T (\nabla(\mathbf{m}_{hk}^- + \theta k \mathbf{v}_{hk}^-), \nabla \phi_h) \\ &\quad + \int_0^T (\bar{\mathbf{H}}_{hk}, \phi_h) + \int_0^T (\boldsymbol{\pi}(\mathbf{m}_{hk}^-), \phi_h) \\ \varepsilon_0 \int_0^T ((\mathbf{E}_{hk})_t, \psi_h) - \int_0^T (\bar{\mathbf{H}}_{hk}, \nabla \times \psi_h) + \sigma \int_0^T (\chi_\Omega \bar{\mathbf{E}}_{hk}, \psi_h) &= - \int_0^T (\bar{\mathbf{J}}_{hk}, \psi_h) \\ \mu_0 \int_0^T ((\mathbf{H}_{hk})_t, \zeta_h) + \int_0^T (\nabla \times \bar{\mathbf{E}}_{hk}, \zeta_h) &= -\mu_0 \int_0^T (\mathbf{v}_{hk}^-, \zeta_h). \end{aligned}$$

As in the proof of Theorem 2.3.1, boundedness of the involved quantities in combination with the approximation properties of the nodal interpolation operator, for the LLG part this yields

$$\begin{aligned} \int_0^T ((\alpha \mathbf{v}_{hk}^- + \mathbf{m}_{hk}^- \times \mathbf{v}_{hk}^-), (\mathbf{m}_{hk}^- \times \varphi)) + k \theta \int_0^T (\nabla \mathbf{v}_{hk}^-, \nabla(\mathbf{m}_{hk}^- \times \varphi)) \\ + C_e \int_0^T (\nabla \mathbf{m}_{hk}^-, \nabla(\mathbf{m}_{hk}^- \times \varphi)) - \int_0^T (\bar{\mathbf{H}}_{hk}, (\mathbf{m}_{hk}^- \times \varphi)) - \int_0^T (\boldsymbol{\pi}(\mathbf{m}_{hk}^-), (\mathbf{m}_{hk}^- \times \varphi)) \\ = \mathcal{O}(h) \end{aligned}$$

Passing to the limit and using the strong $\mathbf{L}^2(\Omega_T)$ -convergence of $(\mathbf{m}_{hk}^- \times \varphi)$ towards $(\mathbf{m} \times \varphi)$, we get

$$\begin{aligned} \int_0^T ((\alpha \mathbf{v}_{hk}^- + \mathbf{m}_{hk}^- \times \mathbf{v}_{hk}^-), (\mathbf{m}_{hk}^- \times \varphi)) &\longrightarrow \int_0^T ((\alpha \mathbf{m}_t + \mathbf{m} \times \mathbf{m}_t), (\mathbf{m} \times \varphi)), \\ k \theta \int_0^T (\nabla \mathbf{v}_{hk}^-, \nabla(\mathbf{m}_{hk}^- \times \varphi)) &\longrightarrow 0, \quad \text{and} \\ \int_0^T (\nabla \mathbf{m}_{hk}^-, \nabla(\mathbf{m}_{hk}^- \times \varphi)) &\longrightarrow \int_0^T (\nabla \mathbf{m}, \nabla(\mathbf{m} \times \varphi)), \end{aligned}$$

as in Lemma 2.3.9. For the second limit, we have used the boundedness of $k \|\nabla \mathbf{v}_{hk}^-\|_{\mathbf{L}^2(\Omega_T)}^2$ for $\theta \in (1/2, 1]$, see Lemma 4.2.6. The weak convergence properties of $\bar{\mathbf{H}}_{hk}$ and $\boldsymbol{\pi}(\mathbf{m}_{hk}^-)$

from (4.2.11) now yield

$$\begin{aligned} \int_0^T (\bar{\mathbf{H}}_{hk}, (\mathbf{m}_{hk}^- \times \boldsymbol{\varphi})) &\longrightarrow \int_0^T (\mathbf{H}, (\mathbf{m} \times \boldsymbol{\varphi})) \quad \text{and} \\ \int_0^T (\boldsymbol{\pi}(\mathbf{m}_{hk}^-), (\mathbf{m}_{hk}^- \times \boldsymbol{\varphi})) &\longrightarrow \int_0^T (\boldsymbol{\pi}(\mathbf{m}), (\mathbf{m} \times \boldsymbol{\varphi})). \end{aligned}$$

So far, we have thus proved

$$\begin{aligned} \int_0^T ((\alpha \mathbf{m}_t + \mathbf{m} \times \mathbf{m}_t), (\mathbf{m} \times \boldsymbol{\varphi})) &= -C_e \int_0^T (\nabla \mathbf{m}, \nabla (\mathbf{m} \times \boldsymbol{\varphi})) \\ &\quad + \int_0^T (\mathbf{H}, (\mathbf{m} \times \boldsymbol{\varphi})) + \int_0^T (\boldsymbol{\pi}(\mathbf{m}), (\mathbf{m} \times \boldsymbol{\varphi})) \end{aligned}$$

As in Lemma 2.3.9, we conclude (4.1.2). The equality $\mathbf{m}(0, \cdot) = \mathbf{m}^0$ in the trace sense again follows from the weak convergence $\mathbf{m}_{hk} \rightharpoonup \mathbf{m}$ in $\mathbf{H}^1(\Omega_T)$ and thus weak convergence of the traces. Using the weak convergence $\mathbf{m}_h^0 \rightharpoonup \mathbf{m}^0$ in $\mathbf{L}^2(\Omega)$, we finally identify the sought limit. For the Maxwell part (4.1.3)–(4.1.4) of Definition 4.1.1, we proceed as in [BBP08]. Given the above definition of the test functions, (4.2.5b) implies

$$\begin{aligned} \varepsilon_0 \int_0^T ((\mathbf{E}_{hk})_t, \boldsymbol{\psi}_h) - \int_0^T (\bar{\mathbf{H}}_{hk}, \nabla \times \boldsymbol{\psi}_h) + \sigma \int_0^T (\chi_\Omega \bar{\mathbf{E}}_{hk}, \boldsymbol{\psi}_h) &= \int_0^T (\bar{\mathbf{J}}_{hk}, \boldsymbol{\psi}_h) \\ \mu_0 \int_0^T ((\mathbf{H}_{hk})_t, \boldsymbol{\zeta}_h) + \int_0^T (\nabla \times \bar{\mathbf{E}}_{hk}, \boldsymbol{\zeta}_h) &= -\mu_0 \int_0^T (\mathbf{v}_{hk}^-, \boldsymbol{\zeta}_h). \end{aligned}$$

We now consider each of those two terms separately. For the first term of the first equation, we integrate by parts in time and get

$$\int_0^T ((\mathbf{E}_{hk})_t, \boldsymbol{\psi}_h) = - \int_0^T (\mathbf{E}_{hk}, (\boldsymbol{\psi}_h)_t) + \underbrace{(\mathbf{E}_{hk}(T, \cdot), \boldsymbol{\psi}_h(T, \cdot))}_{=0} - (\mathbf{E}_h^0, \boldsymbol{\psi}_h(0, \cdot)),$$

where the second term on the right-hand side vanishes due to the temporal boundary conditions. Passing to the limit on the right-hand side, we see

$$\int_0^T ((\mathbf{E}_{hk})_t, \boldsymbol{\psi}_h) \longrightarrow - \int_0^T (\mathbf{E}, \boldsymbol{\psi}_t) - (\mathbf{E}^0, \boldsymbol{\psi}(0, \cdot)), \quad (4.2.14)$$

where we have used the assumed convergence of the initial data. For the first term in the second equation we proceed analogously. The convergence of the terms

$$\begin{aligned} \int_0^T (\bar{\mathbf{H}}_{hk}, \nabla \times \boldsymbol{\psi}_h) &\longrightarrow \int_0^T (\mathbf{H}, \nabla \times \boldsymbol{\psi}), \\ \int_0^T (\chi_\Omega \bar{\mathbf{E}}_{hk}, \boldsymbol{\psi}_h) &\longrightarrow \int_0^T (\chi_\Omega \mathbf{E}, \boldsymbol{\psi}), \\ \int_0^T (\bar{\mathbf{J}}_{hk}, \boldsymbol{\psi}_h) &\longrightarrow \int_0^T (\mathbf{J}, \boldsymbol{\psi}), \quad \text{and} \\ \int_0^T (\mathbf{v}_{hk}^-, \boldsymbol{\zeta}_h) &\longrightarrow \int_0^T (\mathbf{m}_t, \boldsymbol{\zeta}) \end{aligned}$$

is straightforward. It remains to analyze the second term in the second equation. Using $\nabla \times \bar{\mathbf{E}}_{hk}(t) \in \mathcal{Y}_h$ and the orthogonality properties of $\mathcal{I}_{\mathcal{Y}_h}$, we deduce

$$\begin{aligned} \int_0^T (\nabla \times \bar{\mathbf{E}}_{hk}, \zeta_h) &= \int_0^T (\nabla \times \bar{\mathbf{E}}_{hk}, \zeta) - \int_0^T (\nabla \times \bar{\mathbf{E}}_{hk}, (1 - \mathcal{I}_{\mathcal{Y}_h})\zeta) \\ &= \int_0^T (\nabla \times \bar{\mathbf{E}}_{hk}, \zeta) = \int_0^T (\bar{\mathbf{E}}_{hk}, \nabla \times \zeta) \longrightarrow \int_0^T (\mathbf{E}, \nabla \times \zeta). \end{aligned}$$

For the last equality, we have used the boundary condition $\mathbf{E}_{hk} \times \mathbf{n} = 0$ on $\partial\hat{\Omega}_T$ and integration by parts. This yields (4.1.3) and (4.1.4). It remains to show the energy estimate (4.1.5). From the discrete energy estimate (4.2.12), we get for any $t' \in [0, T]$ with $t' \in [t_j, t_{j+1})$

$$\begin{aligned} &\|\nabla \mathbf{m}_{hk}^+(t')\|_{\mathbf{L}^2(\Omega)}^2 + \|\mathbf{v}_{hk}^-\|_{\mathbf{L}^2(\Omega_{t'})}^2 + \|\bar{\mathbf{H}}_{hk}(t')\|_{\mathbf{L}^2(\hat{\Omega})}^2 + \|\bar{\mathbf{E}}_{hk}(t')\|_{\mathbf{L}^2(\hat{\Omega})}^2 \\ &= \|\nabla \mathbf{m}_{hk}^+(t')\|_{\mathbf{L}^2(\Omega)}^2 + \int_0^{t'} \|\mathbf{v}_{hk}^-(s)\|_{\mathbf{L}^2(\Omega)}^2 + \|\bar{\mathbf{H}}_{hk}(t')\|_{\mathbf{L}^2(\hat{\Omega})}^2 + \|\bar{\mathbf{E}}_{hk}(t')\|_{\mathbf{L}^2(\hat{\Omega})}^2 \\ &\leq \|\nabla \mathbf{m}_{hk}^+(t')\|_{\mathbf{L}^2(\Omega)}^2 + \int_0^{t_{j+1}} \|\mathbf{v}_{hk}^-(s)\|_{\mathbf{L}^2(\Omega)}^2 + \|\bar{\mathbf{H}}_{hk}(t')\|_{\mathbf{L}^2(\hat{\Omega})}^2 + \|\bar{\mathbf{E}}_{hk}(t')\|_{\mathbf{L}^2(\hat{\Omega})}^2 \\ &\leq 2C_{22} \end{aligned}$$

Integration in time thus yields for any measurable set $\mathfrak{J} \subseteq [0, T]$

$$\int_{\mathfrak{J}} \|\nabla \mathbf{m}_{hk}^+(t')\|_{\mathbf{L}^2(\Omega)}^2 + \int_{\mathfrak{J}} \|\mathbf{v}_{hk}^-\|_{\mathbf{L}^2(\Omega_{t'})}^2 + \int_{\mathfrak{J}} \|\bar{\mathbf{H}}_{hk}(t')\|_{\mathbf{L}^2(\hat{\Omega})}^2 + \int_{\mathfrak{J}} \|\bar{\mathbf{E}}_{hk}(t')\|_{\mathbf{L}^2(\hat{\Omega})}^2 \leq 2 \int_{\mathfrak{J}} C_{22}$$

whence weak lower semi-continuity leads to

$$\int_{\mathfrak{J}} \|\nabla \mathbf{m}\|_{\mathbf{L}^2(\Omega)}^2 + \int_{\mathfrak{J}} \|\mathbf{m}_t\|_{\mathbf{L}^2(\Omega_{t'})}^2 + \int_{\mathfrak{J}} \|\mathbf{H}\|_{\mathbf{L}^2(\hat{\Omega})}^2 + \int_{\mathfrak{J}} \|\mathbf{E}\|_{\mathbf{L}^2(\hat{\Omega})}^2 \leq 2 \int_{\mathfrak{J}} C_{22}.$$

The desired result now follows from standard measure theory, see e.g. [Els11, IV, Thm. 4.4]. \square

Remark. Note that, with the above analysis, we do not get the convergence of γ_{hk}^\pm towards γ for $\gamma \in \{\mathbf{E}, \mathbf{H}\}$ as we do not control $\sum \|\gamma_h^{j+1} - \gamma_h^j\|_{\mathbf{L}^2}^2$. This is somewhat unexpected as we know that γ_{hk}^\pm do converge by boundedness — at least for a subsequence. Theoretically, however, the limits of γ_{hk}^+ and γ_{hk}^- could be different.

4.2.2. Analysis of fully decoupled Algorithm 4.2.2

In this Section, we finally show convergence of the fully decoupled Algorithm 4.2.2. While the analysis seems to be slightly more involved at first glance, we again stress that, due to decoupling, this algorithm has large benefits from an implementational point of view. As before, the proof consists of three steps and we start by verifying the boundedness of the computational quantities.

Step 1: Boundedness of the discrete quantities.

Lemma 4.2.8. *There exists $k_0 > 0$ such that for all $k < k_0$, the discrete quantities $(\mathbf{m}_h^j, \mathbf{E}_h^j, \mathbf{H}_h^j) \in \mathcal{M}_h \times \mathcal{X}_h \times \mathcal{Y}_h$ fulfill*

$$\begin{aligned} \|\nabla \mathbf{m}_h^j\|_{L^2(\Omega)}^2 + k \sum_{i=0}^{j-1} \|\mathbf{v}_h^i\|_{L^2(\Omega)}^2 + \|\mathbf{H}_h^j\|_{L^2(\hat{\Omega})}^2 + \|\mathbf{E}_h^j\|_{L^2(\hat{\Omega})}^2 + (\theta - 1/2)k^2 \sum_{i=0}^{j-1} \|\nabla \mathbf{v}_h^i\|_{L^2(\Omega)}^2 \\ + \sum_{i=0}^{j-1} (\|\mathbf{H}_h^{i+1} - \mathbf{H}_h^i\|_{L^2(\hat{\Omega})}^2 + \|\mathbf{E}_h^{i+1} - \mathbf{E}_h^i\|_{L^2(\hat{\Omega})}^2) \leq C_{27} \end{aligned} \quad (4.2.15)$$

for each $j = 0, \dots, N$ and some constant $C_{27} > 0$ that only depends on $|\hat{\Omega}|$, on $|\Omega|$, as well as on C_π .

Proof. Again, the proof relies on a clever choice of test functions. For Maxwell's equations, i.e. step (ii) of Algorithm 4.2.2, we choose $(\boldsymbol{\psi}_h, \boldsymbol{\zeta}_h) = (\mathbf{E}_h^{i+1}, \mathbf{H}_h^{i+1})$ as special pair of test functions and get from (4.2.5b)–(4.2.5c)

$$\begin{aligned} \frac{\varepsilon_0}{k}(\mathbf{E}_h^{i+1} - \mathbf{E}_h^i, \mathbf{E}_h^{i+1}) - (\mathbf{H}_h^{i+1}, \nabla \times \mathbf{E}_h^{i+1}) + \sigma(\chi_\Omega \mathbf{E}_h^{i+1}, \mathbf{E}_h^{i+1}) = -(\mathbf{J}^i, \mathbf{E}_h^{i+1}) \quad \text{and} \\ \frac{\mu_0}{k}(\mathbf{H}_h^{i+1} - \mathbf{H}_h^i, \mathbf{H}_h^{i+1}) + (\nabla \times \mathbf{E}_h^{i+1}, \mathbf{H}_h^{i+1}) = -\mu_0(\mathbf{v}_h^i, \mathbf{H}_h^{i+1}). \end{aligned}$$

Adding up those two equations (and multiplying by $1/C_e$), we therefore see

$$\begin{aligned} \frac{\varepsilon_0}{kC_e}(\mathbf{E}_h^{i+1} - \mathbf{E}_h^i, \mathbf{E}_h^{i+1}) + \frac{\sigma}{C_e}\|\mathbf{E}_h^{i+1}\|_{L^2(\Omega)}^2 + \frac{\mu_0}{kC_e}(\mathbf{H}_h^{i+1} - \mathbf{H}_h^i, \mathbf{H}_h^{i+1}) \\ = -\frac{\mu_0}{C_e}(\mathbf{v}_h^i, \mathbf{H}_h^i) + \frac{\mu_0}{C_e}(\mathbf{v}_h^i, \mathbf{H}_h^i - \mathbf{H}_h^{i+1}) - \frac{1}{C_e}(\mathbf{J}^i, \mathbf{E}_h^{i+1}). \end{aligned} \quad (4.2.16)$$

The LLG equation (4.2.5a) is again tested with $\boldsymbol{\varphi}_i = \mathbf{v}_h^i \in \mathcal{K}_{\mathbf{m}_h^i}$. In complete analogy to before, we get

$$\alpha(\mathbf{v}_h^i, \mathbf{v}_h^i) + \underbrace{((\mathbf{m}_h^i \times \mathbf{v}_h^i), \mathbf{v}_h^i)}_{=0} = -C_e(\nabla(\mathbf{m}_h^i + \theta k \mathbf{v}_h^i), \nabla \mathbf{v}_h^i) + (\mathbf{H}_h^i, \mathbf{v}_h^i) + (\pi(\mathbf{m}_h^i), \mathbf{v}_h^i),$$

whence

$$\frac{\alpha k}{C_e}\|\mathbf{v}_h^i\|_{L^2(\Omega)}^2 + \theta k^2\|\nabla \mathbf{v}_h^i\|_{L^2(\Omega)}^2 = -k(\nabla \mathbf{m}_h^i, \nabla \mathbf{v}_h^i) + \frac{k}{C_e}(\mathbf{H}_h^i, \mathbf{v}_h^i) + \frac{k}{C_e}(\pi(\mathbf{m}_h^i), \mathbf{v}_h^i).$$

Again, we utilize the discrete energy decay stemming from the angle condition (2.3.1) to see

$$\begin{aligned} \frac{1}{2}\|\nabla \mathbf{m}_h^{i+1}\|_{L^2(\Omega)}^2 &\leq \frac{1}{2}\|\nabla \mathbf{m}_h^i\|_{L^2(\Omega)}^2 + k(\nabla \mathbf{m}_h^i, \nabla \mathbf{v}_h^i) + \frac{k^2}{2}\|\nabla \mathbf{v}_h^i\|_{L^2(\Omega)}^2 \\ &= \frac{1}{2}\|\nabla \mathbf{m}_h^i\|_{L^2(\Omega)}^2 - (\theta - 1/2)k^2\|\nabla \mathbf{v}_h^i\|_{L^2(\Omega)}^2 \\ &\quad - \frac{\alpha k}{C_e}\|\mathbf{v}_h^i\|_{L^2(\Omega)}^2 + \frac{k}{C_e}(\mathbf{H}_h^i, \mathbf{v}_h^i) + \frac{k}{C_e}(\pi(\mathbf{m}_h^i), \mathbf{v}_h^i). \end{aligned}$$

Multiplying the last estimate by μ_0/k and adding (4.2.16), we obtain

$$\begin{aligned} \frac{\mu_0}{2k}(\|\nabla \mathbf{m}_h^{i+1}\|_{L^2(\Omega)}^2 - \|\nabla \mathbf{m}_h^i\|_{L^2(\Omega)}^2) + (\theta - 1/2)\mu_0 k\|\nabla \mathbf{v}_h^i\|_{L^2(\Omega)}^2 + \frac{\alpha \mu_0}{C_e}\|\mathbf{v}_h^i\|_{L^2(\Omega)}^2 \\ + \frac{\varepsilon_0}{k C_e}(\mathbf{E}_h^{i+1} - \mathbf{E}_h^i, \mathbf{E}_h^{i+1}) + \frac{\sigma}{C_e}\|\mathbf{E}_h^{i+1}\|_{L^2(\Omega)}^2 + \frac{\mu_0}{k C_e}(\mathbf{H}_h^{i+1} - \mathbf{H}_h^i, \mathbf{H}_h^{i+1}) \\ \leq \frac{\mu_0}{C_e}(\mathbf{H}_h^i - \mathbf{H}_h^{i+1}, \mathbf{v}_h^i) - \frac{1}{C_e}(\mathbf{J}^i, \mathbf{E}_h^{i+1}) + \frac{\mu_0}{C_e}(\pi(\mathbf{m}_h^i), \mathbf{v}_h^i). \end{aligned}$$

Multiplying the above equation by k , summing up over the time intervals, and exploiting Abel's summation from Lemma A.1.3 for the \mathbf{E}_h^i and \mathbf{H}_h^i scalar-products, this yields

$$\begin{aligned}
 & \frac{\mu_0}{2} \|\nabla \mathbf{m}_h^j\|_{L^2(\Omega)}^2 + (\theta - 1/2) \mu_0 k^2 \sum_{i=0}^{j-1} \|\nabla \mathbf{v}_h^i\|_{L^2(\Omega)}^2 + \frac{\alpha k \mu_0}{C_e} \sum_{i=0}^{j-1} \|\mathbf{v}_h^i\|_{L^2(\Omega)}^2 + \frac{\varepsilon_0}{2C_e} \|\mathbf{E}_h^j\|_{L^2(\hat{\Omega})}^2 \\
 & + \frac{\varepsilon_0}{2C_e} \sum_{i=0}^{j-1} \|\mathbf{E}_h^{i+1} - \mathbf{E}_h^i\|_{L^2(\hat{\Omega})}^2 + \frac{k\sigma}{C_e} \sum_{i=0}^{j-1} \|\mathbf{E}_h^{i+1}\|_{L^2(\Omega)}^2 + \frac{\mu_0}{2C_e} \|\mathbf{H}_h^j\|_{L^2(\hat{\Omega})}^2 + \frac{\mu_0}{2C_e} \sum_{i=0}^{j-1} \|\mathbf{H}_h^{i+1} - \mathbf{H}_h^i\|_{L^2(\hat{\Omega})}^2 \\
 & \leq \frac{k\mu_0}{C_e} \sum_{i=0}^{j-1} (\mathbf{H}_h^i - \mathbf{H}_h^{i+1}, \mathbf{v}_h^i) - \frac{k}{C_e} \sum_{i=0}^{j-1} (\mathbf{J}^i, \mathbf{E}_h^{i+1}) + \frac{\mu_0 k}{C_e} \sum_{i=0}^{j-1} (\pi(\mathbf{m}_h^i), \mathbf{v}_h^i) \\
 & + \underbrace{\frac{\mu_0}{2} \|\nabla \mathbf{m}_h^0\|_{L^2(\Omega)}^2 + \frac{\varepsilon_0}{2C_e} \|\mathbf{E}_h^0\|_{L^2(\hat{\Omega})}^2 + \frac{\mu_0}{2C_e} \|\mathbf{H}_h^0\|_{L^2(\hat{\Omega})}^2}_{=: \mathcal{E}_h^0}
 \end{aligned}$$

for any $j \in 1, \dots, N$. By use of the inequalities of Young and Hölder, the first part of the right-hand side can be estimated by

$$\begin{aligned}
 & \frac{k\mu_0}{C_e} \sum_{i=0}^{j-1} (\mathbf{H}_h^i - \mathbf{H}_h^{i+1}, \mathbf{v}_h^i) - \frac{k}{C_e} \sum_{i=0}^{j-1} (\mathbf{J}^i, \mathbf{E}_h^{i+1}) + \frac{\mu_0 k}{C_e} \sum_{i=0}^{j-1} (\pi(\mathbf{m}_h^i), \mathbf{v}_h^i) \\
 & \leq \frac{k\mu_0}{C_e} \sum_{i=0}^{j-1} \frac{1}{2\varepsilon} (\|\pi(\mathbf{m}_h^i)\|_{L^2(\Omega)}^2 + \|\mathbf{H}_h^{i+1} - \mathbf{H}_h^i\|_{L^2(\hat{\Omega})}^2) + \frac{\varepsilon\mu_0 k}{C_e} \sum_{i=0}^{j-1} \|\mathbf{v}_h^i\|_{L^2(\Omega)}^2 \\
 & + \frac{k\nu}{C_e} \sum_{i=0}^{j-1} \|\mathbf{E}_h^{i+1}\|_{L^2(\hat{\Omega})}^2 + \frac{k}{4\nu C_e} \sum_{i=0}^{j-1} \|\mathbf{J}^i\|_{L^2(\hat{\Omega})}^2,
 \end{aligned}$$

for any $\varepsilon, \nu > 0$. Here, we used $\|\mathbf{H}_h^{i+1} - \mathbf{H}_h^i\|_{L^2(\Omega)}^2 \leq \|\mathbf{H}_h^{i+1} - \mathbf{H}_h^i\|_{L^2(\hat{\Omega})}^2$. The combination of the last two estimates yields

$$\begin{aligned}
 & \frac{\mu_0}{2} \|\nabla \mathbf{m}_h^j\|_{L^2(\Omega)}^2 + (\theta - 1/2) \mu_0 k^2 \sum_{i=0}^{j-1} \|\nabla \mathbf{v}_h^i\|_{L^2(\Omega)}^2 + \frac{\alpha k \mu_0}{C_e} \sum_{i=0}^{j-1} \|\mathbf{v}_h^i\|_{L^2(\Omega)}^2 + \frac{\varepsilon_0}{2C_e} \|\mathbf{E}_h^j\|_{L^2(\hat{\Omega})}^2 \\
 & + \frac{\varepsilon_0}{2C_e} \sum_{i=0}^{j-1} \|\mathbf{E}_h^{i+1} - \mathbf{E}_h^i\|_{L^2(\hat{\Omega})}^2 + \frac{k\sigma}{C_e} \sum_{i=0}^{j-1} \|\mathbf{E}_h^{i+1}\|_{L^2(\Omega)}^2 + \frac{\mu_0}{2C_e} \|\mathbf{H}_h^j\|_{L^2(\hat{\Omega})}^2 + \frac{\mu_0}{2C_e} \sum_{i=0}^{j-1} \|\mathbf{H}_h^{i+1} - \mathbf{H}_h^i\|_{L^2(\hat{\Omega})}^2 \\
 & \leq \frac{\mu_0 k}{2C_e \varepsilon} \sum_{i=0}^{j-1} (\|\pi(\mathbf{m}_h^i)\|_{L^2(\Omega)}^2 + \|\mathbf{H}_h^{i+1} - \mathbf{H}_h^i\|_{L^2(\hat{\Omega})}^2) + \frac{\varepsilon\mu_0 k}{C_e} \sum_{i=0}^{j-1} \|\mathbf{v}_h^i\|_{L^2(\Omega)}^2 \\
 & + \frac{\nu k}{\nu C_e} \sum_{i=0}^{j-1} \|\mathbf{E}_h^{i+1}\|_{L^2(\hat{\Omega})}^2 + \frac{k}{4\nu C_e} \sum_{i=0}^{j-1} \|\mathbf{J}^i\|_{L^2(\hat{\Omega})}^2 + \mathcal{E}_h^0.
 \end{aligned}$$

As before, the term $\frac{k\nu}{C_e} \sum_{i=0}^{j-1} \|\mathbf{E}_h^{i+1}\|_{L^2(\hat{\Omega})}^2$ on the right-hand side cannot be absorbed by the term $\frac{k\sigma}{C_e} \sum_{i=0}^{j-1} \|\mathbf{E}_h^{i+1}\|_{L^2(\Omega)}^2$ on the left hand-side, since the latter consists only of contributions on the smaller domain Ω . Again, we thus artificially enlarge the first term by

$$\frac{k\nu}{C_e} \sum_{i=0}^{j-1} \|\mathbf{E}_h^{i+1}\|_{L^2(\hat{\Omega})}^2 \leq \frac{2k\nu}{C_e} \sum_{i=0}^{j-1} \|\mathbf{E}_h^{i+1} - \mathbf{E}_h^i\|_{L^2(\hat{\Omega})}^2 + \frac{2k\nu}{C_e} \sum_{i=0}^{j-1} \|\mathbf{E}_h^i\|_{L^2(\hat{\Omega})}^2$$

and absorb the first sum into the corresponding quantity on the left-hand side. With

$$C_{\mathbf{v}} := \frac{\mu_0 k}{C_e}(\alpha - \varepsilon), \quad C_{\mathbf{H}} := \frac{\mu_0}{2C_e}\left(1 - \frac{k}{\varepsilon}\right), \quad \text{and} \quad C_{\mathbf{E}} := \frac{1}{2C_e}(\varepsilon_0 - 4k\nu),$$

this yields

$$\begin{aligned} a_j &:= \frac{\mu_0}{2} \|\nabla \mathbf{m}_h^j\|_{L^2(\Omega)}^2 + (\theta - 1/2) \mu_0 k^2 \sum_{i=0}^{j-1} \|\nabla \mathbf{v}_h^i\|_{L^2(\Omega)}^2 + C_{\mathbf{v}} \sum_{i=0}^{j-1} \|\mathbf{v}_h^i\|_{L^2(\Omega)}^2 + \frac{\varepsilon_0}{2C_e} \|\mathbf{E}_h^j\|_{L^2(\hat{\Omega})}^2 \\ &\quad + C_{\mathbf{E}} \sum_{i=0}^{j-1} \|\mathbf{E}_h^{i+1} - \mathbf{E}_h^i\|_{L^2(\hat{\Omega})}^2 + \frac{k\sigma}{C_e} \sum_{i=0}^{j-1} \|\mathbf{E}_h^{i+1}\|_{L^2(\Omega)}^2 + \frac{\mu_0}{2C_e} \|\mathbf{H}_h^j\|_{L^2(\hat{\Omega})}^2 + C_{\mathbf{H}} \sum_{i=0}^{j-1} \|\mathbf{H}_h^{i+1} - \mathbf{H}_h^i\|_{L^2(\hat{\Omega})}^2 \\ &\leq \underbrace{\mathcal{E}_h^0 + \frac{k\mu_0}{4C_e\varepsilon} \sum_{i=0}^{j-1} \|\boldsymbol{\pi}(\mathbf{m}_h^i)\|_{L^2(\Omega)}^2 + \frac{\nu k}{C_e} \sum_{i=0}^{j-1} \|\mathbf{J}^i\|_{L^2(\hat{\Omega})}^2 + \frac{2k\nu}{C_e} \sum_{i=0}^{j-1} \|\mathbf{E}_h^i\|_{L^2(\hat{\Omega})}^2}_{=:b} \\ &\leq b + \frac{4k\nu}{\varepsilon_0} \sum_{i=0}^{j-1} a_i. \end{aligned}$$

In order to show the desired result, we have to ensure that there are choices of $\varepsilon > 0$ and $\nu > 0$, such that the constants $C_{\mathbf{v}}$, $C_{\mathbf{H}}$, and $C_{\mathbf{E}}$ are positive, i.e.

$$(\alpha - \varepsilon) > 0, \quad \left(1 - \frac{k}{\varepsilon}\right) > 0, \quad \text{and} \quad (\varepsilon_0 - 4k\nu) > 0$$

which is equivalent to $k < \varepsilon < \alpha$ and $\nu < \varepsilon_0/4k_0 \leq \varepsilon_0/4k$. The application of the discrete Gronwall inequality from Lemma A.1.2 yields $a_j \leq C$ and thus proves the desired result. \square

We can now conclude the existence of weakly convergent subsequences.

Step 2:

Lemma 4.2.9. *There exist functions $(\mathbf{m}, \mathbf{H}, \mathbf{E}) \in H^1(\Omega_T, \mathbb{S}^2) \times L^2(\hat{\Omega}_T) \times L^2(\hat{\Omega}_T)$ such that*

$$\mathbf{m}_{hk} \xrightarrow{\text{sub}} \mathbf{m} \text{ in } H^1(\Omega_T), \quad (4.2.17a)$$

$$\mathbf{m}_{hk}, \mathbf{m}_{hk}^{\pm}, \overline{\mathbf{m}}_{hk} \xrightarrow{\text{sub}} \mathbf{m} \text{ in } L^2(H^1(\Omega)), \quad (4.2.17b)$$

$$\mathbf{m}_{hk}, \mathbf{m}_{hk}^{\pm}, \overline{\mathbf{m}}_{hk} \xrightarrow{\text{sub}} \mathbf{m} \text{ in } L^2(\Omega_T), \quad (4.2.17c)$$

$$\mathbf{H}_{hk}, \mathbf{H}_{hk}^{\pm}, \overline{\mathbf{H}}_{hk} \xrightarrow{\text{sub}} \mathbf{H} \text{ in } L^2(\hat{\Omega}_T), \quad (4.2.17d)$$

$$\mathbf{E}_{hk}, \mathbf{E}_{hk}^{\pm}, \overline{\mathbf{E}}_{hk} \xrightarrow{\text{sub}} \mathbf{H} \text{ in } L^2(\hat{\Omega}_T), \quad (4.2.17e)$$

where the subsequences are succesively constructed, i.e. for arbitrary mesh-sizes $h \rightarrow 0$ and timestep-sizes $k \rightarrow 0$ there exist subindices h_n, k_n for which the above convergence properties are satisfied simultaneously. In addition, there exist some $\mathbf{v} \in L^2(\Omega_T)$ with

$$\mathbf{v}_{hk}^- \xrightarrow{\text{sub}} \mathbf{v} \text{ in } L^2(\Omega_T) \quad (4.2.18)$$

for the same subsequence as above.

Proof. The proof is completely analogue to the one of Lemma 4.2.7 and Lemma 2.3.5, respectively. The limits of \mathbf{H}_{hk}^\pm and \mathbf{E}_{hk}^\pm are identified using the boundedness of the quantities $\sum_{i=0}^{j-1} (\|\mathbf{H}_h^{i+1} - \mathbf{H}_h^i\|_{\mathbf{L}^2(\widehat{\Omega})}^2 + \|\mathbf{E}_h^{i+1} - \mathbf{E}_h^i\|_{\mathbf{L}^2(\widehat{\Omega})}^2)$ in combination with Lemma 2.2.5. Usage of the midpoint rule can thus be avoided in this case. \square

From Lemma 2.3.6, we again deduce that the limiting function \mathbf{v} equals the time derivative of the magnetization \mathbf{m} almost everywhere in Ω_T . This concludes Step 2 of the convergence analysis and thus the proof of Theorem 4.2.5 part *a*.

Step 3: Identification of the weak limits.

Proof of Theorem 4.2.5 part b for Algorithm 4.2.2. Consider arbitrary functions $\varphi \in C^\infty(\overline{\Omega_T})$, $\psi \in C_c^\infty([0, T]; C^\infty(\widehat{\Omega}) \cap \mathbf{H}_0(\text{curl}, \widehat{\Omega}))$, and $\zeta \in C_c^\infty([0, T]; C^\infty(\widehat{\Omega}))$. We now define test functions by $(\phi_h, \psi_h, \zeta_h)(t, \cdot) := (\mathcal{I}_h(\mathbf{m}_{hk}^- \times \varphi), \mathcal{I}_{\mathcal{X}_h} \psi, \mathcal{I}_{\mathcal{Y}_h} \zeta)(t, \cdot)$. Recall that the \mathbf{L}^2 -orthogonal projection $\mathcal{I}_{\mathcal{Y}_h} : \mathbf{L}^2(\widehat{\Omega}) \rightarrow \mathcal{Y}_h$ satisfies $(\mathbf{u} - \mathcal{I}_{\mathcal{Y}_h} \mathbf{u}, \mathbf{y}_h) = 0$ for all $\mathbf{y}_h \in \mathcal{Y}_h$ and all $\mathbf{u} \in \mathbf{L}^2(\widehat{\Omega})$. Equation (4.2.5a) of Algorithm 4.2.2 implies

$$\begin{aligned} \alpha \int_0^T (\mathbf{v}_{hk}^-, \phi_h) + \int_0^T ((\mathbf{m}_{hk}^- \times \mathbf{v}_{hk}^-), \phi_h) &= -C_e \int_0^T (\nabla(\mathbf{m}_{hk}^- + \theta k \mathbf{v}_{hk}^-), \nabla \phi_h) \\ &\quad + \int_0^T (\mathbf{H}_{hk}^-, \phi_h) + \int_0^T (\pi(\mathbf{m}_{hk}^-), \phi_h) \end{aligned}$$

As in the proof of Theorem 2.3.1, boundedness of the discrete quantities and the approximation properties of the nodal interpolation operator yield

$$\begin{aligned} &\int_0^T ((\alpha \mathbf{v}_{hk}^- + \mathbf{m}_{hk}^- \times \mathbf{v}_{hk}^-), (\mathbf{m}_{hk}^- \times \varphi)) + k\theta C_e \int_0^T (\nabla \mathbf{v}_{hk}^-, \nabla(\mathbf{m}_{hk}^- \times \varphi)) \\ &\quad + C_e \int_0^T (\nabla \mathbf{m}_{hk}^-, \nabla(\mathbf{m}_{hk}^- \times \varphi)) - \int_0^T (\mathbf{H}_{hk}^-, (\mathbf{m}_{hk}^- \times \varphi)) - \int_0^T (\pi(\mathbf{m}_{hk}^-), (\mathbf{m}_{hk}^- \times \varphi)) \\ &= \mathcal{O}(h) \end{aligned}$$

Verbatim to the previous section, passing to the limit yields

$$\begin{aligned} \int_0^T ((\alpha \mathbf{v}_{hk}^- + \mathbf{m}_{hk}^- \times \mathbf{v}_{hk}^-), (\mathbf{m}_{hk}^- \times \varphi)) &\longrightarrow \int_0^T ((\alpha \mathbf{m}_t + \mathbf{m} \times \mathbf{m}_t), (\mathbf{m} \times \varphi)), \\ k\theta \int_0^T (\nabla \mathbf{v}_{hk}^-, \nabla(\mathbf{m}_{hk}^- \times \varphi)) &\longrightarrow 0, \\ \int_0^T (\nabla \mathbf{m}_{hk}^-, \nabla(\mathbf{m}_{hk}^- \times \varphi)) &\longrightarrow \int_0^T (\nabla \mathbf{m}, \nabla(\mathbf{m} \times \varphi)), \quad \text{and} \\ \int_0^T (\pi(\mathbf{m}_{hk}^-), (\mathbf{m}_{hk}^- \times \varphi)) &\longrightarrow \int_0^T (\pi(\mathbf{m}), (\mathbf{m} \times \varphi)). \end{aligned}$$

Again, this is where we have used the boundedness of $k\|\nabla \mathbf{v}_{hk}^-\|_{\mathbf{L}^2(\Omega_T)}^2$ for $\theta \in (1/2, 1]$. Contrary to the coupled algorithm, we now have convergence of \mathbf{H}_{hk}^- and may thus directly conclude

$$\int_0^T (\mathbf{H}_{hk}^-, (\mathbf{m}_{hk}^- \times \varphi)) \longrightarrow \int_0^T (\mathbf{H}, (\mathbf{m} \times \varphi)).$$

So far, we thus have proved

$$\begin{aligned} \int_0^T ((\alpha \mathbf{m}_t + \mathbf{m} \times \mathbf{m}_t), (\mathbf{m} \times \boldsymbol{\varphi})) &= -C_e \int_0^T (\nabla \mathbf{m}, \nabla (\mathbf{m} \times \boldsymbol{\varphi})) \\ &\quad + \int_0^T (\mathbf{H}, (\mathbf{m} \times \boldsymbol{\varphi})) + \int_0^T (\boldsymbol{\pi}(\mathbf{m}), (\mathbf{m} \times \boldsymbol{\varphi})), \end{aligned}$$

and verbatim arguments as in the previous section show (4.1.2). For the Maxwell part (4.1.3)–(4.1.4) of Definition 4.1.1, we again follow the lines of [BBP08] and proceed as in the previous section. Given the above definition of the test functions, (4.2.5b) implies

$$\begin{aligned} \varepsilon_0 \int_0^T ((\mathbf{E}_{hk})_t, \boldsymbol{\psi}_h) - \int_0^T (\mathbf{H}_{hk}^+, \nabla \times \boldsymbol{\psi}_h) + \sigma \int_0^T (\chi_\Omega \mathbf{E}_{hk}^+, \boldsymbol{\psi}_h) &= \int_0^T (\mathbf{J}_{hk}^-, \boldsymbol{\psi}_h) \\ \mu_0 \int_0^T ((\mathbf{H}_{hk})_t, \boldsymbol{\zeta}_h) + \int_0^T (\nabla \times \mathbf{E}_{hk}^+, \boldsymbol{\zeta}_h) &= -\mu_0 \int_0^T (\mathbf{v}_{hk}^-, \boldsymbol{\zeta}_h). \end{aligned}$$

As before, we see

$$\int_0^T ((\mathbf{E}_{hk})_t, \boldsymbol{\psi}_h) \longrightarrow - \int_0^T (\mathbf{E}, \boldsymbol{\psi}_t) - (\mathbf{E}^0, \boldsymbol{\psi}(0, \cdot)), \quad (4.2.19)$$

where we have used the assumed convergence of the initial data. For the first term in the second equation we proceed analogously. The convergence of the terms

$$\begin{aligned} \int_0^T (\mathbf{H}_{hk}^+, \nabla \times \boldsymbol{\psi}_h) &\longrightarrow \int_0^T (\mathbf{H}, \nabla \times \boldsymbol{\psi}), \\ \int_0^T (\chi_\Omega \mathbf{E}_{hk}^+, \boldsymbol{\psi}_h) &\longrightarrow \int_0^T (\chi_\Omega \mathbf{E}, \boldsymbol{\psi}), \\ \int_0^T (\mathbf{J}_{hk}^-, \boldsymbol{\psi}_h) &\longrightarrow \int_0^T (\mathbf{J}, \boldsymbol{\psi}), \quad \text{and} \\ \int_0^T (\mathbf{v}_{hk}^-, \boldsymbol{\zeta}_h) &\longrightarrow \int_0^T (\mathbf{m}_t, \boldsymbol{\zeta}) \end{aligned}$$

follows as before and here, we exploit knowledge of the limits of \mathbf{H}_{hk}^+ and \mathbf{E}_{hk}^+ . As before, we finally deduce the estimate

$$\begin{aligned} \int_0^T (\nabla \times \mathbf{E}_{hk}^+, \boldsymbol{\zeta}_h) &= \int_0^T (\nabla \times \mathbf{E}_{hk}^+, \boldsymbol{\zeta}) - \int_0^T \underbrace{(\nabla \times \mathbf{E}_{hk}^+, (1 - \mathcal{I}_{\mathcal{Y}_h}) \boldsymbol{\zeta})}_{=0} \\ &= \int_0^T (\nabla \times \mathbf{E}_{hk}^+, \boldsymbol{\zeta}) = \int_0^T (\mathbf{E}_{hk}^+, \nabla \times \boldsymbol{\zeta}) \longrightarrow \int_0^T (\mathbf{E}, \nabla \times \boldsymbol{\zeta}), \end{aligned}$$

where we again used the properties of the orthogonal projection and the boundary condition $\mathbf{E}_{hk}^+ \times \mathbf{n} = 0$ on $\partial \widehat{\Omega}_T$ and integration by parts. This yields (4.1.3) and (4.1.4).

As for the energy estimate (4.1.5) and contrary to the previous section, we can now directly estimate the limits of \mathbf{E}_{hk}^+ resp. \mathbf{H}_{hk}^+ . From the discrete energy estimate (5.3.5), we get for

any $t' \in [0, T]$ with $t' \in [t_j, t_{j+1})$

$$\begin{aligned}
 & \|\nabla \mathbf{m}_{hk}^+(t')\|_{\mathbf{L}^2(\Omega)}^2 + \|\mathbf{v}_{hk}^-\|_{\mathbf{L}^2(\Omega_{t'})}^2 + \|\mathbf{H}_{hk}^+(t')\|_{\mathbf{L}^2(\widehat{\Omega})}^2 + \|\mathbf{E}_{hk}^+(t')\|_{\mathbf{L}^2(\widehat{\Omega})}^2 \\
 &= \|\nabla \mathbf{m}_{hk}^+(t')\|_{\mathbf{L}^2(\Omega)}^2 + \int_0^{t'} \|\mathbf{v}_{hk}^-(s)\|_{\mathbf{L}^2(\Omega)}^2 + \|\mathbf{H}_{hk}^+(t')\|_{\mathbf{L}^2(\widehat{\Omega})}^2 + \|\mathbf{E}_{hk}^+(t')\|_{\mathbf{L}^2(\widehat{\Omega})}^2 \\
 &\leq \|\nabla \mathbf{m}_{hk}^+(t')\|_{\mathbf{L}^2(\Omega)}^2 + \int_0^{t_{j+1}} \|\mathbf{v}_{hk}^-(s)\|_{\mathbf{L}^2(\Omega)}^2 + \|\mathbf{H}_{hk}^+(t')\|_{\mathbf{L}^2(\widehat{\Omega})}^2 + \|\mathbf{E}_{hk}^+(t')\|_{\mathbf{L}^2(\widehat{\Omega})}^2 \\
 &\leq C_{27}
 \end{aligned}$$

Integration in time thus yields for any measurable set $\mathfrak{J} \subseteq [0, T]$

$$\int_{\mathfrak{J}} \|\nabla \mathbf{m}_{hk}^+(t')\|_{\mathbf{L}^2(\Omega)}^2 + \int_{\mathfrak{J}} \|\mathbf{v}_{hk}^-\|_{\mathbf{L}^2(\Omega_{t'})}^2 + \int_{\mathfrak{J}} \|\mathbf{H}_{hk}^+(t')\|_{\mathbf{L}^2(\widehat{\Omega})}^2 + \int_{\mathfrak{J}} \|\mathbf{E}_{hk}^+(t')\|_{\mathbf{L}^2(\widehat{\Omega})}^2 \leq \int_{\mathfrak{J}} C_{27}$$

whence weak lower semi-continuity leads to

$$\int_{\mathfrak{J}} \|\nabla \mathbf{m}\|_{\mathbf{L}^2(\Omega)}^2 + \int_{\mathfrak{J}} \|\mathbf{m}_t\|_{\mathbf{L}^2(\Omega_{t'})}^2 + \int_{\mathfrak{J}} \|\mathbf{H}\|_{\mathbf{L}^2(\widehat{\Omega})}^2 + \int_{\mathfrak{J}} \|\mathbf{E}\|_{\mathbf{L}^2(\widehat{\Omega})}^2 \leq \int_{\mathfrak{J}} C_{27}.$$

The desired result now follows from standard measure theory, see e.g. [Els11, IV, Thm. 4.4]. \square

Remark. *At this point we like to emphasize that the decoupling of both equations in Algorithm 4.2.2 yields boundedness of the difference of two subsequent discrete solutions, i.e.*

$$\sum_{i=0}^{j-1} (\|\mathbf{E}_h^{i+1} - \mathbf{E}_h^i\|_{\mathbf{L}^2(\widehat{\Omega})}^2 + \|\mathbf{H}_h^{i+1} - \mathbf{H}_h^i\|_{\mathbf{L}^2(\widehat{\Omega})}^2) \leq C.$$

Those terms, sometimes called artificial damping ease the analysis as they allow to control the limits of \mathbf{E}_{hk}^\pm and \mathbf{H}_{hk}^\pm , respectively. This is yet another strength of the decoupled algorithm and is exploited at several points. In particular the technical use of the midpoint rule for computing the limits can be avoided here. Moreover, the energy estimate (4.1.5) can be proved with the constant from the discrete energy estimate from Lemma 4.2.8, whereas the coupled algorithm enforced an additional factor of 2.

4.2.3. Improved energy estimates

Similar to the result from Section 2.4, the energy bound (4.1.5) can be improved for many (physically relevant) situations. Instead of a uniform bound of the form

$$\|\nabla \mathbf{m}(t')\|_{\mathbf{L}^2(\Omega)}^2 + \|\mathbf{m}_t\|_{\mathbf{L}^2(\Omega_{t'})}^2 + \|\mathbf{E}(t')\|_{\mathbf{L}^2(\widehat{\Omega})}^2 + \|\mathbf{H}(t')\|_{\mathbf{L}^2(\widehat{\Omega})}^2 \leq C,$$

one can obtain a real energy inequality of the kind

$$\mathcal{E}(t') + \|\mathbf{m}_t\|_{\mathbf{L}^2(\Omega)}^2 \leq \mathcal{E}(0)$$

under some additional assumptions and for some meaningful energy term $\mathcal{E}(\cdot)$. This is basically the result of this section, and we again investigate both algorithms individually. This time, we

start with the fully decoupled Algorithm 4.2.2 since the analysis is somewhat more involved. We define the energy term

$$\begin{aligned} \mathcal{E}(t) &:= \mathcal{E}(\mathbf{m}(t), \mathbf{E}(t), \mathbf{H}(t)) \\ &:= \mu_0 \|\nabla \mathbf{m}(t)\|_{\mathbf{L}^2(\Omega)}^2 + \frac{\mu_0}{C_e} \|\mathbf{H}(t)\|_{\mathbf{L}^2(\hat{\Omega})}^2 + \frac{\varepsilon_0}{C_e} \|\mathbf{E}(t)\|_{\mathbf{L}^2(\hat{\Omega})}^2 - \frac{\mu_0}{C_e} (\boldsymbol{\pi}(\mathbf{m}(t)), \mathbf{m}(t)) \end{aligned} \quad (4.2.20)$$

and its discrete counterpart

$$\begin{aligned} \mathcal{E}(\mathbf{m}_h^j, \mathbf{E}_h^j, \mathbf{H}_h^j) \\ := \mu_0 \|\nabla \mathbf{m}_h^j\|_{\mathbf{L}^2(\Omega)}^2 + \frac{\mu_0}{C_e} \|\mathbf{H}_h^j\|_{\mathbf{L}^2(\hat{\Omega})}^2 + \frac{\varepsilon_0}{C_e} \|\mathbf{E}_h^j\|_{\mathbf{L}^2(\hat{\Omega})}^2 - \frac{\mu_0}{C_e} (\boldsymbol{\pi}(\mathbf{m}_h^j), \mathbf{m}_h^j). \end{aligned} \quad (4.2.21)$$

With those notions, we get the following result.

Proposition 4.2.10 (Improved energy estimate for Algorithm 4.2.2). *Let $\boldsymbol{\pi}(\cdot)$ be uniformly Lipschitz continuous and bounded in $\mathbf{L}^4(\Omega)$, i.e. $\|\boldsymbol{\pi}(\mathbf{n})\|_{\mathbf{L}^4(\Omega)} \leq C_{24}$ for all $\mathbf{n} \in \mathbf{L}^2(\Omega)$ with $|\mathbf{n}| \leq 1$ almost everywhere in Ω . Here, C_{24} denotes some uniform constant which only depends on Ω . Let further $\boldsymbol{\pi}(\cdot)$ be self-adjoint. Moreover, we assume $\mathbf{J}_{hk}^- \rightarrow \mathbf{J}$ strongly in $\mathbf{L}^2(\hat{\Omega}_T)$. Then, for the output of Algorithm (4.2.2), we have the energy decay estimate*

$$\mathcal{E}(t') + \frac{2\mu_0}{C_e}(\alpha - \varepsilon) \|\mathbf{m}_t\|_{\mathbf{L}^2(\Omega_{t'})}^2 + \frac{2\sigma}{C_e} \|\mathbf{E}\|_{\mathbf{L}^2(\Omega_{t'})}^2 \leq \mathcal{E}(0) - \frac{2}{C_e} (\mathbf{J}, \mathbf{E})_{\hat{\Omega}_{t'}}, \quad (4.2.22)$$

for almost every $t' \in [0, T]$ and any $\varepsilon > 0$.

Proof. As in the proof of Lemma 4.2.8, there holds

$$\begin{aligned} \mu_0 \|\nabla \mathbf{m}_h^{i+1}\|_{\mathbf{L}^2(\Omega)}^2 &\leq \mu_0 \|\nabla \mathbf{m}_h^i\|_{\mathbf{L}^2(\Omega)}^2 - 2(\theta - \frac{1}{2})\mu_0 k^2 \|\nabla \mathbf{v}_h^i\|_{\mathbf{L}^2(\Omega)}^2 \\ &\quad - \frac{2\alpha\mu_0 k}{C_e} \|\mathbf{v}_h^i\|_{\mathbf{L}^2(\Omega)}^2 - \frac{2\varepsilon_0}{C_e} (\mathbf{E}_h^{i+1} - \mathbf{E}_h^i, \mathbf{E}_h^{i+1}) - \frac{2\sigma k}{C_e} \|\mathbf{E}_h^{i+1}\|_{\mathbf{L}^2(\Omega)}^2 \\ &\quad - \frac{2\mu_0 k}{C_e} (\mathbf{H}_h^{i+1} - \mathbf{H}_h^i, \mathbf{H}_h^{i+1}) + \frac{2\mu_0 k}{C_e} (\mathbf{H}_h^i - \mathbf{H}_h^{i+1}, \mathbf{v}_h^i) \\ &\quad - \frac{2k}{C_e} (\mathbf{J}^i, \mathbf{E}_h^{i+1}) + \frac{2\mu_0 k}{C_e} (\boldsymbol{\pi}(\mathbf{m}_h^i), \mathbf{v}_h^i). \end{aligned}$$

On the other hand, by definition of the discrete energy term, the difference of two subsequent energies can be estimated by

$$\begin{aligned} \mathcal{E}(\mathbf{m}_h^{i+1}, \mathbf{E}_h^{i+1}, \mathbf{H}_h^{i+1}) - \mathcal{E}(\mathbf{m}_h^i, \mathbf{E}_h^i, \mathbf{H}_h^i) \\ = \mu_0 \|\nabla \mathbf{m}_h^{i+1}\|_{\mathbf{L}^2(\Omega)}^2 + \frac{\varepsilon_0}{C_e} \|\mathbf{E}_h^{i+1}\|_{\mathbf{L}^2(\hat{\Omega})}^2 + \frac{\mu_0}{C_e} \|\mathbf{H}_h^{i+1}\|_{\mathbf{L}^2(\hat{\Omega})}^2 - \frac{\mu_0}{C_e} (\boldsymbol{\pi}(\mathbf{m}_h^{i+1}), \mathbf{m}_h^{i+1}) \\ - \mu_0 \|\nabla \mathbf{m}_h^i\|_{\mathbf{L}^2(\Omega)}^2 - \frac{\varepsilon_0}{C_e} \|\mathbf{E}_h^i\|_{\mathbf{L}^2(\hat{\Omega})}^2 - \frac{\mu_0}{C_e} \|\mathbf{H}_h^i\|_{\mathbf{L}^2(\hat{\Omega})}^2 + \frac{\mu_0}{C_e} (\boldsymbol{\pi}(\mathbf{m}_h^i), \mathbf{m}_h^i) =: RHS. \end{aligned}$$

The combination of those two estimates yields

$$\begin{aligned}
 RHS \leq & \mu_0 \|\nabla \mathbf{m}_h^i\|_{L^2(\Omega)}^2 - 2(\theta - \frac{1}{2})\mu_0 k^2 \|\nabla \mathbf{v}_h^i\|_{L^2(\Omega)}^2 - \frac{2\alpha\mu_0 k}{C_e} \|\mathbf{v}_h^i\|_{L^2(\Omega)}^2 \\
 & - \frac{2\varepsilon_0}{C_e} (\mathbf{E}_h^{i+1} - \mathbf{E}_h^i, \mathbf{E}_h^{i+1}) - \frac{2\sigma k}{C_e} \|\mathbf{E}_h^{i+1}\|_{L^2(\Omega)}^2 - \frac{2\mu_0}{C_e} (\mathbf{H}_h^{i+1} - \mathbf{H}_h^i, \mathbf{H}_h^{i+1}) \\
 & + \frac{2\mu_0 k}{C_e} (\mathbf{H}_h^i - \mathbf{H}_h^{i+1}, \mathbf{v}_h^i) - \frac{2k}{C_e} (\mathbf{J}^i, \mathbf{E}_h^{i+1}) + \frac{2\mu_0 k}{C_e} (\pi(\mathbf{m}_h^i), \mathbf{v}_h^i) \\
 & + \frac{\varepsilon_0}{C_e} \|\mathbf{E}_h^{i+1}\|_{L^2(\hat{\Omega})}^2 + \frac{\mu_0}{C_e} \|\mathbf{H}_h^{i+1}\|_{L^2(\hat{\Omega})}^2 - \frac{\mu_0}{C_e} (\pi(\mathbf{m}_h^{i+1}), \mathbf{m}_h^{i+1}) \\
 & - \mu_0 \|\nabla \mathbf{m}_h^i\|_{L^2(\Omega)}^2 - \frac{\varepsilon_0}{C_e} \|\mathbf{E}_h^i\|_{L^2(\hat{\Omega})}^2 - \frac{\mu_0}{C_e} \|\mathbf{H}_h^i\|_{L^2(\hat{\Omega})}^2 + \frac{\mu_0}{C_e} (\pi(\mathbf{m}_h^i), \mathbf{m}_h^i).
 \end{aligned}$$

Next, we recall that by Abel's partial summation A.1.3, we get

$$-\frac{2\varepsilon_0}{C_e} \sum_{i=0}^{j-1} (\mathbf{E}_h^{i+1} - \mathbf{E}_h^i, \mathbf{E}_h^{i+1}) = -\frac{\varepsilon_0}{C_e} \|\mathbf{E}_h^j\|_{L^2(\hat{\Omega})}^2 + \frac{\varepsilon_0}{C_e} \|\mathbf{E}_h^0\|_{L^2(\hat{\Omega})}^2 - \frac{\varepsilon_0}{C_e} \sum_{i=0}^{j-1} \|\mathbf{E}_h^{i+1} - \mathbf{E}_h^i\|_{L^2(\hat{\Omega})}^2,$$

and

$$-\frac{2\mu_0}{C_e} \sum_{i=0}^{j-1} (\mathbf{H}_h^{i+1} - \mathbf{H}_h^i, \mathbf{H}_h^{i+1}) = -\frac{\mu_0}{C_e} \|\mathbf{H}_h^j\|_{L^2(\hat{\Omega})}^2 + \frac{\mu_0}{C_e} \|\mathbf{H}_h^0\|_{L^2(\hat{\Omega})}^2 - \frac{\mu_0}{C_e} \sum_{i=0}^{j-1} \|\mathbf{H}_h^{i+1} - \mathbf{H}_h^i\|_{L^2(\hat{\Omega})}^2.$$

Summing up the energy terms over $i = 0, \dots, j-1$ therefore yields

$$\begin{aligned}
 & \mathcal{E}(\mathbf{m}_h^j, \mathbf{E}_h^j, \mathbf{H}_h^j) - \mathcal{E}(\mathbf{m}_h^0, \mathbf{E}_h^0, \mathbf{H}_h^0) \\
 & \leq -2(\theta - \frac{1}{2})\mu_0 k^2 \sum_{i=0}^{j-1} \|\nabla \mathbf{v}_h^i\|_{L^2(\Omega)}^2 - \frac{2\alpha\mu_0 k}{C_e} \sum_{i=0}^{j-1} \|\mathbf{v}_h^i\|_{L^2(\Omega)}^2 \\
 & \quad - \frac{\varepsilon_0}{C_e} \|\mathbf{E}_h^j\|_{L^2(\hat{\Omega})}^2 + \frac{\varepsilon_0}{C_e} \|\mathbf{E}_h^0\|_{L^2(\hat{\Omega})}^2 - \frac{\varepsilon_0}{C_e} \sum_{i=0}^{j-1} \|\mathbf{E}_h^{i+1} - \mathbf{E}_h^i\|_{L^2(\hat{\Omega})}^2 - \frac{2\sigma k}{C_e} \sum_{i=0}^{j-1} \|\mathbf{E}_h^{i+1}\|_{L^2(\Omega)}^2 \\
 & \quad - \frac{\mu_0}{C_e} \|\mathbf{H}_h^j\|_{L^2(\hat{\Omega})}^2 + \frac{\mu_0}{C_e} \|\mathbf{H}_h^0\|_{L^2(\hat{\Omega})}^2 - \frac{\mu_0}{C_e} \sum_{i=0}^{j-1} \|\mathbf{H}_h^{i+1} - \mathbf{H}_h^i\|_{L^2(\hat{\Omega})}^2 + \frac{2\mu_0 k}{C_e} \sum_{i=0}^{j-1} (\mathbf{H}_h^i - \mathbf{H}_h^{i+1}, \mathbf{v}_h^i) \\
 & \quad - \frac{2k}{C_e} \sum_{i=0}^{j-1} (\mathbf{J}^i, \mathbf{E}_h^{i+1}) + \frac{2\mu_0 k}{C_e} \sum_{i=0}^{j-1} (\pi(\mathbf{m}_h^i), \mathbf{v}_h^i) + \frac{\varepsilon_0}{C_e} \|\mathbf{E}_h^j\|_{L^2(\hat{\Omega})}^2 + \frac{\mu_0}{C_e} \|\mathbf{H}_h^j\|_{L^2(\hat{\Omega})}^2 \\
 & \quad - \frac{\mu_0}{C_e} \sum_{i=0}^{j-1} (\pi(\mathbf{m}_h^{i+1}), \mathbf{m}_h^{i+1}) - \frac{\varepsilon_0}{C_e} \|\mathbf{E}_h^0\|_{L^2(\hat{\Omega})}^2 - \frac{\mu_0}{C_e} \|\mathbf{H}_h^0\|_{L^2(\hat{\Omega})}^2 + \frac{\mu_0}{C_e} \sum_{i=0}^{j-1} (\pi(\mathbf{m}_h^i), \mathbf{m}_h^i).
 \end{aligned}$$

Application of Young's inequality yields for any $\varepsilon > 0$

$$\begin{aligned}
 & -\frac{\mu_0}{C_e} \sum_{i=0}^{j-1} \|\mathbf{H}_h^{i+1} - \mathbf{H}_h^i\|_{L^2(\hat{\Omega})}^2 + \frac{2\mu_0 k}{C_e} \sum_{i=0}^{j-1} (\mathbf{H}_h^i - \mathbf{H}_h^{i+1}, \mathbf{v}_h^i) \\
 & \leq \frac{\mu_0}{C_e} (\frac{k}{2\varepsilon} - 1) \sum_{i=0}^{j-1} \|\mathbf{H}_h^{i+1} - \mathbf{H}_h^i\|_{L^2(\hat{\Omega})}^2 + \frac{2\varepsilon\mu_0 k}{C_e} \sum_{i=0}^{j-1} \|\mathbf{v}_h^i\|_{L^2(\Omega)}^2 \\
 & \leq \frac{2\varepsilon\mu_0 k}{C_e} \sum_{i=0}^{j-1} \|\mathbf{v}_h^i\|_{L^2(\Omega)}^2.
 \end{aligned} \tag{4.2.23}$$

Without loss of generality, we assumed $k/2 < \varepsilon$ here. This can safely be assumed for any ε , since we are interested in the limit $k \rightarrow 0$. Since a couple of terms in the above estimate cancel out, and others can be dropped due to negativity, by exploiting $\theta \in [1/2, 1]$, we end up with

$$\begin{aligned} \mathcal{E}(\mathbf{m}_h^j, \mathbf{E}_h^j, \mathbf{H}_h^j) - \mathcal{E}(\mathbf{m}_h^0, \mathbf{E}_h^0, \mathbf{H}_h^0) &+ \frac{2\mu_0 k}{C_e}(\alpha - \varepsilon) \sum_{i=0}^{j-1} \|\mathbf{v}_h^i\|_{L^2(\Omega)}^2 + \frac{2\sigma k}{C_e} \sum_{i=0}^{j-1} \|\mathbf{E}_h^{i+1}\|_{L^2(\Omega)}^2 \\ &\leq -\frac{2k}{C_e} \sum_{i=0}^{j-1} (\mathbf{J}^i, \mathbf{E}_h^{i+1}) + \frac{2\mu_0 k}{C_e} \sum_{i=0}^{j-1} (\pi(\mathbf{m}_h^i), \mathbf{v}_h^i) - \frac{\mu_0}{C_e} \sum_{i=0}^{j-1} (\pi(\mathbf{m}_h^{i+1}), \mathbf{m}_h^{i+1}) \\ &\quad + \frac{\mu_0}{C_e} \sum_{i=0}^{j-1} (\pi(\mathbf{m}_h^i), \mathbf{m}_h^i). \end{aligned}$$

As in the proof of Lemma 2.4.1, straightforward calculations show

$$\begin{aligned} 2k(\pi(\mathbf{m}_h^i), \mathbf{v}_h^i) - (\pi(\mathbf{m}_h^{i+1}), \mathbf{m}_h^{i+1}) + (\pi(\mathbf{m}_h^i), \mathbf{m}_h^i) \\ = 2k(\pi(\mathbf{m}_h^i), \mathbf{v}_h^i) - (\pi(\mathbf{m}_h^{i+1}) + \pi(\mathbf{m}_h^i), \mathbf{m}_h^{i+1} - \mathbf{m}_h^i) \\ - (\pi(\mathbf{m}_h^{i+1}), \mathbf{m}_h^i) + (\pi(\mathbf{m}_h^i), \mathbf{m}_h^{i+1}) \\ = 2k(\pi(\mathbf{m}_h^i), \mathbf{v}_h^i) - (\pi(\mathbf{m}_h^{i+1}) + \pi(\mathbf{m}_h^i), \mathbf{m}_h^{i+1} - \mathbf{m}_h^i), \end{aligned}$$

due to the assumed self-adjointness of $\pi(\cdot)$. Further estimation shows

$$\begin{aligned} 2k(\pi(\mathbf{m}_h^i), \mathbf{v}_h^i) - (\pi(\mathbf{m}_h^{i+1}) + \pi(\mathbf{m}_h^i), \mathbf{m}_h^{i+1} - \mathbf{m}_h^i) \\ = \underbrace{-2(\pi(\mathbf{m}_h^i), \mathbf{m}_h^{i+1} - \mathbf{m}_h^i - k\mathbf{v}_h^i)}_{=:a} - \underbrace{(\pi(\mathbf{m}_h^{i+1}) - \pi(\mathbf{m}_h^i), \mathbf{m}_h^{i+1} - \mathbf{m}_h^i)}_{=:b}. \end{aligned}$$

Next, we investigate both terms individually. By the assumed L^4 -boundedness of $\pi(\cdot)$, we get as in the proof of Lemma 2.4.1

$$a = -2(\pi(\mathbf{m}_h^i), \mathbf{m}_h^{i+1} - \mathbf{m}_h^i - k\mathbf{v}_h^i) \lesssim k^2 \|\mathbf{v}_h^i\|_{L^2(\Omega)} (\|\mathbf{v}_h^i\|_{L^2(\Omega)} + \|\nabla \mathbf{v}_h^i\|_{L^2(\Omega)}).$$

From the Lipschitz continuity of the general field contribution, we further deduce

$$b = -(\pi(\mathbf{m}_h^{i+1}) - \pi(\mathbf{m}_h^i), \mathbf{m}_h^{i+1} - \mathbf{m}_h^i) \lesssim k^2 \|\mathbf{v}_h^i\|_{L^2(\Omega)}^2.$$

Altogether, we thus derived

$$\begin{aligned} \mathcal{E}(\mathbf{m}_h^j, \mathbf{E}_h^j, \mathbf{H}_h^j) - \mathcal{E}(\mathbf{m}_h^0, \mathbf{E}_h^0, \mathbf{H}_h^0) &+ \frac{2\mu_0 k}{C_e}(\alpha - \varepsilon) \sum_{i=0}^{j-1} \|\mathbf{v}_h^i\|_{L^2(\Omega)}^2 + \frac{2\sigma k}{C_e} \sum_{i=0}^{j-1} \|\mathbf{E}_h^{i+1}\|_{L^2(\Omega)}^2 \\ &\leq -\frac{2k}{C_e} \sum_{i=0}^{j-1} (\mathbf{J}^i, \mathbf{E}_h^{i+1}) + Ck(\|\mathbf{v}_{hk}^-\|_{L^2(\Omega_T)} \|\nabla \mathbf{v}_{hk}^-\|_{L^2(\Omega_T)} + \|\mathbf{v}_{hk}^-\|_{L^2(\Omega_T)}^2). \end{aligned}$$

For any $t' \in [t_j, t_{j+1}]$, we thus get with $\varepsilon < \alpha$

$$\begin{aligned}
 & \mathcal{E}(\mathbf{m}_{hk}^+(t'), \mathbf{E}_{hk}^+(t), \mathbf{H}_{hk}^+(t')) + \frac{2\mu_0}{C_e}(\alpha - \varepsilon) \|\mathbf{v}_{hk}^-\|_{\mathbf{L}^2(\Omega_{t'})}^2 + \frac{2\sigma}{C_e} \|\mathbf{E}_{hk}^+\|_{\mathbf{L}^2(\Omega_{t'})}^2 \\
 &= \mathcal{E}(\mathbf{m}_{hk}^+(t'), \mathbf{E}_{hk}^+(t), \mathbf{H}_{hk}^+(t')) + \frac{2\mu_0}{C_e}(\alpha - \varepsilon) \int_0^{t'} \|\mathbf{v}_{hk}^-(s)\|_{\mathbf{L}^2(\Omega)}^2 + \frac{2\sigma}{C_e} \int_0^{t'} \|\mathbf{E}_{hk}^+(s)\|_{\mathbf{L}^2(\Omega)}^2 \\
 &\leq \mathcal{E}(\mathbf{m}_{hk}^+(t'), \mathbf{E}_{hk}^+(t'), \mathbf{H}_{hk}^+(t')) + \frac{2\mu_0}{C_e}(\alpha - \varepsilon) \int_0^{t_{j+1}} \|\mathbf{v}_{hk}^-(s)\|_{\mathbf{L}^2(\Omega)}^2 + \frac{2\sigma}{C_e} \int_0^{t_{j+1}} \|\mathbf{E}_{hk}^+(s)\|_{\mathbf{L}^2(\Omega)}^2 \\
 &= \mathcal{E}(\mathbf{m}_h^{j+1}, \mathbf{E}_h^{j+1}, \mathbf{H}_h^{j+1}) + \frac{2\mu_0 k}{C_e}(\alpha - \varepsilon) \sum_{i=0}^j \|\mathbf{v}_h^i\|_{\mathbf{L}^2(\Omega)}^2 + \frac{2\sigma k}{C_e} \sum_{i=0}^j \|\mathbf{E}_h^{i+1}\|_{\mathbf{L}^2(\Omega)}^2 \\
 &\leq \mathcal{E}(\mathbf{m}_h^0, \mathbf{E}_h^0, \mathbf{H}_h^0) - \frac{2k}{C_e} \sum_{i=0}^j (\mathbf{J}^i, \mathbf{E}_h^{i+1}) + Ck(\|\mathbf{v}_{hk}^-\|_{\mathbf{L}^2(\Omega_T)} \|\nabla \mathbf{v}_{hk}^-\|_{\mathbf{L}^2(\Omega_T)} + \|\mathbf{v}_{hk}^-\|_{\mathbf{L}^2(\Omega_T)}^2) \\
 &= \mathcal{E}(\mathbf{m}_h^0, \mathbf{E}_h^0, \mathbf{H}_h^0) - \frac{2}{C_e} \sum_{i=0}^j \int_{t_i}^{t_{i+1}} (\mathbf{J}^i, \mathbf{E}_h^{i+1}) + Ck(\|\mathbf{v}_{hk}^-\|_{\mathbf{L}^2(\Omega_T)} \|\nabla \mathbf{v}_{hk}^-\|_{\mathbf{L}^2(\Omega_T)} + \|\mathbf{v}_{hk}^-\|_{\mathbf{L}^2(\Omega_T)}^2) \\
 &= \mathcal{E}(\mathbf{m}_h^0, \mathbf{E}_h^0, \mathbf{H}_h^0) - \frac{2}{C_e} \int_0^{t'} (\mathbf{J}_{hk}^-, \mathbf{E}_{hk}^+) - \frac{2}{C_e} \underbrace{\int_{t'}^{t_{j+1}} (\mathbf{J}_{hk}^-, \mathbf{E}_{hk}^+)}_{=:c} \\
 &\quad + Ck(\|\mathbf{v}_{hk}^-\|_{\mathbf{L}^2(\Omega_T)} \|\nabla \mathbf{v}_{hk}^-\|_{\mathbf{L}^2(\Omega_T)} + \|\mathbf{v}_{hk}^-\|_{\mathbf{L}^2(\Omega_T)}^2).
 \end{aligned}$$

First, we observe that due to non-concentration of Lebesgue measures and boundedness of \mathbf{J}_{hk}^- and \mathbf{E}_{hk}^+ in $\mathbf{L}^2(\widehat{\Omega}_T)$, we have

$$c = \int_{t'}^{t_{j+1}} (\mathbf{J}_{hk}^-, \mathbf{E}_{hk}^+) \xrightarrow{\text{sub}} 0 \quad \text{as } (h, k) \rightarrow (0, 0).$$

Finally, we consider the limiting process. Integrating the above estimate in time over any Borel set $\mathfrak{J} \subseteq [0, T]$, we get

$$\begin{aligned}
 & \int_{\mathfrak{J}} \mathcal{E}(\mathbf{m}_{hk}^+(t'), \mathbf{E}_{hk}^+(t), \mathbf{H}_{hk}^+(t')) + \int_{\mathfrak{J}} \frac{2\mu_0}{C_e}(\alpha - \varepsilon) \|\mathbf{v}_{hk}^-\|_{\mathbf{L}^2(\Omega_{t'})}^2 + \int_{\mathfrak{J}} \frac{2\sigma}{C_e} \|\mathbf{E}_{hk}^+\|_{\mathbf{L}^2(\Omega_{t'})}^2 \\
 &\leq \int_{\mathfrak{J}} \mathcal{E}(\mathbf{m}_h^0, \mathbf{E}_h^0, \mathbf{H}_h^0) - \frac{2}{C_e} \int_{\mathfrak{J}} \int_0^{t'} (\mathbf{J}_{hk}^-, \mathbf{E}_{hk}^+) - \frac{2}{C_e} \int_{\mathfrak{J}} \int_{t'}^{t_{j+1}} (\mathbf{J}_{hk}^-, \mathbf{E}_{hk}^+) \\
 &\quad + \int_{\mathfrak{J}} Ck(\|\mathbf{v}_{hk}^-\|_{\mathbf{L}^2(\Omega_T)} \|\nabla \mathbf{v}_{hk}^-\|_{\mathbf{L}^2(\Omega_T)} + \|\mathbf{v}_{hk}^-\|_{\mathbf{L}^2(\Omega_T)}^2).
 \end{aligned}$$

Passing to the limit while using weak lower semi-continuity finally reveals

$$\begin{aligned}
 & \int_{\mathfrak{J}} \mathcal{E}(\mathbf{m}, \mathbf{E}, \mathbf{H}) + \int_{\mathfrak{J}} \frac{2\mu_0}{C_e}(\alpha - \varepsilon) \|\mathbf{m}_t\|_{\mathbf{L}^2(\Omega_{t'})}^2 + \int_{\mathfrak{J}} \frac{2\sigma}{C_e} \|\mathbf{E}\|_{\mathbf{L}^2(\Omega_{t'})}^2 \\
 &\leq \int_{\mathfrak{J}} \mathcal{E}(\mathbf{m}(0), \mathbf{E}(0), \mathbf{H}(0)) - \frac{2}{C_e} \int_{\mathfrak{J}} (\mathbf{J}, \mathbf{E})_{\Omega_{t'}}.
 \end{aligned}$$

Since the set $\mathfrak{J} \subseteq [0, T]$ was arbitrary, this yields the desired result by standard measure theory, i.e. [Els11, IV, Theorem 4.4]. \square

We conclude this section with an analog statement for the coupled Algorithm 4.2.1. As mentioned above, the analysis in this case is slightly simplified since there is no need for the application of Abel's partial summation formula.

Proposition 4.2.11 (Improved energy estimate for Algorithm 4.2.1). *Let $\pi(\cdot)$ be uniformly Lipschitz continuous and bounded in $\mathbf{L}^2(\Omega)$, i.e. $\|\pi(\mathbf{n})\|_{\mathbf{L}^4(\Omega)} \leq C_{25}$ for all $\mathbf{n} \in \mathbf{L}^2(\Omega)$ with $|\mathbf{n}| \leq 1$ almost everywhere in Ω . Here, C_{25} denotes some uniform constant which only depends on Ω . Let further $\pi(\cdot)$ be self-adjoint. Moreover, we assume $\mathbf{J}_{hk}^- \rightarrow \mathbf{J}$ strongly in $\mathbf{L}^2(\hat{\Omega}_T)$. Then, for the output of Algorithm (4.2.1), we have the energy decay estimate*

$$\mathcal{E}(t') + \frac{\mu_0 \alpha}{C_e} \|\mathbf{m}_t\|_{\mathbf{L}^2(\Omega_{t'})}^2 + \frac{\sigma}{C_e} \|\mathbf{E}\|_{\Omega_{t'}}^2 \leq \mathcal{E}(0) - \frac{2}{C_e} (\mathbf{J}, \mathbf{E})_{\hat{\Omega}_{t'}}, \quad (4.2.24)$$

for almost every $t' \in [0, T]$.

Proof. The proof follows the lines of the one of Proposition 4.2.10. We start with a discrete energy estimate as in the proof of Lemma 4.2.6. The output of Algorithm 4.2.1 satisfies

$$\begin{aligned} \mu_0 \|\nabla \mathbf{m}_h^{i+1}\|_{\mathbf{L}^2(\Omega)}^2 &\leq \mu_0 \|\nabla \mathbf{m}_h^i\|_{\mathbf{L}^2(\Omega)}^2 - 2(\theta - \frac{1}{2}) \mu_0 k^2 \|\nabla \mathbf{v}_h^i\|_{\mathbf{L}^2(\Omega)}^2 - \frac{2\alpha\mu_0 k}{C_e} \|\mathbf{v}_h^i\|_{\mathbf{L}^2(\Omega)}^2 \\ &\quad + \frac{2\mu_0 k}{C_e} (\pi(\mathbf{m}_h^i), \mathbf{v}_h^i) - \frac{\varepsilon_0}{C_e} \|\mathbf{E}_h^{i+1}\|_{\mathbf{L}^2(\hat{\Omega})}^2 - \frac{\mu_0}{C_e} \|\mathbf{H}_h^{i+1}\|_{\mathbf{L}^2(\hat{\Omega})}^2 \\ &\quad - \frac{2\sigma k}{C_e} \|\mathbf{E}_h^{i+1/2}\|_{\mathbf{L}^2(\Omega)}^2 + \frac{\varepsilon_0}{C_e} \|\mathbf{E}_h^i\|_{\mathbf{L}^2(\hat{\Omega})}^2 + \frac{\mu_0}{C_e} \|\mathbf{H}_h^i\|_{\mathbf{L}^2(\hat{\Omega})}^2 - \frac{2k}{C_e} (\mathbf{J}^{i+1/2}, \mathbf{E}_h^{i+1/2}). \end{aligned}$$

Analogously to before, this implies

$$\begin{aligned} &\mathcal{E}(\mathbf{m}_h^{i+1}, \mathbf{E}_h^{i+1}, \mathbf{H}_h^{i+1}) - \mathcal{E}(\mathbf{m}_h^i, \mathbf{E}_h^i, \mathbf{H}_h^i) \\ &= \mu_0 \|\nabla \mathbf{m}_h^{i+1}\|_{\mathbf{L}^2(\Omega)}^2 + \frac{\varepsilon_0}{C_e} \|\mathbf{E}_h^{i+1}\|_{\mathbf{L}^2(\hat{\Omega})}^2 + \frac{\mu_0}{C_e} \|\mathbf{H}_h^{i+1}\|_{\mathbf{L}^2(\hat{\Omega})}^2 - \frac{\mu_0}{C_e} (\pi(\mathbf{m}_h^{i+1}), \mathbf{m}_h^{i+1}) \\ &\quad - \mu_0 \|\nabla \mathbf{m}_h^i\|_{\mathbf{L}^2(\Omega)}^2 - \frac{\varepsilon_0}{C_e} \|\mathbf{E}_h^i\|_{\mathbf{L}^2(\hat{\Omega})}^2 - \frac{\mu_0}{C_e} \|\mathbf{H}_h^i\|_{\mathbf{L}^2(\hat{\Omega})}^2 + \frac{\mu_0}{C_e} (\pi(\mathbf{m}_h^i), \mathbf{m}_h^i) \\ &\leq -\frac{2\alpha\mu_0 k}{C_e} \|\mathbf{v}_h^i\|_{\mathbf{L}^2(\Omega)}^2 - \frac{2\sigma k}{C_e} \|\mathbf{E}_h^{i+1/2}\|_{\mathbf{L}^2(\Omega)}^2 - \frac{2k}{C_e} (\mathbf{J}^{i+1/2}, \mathbf{E}_h^{i+1/2}) \\ &\quad + \frac{2\mu_0 k}{C_e} (\pi(\mathbf{m}_h^i), \mathbf{v}_h^i) - \frac{\mu_0}{C_e} (\pi(\mathbf{m}_h^{i+1}), \mathbf{m}_h^{i+1}) + \frac{\mu_0}{C_e} (\pi(\mathbf{m}_h^i), \mathbf{m}_h^i). \end{aligned}$$

Here, we exploited $\theta \in [1/2, 1]$. The last three terms on the right-hand side are estimated as in the above proof. We again deduce

$$\begin{aligned} &\frac{2\mu_0 k}{C_e} (\pi(\mathbf{m}_h^i), \mathbf{v}_h^i) - \frac{\mu_0}{C_e} (\pi(\mathbf{m}_h^{i+1}), \mathbf{m}_h^{i+1}) + \frac{\mu_0}{C_e} (\pi(\mathbf{m}_h^i), \mathbf{m}_h^i) \\ &\leq Ck^2 (\|\mathbf{v}_h^i\|_{\mathbf{L}^2(\Omega)} \|\nabla \mathbf{v}_h^i\|_{\mathbf{L}^2(\Omega)} + \|\mathbf{v}_h^i\|_{\mathbf{L}^2(\Omega)}^2) \end{aligned}$$

whence in total and after summing up

$$\begin{aligned} &\mathcal{E}(\mathbf{m}_h^j, \mathbf{E}_h^j, \mathbf{H}_h^j) + \frac{2\alpha\mu_0 k}{C_e} \sum_{i=0}^{j-1} \|\mathbf{v}_h^i\|_{\mathbf{L}^2(\Omega)}^2 + \frac{2\sigma k}{C_e} \sum_{i=0}^{j-1} \|\mathbf{E}_h^{i+1/2}\|_{\mathbf{L}^2(\Omega)}^2 \\ &\leq \mathcal{E}(\mathbf{m}_h^0, \mathbf{E}_h^0, \mathbf{H}_h^0) - \frac{2k}{C_e} \sum_{i=0}^{j-1} (\mathbf{J}^{i+1/2}, \mathbf{E}_h^{i+1/2}) + Ck (\|\mathbf{v}_{hk}^-\|_{\mathbf{L}^2(\Omega_T)} \|\nabla \mathbf{v}_{hk}^-\|_{\mathbf{L}^2(\Omega_T)} + \|\mathbf{v}_{hk}^-\|_{\mathbf{L}^2(\Omega_T)}^2). \end{aligned}$$

While the remainder of the proof is pretty similar to the one of Algorithm 4.2.2, we stress that in this case, we do not have a priori information on the convergence of \mathbf{E}_{hk}^\pm and \mathbf{H}_{hk}^\pm , respectively. The remedy is to apply the known convergence of the midpoint evaluations. For $t' \in [t_j, t_{j+1})$, we have

$$\begin{aligned}
 & \mathcal{E}(\mathbf{m}_{hk}^+(t'), \bar{\mathbf{E}}_{hk}(t'), \bar{\mathbf{H}}_{hk}(t')) + \mathcal{E}(\mathbf{m}_{hk}^-(t'), \bar{\mathbf{E}}_{hk}(t'), \bar{\mathbf{H}}_{hk}(t')) \\
 & \sim \|\nabla \mathbf{m}_h^{j+1}\|_{L^2(\Omega)}^2 + \|\mathbf{E}_h^{j+1/2}\|_{L^2(\hat{\Omega})}^2 + \|\mathbf{H}_h^{j+1/2}\|_{L^2(\hat{\Omega})}^2 + (\pi(\mathbf{m}_h^{j+1}), \mathbf{m}_h^{j+1}) \\
 & \quad + \|\nabla \mathbf{m}_h^j\|_{L^2(\Omega)}^2 + \|\mathbf{E}_h^{j+1/2}\|_{L^2(\hat{\Omega})}^2 + \|\mathbf{H}_h^{j+1/2}\|_{L^2(\hat{\Omega})}^2 + (\pi(\mathbf{m}_h^j), \mathbf{m}_h^j) \\
 & \leq \|\nabla \mathbf{m}_h^{j+1}\|_{L^2(\Omega)}^2 + \|\nabla \mathbf{m}_h^j\|_{L^2(\Omega)}^2 + \|\mathbf{E}_h^{j+1}\|_{L^2(\hat{\Omega})}^2 + \|\mathbf{E}_h^j\|_{L^2(\hat{\Omega})}^2 + \|\mathbf{H}_h^{j+1}\|_{L^2(\hat{\Omega})}^2 + \|\mathbf{H}_h^j\|_{L^2(\hat{\Omega})}^2 \\
 & \quad + (\pi(\mathbf{m}_h^{j+1}), \mathbf{m}_h^{j+1}) + (\pi(\mathbf{m}_h^j), \mathbf{m}_h^j) \\
 & \sim \mathcal{E}(\mathbf{m}_{hk}^+(t'), \mathbf{E}_{hk}^+(t'), \mathbf{H}_{hk}^+(t')) + \mathcal{E}(\mathbf{m}_{hk}^-(t'), \mathbf{E}_{hk}^-(t'), \mathbf{H}_{hk}^-(t')).
 \end{aligned}$$

Analogously to before, this yields

$$\begin{aligned}
 & \mathcal{E}(\mathbf{m}_{hk}^+(t'), \bar{\mathbf{E}}_{hk}(t'), \bar{\mathbf{H}}_{hk}(t')) + \mathcal{E}(\mathbf{m}_{hk}^-(t'), \bar{\mathbf{E}}_{hk}(t'), \bar{\mathbf{H}}_{hk}(t')) + \frac{2\alpha\mu_0}{C_e} \|\mathbf{v}_{hk}^-\|_{L^2(\Omega_{t'})}^2 + \frac{2\sigma}{C_e} \|\bar{\mathbf{E}}_{hk}\|_{L^2(\Omega_{t'})}^2 \\
 & \leq 2\mathcal{E}(\mathbf{m}_h^0, \mathbf{E}_h^0, \mathbf{H}_h^0) + 2Ck(\|\mathbf{v}_{hk}^-\|_{L^2(\Omega_T)} \|\nabla \mathbf{v}_{hk}^-\|_{L^2(\Omega_T)} + \|\mathbf{v}_{hk}^-\|_{L^2(\Omega_T)}^2) \\
 & \quad - \underbrace{\frac{2k}{C_e} \sum_{i=0}^{j-1} (\mathbf{J}^{i+1/2}, \mathbf{E}_h^{i+1/2})}_{=:a} - \underbrace{\frac{2k}{C_e} \sum_{i=0}^j (\mathbf{J}^{i+1/2}, \mathbf{E}_h^{i+1/2})}_{=:b}.
 \end{aligned}$$

The last two terms on the right-hand side can be further estimated by

$$\begin{aligned}
 a &= -\frac{2}{C_e} \int_0^{t_j} (\bar{\mathbf{J}}_{hk}, \bar{\mathbf{E}}_{hk}) = -\frac{2}{C_e} \int_0^{t'} (\bar{\mathbf{J}}_{hk}, \bar{\mathbf{E}}_{hk}) + \int_{t_j}^{t'} (\bar{\mathbf{J}}_{hk}, \bar{\mathbf{E}}_{hk}), \quad \text{and} \\
 b &= -\frac{2}{C_e} \int_0^{t_{j+1}} (\bar{\mathbf{J}}_{hk}, \bar{\mathbf{E}}_{hk}) = -\frac{2}{C_e} \int_0^{t'} (\bar{\mathbf{J}}_{hk}, \bar{\mathbf{E}}_{hk}) - \int_{t'}^{t_{j+1}} (\bar{\mathbf{J}}_{hk}, \bar{\mathbf{E}}_{hk}).
 \end{aligned}$$

Again, non-concentration of Lebesgue measures reveals

$$\int_{t_j}^{t'} (\bar{\mathbf{J}}_{hk}, \bar{\mathbf{E}}_{hk}) - \int_{t'}^{t_{j+1}} (\bar{\mathbf{J}}_{hk}, \bar{\mathbf{E}}_{hk}) \xrightarrow{\text{sub}} 0 \quad \text{as } (h, k) \rightarrow (0, 0).$$

Integration over any Borel set $\mathfrak{J} \subseteq [0, T]$ and passing to the limit, we finally deduce

$$\begin{aligned}
 2 \int_{\mathfrak{J}} \mathcal{E}(\mathbf{m}, \mathbf{E}, \mathbf{H}) + \frac{2\mu_0}{C_e} \int_{\mathfrak{J}} \|\mathbf{m}_t\|_{L^2(\Omega_{t'})}^2 + \frac{2\sigma}{C_e} \int_{\mathfrak{J}} \|\mathbf{E}\|_{L^2(\Omega_{t'})}^2 \\
 \leq 2 \int_{\mathfrak{J}} \mathcal{E}(\mathbf{m}(0), \mathbf{E}(0), \mathbf{H}(0)) - \frac{4}{C_e} \int_{\mathfrak{J}} (\mathbf{J}, \mathbf{E})_{\Omega_{t'}}.
 \end{aligned}$$

Since the integration domain $\mathfrak{J} \subseteq [0, T]$ was arbitrary, the result again follows from [Els11, IV, Theorem 4.4]. \square

Remark . We briefly remark on the derived results in comparison to each other and the available literature.

- a) In comparison to the estimate (4.2.22), the previous estimate (4.2.24) has only a factor 1 for the second and third term on the left hand side. This is due to the fact that we do not have any result on the convergence of \mathbf{E}_{hk}^\pm and \mathbf{H}_{hk}^\pm , respectively. The remedy we used is to estimate the midpoint evaluation by the sum of the upper- and lower-bound estimation. Finally, we employed the limiting process for the midpoint evaluation. Another ansatz would be to directly work with the midpoint evaluation in $\mathcal{E}(\cdot)$, i.e. also use $\nabla \overline{\mathbf{m}}_{hk}$. This would, however, lead to the additional term

$$(\pi(\overline{\mathbf{m}}_{hk}), \overline{\mathbf{m}}_{hk}),$$

which then needs to be controlled. This problem could be circumvented if we knew convergence of $\mathbf{E}_{hk}^\pm \rightarrow \mathbf{E}$ and $\mathbf{H}_{hk}^\pm \rightarrow \mathbf{H}$, respectively which is the case for Algorithm 4.2.2. Here, the drawback is an additional damping term ε in front of \mathbf{m}_t .

- b) In [BBP08], the energy estimate seems to be somewhat nicer at first glance, as it reads

$$\mathcal{E}(t') + \mu_0 \alpha \|\mathbf{m}_t\|_{\mathbf{L}^2(\Omega_{t'})}^2 + \sigma \|\mathbf{E}\|_{\mathbf{L}^2(\Omega_{t'})}^2 \leq \mathcal{E}(0) - (\mathbf{J}, \mathbf{E})_{\Omega_{t'}},$$

i.e. we do not have a factor $2/C_e$ in front of the terms outside of $\mathcal{E}(\cdot)$. This is, however, not true, since the energy term in [BBP08] is defined with an additional factor $1/2$ in comparison to our energy functional here. This means that the factor 2 is simply hidden in $\mathcal{E}(\cdot)$. Moreover, the exchange constant C_e is set to be 1 in [BBP08].

Coupling to the eddy-current equation

In the last chapter, we treated coupling of the LLG equation to the full Maxwell system, and particular focus was laid on the possibility of decoupling both problems. In that regard, the proposed algorithm has a major advantage compared to e.g. the midpoint scheme algorithm for MLLG which was analyzed in [BBP08]. In this short chapter, we aim to transfer this advantages to the eddy-current problem below. As already mentioned in Section 1.4.2, the time derivative of the electric field can sometimes be neglected (especially for low-frequency problems) which leads to the eddy-current simplification

$$\mu_0 \mathbf{H}_t + \frac{1}{\sigma} \nabla \times (\nabla \times \mathbf{H}) = -\mu_0 \mathbf{m}_t. \quad (5.0.1)$$

An unconditionally convergent integrator for the coupled system of LLG with the eddy-current equation (5.0.1) has first been proposed by LE and TRAN in [LT12]. In this work, the authors employed the tangent plane scheme for the LLG part and existence of weak solutions was shown for a simplified effective field. The integrator is, however, still coupled and thus enforces the solution of one large linear system, instead of two small and subsequent linear systems per time step. In this chapter, we combine the results from Chapter 4 and [LT12] to derive a fully decoupled scheme for the eddy-current-LLG problem. As before, this has a huge impact on implementational applicability as existing LLG solvers, as well as preconditioners for either equation can easily be reused. Moreover, in comparison to the full Maxwell system and analogously to [LT12], one derives higher time-regularity for the magnetic field \mathbf{H} , cf. Theorem 5.3.1 below. The results from this chapter have partially been published in [LPPT13].

5.1. The eddy-current-LLG system

We consider the Landau-Lifshitz-Gilbert equation coupled with the eddy-current equation (ELLG), i.e.

$$\mathbf{m}_t - \alpha \mathbf{m} \times \mathbf{m}_t = -\mathbf{m} \times \mathbf{h}_{\text{eff}} \quad \text{in } \Omega_T := (0, T) \times \Omega, \quad (5.1.1a)$$

$$\mu_0 \mathbf{H}_t + \sigma^{-1} \nabla \times (\nabla \times \mathbf{H}) = -\mu_0 \mathbf{m}_t \quad \text{in } \hat{\Omega}_T := (0, T) \times \hat{\Omega}, \quad (5.1.1b)$$

where the effective field reads $\mathbf{h}_{\text{eff}} = C_e \Delta \mathbf{m} + \mathbf{H} + \boldsymbol{\pi}(\mathbf{m})$. Again, we neglect a time-dependent field contribution, as well as a spatial approximation $\boldsymbol{\pi}_h$ of $\boldsymbol{\pi}$. The rigorous inclusion of such an

approximation is, however, straightforward with the techniques from Chapter 2. Analogously to the other chapters, the case $\mathbf{h}_{\text{eff}} = C_e \Delta \mathbf{m} + \mathbf{H} + C_a D\Phi(\mathbf{m}) + \mathbf{f}$ is particularly covered. The above System 4.1.1 describes the evolution of the magnetization of a ferromagnetic body that occupies the domain $\Omega \Subset \widehat{\Omega} \subseteq \mathbb{R}^3$ for some given parameters $\alpha, \mu_0, \sigma \geq 0$.

As for the MLLG case, we assume $\widehat{\Omega} \subset \mathbb{R}^3$ to be bounded with perfectly conducting outer surface $\partial\widehat{\Omega}$ into which the ferromagnet $\Omega \Subset \widehat{\Omega}$ is embedded, and $\widehat{\Omega} \setminus \overline{\Omega}$ is assumed to be vacuum. Similar to the full Maxwell-LLG problem, the ELLG system (4.1.1) is supplemented by initial conditions

$$\mathbf{m}(0, \cdot) = \mathbf{m}^0 \text{ in } \Omega \quad \text{and} \quad \mathbf{H}(0, \cdot) = \mathbf{H}^0 \text{ in } \widehat{\Omega} \quad (5.1.1c)$$

as well as boundary conditions

$$\partial_{\mathbf{n}} \mathbf{m} = 0 \text{ on } \partial\Omega_T, \quad (\nabla \times \mathbf{H}) \times \mathbf{n} = 0 \text{ on } \partial\widehat{\Omega}_T. \quad (5.1.1d)$$

In analogy to [LT12] and Chapter 4, we assume the given data to satisfy

$$\mathbf{m}^0 \in \mathbf{H}^1(\Omega, \mathbb{S}^2), \quad \mathbf{H}^0 \in \mathbf{H}(\text{curl}; \widehat{\Omega}) \quad (5.1.1e)$$

as well as

$$\text{div}(\mathbf{H}^0 + \chi_{\Omega} \mathbf{m}^0) = 0 \quad \text{in } \widehat{\Omega}, \quad \langle \mathbf{H}^0 + \chi_{\Omega} \mathbf{m}^0, \mathbf{n} \rangle = 0 \quad \text{on } \partial\widehat{\Omega}. \quad (5.1.1f)$$

We now recall the notion of a weak solution of (4.1.1a)–(4.1.1b) from [LT12] which extends [AS92] from the pure LLG to ELLG .

Definition 5.1.1. *Given (5.1.1e)–(5.1.1f), the tuple (\mathbf{m}, \mathbf{H}) is called a weak solution of ELLG if,*

- (i) $\mathbf{m} \in \mathbf{H}^1(\Omega_T)$ with $|\mathbf{m}| = 1$ almost everywhere in Ω_T ;
- (ii) $\mathbf{H}, \mathbf{H}_t, \nabla \times \mathbf{H} \in \mathbf{L}^2(\widehat{\Omega}_T)$, i.e. $\mathbf{H} \in H^1(\mathbf{L}^2)$ and $\nabla \times \mathbf{H} \in \mathbf{L}^2(\widehat{\Omega}_T)$ in the weak sense;
- (iii) for all $\varphi \in C^\infty(\overline{\Omega_T})$ and $\zeta \in C^\infty(\widehat{\Omega}_T)$, we have

$$\begin{aligned} \int_{\Omega_T} \mathbf{m}_t \cdot \varphi - \alpha \int_{\Omega_T} (\mathbf{m} \times \mathbf{m}_t) \cdot \varphi &= -C_e \int_{\Omega_T} (\nabla \mathbf{m} \times \mathbf{m}) \cdot \nabla \varphi \\ &\quad + \int_{\Omega_T} (\mathbf{H} \times \mathbf{m}) \cdot \varphi + \int_{\Omega_T} (\boldsymbol{\pi}(\mathbf{m}) \times \mathbf{m}) \cdot \varphi, \end{aligned} \quad (5.1.2)$$

$$\mu_0 \int_{\widehat{\Omega}_T} \mathbf{H}_t \cdot \zeta + \sigma^{-1} \int_{\widehat{\Omega}_T} (\nabla \times \mathbf{H}) \cdot (\nabla \times \zeta) = -\mu_0 \int_{\Omega_T} \mathbf{m}_t \cdot \zeta; \quad (5.1.3)$$

- (iv) there holds $\mathbf{m}(0, \cdot) = \mathbf{m}^0$ and $\mathbf{H}(0, \cdot) = \mathbf{H}^0$ in the sense of traces;
- (v) for almost all $t' \in [0, T]$, we have bounded energy

$$\|\nabla \mathbf{m}(t')\|_{\mathbf{L}^2(\Omega)}^2 + \|\mathbf{m}_t\|_{\mathbf{L}^2(\Omega_{t'})}^2 + \|\mathbf{H}(t')\|_{\mathbf{L}^2(\widehat{\Omega})}^2 + \|(\nabla \times \mathbf{H})(t')\|_{\mathbf{L}^2(\widehat{\Omega})}^2 + \|\mathbf{H}_t\|_{\mathbf{L}^2(\widehat{\Omega}_{t'})}^2 \leq C_{26}, \quad (5.1.4)$$

where $C_{26} > 0$ is independent of t' .

Remark. Under the usual additional assumptions on the general operator $\pi(\cdot)$, namely boundedness in $\mathbf{L}^4(\Omega)$ and self-adjointness, one can derive the improved energy estimate

$$\mathcal{E}(t') + \frac{\mu_0}{C_e}(\alpha - 2\varepsilon)\|\mathbf{m}_t\|_{\mathbf{L}^2(\widehat{\Omega}_{t'})}^2 + \frac{\mu_0\alpha}{C_e}\|\mathbf{H}_t\|_{\mathbf{L}^2(\widehat{\Omega}_{t'})}^2 + \frac{2}{\sigma C_e}\|\nabla \times \mathbf{H}\|_{\mathbf{L}^2(\widehat{\Omega}_{t'})}^2 \leq \mathcal{E}(0),$$

with

$$\mathcal{E}(t') = \mu_0\|\nabla \mathbf{m}(t')\|_{\mathbf{L}^2(\Omega)}^2 + \frac{\mu_0}{C_e}\|\mathbf{H}(t')\|_{\mathbf{L}^2(\widehat{\Omega})}^2 + \frac{\alpha}{C_e\sigma}\|(\nabla \times \mathbf{H})(t')\|_{\mathbf{L}^2(\widehat{\Omega})}^2 - \frac{\mu_0}{C_e}(\pi(\mathbf{m}(t')), \mathbf{m}(t')).$$

This result is formally stated and proved in Section 5.3.1. The additional assumptions are particularly fulfilled if $\pi(\cdot)$ denotes the uniaxial anisotropy.

Remark. We emphasize the additional regularity $\mathbf{H}_t \in \mathbf{L}^2(\widehat{\Omega}_T)$ and $\nabla \times \mathbf{H} \in \mathbf{L}^2(\widehat{\Omega}_T)$ for the derivative and the curl of the magnetic field \mathbf{H} . If LLG is coupled to the full Maxwell system, the current analysis of weak solvers provides only the reduced regularity $\mathbf{E}, \mathbf{H} \in \mathbf{L}^2(\widehat{\Omega}_T)$ for the electric and magnetic field, see [BBP08, BPP13].

5.2. Preliminaries and numerical algorithm

The LLG equation is discretized in the tangent space $\mathcal{K}_{\mathbf{m}_h^j}$, as before. For the eddy-current part, we employ the space \mathcal{X}_h of lowest order edge elements of Nédélec's first family. It is well-known [Néd80, Mon08], that this is a subspace of

$$\mathbf{H}(\text{curl}; \widehat{\Omega}) := \{\boldsymbol{\varphi} \in \mathbf{L}^2(\widehat{\Omega}) : \nabla \times \boldsymbol{\varphi} \in \mathbf{L}^2(\widehat{\Omega})\}.$$

Similarly to the MLLG-case, we propose the following fully decoupled algorithm:

Algorithm 5.2.1. *Input: Initial data \mathbf{m}^0 and \mathbf{H}^0 , parameter $0 \leq \theta \leq 1$, counter $i = 0$. For all $i = 0, \dots, N - 1$ iterate:*

(i) *Compute unique solution $\mathbf{v}_h^i \in \mathcal{K}_{\mathbf{m}_h^i}$ such that for all $\phi_h \in \mathcal{K}_{\mathbf{m}_h^i}$ there holds*

$$\begin{aligned} \alpha(\mathbf{v}_h^i, \phi_h) + ((\mathbf{m}_h^i \times \mathbf{v}_h^i), \phi_h) + C_e(\theta k \nabla \mathbf{v}_h^i, \nabla \phi_h) = -C_e(\nabla \mathbf{m}_h^i, \nabla \phi_h) \\ + (\mathbf{H}_h^i, \phi_h) + (\pi(\mathbf{m}_h^i), \phi_h). \end{aligned} \quad (5.2.1a)$$

(ii) *Define $\mathbf{m}_h^{i+1} \in \mathcal{M}_h$ nodewise by $\mathbf{m}_h^{i+1}(\mathbf{z}) = \frac{\mathbf{m}_h^i(\mathbf{z}) + k\mathbf{v}_h^i(\mathbf{z})}{|\mathbf{m}_h^i(\mathbf{z}) + k\mathbf{v}_h^i(\mathbf{z})|}$ for all $\mathbf{z} \in \mathcal{N}_h$.*

(iii) *Compute unique solution $\mathbf{H}_h^{i+1} \in \mathcal{X}_h$ such that for all $\boldsymbol{\zeta}_h \in \mathcal{X}_h$ there holds*

$$\mu_0(d_t \mathbf{H}_h^{i+1}, \boldsymbol{\zeta}_h) + \sigma^{-1}(\nabla \times \mathbf{H}_h^{i+1}, \nabla \times \boldsymbol{\zeta}_h) = -\mu_0(\mathbf{v}_h^i, \boldsymbol{\zeta}_h). \quad (5.2.1b)$$

The following lemma states that the above algorithm is indeed well-defined.

Lemma 5.2.2. *Algorithm 5.2.1 is well-defined in the sense that it admits a unique solution $(\mathbf{v}_h^i, \mathbf{m}_h^{i+1}, \mathbf{H}_h^{i+1})$ at each step $i = 0, \dots, N - 1$ of the iterative loop. Moreover, we have $\|\mathbf{m}_h^i\|_{\mathbf{L}^\infty(\Omega)} = 1$ for each $i = 0, \dots, N$.*

Proof. Unique solvability of (5.2.1a)–(5.2.1b) directly follows from the linearity of the right-hand sides, positive definiteness of the left-hand sides, and finite space dimension, cf. e.g. proof of Lemma 4.2.4. Due to the Pythagoras theorem and the pointwise orthogonality from $\mathcal{K}_{\mathbf{m}_h^i}$, we further get $|\mathbf{m}_h^i(\mathbf{z}) + k\mathbf{v}_h^i(\mathbf{z})|^2 = |\mathbf{m}_h^i(\mathbf{z})|^2 + k|\mathbf{v}_h^i(\mathbf{z})|^2 \geq 1$, and thus also step (ii) of the algorithm is well-defined. The boundedness of $\|\mathbf{m}_h^i\|_{\mathbf{L}^\infty(\Omega)} = 1$ finally follows from normalization at the grid points and use of barycentric coordinates, cf. [Gol12, Lemma 3.2.6]. \square

5.3. Convergence analysis

In this section, we consider the convergence properties of the above algorithm and show that it indeed converges towards a weak solution of the coupled ELLG system. As usual, the proof is constructive in the sense that it also shows existence of weak solutions of ELLG.

Throughout, we assume that the spatial meshes \mathcal{T}_h are uniformly shape regular and satisfy the angle condition

$$\int_{\Omega} \nabla \eta_i \cdot \nabla \eta_j \leq 0 \quad \text{for all hat functions } \eta_i, \eta_j \in \mathcal{S}^1(\mathcal{T}_h) \text{ with } i \neq j. \quad (5.3.1)$$

As before, we denote by \mathcal{T}_h the triangulation of the domain Ω which is the restriction of the triangulation $\mathcal{T}_h^{\hat{\Omega}}$ of $\hat{\Omega}$.

We now formulate the main result of this chapter

Theorem 5.3.1. (a) Suppose that there exists a constant $C_\pi > 0$ which only depends on $|\Omega|$ such that the general energy contribution $\pi(\cdot)$ is uniformly bounded

$$\|\pi(\mathbf{n})\|_{\mathbf{L}^2(\Omega)}^2 \leq C_\pi, \quad \text{for all } \mathbf{n} \in \mathbf{L}^2(\Omega) \text{ with } \|\mathbf{n}\|_{\mathbf{L}^2(\Omega)}^2 \leq 1. \quad (5.3.2)$$

Moreover, for the initial data, we assume

$$\mathbf{m}_h^0 \rightharpoonup \mathbf{m}^0 \quad \text{weakly in } \mathbf{H}^1(\Omega), \quad \text{as well as} \quad \mathbf{H}_h^0 \rightharpoonup \mathbf{H}^0 \quad \text{weakly in } \mathbf{H}(\text{curl}, \hat{\Omega}). \quad (5.3.3)$$

Then, we have strong subconvergence of \mathbf{m}_{hk}^- towards some function \mathbf{m} in $\mathbf{L}^2(\hat{\Omega}_T)$.

(b) In addition to the above, we assume

$$\pi(\mathbf{m}_{hk}^-) \rightharpoonup \pi(\mathbf{m}) \quad \text{weakly subconvergent in } \mathbf{L}^2(\Omega_T). \quad (5.3.4)$$

Then, the computed FE solutions $(\mathbf{m}_{hk}, \mathbf{H}_{hk})$ admit subsequences which are weakly convergent in $\mathbf{H}^1(\Omega_T) \times (H^1(\mathbf{L}^2(\hat{\Omega})) \cap L^2(\mathbf{H}(\text{curl}, \hat{\Omega})))$ towards a weak solution (\mathbf{m}, \mathbf{H}) of ELLG. In particular, this yields existence of weak solutions and each accumulation point of $(\mathbf{m}_{hk}, \mathbf{H}_{hk})$ is a weak solution of ELLG in the sense of Definition 5.1.1.

Again, we have to show the three steps:

- (i) Boundedness of the discrete quantities and energies.
- (ii) Existence of weakly convergent subsequences.
- (iii) Identification of the limits with a weak solution of ELLG.

Step 1:

Lemma 5.3.2. *For all $k < \alpha/2$, the discrete quantities $(\mathbf{m}_h^j, \mathbf{v}_h^j, \mathbf{H}_h^j) \in \mathcal{M}_h \times \mathcal{K}_{\mathbf{m}_h^j} \times \mathcal{X}_h$ fulfill*

$$\begin{aligned} & \|\nabla \mathbf{m}_h^j\|_{\mathbf{L}^2(\Omega)}^2 + k \sum_{i=0}^{j-1} \|\mathbf{v}_h^i\|_{\mathbf{L}^2(\Omega)}^2 + (\theta - 1/2)k^2 \sum_{i=0}^{j-1} \|\nabla \mathbf{v}_h^i\|_{\mathbf{L}^2(\Omega)}^2 + \|\mathbf{H}_h^j\|_{\mathbf{L}^2(\widehat{\Omega})}^2 + \|\nabla \times \mathbf{H}_h^j\|_{\mathbf{L}^2(\widehat{\Omega})}^2 \\ & + \sum_{i=0}^{j-1} \|\mathbf{H}_h^{i+1} - \mathbf{H}_h^i\|_{\mathbf{L}^2(\widehat{\Omega})}^2 + k \sum_{i=0}^{j-1} \|d_t \mathbf{H}_h^{i+1}\|_{\mathbf{L}^2(\widehat{\Omega})}^2 + k \sum_{i=0}^{j-1} \|\nabla \times \mathbf{H}_h^{i+1}\|_{\mathbf{L}^2(\widehat{\Omega})}^2 \\ & + \sum_{i=0}^{j-1} \|\nabla \times (\mathbf{H}_h^{i+1} - \mathbf{H}_h^i)\|_{\mathbf{L}^2(\widehat{\Omega})}^2 \leq C_{27} \end{aligned} \quad (5.3.5)$$

for each $j = 0, \dots, N$ and some constant $C_{27} > 0$ that only depends on $|\widehat{\Omega}|$, on $|\Omega|$, as well as on C_π .

Proof. For the eddy-current equation (5.2.1b) in step (iii) of Algorithm 5.2.1, we choose $\boldsymbol{\zeta}_h = \mathbf{H}_h^{i+1}$ as test function and multiply by $\frac{k}{C_e}$ to get

$$\frac{\mu_0}{C_e}(\mathbf{H}_h^{i+1} - \mathbf{H}_h^i, \mathbf{H}_h^{i+1}) + \frac{k}{\sigma C_e} \|\nabla \times \mathbf{H}_h^{i+1}\|_{\mathbf{L}^2(\widehat{\Omega})}^2 = -\frac{\mu_0 k}{C_e}(\mathbf{v}_h^i, \mathbf{H}_h^i) + \frac{\mu_0 k}{C_e}(\mathbf{v}_h^i, \mathbf{H}_h^i - \mathbf{H}_h^{i+1}). \quad (5.3.6)$$

The LLG equation (5.2.1a) is tested with $\boldsymbol{\varphi}_h = \mathbf{v}_h^i \in \mathcal{K}_{\mathbf{m}_h^i}$. With $((\mathbf{m}_h^i \times \mathbf{v}_h^i), \mathbf{v}_h^i) = 0$, this yields after multiplication with $\frac{\mu_0 k}{C_e} > 0$

$$\frac{\mu_0 \alpha k}{C_e} \|\mathbf{v}_h^i\|_{\mathbf{L}^2(\Omega)}^2 + \mu_0 \theta k^2 \|\nabla \mathbf{v}_h^i\|_{\mathbf{L}^2(\Omega)}^2 = -\mu_0 k (\nabla \mathbf{m}_h^i, \nabla \mathbf{v}_h^i) + \frac{\mu_0 k}{C_e}(\mathbf{H}_h^i, \mathbf{v}_h^i) + \frac{\mu_0 k}{C_e}(\pi(\mathbf{m}_h^i), \mathbf{v}_h^i).$$

As in the previous chapters, the angle condition gives $\|\nabla \mathbf{m}_h^{i+1}\|_{\mathbf{L}^2(\Omega)}^2 \leq \|\nabla(\mathbf{m}_h^i + k\mathbf{v}_h^i)\|_{\mathbf{L}^2(\Omega)}^2$, whence

$$\begin{aligned} \frac{\mu_0}{2} \|\nabla \mathbf{m}_h^{i+1}\|_{\mathbf{L}^2(\Omega)}^2 & \leq \frac{\mu_0}{2} \|\nabla \mathbf{m}_h^i\|_{\mathbf{L}^2(\Omega)}^2 + \mu_0 k (\nabla \mathbf{m}_h^i, \nabla \mathbf{v}_h^i) + \frac{\mu_0 k^2}{2} \|\nabla \mathbf{v}_h^i\|_{\mathbf{L}^2(\Omega)}^2 \\ & \leq \frac{\mu_0}{2} \|\nabla \mathbf{m}_h^i\|_{\mathbf{L}^2(\Omega)}^2 - \mu_0 (\theta - 1/2) k^2 \|\nabla \mathbf{v}_h^i\|_{\mathbf{L}^2(\Omega)}^2 \\ & \quad - \frac{\alpha \mu_0 k}{C_e} \|\mathbf{v}_h^i\|_{\mathbf{L}^2(\Omega)}^2 + \frac{\mu_0 k}{C_e}(\mathbf{H}_h^i, \mathbf{v}_h^i) + \frac{\mu_0 k}{C_e}(\pi(\mathbf{m}_h^i), \mathbf{v}_h^i). \end{aligned} \quad (5.3.7)$$

Combining (5.3.6)–(5.3.7), we obtain

$$\begin{aligned} & \frac{\mu_0}{2} (\|\nabla \mathbf{m}_h^{i+1}\|_{\mathbf{L}^2(\Omega)}^2 - \|\nabla \mathbf{m}_h^i\|_{\mathbf{L}^2(\Omega)}^2) + \mu_0 (\theta - 1/2) k^2 \|\nabla \mathbf{v}_h^i\|_{\mathbf{L}^2(\Omega)}^2 + \frac{\alpha \mu_0 k}{C_e} \|\mathbf{v}_h^i\|_{\mathbf{L}^2(\Omega)}^2 \\ & \quad + \frac{\mu_0}{C_e}(\mathbf{H}_h^{i+1} - \mathbf{H}_h^i, \mathbf{H}_h^{i+1}) + \frac{k}{\sigma C_e} \|\nabla \times \mathbf{H}_h^{i+1}\|_{\mathbf{L}^2(\widehat{\Omega})}^2 \\ & \leq \frac{\mu_0 k}{C_e}(\mathbf{v}_h^i, \mathbf{H}_h^i - \mathbf{H}_h^{i+1}) + \frac{\mu_0 k}{C_e}(\pi(\mathbf{m}_h^i), \mathbf{v}_h^i). \end{aligned}$$

Summing up over $i = 0, \dots, j-1$, and exploiting Abel's summation from Lemma A.1.3 for the

\mathbf{H}_h^i scalar product as well as the inequalities of Young and Hölder, this yields for any $\varepsilon > 0$

$$\begin{aligned}
 & \frac{\mu_0}{2} \|\nabla \mathbf{m}_h^j\|_{L^2(\Omega)}^2 + (\theta - 1/2) \mu_0 k^2 \sum_{i=0}^{j-1} \|\nabla \mathbf{v}_h^i\|_{L^2(\Omega)}^2 + \frac{\alpha k \mu_0}{C_e} \sum_{i=0}^{j-1} \|\mathbf{v}_h^i\|_{L^2(\Omega)}^2 + \frac{\mu_0}{2C_e} \|\mathbf{H}_h^j\|_{L^2(\hat{\Omega})}^2 \\
 & + \frac{\mu_0}{2C_e} \sum_{i=0}^{j-1} \|\mathbf{H}_h^{i+1} - \mathbf{H}_h^i\|_{L^2(\hat{\Omega})}^2 + \frac{k}{\sigma C_e} \sum_{i=0}^{j-1} \|\nabla \times \mathbf{H}_h^{i+1}\|_{L^2(\hat{\Omega})}^2 \\
 & \leq \frac{\mu_0 k}{2\varepsilon C_e} \sum_{i=0}^{j-1} (\|\pi(\mathbf{m}_h^i)\|_{L^2(\Omega)}^2 + \|\mathbf{H}_h^{i+1} - \mathbf{H}_h^i\|_{L^2(\hat{\Omega})}^2) + \frac{\varepsilon \mu_0 k}{C_e} \sum_{i=0}^{j-1} \|\mathbf{v}_h^i\|_{L^2(\Omega)}^2 \\
 & + \frac{\mu_0}{2} (\|\nabla \mathbf{m}_h^0\|_{L^2(\Omega)}^2 + \frac{1}{C_e} \|\mathbf{H}_h^0\|_{L^2(\hat{\Omega})}^2).
 \end{aligned}$$

With the notation $C_{\mathbf{v}}^k := \frac{2\mu_0 k}{C_e}(\alpha - \varepsilon)$, and $C_{\mathbf{H}}^k := \frac{\mu_0}{C_e}(1 - \frac{k}{2\varepsilon})$, this yields

$$\begin{aligned}
 & \mu_0 \|\nabla \mathbf{m}_h^j\|_{L^2(\Omega)}^2 + 2(\theta - 1/2) \mu_0 k^2 \sum_{i=0}^{j-1} \|\nabla \mathbf{v}_h^i\|_{L^2(\Omega)}^2 + C_{\mathbf{v}}^k \sum_{i=0}^{j-1} \|\mathbf{v}_h^i\|_{L^2(\Omega)}^2 \\
 & + \frac{\mu_0}{C_e} \|\mathbf{H}_h^j\|_{L^2(\hat{\Omega})}^2 + C_{\mathbf{H}}^k \sum_{i=0}^{j-1} \|\mathbf{H}_h^{i+1} - \mathbf{H}_h^i\|_{L^2(\hat{\Omega})}^2 + \frac{2k}{\sigma C_e} \sum_{i=0}^{j-1} \|\nabla \times \mathbf{H}_h^{i+1}\|_{L^2(\hat{\Omega})}^2 \\
 & \leq \frac{\mu_0 k}{2\varepsilon C_e} \sum_{i=0}^{j-1} \|\pi(\mathbf{m}_h^i)\|_{L^2(\Omega)}^2 + \mu_0 \|\nabla \mathbf{m}_h^0\|_{L^2(\Omega)}^2 + \frac{\mu_0}{C_e} \|\mathbf{H}_h^0\|_{L^2(\hat{\Omega})}^2.
 \end{aligned} \tag{5.3.8}$$

Next, we test with $\zeta_h = \mathbf{d}_t \mathbf{H}_h^{i+1}$ in (5.2.1b) to obtain after multiplication by $2k$

$$2\mu_0 k \|\mathbf{d}_t \mathbf{H}_h^{i+1}\|_{L^2(\hat{\Omega})}^2 + 2\sigma^{-1} (\nabla \times \mathbf{H}_h^{i+1}, \nabla \times (\mathbf{H}_h^{i+1} - \mathbf{H}_h^i)) = -2\mu_0 k (\mathbf{v}_h^i, \mathbf{d}_t \mathbf{H}_h^{i+1}).$$

The right-hand side can further be estimated by

$$-2\mu_0 k (\mathbf{v}_h^i, \mathbf{d}_t \mathbf{H}_h^{i+1}) \leq \mu_0 k \|\mathbf{v}_h^i\|_{L^2(\Omega)}^2 + \mu_0 k \|\mathbf{d}_t \mathbf{H}_h^{i+1}\|_{L^2(\hat{\Omega})}^2.$$

Abel's summation thus yields

$$\begin{aligned}
 & \mu_0 k \sum_{i=0}^{j-1} \|\mathbf{d}_t \mathbf{H}_h^{i+1}\|_{L^2(\hat{\Omega})}^2 + \sigma^{-1} \|\nabla \times \mathbf{H}_h^j\|_{L^2(\hat{\Omega})}^2 + \sigma^{-1} \sum_{i=0}^{j-1} \|\nabla \times (\mathbf{H}_h^{i+1} - \mathbf{H}_h^i)\|_{L^2(\hat{\Omega})}^2 \\
 & \leq \sigma^{-1} \|\nabla \times \mathbf{H}_h^0\|_{L^2(\hat{\Omega})}^2 + \mu_0 k \sum_{i=0}^{j-1} \|\mathbf{v}_h^i\|_{L^2(\Omega)}^2.
 \end{aligned} \tag{5.3.9}$$

Finally, we weight (5.3.9) by α/C_e and add (5.3.8). The last term on the right-hand side of (5.3.9) can be absorbed by the corresponding term on the left-hand side of (5.3.8). For the desired result, we have to ensure that there is a choice of ε such that the $C_{\mathbf{v}}^k - \mu_0 k \alpha / C_e$, and $C_{\mathbf{H}}^k$ are positive, i.e. $(\alpha - 2\varepsilon) > 0$ and $(1 - \frac{k}{\varepsilon}) > 0$. This is, however, equivalent to $k < \varepsilon < \alpha/2$. From the assumed convergence of the initial data (5.3.3) as well as (5.3.2), we know that the right-hand side is uniformly bounded, which concludes the proof. \square

Next, we conclude the existence of weakly convergent subsequences.

Step 2:

Lemma 5.3.3. *There exist functions $(\mathbf{m}, \mathbf{H}) \in \mathbf{H}^1(\Omega_T) \times (H^1(\mathbf{L}^2) \cap L^2(\mathbf{H}(\text{curl})))$, with $|\mathbf{m}| = 1$ almost everywhere in Ω such that up to extraction of a subsequence, there holds*

$$\mathbf{m}_{hk} \xrightarrow{\text{sub}} \mathbf{m} \text{ in } \mathbf{H}^1(\Omega_T), \quad (5.3.10a)$$

$$\mathbf{m}_{hk}, \mathbf{m}_{hk}^\pm \xrightarrow{\text{sub}} \mathbf{m} \text{ in } L^2(\mathbf{H}^1(\Omega)), \quad (5.3.10b)$$

$$\mathbf{m}_{hk}, \mathbf{m}_{hk}^\pm \xrightarrow{\text{sub}} \mathbf{m} \text{ in } \mathbf{L}^2(\Omega_T), \quad (5.3.10c)$$

$$\mathbf{H}_{hk} \xrightarrow{\text{sub}} \mathbf{H} \text{ in } H^1(\mathbf{L}^2(\widehat{\Omega})) \cap L^2(\mathbf{H}(\text{curl}, \widehat{\Omega})), \quad (5.3.10d)$$

$$\mathbf{H}_{hk}^\pm \xrightarrow{\text{sub}} \mathbf{H} \text{ in } L^2(\mathbf{H}(\text{curl}, \widehat{\Omega})), \quad (5.3.10e)$$

$$\mathbf{v}_{hk}^- \xrightarrow{\text{sub}} \mathbf{m}_t \text{ in } \mathbf{L}^2(\Omega_T). \quad (5.3.10f)$$

Here, the subsequences are constructed successively, i.e. for arbitrary mesh-sizes $h \rightarrow 0$, and time-step sizes $k \rightarrow 0$ there exist subindices h_ℓ, k_ℓ for which the above convergence properties (5.3.10) are satisfied simultaneously.

Proof. Analogously to Lemma 4.2.9, the proof of (5.3.10a)–(5.3.10e) directly follows from the boundedness of the discrete quantities from Lemma 5.3.2 in combination with the continuous inclusions $\mathbf{H}^1(\Omega_T) \subseteq L^2(\mathbf{H}^1(\Omega)) \subseteq \mathbf{L}^2(\Omega_T)$ and $H^1(\mathbf{L}^2(\widehat{\Omega})) \cap L^2(\mathbf{H}(\text{curl}, \widehat{\Omega})) \subseteq \mathbf{L}^2(\widehat{\Omega}_T)$. As in Lemma 2.3.6, we get (5.3.10a). The length constraint of the limiting function \mathbf{m} finally follows by direct calculation. \square

Now, we have collected all ingredients for the proof of our main theorem.

Step 3:

Proof of Theorem 5.3.1. Let $\varphi \in C^\infty(\overline{\Omega_T})$ and $\zeta \in C^\infty(\widehat{\Omega}_T)$ be arbitrary. We define test functions by $(\phi_h, \zeta_h)(t, \cdot) := (\mathcal{I}_h(\mathbf{m}_{hk}^- \times \varphi), \mathcal{I}_{\mathcal{X}_h} \zeta)(t, \cdot)$. Obviously, for any $t \in [t_j, t_{j+1})$, we have $(\phi_h, \zeta_h) \in (\mathcal{K}_{\mathbf{m}_h^j}, \mathcal{X}_h)$. Equation (5.2.1a) of Algorithm 5.2.1 now implies

$$\begin{aligned} \alpha \int_0^T (\mathbf{v}_{hk}^-, \phi_h) + \int_0^T ((\mathbf{m}_{hk}^- \times \mathbf{v}_{hk}^-), \phi_h) &= -C_e \int_0^T (\nabla(\mathbf{m}_{hk}^- + \theta k \mathbf{v}_{hk}^-), \nabla \phi_h) \\ &\quad + \int_0^T (\mathbf{H}_{hk}^-, \phi_h) + \int_0^T (\pi(\mathbf{m}_{hk}^-), \phi_h) \end{aligned}$$

As in Chapter 2, passing to the limit and using the strong $\mathbf{L}^2(\Omega_T)$ -convergence of $(\mathbf{m}_{hk}^- \times \varphi)$ towards $(\mathbf{m} \times \varphi)$, in combination with Lemma 5.3.3 and the weak convergence property (5.3.4) of $\pi(\mathbf{m}_{hk}^-)$, this yields

$$\begin{aligned} \int_0^T ((\alpha \mathbf{m}_t + \mathbf{m} \times \mathbf{m}_t), (\mathbf{m} \times \varphi)) &= -C_e \int_0^T (\nabla \mathbf{m}, \nabla(\mathbf{m} \times \varphi)) \\ &\quad + \int_0^T (\mathbf{H}, (\mathbf{m} \times \varphi)) + \int_0^T (\pi(\mathbf{m}), (\mathbf{m} \times \varphi)) \end{aligned}$$

Exploiting basic properties of the cross product, we conclude (4.1.2). The equality $\mathbf{m}(0, \cdot) = \mathbf{m}^0$ in the trace sense follows from the weak convergence $\mathbf{m}_{hk} \rightharpoonup \mathbf{m}$ in $\mathbf{H}^1(\Omega_T)$. Analogously, we get $\mathbf{H}(0, \cdot) = \mathbf{H}^0$ in the trace sense. For the eddy-current part, (5.2.1b) implies

$$\mu_0 \int_0^T ((\mathbf{H}_{hk})_t, \zeta_h) + \sigma^{-1} \int_0^T (\nabla \times \mathbf{H}_{hk}^+, \nabla \times \zeta_h) = -\mu_0 \int_0^T (\mathbf{v}_{hk}^-, \zeta_h).$$

The convergence properties from Lemma 6.2.11 in combination with the properties of the interpolation operator $\mathcal{I}_{\mathcal{X}_h}$ from (4.2.1) now reveal

$$\begin{aligned} \int_0^T ((\mathbf{H}_{hk})_t, \boldsymbol{\zeta}_h) &\longrightarrow \int_0^T (\mathbf{H}_t, \boldsymbol{\zeta}), \\ \int_0^T (\nabla \times \mathbf{H}_{hk}^+, \nabla \times \boldsymbol{\zeta}_h) &\longrightarrow \int_0^T (\nabla \times \mathbf{H}, \nabla \times \boldsymbol{\zeta}), \quad \text{and} \\ \int_0^T (\mathbf{v}_{hk}^-, \boldsymbol{\zeta}_h) &\longrightarrow (\mathbf{m}_t, \boldsymbol{\zeta}), \end{aligned}$$

whence (4.1.3).

It remains to show the energy estimate (5.1.4) which follows from the discrete energy estimate (5.3.5) together with weak lower semi-continuity. This yields the desired result. \square

5.3.1. Improved energy estimate

In the spirit of the Sections 2.4 and 4.2.3, the energy estimate (5.1.4) for the ELLG problem can also be refined for many physically relevant cases. To that end, we define the energy term

$$\mathcal{E}(t) := \mathcal{E}(\mathbf{m}(t), \mathbf{H}(t)) \quad (5.3.11)$$

$$= \mu_0 \|\nabla \mathbf{m}(t)\|_{\mathbf{L}^2(\Omega)}^2 + \frac{\mu_0}{C_e} \|\mathbf{H}(t)\|_{\mathbf{L}^2(\hat{\Omega})}^2 + \frac{\alpha}{C_e \sigma} \|\nabla \times \mathbf{H}(t)\|_{\mathbf{L}^2(\hat{\Omega})}^2 - \frac{\mu_0}{C_e} (\boldsymbol{\pi}(\mathbf{m}(t)), \mathbf{m}(t)) \quad (5.3.12)$$

and the discrete version

$$\mathcal{E}(\mathbf{m}_h^j, \mathbf{H}_h^j) \quad (5.3.13)$$

$$:= \mu_0 \|\nabla \mathbf{m}_h^j\|_{\mathbf{L}^2(\Omega)}^2 + \frac{\mu_0}{C_e} \|\mathbf{H}_h^j\|_{\mathbf{L}^2(\hat{\Omega})}^2 + \frac{\alpha}{C_e \sigma} \|\nabla \times \mathbf{H}_h^j\|_{\mathbf{L}^2(\hat{\Omega})}^2 - \frac{\mu_0}{C_e} (\boldsymbol{\pi}(\mathbf{m}_h^j), \mathbf{m}_h^j). \quad (5.3.14)$$

With these quantities, we derive a result that is in analogy to the MLLG case.

Proposition 5.3.4 (Improved energy estimate for Algorithm 5.2.1). *Let $\boldsymbol{\pi}(\cdot)$ be uniformly Lipschitz continuous and bounded in $\mathbf{L}^4(\Omega)$, i.e. $\|\boldsymbol{\pi}(\mathbf{n})\|_{\mathbf{L}^4(\Omega)} \leq C_{28}$ for all $\mathbf{n} \in \mathbf{L}^2(\Omega)$ with $|\mathbf{n}| \leq 1$ almost everywhere in Ω . Here, C_{28} denotes some uniform constant which only depends on Ω . Let further $\boldsymbol{\pi}(\cdot)$ be self-adjoint. Then, for the output of Algorithm (4.2.2), we have the energy decay estimate*

$$\mathcal{E}(t') + \frac{\mu_0}{C_e} (\alpha - 2\varepsilon) \|\mathbf{m}_t\|_{\mathbf{L}^2(\Omega_{t'})}^2 + \frac{\mu_0 \alpha}{C_e} \|\mathbf{H}_t\|_{\mathbf{L}^2(\hat{\Omega}_{t'})}^2 + \frac{2}{\sigma C_e} \|\nabla \times \mathbf{H}\|_{\mathbf{L}^2(\hat{\Omega}_{t'})}^2 \leq \mathcal{E}(0), \quad (5.3.15)$$

for almost every $t' \in [0, T]$ and any $\varepsilon > 0$.

Proof. The proof follows the same lines as the ones in Section 4.2.3 and we only give the relevant changes here. As in the proof of Lemma 5.3.2, we have

$$\begin{aligned} &\frac{\mu_0}{2} (\|\nabla \mathbf{m}_h^{i+1}\|_{\mathbf{L}^2(\Omega)}^2 - \|\nabla \mathbf{m}_h^i\|_{\mathbf{L}^2(\Omega)}^2) + \mu_0 (\theta - 1/2) k^2 \|\nabla \mathbf{v}_h^i\|_{\mathbf{L}^2(\Omega)}^2 + \frac{\alpha \mu_0 k}{C_e} \|\mathbf{v}_h^i\|_{\mathbf{L}^2(\Omega)}^2 \\ &\quad + \frac{\mu_0}{C_e} (\mathbf{H}_h^{i+1} - \mathbf{H}_h^i, \mathbf{H}_h^{i+1}) + \frac{k}{\sigma C_e} \|\nabla \times \mathbf{H}_h^{i+1}\|_{\mathbf{L}^2(\hat{\Omega})}^2 \\ &\leq \frac{\mu_0 k}{C_e} (\mathbf{v}_h^i, \mathbf{H}_h^i - \mathbf{H}_h^{i+1}) + \frac{\mu_0 k}{C_e} (\boldsymbol{\pi}(\mathbf{m}_h^i), \mathbf{v}_h^i) \end{aligned}$$

and thus

$$\begin{aligned}
& \mathcal{E}(\mathbf{m}_h^{i+1}, \mathbf{H}_h^{i+1}) - \mathcal{E}(\mathbf{m}_h^i, \mathbf{H}_h^i) \\
&= \mu_0 \|\nabla \mathbf{m}_h^{i+1}\|_{L^2(\Omega)}^2 + \frac{\mu_0}{C_e} \|\mathbf{H}_h^{i+1}\|_{L^2(\hat{\Omega})}^2 + \frac{\alpha}{C_e \sigma} \|\nabla \times \mathbf{H}_h^{i+1}\|_{L^2(\hat{\Omega})}^2 - \frac{\mu_0}{C_e} (\pi(\mathbf{m}_h^{i+1}), \mathbf{m}_h^{i+1}) \\
&- \mu_0 \|\nabla \mathbf{m}_h^i\|_{L^2(\Omega)}^2 + \frac{\mu_0}{C_e} \|\mathbf{H}_h^i\|_{L^2(\hat{\Omega})}^2 + \frac{\alpha}{C_e \sigma} \|\nabla \times \mathbf{H}_h^i\|_{L^2(\hat{\Omega})}^2 - \frac{\mu_0}{C_e} (\pi(\mathbf{m}_h^i), \mathbf{m}_h^i) \\
&\leq -2\mu_0(\theta - 1/2)k^2 \|\nabla \mathbf{v}_h^i\|_{L^2(\Omega)}^2 - \frac{2\alpha\mu_0 k}{C_e} \|\mathbf{v}_h^i\|_{L^2(\Omega)}^2 - \frac{2k}{\sigma C_e} \|\nabla \times \mathbf{H}_h^{i+1}\|_{L^2(\hat{\Omega})}^2 \\
&- \frac{2\mu_0}{C_e} (\mathbf{H}_h^{i+1} - \mathbf{H}_h^i, \mathbf{H}_h^{i+1}) + \frac{2\mu_0 k}{C_e} (\mathbf{v}_h^i, \mathbf{H}_h^i - \mathbf{H}_h^{i+1}) + \frac{2\mu_0 k}{C_e} (\pi(\mathbf{m}_h^i), \mathbf{v}_h^i) \\
&+ \frac{\mu_0}{C_e} \|\mathbf{H}_h^{i+1}\|_{L^2(\hat{\Omega})}^2 + \frac{\alpha}{C_e \sigma} \|\nabla \times \mathbf{H}_h^{i+1}\|_{L^2(\hat{\Omega})}^2 - \frac{\mu_0}{C_e} (\pi(\mathbf{m}_h^{i+1}), \mathbf{m}_h^{i+1}) \\
&- \frac{\mu_0}{C_e} \|\mathbf{H}_h^i\|_{L^2(\hat{\Omega})}^2 - \frac{\alpha}{C_e \sigma} \|\nabla \times \mathbf{H}_h^i\|_{L^2(\hat{\Omega})}^2 + \frac{\mu_0}{C_e} (\pi(\mathbf{m}_h^i), \mathbf{m}_h^i).
\end{aligned}$$

Summing up over $i = 0, \dots, j-1$, we thus get analogously to Section 4.2.3.

$$\begin{aligned}
& \mathcal{E}(\mathbf{m}_h^j, \mathbf{H}_h^j) - \mathcal{E}(\mathbf{m}_h^0, \mathbf{H}_h^0) + \frac{2\alpha\mu_0 k}{C_e} \sum_{i=0}^{j-1} \|\mathbf{v}_h^i\|_{L^2(\Omega)}^2 + \frac{2k}{\sigma C_e} \sum_{i=0}^{j-1} \|\nabla \times \mathbf{H}_h^{i+1}\|_{L^2(\hat{\Omega})}^2 \\
&\leq -\frac{\mu_0}{C_e} \sum_{i=0}^{j-1} \|\mathbf{H}_h^{i+1} - \mathbf{H}_h^i\|_{L^2(\hat{\Omega})}^2 + \frac{2\mu_0 k}{C_e} \sum_{i=0}^{j-1} (\mathbf{H}_h^i - \mathbf{H}_h^{i+1}, \mathbf{v}_h^i) \\
&+ \frac{2\mu_0 k}{C_e} \sum_{i=0}^{j-1} (\pi(\mathbf{m}_h^i), \mathbf{v}_h^i) - \frac{\mu_0}{C_e} \sum_{i=0}^{j-1} (\pi(\mathbf{m}_h^{i+1}), \mathbf{m}_h^{i+1}) + \frac{\mu_0}{C_e} \sum_{i=0}^{j-1} (\pi(\mathbf{m}_h^i), \mathbf{m}_h^i) \\
&+ \frac{\alpha}{C_e \sigma} \|\nabla \times \mathbf{H}_h^j\|_{L^2(\hat{\Omega})}^2 - \frac{\alpha}{C_e \sigma} \|\nabla \times \mathbf{H}_h^0\|_{L^2(\hat{\Omega})}^2.
\end{aligned}$$

Here, we employed Abel's summation by parts from Lemma A.1.3 and $\theta \in (1/2, 1]$. The first two terms on the right hand side are estimated as in (4.2.23) by

$$-\frac{\mu_0}{C_e} \sum_{i=0}^{j-1} \|\mathbf{H}_h^{i+1} - \mathbf{H}_h^i\|_{L^2(\hat{\Omega})}^2 + \frac{2\mu_0 k}{C_e} \sum_{i=0}^{j-1} (\mathbf{H}_h^i - \mathbf{H}_h^{i+1}, \mathbf{v}_h^i) \leq \frac{2\varepsilon\mu_0 k}{C_e} \sum_{i=0}^{j-1} \|\mathbf{v}_h^i\|_{L^2(\Omega)}^2.$$

Next, as in the proof of Lemma 5.3.2, we have

$$\begin{aligned}
& \frac{\mu_0 \alpha k}{C_e} \sum_{i=0}^{j-1} \|\mathbf{d}_t \mathbf{H}_h^{i+1}\|_{L^2(\hat{\Omega})}^2 + \frac{\alpha}{\sigma C_e} \|\nabla \times \mathbf{H}_h^j\|_{L^2(\hat{\Omega})}^2 + \frac{\alpha}{\sigma C_e} \sum_{i=0}^{j-1} \|\nabla \times (\mathbf{H}_h^{i+1} - \mathbf{H}_h^i)\|_{L^2(\hat{\Omega})}^2 \\
&\leq \frac{\alpha}{\sigma C_e} \|\nabla \times \mathbf{H}_h^0\|_{L^2(\hat{\Omega})}^2 + \frac{\alpha\mu_0 k}{C_e} \sum_{i=0}^{j-1} \|\mathbf{v}_h^i\|_{L^2(\Omega)}^2,
\end{aligned}$$

and the combination of the last estimates therefore yields

$$\begin{aligned}
& \mathcal{E}(\mathbf{m}_h^j, \mathbf{H}_h^j) - \mathcal{E}(\mathbf{m}_h^0, \mathbf{H}_h^0) + \frac{\mu_0 k}{C_e} (\alpha - 2\varepsilon) \sum_{i=0}^{j-1} \|\mathbf{v}_h^i\|_{L^2(\Omega)}^2 + \frac{2k}{\sigma C_e} \sum_{i=0}^{j-1} \|\nabla \times \mathbf{H}_h^{i+1}\|_{L^2(\hat{\Omega})}^2 \\
& + \frac{\mu_0 \alpha k}{C_e} \sum_{i=0}^{j-1} \|\mathbf{d}_t \mathbf{H}_h^{i+1}\|_{L^2(\hat{\Omega})}^2 \\
& \leq \frac{2\mu_0 k}{C_e} \sum_{i=0}^{j-1} (\pi(\mathbf{m}_h^i), \mathbf{v}_h^i) - \frac{\mu_0}{C_e} \sum_{i=0}^{j-1} (\pi(\mathbf{m}_h^{i+1}), \mathbf{m}_h^{i+1}) + \frac{\mu_0}{C_e} \sum_{i=0}^{j-1} (\pi(\mathbf{m}_h^i), \mathbf{m}_h^i).
\end{aligned}$$

The remainder of the proof now follows verbatim to the one of proposition 4.2.10. \square

5.4. Numerical experiments

We conclude the chapters on coupling of LLG with variants of the Maxwell equations with some numerical experiments. Before we come to the actual investigation of those, however, we like to comment on some implementational details. Throughout this section, we used Algorithm 5.2.1, i.e. we implemented the coupling of LLG to the eddy-current equation where the algorithm fully decouples both equations. For numerical experiments including the full Maxwell system, i.e. Algorithm 4.2.1 or Algorithm 4.2.2, we refer to [BPP13]. There, also a comparison to the midpoint scheme is discussed.

As mentioned above, we used lowest order edge elements to discretize the eddy-current equation. For Nédélec elements, the basis functions take the form

$$\Phi_k = \lambda_i \nabla \lambda_j - \lambda_j \nabla \lambda_i,$$

cf. [Néd80, Mon08]. Here, Φ_k denotes the k -th edge given by $[i, j]$ and λ_i, λ_j are the barycentric coordinates, i.e. the P1-hat functions of the corresponding nodes of the tetrahedral mesh. Note, that the orientation of the edge is fixed once and for all at the beginning. If the system matrices are to be assembled elementwise, one thus has to ensure that the orientation is the same for each adjacent element.

Straightforward calculations easily show

$$\nabla \times \Phi_k = 2 \nabla \lambda_i \times \nabla \lambda_j$$

which can directly be exploited for the curl-curl matrix to compute the integral

$$\int_T \nabla \times \Phi_k \cdot \nabla \times \Phi_\ell.$$

As for the mass matrix, we need to compute the entry

$$\int_T \Phi_i \cdot \Phi_j = \int_T (\lambda_{i_1} \lambda_{j_1} \nabla \lambda_{i_2} \nabla \lambda_{j_2} - \lambda_{i_1} \lambda_{j_2} \nabla \lambda_{i_2} \nabla \lambda_{j_1} - \lambda_{i_2} \lambda_{j_1} \nabla \lambda_{i_1} \nabla \lambda_{j_2} + \lambda_{i_2} \lambda_{j_2} \nabla \lambda_{i_1} \nabla \lambda_{j_1}),$$

where $i = [i_1, i_2]$ and $j = [j_1, j_2]$. To that end, we exploit

$$\int_T \lambda_i \lambda_j = (1 + (i == j)) |T| / 20,$$

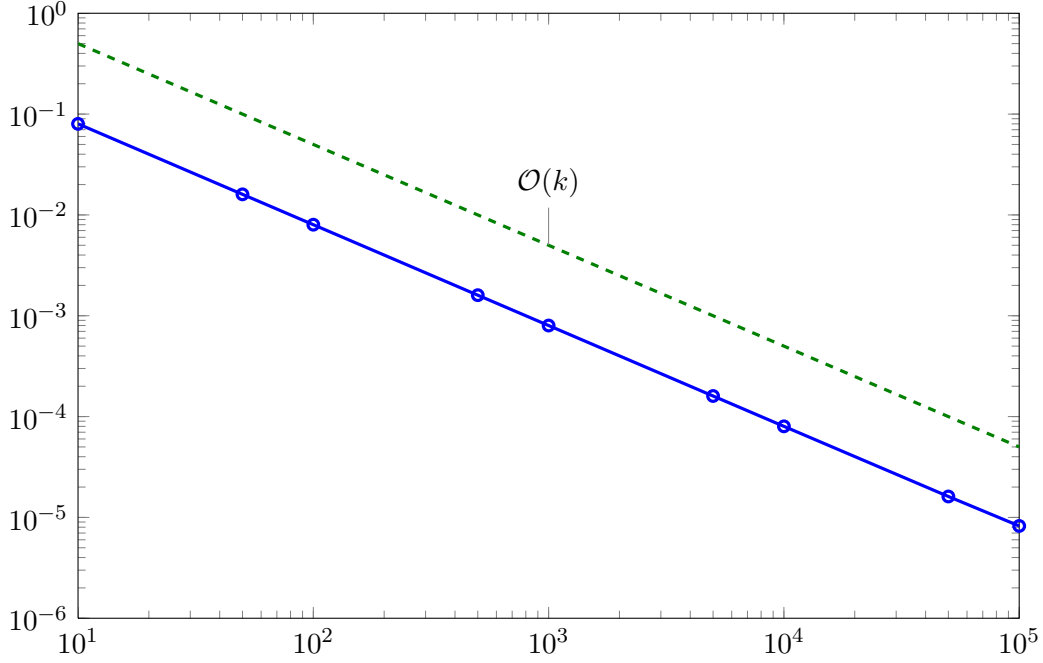


Figure 5.1.: Decay of $\text{Err}(\mathbf{u})$ for uniform refinement in time with $P = 320$ spatial elements and $N \in \{10, 50, 100, 500, 1000, 5000, 10000, 50000, 100000\}$. As expected, we observe linear behaviour.

cf. [Che08], and compute the scalar product of the corresponding gradients directly. For more details, the interested reader is referred to [Che08] and the very comprehensive open source *iFEM* package [Web1] which was also helpful for our implementation. Some details on the implementation including the coupling to LLG can also be found in [LT13].

Finally, the transfer matrix T with

$$T_{ij} = \int_{\hat{\Omega}} \Phi_i \cdot \varphi_j$$

needs to be computed in order to realize the coupling terms. Note here, that the basis functions for the edge elements are already three-dimensional, and one thus also needs to use the three-dimensional P1-hat functions

$$\begin{pmatrix} \varphi \\ 0 \\ 0 \end{pmatrix}, \begin{pmatrix} 0 \\ \varphi \\ 0 \end{pmatrix}, \text{ and } \begin{pmatrix} 0 \\ 0 \\ \varphi \end{pmatrix}.$$

The transfer matrix T is thus a block-full matrix and for each element $E \in \mathcal{T}_h$, the corresponding element matrix T_E is of the size 6×12 . Again, the integral for each entry can directly be computed.

5.4.1. General performance

In this first series of experiments, we aim to test the performance as well as the implementation of our Nedélec scheme for the discretization of the eddy-current equation. To that end, we

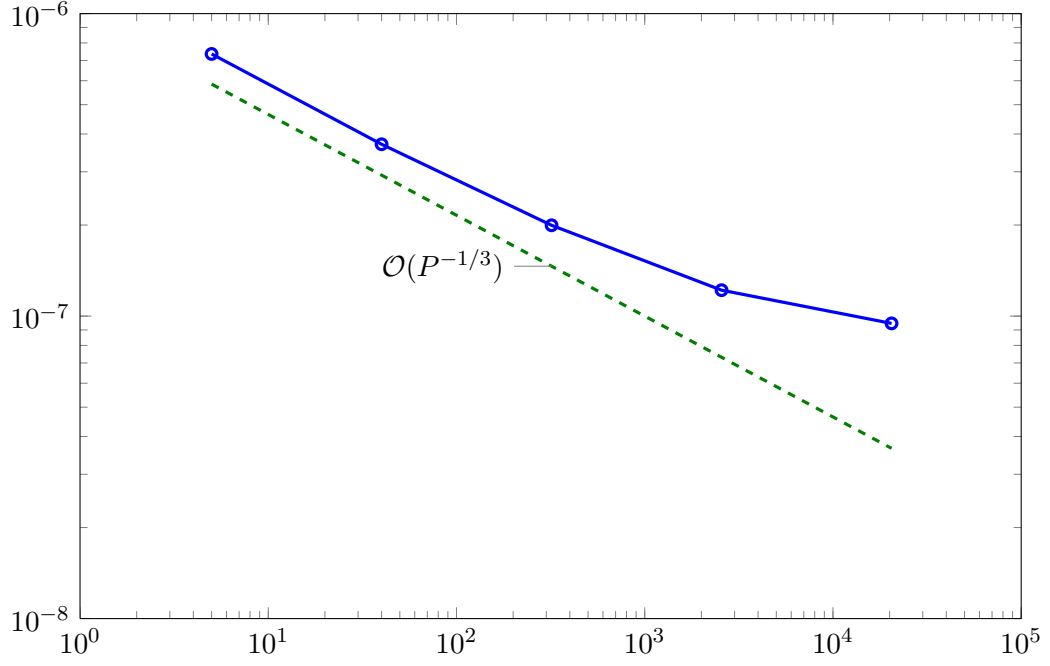


Figure 5.2.: Decay of $\text{Err}(\mathbf{u})$ for uniform refinement in space with $N = 1000$ time steps and $P \in \{5, 40, 320, 2560, 20480\}$. We observe linear decay in the beginning which is then dominated by the temporal error.

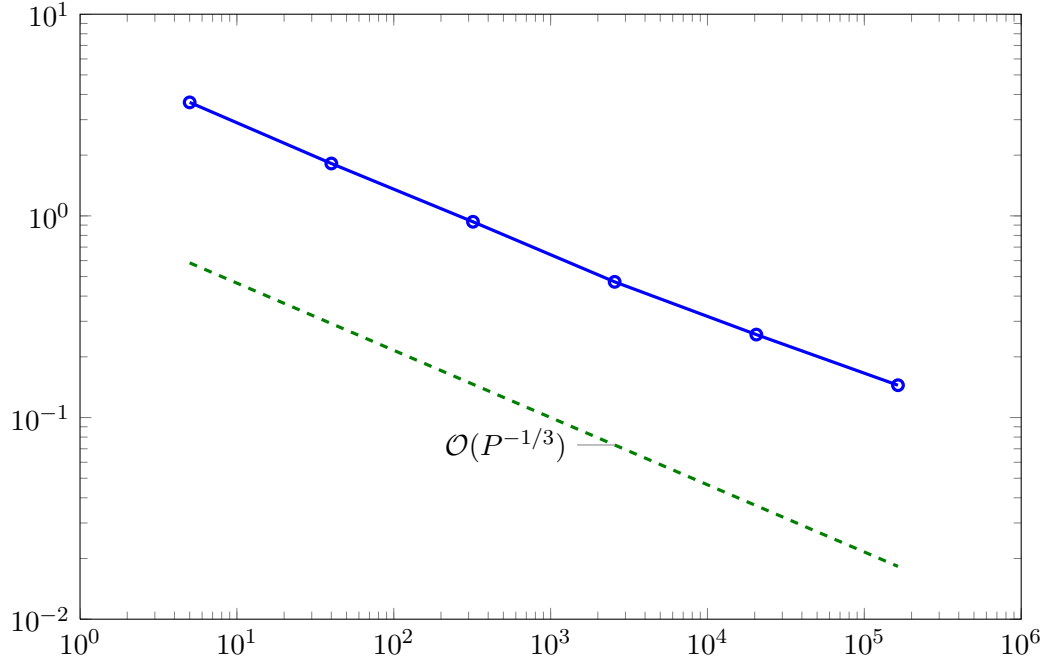


Figure 5.3.: Decay of $\text{Err}(\mathbf{u})$ for stationary problem and uniform refinement with $P \in \{5, 40, 320, 2560, 20480, 163840\}$. As expected, we observe linear decay of the error.

prescribe an exact solution and investigate the convergence rate with respect to time and space. For given

$$\mathbf{u} = \begin{pmatrix} u_1 \\ u_2 \\ u_3 \end{pmatrix} = \begin{pmatrix} at \cos(bx) \\ -at \sin(by) \\ at(2bz + 1) \end{pmatrix},$$

with varying parameters a and b , we compute \mathbf{f} such that there holds

$$\mathbf{u}_t + \nabla \times (\nabla \times \mathbf{u}) = \mathbf{f}.$$

Note that \mathbf{u} is chosen in such a way that $\nabla \times \mathbf{u} = 0$ whence the boundary condition $(\nabla \times \mathbf{u}) \times \mathbf{n} = 0$ is automatically fulfilled. As initial condition \mathbf{u}^0 serves the temporal trace of the prescribed solution, i.e.

$$\mathbf{u}^0 = \mathbf{u}(0) = \begin{pmatrix} 0 \\ 0 \\ 0 \end{pmatrix}.$$

Convergence in time

In a first experiment, we consider the temporal convergence rate of our scheme. On the cube $\widehat{\Omega} = [-1, 1]^3$, we solve the above equation for the time interval $(0, 2)$. To minimize the influence of the spatial error, we choose $a = 0.1$ and $b = 0.00001$. We carry out the computations on a mesh with $P = 320$ tetrahedra and varying amount of time steps $N \in \{10, 50, 100, 500, 1000, 5000, 10000, 50000, 100000\}$. In each case we compute the error as

$$\text{Err}(\mathbf{u}) = \max_j \|\mathbf{u}_h^j - \mathbf{u}(t_j)\|_{L^2(\widehat{\Omega})} + \|\nabla \times (\mathbf{u}_h^j - \mathbf{u}(t_j))\|_{L^2(\widehat{\Omega})}.$$

The results are given in Table 5.1 and visualized in Figure 5.1. As expected, we observe linear decay of the error as the amount of time steps increases.

	Timesteps								
	10	50	100	500	1000	5000	10000	50000	100000
Err(\mathbf{u})	0.08	0.016	0.008	0.0016	8.0003e-4	1.6004e-4	8.0050e-5	1.6130e-5	8.2292e-6

Table 5.1.: Err(\mathbf{u}) for varying time steps.

Convergence in space

Next, we investigate the convergence behaviour of our scheme as the spatial mesh parameter h tends to zero. To that end, we aim to minimize the effect of the temporal error and choose $a = 0.001$ and $b = 0.00001$. As computational domain, we choose $\widehat{\Omega} = [-1, 1]^3$ and $(0, 1)$ for the time interval. Throughout the computations, we choose $k = 0.001$, i.e. we make 1000 time steps. The error for varying amount of spatial elements $P \in \{5, 40, 320, 2560, 20480\}$ is given in Table 5.2 and visualized in Figure 5.2. As before, we observe linear decay of the error in

	Spatial elements				
	5	40	320	2560	20480
Err(\mathbf{u})	0.7356e-6	0.37e-6	0.1997e-6	0.1218e-6	0.0946e-6

Table 5.2.: Err(\mathbf{u}) for varying amount of spatial elements.

the beginning. As the spatial mesh gets finer, however, the temporal error becomes more and more dominant and the convergence rate decreases.

Finally, we completely neglect the temporal error and consider the stationary problem

$$\mathbf{u} + \nabla \times (\nabla \times \mathbf{u}) = \mathbf{f}$$

on $[-1, 1]^3$. We choose

$$\mathbf{u} = \begin{pmatrix} u_1 \\ u_2 \\ u_3 \end{pmatrix} = \begin{pmatrix} \cos(x) \\ -\sin(y) \\ 2z + 1 \end{pmatrix} = \mathbf{f}.$$

The values of the error for this experiment are given in Table 5.3 and the results are visualized in Figure 5.3. This time, we observe linear decay of the spatial error.

	Spatial elements					
	5	40	320	2560	20480	163840
Err(\mathbf{u})	3.6543	1.8184	0.9348	0.4708	0.2579	0.1446

Table 5.3.: Err(\mathbf{u}) for varying amount of spatial elements.

Altogether, our numerical results concur with those from theory.

5.4.2. Finite time blowup in 3D

In the second experiment, we investigate the full ELLG System (5.1.1) on the shifted unit cube $\Omega = \widehat{\Omega} = [-0.5, 0.5]^3$ and the time interval $(0, 0.1)$. We consider a problem similar to the one treated in [BBP08, LT12]. As initial condition, we choose

$$\mathbf{m}^0(\mathbf{x}) := \begin{cases} (0, 0, -1) & |\mathbf{x}^*| \geq 1/2, \\ (2\mathbf{x}^*A, A^2 - |\mathbf{x}^*|^2)/(A^2 + |\mathbf{x}^*|^2) & |\mathbf{x}^*| \leq 1/2, \end{cases}$$

with $\mathbf{x}^* = (x_1, x_2)$ and $A = (1 - 2|\mathbf{x}^*|)^4/4$. The initial magnetization is chosen in such a way, that it produces a singularity around the $(x_1, x_2) = (0, 0)$ line, similarly to the 2D example from Section 3.3.2. The initial state is visualized in the top left of Figure 5.4.

In order to perform a physically relevant simulation, we further need to ensure, that \mathbf{m}^0 and \mathbf{H}^0 fulfill condition (5.1.1f). To that end, we take

$$\mathbf{H}^0 = \mathbf{H}_\star^0 - \chi_\Omega \mathbf{m}^0,$$

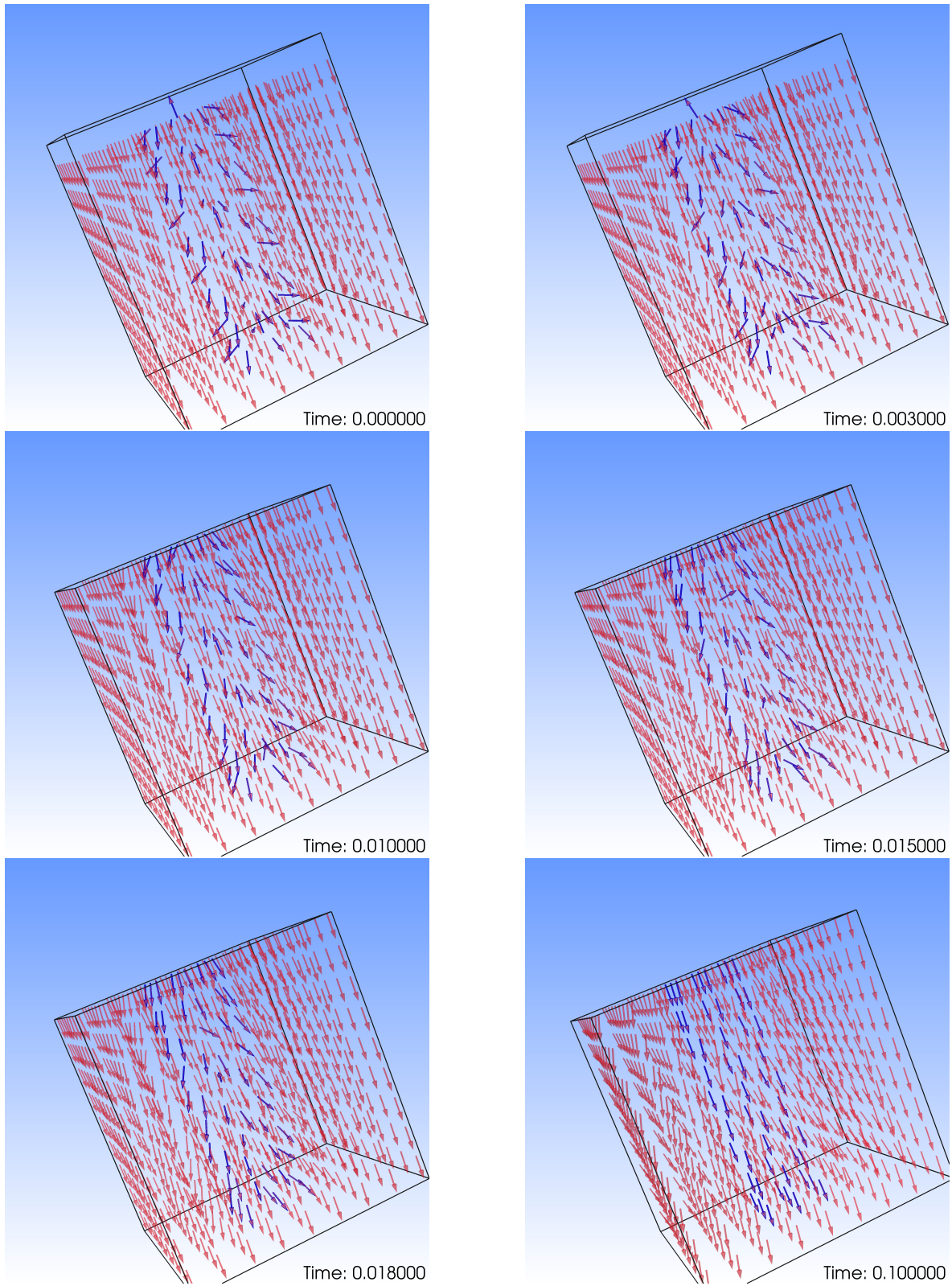


Figure 5.4.: Evolution of the magnetization with $H_s = 30$. We observe blowup behavior and alignment of the magnetization in $(0,0,-1)$ -direction afterwards.

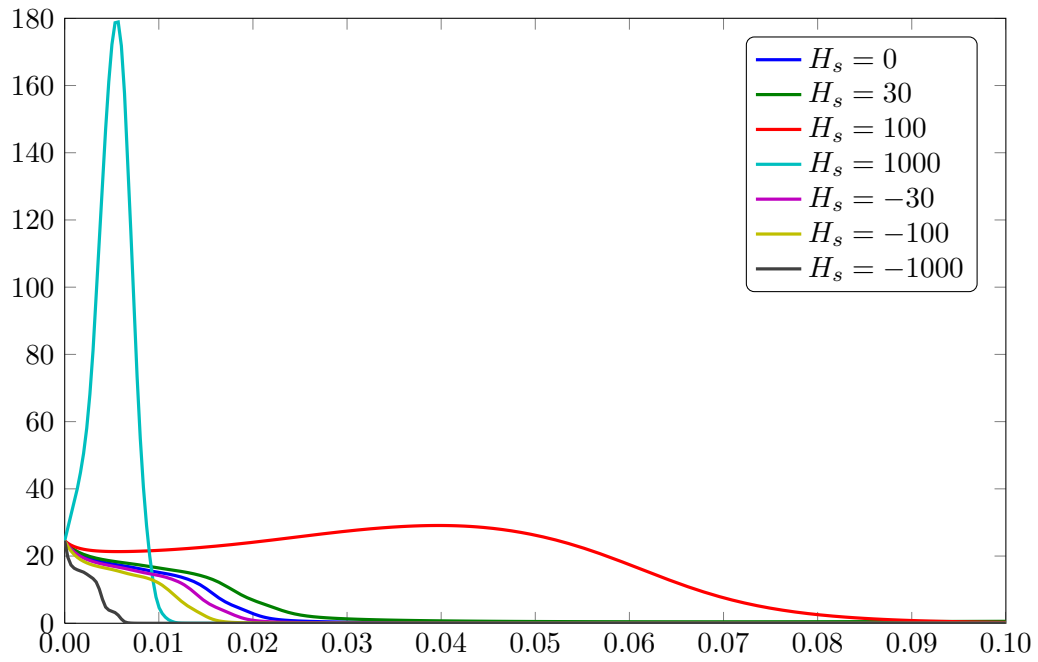


Figure 5.5.: Exchange energy $\mathcal{E}_{\text{exch}} = \|\nabla \mathbf{m}(t)\|_{\mathbf{L}^2(\Omega)}^2$ plotted over time.

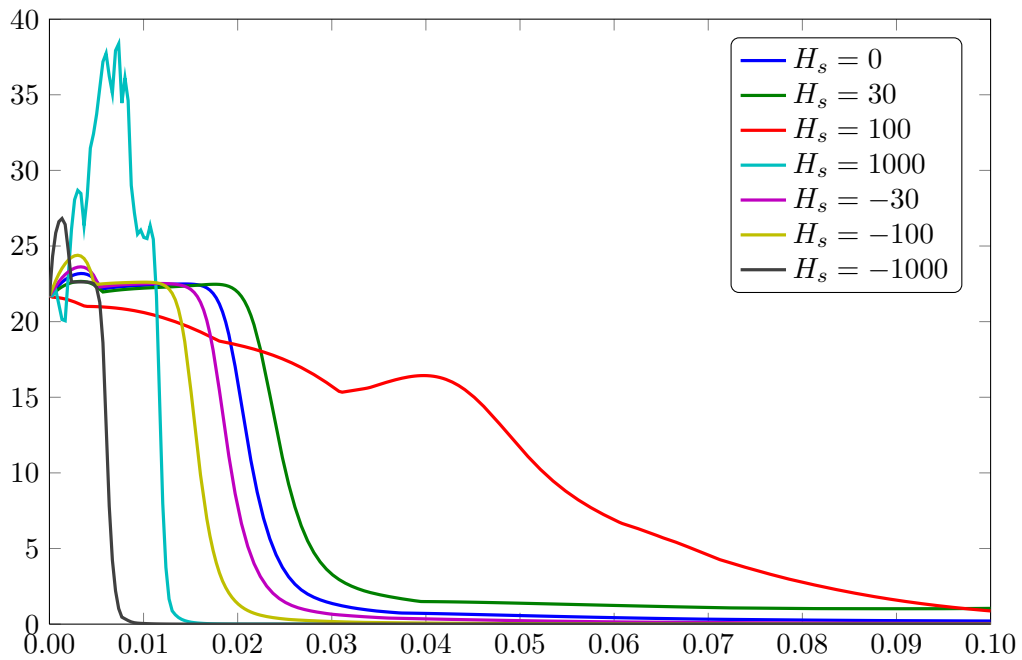
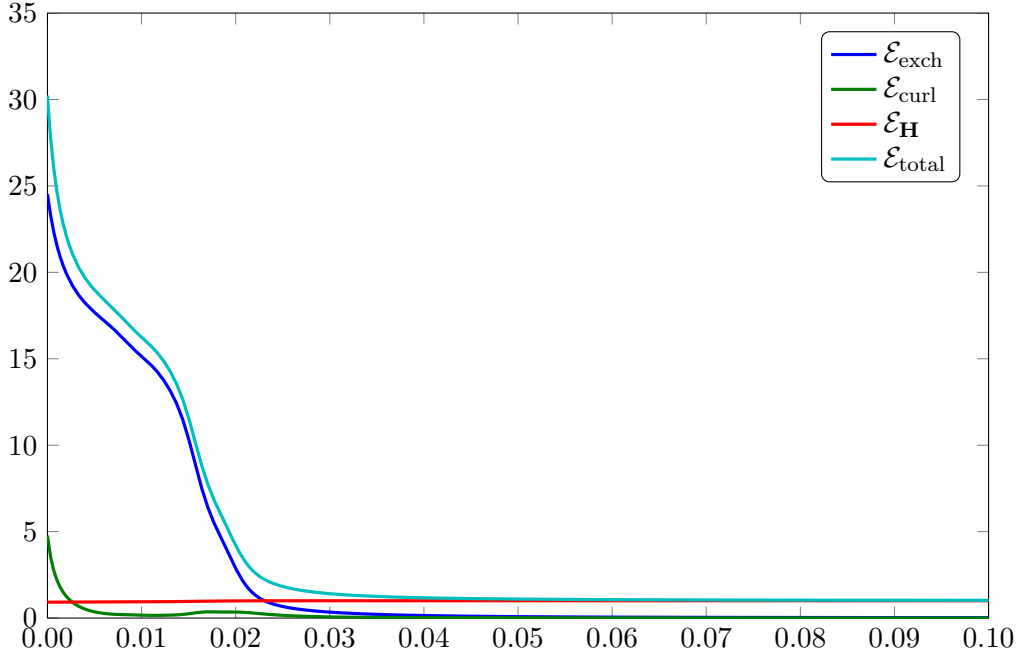
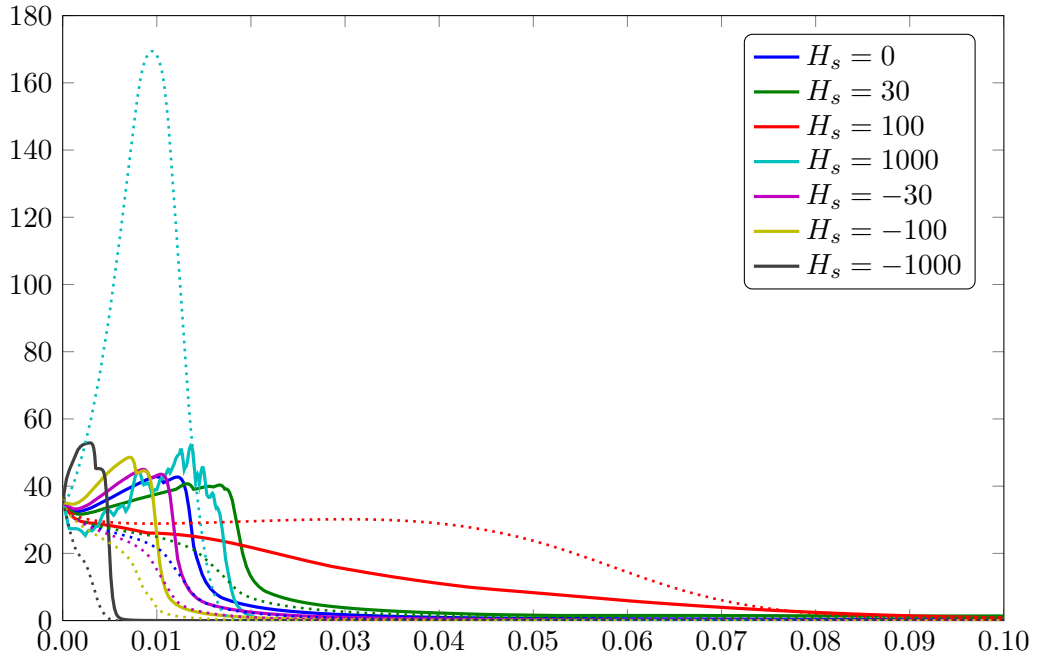


Figure 5.6.: Maximum norm $\|\nabla \mathbf{m}(t)\|_{\mathbf{L}^\infty(\Omega)}$ plotted over time.

Figure 5.7.: Different energy contributions for $H_s = 0$ plotted over time.Figure 5.8.: Exchange energy (solid) and $W^{1,\infty}(\Omega)$ -seminorm (dotted) for simulation on refined mesh with $P = 20480$ elements.

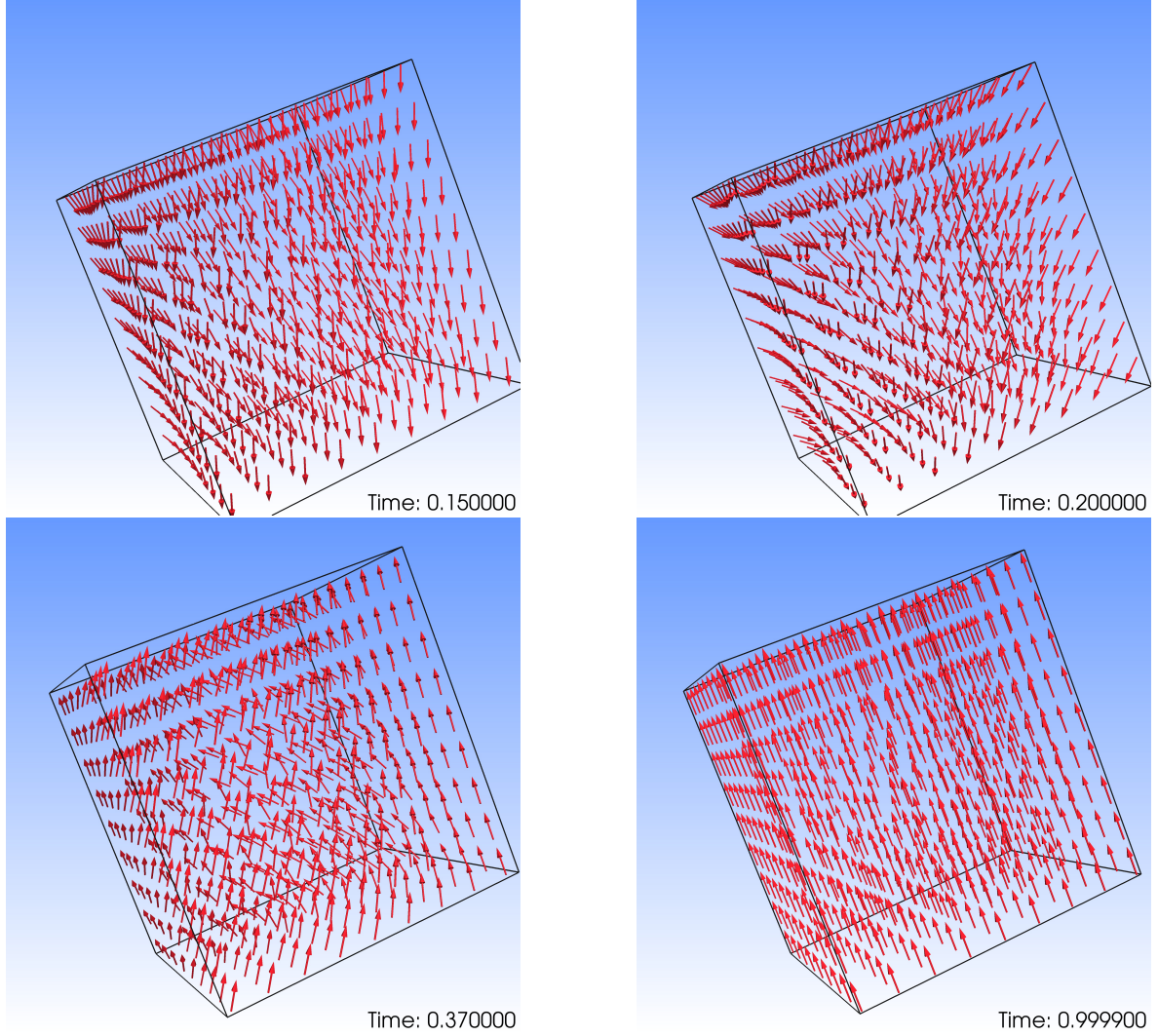


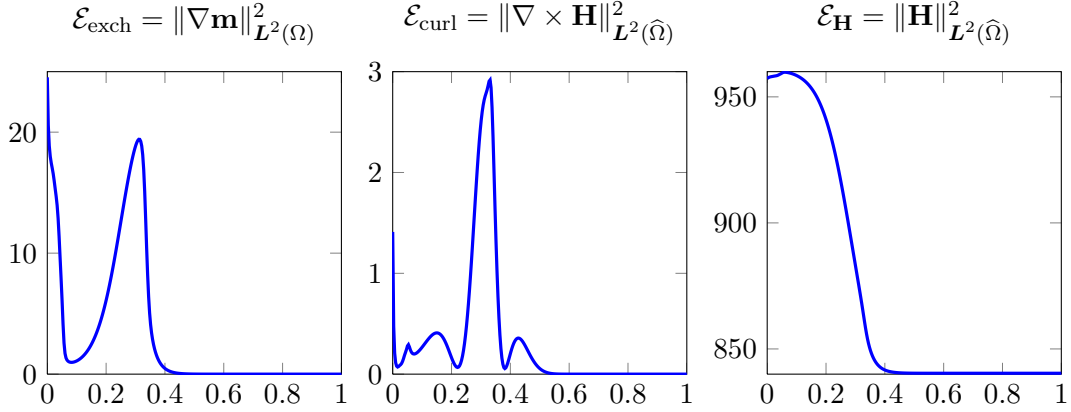
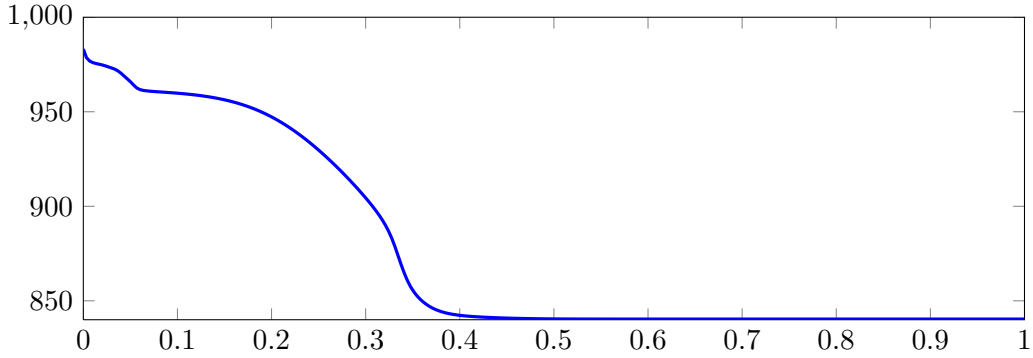
Figure 5.9.: Evolution of the magnetization with $H_s = 30$ after $T = 0.15$. We observe realignment of the magnetization in $(0, 0, 1)$ -direction.

for some \mathbf{H}_\star^0 with $\operatorname{div} \mathbf{H}_\star^0 = 0$ in $\widehat{\Omega}$. For simplicity, we choose \mathbf{H}_\star^0 to be the constant

$$\mathbf{H}_\star^0(\mathbf{x}) = \begin{pmatrix} 0 \\ 0 \\ H_s \end{pmatrix}$$

for varying parameters $H_s \in \{-1000, -100, -30, 0, 30, 100, 1000\}$. As Gilbert damping parameter, we employ $\alpha = 1$. Note, that $\alpha = 1$ corresponds to $\alpha/(1 + \alpha^2) = 0.5$ as coefficient of the damping term. As spatial mesh size, we use $h \approx 0.07$, i.e. a mesh with $P = 2560$ tetrahedral elements. Throughout, we employ $N = 1000$ time steps.

The evolution of the magnetization over the time interval $(0, 0.1)$ is visualized in Figure 5.4 for $H_s = 30$. As expected, we see that the magnetization in the vicinity of $(x_1, x_2) = (0, 0)$ slowly aligns parallel to $(0, 0, -1)$ creating a singularity at $(0, 0, 0)$ which induces a blowup in the $W^{1,\infty}(\Omega)$ -norm. Finally, the singularity gets resolved and the magnetization aligns

Figure 5.10.: Different energy contributions for $H_s = 30$ and extended simulation time.Figure 5.11.: Total energy $\mathcal{E}_{\text{total}} = \mathcal{E}_{\text{exch}} + \mathcal{E}_{\text{curl}} + \mathcal{E}_{\mathbf{H}}$ for $H_s = 30$ on the extended time interval.

parallel to $(0, 0, -1)$.

Figure 5.5 displays the exchange energy $\|\nabla \mathbf{m}(t, \cdot)\|_{L^2(\Omega)}^2$ of the magnetization plotted over time. Note that in the cases $H_s = 100$ and $H_s = 1000$, the magnetization directly aligns in $(0, 0, 1)$ -direction. The results are in good agreement with those from [BBP08]. Figure 5.6 displays the $W^{1,\infty}(\Omega)$ -norm of the magnetization. As expected, we observe that the empirical blowup time decreases as the magnetic field gets stronger in $(0, 0, -1)$ -direction, i.e. the magnetization aligns faster.

In the cases $H_s = 100$ and $H_s = 1000$ on the other hand, \mathbf{m} gets aligned in $(0, 0, 1)$ direction, due to the influence of the magnetic field. In case of a moderate magnetic field $H_s = 100$, this takes longer as the majority of the magnetization needs to be realigned and the field is not too strong yet.

In Figure 5.7, we plot the different energy contributions

$$\begin{aligned}\mathcal{E}_{\text{exch}} &= \|\nabla \mathbf{m}\|_{L^2(\Omega)}^2, \\ \mathcal{E}_{\text{curl}} &= \|\nabla \times \mathbf{H}\|_{L^2(\hat{\Omega})}^2, \\ \mathcal{E}_{\mathbf{H}} &= \|\mathbf{H}\|_{L^2(\hat{\Omega})}^2, \quad \text{and} \\ \mathcal{E}_{\text{total}} &= \mathcal{E}_{\text{exch}} + \mathcal{E}_{\text{curl}} + \mathcal{E}_{\mathbf{H}}\end{aligned}$$

for $H_s = 0$ over time. As expected, we observe a monotone decay of the total energy. Moreover, the exchange contribution is the dominant term in this case.

In Figure 5.8, the same data are visualized for a refined spatial mesh of $P = 20480$ tetrahedral elements. The exchange energy $\mathcal{E}_{\text{exch}}$ is given by the solid lines, whereas the dotted lines (of the same color) denote the corresponding $W^{1,\infty}(\Omega)$ -norms. Similarly to the 2D case from Section 3.3.2, we observe that the time as well as the magnitude of the blowup change if the spatial mesh-size h is decreased.

The case $H_s = 30$ has a special role as the field points in positive $(0, 0, 1)$ -direction and yet we observe that the magnetization aligns in the direction of $(0, 0, -1)$, cf. Figure 5.4. The same behaviour was already observed in [BBP08] and there, the authors conjectured that the magnetization would eventually realign in $(0, 0, 1)$ -direction. While such a behaviour could be divined from their experiment, they did not compute far enough to actually check it. With our experiment, we can now confirm their conjecture for this case as we observe that after $T = 0.1$, the magnetization starts to form a x_3 -centered vortex and then slowly starts to point upwards in the direction of $(0, 0, 1)$. The dynamical behaviour after $T = 0.1$ is visualized in Figure 5.9.

The different energy contributions for the case $H_s = 30$ are visualized in Figure 5.10 over the extended time interval $(0, 1)$. One easily observes that the exchange energy monotonously decreases at the beginning until the alignment in $(0, 0, -1)$ -direction is reached. After $T = 0.1$, however, the exchange- as well as the curl-part of the energy show a peak until they finally drop to zero again. This corresponds to the remagnetization process in $(0, 0, 1)$ -direction. Figure 5.11 finally visualizes the total energy throughout the extended experiment and, as expected, we observe monotone decay of the total energy.

5.4.3. Remarks on known stable states

Finally, we solve a problem for which the stable limiting states are known. In a first experiment, we consider $\Omega = \hat{\Omega} = [-1, 1]^3$ on $(0, 0.2)$ and the initial condition

$$\mathbf{m}^0 = \begin{cases} (0, 0, 1) & x_1 \leq 0, \\ (0, 0, -1) & x_1 \geq 0. \end{cases}$$

Note, that this initial magnetization is not formally covered by theory as $\mathbf{m}^0 \notin \mathbf{H}^1(\Omega)$. We stress, however, that as soon as the initial state is surpassed, the magnetization becomes $\mathbf{H}^1(\Omega)$. We furthermore choose

$$\mathbf{H}^0 = -\mathbf{m}^0,$$

$\alpha = 1$, $P = 2560$ spatial elements and $N = 1000$ time steps.

The dynamic behaviour of the magnetization is visualized in Figure 5.12. As expected, we observe that, after a short while, a vortex is formed as stable state. The different energy contributions plotted over time are visualized in Figure 5.13 and the total energy is depicted in Figure 5.14. Again, we observe a monotone decay of the involved energy.

Next, we start with an initial magnetization that is homogeneously aligned in $(0, 0, 1)$ -direction. This time, we investigate $\Omega = [-0.125, 0.125]^3$ and $\hat{\Omega} = [-1, 1]^3$ on the time interval $(0, 0.5)$. As the LLG domain Ω needs to have a higher resolution than $\hat{\Omega}$, we employ an adaptively refined mesh that is dense within Ω and becomes coarser towards the boundary

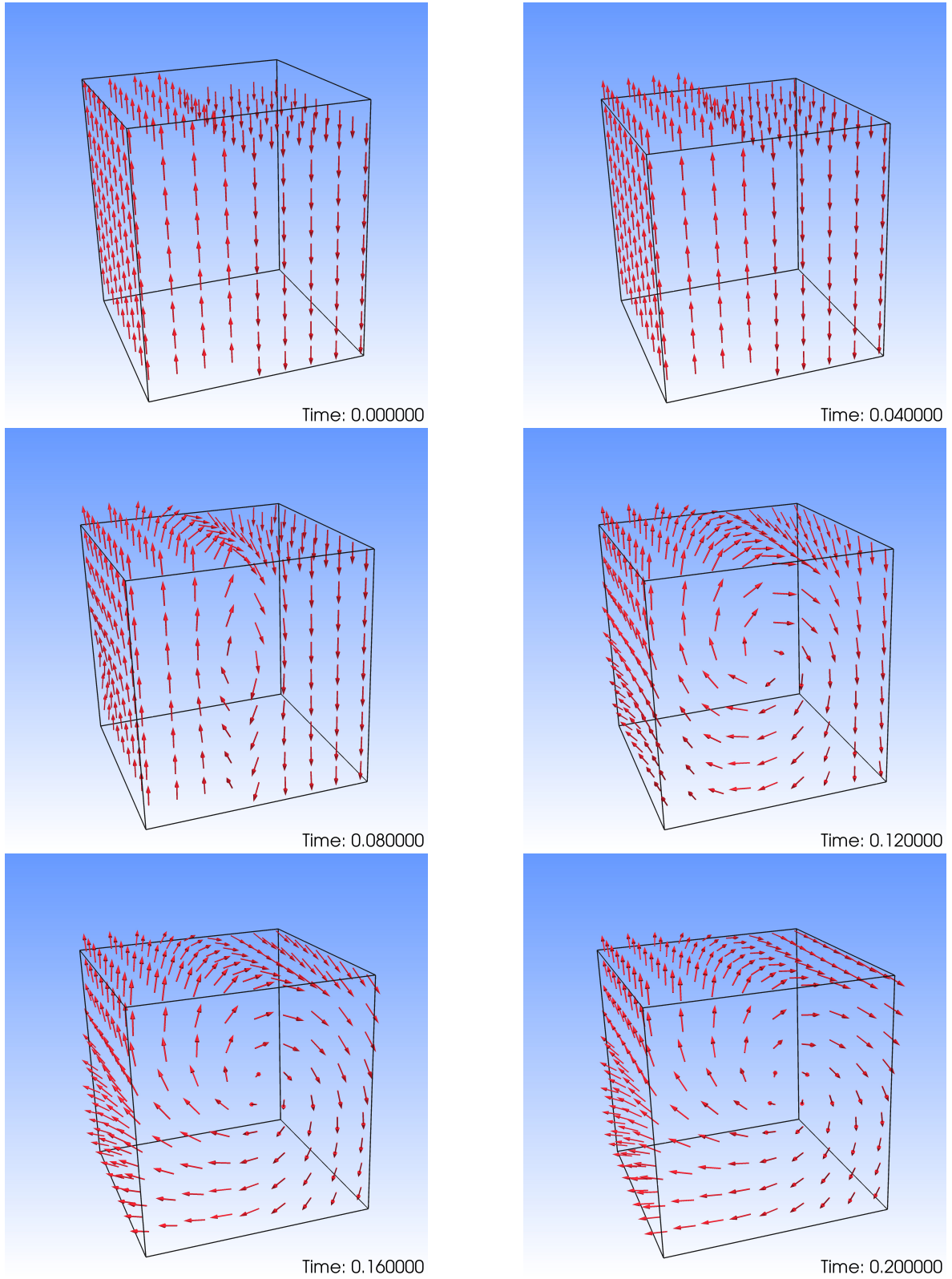


Figure 5.12.: Dynamic behaviour of the magnetization that leads to a vortex state.

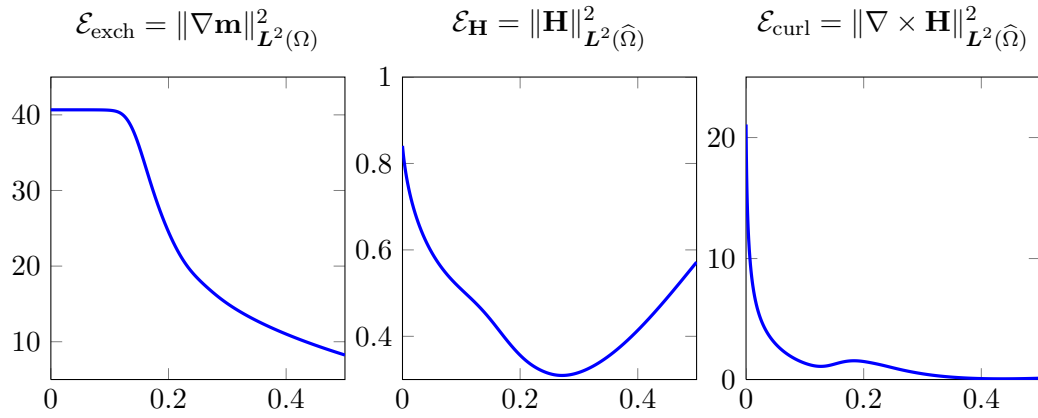


Figure 5.13.: Different energy contributions for vortex state plotted over time.

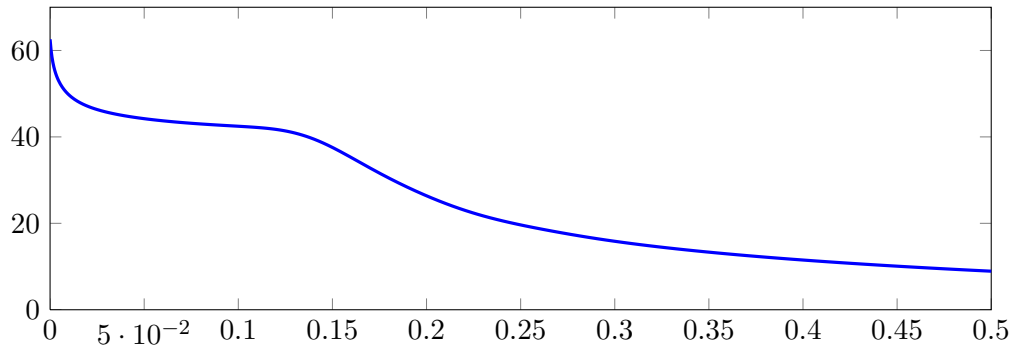


Figure 5.14.: Total energy $\mathcal{E}_{\text{total}} = \mathcal{E}_{\text{exch}} + \mathcal{E}_{\text{curl}} + \mathcal{E}_{\mathbf{H}}$ of vortex state plotted over time.

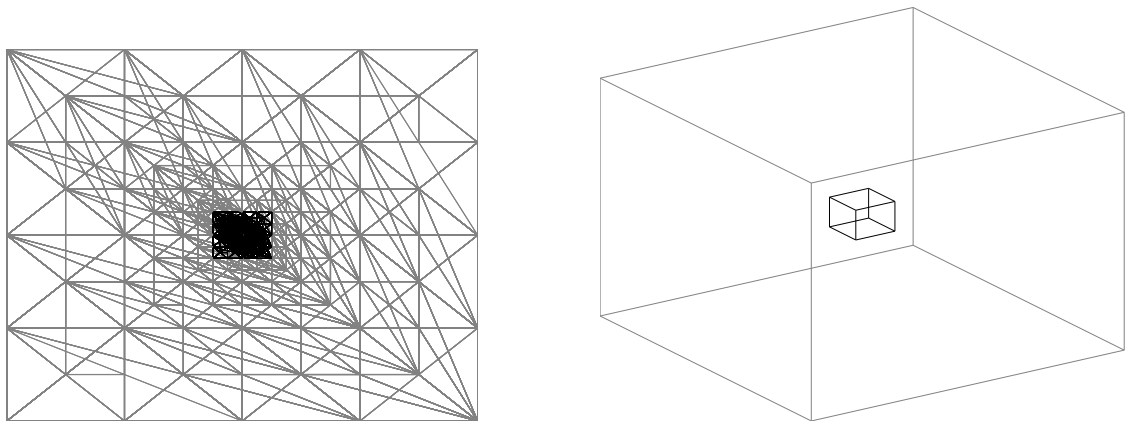


Figure 5.15.: Graded mesh for flower state computation as projection (left). The two domains Ω and $\hat{\Omega}$ as 3D view (right).

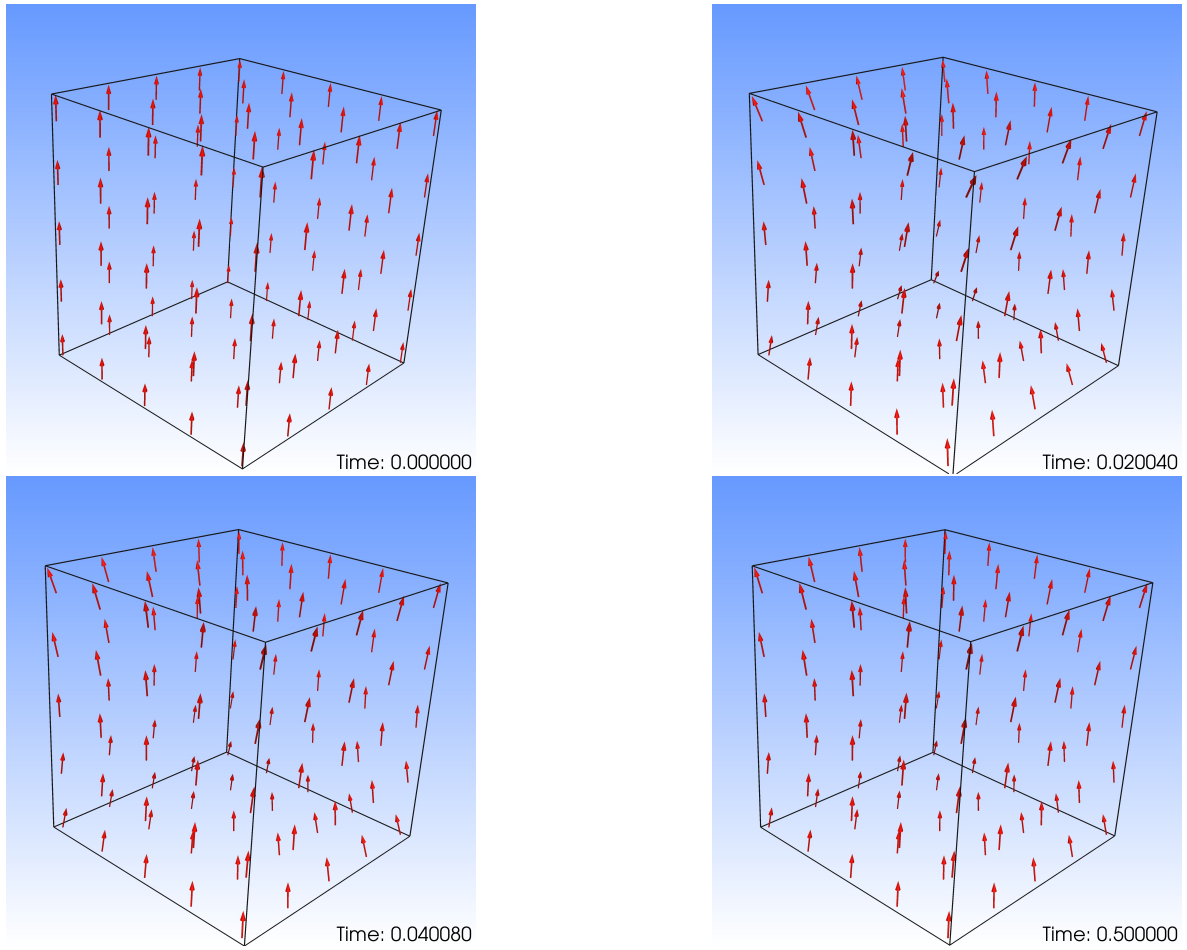


Figure 5.16.: Dynamic behaviour of the magnetization that leads to a flower state.

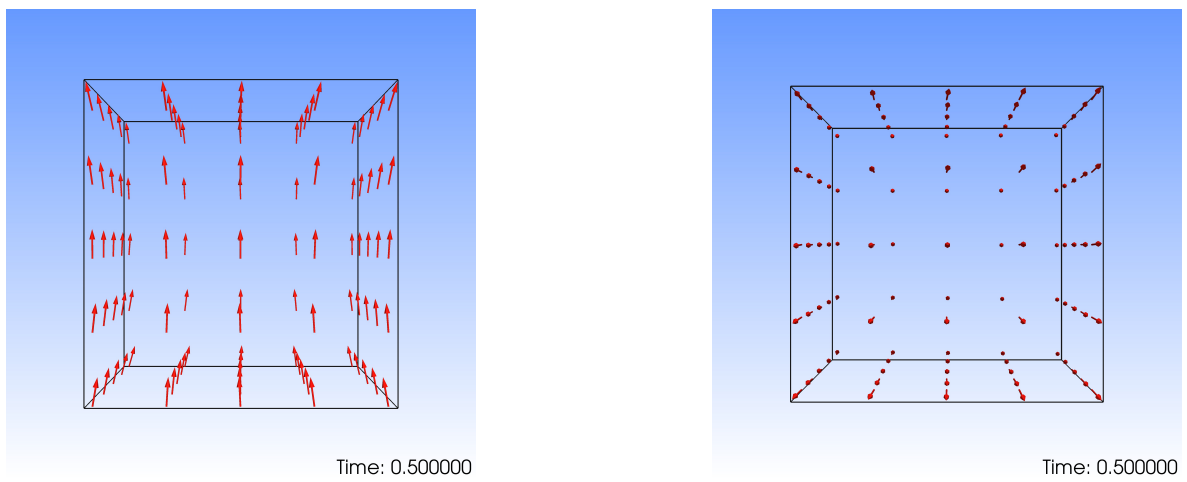


Figure 5.17.: Symmetric flower state from lateral view (left) and top view (right).

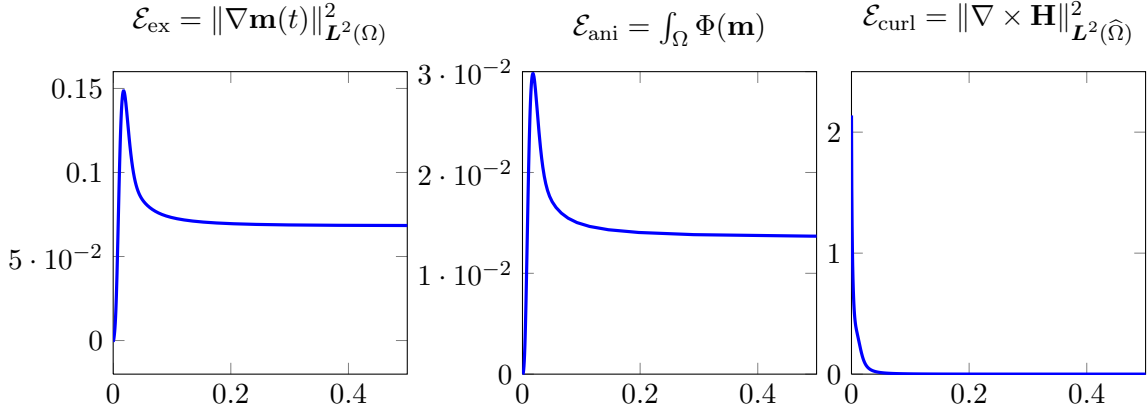


Figure 5.18.: Different energy contributions of the flower state.

of the larger domain $\hat{\Omega}$. Figure 5.15 shows a 2D projection of the adaptive mesh (left) and a 3D view of the two domains (right), where Ω is marked black and $\hat{\Omega}$ is visualized in grey.

Again, we choose $\alpha = 1$ and employ

$$\mathbf{H}^0(\mathbf{x}) = \begin{cases} -\mathbf{m}^0(\mathbf{x}) & \mathbf{x} \in \Omega, \\ 0 & \mathbf{x} \in \hat{\Omega} \setminus \Omega. \end{cases}$$

Moreover, we include uniaxial anisotropy in x_3 -direction with

$$\Phi(\mathbf{m}) = -(\mathbf{e}, \mathbf{m})^2$$

into this simulation. Here, \mathbf{e} denotes the easy axis.

The dynamic behaviour of the magnetization is shown in Figure 5.16 and we observe, that the stable state for this setting is the well-known (symmetric) flower state. Figure 5.17 shows a side- and a top view of the final state.

The different energy contributions are plotted over time in Figure 5.18 and the total energy is visualized in Figure 5.19. Again, we observe monotonously decreasing energy towards the stable state.

Finally, as we increase the size of the sample domains Ω and $\hat{\Omega}$ with a factor of 1.4, we observe that the symmetric flower state vanishes and we derive a twisted flower state instead. This behaviour is described in detail in [Gol12] and the final state is visualized in Figure 5.20.

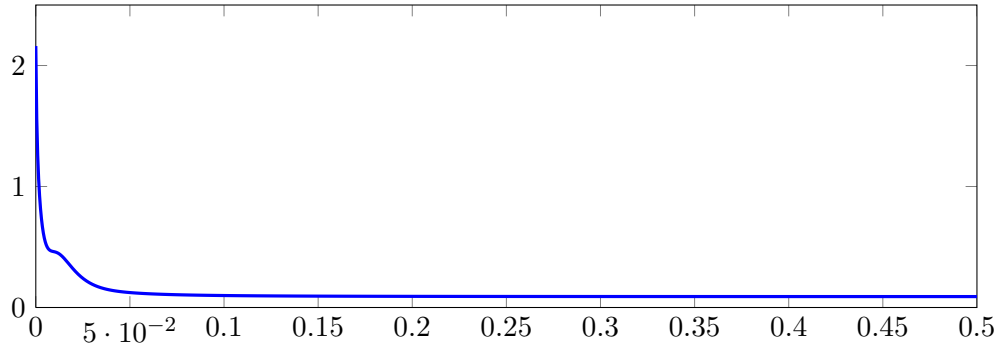


Figure 5.19.: Total energy $\mathcal{E}_{\text{total}} = \mathcal{E}_{\text{exch}} + \mathcal{E}_{\text{curl}} + \mathcal{E}_{\mathbf{H}} + \mathcal{E}_{\text{ani}}$ of flower state.

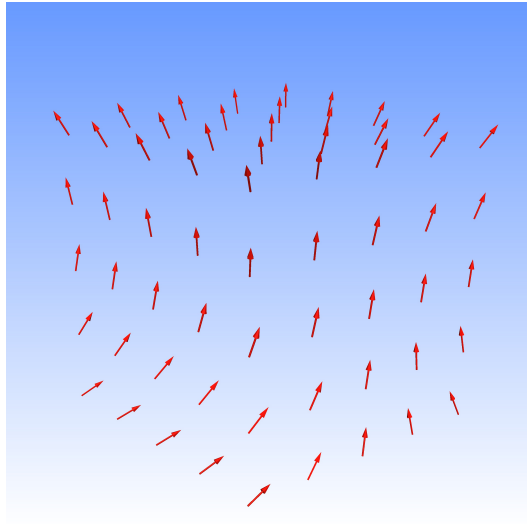


Figure 5.20.: Twisted flower state.

LLG with magnetostriction

So far, we have seen that the elegance and the mathematical advantages of the original work [Alo08a] from ALOUGES can be carried over to more general effective fields, as well as coupling to certain variants of Maxwell's equations. The goal of such generalizations has been, and must always be, the realization of more realistic simulations. Another interesting physical effect, which is not negligible at least for certain materials like Terfenol-D, is the magnetoelastic interaction or *magnetostriction*. Roughly speaking, this additional field contribution models the circumstance that the deformation of a magnetic material influences the magnetic field and hence the magnetization. It thus models somehow the inverse of the effect that a magnet can be deformed if it is exposed to a strong magnetic field. The inclusion of this effect together with the derivation of an unconditionally convergent numerical scheme in spirit of the previous approaches will be the goal of this chapter.

Incorporating magnetostriction requires coupling to the conservation of momentum equation. Here the coupling is, however, less straightforward compared to the previous chapters. This is mainly because of the structure of the coupling operator $\mathbf{h}_{\mathbf{m}}$ below, which is simply more complicated than before. In particular, we deal with a nonlinear coupling operator, which does not only depend on the solution of the second equation, but rather on its spatial derivative. The results of this chapter have partially been published in [BPPR13]. For strong LLG solvers coupled with magnetostriction (LLGM), we refer to [Bañ05a, Bañ05b, BS06, Bañ08]. A weak integrator for the LLGM problem which is based on the midpoint scheme is found in [Roc12].

6.1. Elasticity model and problem formulation

For the evolution of the magnetization on Ω_T , we again consider the LLG equation

$$\mathbf{m}_t - \alpha \mathbf{m} \times \mathbf{m}_t = -\mathbf{m} \times \mathbf{h}_{\text{eff}}, \quad (6.1.1a)$$

where the effective field reads

$$\mathbf{h}_{\text{eff}} = C_e \Delta \mathbf{m} + \mathbf{h}_{\mathbf{m}} + \boldsymbol{\pi}(\mathbf{m}) \quad (6.1.1b)$$

and consists of the exchange contribution $\Delta \mathbf{m}$, the generalized contribution $\boldsymbol{\pi}(\mathbf{m})$, and the magnetostrictive component $\mathbf{h}_{\mathbf{m}}$, which will be specified below. Again, the general contribution is only assumed to fulfill the two properties (6.2.5) and (6.2.6) below and thus particularly

includes the case

$$\mathbf{h}_{\text{eff}} = C_e \Delta \mathbf{m} + \mathbf{h}_m + C_{\text{ani}} D\Phi(\mathbf{m}) + P(\mathbf{m}) - \mathbf{f}.$$

To keep the presentation simple, we did not include the additional coupling to the full Maxwell system or the eddy-current simplification as in the Chapters 4 or 5. We stress, however, that this extension is straightforward and, with the combined techniques, one could consider a coupled system of full Maxwell-LLG with the conservation of momentum equation to account for magnetostrictive effects. Moreover, with the techniques from Chapter 3, it is straightforward to rigorously include a numerical approximation $\pi_h(\cdot)$ of $\pi(\cdot)$ into the convergence analysis.

As usual, (6.1.1) is supplemented by the initial and boundary conditions

$$\mathbf{m}(0) = \mathbf{m}^0 \in \mathbf{H}^1(\Omega; \mathbb{S}^2) \quad \text{and} \quad \partial_n \mathbf{m} = 0 \text{ on } (0, T) \times \partial\Omega. \quad (6.1.1c)$$

For modeling the magnetostrictive component, we follow the approach of [Vis85]. Here, the magnetostrictive field reads

$$\mathbf{h}_m : \Omega_T \rightarrow \mathbb{R}^3, \quad (\mathbf{h}_m)_q = (\mathbf{h}_m(\mathbf{u}, \mathbf{m}))_q := \sum_{i,j,p=1}^3 \lambda_{ijpq}^m \sigma_{ij}(\mathbf{m})_p, \quad (6.1.2)$$

where $(\cdot)_p$ denotes the p -th component of a vector field. We implicitly assume linear dependence of the stress tensor $\boldsymbol{\sigma} = \{\sigma_{ij}\}$ on the elastic part of the total strain $\boldsymbol{\varepsilon}^e = \{\varepsilon_{ij}^e\}$ which is the converse form of Hook's law, i.e.

$$\boldsymbol{\sigma} := \boldsymbol{\lambda}^e \boldsymbol{\varepsilon}^e(\mathbf{u}, \mathbf{m}) : \Omega_T \longrightarrow \mathbb{R}^{3 \times 3}, \quad \sigma_{ij} = \sum_{p,q=1}^3 \lambda_{ijpq}^e \varepsilon_{pq}^e, \quad (6.1.3)$$

$$\boldsymbol{\varepsilon}^e(\mathbf{u}, \mathbf{m}) := \boldsymbol{\varepsilon}(\mathbf{u}) - \boldsymbol{\varepsilon}^m(\mathbf{m}) : \Omega_T \longrightarrow \mathbb{R}^{3 \times 3}. \quad (6.1.4)$$

Here, $\mathbf{u} : \Omega_T \rightarrow \mathbb{R}^3$ denotes the *displacement vector field* from the conservation of momentum equation (6.1.8) below. The *total strain* is defined by the symmetric part of the gradient of \mathbf{u} , i.e.

$$\varepsilon_{ij}(\mathbf{u}) := \frac{1}{2} \left(\frac{\partial u_i}{\partial x_j} + \frac{\partial u_j}{\partial x_i} \right), \quad (6.1.5)$$

and the magnetic part of the total strain by

$$\boldsymbol{\varepsilon}^m(\mathbf{m}) := \boldsymbol{\lambda}^m \mathbf{m} \mathbf{m}^T : \Omega_T \longrightarrow \mathbb{R}^{3 \times 3}, \quad \varepsilon_{ij}^m(\mathbf{m}) = \sum_{p,q=1}^3 \lambda_{ijpq}^m (\mathbf{m})_p (\mathbf{m})_q. \quad (6.1.6)$$

In addition, we assume both material tensors $\boldsymbol{\lambda} \in \{\boldsymbol{\lambda}^e, \boldsymbol{\lambda}^m\}$ to be symmetric ($\lambda_{ijpq} = \lambda_{jipq} = \lambda_{ijqp} = \lambda_{pqij}$) and positive definite

$$\sum_{i,j,p,q=1}^3 \lambda_{ijpq} \xi_{ij} \xi_{pq} \geq \lambda^* \sum_{i,j=1}^3 \xi_{ij}^2 \quad (6.1.7)$$

with bounded entries, i.e. there exists some $\bar{\lambda}$ with $\lambda_{ijpq}^e, \lambda_{ijpq}^m \leq \bar{\lambda}$ for any $i, j, p, q = 1, 2, 3$. The stress tensor $\boldsymbol{\sigma}$ and the displacement field \mathbf{u} (where we assume no external forces) are finally coupled via the conservation of momentum equation

$$\rho \mathbf{u}_{tt} - \nabla \cdot \boldsymbol{\sigma} = 0 \quad \text{in } \Omega_T. \quad (6.1.8a)$$

Here, we assume the mass density $\varrho > 0$ to be constant and independent of the deformation. Equation (6.1.8a) is additionally supplemented by the initial and boundary conditions

$$\mathbf{u}(0) = \mathbf{u}^0 \text{ in } \Omega, \quad \mathbf{u}_t(0) = \dot{\mathbf{u}}^0 \text{ in } \Omega, \quad \text{and} \quad \mathbf{u} = 0 \text{ on } \partial\Omega. \quad (6.1.8b)$$

Altogether, we thus aim to solve the coupled problem

$$\begin{cases} \mathbf{m}_t - \alpha \mathbf{m} \times \mathbf{m}_t = -\mathbf{m} \times \mathbf{h}_{\text{eff}} \\ \varrho \mathbf{u}_{tt} - \nabla \cdot \boldsymbol{\sigma} = 0 \end{cases} \quad (6.1.9)$$

of the LLG equation with magnetostriction (LLGM) subject to the stated initial and boundary conditions.

Using the above boundary conditions, Hook's relation (6.1.3), the definition of the total strain tensor (6.1.4), and the symmetry of the tensors $\boldsymbol{\lambda}^e$ and $\boldsymbol{\lambda}^m$, we obtain the following result:

Lemma 6.1.1. *The weak formulation of (6.1.8a) is given by*

$$(\varrho \mathbf{u}_{tt}(t), \boldsymbol{\varphi}) + (\boldsymbol{\lambda}^e \boldsymbol{\varepsilon}(\mathbf{u})(t), \boldsymbol{\varepsilon}(\boldsymbol{\varphi})) = (\boldsymbol{\lambda}^e \boldsymbol{\varepsilon}^m(\mathbf{m})(t), \boldsymbol{\varepsilon}(\boldsymbol{\varphi})), \quad (6.1.10)$$

for any testfunction $\boldsymbol{\varphi} \in \mathbf{H}_0^1(\Omega)$.

Proof. Multiplication with a testfunction $\boldsymbol{\varphi} \in \mathbf{H}_0^1(\Omega)$ and intergration over Ω yields

$$(\varrho \mathbf{u}_{tt}(t), \boldsymbol{\varphi}) - (\nabla \cdot \boldsymbol{\lambda}^e \boldsymbol{\varepsilon}(\mathbf{u})(t), \boldsymbol{\varphi}) = -(\nabla \cdot \boldsymbol{\lambda}^e \boldsymbol{\varepsilon}^m(\mathbf{m})(t), \boldsymbol{\varphi}).$$

Componentwise integration by parts now shows for the second term on the left hand side

$$\begin{aligned} (\nabla \cdot \boldsymbol{\lambda}^e \boldsymbol{\varepsilon}(\mathbf{u})(t), \boldsymbol{\varphi}) &= \int_{\Omega} \begin{pmatrix} \partial_{x_1}[\lambda^e \varepsilon(\mathbf{u})]_{11}(t) + \partial_{x_2}[\lambda^e \varepsilon(\mathbf{u})]_{12}(t) + \partial_{x_3}[\lambda^e \varepsilon(\mathbf{u})]_{13}(t) \\ \partial_{x_1}[\lambda^e \varepsilon(\mathbf{u})]_{21}(t) + \partial_{x_2}[\lambda^e \varepsilon(\mathbf{u})]_{22}(t) + \partial_{x_3}[\lambda^e \varepsilon(\mathbf{u})]_{23}(t) \\ \partial_{x_1}[\lambda^e \varepsilon(\mathbf{u})]_{31}(t) + \partial_{x_2}[\lambda^e \varepsilon(\mathbf{u})]_{32}(t) + \partial_{x_3}[\lambda^e \varepsilon(\mathbf{u})]_{33}(t) \end{pmatrix} \cdot \begin{pmatrix} \varphi_1 \\ \varphi_2 \\ \varphi_3 \end{pmatrix} \\ &= \int_{\Omega} \sum_i \partial_{x_i}[\lambda^e \varepsilon(\mathbf{u})]_{1i}(t) \varphi_1 + \int_{\Omega} \sum_i \partial_{x_i}[\lambda^e \varepsilon(\mathbf{u})]_{2i}(t) \varphi_2 + \int_{\Omega} \sum_i \partial_{x_i}[\lambda^e \varepsilon(\mathbf{u})]_{3i}(t) \varphi_3 \\ &= \int_{\Omega} \sum_j \sum_i \partial_{x_i}[\lambda^e \varepsilon(\mathbf{u})]_{ji}(t) \varphi_j \\ &\stackrel{\text{i.p.}}{=} - \int_{\Omega} \sum_j \sum_i [\lambda^e \varepsilon(\mathbf{u})]_{ji}(t) \frac{\partial \varphi_j}{\partial x_i} + \underbrace{\int_{\Gamma} \sum_j \sum_i [\lambda^e \varepsilon(\mathbf{u})]_{ji}(t) \varphi_j \cdot n}_{=0} \\ &= - \int_{\Omega} \sum_i [\lambda^e \varepsilon(\mathbf{u})]_{1i}(t) \frac{\partial \varphi_1}{\partial x_i} + \sum_i [\lambda^e \varepsilon(\mathbf{u})]_{2i}(t) \frac{\partial \varphi_2}{\partial x_i} + \sum_i [\lambda^e \varepsilon(\mathbf{u})]_{3i}(t) \frac{\partial \varphi_3}{\partial x_i} \\ &= - \int_{\Omega} \begin{pmatrix} [\lambda^e \varepsilon(\mathbf{u})]_{11}(t) & [\lambda^e \varepsilon(\mathbf{u})]_{12}(t) & [\lambda^e \varepsilon(\mathbf{u})]_{13}(t) \\ [\lambda^e \varepsilon(\mathbf{u})]_{21}(t) & [\lambda^e \varepsilon(\mathbf{u})]_{22}(t) & [\lambda^e \varepsilon(\mathbf{u})]_{23}(t) \\ [\lambda^e \varepsilon(\mathbf{u})]_{31}(t) & [\lambda^e \varepsilon(\mathbf{u})]_{32}(t) & [\lambda^e \varepsilon(\mathbf{u})]_{33}(t) \end{pmatrix} : \begin{pmatrix} \frac{\partial \varphi_1}{\partial x_1} & \frac{\partial \varphi_1}{\partial x_2} & \frac{\partial \varphi_1}{\partial x_3} \\ \frac{\partial \varphi_2}{\partial x_1} & \frac{\partial \varphi_2}{\partial x_2} & \frac{\partial \varphi_2}{\partial x_3} \\ \frac{\partial \varphi_3}{\partial x_1} & \frac{\partial \varphi_3}{\partial x_2} & \frac{\partial \varphi_3}{\partial x_3} \end{pmatrix} \\ &= -(\boldsymbol{\lambda}^e \boldsymbol{\varepsilon}(\mathbf{u})(t), \nabla \boldsymbol{\varphi}), \end{aligned}$$

where we implicitly use the frobenius scalar product. Completely analogously, one gets

$$(\nabla \cdot \boldsymbol{\lambda}^e \boldsymbol{\varepsilon}^m(\mathbf{m})(t), \boldsymbol{\varphi}) = -(\boldsymbol{\lambda}^e \boldsymbol{\varepsilon}^m(\mathbf{m})(t), \nabla \boldsymbol{\varphi}).$$

It therefore remains to show the equality

$$(\boldsymbol{\lambda}^e \boldsymbol{\varepsilon}(\mathbf{u})(t), \nabla \varphi) = (\boldsymbol{\lambda}^e \boldsymbol{\varepsilon}(\mathbf{u})(t), \boldsymbol{\varepsilon}(\varphi)).$$

To that end, we recall that, for the frobenius scalar product, there holds

$$A : B = \text{tr}(A^T B),$$

from which we deduce

$$\begin{aligned} \text{tr}(\boldsymbol{\lambda}^e \boldsymbol{\varepsilon}(\mathbf{u})^T(t) \nabla \varphi) &= \text{tr} \left(\begin{pmatrix} [\lambda^e \varepsilon(\mathbf{u})]_{11}(t) & [\lambda^e \varepsilon(\mathbf{u})]_{21}(t) & [\lambda^e \varepsilon(\mathbf{u})]_{31}(t) \\ [\lambda^e \varepsilon(\mathbf{u})]_{12}(t) & [\lambda^e \varepsilon(\mathbf{u})]_{22}(t) & [\lambda^e \varepsilon(\mathbf{u})]_{32}(t) \\ [\lambda^e \varepsilon(\mathbf{u})]_{13}(t) & [\lambda^e \varepsilon(\mathbf{u})]_{23}(t) & [\lambda^e \varepsilon(\mathbf{u})]_{33}(t) \end{pmatrix} \begin{pmatrix} \frac{\partial \varphi_1}{\partial x_1} & \frac{\partial \varphi_1}{\partial x_2} & \frac{\partial \varphi_1}{\partial x_3} \\ \frac{\partial \varphi_2}{\partial x_1} & \frac{\partial \varphi_2}{\partial x_2} & \frac{\partial \varphi_2}{\partial x_3} \\ \frac{\partial \varphi_3}{\partial x_1} & \frac{\partial \varphi_3}{\partial x_2} & \frac{\partial \varphi_3}{\partial x_3} \end{pmatrix} \right) \\ &= \text{tr} \left(\begin{pmatrix} \sum_i [\lambda^e \varepsilon(\mathbf{u})]_{i1}(t) \frac{\partial \varphi_i}{\partial x_1} & \sum_i [\lambda^e \varepsilon(\mathbf{u})]_{i1}(t) \frac{\partial \varphi_i}{\partial x_2} & \sum_i [\lambda^e \varepsilon(\mathbf{u})]_{i1}(t) \frac{\partial \varphi_i}{\partial x_3} \\ \sum_i [\lambda^e \varepsilon(\mathbf{u})]_{i2}(t) \frac{\partial \varphi_i}{\partial x_1} & \sum_i [\lambda^e \varepsilon(\mathbf{u})]_{i2}(t) \frac{\partial \varphi_i}{\partial x_2} & \sum_i [\lambda^e \varepsilon(\mathbf{u})]_{i2}(t) \frac{\partial \varphi_i}{\partial x_3} \\ \sum_i [\lambda^e \varepsilon(\mathbf{u})]_{i3}(t) \frac{\partial \varphi_i}{\partial x_1} & \sum_i [\lambda^e \varepsilon(\mathbf{u})]_{i3}(t) \frac{\partial \varphi_i}{\partial x_2} & \sum_i [\lambda^e \varepsilon(\mathbf{u})]_{i3}(t) \frac{\partial \varphi_i}{\partial x_3} \end{pmatrix} \right) \\ &= \sum_i [\lambda^e \varepsilon(\mathbf{u})]_{i1}(t) \frac{\partial \varphi_i}{\partial x_1} + \sum_i [\lambda^e \varepsilon(\mathbf{u})]_{i2}(t) \frac{\partial \varphi_i}{\partial x_2} + \sum_i [\lambda^e \varepsilon(\mathbf{u})]_{i3}(t) \frac{\partial \varphi_i}{\partial x_3}, \end{aligned}$$

as well as

$$\begin{aligned} \text{tr}(\boldsymbol{\lambda}^e \boldsymbol{\varepsilon}(\mathbf{u})^T(t) (\frac{1}{2}(\nabla \varphi + \nabla \varphi^T))) &= \text{tr} \left(\boldsymbol{\varepsilon}(\mathbf{u})^T(t) \frac{1}{2} \begin{pmatrix} 2 \frac{\partial \varphi_1}{\partial x_1} & \frac{\partial \varphi_1}{\partial x_2} + \frac{\partial \varphi_2}{\partial x_1} & \frac{\partial \varphi_1}{\partial x_3} + \frac{\partial \varphi_3}{\partial x_1} \\ \frac{\partial \varphi_2}{\partial x_1} + \frac{\partial \varphi_1}{\partial x_2} & 2 \frac{\partial \varphi_2}{\partial x_2} & \frac{\partial \varphi_2}{\partial x_3} + \frac{\partial \varphi_3}{\partial x_2} \\ \frac{\partial \varphi_3}{\partial x_1} + \frac{\partial \varphi_1}{\partial x_3} & \frac{\partial \varphi_3}{\partial x_2} + \frac{\partial \varphi_2}{\partial x_3} & 2 \frac{\partial \varphi_3}{\partial x_3} \end{pmatrix} \right) \\ &= \sum_i [\lambda^e \varepsilon(\mathbf{u})]_{i1}(t) \frac{1}{2} \left(\frac{\partial \varphi_i}{\partial x_1} + \frac{\partial \varphi_1}{\partial x_i} \right) \\ &\quad + \sum_i [\lambda^e \varepsilon(\mathbf{u})]_{i2}(t) \frac{1}{2} \left(\frac{\partial \varphi_i}{\partial x_2} + \frac{\partial \varphi_2}{\partial x_i} \right) \\ &\quad + \sum_i [\lambda^e \varepsilon(\mathbf{u})]_{i3}(t) \frac{1}{2} \left(\frac{\partial \varphi_i}{\partial x_3} + \frac{\partial \varphi_3}{\partial x_i} \right). \end{aligned}$$

The symmetry of $\boldsymbol{\lambda}^e \boldsymbol{\varepsilon}(\mathbf{u})(t)$, i.e. $[\lambda^e \varepsilon(\mathbf{u})]_{ij}(t) = [\lambda^e \varepsilon(\mathbf{u})]_{ji}(t)$ concludes the desired result. The right hand side is estimated in complete analogy. \square

Given these notations, we now define the notion of a weak solution for the coupled LLGM system (6.1.9), which goes back to [CEF11]. Note that, analogously to Chapter 4, where coupling to the full Maxwell system was considered, the highest time derivative of the second equation is enforced only in a weak sense. That is to say, we perform integration by parts in time and use suitable testfunctions which vanish at the upper time boundary.

Definition 6.1.2. *The tuple (\mathbf{m}, \mathbf{u}) is called a weak solution of LLG with magnetostriction, if for all $T > 0$,*

(i) $\mathbf{m} \in \mathbf{H}^1(\Omega_T)$ with $|\mathbf{m}| = 1$ almost everywhere in Ω_T and $\mathbf{u} \in H^1(\Omega_T)$;

(ii) for all $\phi \in C^\infty(\overline{\Omega_T})$ and $\zeta \in C_c^\infty([0, T]; C_c^\infty(\Omega))$, we have

$$\begin{aligned} \int_{\Omega_T} \mathbf{m}_t \cdot \phi - \alpha \int_{\Omega_T} (\mathbf{m} \times \mathbf{m}_t) \cdot \phi &= -C_e \int_{\Omega_T} (\nabla \mathbf{m} \times \mathbf{m}) \cdot \nabla \phi \\ &\quad + \int_{\Omega_T} (\mathbf{h}_m \times \mathbf{m}) \cdot \phi + \int_{\Omega_T} (\boldsymbol{\pi}(\mathbf{m}) \times \mathbf{m}) \cdot \phi \end{aligned} \quad (6.1.11)$$

$$- \varrho \int_{\Omega_T} \mathbf{u}_t \cdot \zeta_t + \int_{\Omega_T} \lambda^e \boldsymbol{\varepsilon}(\mathbf{u}) \cdot \boldsymbol{\varepsilon}(\zeta) = \int_{\Omega_T} \lambda^e \boldsymbol{\varepsilon}(\mathbf{m}) \cdot \boldsymbol{\varepsilon}(\zeta) + \int_{\Omega} \dot{\mathbf{u}}^0 \cdot \zeta(0, \cdot); \quad (6.1.12)$$

(iii) there holds $\mathbf{m}(0, \cdot) = \mathbf{m}^0$ and $\mathbf{u}(0, \cdot) = \mathbf{u}_0$ in the sense of traces;

(iv) for almost all $t' \in (0, T)$, we have bounded energy

$$\|\nabla \mathbf{m}(t')\|_{\mathbf{L}^2(\Omega)}^2 + \|\mathbf{m}_t\|_{\mathbf{L}^2(\Omega_{t'})}^2 + \|\nabla \mathbf{u}(t')\|_{\mathbf{L}^2(\Omega)}^2 + \|\mathbf{u}_t(t')\|_{\mathbf{L}^2(\Omega)}^2 \leq C_{29}, \quad (6.1.13)$$

where C_{29} is independent of t' and depends only on $|\Omega|, \mathbf{m}_0, \mathbf{u}_0$, and $\dot{\mathbf{u}}_0$.

6.2. Preliminaries and numerical integrator

For spatial discretization, we again employ the tangent space $\mathcal{K}_{\mathbf{m}_h^j}$ for the LLG equation. Concerning the equation of magnetoelasticity, we consider

$$\mathcal{S}_0^1(\mathcal{T}_h) := \mathcal{S}^1(\mathcal{T}_h) \cap H_0^1(\Omega).$$

In addition, let $\mathbf{m}_h^0 \in \mathcal{M}_h$ and $\mathbf{u}_h^0, \dot{\mathbf{u}}_h^0 \in \mathcal{S}_0^1(\mathcal{T}_h)$ be suitable approximations of the initial data obtained e.g. by projection. Further requirements on those initial data are specified below in Theorem 6.2.3. Moreover, we define $d_t \mathbf{u}_h^0$ as $\dot{\mathbf{u}}_h^0$.

The time derivative in (6.1.10) is finally discretized by means of the difference quotient of second order which is denoted by

$$d_t z_i = \frac{z_i - z_{i-1}}{k}, \quad d_t^2 z_i = \frac{d_t z_i - d_t z_{i-1}}{k} = \frac{z_i - 2z_{i-1} + z_{i-2}}{k^2}, \quad (6.2.1)$$

for any discrete function $z_i \approx z(t_i)$.

With these notations, we propose the following fully decoupled tangent plane scheme for the LLGM problem.

Algorithm 6.2.1. *Input: Initial data $\mathbf{m}_h^0, \mathbf{u}_h^0$ and $\dot{\mathbf{u}}_h^0$, parameter $0 \leq \theta \leq 1, \alpha > 0$. For $\ell = 0, \dots, N-1$ iterate:*

(i) *Compute unique solution $\mathbf{v}_h^\ell \in \mathcal{K}_{\mathbf{m}_h^\ell}$ such that for all $\boldsymbol{\varphi}_h \in \mathcal{K}_{\mathbf{m}_h^\ell}$, we have*

$$\alpha(\mathbf{v}_h^\ell, \boldsymbol{\varphi}_h) + ((\mathbf{m}_h^\ell \times \mathbf{v}_h^\ell), \boldsymbol{\varphi}_h) = -C_e(\nabla(\mathbf{m}_h^\ell + \theta k \mathbf{v}_h^\ell), \nabla \boldsymbol{\varphi}_h) + (\mathbf{h}_m(\mathbf{u}_h^\ell, \mathbf{m}_h^\ell), \boldsymbol{\varphi}_h) + (\boldsymbol{\pi}(\mathbf{m}_h^\ell), \boldsymbol{\varphi}_h). \quad (6.2.2)$$

(ii) *Define $\mathbf{m}_h^{\ell+1} \in \mathcal{M}_h$ nodewise by $\mathbf{m}_h^{\ell+1}(\mathbf{z}) = \frac{\mathbf{m}_h^\ell(\mathbf{z}) + k \mathbf{v}_h^\ell(\mathbf{z})}{|\mathbf{m}_h^\ell(\mathbf{z}) + k \mathbf{v}_h^\ell(\mathbf{z})|}$ for all $\mathbf{z} \in \mathcal{N}_h$.*

(iii) *Compute unique solution $\mathbf{u}_h^{\ell+1} \in \mathcal{S}_0^1(\mathcal{T}_h)$ such that for all $\boldsymbol{\psi}_h \in \mathcal{S}_0^1(\mathcal{T}_h)$, we have*

$$\varrho(d_t^2 \mathbf{u}_h^{\ell+1}, \boldsymbol{\psi}_h) + (\boldsymbol{\lambda}^e \boldsymbol{\varepsilon}(\mathbf{u}_h^{\ell+1}), \boldsymbol{\varepsilon}(\boldsymbol{\psi}_h)) = (\boldsymbol{\lambda}^e \boldsymbol{\varepsilon}^m(\mathbf{m}_h^{\ell+1}), \boldsymbol{\varepsilon}(\boldsymbol{\psi}_h)). \quad (6.2.3)$$

In the above algorithm, the discrete magnetostrictive contribution is given by

$$[\mathbf{h}_m(\mathbf{u}_h^\ell, \mathbf{m}_h^\ell)]_q := \sum_{i,j,p=1}^3 \lambda_{ijpq}^m \sigma_{ij}^\ell(\mathbf{m}_h^\ell)_p, \quad \text{with} \quad \boldsymbol{\sigma}^\ell = \boldsymbol{\lambda}^e(\boldsymbol{\varepsilon}(\mathbf{u}_h^\ell) - \boldsymbol{\varepsilon}^m(\mathbf{m}_h^\ell)).$$

Exploiting that we solve each of the two equations separately, we can immediately state well-posedness of Algorithm 6.2.1.

Lemma 6.2.2. *Algorithm 6.2.1 is well defined, i.e. it admits a tuple of unique discrete solutions $(\mathbf{v}_h^\ell, \mathbf{m}_h^{\ell+1}, \mathbf{u}_h^{\ell+1})$ in each step $\ell = 0, \dots, N-1$ of the iteration. Moreover, we have $\|\mathbf{m}_h^\ell\|_{L^\infty(\Omega)} = 1$ for all $\ell = 1, \dots, N$.*

Proof. We first show solvability of (6.2.2). We define the bilinear form

$$a_1^\ell(\cdot, \cdot) : \mathcal{K}_{\mathbf{m}_h^\ell} \times \mathcal{K}_{\mathbf{m}_h^\ell} \rightarrow \mathbb{R}, \quad a_1^\ell(\boldsymbol{\phi}, \boldsymbol{\varphi}) := \alpha(\boldsymbol{\phi}, \boldsymbol{\varphi}) + \theta C_e k (\nabla \boldsymbol{\phi}, \nabla \boldsymbol{\varphi}) + ((\mathbf{m}_h^\ell \times \boldsymbol{\phi}), \boldsymbol{\varphi})$$

and the linear functional

$$L_1^\ell(\boldsymbol{\varphi}) := C_e(\nabla \mathbf{m}_h^\ell, \nabla \boldsymbol{\varphi}) + (\mathbf{h}_m(\mathbf{u}_h^\ell, \mathbf{m}_h^\ell), \boldsymbol{\varphi}) + (\boldsymbol{\pi}(\mathbf{m}_h^\ell), \boldsymbol{\varphi}).$$

Then, (6.2.2) is equivalent to

$$a_1^\ell(\mathbf{v}_h^\ell, \boldsymbol{\varphi}_h) = L_1^\ell(\boldsymbol{\varphi}_h) \text{ for all } \boldsymbol{\varphi}_h \in \mathcal{K}_{\mathbf{m}_h^\ell}.$$

Note that $a_1^\ell(\cdot, \cdot)$ is positive definite for $\alpha > 0$, i.e. $a_1^\ell(\boldsymbol{\varphi}, \boldsymbol{\varphi}) \geq \alpha \|\boldsymbol{\varphi}\|_{L^2(\Omega)}^2$. Thus, by exploiting finite dimension, we see that there exists a unique $\mathbf{v}_h^\ell \in \mathcal{K}_{\mathbf{m}_h^\ell}$ which solves (6.2.2). Due to pointwise orthogonality of \mathbf{m}_h^ℓ and \mathbf{v}_h^ℓ , and the Pythagoras theorem, we get $|\mathbf{m}_h^\ell(\mathbf{z}) + k \mathbf{v}_h^\ell(\mathbf{z})|^2 = |\mathbf{m}_h^\ell(\mathbf{z})|^2 + k^2 |\mathbf{v}_h^\ell(\mathbf{z})|^2 \geq 1$ and thus even step (ii) of the above algorithm is well-defined. The bound $\|\mathbf{m}_h^\ell\|_{L^\infty(\Omega)} = 1$ can be seen by the normalization at the grid points in combination with barycentric coordinates and the convexity of each tetrahedron.

For the second equation (6.2.3), we consider the bilinear form

$$a_2(\cdot, \cdot) : \mathcal{S}_0^1(\mathcal{T}_h) \times \mathcal{S}_0^1(\mathcal{T}_h) \rightarrow \mathbb{R}, \quad a_2(\zeta, \psi) := \frac{\rho}{k^2}(\zeta, \psi) + (\lambda^e \varepsilon(\zeta), \varepsilon(\psi))$$

and the linear functional

$$L_2^\ell(\psi) = (\lambda^e \varepsilon^m(\mathbf{m}_h^{\ell+1}), \varepsilon(\psi)) + \frac{\rho}{k}(\mathbf{d}_t \mathbf{u}_h^\ell, \psi) + \frac{\rho}{k^2}(\mathbf{u}_h^\ell, \psi),$$

According to (6.1.7) and Korn's inequality [BS08, Thm. 11.2.16], it holds that

$$\begin{aligned} a_2(\psi, \psi) &= \frac{\rho}{k^2} \|\psi\|_{\mathbf{L}^2(\Omega)}^2 + (\lambda^e \varepsilon(\psi), \varepsilon(\psi)) \\ &\geq \frac{\rho}{k^2} \|\psi\|_{\mathbf{L}^2(\Omega)}^2 + \lambda^* (\varepsilon(\psi), \varepsilon(\psi)) \\ &= \frac{\rho}{k^2} \|\psi\|_{\mathbf{L}^2(\Omega)}^2 + \lambda^* \|\varepsilon(\psi)\|_{\mathbf{L}^2(\Omega)}^2 \\ &\gtrsim \|\psi\|_{\mathbf{H}^1(\Omega)}^2. \end{aligned}$$

With this notation, (6.2.3) is equivalent to

$$a_2(\mathbf{u}_h^{\ell+1}, \psi_h) = L_2^\ell(\psi_h) \text{ for all functions } \psi_h \in \mathcal{S}_0^1(\mathcal{T}_h),$$

and hence, admits a unique solution $\mathbf{u}_h^{\ell+1} \in \mathcal{S}_0^1(\mathcal{T}_h)$ in each step of the loop. The length constraint finally follows as before, cf. e.g. Lemma 5.2.2. \square

6.2.1. Convergence analysis

Next, we show that the sequence of discrete solutions from Algorithm 6.2.1 indeed converges towards a weak solution of LLGM in the sense of Definition 6.1.2. As usual, we assume the triangulation to fulfill the angle condition

$$\int_{\Omega} \nabla \eta_i \cdot \nabla \eta_j \leq 0 \quad \text{for all hat functions } \eta_i, \eta_j \in \mathcal{S}^1(\mathcal{T}_h) \text{ with } i \neq j. \quad (6.2.4)$$

Moreover, and in addition to the standard notation, for $t \in [t_\ell, t_{\ell+1})$, we define

$$\dot{\mathbf{u}}_{hk}(t, \mathbf{x}) := \mathbf{d}_t \mathbf{u}_h^\ell(\mathbf{x}) + (t - t_\ell) \mathbf{d}_t^2 \mathbf{u}_h^{\ell+1}(\mathbf{x}), \quad \dot{\mathbf{u}}_{hk}^-(t, \mathbf{x}) := \mathbf{d}_t \mathbf{u}_h^\ell(\mathbf{x}), \quad \dot{\mathbf{u}}_{hk}^+(t, \mathbf{x}) := \mathbf{d}_t \mathbf{u}_h^{\ell+1}(\mathbf{x}).$$

The next statement is the main theorem of this chapter and particularly includes the main result from [CEF11].

Theorem 6.2.3. (a) *Let $\theta \in (1/2, 1]$ and suppose that the meshes \mathcal{T}_h are uniformly shape regular and satisfy the angle condition (6.2.4). Moreover, let the general energy contribution π be uniformly bounded in $\mathbf{L}^2(\Omega_T)$, i.e.*

$$\|\pi(\mathbf{n})\|_{\mathbf{L}^2(\Omega)}^2 \leq C_\pi \quad \text{for all } |\mathbf{n}| \in \mathbf{L}^2(\Omega) \text{ with } \mathbf{n} \leq 1 \text{ a.e. in } \Omega, \quad (6.2.5)$$

with an \mathbf{n} -independent constant $C_\pi > 0$ and assume weak convergence of the initial data, i.e. $\mathbf{m}_h^0 \rightharpoonup \mathbf{m}^0, \mathbf{u}_h^0 \rightharpoonup \mathbf{u}^0$ in $\mathbf{H}^1(\Omega)$, as well as $\dot{\mathbf{u}}_h^0 \rightharpoonup \dot{\mathbf{u}}^0$ in $\mathbf{L}^2(\Omega)$ as $h \rightarrow 0$. Under these assumptions, we have strong $\mathbf{L}^2(\Omega_T)$ -convergence of \mathbf{m}_{hk}^- towards some function $\mathbf{m} \in \mathbf{H}^1(\Omega_T)$.

(b) Suppose that, in addition to the above assumptions, we have

$$\pi(\mathbf{m}_{hk}^-) \rightharpoonup \pi(\mathbf{m}) \quad \text{weakly subconvergent in } \mathbf{L}^2(\Omega_T). \quad (6.2.6)$$

Then, the computed FE solutions $(\mathbf{m}_{hk}, \mathbf{u}_{hk})$ are weakly subconvergent in $\mathbf{H}^1(\Omega_T) \times \mathbf{H}^1(\Omega_T)$ towards some functions (\mathbf{m}, \mathbf{u}) , and those weak limits (\mathbf{m}, \mathbf{u}) are a weak solution of LLG with magnetostriction. In particular, weak solutions exist and each weak accumulation point of $(\mathbf{m}_{hk}, \mathbf{u}_{hk})$ is a weak solution in the sense of Definition 6.1.2.

The proof follows exactly the same three steps as the one for pure LLG or coupling to the different variants of Maxwell's equations. Those three steps incorporate the classic convergence strategy that was also employed in the seminal works [BP06, Alo08a]. The approach here is, however, somewhat different, since including magnetostriction is less straightforward than e.g. the Maxwell system. For the MLLG system from Chapter 4 and the ELLG system from Chapter 5, the coupling of LLG and Maxwell's equations is simply done via $(\mathbf{H}_h^j, \mathbf{v}_h^j)$. In contrast to this, here the coupling operators between (6.2.2) and (6.2.3) are different, and therefore the equations cannot simply be inserted into each other. Consequently, boundedness has to be shown individually for both problems (Lemma 6.2.5 and Proposition 6.2.8 below.) The remainder is then finally estimated via Gronwall's lemma.

Step 1:

First, we show that the discrete quantities remain bounded. To that end, we take a closer look at the magnetostrictive contribution.

Lemma 6.2.4. *The discrete magnetostrictive component can be estimated by the total strain of the discrete displacement, i.e.*

$$\|\mathbf{h}_m(\mathbf{u}_h^\ell, \mathbf{m}_h^\ell)\|_{\mathbf{L}^2(\Omega)}^2 \leq C_{30} \|\boldsymbol{\varepsilon}(\mathbf{u}_h^\ell)\|_{\mathbf{L}^2(\Omega)}^2 + C_{31}, \quad (6.2.7)$$

for some constants $C_{30}, C_{31} > 0$ that depend only on $\bar{\lambda}$.

Proof. By definition of the magnetostrictive part, we immediately get

$$\|\mathbf{h}_m(\mathbf{u}_h^\ell, \mathbf{m}_h^\ell)\|_{\mathbf{L}^2(\Omega)}^2 \lesssim \bar{\lambda} \|\mathbf{m}_h^\ell\|_{\mathbf{L}^\infty(\Omega)}^2 \|\boldsymbol{\sigma}^\ell\|_{\mathbf{L}^2(\Omega)}^2 \lesssim \|\boldsymbol{\sigma}^\ell\|_{\mathbf{L}^2(\Omega)}^2$$

due to the normalization step. From the definition of the discrete stress tensor and the boundedness of the material tensors, we additionally get

$$\|\boldsymbol{\sigma}^\ell\|_{\mathbf{L}^2(\Omega)}^2 \lesssim \bar{\lambda} (\|\boldsymbol{\varepsilon}(\mathbf{u}_h^\ell)\|_{\mathbf{L}^2(\Omega)}^2 + \|\boldsymbol{\varepsilon}^m(\mathbf{m}_h^\ell)\|_{\mathbf{L}^2(\Omega)}^2) \lesssim \|\boldsymbol{\varepsilon}(\mathbf{u}_h^\ell)\|_{\mathbf{L}^2(\Omega)}^2 + C.$$

This yields the assertion. \square

With the result of the last lemma, we gain the following knowledge about the magnetization and its discrete derivative.

Lemma 6.2.5. *For $j = 1, \dots, N$, there holds*

$$\begin{aligned} \|\nabla \mathbf{m}_h^j\|_{\mathbf{L}^2(\Omega)}^2 + (\theta - \frac{1}{2})k^2 \sum_{\ell=0}^{j-1} \|\nabla \mathbf{v}_h^\ell\|_{\mathbf{L}^2(\Omega)}^2 + k \sum_{\ell=0}^{j-1} \|\mathbf{v}_h^\ell\|_{\mathbf{L}^2(\Omega)}^2 \\ \leq C_{32} (\|\nabla \mathbf{m}_h^0\|_{\mathbf{L}^2(\Omega)}^2 + k \sum_{\ell=0}^{j-1} \|\boldsymbol{\varepsilon}(\mathbf{u}_h^\ell)\|_{\mathbf{L}^2(\Omega)}^2 + C_{33}), \end{aligned} \quad (6.2.8)$$

for constants $C_{32}, C_{33} > 0$ that depend only on C_π as well as C_{30} and C_{31} from the previous lemma.

Proof. As before, in (6.2.2), we use the special test function $\varphi_h = \mathbf{v}_h^\ell \in \mathcal{K}_{\mathbf{m}_h^\ell}$ and exploit the angle condition (6.2.4) to see

$$\begin{aligned} \frac{1}{2} \|\nabla \mathbf{m}_h^{\ell+1}\|_{\mathbf{L}^2(\Omega)}^2 &\leq \frac{1}{2} \|\nabla \mathbf{m}_h^\ell\|_{\mathbf{L}^2(\Omega)}^2 + k(\nabla \mathbf{m}_h^\ell, \nabla \mathbf{v}_h^\ell) + \frac{k^2}{2} \|\nabla \mathbf{v}_h^\ell\|_{\mathbf{L}^2(\Omega)}^2 \\ &\leq \frac{1}{2} \|\nabla \mathbf{m}_h^\ell\|_{\mathbf{L}^2(\Omega)}^2 - (\theta - 1/2) k^2 \|\nabla \mathbf{v}_h^\ell\|_{\mathbf{L}^2(\Omega)}^2 \\ &\quad - \frac{\alpha k}{C_e} \|\mathbf{v}_h^\ell\|_{\mathbf{L}^2(\Omega)}^2 + \frac{k}{C_e} (\mathbf{h}_m(\mathbf{u}_h^\ell, \mathbf{m}_h^\ell), \mathbf{v}_h^\ell) + \frac{k}{C_e} (\boldsymbol{\pi}(\mathbf{m}_h^\ell), \mathbf{v}_h^\ell). \end{aligned} \quad (6.2.9)$$

Analogously to before, we sum up over the time intervals from 0 to $j-1$, which, in combination with Lemma 6.2.4 yields for any $\nu > 0$

$$\begin{aligned} \frac{1}{2} \|\nabla \mathbf{m}_h^j\|_{\mathbf{L}^2(\Omega)}^2 + \frac{k}{C_e} (\alpha - \nu) \sum_{\ell=0}^{j-1} \|\mathbf{v}_h^\ell\|_{\mathbf{L}^2(\Omega)}^2 + (\theta - \frac{1}{2}) k^2 \sum_{\ell=0}^{j-1} \|\nabla \mathbf{v}_h^\ell\|_{\mathbf{L}^2(\Omega)}^2 \\ \lesssim \frac{1}{2} \|\nabla \mathbf{m}_h^0\|_{\mathbf{L}^2(\Omega)}^2 + \frac{k C_{30}}{4 C_e \nu} \sum_{\ell=0}^{j-1} (\|\boldsymbol{\varepsilon}(\mathbf{u}_h^\ell)\|_{\mathbf{L}^2(\Omega)}^2 + C_{31}) + C_\pi \end{aligned}$$

Taking $\nu < \alpha$ thus yields the desired result. \square

Given the last two lemmata, we now aim to show boundedness of the discrete quantities involved in equation (6.2.3), i.e. boundedness of the discrete displacement approximations. We start with a two technical results concerning the material tensors and the magnetic part of the total strain.

Lemma 6.2.6. *There holds*

$$\|\boldsymbol{\lambda}^e A\|_{\mathbf{L}^2(\Omega)}^2 \leq C \|A\|_{\mathbf{L}^2(\Omega)}^2 \quad \text{and} \quad (6.2.10)$$

$$\|\boldsymbol{\lambda}^m A\|_{\mathbf{L}^2(\Omega)}^2 \leq C \|A\|_{\mathbf{L}^2(\Omega)}^2, \quad (6.2.11)$$

for all $A \in \mathbb{R}^{3 \times 3}$ and for a constant $C > 0$ that only depends on the entries of $\boldsymbol{\lambda}^e$ and $\boldsymbol{\lambda}^m$.

Proof. By definition, there holds

$$\begin{aligned} \|\boldsymbol{\lambda}^e A\|_{\mathbf{L}^2(\Omega)}^2 &= \sum_{i,j=1}^3 \|(\boldsymbol{\lambda}^e A)_{ij}\|_{\mathbf{L}^2(\Omega)}^2 \\ &= \sum_{i,j=1}^3 \left\| \sum_{k,l=1}^3 \lambda_{ijkl}^e A_{kl} \right\|_{\mathbf{L}^2(\Omega)}^2 \\ &\leq C \sum_{i,j=1}^3 \sum_{k,l=1}^3 \|A_{kl}\|_{\mathbf{L}^2(\Omega)}^2 \\ &\lesssim \|A\|_{\mathbf{L}^2(\Omega)}^2. \end{aligned}$$

This yields the first inequality. The second one follows verbatim. \square

Lemma 6.2.7. *The magnetic part of the total strain depends lipshitz-continuously on the magnetization, i.e. for any $k = 0, \dots, N-1$, there holds*

$$\|\boldsymbol{\varepsilon}^m(\mathbf{m}_h^{k+1}) - \boldsymbol{\varepsilon}^m(\mathbf{m}_h^k)\|_{\mathbf{L}^2(\Omega)} \leq C \|\mathbf{m}_h^{k+1} - \mathbf{m}_h^k\|_{\mathbf{L}^2(\Omega)}, \quad (6.2.12)$$

where the constant $C > 0$ depends only on $|\Omega|$.

Proof. We show the result componentwise for ε_{ij}^m . By definition, we have

$$\begin{aligned} \|\varepsilon_{ij}^m(\mathbf{m}_h^{k+1}) - \varepsilon_{ij}^m(\mathbf{m}_h^k)\|_{\mathbf{L}^2(\Omega)} &= \left\| \sum_{p\ell} \lambda_{ijp\ell}^m ((\mathbf{m}_h^{k+1})_p (\mathbf{m}_h^{k+1})_\ell - (\mathbf{m}_h^k)_p (\mathbf{m}_h^k)_\ell) \right\|_{\mathbf{L}^2(\Omega)} \\ &\sim \left\| \sum_{p\ell} ((\mathbf{m}_h^{k+1})_p (\mathbf{m}_h^{k+1})_\ell - (\mathbf{m}_h^k)_p (\mathbf{m}_h^k)_\ell) \right\|_{\mathbf{L}^2(\Omega)} \\ &= \left\| \sum_{p\ell} ((\mathbf{m}_h^{k+1})_p - (\mathbf{m}_h^k)_p) (\mathbf{m}_h^{k+1})_\ell + (\mathbf{m}_h^k)_p ((\mathbf{m}_h^{k+1})_\ell - (\mathbf{m}_h^k)_\ell) \right\|_{\mathbf{L}^2(\Omega)} \\ &= \left\| \sum_{p\ell} ((\mathbf{m}_h^{k+1})_p - (\mathbf{m}_h^k)_p) (\mathbf{m}_h^{k+1})_\ell + (\mathbf{m}_h^k)_p ((\mathbf{m}_h^{k+1})_\ell - (\mathbf{m}_h^k)_\ell) \right\|_{\mathbf{L}^2(\Omega)} \\ &\leq \sum_{p\ell} (\|(\mathbf{m}_h^{k+1})_p - (\mathbf{m}_h^k)_p\|_{\mathbf{L}^2(\Omega)} + \|(\mathbf{m}_h^{k+1})_\ell - (\mathbf{m}_h^k)_\ell\|_{\mathbf{L}^2(\Omega)}) \\ &= \sum_p (\|(\mathbf{m}_h^{k+1})_p - (\mathbf{m}_h^k)_p\|_{\mathbf{L}^2(\Omega)} + \|(\mathbf{m}_h^{k+1})_1 - (\mathbf{m}_h^k)_1\|_{\mathbf{L}^2(\Omega)} \\ &\quad + \|(\mathbf{m}_h^{k+1})_2 - (\mathbf{m}_h^k)_2\|_{\mathbf{L}^2(\Omega)} + \|(\mathbf{m}_h^{k+1})_3 - (\mathbf{m}_h^k)_3\|_{\mathbf{L}^2(\Omega)}) \\ &\sim \|\mathbf{m}_h^{k+1} - \mathbf{m}_h^k\|_{\mathbf{L}^2(\Omega)}. \end{aligned}$$

Here, we only exploited the uniform boundedness of \mathbf{m}_h^k and \mathbf{m}_h^{k+1} , i.e. $\|\mathbf{m}_h^k\|_{\mathbf{L}^\infty(\Omega)} = 1$ for any $k \in 0, \dots, N-1$. \square

The statement of the following result is basically found in [BS06, Lemma 3]. There, however, the focus is on strong solutions of LLG and a different integrator, so that the proof and the overall analysis differs.

Proposition 6.2.8. *For any $j = 1, \dots, N$ and $\frac{1}{2} \leq \theta \leq 1$, there holds*

$$\|d_t \mathbf{u}_h^j\|_{\mathbf{L}^2(\Omega)}^2 + \sum_{\ell=1}^j \|d_t \mathbf{u}_h^\ell - d_t \mathbf{u}_h^{\ell-1}\|_{\mathbf{L}^2(\Omega)}^2 + \|\boldsymbol{\varepsilon}(\mathbf{u}_h^j)\|_{\mathbf{L}^2(\Omega)}^2 + \sum_{\ell=1}^j \|\boldsymbol{\varepsilon}(\mathbf{u}_h^\ell) - \boldsymbol{\varepsilon}(\mathbf{u}_h^{\ell-1})\|_{\mathbf{L}^2(\Omega)}^2 \leq C_{34} \quad (6.2.13)$$

for some h and k independent constant $C_{34} > 0$ which depends only on $\boldsymbol{\lambda}^*$ and the constants C_{32} and C_{33} from Lemma 6.2.5.

Proof. We use $\boldsymbol{\psi}_h = \mathbf{u}_h^{\ell+1} - \mathbf{u}_h^\ell$ as test function in (6.2.3) and sum up for $\ell = 0, \dots, j-1$ to see

$$\varrho(d_t \mathbf{u}_h^{\ell+1} - d_t \mathbf{u}_h^\ell, d_t \mathbf{u}_h^{\ell+1}) + (\boldsymbol{\lambda}^e \boldsymbol{\varepsilon}(\mathbf{u}_h^{\ell+1}), \boldsymbol{\varepsilon}(\mathbf{u}_h^{\ell+1}) - \boldsymbol{\varepsilon}(\mathbf{u}_h^\ell)) = (\boldsymbol{\lambda}^e \boldsymbol{\varepsilon}^m(\mathbf{m}_h^{\ell+1}), \boldsymbol{\varepsilon}(\mathbf{u}_h^{\ell+1}) - \boldsymbol{\varepsilon}(\mathbf{u}_h^\ell)).$$

Abel's summation from Lemma A.1.3 in combination with the positive definiteness (6.1.7) and symmetry of λ^e now yields

$$\begin{aligned} & \|d_t \mathbf{u}_h^j\|_{L^2(\Omega)}^2 + \sum_{\ell=1}^j \|d_t \mathbf{u}_h^\ell - d_t \mathbf{u}_h^{\ell-1}\|_{L^2(\Omega)}^2 + \|\boldsymbol{\varepsilon}(\mathbf{u}_h^j)\|_{L^2(\Omega)}^2 + \sum_{\ell=1}^j \|\boldsymbol{\varepsilon}(\mathbf{u}_h^\ell) - \boldsymbol{\varepsilon}(\mathbf{u}_h^{\ell-1})\|_{L^2(\Omega)}^2 \\ & \leq \tilde{C} + C \sum_{\ell=1}^j (\lambda^e \boldsymbol{\varepsilon}^m(\mathbf{m}_h^\ell), \boldsymbol{\varepsilon}(\mathbf{u}_h^\ell) - \boldsymbol{\varepsilon}(\mathbf{u}_h^{\ell-1})), \end{aligned}$$

for some generic constants $C, \tilde{C} > 0$. Note that the terms $\|d_t \mathbf{u}_h^0\|_{L^2(\Omega)}^2 = \|\dot{\mathbf{u}}_h^0\|_{L^2(\Omega)}^2$ and $\|\boldsymbol{\varepsilon}(\mathbf{u}_h^0)\|_{L^2(\Omega)}^2$ are uniformly bounded due to the assumed convergence of these initial data and are hidden in the constant \tilde{C} .

Next, we rewrite the sum on the right-hand side as

$$\begin{aligned} & \sum_{\ell=1}^j (\lambda^e \boldsymbol{\varepsilon}^m(\mathbf{m}_h^\ell), \boldsymbol{\varepsilon}(\mathbf{u}_h^\ell) - \boldsymbol{\varepsilon}(\mathbf{u}_h^{\ell-1})) \\ & = (\lambda^e \boldsymbol{\varepsilon}^m(\mathbf{m}_h^j), \boldsymbol{\varepsilon}(\mathbf{u}_h^j)) - (\lambda^e \boldsymbol{\varepsilon}^m(\mathbf{m}_h^1), \boldsymbol{\varepsilon}(\mathbf{u}_h^0)) - \sum_{\ell=1}^{j-1} (\lambda^e \boldsymbol{\varepsilon}^m(\mathbf{m}_h^{\ell+1}) - \lambda^e \boldsymbol{\varepsilon}^m(\mathbf{m}_h^\ell), \boldsymbol{\varepsilon}(\mathbf{u}_h^\ell)) \\ & = (\lambda^e \boldsymbol{\varepsilon}^m(\mathbf{m}_h^j), \boldsymbol{\varepsilon}(\mathbf{u}_h^j)) - (\lambda^e \boldsymbol{\varepsilon}^m(\mathbf{m}_h^1), \boldsymbol{\varepsilon}(\mathbf{u}_h^0)) - k \sum_{\ell=1}^{j-1} (\lambda^e d_t \boldsymbol{\varepsilon}^m(\mathbf{m}_h^{\ell+1}), \boldsymbol{\varepsilon}(\mathbf{u}_h^\ell)). \end{aligned}$$

For any $\eta > 0$ and with Lemma 6.2.6, we further get

$$\begin{aligned} & \|d_t \mathbf{u}_h^j\|_{L^2(\Omega)}^2 + \sum_{\ell=1}^j \|d_t \mathbf{u}_h^\ell - d_t \mathbf{u}_h^{\ell-1}\|_{L^2(\Omega)}^2 + \|\boldsymbol{\varepsilon}(\mathbf{u}_h^j)\|_{L^2(\Omega)}^2 + \sum_{\ell=1}^j \|\boldsymbol{\varepsilon}(\mathbf{u}_h^\ell) - \boldsymbol{\varepsilon}(\mathbf{u}_h^{\ell-1})\|_{L^2(\Omega)}^2 \\ & \lesssim 1 + k \sum_{\ell=1}^{j-1} \|d_t \boldsymbol{\varepsilon}^m(\mathbf{m}_h^{\ell+1})\|_{L^2(\Omega)}^2 + k \sum_{\ell=1}^{j-1} \|\boldsymbol{\varepsilon}(\mathbf{u}_h^\ell)\|_{L^2(\Omega)}^2 + \frac{1}{4\eta} \|\boldsymbol{\varepsilon}^m(\mathbf{m}_h^j)\|_{L^2(\Omega)}^2 \\ & \quad + \eta \|\boldsymbol{\varepsilon}(\mathbf{u}_h^j)\|_{L^2(\Omega)}^2 + \|\boldsymbol{\varepsilon}^m(\mathbf{m}_h^1)\|_{L^2(\Omega)}^2 + \|\boldsymbol{\varepsilon}(\mathbf{u}_h^0)\|_{L^2(\Omega)}^2. \end{aligned}$$

For sufficiently small η , this can be simplified to

$$\begin{aligned} & \|d_t \mathbf{u}_h^j\|_{L^2(\Omega)}^2 + \sum_{\ell=1}^j \|d_t \mathbf{u}_h^\ell - d_t \mathbf{u}_h^{\ell-1}\|_{L^2(\Omega)}^2 + \|\boldsymbol{\varepsilon}(\mathbf{u}_h^j)\|_{L^2(\Omega)}^2 + \sum_{\ell=1}^j \|\boldsymbol{\varepsilon}(\mathbf{u}_h^\ell) - \boldsymbol{\varepsilon}(\mathbf{u}_h^{\ell-1})\|_{L^2(\Omega)}^2 \\ & \lesssim 1 + k \left(\sum_{\ell=1}^{j-1} \|d_t \boldsymbol{\varepsilon}^m(\mathbf{m}_h^{\ell+1})\|_{L^2(\Omega)}^2 + \sum_{\ell=1}^{j-1} \|\boldsymbol{\varepsilon}(\mathbf{u}_h^\ell)\|_{L^2(\Omega)}^2 \right). \end{aligned}$$

Here, we again used convergence of the initial data. Next, Lemma 6.2.7 yields

$$\|d_t \boldsymbol{\varepsilon}^m(\mathbf{m}_h^\ell)\|_{L^2(\Omega)}^2 \lesssim \|d_t \mathbf{m}_h^\ell\|_{L^2(\Omega)}^2.$$

In combination with

$$\|d_t \mathbf{m}_h^\ell\|_{L^2(\Omega)}^2 = \left\| \frac{\mathbf{m}_h^\ell - \mathbf{m}_h^{\ell-1}}{k} \right\|_{L^2(\Omega)}^2 \leq \|\mathbf{v}_h^{\ell-1}\|_{L^2(\Omega)}^2,$$

from Lemma 2.2.3, this results in

$$\begin{aligned} & \|d_t \mathbf{u}_h^j\|_{L^2(\Omega)}^2 + \sum_{\ell=1}^j \|d_t \mathbf{u}_h^\ell - d_t \mathbf{u}_h^{\ell-1}\|_{L^2(\Omega)}^2 + \|\boldsymbol{\varepsilon}(\mathbf{u}_h^j)\|_{L^2(\Omega)}^2 + \sum_{\ell=1}^j \|\boldsymbol{\varepsilon}(\mathbf{u}_h^\ell) - \boldsymbol{\varepsilon}(\mathbf{u}_h^{\ell-1})\|_{L^2(\Omega)}^2 \\ & \lesssim 1 + k \left(\sum_{\ell=1}^{j-1} \|\mathbf{v}_h^\ell\|_{L^2(\Omega)}^2 + \sum_{\ell=1}^{j-1} \|\boldsymbol{\varepsilon}(\mathbf{u}_h^\ell)\|_{L^2(\Omega)}^2 \right). \end{aligned}$$

Next, we apply Lemma 6.2.5 to see

$$\begin{aligned} & \|d_t \mathbf{u}_h^j\|_{L^2(\Omega)}^2 + \sum_{\ell=1}^j \|d_t \mathbf{u}_h^\ell - d_t \mathbf{u}_h^{\ell-1}\|_{L^2(\Omega)}^2 + \|\boldsymbol{\varepsilon}(\mathbf{u}_h^j)\|_{L^2(\Omega)}^2 + \sum_{\ell=1}^j \|\boldsymbol{\varepsilon}(\mathbf{u}_h^\ell) - \boldsymbol{\varepsilon}(\mathbf{u}_h^{\ell-1})\|_{L^2(\Omega)}^2 \\ & \lesssim 1 + (\|\nabla \mathbf{m}_h^0\|_{L^2(\Omega)}^2 + k \sum_{\ell=0}^{j-1} \|\boldsymbol{\varepsilon}(\mathbf{u}_h^\ell)\|_{L^2(\Omega)}^2 + k \sum_{\ell=1}^{j-1} \|\boldsymbol{\varepsilon}(\mathbf{u}_h^\ell)\|_{L^2(\Omega)}^2) \\ & \lesssim 1 + k \sum_{\ell=0}^{j-1} \|\boldsymbol{\varepsilon}(\mathbf{u}_h^\ell)\|_{L^2(\Omega)}^2. \end{aligned}$$

Application of a discrete version of Gronwall's Lemma A.1.2 finally yields the assertion. \square

In order to show the desired $\mathbf{H}^1(\Omega_T)$ -convergence of \mathbf{u} , we still need to show uniform boundedness of the $\mathbf{L}^2(\Omega_T)$ -part. This result is stated in the next corollary.

Corollary 6.2.9. *Due to the boundary conditions employed, the Poincaré inequality in combination with Korn's inequality shows*

$$\begin{aligned} \|\mathbf{u}_h^j\|_{L^2(\Omega)}^2 + \sum_{\ell=1}^j \|\mathbf{u}_h^\ell - \mathbf{u}_h^{\ell-1}\|_{L^2(\Omega)}^2 & \leq C_{35} (\|\nabla \mathbf{u}_h^j\|_{L^2(\Omega)}^2 + \sum_{\ell=1}^j \|\nabla(\mathbf{u}_h^\ell - \mathbf{u}_h^{\ell-1})\|_{L^2(\Omega)}^2) \\ & \leq C_{35} (\|\boldsymbol{\varepsilon}(\mathbf{u}_h^j)\|_{L^2(\Omega)}^2 + \sum_{\ell=1}^j \|\boldsymbol{\varepsilon}(\mathbf{u}_h^\ell - \mathbf{u}_h^{\ell-1})\|_{L^2(\Omega)}^2) \end{aligned} \quad (6.2.14)$$

for any $j = 1, \dots, N$, where the constant $C_{35} > 0$ stems from Poincaré's inequality and thus only depends on the diameter of Ω . According to Proposition 6.2.8, the right-hand side of (6.2.14) is uniformly bounded. \square

Proposition 6.2.8 now immediately yields boundedness of the discrete magnetizations.

Corollary 6.2.10. *For any $j = 1, \dots, N$, there holds*

$$\|\nabla \mathbf{m}_h^j\|_{L^2(\Omega)}^2 + k \sum_{\ell=0}^{j-1} \|\mathbf{v}_h^\ell\|_{L^2(\Omega)}^2 + \left(\theta - \frac{1}{2}\right) k^2 \sum_{\ell=0}^{j-1} \|\nabla \mathbf{v}_h^\ell\|_{L^2(\Omega)}^2 \leq C_{36} \quad (6.2.15)$$

for some constant $C_{36} > 0$ which depends only on C_{32} , C_{33} , and C_{34} .

Proof. From Lemma 6.2.5, we get

$$\begin{aligned} & \|\nabla \mathbf{m}_h^j\|_{L^2(\Omega)}^2 + \left(\theta - \frac{1}{2}\right) k^2 \sum_{\ell=0}^{j-1} \|\nabla \mathbf{v}_h^\ell\|_{L^2(\Omega)}^2 + k \sum_{\ell=0}^{j-1} \|\mathbf{v}_h^\ell\|_{L^2(\Omega)}^2 \\ & \leq C_{32} (\|\nabla \mathbf{m}_h^0\|_{L^2(\Omega)}^2 + k \sum_{\ell=0}^{j-1} \|\boldsymbol{\varepsilon}(\mathbf{u}_h^\ell)\|_{L^2(\Omega)}^2 + C_{33}), \end{aligned}$$

By utilizing Proposition 6.2.8, we see $k \sum_{\ell=0}^{j-1} \|\varepsilon(\mathbf{u}_h^\ell)\|_{\mathbf{L}^2(\Omega)}^2 \leq |T|C_{34}$. The uniform boundedness of $\|\nabla \mathbf{m}_h^0\|_{\mathbf{L}^2(\Omega)}$ concludes the proof. \square

Step 2:

Next, we deduce the existence of convergent subsequences.

Lemma 6.2.11. *Let $1/2 \leq \theta \leq 1$. Then, there exist functions $(\mathbf{m}, \mathbf{u}, \dot{\mathbf{u}}) \in \mathbf{H}^1(\Omega_T, \mathbb{S}^2) \times \mathbf{H}^1(\Omega_T) \times \mathbf{L}^2(\Omega_T)$ such that*

$$\mathbf{m}_{hk} \xrightarrow{\text{sub}} \mathbf{m} \text{ in } \mathbf{H}^1(\Omega_T) \quad (6.2.16a)$$

$$\mathbf{m}_{hk}, \mathbf{m}_{hk}^\pm \xrightarrow{\text{sub}} \mathbf{m} \text{ in } \mathbf{L}^2(\mathbf{H}^1), \quad (6.2.16b)$$

$$\mathbf{m}_{hk}, \mathbf{m}_{hk}^\pm \xrightarrow{\text{sub}} \mathbf{m} \text{ in } \mathbf{L}^2(\Omega_T) \quad (6.2.16c)$$

$$\mathbf{m}_{hk}, \mathbf{m}_{hk}^\pm \xrightarrow{\text{sub}} \mathbf{m} \text{ pointwise almost everywhere in } \Omega_T, \quad (6.2.16d)$$

$$\mathbf{u}_{hk} \xrightarrow{\text{sub}} \mathbf{u} \text{ in } \mathbf{H}^1(\Omega_T) \quad (6.2.16e)$$

$$\mathbf{u}_{hk}, \mathbf{u}_{hk}^\pm \xrightarrow{\text{sub}} \mathbf{u} \text{ in } \mathbf{L}^2(\mathbf{H}^1), \quad (6.2.16f)$$

$$\mathbf{u}_{hk}, \mathbf{u}_{hk}^\pm \xrightarrow{\text{sub}} \mathbf{u} \text{ in } \mathbf{L}^2(\Omega_T) \quad (6.2.16g)$$

$$\dot{\mathbf{u}}_{hk}, \dot{\mathbf{u}}_{hk}^\pm \xrightarrow{\text{sub}} \dot{\mathbf{u}} \text{ in } \mathbf{L}^2(\Omega_T). \quad (6.2.16h)$$

Here, the convergence is to be understood for a subsequence of the corresponding sequences which is successively constructed, i.e. for arbitrary spatial mesh-size $h \rightarrow 0$ and time step-size $k \rightarrow 0$, there exist subindices h_n, k_n , for which the above convergence properties are satisfied simultaneously. In addition, there holds

$$\mathbf{v}_{hk}^- \xrightarrow{\text{sub}} \mathbf{m}_t \text{ in } \mathbf{L}^2(\Omega_T) \quad (6.2.17)$$

again for the same subsequence as above.

Proof. From Proposition 6.2.8, Corollary 6.2.9, and Corollary 6.2.10, we see that

$$\begin{aligned} \sum_{\ell=0}^{j-1} \|\mathbf{m}_h^{\ell+1} - \mathbf{m}_h^\ell\|_{\mathbf{L}^2(\Omega)}^2 &+ \sum_{\ell=0}^{j-1} \|\mathbf{u}_h^{\ell+1} - \mathbf{u}_h^\ell\|_{\mathbf{L}^2(\Omega)}^2 \\ &+ \sum_{\ell=0}^{j-1} \|\varepsilon(\mathbf{u}_h^{\ell+1}) - \varepsilon(\mathbf{u}_h^\ell)\|_{\mathbf{L}^2(\Omega)}^2 + \sum_{\ell=0}^{j-1} \|\mathbf{d}_t(\mathbf{u}_h^{\ell+1}) - \mathbf{d}_t(\mathbf{u}_h^\ell)\|_{\mathbf{L}^2(\Omega)}^2 \end{aligned}$$

is uniformly bounded. For the first sum, we used the inequality

$$\|\mathbf{m}_h^{\ell+1} - \mathbf{m}_h^\ell\|_{\mathbf{L}^2(\Omega)}^2 \leq C_v^2 k^2 \|\mathbf{v}_h^\ell\|_{\mathbf{L}^2(\Omega)}^2$$

from Lemma 2.2.3. Boundedness of the discrete quantities from Proposition 6.2.8, Corollary 6.2.9, and Corollary 6.2.10 and verbatim analysis from the previous chapters thus show the \mathbf{L}^2 - and \mathbf{H}^1 -convergence properties. By use of the Weyl theorem, we may extract yet another subsequence of $\mathbf{m}_{hk}, \mathbf{m}_{hk}^\pm$ to see pointwise convergence, i.e. (6.2.16d). Finally, the length preservation constraint follows as before and the identification of the limit of \mathbf{v} from Lemma 2.3.6. \square

Step 3:

In the remainder of this chapter, we will prove that the limiting tuple (\mathbf{m}, \mathbf{u}) is indeed a weak solution in the sense of Definition 6.1.2.

Proof of Theorem 6.2.3. Let $(\boldsymbol{\zeta}, \boldsymbol{\psi}) \in C^\infty(\Omega_T) \times C_c^\infty([0, T]; C_c^\infty(\Omega))$ be arbitrary. We define testfunctions by $(\boldsymbol{\varphi}_h, \boldsymbol{\psi}_h)(t, \cdot) := (\mathcal{I}_h(\mathbf{m}_{hk}^- \times \boldsymbol{\zeta}), \mathcal{I}_h \boldsymbol{\psi})(t, \cdot)$. We integrate equation (6.2.2) in time to obtain

$$\begin{aligned} \alpha \int_0^T (\mathbf{v}_{hk}^-, \boldsymbol{\varphi}_h) + \int_0^T ((\mathbf{m}_{hk}^- \times \mathbf{v}_{hk}^-), \boldsymbol{\varphi}_h) &= -C_e \int_0^T (\nabla(\mathbf{m}_{hk}^- + \theta k \mathbf{v}_{hk}^-), \nabla \boldsymbol{\varphi}_h) \\ &+ \int_0^T (\mathbf{h}_m(\mathbf{u}_{hk}^-, \mathbf{m}_{hk}^-), \boldsymbol{\varphi}_h) + \int_0^T (\boldsymbol{\pi}(\mathbf{m}_{hk}^-), \boldsymbol{\varphi}_h), \end{aligned}$$

where the magnetostrictive component is again given by

$$[\mathbf{h}_m(\mathbf{u}_{hk}^-, \mathbf{m}_{hk}^-)]_\ell := \sum_{i,j,p} \lambda_{ijpq}^m \sigma^{hk} i j (\mathbf{m}_{hk}^-)_p, \quad \text{with} \quad \sigma^{hk} = \boldsymbol{\lambda}^e(\boldsymbol{\varepsilon}(\mathbf{u}_{hk}^-) - \boldsymbol{\varepsilon}^m(\mathbf{m}_{hk}^-)).$$

As before, the definition $\boldsymbol{\varphi}_h(t, \cdot) := \mathcal{I}_h(\mathbf{m}_{hk}^- \times \boldsymbol{\zeta})(t, \cdot)$ and the approximation properties of the nodal interpolation operator show

$$\begin{aligned} \int_0^T ((\alpha \mathbf{v}_{hk}^- + \mathbf{m}_{hk}^- \times \mathbf{v}_{hk}^-), (\mathbf{m}_{hk}^- \times \boldsymbol{\zeta})) + k \theta \int_0^T (\nabla \mathbf{v}_{hk}^-, \nabla(\mathbf{m}_{hk}^- \times \boldsymbol{\zeta})) \\ + C_e \int_0^T (\nabla \mathbf{m}_{hk}^-, \nabla(\mathbf{m}_{hk}^- \times \boldsymbol{\zeta})) \\ - \int_0^T (\mathbf{h}_m(\mathbf{u}_{hk}^-, \mathbf{m}_{hk}^-), (\mathbf{m}_{hk}^- \times \boldsymbol{\zeta})) \\ - \int_0^T (\boldsymbol{\pi}(\mathbf{m}_{hk}^-), (\mathbf{m}_{hk}^- \times \boldsymbol{\zeta})) \\ = \mathcal{O}(h), \end{aligned}$$

and we estimate the first three terms on the left hand side as above. Next, the weak convergence of $\boldsymbol{\pi}(\mathbf{m}_{hk}^-)$ from (6.2.6) yields

$$\int_0^T (\boldsymbol{\pi}(\mathbf{m}_{hk}^-), (\mathbf{m}_{hk}^- \times \boldsymbol{\zeta})) \longrightarrow \int_0^T (\boldsymbol{\pi}(\mathbf{m}), (\mathbf{m} \times \boldsymbol{\zeta})),$$

and it therefore only remains to consider the magnetostrictive component. Here, we have to show

$$\mathbf{h}_m(\mathbf{u}_{hk}^-, \mathbf{m}_{hk}^-) \xrightarrow{\text{sub}} \mathbf{h}_m(\mathbf{u}, \mathbf{m}) \quad \text{weakly in } L^2(\Omega_T),$$

where it obviously suffices to show the desired property componentwise. A straightforward computation analogously to Lemma 6.2.7 proves

$$\|\boldsymbol{\varepsilon}^m(\mathbf{m}_{hk}^-) - \boldsymbol{\varepsilon}^m(\mathbf{m})\|_{L^2(\Omega_T)}^2 \lesssim \|\mathbf{m}_{hk}^- - \mathbf{m}\|_{L^2(\Omega_T)}^2$$

The pointwise convergence of \mathbf{m}_{hk}^- from (6.2.16d) in combination with Lebesgue's dominated convergence theorem, now yields the strong convergence $\mathbf{m}_{hk}^- \boldsymbol{\zeta} \rightarrow \mathbf{m} \boldsymbol{\zeta}$ (which even holds componentwise for any set of indices). For any indices $i, j, p, \ell = 1, 2, 3$ this shows

$$((\boldsymbol{\varepsilon}^m(\mathbf{m}_{hk}^-))_{ij}(\mathbf{m}_{hk}^-)_p, \boldsymbol{\zeta}_\ell) \longrightarrow (\boldsymbol{\varepsilon}^m(\mathbf{m})_{ij} \mathbf{m}_p, \boldsymbol{\zeta}_\ell).$$

By definition of the magnetostrictive component it therefore only remains to show

$$(\boldsymbol{\varepsilon}(\mathbf{u}_{hk}^-))_{ij}(\mathbf{m}_{hk}^-)_p \xrightarrow{\text{sub}} \boldsymbol{\varepsilon}(\mathbf{u})_{ij} \mathbf{m}_p \quad \text{weakly in } \mathbf{L}^2(\Omega_T)$$

for any combination $i, j, p = 1, 2, 3$ of indices. Analogously to above, this can be seen by

$$((\boldsymbol{\varepsilon}(\mathbf{u}_{hk}^-))_{ij}(\mathbf{m}_{hk}^-)_p, \boldsymbol{\zeta}_\ell) = (\boldsymbol{\varepsilon}(\mathbf{u}_{hk}^-)_{ij}, (\mathbf{m}_{hk}^-)_p \boldsymbol{\zeta}_\ell) \xrightarrow{\text{sub}} (\boldsymbol{\varepsilon}(\mathbf{u})_{ij}, \mathbf{m}_p \boldsymbol{\zeta}_\ell) = (\boldsymbol{\varepsilon}(\mathbf{u})_{ij} \mathbf{m}_p, \boldsymbol{\zeta}_\ell)$$

for all $\boldsymbol{\zeta} \in C^\infty(\Omega_T)$, where the convergence of $\boldsymbol{\varepsilon}(\mathbf{u}_{hk}^-)$ towards $\boldsymbol{\varepsilon}(\mathbf{u})$ particularly follows from the convergence of \mathbf{u}_{hk}^- towards \mathbf{u} in $L^2(\mathbf{H}^1)$. So far, we have thus proved

$$\begin{aligned} \int_0^T ((\alpha \mathbf{m}_t + \mathbf{m} \times \mathbf{m}_t), (\mathbf{m} \times \boldsymbol{\zeta})) &= -C_e \int_0^T (\nabla \mathbf{m}, \nabla(\mathbf{m} \times \boldsymbol{\zeta})) \\ &\quad + \int_0^T (\mathbf{h}_m(\mathbf{u}, \mathbf{m}), (\mathbf{m} \times \boldsymbol{\zeta})) + \int_0^T (\boldsymbol{\pi}(\mathbf{m}), (\mathbf{m} \times \boldsymbol{\zeta})), \end{aligned}$$

and we conclude (6.1.11) with the standard arguments from above. Again, the equality $\mathbf{m}(0, \cdot) = \mathbf{m}^0$ in the trace sense follows from the weak convergence $\mathbf{m}_{hk} \rightharpoonup \mathbf{m}$ in $\mathbf{H}^1(\Omega_T)$ and thus weak convergence of the traces. The equality $\mathbf{u}(0, \cdot) = \mathbf{u}^0$ follows analogously.

In order to prove (6.1.12), we argue similarly. From (6.2.3), we obtain

$$\int_0^T ((\dot{\mathbf{u}}_{hk})_t, \boldsymbol{\psi}_h) + \int_0^T (\boldsymbol{\lambda}^e \boldsymbol{\varepsilon}(\mathbf{u}_{hk}^+), \boldsymbol{\varepsilon}(\boldsymbol{\psi}_h)) = \int_0^T (\boldsymbol{\lambda}^e \boldsymbol{\varepsilon}^m(\mathbf{m}_{hk}^+), \boldsymbol{\varepsilon}(\boldsymbol{\psi}_h)).$$

For the first summand on the left-hand side, we perform integration by parts in time and get

$$\int_0^T ((\dot{\mathbf{u}}_{hk})_t, \boldsymbol{\psi}_h) = - \int_0^T (\dot{\mathbf{u}}_{hk}, (\boldsymbol{\psi}_h)_t) + \underbrace{(\dot{\mathbf{u}}_{hk}(T, \cdot), \boldsymbol{\psi}_h(T, \cdot))}_{=0} - \underbrace{(\dot{\mathbf{u}}_{hk}(0, \cdot), \boldsymbol{\psi}_h(0, \cdot))}_{=\dot{\mathbf{u}}_h^0}.$$

Passing to the limit $(h, k) \rightarrow 0$, we see

$$\int_0^T ((\dot{\mathbf{u}}_{hk})_t, \boldsymbol{\psi}_h) \xrightarrow{\text{sub}} - \int_0^T (\dot{\mathbf{u}}, \boldsymbol{\psi}_t) - (\dot{\mathbf{u}}(0, \cdot), \boldsymbol{\psi}(0, \cdot)).$$

Here, we have used the assumed convergence of the initial data. It remains to identify the limiting function $\dot{\mathbf{u}}$. From (6.2.16h) and the definition of $\dot{\mathbf{u}}_{hk}^+$, we get $\dot{\mathbf{u}}_{hk}^+ = \partial_t \mathbf{u}_{hk}$, and therefore, by use of weak lower semi-continuity, conclude

$$\|\dot{\mathbf{u}} - \partial_t \mathbf{u}\|_{\mathbf{L}^2(\Omega_T)}^2 \leq \liminf_{(h,k) \rightarrow (0,0)} \|\dot{\mathbf{u}}_{hk}^+ - \partial_t \mathbf{u}_{hk}\|_{\mathbf{L}^2(\Omega_T)}^2 = 0$$

whence $\dot{\mathbf{u}} = \partial_t \mathbf{u}$ almost everywhere in Ω_T . The convergence of the terms

$$\begin{aligned} \int_0^T (\boldsymbol{\lambda}^e \boldsymbol{\varepsilon}(\mathbf{u}_{hk}^+), \boldsymbol{\varepsilon}(\boldsymbol{\psi}_h)) &\xrightarrow{\text{sub}} \int_0^T (\boldsymbol{\lambda}^e \boldsymbol{\varepsilon}(\mathbf{u}), \boldsymbol{\varepsilon}(\boldsymbol{\psi})) \quad \text{and} \\ \int_0^T (\boldsymbol{\lambda}^e \boldsymbol{\varepsilon}^m(\mathbf{m}_{hk}^+), \boldsymbol{\varepsilon}(\boldsymbol{\psi}_h)) &\xrightarrow{\text{sub}} \int_0^T (\boldsymbol{\lambda}^e \boldsymbol{\varepsilon}^m(\mathbf{m}), \boldsymbol{\varepsilon}(\boldsymbol{\psi})) \end{aligned}$$

is straightforward. In summary, we have thus shown (6.1.12).

Finally, standard techniques show the energy estimate (6.1.13). From the discrete energy estimates (6.2.13) and (6.2.15), in combination with Korn's inequality, we get for any $t' \in [0, T]$ with $t' \in [t_\ell, t_{\ell+1})$

$$\begin{aligned}
 & \|\nabla \mathbf{m}_{hk}^+(t')\|_{\mathbf{L}^2(\Omega)}^2 + \|\mathbf{v}_{hk}^-\|_{\mathbf{L}^2(\Omega_{t'})}^2 + \|\nabla \mathbf{u}_{hk}^+(t')\|_{\mathbf{L}^2(\Omega)}^2 + \|\dot{\mathbf{u}}_{hk}^+(t')\|_{\mathbf{L}^2(\Omega)}^2 \\
 &= \|\nabla \mathbf{m}_{hk}^+(t')\|_{\mathbf{L}^2(\Omega)}^2 + \int_0^{t'} \|\mathbf{v}_{hk}^-(t)\|_{\mathbf{L}^2(\Omega)}^2 + \|\nabla \mathbf{u}_{hk}^+(t')\|_{\mathbf{L}^2(\Omega)}^2 + \|\dot{\mathbf{u}}_{hk}^+(t')\|_{\mathbf{L}^2(\Omega)}^2 \\
 &\leq \|\nabla \mathbf{m}_{hk}^+(t')\|_{\mathbf{L}^2(\Omega)}^2 + \int_0^{t_{\ell+1}} \|\mathbf{v}_{hk}^-(t)\|_{\mathbf{L}^2(\Omega)}^2 + \|\nabla \mathbf{u}_{hk}^+(t')\|_{\mathbf{L}^2(\Omega)}^2 + \|\dot{\mathbf{u}}_{hk}^+(t')\|_{\mathbf{L}^2(\Omega)}^2 \\
 &\leq \tilde{C},
 \end{aligned}$$

for some constant \tilde{C} which is independent of h and k . Integration in time thus yields for any measurable set $\mathfrak{J} \subseteq [0, T]$

$$\int_{\mathfrak{J}} \|\nabla \mathbf{m}_{hk}^+(t')\|_{\mathbf{L}^2(\Omega)}^2 + \int_{\mathfrak{J}} \|\mathbf{v}_{hk}^-\|_{\mathbf{L}^2(\Omega_{t'})}^2 + \int_{\mathfrak{J}} \|\nabla \mathbf{u}_{hk}^+(t')\|_{\mathbf{L}^2(\Omega)}^2 + \int_{\mathfrak{J}} \|\dot{\mathbf{u}}_{hk}^+(t')\|_{\mathbf{L}^2(\Omega)}^2 \leq \int_{\mathfrak{J}} \tilde{C}.$$

Weak semi-continuity now shows

$$\int_{\mathfrak{J}} \|\nabla \mathbf{m}(t')\|_{\mathbf{L}^2(\Omega)}^2 + \int_{\mathfrak{J}} \|\mathbf{m}_t\|_{\mathbf{L}^2(\Omega_{t'})}^2 + \int_{\mathfrak{J}} \|\nabla \mathbf{u}(t')\|_{\mathbf{L}^2(\Omega)}^2 + \int_{\mathfrak{J}} \|\mathbf{u}_t(t')\|_{\mathbf{L}^2(\Omega)}^2 \leq \int_{\mathfrak{J}} \tilde{C}.$$

Standard measure theory, cf. e.g. [Els11, IV, Theorem 4.4] concludes the proof. \square

Remark. Under certain regularity assumptions, namely

$$\begin{aligned}
 & \nabla \mathbf{u} \in \mathbf{L}^\infty(\Omega_T), \\
 & \partial_t \mathbf{u} \in L^2(\mathbf{H}^2), \text{ and} \\
 & \partial_{tt} \mathbf{u} \in L^2(\mathbf{L}^2),
 \end{aligned}$$

in combination with the stability assumptions

$$\begin{aligned}
 k \sum_{i=1}^{j-1} \|d_t^2 \mathbf{m}_h^{i+1}\|_{\mathbf{L}^2(\Omega)}^2 &\lesssim 1 + k \sum_{i=1}^{j-1} \|d_t \boldsymbol{\varepsilon}(\mathbf{u}_h^i)\|_{\mathbf{L}^2(\Omega)}^2, \\
 \|\mathbf{v}_h^0\|_{\mathbf{L}^2(\Omega)}^2 &\leq C, \text{ and} \\
 \|\mathbf{v}_h^{N-1}\|_{\mathbf{L}^2(\Omega)}^2 &\leq C,
 \end{aligned}$$

strong convergence

$$\|\mathbf{u}_{hk} - \mathbf{u}\|_{\mathbf{H}^1(\Omega_T)} \xrightarrow{\text{sub}} 0$$

can be achieved for a subsequence. Here, \mathbf{u} denotes a weak solution of the conservation of momentum equation in the sense of Definition 6.1.2. To that end, the magnetostrictive component can be treated as a time-dependent contribution, and the properties (2.3.30)–(2.3.31) can be shown by an extended analysis based on [Bañ05b]. The strong convergence property for \mathbf{u}_{hk} then follows along the way. To the best of our knowledge, a proof of the above assumptions is, however, mathematically open. For more details, the interested reader is referred to [PHPS12].

6.3. Numerical experiments

We conclude the analytic investigation of the coupled system of LLG with the conservation of momentum equation with a short section of computational experiments. Throughout, we implemented Algorithm 6.2.1. As before, visualization of 3D data is carried out in PARAVIEW, cf. [Webc].

6.3.1. General performance

Before we come to the first experiment, we want to comment on the implementation of the system matrix $A \in \mathbb{R}^{3N \times 3N}$ with

$$A_{ij} = \int_{\Omega} (\lambda^e \varepsilon(\eta_i), \varepsilon(\eta_j)),$$

where η_i and η_j denote the nodal basis functions on \mathbf{z}_i and \mathbf{z}_j , respectively, and $N = \#\mathcal{N}$ denotes the number of nodes. Throughout, we work on a three-dimensional spatial domain. Therefore, for each node $\mathbf{z}_j \in \mathcal{N}$, we have the three basis functions

$$\eta_1^j = \begin{pmatrix} \eta^j \\ 0 \\ 0 \end{pmatrix}, \eta_2^j = \begin{pmatrix} 0 \\ \eta^j \\ 0 \end{pmatrix}, \text{ and } \eta_3^j = \begin{pmatrix} 0 \\ 0 \\ \eta^j \end{pmatrix}.$$

For the entries of the standard stiffness matrix as it occurs in LLG, for example, one thus gets

$$\nabla \eta_1^j = \begin{pmatrix} \frac{\partial \eta}{\partial x_1} & \frac{\partial \eta}{\partial x_2} & \frac{\partial \eta}{\partial x_3} \\ 0 & 0 & 0 \\ 0 & 0 & 0 \end{pmatrix}, \nabla \eta_2^j = \begin{pmatrix} 0 & 0 & 0 \\ \frac{\partial \eta}{\partial x_1} & \frac{\partial \eta}{\partial x_2} & \frac{\partial \eta}{\partial x_3} \\ 0 & 0 & 0 \end{pmatrix}, \text{ and } \nabla \eta_3^j = \begin{pmatrix} 0 & 0 & 0 \\ 0 & 0 & 0 \\ \frac{\partial \eta}{\partial x_1} & \frac{\partial \eta}{\partial x_2} & \frac{\partial \eta}{\partial x_3} \end{pmatrix}.$$

For different components i, i' of η^j , we thus always get $\nabla \eta_i^j : \nabla \eta_{i'}^j = 0$ and therefore $(\nabla \eta_i^j, \nabla \eta_{i'}^j) = 0$. By some clever enumeration of the nodes and indices, namely by separating x_1, x_2 and x_3 components, the stiffness matrix gets the elegant block-diagonal shape

$$S = \begin{matrix} & \begin{matrix} x_1 & x_2 & x_3 \end{matrix} \\ \begin{matrix} x_1 \\ x_2 \\ x_3 \end{matrix} & \begin{pmatrix} \tilde{S} & 0 & 0 \\ 0 & \tilde{S} & 0 \\ 0 & 0 & \tilde{S} \end{pmatrix} \end{matrix},$$

where \tilde{S} is the 1D stiffness matrix. Exploiting MATLAB's `spy`-command, we can see that this is indeed the case and for the data from the second experiment below, the structure of the stiffness matrix is given in Figure 6.1.

For the system matrix A from the conservation of momentum equation, however, this is not the case anymore. Even if we neglect the tensorial multiplication with λ^e , we get

$$\varepsilon(\eta_1^j) = \begin{pmatrix} \frac{\partial \eta}{\partial x_1} & \frac{1}{2} \frac{\partial \eta}{\partial x_2} & \frac{1}{2} \frac{\partial \eta}{\partial x_3} \\ \frac{1}{2} \frac{\partial \eta}{\partial x_2} & 0 & 0 \\ \frac{1}{2} \frac{\partial \eta}{\partial x_3} & 0 & 0 \end{pmatrix}, \varepsilon(\eta_2^j) = \begin{pmatrix} 0 & \frac{1}{2} \frac{\partial \eta}{\partial x_1} & 0 \\ \frac{1}{2} \frac{\partial \eta}{\partial x_1} & \frac{\partial \eta}{\partial x_2} & \frac{1}{2} \frac{\partial \eta}{\partial x_3} \\ 0 & \frac{1}{2} \frac{\partial \eta}{\partial x_3} & 0 \end{pmatrix}, \text{ and } \\ \varepsilon(\eta_3^j) = \begin{pmatrix} 0 & 0 & \frac{1}{2} \frac{\partial \eta}{\partial x_1} \\ 0 & 0 & \frac{1}{2} \frac{\partial \eta}{\partial x_2} \\ \frac{1}{2} \frac{\partial \eta}{\partial x_1} & \frac{1}{2} \frac{\partial \eta}{\partial x_2} & \frac{\partial \eta}{\partial x_3} \end{pmatrix}.$$

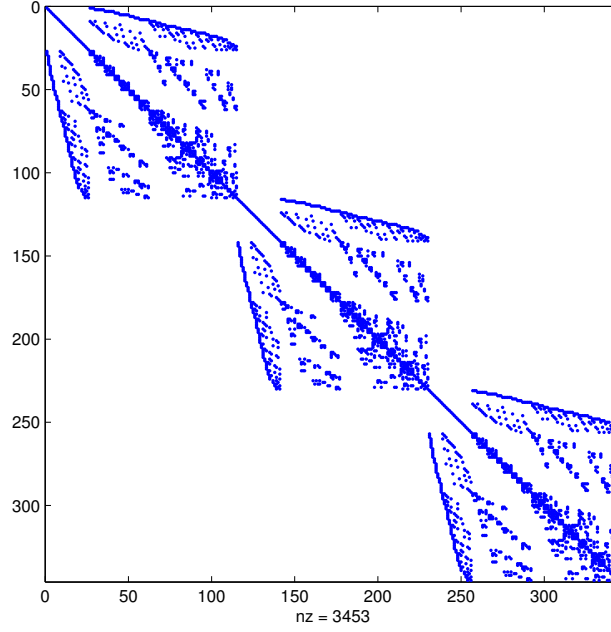


Figure 6.1.: Sparsity pattern of the stiffness matrix.

The system matrix A from the conservation of momentum equation thus even has entries in parts which correspond to different components of the solution. More precisely, A is a block-full matrix. It is, however, still sparse due to the finite overlap of the supports of the different hat functions. The structure of the elasticity matrix for the data from the second example below is visualized in Figure 6.2.

Convergence in time

	Timesteps							
	10	50	100	500	1000	5000	10000	50000
Err(\mathbf{u})	17.5860	5.5100	3.2414	0.7743	0.3985	0.0824	0.0429	0.0165

Table 6.1.: Err(\mathbf{u}) for varying time steps.

In a first experiment, we aim to investigate the convergence order in time and space for the conservation of momentum equation. To that end, we prescribe the exact solution

$$\mathbf{u}(t, x_1, x_2, x_3) = \begin{pmatrix} u_1 \\ u_2 \\ u_3 \end{pmatrix} (t, x_1, x_2, x_3) \quad \text{and} \quad \mathbf{m}(t, x_1, x_2, x_3) = \begin{pmatrix} m_1 \\ m_2 \\ m_3 \end{pmatrix} (t, x_1, x_2, x_3)$$

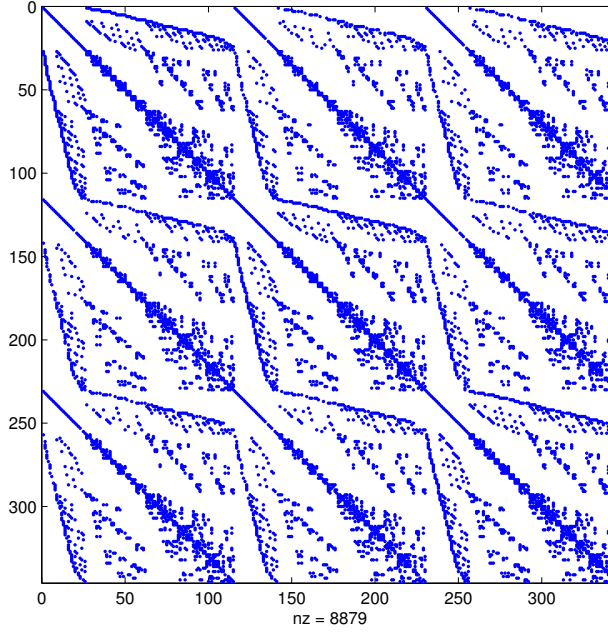


Figure 6.2.: Sparsity pattern of the system matrix A from the conservation of momentum equation.

with

$$\begin{aligned}
 m_1(t, x_1, x_2, x_3) &:= \sin(ct + dx_1) \cos(ct + d(x_2 + x_3)) \\
 m_2(t, x_1, x_2, x_3) &:= \cos(ct + dx_1) \cos(ct + d(x_2 + x_3)) \\
 m_3(t, x_1, x_2, x_3) &:= \sin(ct + d(x_2 + x_3)) \\
 u_1(t, x_1, x_2, x_3) &:= \sin(a(x_1x_2 + x_3) + bt) \\
 u_2(t, x_1, x_2, x_3) &:= \cos(a(x_3x_1 + x_2) + bt) \\
 u_3(t, x_1, x_2, x_3) &:= \sin(a(x_2x_3 + x_1) + bt) + \cos(a(x_2x_3 + x_1) + bt)
 \end{aligned}$$

and solve (6.2.3) on the cube $[-1, 1]^3$ with $\varrho = 1$ and $\mathbf{h}_{\text{eff}} = \Delta \mathbf{m} + \mathbf{h}_{\mathbf{m}}$. For the tensors $\boldsymbol{\lambda}^e, \boldsymbol{\lambda}^m$, we use

$$\lambda_{ijkl}^e = \lambda_{ijkl}^m = C \delta_{ik} \delta_{jl}$$

and $C = 1$. For the time interval $[0, T]$, we choose $T = 3$. To minimize the spatial error, we further set $a = 0.01, b = 4/3\pi, c = 2\pi, d = 0.01$. The corresponding right-hand side was calculated with MATHEMATICA. The dynamic behaviour of the displacement \mathbf{u} is visualized in Figure 6.3. For $P = 320$ spatial elements, we investigate the temporal error for varying time steps and find linear error decay for $\text{Err}(\mathbf{u})$, cf. Table 6.1. The results are also visualized in Figure 6.4.

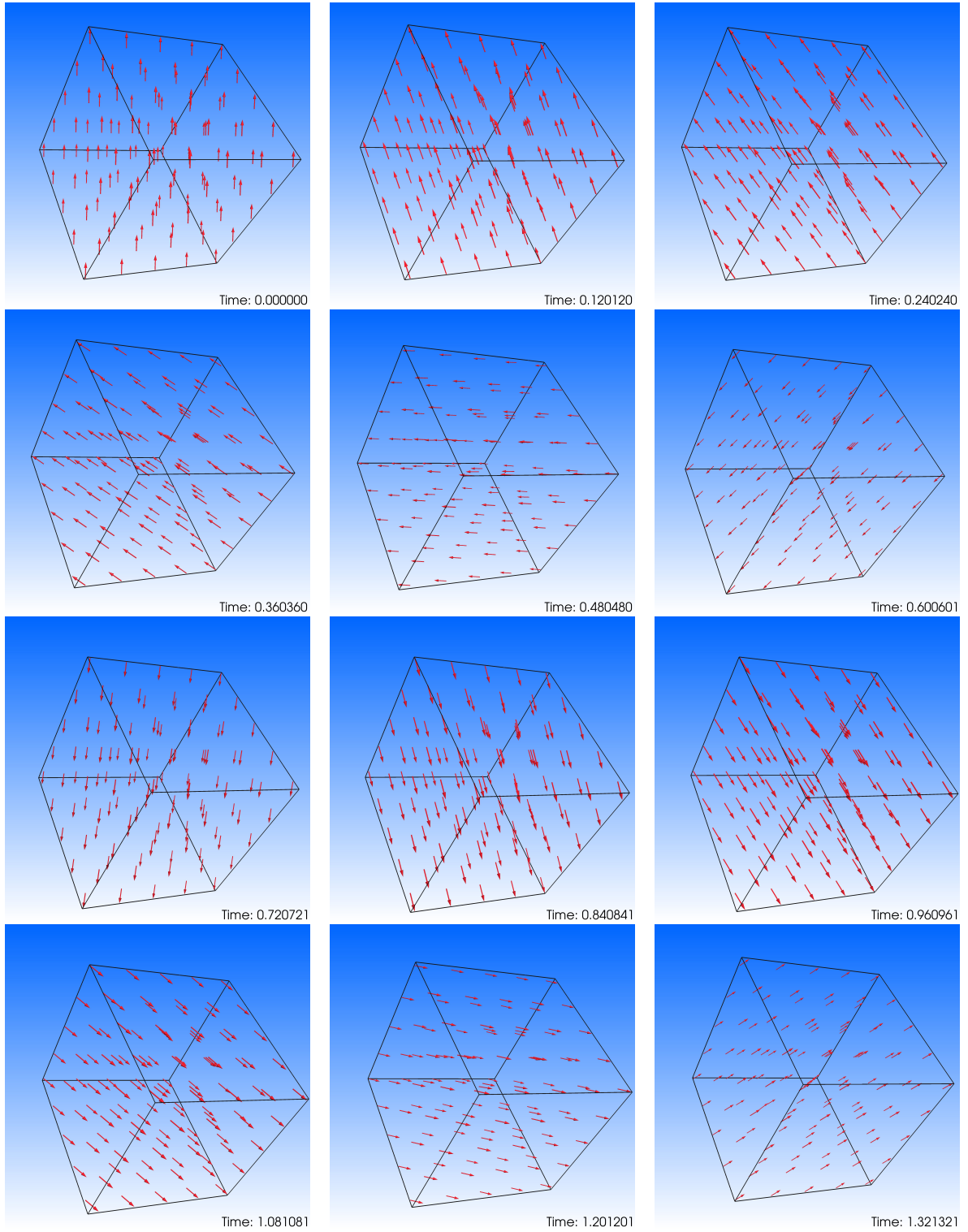


Figure 6.3.: Evolution of the displacement for $P = 320$ spatial elements and $N = 100$ time steps.

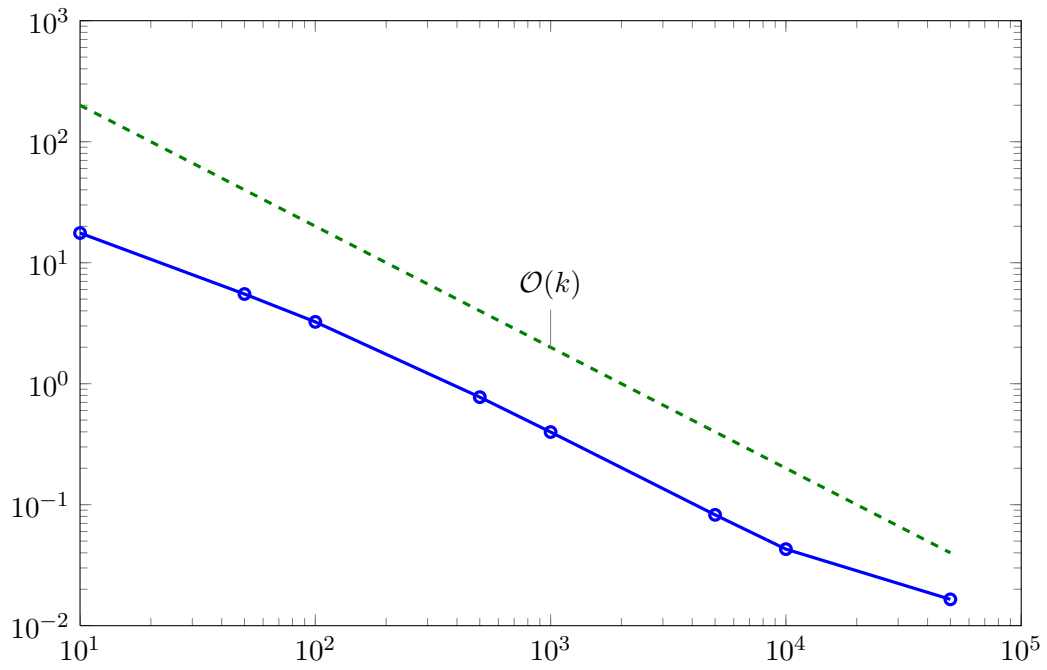


Figure 6.4.: Error decay for uniform refinement in time with $P = 320$ spatial elements. As expected, we observe linear behaviour.

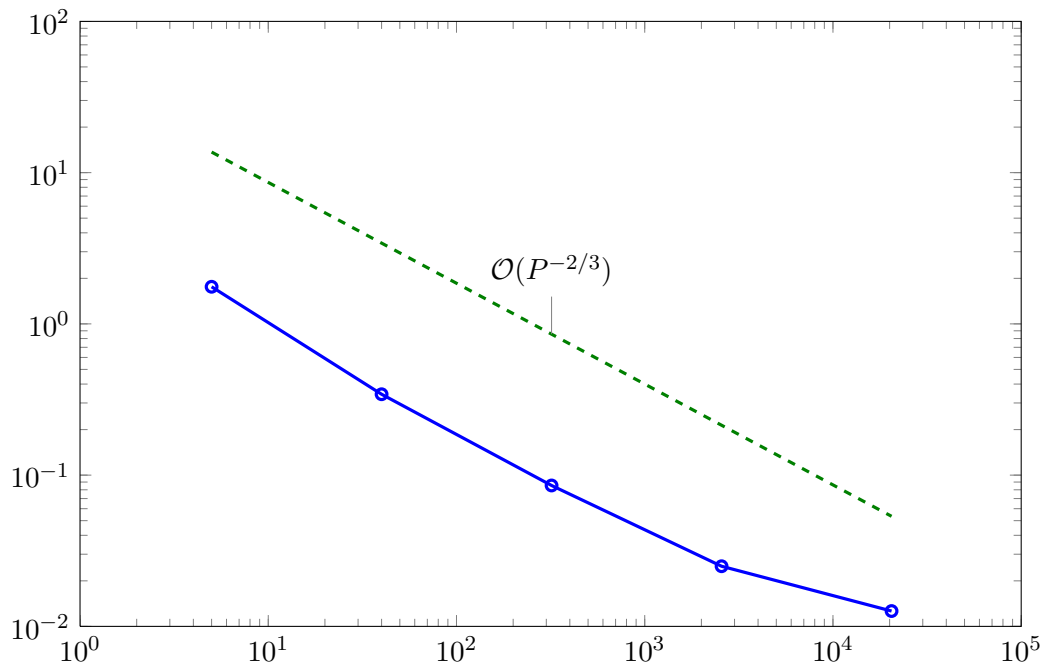
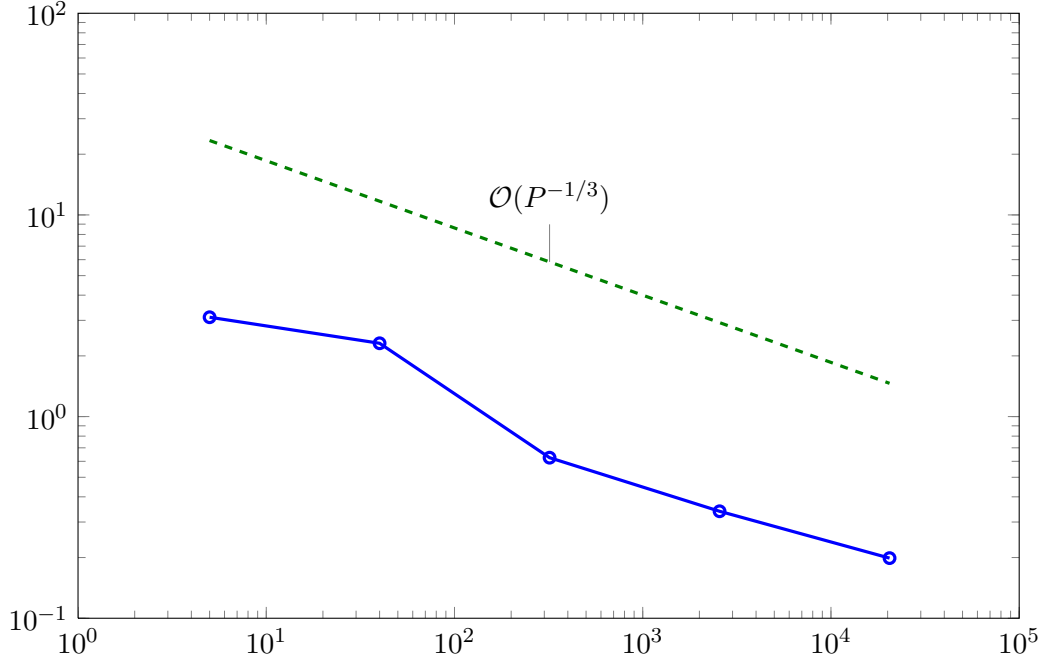


Figure 6.5.: Decay of the spatial error in L^2 -norm plotted over the amount of spatial elements.

Figure 6.6.: Decay of the spatial error in \mathbf{H}^1 -norm plotted over the amount of spatial elements.

Convergence in space

In the next experiment, we aim to investigate the spatial convergence rate. To that end, we use a fixed amount of 1000 time steps and choose the parameter setting to be $a = 0.5, b = \pi, c = \pi$, and $d = 0.5$. For varying amounts $P \in \{5, 40, 320, 2560, 20480\}$ of spatial elements, we compare the error in \mathbf{H}^1 and \mathbf{L}^2 norm, cf. Table 6.2.

	Spatial elements				
	5	40	320	2560	20480
$\max_{t \in [0, T]} \ \mathbf{u}(t) - \mathbf{u}_{hk}(t)\ _{\mathbf{L}^2(\Omega)}$	1.7596	0.3426	0.0854	0.0250	0.0126
$\max_{t \in [0, T]} \ \mathbf{u}(t) - \mathbf{u}_{hk}(t)\ _{\mathbf{H}^1(\Omega)}$	3.1090	2.3096	0.6254	0.3392	0.1987

Table 6.2.: Spatial error in \mathbf{L}^2 - and \mathbf{H}^1 -norm, respectively.

The \mathbf{L}^2 -error is visualized in Figure 6.5 and the \mathbf{H}^1 -error is visualized in Figure 6.6. As expected, we observe quadratic decay in the \mathbf{L}^2 -norm, and linear decay for \mathbf{H}^1 . We like to emphasize, that the \mathbf{L}^2 -norm of the error is actually the correct quantity to investigate here, as the above analysis only yields norm convergence in \mathbf{L}^2 rather than \mathbf{H}^1 . The computational results, however, suggest, that \mathbf{u}_{hk} converges towards \mathbf{u} normwise even in \mathbf{H}^1 .

Finally, we completely neglect the temporal error and consider the stationary problem

$$-\nabla \cdot \boldsymbol{\sigma} = \mathbf{f} \quad (6.3.1)$$

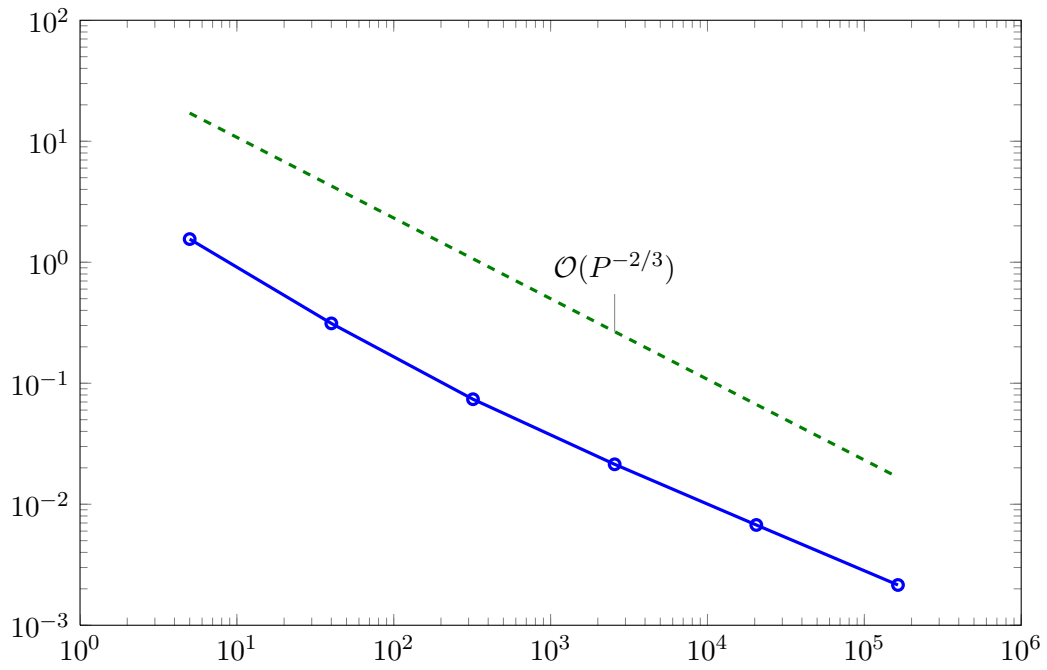


Figure 6.7.: Error decay in L^2 -norm for the stationary problem plotted over the amount of spatial elements.

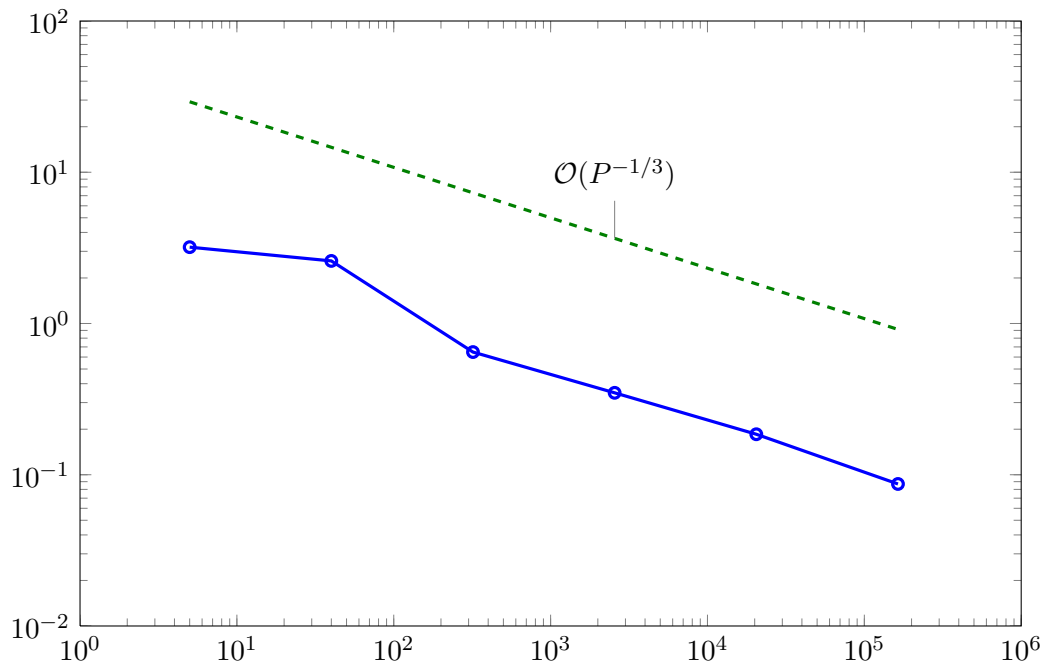


Figure 6.8.: Error decay in H^1 -norm for the stationary problem plotted over the amount of spatial elements.

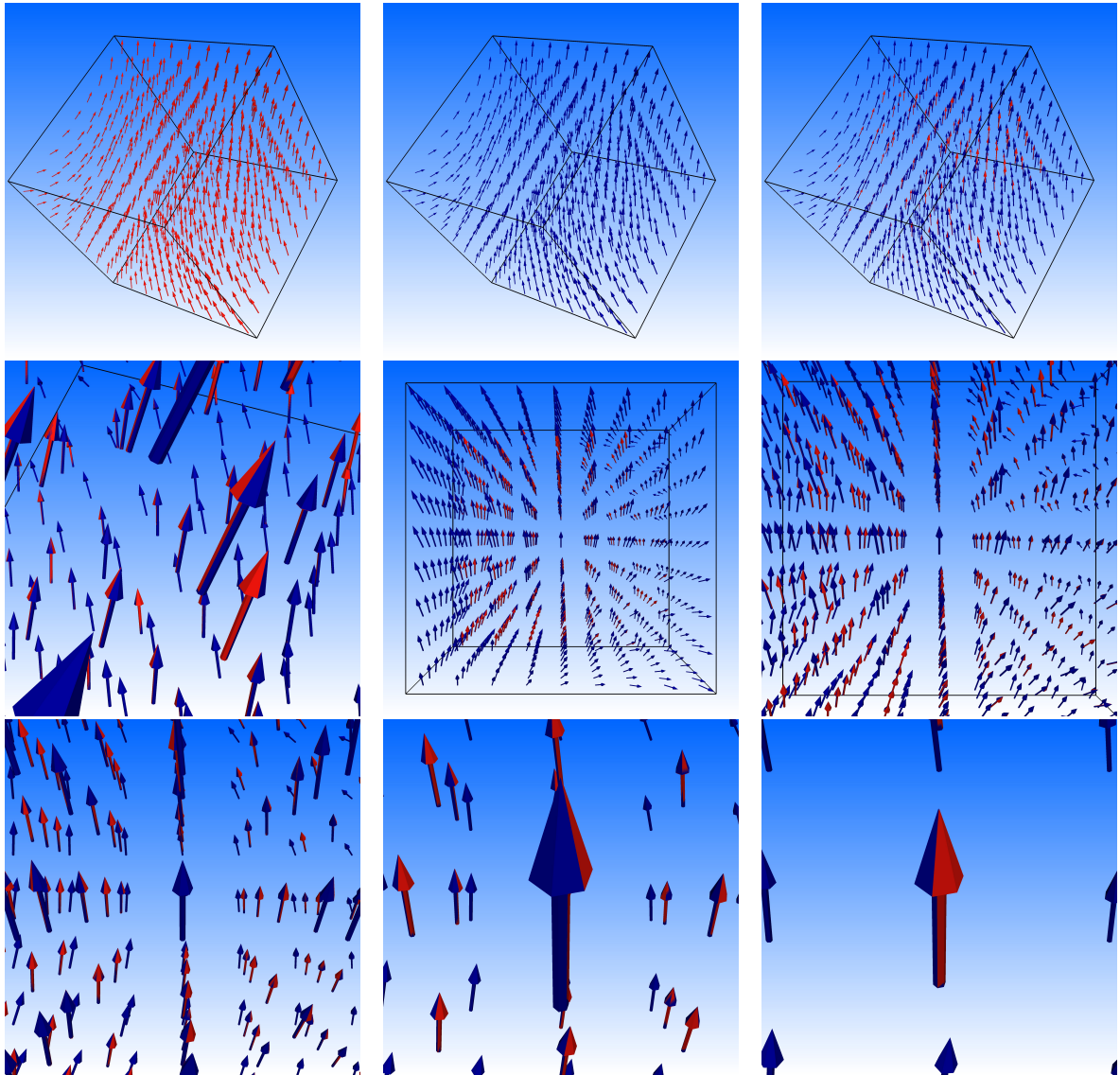


Figure 6.9.: Visualization of the exact stationary solution (red) and its numerical approximation (blue).

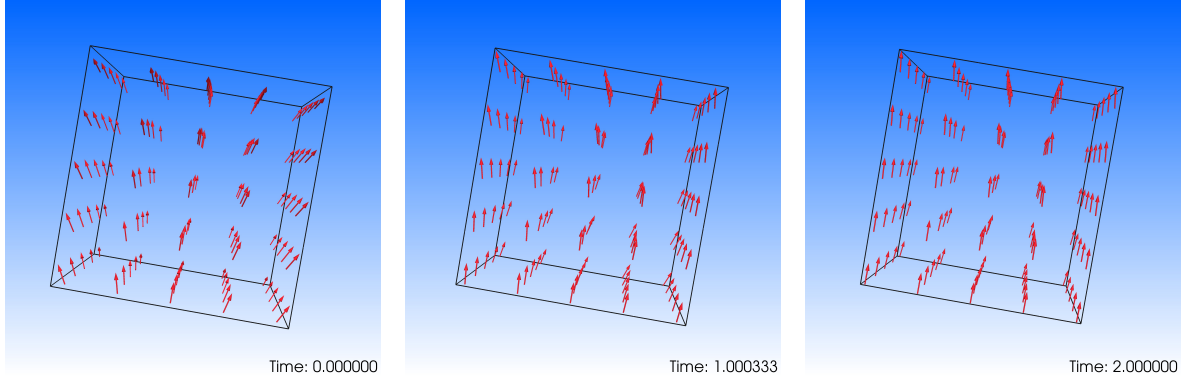


Figure 6.10.: Dynamic behaviour of the magnetization for small magnetostriction with $C_\lambda = 1$.

for the above data with $t = 0$. In this example, we thus test the system matrix A with

$$A_{ij} = \int_{\Omega} (\lambda^e \varepsilon(\eta_i), \varepsilon(\eta_j)).$$

Moreover, we neglect the dependence on the magnetization \mathbf{m} , i.e. we solve

$$(\lambda^e \varepsilon(\mathbf{u}_h), \varepsilon(\boldsymbol{\psi}_h)) = (\mathbf{f}, \boldsymbol{\psi}_h) \quad \text{for all } \boldsymbol{\psi}_h \in \mathcal{S}^1(\mathcal{T}_h), \quad (6.3.2)$$

where the boundary data is given by the trace of the prescribed solution from above. Again, the exact right-hand side was computed with MATHEMATICA. The exact- and the numerical solutions are visualized in Figure 6.9. The exact solution is represented by the red arrows, whereas the numerical solution is represented by the blue arrows. In the third picture of the top row, both solutions are visualized simultaneously and as expected, they nearly coincide. The other images from Figure 6.9 show closeup snapshots of the solution and confirm, that the approximated solution is in good agreement with the exact one for $P = 2560$ elements.

Again, we investigate the decay of the error for varying spatial resolution and the \mathbf{H}^1 - and \mathbf{L}^2 errors are given in Table 6.3. As in the evolutionary case, the errors are visualized in the Figures 6.7 and 6.8. Again, we observe the expected convergence behaviour.

	Spatial elements					
	5	40	320	2560	20480	163840
$\ \mathbf{u} - \mathbf{u}_h\ _{\mathbf{L}^2(\Omega)}$	1.5545	0.3124	0.0738	0.0214	0.0067	0.0022
$\ \mathbf{u} - \mathbf{u}_h\ _{\mathbf{H}^1(\Omega)}$	3.1970	2.5926	0.6474	0.3481	0.1853	0.0869

Table 6.3.: Spatial error in \mathbf{L}^2 - and \mathbf{H}^1 -norm for stationary problem.

6.3.2. Some thoughts on energy

In the next experiment, we consider the coupled system of LLG with the conservation of momentum equation and investigate the influence of increasing magnetostriction on the total energy of the system. To that end, we employ the initial data

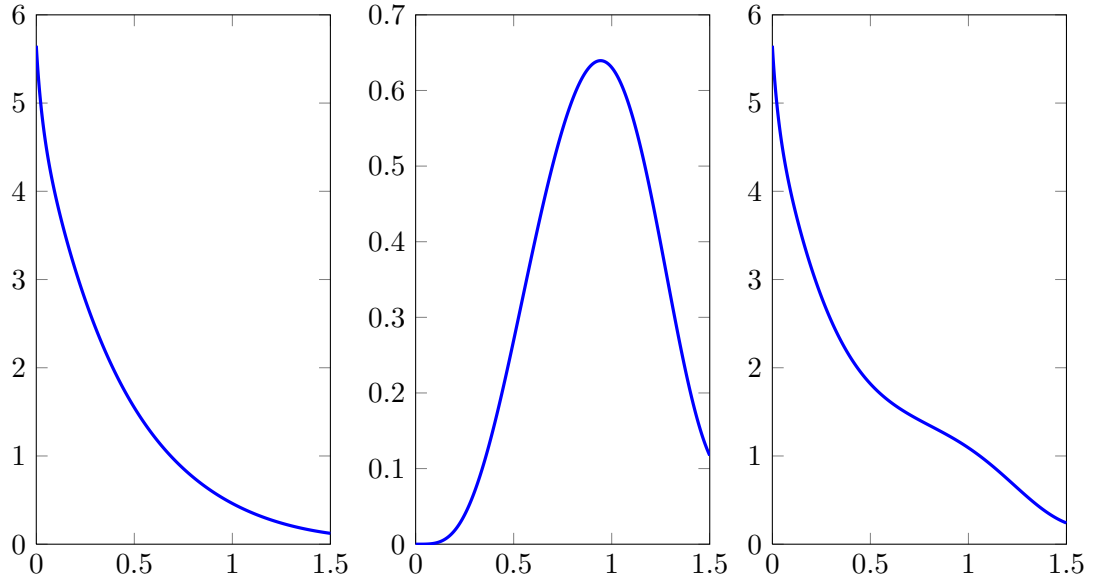


Figure 6.11.: Energy contributions $\mathcal{E}_{\text{exch}}$ (*left*), $\mathcal{E}_{\text{elastic}}$ (*middle*), and $\mathcal{E}_{\text{total}}$ (*right*) for $C_\lambda = 1$. Clearly, the exchange contribution is dominant.

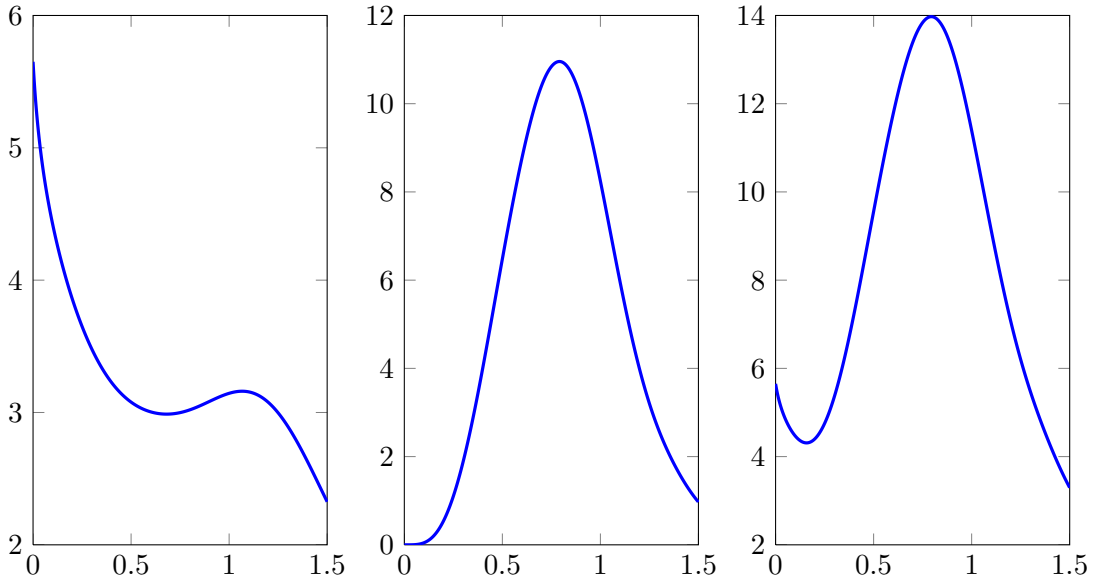


Figure 6.12.: Energy contributions $\mathcal{E}_{\text{exch}}$ (*left*), $\mathcal{E}_{\text{elastic}}$ (*middle*), and $\mathcal{E}_{\text{total}}$ (*right*) for $C_\lambda = 2$. Influence of the magnetostriction is clearly visible.

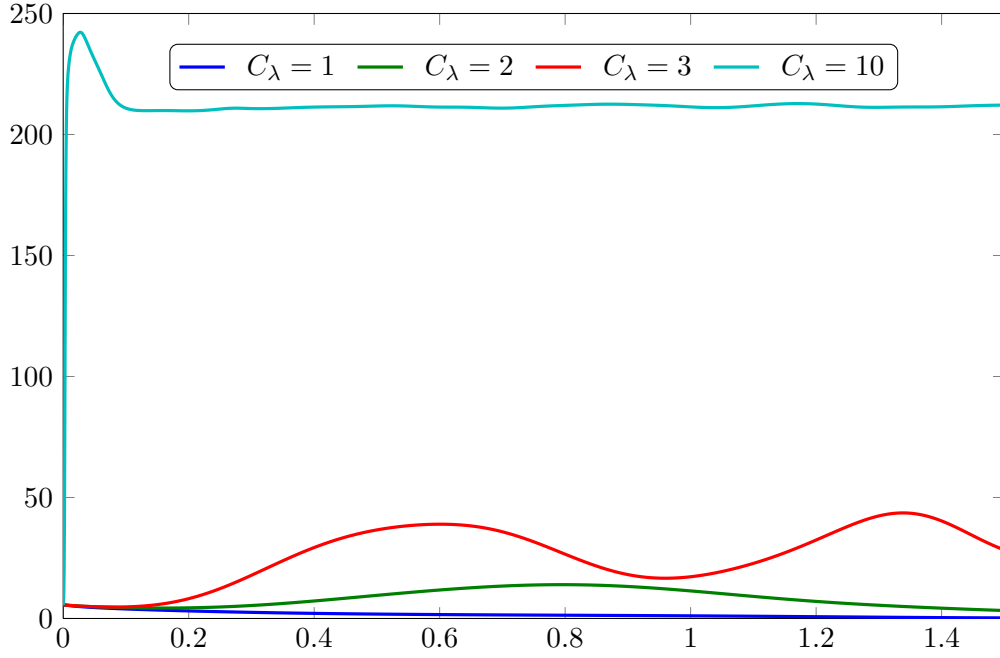


Figure 6.13.: Total energy $\mathcal{E}_{\text{total}}$ for different values of $C_\lambda \in \{1, 2, 3, 10\}$ plotted over time.

$$\begin{aligned} m_1^0(x_1, x_2, x_3) &:= \sin(1/2x_1) \cos(1/2(x_2 + x_3)), \\ m_2^0(x_1, x_2, x_3) &:= \cos(1/2x_1) \cos(1/2(x_2 + x_3)), \\ m_3^0(x_1, x_2, x_3) &:= \sin(1/2(x_2 + x_3)), \end{aligned}$$

$$\mathbf{u}^0(x_1, x_2, x_3) := \begin{pmatrix} 0 \\ 0 \\ 0 \end{pmatrix}, \quad \text{and} \quad \dot{\mathbf{u}}^0(x_1, x_2, x_3) := \begin{pmatrix} 0 \\ 0 \\ 0 \end{pmatrix}.$$

We apply the tensors

$$\lambda_{ijkl}^e = \lambda_{ijkl}^m = C_\lambda \delta_{ik} \delta_{jl}$$

with increasing $C_\lambda \in \{1, 2, 3, 10\}$ and consider the time interval $[0, T]$ with $T = 1.5$ for $\alpha = 1$, $P = 2560$, and $N = 1000$. For our simulation, we include the exchange effect, as well as the magnetostrictive component, i.e. $\mathbf{h}_{\text{eff}} = \Delta \mathbf{m} + \mathbf{h}_m$. Moreover, we consider the exchange energy

$$\mathcal{E}_{\text{exch}}(\mathbf{m}, t) = \frac{1}{2} \|\nabla \mathbf{m}(t, \cdot)\|_{\mathbf{L}^2(\Omega)}^2, \quad (6.3.3)$$

the elastic energy

$$\mathcal{E}_{\text{elastic}}(\mathbf{u}, t) = \frac{1}{2} \|\boldsymbol{\varepsilon}(\mathbf{u}(t, \cdot))\|_{\mathbf{L}^2(\Omega)}^2 \quad (6.3.4)$$

and the total energy

$$\mathcal{E}_{\text{total}} = \mathcal{E}_{\text{exch}} + \mathcal{E}_{\text{elastic}}. \quad (6.3.5)$$

For small $C_\lambda = 1$, the exchange contribution is dominant, and we observe that the magnetization slowly aligns parallel. This is visualized in Figure 6.10. The energy contributions $\mathcal{E}_{\text{exch}}$, $\mathcal{E}_{\text{elastic}}$, and $\mathcal{E}_{\text{total}}$ are plotted over time in Figure 6.11. As expected, the exchange energy is minimized. In the next step, we set $C_\lambda = 2$ and again compare the energy contributions in Figure 6.12. This time, the influence of the magnetostrictive component is clearly visible and the exchange energy is not dominant anymore, after a short while.

Finally, in Figure 6.13, we plot $\mathcal{E}_{\text{total}}$ for different values of $C_\lambda \in \{1, 2, 3, 10\}$ over time. In any case and as predicted by theory the total energy is uniformly bounded. Note, that we cannot expect the total energy $\mathcal{E}_{\text{total}}$ to decrease or even vanish, as we only proved boundedness of $\mathcal{E}_{\text{total}}$ by some constant that strongly depends on C_λ . Altogether, our results are in good agreement with similar observations in [Roc12, Section 4.2.5].

6.3.3. Effects on hysteresis

Finally, we investigate the effects of magnetostriction on hysteresis. To that end, we compute an academic example in 2D. On $[-0.5, 0.5]^2$ and the time interval $(0, 3)$, we solve Algorithm 6.2.1 with

$$\mathbf{h}_{\text{eff}} = 0.5\Delta\mathbf{m} + \mathbf{h}_{\mathbf{m}} + \mathbf{h}_{\mathbf{a}} + \mathbf{f},$$

where $\mathbf{h}_{\mathbf{a}}$ denotes the uniaxial anisotropy in x_3 -direction with $C_{\text{ani}} = 50$. For the material tensors, we choose the simplified

$$\lambda_{ijkl}^m = \lambda_{ijkl}^e = \begin{cases} C_\lambda & i = j = k = l \in \{1, 2\}, \\ 0 & \text{else.} \end{cases}$$

Thus, the magnetostrictive contribution of the effective field simplifies to

$$(\mathbf{h}_{\mathbf{m}})_i = \lambda_{iii}^m \sigma_{ii}(\mathbf{m})_i = C_\lambda \sigma_{ii}(\mathbf{m})_i.$$

Moreover, the external field \mathbf{f} is not constant in time but has the form $\mathbf{f}(t) = \mu(t)C_{\mathbf{f}}[-0.5, 0, -1]$ with $C_{\mathbf{f}} = 100$ and where $\mu(t)$ is slowly increased from 0 to 2. Afterwards, it is decreased until -2 and then again increased until 2 and so on. The inertial remagnetization process into the direction of the applied field is characteristic for the corresponding material and is visualized by means of a hysteresis loop, see e.g. [Gol12, Section 6.1] for details. Initially, the magnetization is homogeneously oriented in easy-axis direction, and the displacement is neglected, i.e.

$$\mathbf{m}^0 := \begin{pmatrix} 0 \\ 0 \\ 1 \end{pmatrix}, \mathbf{u}^0 := \begin{pmatrix} 0 \\ 0 \\ 0 \end{pmatrix}, \text{ and } \dot{\mathbf{u}}^0 := \begin{pmatrix} 0 \\ 0 \\ 0 \end{pmatrix}.$$

As discretization parameters, we choose $h = 1/16$ and $N = 10000$ time steps and $\alpha = 1$. The results for different values of $C_\lambda \in \{0, 1, 2, 3, 4, 5, 6\}$ are visualized in Figure 6.14 where we plot the average magnetization in x_3 -direction over the strength of the applied field. We see the typical hysteresis loop, and we clearly observe that coercivity increases as we increase C_λ .

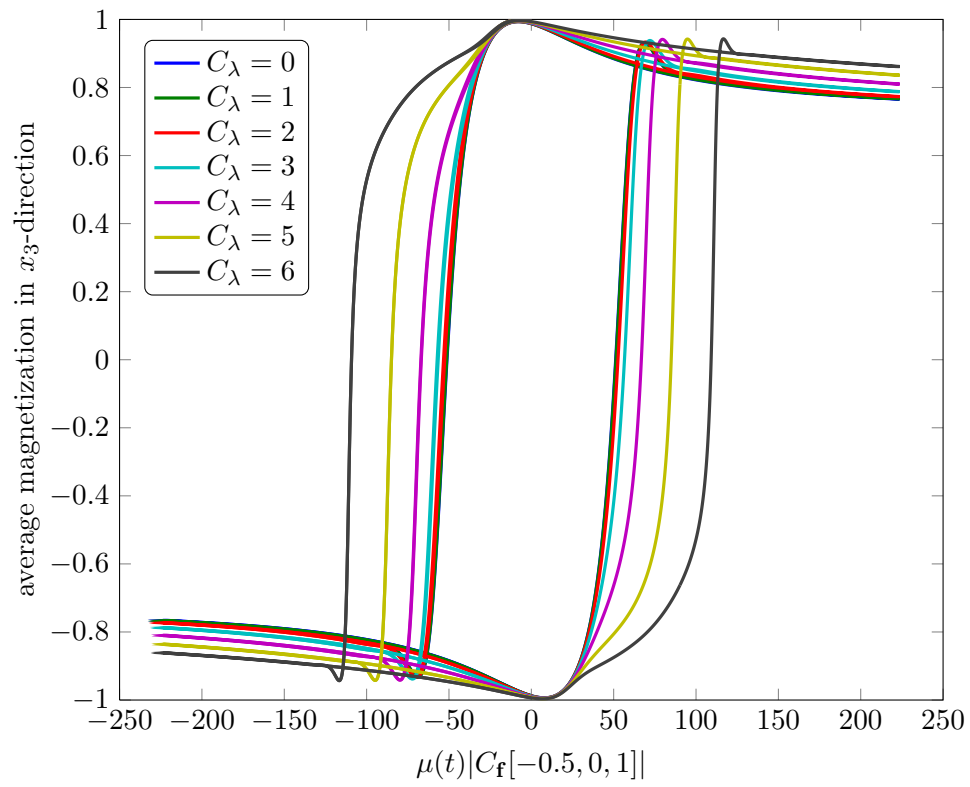


Figure 6.14.: Hysteresis loop for different values of C_λ . Clearly, the coercivity increases as C_λ is increased.

Outlook and open questions

With this work, we contribute to the field of dynamical micromagnetism by means of analytical and numerical results. Starting from the notion of a weak solution in [AS92] and the subsequent scheme proposed by ALOUGES in [Alo08a], we constructed numerical integrators for a wide variety of problems. The main leitmotif has always been to construct a numerical integrator which is applicable to as many situations as possible. To that end, we did an abstract convergence analysis and derived a set of assumptions a field contribution needs to fulfill in order for the scheme to be convergent. Instead of investigating each classic or possible future field contribution individually, one now has a checklist of two easily verifiable conditions to be checked without to even have to look at the convergence analysis. Concretely, one has to ensure that the field operator $\pi(\cdot)$ is uniformly bounded in $\mathbf{L}^2(\Omega)$, i.e.

$$\|\pi(\mathbf{n})\|_{\mathbf{L}^2(\Omega)} \lesssim \|\mathbf{n}\|_{\mathbf{L}^2(\Omega)}$$

for all $\mathbf{n} \in \mathbf{L}^2(\Omega)$ with $|\mathbf{n}| \leq 1$ almost everywhere. Moreover, one needs to verify the weak convergence property

$$\pi(\mathbf{n}_{hk}) \xrightarrow{\text{sub}} \pi(\mathbf{n}) \quad \text{weakly in } \mathbf{L}^2(\Omega_T),$$

provided the sequence \mathbf{n}_{hk} strongly subconverges towards \mathbf{n} in $\mathbf{L}^2(\Omega_T)$. It can be verified that the classic field contributions *anisotropy*, *strayfield*, and *external field* fall into this category. Furthermore, we could even show that the multiscale ansatz introduced by BRUCKNER [Bru13] is covered by our approach. This result gives both, a better understanding of the line of proof as well as a straightforward applicability for future developments.

In the next step, we investigated LLG coupled to various other PDEs to account for multiple micromagnetic effects. More precisely, we investigated coupling to the full Maxwell system, the eddy-current equation, and the conservation of momentum equation. In all cases, we were able to derive an unconditionally convergent integrator which numerically decouples both equations. That is to say instead of one large (and possibly nonlinear) system, we subsequently solve two smaller linear problems, one for LLG in the spirit of [Alo08a] and one for the coupled equation. The sequence of discrete solutions is then still guaranteed to weakly subconverge towards a weak solution of the full coupled problem without any condition on the discretization parameters. Altogether, we considered coupling to various model problems, namely

- coupling to a linear second order hyperbolic PDE (full Maxwell system),
- coupling to a linear second order parabolic PDE (eddy-current equation),
- coupling with a nonlinear coupling operator (magnetostriction).

Finally, we investigated the conditions under which more physically relevant (yet mathematically unnecessary) energy estimates can be derived. For the 3D case, it turned out that those are uniform $\mathbf{L}^4(\Omega)$ -boundedness as well as self-adjointness of the corresponding field contribution. As far as the classical field contributions are concerned, this is the case for uniaxial anisotropy or the magnetostatic strayfield, which is in good agreement to the available literature, see e.g. [Alo08a, BP06].

Despite its optimistic title, a single work cannot give a concluding answer to all questions in dynamical micromagnetism. On the contrary, it behaves as always in mathematics, for each answered question, two new ones pop up, and we like to give a short outlook here.

- The most obvious issue seems to be a general analysis of the coupling operator. For stationary LLG field contributions, we derived a list of requirements that need to be satisfied to ensure unconditional convergence. The question for such a set of minimal assumptions for the coupling operator thus seems straightforward. Allowedly, with the magnetostrictive component, we treated quite a complicated coupling operator as it is nonlinear and additionally depends on the spatial derivative of the solution from the second PDE. It would be interesting, however, to push the boundaries of our analysis and see under which circumstances coupling to other PDEs still leads to an unconditionally convergent scheme.
- In the context of the first point, one could investigate the decoupling of the two problems in a more general fashion to understand in which cases such a result is possible. In all cases, we managed to derive a stable bound for the difference of two subsequent solutions, e.g. for the eddy-current case

$$\sum_{i=0}^N \|\mathbf{H}_h^{i+1} - \mathbf{H}_h^i\|_{\mathbf{L}^2(\hat{\Omega})}^2 \leq C.$$

While one may expect that such an estimate is a necessary condition for a decoupled scheme, it remains unclear whether it is also sufficient in general.

- In terms of efficiency of the proposed integrator, there remains the important question of convergence order. While we did not make any statement on the convergence rate of our schemes, they are generically of order 1 in both, space and time. Higher order extensions in space or time are hindered by technical difficulties. The recent work [AKST12] is a good starting point for a second order scheme in time, but there is still some work to do. In this context, it would be especially interesting to see if one can still decouple the coupled problems, if the discretization is of higher order.
- As mentioned in the introduction, we basically find two competing integrators in the literature at the moment, the tangent plane scheme [Alo08a] and the midpoint scheme [BP06], both of which have distinguished advantages and disadvantages. For the tangent plane scheme those are:

-
- advantages
 - * linear scheme
 - * unconditional convergence
 - * decoupling rigorously analyzed
 - disadvantages
 - * artificial damping
 - * current scheme only of first order in time
 - * angle condition on mesh

For the midpoint scheme, on the other hand, one has:

- advantages
 - * no artificial damping
 - * formally of second order in time
- disadvantages
 - * requires condition on mesh parameters in practice for reliable fixed point iteration
 - * decoupling not rigorously analyzed in the literature so far

It would thus be nice to have criteria that indicate which integrator would be the most suitable in which situation. To that end, the work [BPPR13] provides some computational comparison, but more studies are in order.

- Finally, and independently of the concrete integrators derived in this thesis, there are open questions concerning the analysis of weakly convergent integrators of LLG: Is it possible to deduce convergence of the whole sequence rather than only a subsequence? At least in our computations, we always observe that the complete sequence converges. Other questions concern strong convergence or even the non-uniqueness of weak solutions. The original work [AS92] proves non-uniqueness only in the case $\mathbf{h}_{\text{eff}} = \Delta \mathbf{m}$. Maybe this result could be weakened if other field contributions come into play.

For stationary problems in micromagnetics, for instance, uniqueness of minimizers follows mathematically from the interplay of anisotropy and the demagnetization field, see e.g. [DP98, FLMP12].

Altogether, we derived very nice results, but ultimately this thesis leaves much space for further research. On the other hand, this is what makes a topic interesting for future mathematicians in the first place.

Appendix A

Appendix

A.1. Equalities and inequalities

Lemma A.1.1 (Gronwall). *Let $r(t), h(t), y(t)$ be continuous functions on the interval $[a, b]$ with $r(t), h(t) \geq 0$. Assume that for $a \leq t \leq b$, there holds*

$$y(t) \leq h(t) + \int_a^t r(s)y(s) ds.$$

Then, we have

$$y(t) \leq h(t) + \int_a^t h(s)r(s) \exp \left(\int_s^t r(q)r(q) dq \right) ds.$$

If we further have $r(s) = C$ and h non-decreasing, then we additionally get

$$y(t) \leq h(t) \exp (C(t-a)),$$

for $a \leq t \leq b$.

Proof. The proof can be found in [Pla00, Lemma 8.13]. □

Lemma A.1.2 (Gronwall — discrete version). *Let $h_0, \dots, h_{r-1} > 0$ and $\alpha \geq 0, \beta \geq 0$ be given. Assume further that for v_0, \dots, v_r the following inequalities are satisfied:*

$$|v_0| \leq \alpha, \quad |v_\ell| \leq \alpha + \beta \sum_{j=0}^{\ell-1} h_j |v_j| \quad \text{for all } \ell = 1, \dots, r.$$

Then, there holds

$$|v_\ell| \leq \alpha \exp \left(\beta \sum_{j=0}^{\ell-1} h_j \right) \quad \text{for all } \ell = 0, 1, \dots, r.$$

Proof. The proof can be found in [Pla00, Lemma 8.14]. □

Lemma A.1.3. (*Abel's summation by parts*) Let \mathcal{X} be a Hilbert space with scalar product (\cdot, \cdot) and induced norm $\|\cdot\|^2 = (\cdot, \cdot)$. Moreover, let $v_\ell \in \mathcal{X}$ for all $\ell = 0, \dots, j$ for some $j \in \mathbb{N}$ with $j \geq 0$. Then there holds

$$\sum_{\ell=0}^{j-1} (v_{\ell+1} - v_\ell, v_{\ell+1}) = \frac{1}{2} \|v_j\|^2 - \frac{1}{2} \|v_0\|^2 + \frac{1}{2} \sum_{\ell=0}^{j-1} \|v_{\ell+1} - v_\ell\|^2. \quad (\text{A.1.1})$$

Proof. The proof follows by direct calculation. We have

$$\begin{aligned} 2(v_{\ell+1} - v_\ell, v_{\ell+1}) &= (v_{\ell+1}, v_{\ell+1} - v_\ell) + (v_{\ell+1} - v_\ell, v_{\ell+1}) \\ &= (v_{\ell+1}, v_{\ell+1}) - (v_{\ell+1}, v_\ell) + (v_{\ell+1} - v_\ell, v_{\ell+1}) \\ &= (v_{\ell+1}, v_{\ell+1}) - (v_{\ell+1}, v_\ell) + (v_{\ell+1} - v_\ell, v_{\ell+1}) - (v_\ell, v_\ell) + (v_\ell, v_\ell) \\ &= (v_{\ell+1}, v_{\ell+1}) - (v_\ell, v_\ell) + (v_{\ell+1} - v_\ell, v_{\ell+1}) - (v_{\ell+1} - v_\ell, v_\ell) \\ &= (v_{\ell+1}, v_{\ell+1}) - (v_\ell, v_\ell) + (v_{\ell+1} - v_\ell, v_{\ell+1} - v_\ell). \end{aligned}$$

Summing up and exploiting the telescopic sum yields the assertion. \square

Lemma A.1.4 (Hölder inequality). Let $p_j \in [1, \infty]$ for $j = 1, \dots, m$ and $\frac{1}{r} = \sum_{j=1}^m \frac{1}{p_j}$. Let further $f_j \in L^{p_j}(X)$ for $j = 1, \dots, m$. Then, there holds

$$\left\| \prod_{j=1}^m f_j \right\|_{L^r(X)} \leq \prod_{j=1}^m \|f_j\|_{L^{p_j}(X)}. \quad (\text{A.1.2})$$

Proof. The proof is found e.g. in [Eva02, B.2]. \square

Lemma A.1.5. (*Cauchy inequality with ε - sometimes also Young inequality with ε*) For $a, b \in \mathbb{R}$, we have for any $\varepsilon > 0$

$$ab \leq \varepsilon a^2 + \frac{b^2}{4\varepsilon}. \quad (\text{A.1.3})$$

Proof. The proof can be found at [Eva02, Appendix B.2, a and b]. \square

Lemma A.1.6. Let $\zeta, \eta \in L^2(\mathbf{H}^1)$. Then there holds

$$(\nabla \zeta, \nabla(\zeta \times \eta)) = (\nabla \zeta, (\zeta \times \nabla \eta)). \quad (\text{A.1.4})$$

Here, the cross product of ζ and the Jacobian $\nabla \eta$ is given as

$$\begin{aligned} \zeta \times \nabla \eta &= \begin{pmatrix} \zeta_1 \\ \zeta_2 \\ \zeta_3 \end{pmatrix} \times \begin{pmatrix} \nabla \eta_1 \\ \nabla \eta_2 \\ \nabla \eta_3 \end{pmatrix} = \begin{pmatrix} \zeta_2 \nabla \eta_2 - \zeta_3 \nabla \eta_1 \\ \zeta_3 \nabla \eta_1 - \zeta_1 \nabla \eta_3 \\ \zeta_1 \nabla \eta_2 - \zeta_2 \nabla \eta_1 \end{pmatrix} \\ &= \begin{pmatrix} \zeta_2 \partial_{x_1} \eta_3 - \zeta_3 \partial_{x_1} \eta_2 & \cdots & \zeta_2 \partial_{x_3} \eta_2 - \zeta_3 \partial_{x_3} \eta_1 \\ \vdots & \ddots & \vdots \\ \zeta_1 \partial_{x_1} \eta_2 - \zeta_2 \partial_{x_1} \eta_1 & \cdots & \zeta_1 \partial_{x_3} \eta_2 - \zeta_2 \partial_{x_3} \eta_1 \end{pmatrix}. \end{aligned}$$

Proof. The proof is straightforward and follows from direct calculations. The elaborated arguments can be found, e.g. in [Gol12, Lemma 2.0.10]. \square

Lemma A.1.7 (Properties of the cross product). *For $u, v, w \in \mathbb{R}^3$, the following properties are true.*

- (i) $u \times u = 0$.
- (ii) $u \times v = -v \times u$.
- (iii) $\langle u, u \times v \rangle = 0$.
- (iv) $u \times (v \times w) = \langle u, w \rangle v - \langle u, v \rangle w$.
- (v) $\langle u \times v, w \rangle = \langle w \times u, v \rangle = \langle v \times w, u \rangle$.
- (vi) $\langle u \times (v \times w) + v \times (w \times u) + w \times (u \times v) \rangle = 0$.

Proof. The proof follows by straightforward computations. \square

Theorem A.1.8 (Korn's inequality). *There exists a positive $C > 0$ such that*

$$\|\varepsilon(\mathbf{u})\|_{L^2(\Omega)} + \|\mathbf{u}\|_{L^2(\Omega)} \geq C\|\mathbf{u}\|_{H^1(\Omega)}, \quad (\text{A.1.5})$$

where ε denotes the symmetric part of the gradient from (6.1.5).

Proof. The proof can be found in [BS08, Theorem 11.2.16]. \square

A.2. Functional analytic facts

Theorem A.2.1. *Let \mathcal{X} be a reflexive space. Then each bounded sequence $(x_n) \subset \mathcal{X}$ admits a weakly convergent subsequence, i.e. there exists some $x \in \mathcal{X}$ such that*

$$x_n \xrightarrow{\text{sub}} x \quad \text{weakly in } \mathcal{X}. \quad (\text{A.2.1})$$

Proof. The proof can be found in [Wer00, Theorem III.3.7]. \square

Theorem A.2.2 (Lebesgue dominated convergence). *On the open domain X , we consider measurable functions $f, f_n : X \rightarrow \mathbb{K}$ with $f_n \rightarrow f$ almost everywhere. Let further g be an integrable and measurable function such that for all $n \in \mathbb{N}$, we have $|f_n| \leq g$ almost everywhere. Then f and f_n are integrable and there holds*

$$\lim_{n \rightarrow \infty} \int_X f_n = \int_X f \quad (\text{A.2.2})$$

and, in particular

$$\lim_{n \rightarrow \infty} \int_X |f_n - f| = 0, \quad (\text{A.2.3})$$

i.e. f_n converges towards f even in $L^1(X)$.

Proof. The proof can be found in [Els11, IV, Theorem 5.2]. \square

The dominated convergence theorem even allows an extension in $L^p(X)$.

Corollary A.2.3 (Dominated convergence in L^p). *Let $0 < p < \infty$, $f_n, f : X \rightarrow \mathbb{K}$ measurable for some open domain X , with $f_n \rightarrow f$ almost everywhere. Let further $g \in L^p(X)$ with $|f_n| \leq g$ almost everywhere. Then $f_n, f \in L^p(X)$ and f_n converges towards f even in $L^p(x)$, i.e.*

$$\lim_{n \rightarrow \infty} \|f_n - f\|_{L^p(X)} = 0. \quad (\text{A.2.4})$$

Proof. The proof for an even more general version of this result can be found in [Els11, VI, Theorem 5.3]. \square

Theorem A.2.4 (Rellich-Kondrachov compactness theorem). *Let Ω be an open and bounded subset of \mathbb{R}^n with Lipschitz boundary. Then, the embedding*

$$H^1(\Omega) \hookrightarrow L^2(\Omega)$$

is compact.

Proof. Then proof can be found e.g. in [McL00, Theorem 3.27]. \square

Lemma A.2.5 (Convergence of the product). *Let $1 \leq p, q, r \leq \infty$, $1/p + 1/q = 1/r$, and $f_n \in L^p(X)$, $g_n \in L^q(X)$ with*

$$\lim_{n \rightarrow \infty} \|f_n - f\|_{L^p(X)} = 0, \quad \text{and} \quad \lim_{n \rightarrow \infty} \|g_n - g\|_{L^q(X)} = 0. \quad (\text{A.2.5})$$

Then, there holds

$$\lim_{n \rightarrow \infty} \|f_n g_n - f g\|_{L^r(X)} = 0, \quad (\text{A.2.6})$$

i.e. the product converges strongly in $L^r(X)$. For $1/p + 1/q = 1$, there particularly holds

$$\lim_{n \rightarrow \infty} \|f_n g_n - f g\|_{L^1(X)} = 0. \quad (\text{A.2.7})$$

Proof. The proof is done by straightforward calculation using Hölders inequality from Lemma A.1.4. There holds

$$\begin{aligned} \|f_n g_n - f g\|_{L^r(X)} &= \|(f_n - f)g_n + (g_n - g)f\|_{L^r(X)} \\ &\leq \|(f_n - f)g_n\|_{L^r(X)} + \|(g_n - g)f\|_{L^r(X)} \\ &\leq \|f_n - f\|_{L^p(X)} \|g_n\|_{L^q(X)} + \|g_n - g\|_{L^q(X)} \|f\|_{L^p(X)} \longrightarrow 0. \end{aligned}$$

This concludes the proof. \square

Lemma A.2.6 (Riesz). *Let $0 < p < \infty$ and let (f_n) be a sequence in $L^p(\Omega)$ which converges towards some function $f \in L^p(\Omega)$, i.e.*

$$\|f_n - f\|_{L^p(\Omega)} \rightarrow 0.$$

Then, (f_n) converges towards f even in measure.

Proof. The proof can be found in [Els11, Satz VI 4.3]. \square

Lemma A.2.7 (Weyl). *Let $0 < p \leq \infty$ and $(f_n)_n \in L^p(\Omega)$ be a convergent sequence in $L^p(\Omega)$ with limit $f \in L^p(\Omega)$. Then, there exists a subsequence $(f_{n_k})_k$ of $(f_n)_n$ which converges towards f pointwise almost everywhere in Ω .*

Proof. The proof follows from Lemma A.2.6 and is found e.g. in [Els11, VI, Korollar 2.7]. \square

Lemma A.2.8. *Let X be a Hilbert space, and let $(x_n)_n, (y_n)_n \subset X$ be weakly resp. strongly convergent subsequences with limits $x, y \in X$, i.e.*

$$\begin{aligned} x_n &\longrightarrow x && \text{strongly in } X, \\ y_n &\rightharpoonup y && \text{weakly in } X. \end{aligned}$$

Then, there holds $(x_n, y_n)_X \longrightarrow (x, y)$.

Proof. There holds

$$\begin{aligned} |(x_n, y_n)_X - (x, y)_X| &= |(x_n, y_n)_X - (x, y_n)_X + (x, y_n - y)_X| \\ &= |(x_n - x, y_n)_X + (x, y_n - y)_X| \longrightarrow 0 \end{aligned}$$

due to boundedness of $(y_n)_n$ in X and strong convergence of x_n . \square

Lemma A.2.9. *Let Ω be a bounded domain in \mathbb{R}^d and $a_n \subseteq H^1(\Omega)$ a weakly convergent sequence with limit $a \in H^1(\Omega)$. Then, there holds*

$$\begin{aligned} a_n &\longrightarrow a && \text{strongly in } L^2(\Omega) \quad \text{and} \\ \nabla a_n &\rightharpoonup \nabla a && \text{weakly in } L^2(\Omega), \end{aligned}$$

i.e. the individual contributions of the norm are also convergent.

Proof. The first result is a direct consequence of the Rellich-Kondrachov theorem A.2.4. To see the second one, we argue as follows: Due to boundedness of weakly convergent sequences, from $\|a_n\|_{H^1(\Omega)}^2 = \|a_n\|_{L^2(\Omega)}^2 + \|\nabla a_n\|_{L^2(\Omega)}^2 \leq C < \infty$, we get $\|\nabla a_n\|_{L^2(\Omega)} \leq C$. This, however yields the existence of a function $A \in L^2(\Omega)$ with

$$\nabla a_n \xrightarrow{\text{sub}} A \text{ weakly in } L^2(\Omega).$$

It remains to investigate the equality $A = \nabla a$. From weak convergence in $L^2(\Omega)$, we get for any testfunction $\varphi \in C_c^\infty(\Omega)$

$$\lim_n (\nabla a_n, \varphi) = (A, \varphi)$$

and via integration by parts thus

$$\int_\Omega A \varphi = \lim_n \int_\Omega \nabla a_n \varphi = - \lim_n \int_\Omega a_n \operatorname{div} \varphi = - \int_\Omega a \operatorname{div} \varphi = \int_\Omega \nabla a \varphi.$$

Since the testfunction $\varphi \in C_c^\infty(\Omega)$ was arbitrary, this yields $A = \nabla a$. Moreover, the limit is the same for each subsequence, and hence the entire sequence is convergent which is the desired result. \square

The following Lemma considers the convergence of the product of a weakly L^1 -convergent sequence and a strongly L^2 -convergent sequence.

Lemma A.2.10. *Let Ω be a bounded domain. Let further $a_n \in L^2(\Omega)$ be bounded and $b_n \subseteq L^2(\Omega)$ with*

$$\begin{aligned} a_n &\rightharpoonup a \text{ weakly in } L^1(\Omega) \text{ and} \\ b_n &\longrightarrow b \text{ strongly in } L^2(\Omega). \end{aligned}$$

Then, there holds

$$(a_n, b_n) \longrightarrow (a, b),$$

where (\cdot, \cdot) denotes the L^2 -scalar product.

Proof. From the boundedness of a_n in $L^2(\Omega)$, we deduce the existence of a function $A \in L^2(\Omega)$ with

$$a_n \xrightarrow{\text{sub}} A \text{ in } L^2(\Omega).$$

From the definition of weak limits, we get

$$\begin{aligned} (a_n, \varphi) &\longrightarrow (A, \varphi) \quad \text{for all } \varphi \in L^2(\Omega) \supseteq C_c^\infty(\Omega) \text{ and} \\ (a_n, \varphi) &\longrightarrow (a, \varphi) \quad \text{for all } \varphi \in L^\infty(\Omega) \supseteq C_c^\infty(\Omega) \end{aligned}$$

and thus

$$(A - a, \varphi) \equiv 0 \quad \text{for all } \varphi \in C_c^\infty(\Omega)$$

and hence $A = a$ in $L^2(\Omega)$. As this argument holds for any subsequence of a_n , we conclude convergence of the entire sequence. Exploiting Lemma A.2.8, we conclude the desired result. \square

Lemma A.2.11 (Mazur). *Let (x_n) be a weakly convergent sequence in a normed vector space X with $x_n \rightharpoonup x$. Then, the limit x lies within the closed convex hull of the members of x_n , i.e. $x \in \overline{\text{conv}}\{x_n : n \in \mathbb{N}\}$.*

Proof. The proof can be found in [RR04, Theorem 10.19]. \square

By definition, the space $L^2(\mathbf{H}^1)$ contains all functions $\mathbf{u} : [0, T] \rightarrow \mathbf{H}^1(\Omega)$, cf. e.g. [Eva02, Section 5.9.2]. We thus have

$$\begin{aligned} \mathbf{u} &: [0, T] \longrightarrow \mathbf{H}^1(\Omega), \\ \mathbf{u}(t) &\in \mathbf{H}^1(\Omega) \text{ and therefore } \mathbf{u}(t)(x) \in \mathbb{R}^3. \end{aligned}$$

For a given function $\mathbf{u} \in L^2(\mathbf{H}^1)$, the function defined on the time-space cylinder $\tilde{\mathbf{u}} \in L^2(\Omega_T)$ with one weak spatial derivative is implicitly defined by

$$\begin{aligned} \tilde{\mathbf{u}} &: \Omega_T \longrightarrow \mathbb{R}^3, \\ \tilde{\mathbf{u}}(t, \mathbf{x}) &= \mathbf{u}(t)(\mathbf{x}). \end{aligned}$$

To ease the presentation, as usually done in literature, we will notationally not further distinguish between \mathbf{u} and $\tilde{\mathbf{u}}$. The next result now states that for such functions, one can interchange the spatial derivative and the time evaluation (at least if they are smooth enough).

Lemma A.2.12. *Let $\mathbf{u} \in C(C^1)$ and $\tilde{\mathbf{u}}$ be defined as above, then we have*

$$(\nabla \tilde{\mathbf{u}})(t, \mathbf{x}) = (\nabla \mathbf{u}(t))(\mathbf{x}), \quad (\text{A.2.8})$$

i.e. the evaluation in time and the weak spatial gradient interchange. To ease the presentation, we write

$$(\nabla \mathbf{u})(t, \mathbf{x}) = (\nabla \mathbf{u}(t))(\mathbf{x}).$$

Proof. The proof is done by straightforward calculation. It obviously remains to show the desired result for one partial derivative. By definition we get

$$\begin{aligned} \frac{\partial \tilde{\mathbf{u}}}{\partial x_1}(t, x_1, x_2, x_3) &= \lim_{h \rightarrow 0} \frac{\tilde{\mathbf{u}}(t, x_1 + h, x_2, x_3) - \tilde{\mathbf{u}}(t, x_1, x_2, x_3)}{h} \\ &= \lim_{h \rightarrow 0} \frac{\mathbf{u}(t)(x_1 + h, x_2, x_3) - \mathbf{u}(t)(x_1, x_2, x_3)}{h} \\ &= \frac{\partial \mathbf{u}(t)}{\partial x_1}(x_1, x_2, x_3). \end{aligned}$$

□

Remark. *Note, that we only apply the last result for smooth functions, i.e. strong derivatives. Formally, the proof is not sufficient for weak gradients.*

A.3. What else?

Lemma A.3.1. *Let $\{s_{mn}\}_{mn} \subset \mathbb{R}$ be a convergent doublesequence with simultaneous limit $\lim_{(m,n) \rightarrow (\infty, \infty)} s_{mn} = s$ and assume further that the limit $s_m := \lim_{n \rightarrow \infty} s_{mn}$ exists in \mathbb{R} for all $m \in \mathbb{N}_0$. Then, the limit $\lim_{m \rightarrow \infty} s_m$ exists in \mathbb{R} , and there holds*

$$\lim_{m \rightarrow \infty} s_m = \lim_{m \rightarrow \infty} \left(\lim_{n \rightarrow \infty} s_{mn} \right) = \lim_{(m,n) \rightarrow (\infty, \infty)} s_{mn} = s.$$

Proof. The proof can be found e.g. in [Sch11, Satz 3.6.6].

□

List of Figures

1.1. Basic functionality of a magnetic hard drive.	2
1.2. Precession part and damping part of the LLG equation	5
1.3. Evolution of the magnetization, where precession and damping are taken into account.	6
1.4. Example geometry which demonstrates model separation into LLG region Ω_1 and Maxwell region Ω_2	11
3.1. Example geometry which demonstrates model separation into LLG region Ω_1 and Maxwell region Ω_2	71
3.2. Magnetization dynamics on $[0, 3]$ for the above example.	79
3.3. Spatial error for $k = 0.01$. As expected, linear decay is observed.	80
3.4. Temporal error for $P = 20480$ spatial elements. As expected, linear decay is observed.	80
3.5. Magnetization dynamics on $[0, 0.03]$ for $h = 1/32$ and $k = 0.00001$	83
3.6. Magnetization dynamics on $[0, 0.03]$ in lateral view.	84
3.7. Different empirical blowup times for $h \in \{1/8, 1/16, 1/32, 1/64, 1/96, 1/128\}$ and $k = 0.00001$	85
3.8. Empirical blowup times for $k \in \{10^{-2}, 10^{-3}, 10^{-4}, 10^{-5}, 10^{-6}\}$ and $h = 1/32$	85
3.9. Different empirical blowup times for $\alpha \in \{1, 1/32, 1/64, 1/128, 1/256, 1/512\}$, $k = 0.00001$, and $h = 1/32$	86
3.10. Empirical blowup times for $s \in \{1, 2, 3, 4, 5, 6\}$, $\alpha = 1$, $k = 0.0001$, and $h = 1/32$	86
3.11. Energy $\mathcal{E}(\mathbf{m}, t)$ for different configurations of mesh parameters and $\alpha = 1$, $s = 4$ plotted over time.	87
3.12. Condition numbers of M and the full matrix from (3.3.1) for $\alpha = 1$ plotted over the simulation time.	88
3.13. Magnetization dynamics as 2D projection on $[0, 2]$ for $\alpha = 1$ (white) and $\alpha = 0$ (red). Initial state is visualized in the top left picture	90
3.14. Condition numbers of M and the full matrix from (3.3.1) for $\alpha = 0$ plotted over the simulation time.	91
3.15. Energy $\mathcal{E}(\mathbf{m}, t)$ for different values of θ plotted over time. Energy computed with the midpoint scheme is plotted for comparison (dark blue).	93
5.1. Decay of $\text{Err}(\mathbf{u})$ for uniform refinement in time with $P = 320$ spatial elements for different time steps. As expected, we observe linear behaviour.	133

5.2.	Decay of $\text{Err}(\mathbf{u})$ for uniform refinement in space with $N = 1000$ time steps and $P \in \{5, 40, 320, 2560, 20480\}$. We observe linear decay in the beginning which is then dominated by the temporal error.	134
5.3.	Error decay for $P \in \{5, 40, 320, 2560, 20480, 163840\}$	134
5.4.	Evolution of the magnetization with $H_s = 30$. We observe blowup behavior and alignment of the magnetization in $(0, 0, -1)$ -direction afterwards.	137
5.5.	Exchange energy $\mathcal{E}_{\text{exch}} = \ \nabla \mathbf{m}(t)\ _{\mathbf{L}^2(\Omega)}^2$ plotted over time.	138
5.6.	Maximum norm $\ \nabla \mathbf{m}(t)\ _{\mathbf{L}^\infty(\Omega)}$ plotted over time.	138
5.7.	Different energy contributions for $H_s = 0$ plotted over time.	139
5.8.	Exchange energy (solid) and $W^{1,\infty}(\Omega)$ -seminorm (dotted) for simulation on refined mesh with $P = 20480$ elements.	139
5.9.	Evolution of the magnetization with $H_s = 30$ after $T = 0.15$. We observe realignment of the magnetization in $(0, 0, 1)$ -direction.	140
5.10.	Different energy contributions for $H_s = 30$ and extended simulation time. . . .	141
5.11.	Total energy $\mathcal{E}_{\text{total}} = \mathcal{E}_{\text{exch}} + \mathcal{E}_{\text{curl}} + \mathcal{E}_{\mathbf{H}}$ for $H_s = 30$ on the extended time interval.	141
5.12.	Dynamic behaviour of the magnetization that leads to a vortex state.	143
5.13.	Different energy contributions for vortex state plotted over time.	144
5.14.	Total energy $\mathcal{E}_{\text{total}} = \mathcal{E}_{\text{exch}} + \mathcal{E}_{\text{curl}} + \mathcal{E}_{\mathbf{H}}$ of vortex state plotted over time. . . .	144
5.15.	Graded mesh for flower state computation as projection (left). The two domains Ω and $\hat{\Omega}$ as 3D view (right).	144
5.16.	Dynamic behaviour of the magnetization that leads to a flower state.	145
5.17.	Symmetric flower state from lateral view (left) and top view (right).	145
5.18.	Different energy contributions of the flower state.	146
5.19.	Total energy $\mathcal{E}_{\text{total}} = \mathcal{E}_{\text{exch}} + \mathcal{E}_{\text{curl}} + \mathcal{E}_{\mathbf{H}} + \mathcal{E}_{\text{ani}}$ of flower state.	147
5.20.	Twisted flower state.	147
6.1.	Sparsity pattern of the stiffness matrix.	166
6.2.	Sparsity pattern of the system matrix A from the conservation of momentum equation.	167
6.3.	Evolution of the displacement for $P = 320$ spatial elements and $N = 100$ time steps.	168
6.4.	Error decay for uniform refinement in time with $P = 320$ spatial elements. As expected, we observe linear behaviour.	169
6.5.	Decay of the spatial error in \mathbf{L}^2 -norm plotted over the amount of spatial elements for the instationary problem.	169
6.6.	Decay of the spatial error in \mathbf{H}^1 -norm plotted over the amount of spatial elements for the instationary problem.	170
6.7.	Error decay in \mathbf{L}^2 -norm for the stationary problem plotted over the amount of spatial elements.	171
6.8.	Error decay in \mathbf{H}^1 -norm for the stationary problem plotted over the amount of spatial elements.	171
6.9.	Visualization of the exact stationary solution (red) and its numerical approximation (blue).	172
6.10.	Dynamic behaviour of the magnetization for small magnetostriction with $C_\lambda = 1$.	173
6.11.	Energy contributions $\mathcal{E}_{\text{exch}}$ (left), $\mathcal{E}_{\text{elastic}}$ (middle), and $\mathcal{E}_{\text{total}}$ (right) for $C_\lambda = 1$. Clearly, the exchange contribution is dominant.	174

6.12. Energy contributions $\mathcal{E}_{\text{exch}}$ (<i>left</i>), $\mathcal{E}_{\text{elastic}}$ (<i>middle</i>), and $\mathcal{E}_{\text{total}}$ (<i>right</i>) for $C_\lambda = 2$. Influence of the magnetostriction is clearly visible.	174
6.13. Total energy $\mathcal{E}_{\text{total}}$ for different values of $C_\lambda \in \{1, 2, 3, 10\}$ plotted over time. . .	175
6.14. Hysteresis loop for different values of C_λ . Clearly, the coercivity increases as C_λ is increased.	177

List of Tables

3.1. Err(m) for the above example computed with respect to a reference solution. . .	81
5.1. Err(u) for varying time steps.	135
5.2. Err(u) for varying amount of spatial elements.	136
5.3. Err(u) for varying amount of spatial elements.	136
6.1. Err(u) for varying time steps.	166
6.2. Spatial error in \mathbf{L}^2 - and \mathbf{H}^1 -norm, respectively.	170
6.3. Spatial error in \mathbf{L}^2 - and \mathbf{H}^1 -norm for stationary problem.	173

Bibliography

- [AFF⁺13] M. AURADA, M. FEISCHL, T. FÜHRER, M. KARKULIK, J. M. MELENK, and D. PRAETORIUS. *Classical FEM-BEM coupling methods: nonlinearities, well-posedness, and adaptivity*. Computational Mechanics, volume 51, no. 4, pp. 399–419 (2013).
- [AJ06] F. ALOUGES and P. JAISSE. *Convergence of a finite element discretization for the Landau–Lifshitz equations in micromagnetism*. Mathematical Models and Methods in Applied Sciences, volume 16, no. 2, pp. 299–316 (2006).
- [AKST12] F. ALOUGES, E. KRITSIKIS, J. STEINER, and J.-C. TOUSSAINT. *A convergent and precise finite element scheme for Landau-Lifschitz-Gilbert equation*. arXiv.org (2012).
URL <http://arxiv.org/abs/1206.0997>
- [AKT11] F. ALOUGES, E. KRITSIKIS, and J.-C. TOUSSAINT. *A convergent finite element approximation for Landau–Lifschitz–Gilbert equation*. Physica B: Physics of Condensed Matter, pp. 1–5 (2011).
- [Alo08a] F. ALOUGES. *A new finite element scheme for Landau-Lifchitz equations*. Discrete and Continuous Dynamical Systems Series S, volume 1, no. 2, pp. 187–196 (2008).
- [Alo08b] F. ALOUGES. *Mathematical models in micromagnetism: an introduction*. ESAIM: Proceedings, volume 22, pp. 114–117 (2008).
- [AS92] F. ALOUGES and A. SOYEUR. *On global weak solutions for Landau-Lifshitz equations: existence and nonuniqueness*. Nonlinear Analysis: Theory, Methods & Applications, volume 18, no. 11, pp. 1071–1084 (1992).
- [ABN00] H. AMMARI, A. BUFFA, and J. C. NÉDÉLEC. *A Justification of Eddy Currents Model for the Maxwell Equations*. SIAM Journal on Applied Mathematics, volume 60, no. 5, pp. 1805–1823 (2000).
- [Bañ05a] L. BAÑAS. *A numerical method for the Landau-Lifshitz equation with magnetostriiction*. Mathematical Methods in the Applied Sciences, volume 28, no. 16, pp. 1939–1954 (2005).

- [Bañ05b] L. BAÑAS. On dynamical Micromagnetism with Magnetostriction. Ph.D. thesis, University of Ghent (2005).
URL <http://www.ma.hw.ac.uk/~lubomir/pubs/thesis.pdf>
- [Bañ08] L. BAÑAS. *Adaptive techniques for Landau–Lifshitz–Gilbert equation with magnetostriction*. Journal of Computational and Applied Mathematics, volume 215, no. 2, pp. 304–310 (2008).
- [Bañ10] L. BAÑAS. *An efficient multigrid preconditioner for Maxwell’s equations in micromagnetism*. Mathematics and Computers in Simulation, volume 80, no. 8, pp. 1657–1663 (2010).
- [Bar05] S. BARTELS. *Stability and convergence of finite-element approximation schemes for harmonic maps*. SIAM Journal on Numerical Analysis, volume 43, no. 1, pp. 220–238 (electronic) (2005).
- [BBP08] L. BANAS, S. BARTELS, and A. PROHL. *A convergent implicit finite element discretization of the Maxwell–Landau–Lifshitz–Gilbert equation*. SIAM Journal on Numerical Analysis, volume 46, no. 3, pp. 1399–1422 (2008).
- [BBP13] L. BANAS, Z. BRZEŹNIAK, and A. PROHL. *Computational Studies for the Stochastic Landau–Lifshitz–Gilbert Equation*. SIAM Journal on Scientific Computing, volume 35, no. 1, pp. B62–B81 (2013).
- [Ber02] L. BERGER. *Interaction of electrons with spin waves in the bulk and in multilayers (invited)*. Journal of Applied Physics, volume 91, no. 10, pp. 6795–6800 (2002).
- [BFF⁺12] F. BRUCKNER, M. FEISCHL, T. FÜHRER, P. GOLDENITS, M. PAGE, D. PRAETORIUS, and D. SUESS. *Multiscale modeling in micromagnetics: well-posedness and numerical integration*. arXiv.org (2012).
URL <http://arxiv.org/abs/1209.5548>
- [BKP08] S. BARTELS, J. KO, and A. PROHL. *Numerical analysis of an explicit approximation scheme for the Landau–Lifshitz–Gilbert equation*. Mathematics of Computation, volume 77, no. 262, pp. 773–788 (2008).
- [BP06] S. BARTELS and A. PROHL. *Convergence of an implicit finite element method for the Landau–Lifshitz–Gilbert equation*. SIAM Journal on Numerical Analysis, volume 44, no. 4, pp. 1405–1419 (2006).
- [BPP13] L. BAÑAS, M. PAGE, and D. PRAETORIUS. *A convergent linear finite element scheme for the Maxwell–Landau–Lifshitz–Gilbert equation*. arXiv.org (2013).
URL <http://arxiv.org/abs/1303.4009v1>
- [BPPR13] L. BAÑAS, M. PAGE, D. PRAETORIUS, and J. ROCHAT. *On the Landau–Lifshitz–Gilbert equation with magnetostriction*. arXiv.org (2013).
URL <http://arxiv.org/abs/1303.4060v2>
- [BPS08] L. BAÑAS, A. PROHL, and M. SLODIČKA. *Modeling of thermally assisted magnetodynamics*. SIAM Journal on Numerical Analysis, volume 47, no. 1, pp. 551–574 (2008).

-
- [BPS12] L. BAÑAS, A. PROHL, and M. SLODIČKA. *Numerical scheme for augmented Landau-Lifshitz equation in heat assisted recording*. Journal of Computational and Applied Mathematics, volume 236, no. 18, pp. 4775–4787 (2012).
- [Bra07] D. BRAESS. Finite Elemente. Springer Verlag, Berlin, 4th edition (2007).
- [Bru13] F. BRUCKNER. Multiscale Simulation of Magnetic Nanostructures. Ph.D. thesis, Vienna University of Technology (2013).
URL <http://publik.tuwien.ac.at/showentry.php?ID=218324&lang=2>
- [BS05] L. BAÑAS and M. SLODIČKA. *Space discretization for the Landau-Lifshitz-Gilbert equation with magnetostriction*. Computer Methods in Applied Mechanics and Engineering, volume 194, no. 2-5, pp. 467–477 (2005).
- [BS06] L. BAÑAS and M. SLODIČKA. *Error estimates for Landau-Lifshitz-Gilbert equation with magnetostriction*. Applied Numerical Mathematics. An IMACS Journal, volume 56, no. 8, pp. 1019–1039 (2006).
- [BS08] S. BRENNER and R. SCOTT. The Mathematical Theory of Finite Element Methods. Springer Verlag, New York, 3rd edition (2008).
- [BVB⁺] F. BRUCKNER, C. VOGLER, B. BERGMAYER, T. HUBER, M. FUGER, D. SUESS, M. FEISCHL, T. FÜHRER, M. PAGE, and D. PRAETORIUS. *Combining micromagnetism and magnetostatic Maxwell equations for multiscale magnetic simulations*. ASC Report (2013).
URL <http://www.asc.tuwien.ac.at/~mpage/?open=publications&sub=0>
- [CEF11] G. CARBOU, M. A. EFENDIEV, and P. FABRIE. *Global weak solutions for the Landau-Lifshitz equation with magnetostriction*. Mathematical Methods in the Applied Sciences, volume 34, no. 10, pp. 1274–1288 (2011).
- [CF98] G. CARBOU and P. FABRIE. *Time average in micromagnetism*. Journal of Differential Equations, volume 147, no. 2, pp. 383–409 (1998).
- [DP98] C. CARSTENSEN and D. PRAETORIUS. *Numerical analysis for a macroscopic model in micromagnetics*. SIAM Journal on Numerical Analysis, volume 42, no. 6, pp. 2633–2651 (2005).
- [Che08] L. CHEN. *iFEM: an innovative finite element methods package in MATLAB*. Preprint, University of Maryland (2008).
URL <http://www.math.uci.edu/~chenlong/Papers/iFEMpaper.pdf>
- [Cim05] I. CIMRÁK. On the Landau-Lifshitz equation of ferromagnetism. Ph.D. thesis, University of Ghent (2005).
URL <http://www.kst.fri.uniza.sk/~icimrak/thesis/thesis.pdf>
- [Cim07a] I. CIMRÁK. *A Survey on the numerics and computations for the Landau-Lifshitz equation of micromagnetism*. Archives of Computational Methods in Engineering, volume 15, no. 3, pp. 1–37 (2007).
-

- [Cim07b] I. CIMRÁK. *Error analysis of a numerical scheme for 3D Maxwell-Landau-Lifshitz system*. Mathematical Methods in the Applied Sciences, volume 30, no. 14, pp. 1667–1683 (2007).
- [Cim07c] I. CIMRÁK. *Existence, regularity and local uniqueness of the solutions to the Maxwell-Landau-Lifshitz system in three dimensions*. Journal of Mathematical Analysis and Applications, volume 329, no. 2, pp. 1080–1093 (2007).
- [Cim08] I. CIMRÁK. *Regularity properties of the solutions to the 3D Maxwell-Landau-Lifshitz system in weighted Sobolev spaces*. Journal of Computational and Applied Mathematics, volume 215, no. 2, pp. 320–327 (2008).
- [Cos88] M. COSTABEL. *A symmetric method for the coupling of finite elements and boundary elements*. In The mathematics of finite elements and applications, VI (Uxbridge, 1987), pp. 281–288. Academic Press, London (1988).
- [dSM⁺05] M. D’AQUINO, C. SERPICO, and G. MIANO. *Geometrical integration of Landau-Lifshitz-Gilbert equation based on the midpoint rule*. Journal of Computational Physics, volume 209, no. 2, pp. 730–743 (2005).
- [Els11] J. ELSTRODT. Maß- und Integrationstheorie. Springer Verlag, Berlin, 7th edition (2011).
- [Eva02] L. C. EVANS. Partial Differential Equations. American Mathematical Society, Providence, Rhode Island (2002).
- [FLMP12] S. FERRAZ-LEITE, J. M. MELENK, and D. PRAETORIUS. *Numerical quadratic energy minimization bound to convex constraints in thin-film micromagnetics*. Numerische Mathematik, volume 122, no. 1, pp. 101–131 (2012).
- [FK90] D. R. FREDKIN and T. R. KOEHLER. *Hybrid method for computing demagnetizing fields*. Magnetism, IEEE Transactions on, volume 26, no. 2, pp. 415–417 (1990).
- [GC09] C. J. GARCÍA-CERVERA. *Numerical micromagnetics: a review*. Boletín SEMA, no. 39 (2007).
- [GD08] B. GUO and S. DING. Landau-Lifshitz equations. Frontier of Research with the Chinese Academy of Sciences. World Scientific, Singapore, 1st edition (2008).
- [Get08] M. GETZLAFF. Fundamentals of Magnetism. Springer Verlag, Berlin (2008).
- [GHPS] P. GOLDENITS, G. HRKAC, D. PRAETORIUS, and D. SUESS. *An effective Integrator for the Landau-Lifshitz-Gilbert equation*. ASC Report (2012).
URL <http://publik.tuwien.ac.at/showentry.php?ID=206432&lang=2>
- [Gil00] W. GILBERT. *De Magnete, Magneticisque Corporibus, et de Magno Magnete Tellure (Translation from 1893)* (1600).
URL <http://archive.org/details/onloadstonemagne00gilbuoft>
- [Gil55] T. L. GILBERT. *A lagrangian formulation of the gyromagnetic equation of the magnetic field*. Physical Review, pp. 1243–1255 (1955).

- [Gil04] T. L. GILBERT. *A Phenomenological Theory of Damping in Ferromagnetic Materials*. IEEE Transactions on Magnetism, volume 40, no. 6, pp. 3443–3449 (2004).
- [GLT13] B. GOLDYS, K.-N. LE, and T. TRAN. *A finite element approximation for the stochastic Landau-Lifshitz-Gilbert equation*. arXiv.org (2013).
URL <http://arxiv.org/abs/1308.3912>
- [Gol12] P. GOLDENITS. Konvergente numerische Integration der Landau-Lifshitz-Gilbert Gleichung (in German). Ph.D. thesis, Vienna University of Technology (2012).
- [HKC04] J. HO, F. KHANNA, and B. CHOI. *Radiation-Spin Interaction, Gilbert Damping, and Spin Torque*. Physical Review Letters, volume 92, no. 9, p. 097601 (2004).
- [Hrk05] G. HRKAC. Combining Eddy-Current and Micromagnetic Simulations with Finite-Element method. Ph.D. thesis, VDM Verlag Dr. Müller (2005).
- [HS08] A. HUBERT and R. SCHÄFER. Magnetic domains: the analysis of magnetic microstructures. Springer Verlag (2008).
- [HW08] G. C. HSIAO and W. WENDLAND. Boundary integral equations. Springer Verlag, Berlin (2008).
- [JN80] C. JOHNSON and J. C. NÉDÉLEC. *On the coupling of boundary integral and finite element methods*. Mathematics of Computation, volume 35, no. 152, pp. 1063–1079 (1980).
- [KP06] M. KRUZÍK and A. PROHL. *Recent developments in the modeling, analysis, and numerics of ferromagnetism*. SIAM review, volume 48, no. 3, pp. 439–483 (2006).
- [Kro07] H. KRONMÜLLER. General Micromagnetic Theory. John Wiley & Sons, Ltd, Chichester, UK (2007).
- [LL35] L. D. LANDAU and E. LIFSHITZ. *On the theory of the dispersion of magnetic permeability in ferromagnetic bodies*. Physikalische Zeitschrift der Sowjetunion, pp. 153–169 (1935).
- [LPPT13] K.-N. LE, M. PAGE, D. PRAETORIUS, and T. TRAN. *On a decoupled linear FEM integrator for Eddy-current-LLG*. arXiv.org (2013).
URL <http://arxiv.org/abs/1306.3319v1>
- [LT12] K.-N. LE and T. TRAN. *A convergent finite element approximation for the quasi-static Maxwell-Landau-Lifshitz-Gilbert equations*. arXiv.org (2012).
URL <http://arxiv.org/abs/1212.3369>
- [LT13] K.-N. LE and T. TRAN. *A finite element approximation for the quasi-static Maxwell-Landau-Lifshitz-Gilbert equations*. unpublished preprint, pp. 1–14 (2013).
- [Max65] J. C. MAXWELL. *A dynamical theory of the electromagnetic field*. Philosophical Transactions of the Royal Society of London, volume 155, pp. 459–512 (1865).
- [McL00] W. MCLEAN. Strongly elliptic systems and boundary integral equations. Cambridge Univ Press, Cambridge (2000).

- [Mon08] P. MONK. Finite Element Methods for Maxwell's Equations. Oxford Science Publications, Oxford (2008).
- [MV99] P. B. MONK and O. VACUS. *Error estimates for a numerical scheme for ferromagnetic problems*. SIAM Journal on Numerical Analysis, volume 36, no. 3, pp. 696–718 (electronic) (1999).
- [MV01] P. B. MONK and O. VACUS. *Accurate discretization of a non-linear micromagnetic problem*. Computer Methods in Applied Mechanics and Engineering, volume 190, no. 40-41, pp. 5243–5269 (2001).
- [Néd80] J. C. NÉDÉLEC. *Mixed finite elements in \mathbb{R}^3* . Numerische Mathematik, volume 35, no. 3, pp. 315–341 (1980).
- [PHPS12] M. PAGE, G. HRKAC, D. PRAETORIUS, and D. SUESS. *Numerical integrator for the LLG equation with magnetostriction (talk)*. In Mathmod 2012. Vienna (2012).
- [Pla00] R. PLATO. Numerische Mathematik kompakt. Vieweg, Braunschweig (2000).
- [Pop74] H. POPPE. Compactness in General Function Spaces. VEB Deutscher Verlag der Wissenschaften, Berlin (1974).
- [Pra04] D. PRAETORIUS. *Analysis of the operator $\Delta^{-1}\text{div}$ arising in magnetic models*. Journal for Analysis and its Applications, volume 23, no. 3, pp. 589–605 (2004).
- [Pro01] A. PROHL. Computational Micromagnetism. Teubner Verlag, Stuttgart, 1st edition (2001).
- [RR04] M. RENARDY and R. ROGERS. An Introduction to Partial Differential Equations. Springer Verlag, New York, 2nd edition (2004).
- [Roc12] J. ROCHAT. An Implicit Finite Element Method for the Landau-Lifshitz-Gilbert Equation with Exchange and Magnetostriction. Master's thesis, EPFL Lausanne (2012).
- [RZMP81] J. RIVAS, J. ZAMARRO, E. MARTIN, and C. PEREIRA. *Simple approximation for magnetization curves and hysteresis loops*. IEEE Transactions on Magnetics, volume 17, no. 4, pp. 1498–1502 (1981).
- [SSS⁺01] T. SCHREFL, D. SUESS, W. SCHOLZ, H. FORSTER, V. TSIANTOS and J. FIEDLER, editors C. CARSTENSEN, S. FUNKEN, W. HACKBUSCH, R. H. W. HOPPE, and P. MONK. *Finite Element Micromagnetics*. taken from Computational Electromagnetics, Lecture Notes in Computational Science and Engineering. Springer Verlag, Berlin, 1st edition (2001).
- [Sch11] F. SCHULZ. Analysis 1. Oldenbourg Verlag, München, 2nd edition (2011).
- [SS11] S. SAUTER and C. SCHWAB. Boundary element methods. Springer Verlag, Berlin (2011).
- [SZ80] L. R. SCOTT and S. ZHANG. *Finite element interpolation of nonsmooth functions satisfying boundary conditions*. Mathematics of Computation, volume 54, no. 190, pp. 483–493 (1980).

- [Ver93] G. L. VERSCHUUR. Hidden Attraction: The History and Mystery of Magnetism. Oxford University Press, New York (1993).
- [Ver96] R. VERFÜRTH. A Review of A Posteriori Error Estimation and Adaptive Mesh-Refinement Strategies. John Wiley & Sons, Ltd, Chichester (1996).
- [Vis85] A. VISINTIN. *On Landau-Lifshitz' equations for ferromagnetism*. Japan Journal of Applied Mathematics, volume 2, no. 1, pp. 69–84 (1985).
- [Weba] WEBSITE. *iFEM - an innovative finite element method package in MATLAB*. URL <http://ifem.wordpress.com>
- [Webb] WEBSITE. *μ MAG - National Institute of Standards and Technology*. URL <http://www.ctcms.nist.gov/~rdm/mumag.org.html>
- [Webc] WEBSITE. *ParaView*. URL <http://www.paraview.org>
- [Wer00] D. WERNER. Funktionalanalysis. Springer, Berlin, 3rd edition (2000).
- [Woh10] P. WOHLHÜTER. Landau-Lifshitz- und Landau-Lifshitz-Gilbert-Gleichung mit Langevin-Dynamik sowie Spin Transfer Torque. Seminar paper, University of Konstanz (2010).
- [Zei90] E. ZEIDLER. Nonlinear functional analysis and its applications. Springer Verlag, New York (1990).

AUTHOR'S CV

MARCUS PAGE, M.Sc.

Date of birth: 19.06.1984
Place of birth: Groß-Gerau
Citizenship: German
email: `marcus.page@tuwien.ac.at`

EDUCATION

since 6/2010 **Vienna University of Technology**
PhD studies (technical mathematics)

10/2008 - 05/2010 **University of Vienna**
Master studies in mathematics with specialization in
numerical mathematics and scientific computing
Master's thesis (in German): *Schätzerreduktion und Konvergenz
adaptiver FEM für Hindernisprobleme*
Supervisor: Ao. Univ. Prof. Dipl. Math. Dr.techn. Dirk Praetorius

10/2006 – 9/2007 **Nihon University, Tokyo**
Exchange student in Japan

10/2004 – 9/2008 **Darmstadt University of Technology**
Bachelor studies in *Mathematics with Computer Science*
Bachelor's thesis: *Mathematical Approaches to Speech Recognition*
Supervisors: Prof. Dr. Jens Lang, Prof. Dr. Tetsuya Hoya

9/1994 – 6/2003 **Edith-Stein-Schule, Darmstadt**
Abitur with specialization in mathematics and computer science.

PUBLICATIONS AND PROCEEDINGS

Ľ. Bañas, M. Page, D. Praetorius, J. Rochat:
**A decoupled and unconditionally convergent linear FEM integrator for the
Landau-Lifshitz-Gilbert equation with magnetostriction,**
accepted for publication in IMA. J. Numer. Anal. (2014).

M. Feischl, M. Page, D. Praetorius:
Convergence and quasi-optimality of adaptive FEM with inhomogeneous Dirichlet data,
J. Comput. Appl. Math., 255, pp. 481-501 (2014).

M. Aurada, M. Feischl, J. Kemetmüller, M. Page, D. Praetorius:
Each $H^{1/2}$ -stable projection yields convergence and quasi-optimality of adaptive FEM with inhomogeneous Dirichlet data in \mathbb{R}^d ,
M2AN Math. Model. Numer. Anal., 47, pp. 1207-1235 (2013).

F. Bruckner, C. Vogler, B. Bergmair, T. Huber, M. Fuger, D. Süß, M. Feischl, T. Führer, M. Page, D. Praetorius:
Combining micromagnetism and magnetostatic Maxwell equations for multiscale magnetic simulations,
J. Magn. Mater., 343, pp. 163-168 (2013).

M. Feischl, M. Page, D. Praetorius:
Convergence of adaptive FEM for some elliptic obstacle problem with inhomogeneous Dirichlet data,
accepted for publication in Int. J. Numer. Anal. Model. (2013).

M. Page, D. Praetorius:
Convergence of adaptive FEM for some elliptic obstacle problem,
Appl. Anal., 92, pp. 595-615 (2013).

M. Feischl, M. Page, D. Praetorius:
Convergence and quasi-optimality of adaptive FEM with inhomogeneous Dirichlet data,
PAMM: Proceedings in Applied Mathematics and Mechanics, pp. 769-772 (2011).

M. Feischl, M. Page, D. Praetorius:
Convergence of adaptive FEM for elliptic obstacle problems,
PAMM: Proceedings in Applied Mathematics and Mechanics, pp. 767-768 (2011).

C. Brzuska, M. Fischlin, T. Freudenreich, A. Lehmann, M. Page, J. Schelbert, D. Schroeder, F. Volk:
Security of Sanitizable Signatures Revisited,
Lecture Notes in Computer Science, Volume 5443, pp. 317-336 (2009).

PREPRINTS

Ľ. Bañas, M. Page, D. Praetorius:
A convergent linear finite element scheme for the Maxwell-Landau-Lifshitz-Gilbert equations,

ASC Report 09/2013, Institute for Analysis and Scientific Computing, Vienna University of Technology, Wien (2013).

K. Le, M. Page, D. Praetorius, T. Tran:

On a decoupled linear FEM integrator for eddy-current-LLG,

ASC Report 15/2013, Institute for Analysis and Scientific Computing, Vienna University of Technology, Wien (2013).

L. Bañas, M. Page, D. Praetorius:

A general integrator for the Landau-Lifshitz-Gilbert equation,

ASC Report 42/2012, Institute for Analysis and Scientific Computing, Vienna University of Technology, Wien (2012).

F. Bruckner, M. Feischl, T. Führer, P. Goldenits, M. Page, D. Praetorius, D. Süss:

Multiscale Modeling in Micromagnetics: Well-Posedness and Numerical Integration,

ASC Report 34/2012, Institute for Analysis and Scientific Computing, Vienna University of Technology, Wien (2012).

SUPERVISED THESES

M. Mayr (Supervisor: M. Page, D. Praetorius):

MILLG - Ein Löser für die Landau-Lifshitz-Gilbert-Gleichung,

Masterarbeit, Institute for Analysis and Scientific Computing, Vienna University of Technology, Wien (2012).

J. Kemetmüller (Supervisor: M. Page, D. Praetorius):

Vektorisierte Implementierung von P1-FEM in 3D,

Bachelorarbeit, Institute for Analysis and Scientific Computing, Vienna University of Technology, Wien (2012).

ACADEMIC THESES

M. Page (Supervisor: D. Praetorius):

Schätzerreduktion und Konvergenz adaptiver FEM für Hindernisprobleme,

Master's thesis, University of Vienna, Wien (2010).

M. Page (Supervisor: J. Lang, T. Hoya):

Mathematical Approaches to Speech Recognition,

Bachelor's thesis, TU Darmstadt/Nihon University, Darmstadt/Tokyo (2007).